Bio-production d'H2 à haute température chez des modèles de Thermococcales : bases pour des solutions de haute pression optimisées (HPBioHyd)

Jordan Hartunians

DOCTORAT SCIENCES BRETAGNE DE LA MER LOIRE ET DU LITTORAL

UBO
Université de Bretagne Occidentale

THESE DE DOCTORAT DE

L'UNIVERSITE
DE BRETAGNE OCCIDENTALE

ECOLE DOCTORALE N° 598
Sciences de la Mer et du littoral
Spécialité : « *Microbiologie* »

Par
Jordan HARTUNIANS

High temperature H_2 bio-production in *Thermococcales* models: setting up bases for optimized high pressure solutions

HPBioHyd

Thèse présentée et soutenue à Plouzané, le 1er juillet 2020
Unité de recherche : Laboratoire de Microbiologie des Environnements Extrêmes (LM2E UMR6197)

Rapporteurs avant soutenance :

Elizaveta BONCH-OSMOLOVSKAYA
Professor, Russian Academy of Sciences

James HOLDEN
Professor, University of Massachusetts

Composition du Jury :

Elizaveta BONCH-OSMOLOVSKAYA, Professor, Russian Academy of Sciences (Rapporteure)

Alain DUFOUR Professeur, Université de Bretagne-Sud (Président du jury)

Anne GODFROY, Chercheure, IFREMER

Aurore GORLAS, Maître de conférences, Université Paris Saclay

James HOLDEN, Professor, University of Massachusetts (Rapporteur)

Mohamed JEBBAR, Professeur, Université de Bretagne Occidentale (Directeur de thèse)

Long-Fei WU, Directeur de recherche CNRS, Aix-Marseille Université

Invité
Frédéric FRAGNE (Co-directeur de thèse)

The Doctoral School of Marine and Littoral Sciences requires that at least 10 % of the manuscript is written in French. Such paragraphs, found at various places in the book, are direct translations (except for the acknowledgments): no information will be lost by a non-French reader.

L'Ecole Doctorale des Sciences de la Mer et du Littoral demande qu'au moins 10 % du manuscrit soit écrit en langue française. Ces paragraphes, trouvés à divers endroits du document, sont issus d'une traduction directe (à l'exception des remerciements) : aucune information n'est perdue pour un lecteur non-francophone.

Acknowledgements - Remerciements

I want to specially thank the jury for having accepted to take the time to evaluate my work. Thanks to the rapporteurs Elizaveta Bonch-Osmolovskaya and James Holden, and to the examinateurs Alain Dufour, Anne Godfroy, Aurore Gorlas, and Long-Fei Wu for contributing to the discussions about this project.

Merci à l'ANRT d'avoir contribué au financement de ce projet de thèse CIFRE et à la SATT Ouest Valorisation d'avoir géré cette collaboration.

Le projet HPBioHyd est le fruit d'un effort collectif étalé sur plusieurs années; aussi il est important que j'adresse mes remerciements à toutes les personnes ayant apporté leur aide, de près ou de loin.

Merci à Mohamed Jebbar, directeur du LM2E, et Frédéric Fragne, dirigeant d'HP Systems pour la confiance qu'ils m'ont accordée en me permettant de mener ce travail dans les meilleures conditions. Merci également à Didier Flament, co-directeur du LM2E, pour son accueil au sein de son unité.

Je remercie vivement Yann Moalic, sans qui cette collaboration n'aurait pas eu lieu, pour son aide cruciale, ses conseils, son soutien, son investissement, sa disponibilité, ses corrections, sa bonne humeur et le co-encadrement des stagiaires.

Je tiens à adresser mes remerciements à tout le personnel présent et passé d'HP Systems, et notamment à Bertrand Binschtok, Stéphanie Poucineau, Chrystèle Le Gal, Hoang NGuyen Duc, Philippe Ramirez-Hernan, Jean-Mathieu Pauillacq, Romain Flamant, Romain Avril, Serge Theodule, Cédric Vadepied, Gregory Caillaud.

Un grand merci à Raphaël Brizard pour m'avoir lancé sur la manipulation du bioréacteur et d'avoir ensuite soutenu son devenir à mes côtés, ainsi qu'évidemment pour toutes les discussions annexes, et plus récemment son aide significative sur la rédaction de mon manuscrit.

Merci à Erwann Vince pour son soutien technique sur la fin du projet, sa disponibilité et son aide toujours enjouée et volontaire.

Je remercie particulièrement Erwan Roussel pour son expertise technique et scientifique, pour ses nombreuses aides et discussions, son intérêt et son soutien, toujours réactif, disponible et volontaire, qui a également été essentiel à la réalisation de ce travail.

Merci à toutes les stagiaires qui m'ont grandement aidé à l'obtention des résultats présentés dans ce manuscrit, toujours de manière engagée, acharnée et patiente : Marie Naitali, Emeline Vidal, Madina Ahmed, Pauline Grippon, Kateline Letoquart, Anaïs Sire de

Vilar. Merci également à Hamza El Khati qui a pris pied sur le sujet « Evol » un peu plus récemment.

Je tiens à remercier les secrétaires/gestionnaires du LM2E, présentes et passées et notamment Stéphanie Renard et Izabelle Bozec, qui ont toujours été très arrangeantes et à l'écoute.

Merci à Guillaume Lannuzel pour son soutien technique en biologie moléculaire, efficace, organisé, et de bonne humeur.

J'adresse mes remerciements également à Jean-Pierre Donval, pour avoir non seulement toujours tenu son matériel disponible, ce qui a permis à mon travail de survivre aux innombrables pannes des différentes machines utilisées, mais qui a toujours également très volontairement répondu à toutes mes questions, et qui a arrangé de nombreuses mises au point pour que je puisse poursuivre les expérimentations.

Merci à Jérémie Gouriou pour les travaux de dosages de carbone.

Merci à Damien Le Vourc'h pour son implication essentielle dans la conception et la réalisation des tubes d'incubation HP, et à Claude Calvarin pour le travail des prototypes de verre.

Merci à Mathieu Cariou, Yves Quéré, Tomo Murovec pour les impressions 3D des supports de tubes HP.

I am deeply thankful to Dr. Masamitsu Matsumoto, from Syn Corporation, for his kindness and understanding, and for having lended us for a long moment a HP microscopic chamber for tests.

Merci à Karine Alain pour ses discussions, conseils et soutien tout au long du projet, dans de nombreux domaines, scientifiques et techniques.

Merci aux personnes ayant planché sur une suite possible du projet : Bart Gruyaert, Didier Flament, Raphaël Brizard, Erwan Roussel, Jean-Marc Daniel, Mohamed Jebbar.

Merci à Claire Hellio et Alain Dufour, membres du comité de suivi individuel de thèse, pour leurs nombreux conseils.

Merci à Valérie Cueff-Gauchard, Anne Godfroy et Nadège Bienvenu Quintin pour m'avoir fourni souches et conseils.

Un grand merci à tous les chercheurs et à tout le personnel technique du LM2E pour l'aide que vous avez pu m'apporter.

Merci au service informatique de l'IUEM pour sa réactivité.

Je remercie profondément toutes les personnes ayant contribué à créer et maintenir une ambiance saine et stimulante, et éprouver de nombreuses cafetières. Notamment, les doctorants du LM2E, du côté IUEM, et particulièrement Maxime, Jie, Marc et Blandine ; et du côté Ifremer, avec notamment David, Maurane et Elodie. Je n'oublie pas les post-doctorants, Clawisse, Ashley, Gaëlle et plus tôt, Sabrina. Les anciens qui nous ont ouvert la voie, et en particulier Simon, Caro, Flo, Pierre, Mélanie, Charlène, Aline, Kévin, Coraline et évidemment Morgane.

Un merci spécial à Seb pour les innumérables discussions professionnelles, et tout particulièrement pour son aide très importante sur la fin de rédaction ; ainsi que pour les discussions forcément personnelles et cet accompagnement tout le long de ma formation à Brest et ailleurs.

Je remercie, d'une évidence rare, Sarah, pour une foule de choses, dont une coburalité plus que complice, qui a probablement été le soutien le plus solide durant ce projet parfois poussé à bout de Nerf, partageant les plus longues cinétiques de l'histoire de la cinétique. Je lui dois également directement une bonne partie de la qualité de ce manuscrit, évidemment, merci.

Les longues nuits au labo ont souvent été partiellement accompagnées par Yang et Francis, qui tiennent aussi un rôle très important dans la bonne humeur ambiante ; merci à eux également pour leur soutien et leur aide.

Je remercie chaleureusement toute la « compagnie un truc bidon » pour la détente du lundi midi.

Un grand merci à ceux qui m'ont énormément aidé dans la rédaction de ce manuscrit et la réflexion associée, et notamment : Mohamed, Raphaël, Sarah, Sébastien, et Yann.

Enfin, merci à ma famille (notamment Sévan, mes parents et grands-parents), mes proches et mes amis pour leur soutien durant ces trois ans et demi.

N'espérant oublier personne, mais le faisant sûrement, je reste reconnaissant pour tout l'aide et le support qui m'aura été apporté. Merci.

Context

This manuscript describes the work achieved in the frame of a PhD thesis funded by an industrial agreement (CIFRE - *Convention Industrielle de Formation par la Recherche*), which constituted a partnership linking the PhD candidate, the academic Laboratory of Microbiology of Extreme Environments (LM2E (*Laboratoire de Microbiologie des Environnements Extrêmes*, UMR6197)), based in Plouzané (near Brest, France) and the company HP Systems based in Périgny (near La Rochelle, France). It was funded by the ANRT (*Association Nationale de la Recherche et de la Technologie*), with a collaboration managed by the Technologies Transfer Acceleration Society (SATT) Ouest Valorisation. This microbiology project started in March 2017 and ends in July 2020, during which period I was employed by the industrial partner. It represented a full-time work, predominantly performed at the LM2E (European Institute for Marine Studies (IUEM), Plouzané). While the academic research of our lab focusses on the study of extremophile microbiology, HP Systems was specialized in the design and realization of high pressure industrial applications. This collaboration ensued from the original surmise that H_2, an interesting energy carrier, may potentially be produced in an applied fashion from *Thermococcales* in pressurized bioreactors. While the overall goal was applied, attention was given to important fundamental advances. The objectives and organization of the work presented herein are displayed after a state-of-the-art description of literature data that were judged relevant to better comprehend the project and its implications.

Contexte

Ce manuscrit décrit le travail réalisé dans le cadre d'un doctorat financé par une convention CIFRE (Convention Industrielle de Formation par la Recherche), constituant un partenariat reliant le doctorant, le laboratoire académique LM2E UMR6197 (Laboratoire de Microbiologie des Environnements Extrêmes), basé à Plouzané (France) et l'entreprise HP Systems, basée à Périgny (France). Il a été financé par l'ANRT (Association Nationale de la Recherche et de la Technologie), et la collaboration a été gérée par la Société d'Accélération du Transfert de Technologies (SATT) Ouest Valorisation. Ce projet de microbiologie a commencé en mars 2017 et se termine en juillet 2020, période pendant laquelle j'ai été employé par le partenaire industriel, principalement. Cela a représenté un travail à temps-plein, majoritairement réalisé au LM2E (Institut Universitaire Européen de la Mer (IUEM), Plouzané). La recherche académique au LM2E se concentre sur l'étude de la microbiologie des extrêmophiles, et HP Systems était spécialisé dans la conception et la réalisation d'applications industrielles de haute pression. Cette collaboration est née de l'hypothèse originale que l'H_2, in vecteur énergétique intéressant, pourrait potentiellement être produit de manière appliquée par des Thermococcales *en bioréacteur pressurisé. Bien que le but global fût donc appliqué, une attention particulière a été portée aux avancées fondamentales. Les objectifs et l'organisation du travail décrit ici sont présentés après une exploration de l'état de l'art des données de la littérature jugée utile à une meilleure compréhension du projet et de ses implications.*

Table des matières

List of figures

List of tables

Main abbreviations

A

ABC: ATP-binding cassette

ACS: Acetyl-CoA synthetase

Adh: Alcohol dehydrogenase

AFEM: *Association française d'écologie microbienne* (French association for microbial ecology)

AK: Adenylate kinase

AlaAT: Alanine aminotransferase

ALE: Adaptive laboratory evolution (*évolution adaptative en laboratoire*)

ANRT: *Association nationale de la recherche et de la technologie* (national association for research and technology)

AOR: Aldehyde ferredoxin oxidoreductase

ASW: Artificial sea water (*eau de mer artificielle*)

AT: Aminotransferase

B

BHP: HP / HT continuous bioreactor manufactured by HP Systems (*bioréacteur HP/HT continu développé par HP Systems*)

C

Cbt: Cellobiose binding protein

cDNA: complementary DNA

CIFRE: *Convention industrielle de formation par la recherche* (Industrial convention for training by research)

Ct: Cycle threshold

CUT: Carbohydrate uptake transporter

D

DMPD: N,N-dimethyl-1,4-phenylenediamine

E

EAATs: Excitatory amino acid transporters

EMP pathway: Embden-Meyerhof-Parnas pathway

EPA: Ecoisapentaenoic acid

F

FAO: Food and agriculture organization (*organisation des Nations Unies pour l'alimentation et l'agriculture*)

FBA: Flux balance analysis, or Fructose 1,6-biphosphate aldolase

FBPA/ase: Bifunctional fructose 1,6-biphosphatase

FCEV: Fuel cell electric vehicles

FKM/FPM: Fluoro rubber

FHL: Formate hydrogenlyase

FNOR: Ferredoxin:NADP oxidoreductase

FNTs: Formate/nitrite transporters

G

GAP: Glyceraldehyde-3-Phosphate

GAPDH: Glyceraldehyde-3-phosphate dehydrogenase

GAPOR: Glyceraldehyde-3-phosphate ferredoxin oxidoreductase

GDH: Glutamate dehydrogenase

GEM: Genome-scale metabolic model

GLK: Glucokinase

GltS: Glutamate synthase

GS: Glutamine synthetase

GTase: Glucanotransferase

H

H_2: Molecular hydrogen

HMI: Human-machine interface

HSP: Heat shock protein

HP: High pressure

HT: High temperature

I

iGEM: International genetically engineered machine

IPCC: Intergovernmental panel on climate change (*groupe d'experts intergouvernemental sur l'évolution du climat, GIEC*)

K

KBL: 2-amino-3-ketobutyrate ligase

KOR: 2-keto acid oxidoreductase

L

LM2E: *Laboratoire de microbiologie des environnements extrêmes* (Laboratory of microbiology of extreme environments)

M

Mbh: Membrane-bound hydrogenase

Mbs: Membrane-bound sulfane reductase, previously named Mbx

Mbx: Previous name of Mbs

MD system: High affinity maltodextrin ABC-transporter system

Mdx: Maltodextrin

N

NBR: nitrile rubber (acrylonitrile butadiene)

NCBI: National center for biotechnology information

Nfn: NADH-dependent reduced ferredoxin:NADP oxidoreductase

NOX: NAD(P)H oxidase

NPOC: Non-purgeable organic carbon

Nsr: NADPH sulfur reductase

O

OD_{600}: optical density at 600 nm

Opp: di/oligopeptide transporter

P

PCK: Phosphoenolpyruvate carboxykinase

PCR: Polymerase Chain Reaction

Pdo: Protein disulfide oxidoreductase

PEEK: Polyether ether ketone

PEPS: Phosphoenolpyruvate synthetase

PFK: Phosphofructokinase

PGI: Phosphogluco-isomerase

PGK: Phospho-glycerate kinase

PGLM: Phosphoglucomutase

PGM: Phospho-glycerate mutase

PLA: Polylactic acid

PLP: Pyridoxal-5'-phosphate

POR: Pyruvate ferredoxinOxidoreductase

PTFE: polytetrafluoroethylene

PU: Polyurethane

R

RuMP pathway: Ribulose monophosphate pathway

Rubisco: ribulose-1,5-biphosphate carboxylase/oxygenase

S

S°: Elemental sulfur

SCS: ADP-forming succinyl-CoA synthetase

T

Tar: *Thermococcales* aromatic amino acid regulator

Tdh: Threonine dehydrogenase

TGM: *Thermcoccales* glycolytic motif

Tgr: *Thermococcales* glycolytic regulator

TIM: Triose-phosphate isomerase

TM system: Trehalose / maltose high-affinity ABC transporter system

TRM : *Thermococcales* rich *medium*

U

UBO: *Université de Bretagne Occidentale* (University of Western Brittany)

UBOCC: UBO culture collection

V

VME: Vulnerable marine ecosystem

Introduction – State of the art

I. The potential of hydrogen

1. The importance of energy in our modern societies

Energy management has always shaped our societies. This was established in the scholarly works of Wilhelm Ostwald in the early twentieth century (Smil, 2019). Control of energy sources and flows is not only linked to power and the way democracy is entrenched, but also to how technology advances. In 2015, we consumed, globally, 146 000 TWh of primary energy, which represented roughly 25 times more than two centuries before (FIGURE 1) (Ritchie and Roser, 2018). Despite the fact that an unprecedented shift in industrial development was triggered by oil exploitation from 1870, followed by great increases in natural gas, hydroelectricity and coal consumption in the early 19th, it has become clear that the age of fossil fuels is approaching an end (Auzanneau, 2015). Doubtlessly, to reduce our greenhouse gas emissions, low-carbon fuel sources must aid in the transition, as collegially resolved by 195 states during the Paris Climate Agreement of 2015.

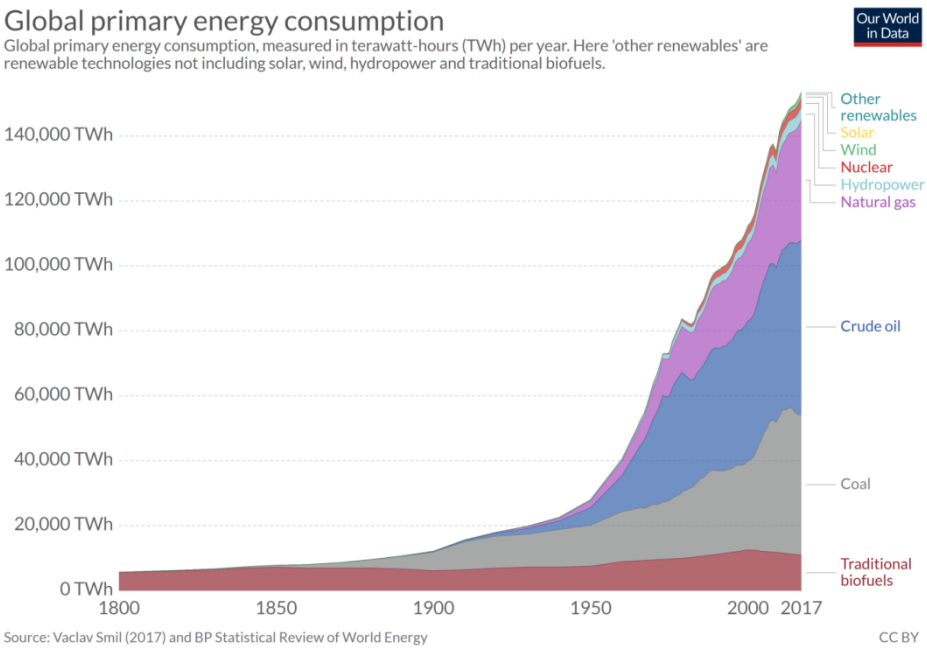

Figure 1: Evolution of the global primary energy consumption, from (Ritchie and Roser, 2018)

For most countries, prosperity and energy are importantly linked, though the exact global tendencies are not clear. Be that as it may, many predictions foresee a continuing increase in the global energy consumption (IEA, 2018; Zeng et al., 2018). The International Panel on Climate Change (IPCC) reports anticipate dramatic consequences to human societies due to a possible rise temperature levels, if this energetic demand is met by current methods, *i.e.* mainly from fossil, carbonized sources. Numerous models forecast rises in sea levels and extreme meteorological events leading to disastrous outcomes on ecological, economical and societal point of views (IPCC, 2018). A shift is thus necessary in order to envision a sustainable future for the people, the biodiversity and their environment.

To solve such change, if we except carbon capture and storage technologies, the possible options are either renewable or nuclear energies, which induce much less CO_2-emissions compared to fossil fuels. Nuclear energy accounts for a major share of many developed countries, especially France, where it holds, since the 1980's, more than 70 % of the electricity mix. It harbors a very high energetic efficiency, reaching, in absolute, more than 10^8 kJ/g, which is many orders of magnitude higher than other fuels (Touran, 2020). Nonetheless, many drawbacks still remain, such as the inherent risk of dramatic explosion, as well as the subsisting technological and political inabilities to properly dispose of waste (Taebi and Roeser, 2019). On another hand, global investment in renewable energy has increased from $ 50 billion per year in 2004 to more than 250 $ billion in 2015, mainly constituted by hydropower, wind and solar energy (Frankfurt School-UNEP Collaborating Centre, 2018). Each solution harbors its proper set of advantages and drawbacks over the other technologies, and each country has different potentialities to develop its own energy mix. This means that on a global scale, it is more accurate to talk about energy transitions than about one uniform transition (IEA, 2019a; I'MTech, 2017).

Lately, a long-known energetic vector has attracted flourishing interest: molecular hydrogen (H_2). Currently used for many other purposes (*e.g.* crude oil desulfurization, electronic device production, fat and oil hydrogenation during oil refining, or as feed stock for chemical productions such as ammonia (Ramachandran and Menon, 1998)), technological progresses have reinstated H_2 for energetic functions.

2. Hydrogen as the modern choice of future energy carrier

Jules Verne discussed the potential of hydrogen as an alternative power source to the unsustainable utilization of fossil fuels, as early as 1874 in his novel "L'Île Mystérieuse" (Verne, 1875). And though H_2 had been chosen, more than 200 years ago, to power the first internal combustion engines (Eckermann, 2001), oil won the race, not demanding as important scientific nor technological breakthrough as hydrogen (Auzanneau, 2015). The latter however received an unprecedented momentum in the last decades, as envisioned as an opportunity to tackle with various energy challenges. Different industrial sectors are concerned by a potential decarbonization effect of H_2, which struggle to reduce their emissions: long-distance transport, chemicals, iron and steel, *etc*. Attempts have occurred in the past to move towards a "hydrogen economy" (*e.g.* (Green, 1982)), but recent lessons from technological innovations having led to successes in other energy fields (solar photovoltaics, wind exploitation, electric vehicles), have shown more potentials for such clean future, and specialists believe that the world economy may convert to hydrogen economy by the end of the century (El-Emam and Özcan, 2019).

Burning H_2 in air should give the following reaction: 2 H_2 (g) + O_2 (g) -> 2 $H_2$0 (l). This combustion produces water, and would release 286 kJ/mol, meaning that molecular hydrogen energy density is of 143 kJ/g, making it higher than most other fuels, generally delivering around 50 kJ/g (Fung, 2005; Wang, 2012). But the growing interest around H_2 for energy does not only stand in its view as a combustible. It is also envisioned to power fuel cells, in which chemical potential energy from a fuel is converted into electrical energy.

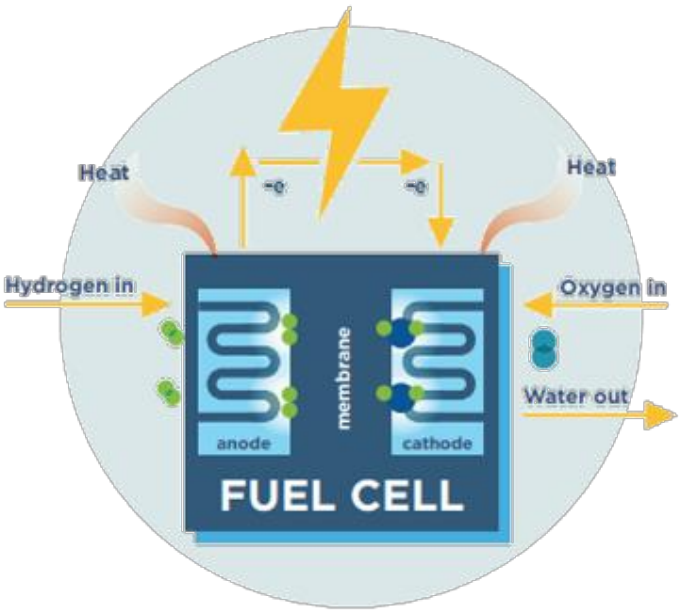

A fuel cell is an electrochemical energy conversion device, utilizing hydrogen and oxygen to generate electricty, heat and water. To such extente, the hydrogen atoms enter at the anode, then are stripped of their electrons in the cathode. The positively charged protons pass through the membrane to the cathode and the negatively charged electrons are forced through a circuit, generating electricity. After passing through the circuit, the electron combine witht the protons and oxygen from the air to generate the fuel cell's byproducts: water and heat.

Figure 2: How fuel cells work (from (FCHEA, 2020)

Efforts have been broadly made towards developing more and more efficient fuel cells, which are already used in various vehicles: personal cars, bikes, planes, postal trucks, public buses, boats (Linde Stories, 2019; Ohnsman, 2020). Nowadays, fuel cells are more efficient in engines than combustion, and we can expect even better yields as technology advances.

Molecular hydrogen, more than a source of energy itself, can serve as a vector, meaning than it can easily, with good yields, store a potential energy and transport it before retransforming it through fuel cells (Krajačić et al., 2008; Mandal and Gregory, 2010). And to this extent, efforts become plural to develop the required infrastructure and technologies to materialize a broad usage (Ortiz Cebolla and Navas, 2019; Popov and Baldynov, 2018). Global sales of fuel cell electric vehicles (FCEV) are exploding, showing a 80 % increase in 2018 compared to 2017, and several countries have announced large targets for FCEV deployment by 2030, which, if followed, would increase the car stock from 11 000 to 2.5 million (FIGURE 3). Hydrogen is indeed the only fuel recognized to date not to produce CO_2 as a byproduct when generating electricity with fuel cells. The use of electric vehicles could hold important influences on air quality (Ahmadi, 2019).

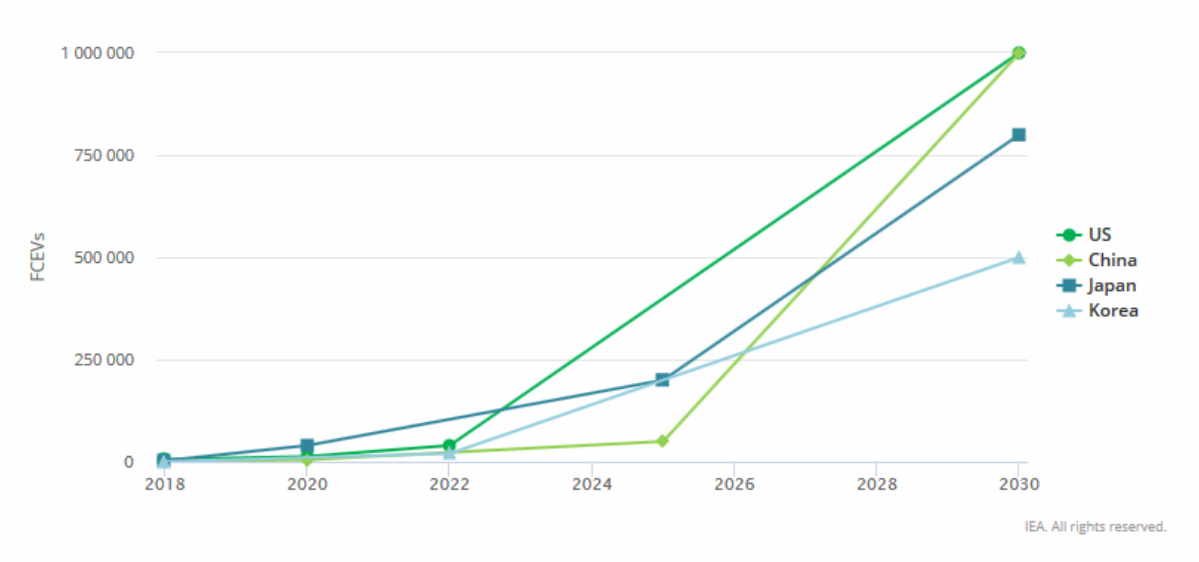

Figure 3: Major targets for fuel cell electric vehicles (from (IEA, 2019b))

Nowadays technologies allow us to produce (sometimes locally (Meillaud, 2020; Nuttall and Bakenne, 2020)), store and use hydrogen efficiently as an energy vector, yet a common effort to develop infrastructures is key to accomplish the transition, understood by industrial and governmental parties (AFP, 2018; Franc and Mateo, 2015; Sun and Shirouzu, 2019; U.S. DOE Hydrogen and Fuel Cells Program, 2020).

One of the major arguments in favor of the hydrogen economy paradigm is that the potential production ways are very diverse, as for example fossil fuels, biomass and non-food crops, nuclear energy, wind, solar, geothermal, hydroelectric. Yet, at the time of writing, almost all of the 70 million tons H_2 produced worldwide ensue from Steam Methane Reforming (SMR), a process based on fossil fuel and emitting CO_2 (IEA, 2019b; Sun et al., 2019). The production is thus not sustainable yet, underlining the urge to develop and adapt alternative methods (Burke, 2018; Glenk and Reichelstein, 2019). Hydrogen can however also be found in natural systems.

3. Hydrogen in natural systems and bio-production processes

Except for some natural vast reservoirs currently considered for exploitation, such as in Bourabougou, Mali (Prinzhofer et al., 2018), molecular hydrogen is rather scarce in nature, and its presence is often considered as a “geological curiosity”. However, if not much

abundant, it is now acknowledged that H_2 can be found in a diversity of natural environments, such as volcanic systems, hydrothermal and geothermal vents (Charlou et al., 2002), ultramafic rocks (Neal and Stanger, 1983), crystalline basements (Parnell and Blamey, 2017a), alkaline igneous complexes (Nivin, 2019), graphite, evaporate and potash deposits (Parnell and Blamey, 2017b), and cataclasites (McMahon et al., 2016). It can emerge from abiotic processes, such as serpentinization (ferromagnesium minerals alteration to serpentine, occurring below 500 °C), graphitization (decomposition of methane to graphite, occurring above 600 °C), radiolysis (dissociation of water by ionizing radiation), cataclasis of silicate minerals (hydromechanical breaks).

At lower temperatures, molecular hydrogen is also part of biological cycles, and can either serve as an electron donor or acceptor. Hydrogen-generating metabolic processes include fermentation (dark or photo-fermentation (Bolatkhan et al., 2019; Reungsang et al., 2018), nitrogen fixation (Bothe et al., 2010), anaerobic carbon monoxide oxidation (Diender et al., 2015), acetate oxidation (Zinder and Koch, 1984), biophotolysis (Ghiasian, 2019). Hydrogen-consuming metabolic processes include hydrogenotrophic methanogenesis, acetogenesis, sulfate reduction, sulfur reduction, iron (III) reduction, aerobic hydrogen oxidation, dehalorespiration, fumarate respiration, denitrification (Gregory et al., 2019). Those types of production and consumptions are often linked in syntrophic relationships (Morris et al., 2013).

In the scope of applied hydrogen production, fermentations are the main types of metabolism considered. They can occur, depending on the hosts, at all temperatures, and be driven by bacterial, eukaryal, and/or archaeal mixed or pure cultures (Dębowski et al., 2014; Pawar and Niel, 2013). They can work with the action of light (photofermentation) or not (dark fermentation). Due to the specificities of each process, two-stage cultures involving both photo- and dark fermentations could be considered (Sağır and Hallenbeck, 2019).

Dark fermentation presents the advantage not to require illumination, which involves large reactors surface areas. Furthermore, fermentative processes involve work in anaerobic conditions, thus not involving mixing O_2 and H_2, which can be highly reactive in some conditions. Some dark fermentative processes can also be naturally linked to carbon monoxide or acetate oxidations. Several studies have also described fermentations by

cultures performed on various wastes, raw or treated. Most of studies of H_2 bio-production *via* dark fermentation concern facultative anaerobic bacteria (*e.g. Enterobacter aerogenes*, *Enterobacter cloacae*, *Escherichia coli*, and *Citrobacter intermedius*, among others) and obligatory anaerobic bacteria (*e.g., Clostridium beijerinckii*, *Clostridium paraputrificum*, and *Ruminococcus albus*, among others) (Hallenbeck and Ghosh, 2009). Most of the works involve mesophilic microorganisms, because of their ease of use and their fast generation rate (Ghimire et al., 2015). However, even though the costs could be slightly higher to heat up the incubators in the first place, performing high temperature cultures shows several advantages for hydrogen synthesis. Among them, high temperatures (80–100 °C) allows to prevent a lot of contaminations, inducing a positive selection for the used strains, decreases *medium* viscosity, enhances its mixing, speeds up the chemical reaction rates, and cancels the need for cooling down the reactor (Pawar and Niel, 2013).

Thermodynamically, it favors the reaction of H_2 production. High temperatures lead to a more entropic system, *i.e.* more energetic, and H_2 production from reducing equivalents by hydrogenases becomes exergonic, so more favorable because spontaneously possible, at high temperatures. Mesophilic temperatures render the reaction possibly endergonic, and consequently favor recycling of reducing equivalents *via* other metabolites (see LIFE IN HOT AREAS, P. 38) (Tang et al., 2008, 2017; Verhaart et al., 2010). Indeed, hyperthermophlic anaerobic bacteria have been reported to reach a yield of up to 80 to 100 % of the maximum theoretical value of 4 mol of H_2 produced per mol of glucose consumed (the so-called Thauer limit (Thauer et al., 1977)), where mesophilic anaerobic bacteria have shown much lower yields.

II. The extreme microbial life of deep hydrothermal vents

The Laboratory of Microbiology of Extreme Environments (LM2E UMR6197) has been observing hydrogenogenic life for several years, since it has specialized in the study of one of the naturally H_2-occuring places: hydrothermal vents.

1. Geochemical, physico-chemical and thermodynamical descriptions of hydrothermal vents

Explored by the scientific community from the 1970's, these habitats are, from a Human's perspective, around the most extreme environments found on Earth. Shallow and deep-sea hydrothermal vents are world-wide distributed, emerge from submarine volcanic activities and occur at mid-ocean ridges, backarc basins, or seamount volcanoes, in both the photic and aphotic zones of the ocean (down to around 6000 m) (FIGURE 4) (Ballard et al., 1975; Corliss et al., 1979; Dick, 2019a; Scott et al., 1974).

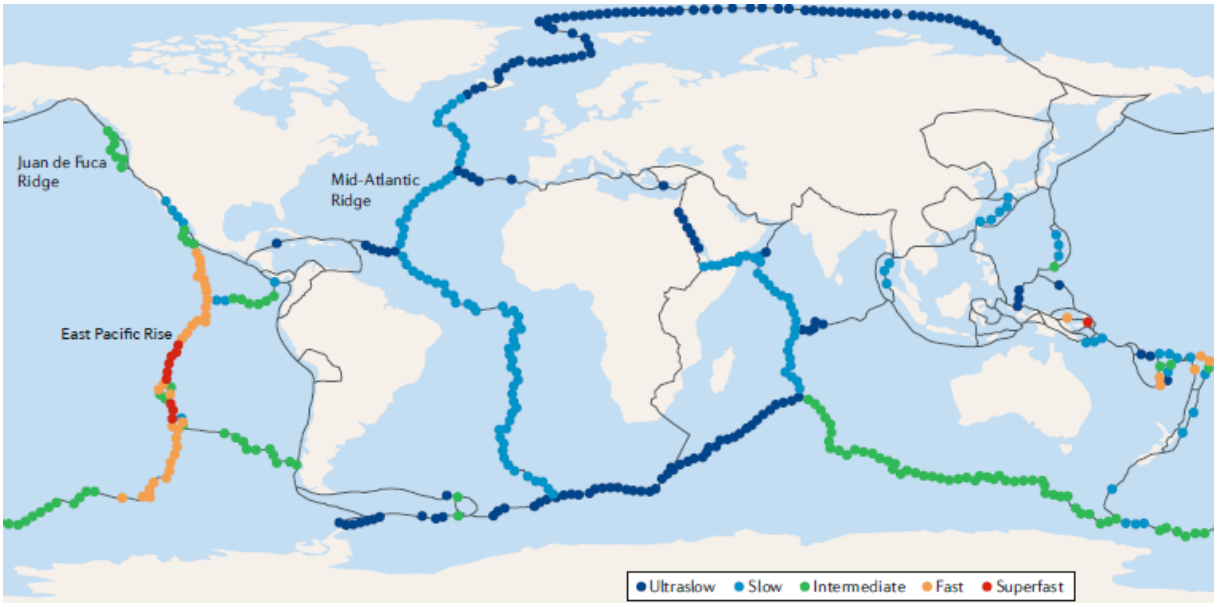

Figure 4: Global distribution of the hydrothermal-vent systems (from (Dick, 2019a))

Locations of confirmed and inferred active deep-sea hydrothermal-vent fields deeper than 200 m. Colors represent spreading rates. Ultraslow: < 20 mm/year. Slow: 20 – 50 mm/year. Intermediate: 50 – 80 mm/year. Fast: 80-140 mm/year. Superfast: > 140 mm/year.

Hydrothermal vents are firstly issued from geological events. When the oceanic crust forms and emerges from ridges, it progressively cools down in contact with the seawater and thus shrinks. Consequently, multiple discontinuities and cavities occur. Then, the dense, cold seawater percolates through them. This water will soon be heated up and react with the rocks to become what is called the hydrothermal fluid. As it approaches the very hot magmatic chambers (around 1200 °C), chemical exchanges intensify, discharging oxygen,

precipitating calcium and sulfates. The fluid enriches in numerous reduced and anoxic species, such as metallic ions (Fe^{2+}, Mn^{2+}, Zn^{2+}, Cu^{2+}), trace metals (Co, Ni, Ge, As, Me, Cd, In, Sn, Te, Au, Sb, Bi, Ag), elemental sulfur, and dissolved gases (CO_2, CH_4, H_2S, CO). This results in a superheated, reduced and acidic fluid, less dense than seawater, thus rapidly flowing upward the faults to discharge in hydrothermal vents, at up to 400 °C. There, chimneys are formed by the contact between hydrothermal fluids and the cold, slightly basic and oxygenated seawater (FIGURE 5). Those geological edifices evolve over time, being determined by fluid end composition, emission temperature and speed.

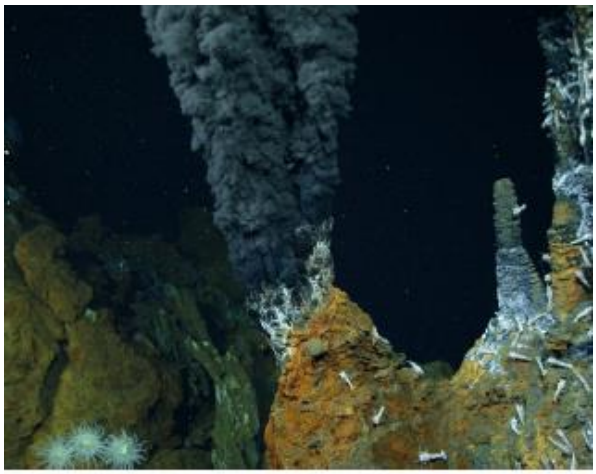

Figure 5: Photo of a black smoker and a chimney habitat (from (Dick, 2019a))

The chemical composition and the temperature of hydrothermal fluids vary according to each site's geological settings, meaning very locally, depending on the nature of the subseafloor fluid circulation network, or of the seafloor (*e.g.* basaltic, mantellic, sedimentary). Particularly, it can be abiotically enriched in hydrogen, due to serpentinization processes (*i.e.* changes of rock structure by addition of water into the crystal structure of the minerals) or magma degassing (Adam and Perner, 2018a). Each chimney itself is highly heterogeneous in its composition, due to the succession of mineral precipitation and dissolution (Charlou et al., 2002; Deborah S. Kelley et al., 2002; Fouquet et al., 1988; Gartman et al., 2011; Haymon, 1983). The hydrothermal plume, corresponding to a mix of hydrothermal fluid and seawater can go up vertically at several hundred meters by density contrast, and can spread up dozens of kilometers in the ocean, following currents, thus dispersing its emissions (Dick, 2019a; Dick et al., 2013). These interactions between the geosphere and the biosphere set the bases for the hydrothermal vent ecosystem (Amend and Shock, 2001).

Especially due to the polymetallic sulfide deposits accumulated around them, these special sites are of growing interest to the deep-sea mining industry (Petersen et al., 2016). But more than constituting geological curiosities, and as better described hereafter, hydrothermal vents host a rich, dense, and meaningful biodiversity. Being able to study them has permitted the scientific community to formulate theories about the origin of life, or the possibility of life on other planets, and has unraveled unknown physiological diversity, to name only few of the consequential interests (Martin et al., 2008). Such areas are thus of a substantial importance, and at many levels, the way we touch and influence them must be managed. In order to organize and control all activities related to mineral resources from the seabed, and other activities such as its exploration, the International Seabed Authority (ISA) was created in 1994 (International Seabed Authority, 2020). On another hand, the Food and Agriculture Organization (FAO) and has classified those sites as Vulnerable Marine Ecosystems (VME) (FAO, 2020). The scientific community still debates whether those peculiar biotopes would be able to quickly recover from mining activities, and precaution is therefore advised regarding their exploitation (Van Dover et al., 2018).

2. Microbial and biological diversity at hydrothermal vents

Hydrothermal vent ecosystems represent rare environments, estimated to fill barely more than the size of Brest (50 km²) (Menini and Van Dover, 2019; Van Dover et al., 2018). They are hypothesized to have hosted the earliest forms of life on Earth (Fiore, 2019; Martin et al., 2008; Toxvaerd, 2019). Life, at vents, has only recently been observed. Fauna was found unexpectedly along the Galapagos Rift, in 1977 (Corliss et al., 1979). The high *in situ* pressure and the distance from photosynthetic primary production led to the belief that the abyss was largely lifeless. Indeed, being completely disassociated from photosynthetic systems, the first links of the food web at hydrothermal vents are chemolithoautotrophic microorganisms. They are often in symbiotic associations with *fauna* (for about 97 %) and are crucial to the whole ecosystems (Tunnicliffe, 1991). For example, the shrimp *Rimicaris exoculata* hosts *Gammaproteobacteria*, *Epsilonproteobacteria*, and *Zetaproteobacteria* in its gill cavity (Jan et al., 2014). Primary producers can also be directly ingested by primary consumers such as grazers, feeding on microbial mats; filter feeders, feeding on free cells or particles emitted by hydrothermal fluids; or detritivorous scavengers (Tunnicliffe, 1991).

Animal life is very dense around hydrothermal vents, which contrasts with the surrounding abyssal seafloor, where individuals are more scarce spread (Desbruyéres et al., 2000; Tunnicliffe, 1991). Generally, a hydrothermal site is dominated by an "engineer" species, mainly belonging to the groups of tube worms (*Alvinellidae* and *Siboglinidae*), mollusks (*Vesicomyidae* and *Mytilidae*) and arthropods (*Cirolanidae*). Those "engineers" influence the habitat by directly or indirectly modulating the nutrient availability for others (Sarrazin and Juniper, 1999). Based on this local habitat micro-diversity, other communities also inhabit the surroundings of hydrothermal vents, such as crustaceans and *meiofauna* (*e.g.* nematods, copepods) (Zeppilli et al., 2018).

How living networks are organized there is highly dependent on each site. The steep temperature and chemical gradients induce rapidly changing conditions, in both temporal and spatial scales, resulting in a wide variety of microhabitats (*e.g.* with fluctuating pH, temperature, salinity). As the conditions vary signifcantly around hydrothermal vents, the associated communities can also be different. Numerical modelling, diversity studies, metagenomics, metatranscriptomics, cell culturing and activity measurements, have indicated that hydrogen and methane as electron donors, and nitrate and oxygen as electron acceptors, are particularly driving microbial diversity and activities (Adam and Perner, 2018b; Fortunato et al., 2018; McCollom, 2007). To a simplified extent, the hydrothermal fluid provides inorganic carbon and electron donors to the primary producers, while the surrounding seawater provides electron acceptors and organic matter to all microbial communities (FIGURE 6). Microbial habitats can be classified into several principal types: hydrothermal edifices, sediments, fauna, and surfaces (of edifices, sediments, animals …).

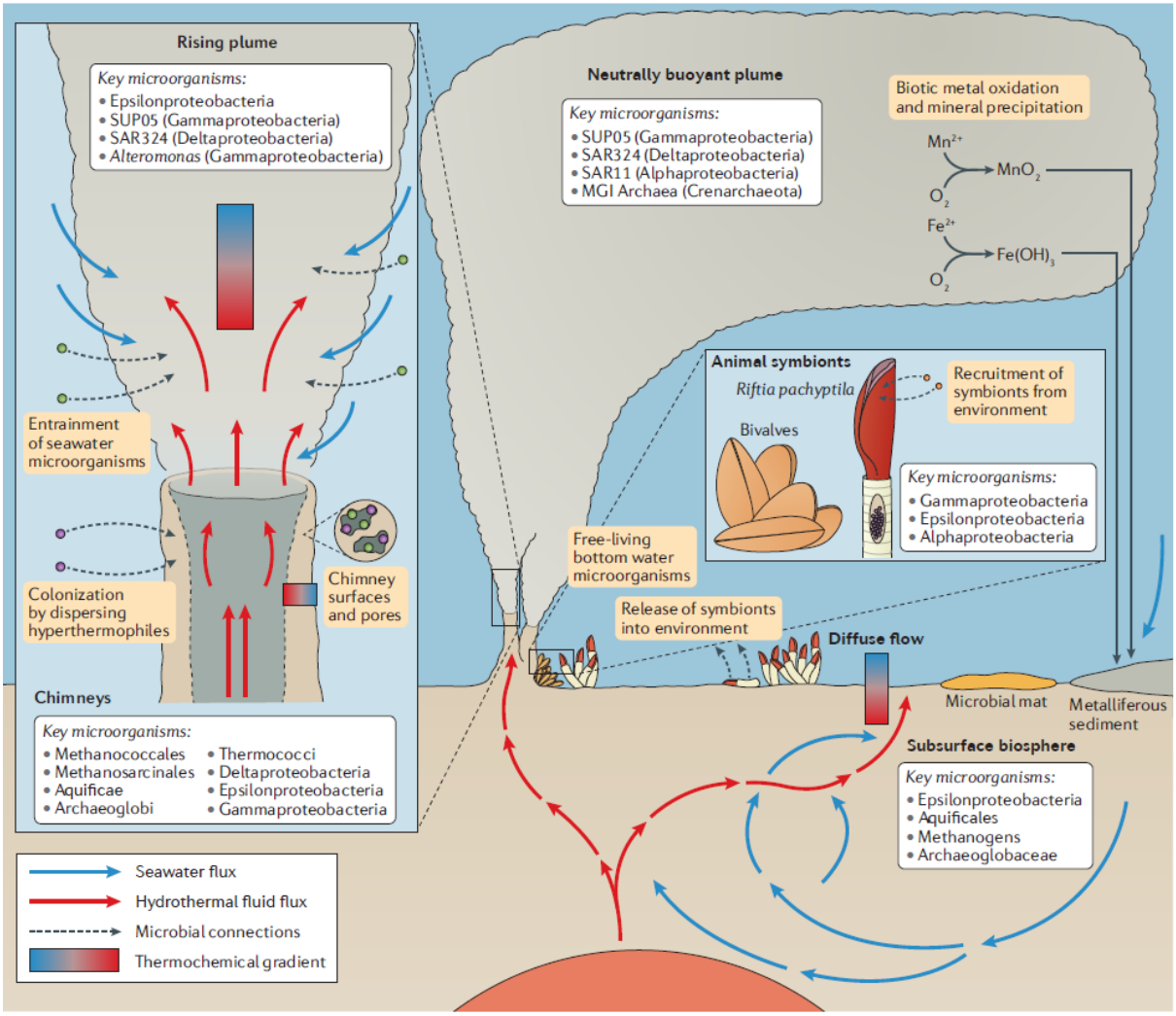

Figure 6: Microbial habitats at deep-sea hydrothermal vents (from (Dick, 2019a))

The main habitats at hydrothermal vents are chimneys, the surrounding subsurface, animals and rising plumes. Hydrothermal fluids move between habitats and mix with cold seawater. Key microorganisms for each habitat represent abundant taxa *observed across multiple vent fields by various cultivation-independent approaches. The red-blue rectangle indicates a thermochemical gradient between anoxic, chemically reducing, hot hydrothermal fluids and oxic, cold seawater. Note that this illustration is generalized, not comprehensive, and it does not represent any particular vent field.*

The way microbial colonization of a hydrothermal vent occurs is uncertain. Because they emerge from fluids at very high temperatures, hydrothermal edifices are initially sterile, but get rapidly colonized when life-compatible conditions are set. It was experimentally shown that hyperthermophilic microorganisms (namely *Pyrococcus furiosus* and *Methanocaldococcus villosus*) adhere to black smoker chimney surfaces using biofilms at the

surface of the chimney (Wirth et al., 2018). Many hyperthermophiles survive long periods of low temperature, and rapidly recover when back in warm environments (Lesongeur et al., 2014; Summit and Baross, 1998). Thus, it is possible that colonization could come from cells remaining in the surrounding cold seawater (Holden et al., 1998). Others hypothesize they were within the seafloor (Colman et al., 2017; Deming and Baross, 1993).

Biological activities around hydrothermal vents are involved, in a broader sense, in the main biogeochemical cycles (carbon, hydrogen, nitrogen, sulfur and iron) (Adam and Perner, 2018b; Holden et al., 2012; Houghton et al., 2019). Many microorganisms isolated from deep-sea hydrothermal vents are (hyper)thermophiles, such as the *Thermococcales*, that are capable of H_2 production and studied herein.

III. Life in hot areas

In the late 1960's, Brock and his team isolated, from Yellowstone hot springs, microorganisms growing well at temperatures higher than 75 °C (Brock and Freeze, 1969). Some strains have then shown potentials to grow at temperatures near the water-boiling point. For example the *Euryarchaeota Methanopyrus kandleri* grows optimally at 100 °C, at atmospheric pressure, and can still divide at 116 °C (Takai et al., 2008), and the *Crenarchaeota Pyrolobus fumarii* has an optimal growth at 106 °C and can withstand up to 113 °C (Blöchl et al., 1997). Along the decades, many studies have intensified our knowledge of the possible adaptations involved in (hyper)thermophily.

Microorganisms are classified as "thermophilic" if they grow optimally at temperatures above 45 °C. This definition has been extended to "hyperthermophilic", concerning ranges above 80 °C (Madigan et al., 2017).

1. What happens when temperature increases?

Changes in temperature, at the very fundamental level, induce modifications of atom interactions in the considered system. However, this will have considerable consequences on

highly integrated systems; including the physiology of a cell and its ecology. The influences of temperature on biological features can be explained at different levels.

As the hyperthermophilic trait of the microorganisms studied during my PhD is important to their metabolism and physiology, it is important to properly understand what happens when temperature increases. Note that pressure will also play a role because it directly affects enthalpy (*i.e.* the total heat content of the system), and will be described later (see LIFE AT HIGH PRESSURE, P. 46).

1.1. Thermodynamical principles

In, 1889, Arrhénius explained that chemical reaction rates are correlated with temperature (Arrhenius, 1889). With increasing temperatures, atoms and molecules move faster, are more likely to encounter and react together, and hold more kinetic energy. At higher temperature, a system is more energetic. To understand what happens biologically in (hyper)thermophiles compared to mesophiles, and how they adapt, it is convenient to grasp the fundamentals of the associated chemistry.

During a chemical reaction, energy changes can be calculated by the Gibbs free energy (noted ΔG). Defined in the 1870's (Gibbs et al., 1874), it is also named the free enthalpy: the difference between the heat released in a process and the heat released for the reversed process. It can be formulated as follows:

$$\Delta G = \Delta H - T\Delta S$$

Where:

ΔH: Change in enthalpy, which corresponds to the heat released or absorbed at constant pressure

T: temperature

ΔS: Change in the entropy

Practically, this notion is useful to determine whether a reaction is favorable or not, while just considering a given thermodynamic system and not its surroundings (which can be abstracted in the case of a biochemical reaction). If $\Delta G > 0$, the chemical reaction demands energy, it is endergonic. If $\Delta G < 0$, the reaction is exergonic, it releases energy.

When increasing temperature, the system is more enthalpic (ΔH increases), but it also influences the second term of the equation, including the entropy change (ΔS). ΔG values for given reactions are thus not the same in a (hyper)thermophilic context than in mesophilic conditions. Whether or not a reaction is favorable can consequently be reversed in some cases, as activation barriers can be relieved. ΔG values of metabolic reactions generally decrease when temperature increases (Amend and Shock, 2001).

Another way to assess the changes in ΔG according to temperature changes is by considering the ΔG values for standard conditions, and the actual chemical composition of the environment of interest (concentrations of products and substrates), such as:

$$\Delta G = \Delta G^{\circ\prime} + RT \ln Q$$

Where:

$\Delta G^{\circ\prime}$: ΔG for standard biological conditions (pH 7, 0.1 MPa, 25 °C)

R: perfect gas universal constant (8.314 $J.mol^{-1}.K^{-1}$)

T: temperature, in Kelvin

Q: reaction quotient, *i.e.* the relative amounts of products and reactants present during a reaction at a particular point in time.

1.2. Thermophilic metabolism

Unlike phototrophic organisms, chemotrophic organisms found around deep-sea hydrothermal vents are driven by *disequilibrium* between reduction-oxidation (redox) reactions. Slow to equilibrate on their own, these reactions are kinetically inhibited but thermodynamically favorable to allow energy flux. The changes in the oxidation states of atoms can be quantified by their midpoint potentials E (in Volt), expressing the aptitude of the giver chemical species (the reducer) to donate electrons to the receiver species (the oxidizer). The more E is negative, the more likely the reducer is to donate electrons.

The electrochemical potential E in a redox reaction is inversely proportionally linked to the Gibbs free energy ΔG by the following formulation:

$$\Delta G = -n\,F\,\Delta E$$

Where:

n : number of electrons transferred

F: Faraday constant (96.552 $kJ.V^{-1}.mol^{-1}$)

ΔE : difference in electrochemical potentials from the two concerned species

Thus, it is possible to calculate the ΔG values by considering the electrochemical potentials of the engaged redox couples.

The way temperature can change the value of ΔG can greatly impact a metabolism, as the sign of ΔG will influence the direction of the reaction. For example, proton reduction by formate would be thermodynamically favorable only in thermophilic conditions. At 80 °C, the corresponding ΔG is -2.6 kJ/mol, whereas +1.3 kJ/mol in standard conditions (Lim et al., 2012).

Principal metabolic reactions kinetics have been assessed at mesophilic conditions several decades ago (Thauer et al., 1977). Higher temperatures were however only considered later, based on the revised Helgeson-Kirkham-Flowers equations of state and combined with experimental data of sound velocity, calorimetry, and other literature analyses (Amend and Shock, 2001). Those calculations also concern the properties at high temperature of many organic compounds: hydrocarbons, acids, alcohols, amides, amines, ketones, aldehydes, chlorinated compound, metal-organic complexes, amino-acids and short peptides, and unfolded proteins (Amend and Shock, 2001). Based on those formulations, thermodynamic properties and chemical affinities of reactions in a hydrothermal context can be calculated with some open-source software, as for example the R package CHNOSZ (Dick, 2019b).

In a metabolic pathway, reactions cannot be only considered independently, as each metabolite concentration locally affects the activity considered in the reaction kinetics. Also, some reactions must occur in the same system to be feasible, as through electron bifurcation. This mechanism is described as the third type of energy conservation (along with substrate-level phosphorylation and electron-transport linked phosphorylation), allowing to perform apparently unfavorable reactions, thermodynamically. For example, in the hyperthermophilic *bacteria Thermotoga maritima*, a NADH-dependent reduced ferredoxin:NADP oxidoreductase, NfnAB, allows, reversibly, the coupling of the endergonic reduction of ferredoxin with NADPH to the exergonic transhydrogenation from NADPH to NAD^+ (Demmer et al., 2015) (see CYTOSOLIC REGULATION OF ELECTRON FLUXES: NFN, P.92). Considered independently, the ferredoxin reduction would not happen favorably, due to their differences in redox potentials (FIGURE 7).

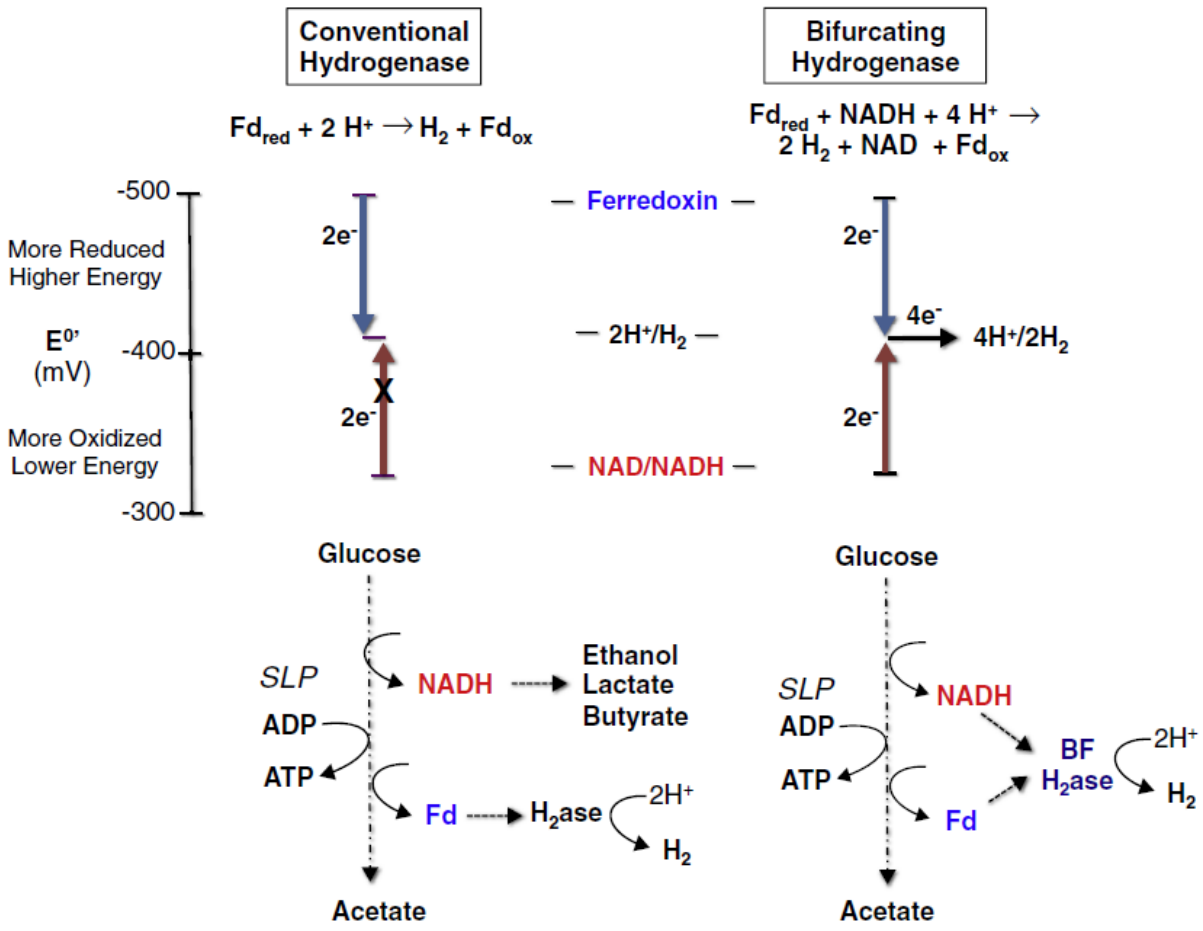

Figure 7: Comparison of the reactions catalyzed by H_2-producing bifurcating and non-bifurcating hydrogenases, and their impacts on the metabolic electron flow and energy conservation (from (Peters et al., 2016))

Upper part: Conventional hydrogenase spontaneously evolves H_2 from the low potential donor reduced ferredoxin (Fd), but oxidation of high potential NADH coupled to proton reduction is an endergonic reaction. The bifurcating hydrogenase catalyzes ferredoxin and NADH oxidation simultaneously to produce H_2.

Low part: Glucose oxidation generates both NADH and reduced Fd and energy is conserved by ATP production via *substrate-level phosphorylation. Conventional hydrogenase oxidizes only reduced Fd, and NADH oxidation must be coupled to the generation of reduced carbon products (from pyruvate) that would otherwise be used for substrate-level phosphorylation. The bifurcating hydrogenase oxidizes both reduced Fd and NADH to generate the maximum amount of H_2 and ATP.*

Note that pH neutrality is affected by temperature (and pressure, to a lower extent). For example, at P_{atm} and 85 °C pH is neutral at 6.26, because H_2O dissociation is linked to temperature and neutrality is defined as the pH value where H^+ and OH^- have the same activity (Amend and Shock, 2001).

1.3. Cellular and molecular adaptations to high temperatures

Temperature variations do not induce changes only at the level of metabolic, biochemical reactions. Many other biological features are also affected, overall leading to different physiologies. For example, cell division time varies with even small temperature changes. In *P. woesei*, a growth temperature of 100 °C results in five times more cell divisions than if incubated at 95 °C (Zillig et al., 1987).

High temperatures increase the risks of denaturation of double-stranded DNA, as well as it flexibility (Driessen et al., 2014; Grogan, 1998; Lindahl and Andersson, 1972; Lindahl and Karlstrom, 1973). Different strategies are used by (hyper)thermophiles to counteract these, such as: better conformational rigidity (Kowalak et al., 1994); histone compaction and nucleosomes (Higashibata et al., 1999); smaller, multi-copy genomes (Bernander, 2000); higher percentages of G and C bases in ribosomal and transfer RNAs (Lambros et al., 2003); positive supercoiling due to reverse gyrase (Atomi et al., 2004a; Catchpole and Forterre; Forterre, 2002); structural compactness (Grosjean and Oshima, 2007); ionic bonds (Imanaka, 2011); and amino acid substitutions (Takami et al., 2004; Xu et al., 2018).

As a higher level of consideration, enzymes are crucial in metabolic pathways. They catalyze reactions that would otherwise require too much activation energy to occur spontaneously, or allow endergonic reactions by coupling exergonic steps. These macromolecular catalysts are mainly proteins. Following the principles stated previously, increases in temperature induce changes in the macroscopic thermodynamics of such molecules. Indeed, thermal stability of a protein or of a protein domain can be measured by the ΔG changes in their folding reactions (Kumar and Nussinov, 2001). Consequently, thermophilic proteins can harbor structural adaptations (*e.g.* more hydrogen bonds and hydrophobic interactions (Imanaka et al., 1986; Macedo-Ribeiro et al., 1996)) to increase stability and compactness, and can also prevent aggregation, use the folding systems of Heat

Shock Proteins (HSP), and adapt their maturation processes to keep active (De Maio et al., 2012; Keese et al., 2010; Rahman et al., 1998; Ritossa, 1962; Thangakani et al., 2012). To preserve viable internal osmotic pressures, all cells accumulate small and soluble organic compounds. Solutes involved in thermophily are called thermolytes and include: polyol-phosphodiesters and alpha-hexose derivatives and other that are specific to hyperthermophiles (*e.g.* β-glutamate) (Neves et al., 2005; Santos et al., 2011).

Post-transcriptional modifications are important in thermal RNA stabilization in some hyperthermophiles, such as *P. furiosus* (Kowalak et al., 1994). Promoters can also be heat-shock inducible, further indicating a possible regulatory adaptation to high temperatures (Keese et al., 2010; Vierke et al., 2003).

As cell membranes are composed of lipids, their rigidity will also be affected by temperature changes. (Hyper)thermophiles have adapted membrane compositions and organizations to counteract this effect and maintain cell integrity (*e.g.* more covalent bonds, use of so-called thermophilic lipids) (Imanaka, 2011; Koga, 2012; Oger and Cario, 2013).

Consequently, many biological differences ensue from those peculiar conditions, in order for (hyper)thermophiles to continue to thrive in such seemingly harsh environments. Additionally, as these extremophiles were investigated for their capacities to withstand high temperatures, they revealed interesting potential biological applications.

2. (Hyper)thermophiles in biotechnology

As described above, the last few decades have witnessed a broad interest from the scientific community in (hyper)thermophiles. Studying their diversity has naturally led to discoveries, from which applications are still being investigated, some having revolutionized scientific and technical practices. One of the most famous examples is the use of the DNA polymerase of *Thermus aquaticus*, whose thermostability has enabled the enhancement of the polymerase chain reaction (PCR) in molecular biology (Saiki et al., 1988). Numerous thermostable enzymes (the so-called "thermozymes" (Vieille and Zeikus, 1996)) have been described, leading to many patents on the potential applications in various fields, such as food, medicine, pharmaceutical and chemical industries. For instance, α-amylases from

Pyrococcus woesei and *Thermococcus profundus* could be used in the sugar industry and for starch processing, cellulases from *P. furiosus* could be used for alcohol production and the fruit industry, and β-galactosidases from *P. woesei* could be used for low-lactose milk production (Mehta et al., 2016; Rekadwad and Khobragade, 2017). More recently, *P. furiosus* was used in microbial fuel cells, generating electricity (Sekar et al., 2017). Therefore, *Thermococcales*, the models considered in this work, are important for industrial applications.

IV. Life at high pressure

Hydrothermal vents are often found in the deep-sea, where another important physical parameter impacts life: pressure. Pressure is defined as the force applied at right angles to the surface of an object per unit area. In piezophile microbiology, pressure is expressed in MPa (1 MPa = 10 bar = 9.81 atm = 769.88 Torr). Most of Earth's biotopes are under elevated hydrostatic pressure. It was estimated that up to 70 % of all cells on our planet could be located in the deep biosphere, where pressure is at least 10 MPa (Magnabosco et al., 2018; Oger and Jebbar, 2010; Whitman et al., 1998). Thermodynamically, in our biotope frame, pressure does not impact on biochemical dynamics, much when compared to temperature, but its variation can still lead to important physiological differences, according to microorganism preferences (FIGURE 8). This feature was observed almost 150 years ago (Certes, 1884), but it is only with the exploration of the deep sea, from the mid-twentieth century, when many piezophilic strains were discovered, that the study of piezophily really advanced (Zobell, 1952; Zobell and Oppenheimer, 1950). While investigators observed that some strains did not survive without pressure, the first recognized obligate piezophile (*Colwellia* sp. MT41) was only described in 1981 (Yayanos et al., 1981).

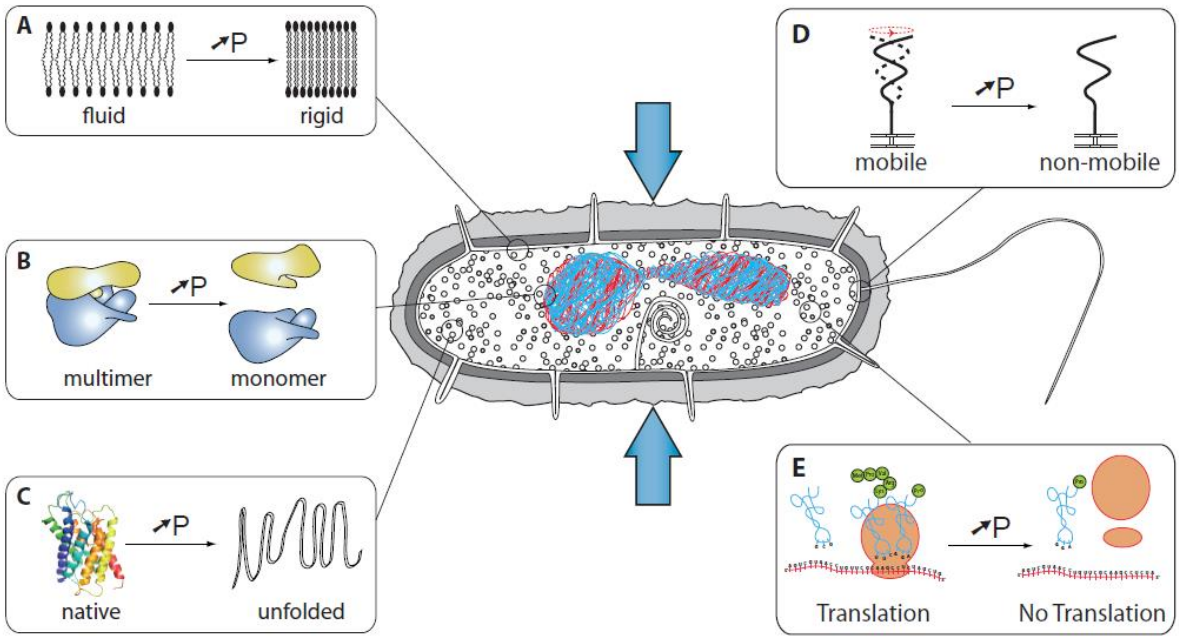

Figure 8: Examples of the effects of high hydrostatic pressure on cells and cellular components (from (Oger and Jebbar, 2010))

A: Lipids in membranes; B: multimeric protein assemblies; C: protein structures; D: cellular motility; E: protein translation by ribosomes.

Piezophiles are defined as strains optimally growing at 10 MPa or more, and are cultivated in high hydrostatic pressure incubators (Jannasch and Taylor, 1984). Most of the piezophilic archaea described are *Thermococcales*, *Methanococcales*, or *Desulfurococcales*. While most of the described archaeal piezophiles are (hyper)thermophiles, known psychrophilic piezophiles are usually bacteria (Fang et al., 2010). Examples of piezophiles growing optimally at mesophilic temperatures are described (*e.g.* (Kaneko et al., 2000; Kobayashi et al., 1998)). Many isolated *Thermococcales* strains are from deep-sea vents, and may show optimal growth at high pressure. For example, *Palaeococcus pacificus* grows optimally at 30 MPa (Zeng et al., 2013), *T. barophilus* at 40 MPa (Marteinsson et al., 1999a; Zeng et al., 2009), and *P. yayanosii* at 52 MPa (Birrien et al., 2011; Zeng et al., 2009). The latter is an obligate piezophile, with a sub-optimal pressure for growth at 20 MPa. The deepest known *Thermococcales* member is *T. piezophilus*, isolated from the Cayman Trough, in the Caribbean Sea, at 4 964 m of depth (Dalmasso et al., 2016)). Although this parameter remains poorly considered in physiological studies of *Thermococcales*, since several species

are only facultative piezophiles (can grow at high pressure but with an optimal growth at P_{atm}), some interesting results have nonetheless emerged.

Interestingly, facultative piezophiles usually habor higher optimal temperature for growth at elevated pressure than at P_{atm} (Holden and Baross, 1995; Marteinsson et al., 1997; Miller et al., 1988a) (FIGURE 9).

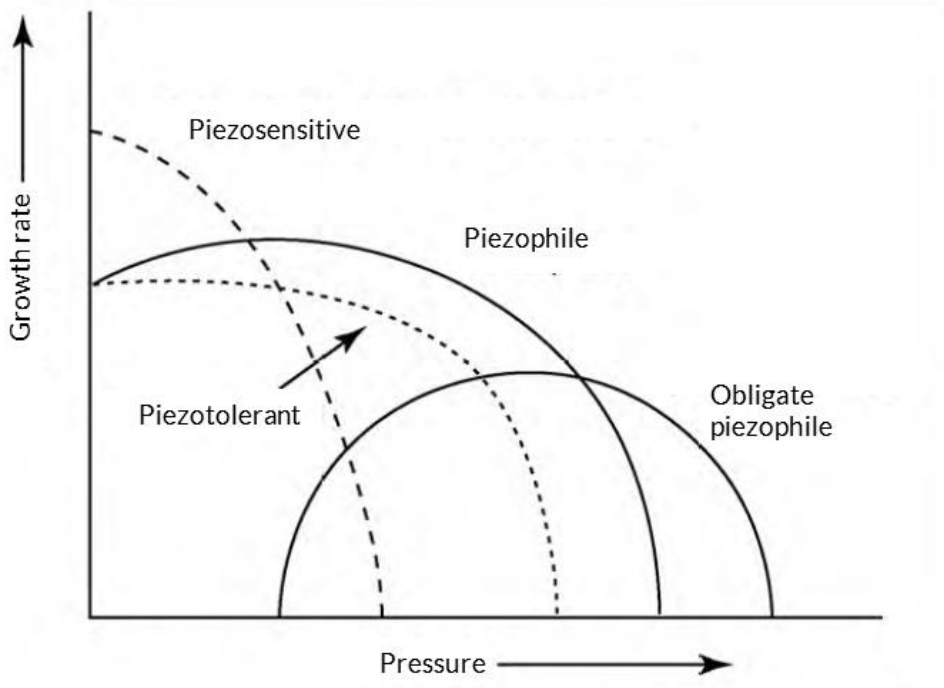

Figure 9: Microbial growth characteristics under high pressure and ensuing classification (adapted from (Fang et al., 2010))

Growth in piezosensitive microorganisms is affected by any positive pressure, while in piezotolerant, growth rate slows down only at higher pressures. Piezophiles have maximum growth rates at high pressure but can still grow at atmospheric pressure, while obligate piezophiles require pressurization to harbor a minimal growth rate.

---

1. Physico-chemical and thermodynamic changes due to high pressure

At pressures experienced by living organisms in natural habitats, *i.e.* between 0.1 MPa to less than 200 MPa, the energy conveyed by increased pressure is quite low compared to

chemical bonds, so intermolecular distances and molecule conformations are affected, but covalent bond distances and bond angles are not influenced. Perturbations of covalent structures of low molecular mass biomolecules or of primary structure of macromolecules would require up to 2 000 MPa of pressure (Oger and Jebbar, 2010; Rivalain et al., 2010).

However, biochemical consequences can result from changes in reaction thermodynamics. Fundamentally, according to Le Chatelier's principle, pressure can influence volume change (ΔV) in a reaction. Consequently, high pressure can inhibit a reaction which would be accompanied by a positive ΔV, such as one forming gas, and can enhance a reaction which would be accompanied by a negative ΔV. Thus, although temperature has a broader impact on such reactions, pressure holds different influences: while increased temperature induces acceleration of a biochemical reaction, pressure can either accelerate, inhibit, or have no effect on the reaction, according to the associated volume changes (Abe and Horikoshi, 2001).

The expression of Gibbs free energy (ΔG) implies a dependence on pressure (see detailed formulas in (Amend and Shock, 2001)). In the shallow layers of the ocean, *i.e.* at lower pressure ranges (typically 0.1 to 10 MPa, corresponding to hundreds of meters of water column), the effect of pressure on ΔG can be ignored. However, for piezophilic life, where optimal pressures for growth are rather in the dozens MPa, the impact of pressure on biochemical reactions should be acknowledged.

When considering gases, pressure influences the Gibbs free energy through the Q term of the following equation:

$$\Delta G = \Delta G° + RT \ln Q$$

Q, the activity, is a function of an activity coefficient. Pressure can influence gas solubility, thus its concentration in the chemical system, and thus its activity (also termed fugacity). For example, at 25 °C, at equilibrium, the activity of H_2 passes from $7.85 .10^{-4}$ at 0.1 MPa (P_{atm}) to $1.93 .10^{-1}$ at 35 MPa (pressure around the average depth of ocean floor) (Amend and LaRowe, 2019; Weatherall et al., 2015). As reviewed in (Amend and Shock, 2001), effects of pressure on Gibbs free energy (ΔG) of biochemical reactions are less than

the effects of temperature. Although pressure is secondary, it is still to be considered in energetics calculations. Energetics of main metabolic microbial reactions regarding pressure, as well as temperature, were calculated and reviewed previously (Amend and Plyasunov, 2001; Amend and Shock, 2001). Experimental evidence indicates the relationship between elevated pressures and metabolism. For example, methanogenesis can occur at higher temperatures when pressurized, in *Methanocaldoccus jannaschii* (Miller et al., 1988a).

2. High pressure effects on piezosensitive and piezophilic organisms

Note: The bibliographical work implied in this 2nd section will be valorized and published within a book chapter on the microbiology of piezophiles (see BOOK CHAPTERS IN PREPARATION, P. 345*).*

From those fundamental changes, many functional differences are induced over biological systems at high pressure. Piezophiles must cope with those extreme conditions, and those adaptations have led to several studies, while some of the exact mechanisms involved are yet to be determined.

2.1. Effects on proteins

The major effects of high pressure on proteins are compression and unfolding, which possibly lead to modulation or impairment of their functions (Bridgman, 1914; Ichiye, 2018). Multimeric proteins, such as ribosomes, can dissociate under high pressure, which may be a major reason for piezosensitivity (Gross and Jaenicke, 1994; Mozhaev et al., 1996). When pressure increases, proteins can either stabilize or weaken (Abe and Horikoshi, 2001; Boonyaratanakornkit et al., 2002; Chen and Makhatadze, 2017). For example, in *Methanocaldococcus jannaschii*, a piezophilic model, pressure stabilizes hydrogenases, but acts oppositely on homologs of the same order, in *Methanotorris igneus*, a strain isolated from shallow areas (Hei and Clark, 1994). Glutamate dehydrogenase from *T. litoralis* is stabilized by high pressure (Sun et al., 2001). DNA polymerases from *Pyrococcus* and *Thermus* species are stabilized at high pressure (Summit et al., 1998).

Changes of protein structures due to high pressure depend on the type of interactions between side-chains and between side-chains and the surrounding water. If those interactions are mainly electrostatic, then unfolding would be accompanied by negative volume changes, and thus are more likely to occur at elevated pressure. If interactions are mainly hydrophobic however, then unfolding is accompanied by positive volume changes, and pressure more likely induces protein stabilization. Experimental proof of the importance of ion-pair networks has been described for *Thermococcales* models, noticeably, by comparing glutamate dehydrogenases (Sun et al., 1999; Vetriani et al., 1998).

It was thus proposed that limits of pressure for growth could rely on volume required by biological machinery. For example, in *E. coli*, ribosome dissociation is accompanied by a negative volume change, and spontaneously happens over 600 MPa, thus inhibiting protein synthesis (Gross et al., 1993). Nevertheless, computational analyses later refuted this hypothesis, revealing that no significant ΔV could be observed between piezophiles and non-piezophiles, and no evolutionary pattern for this feature was detected (testing across thermophiles, psychrophiles, mesophiles, thermos-piezophiles and psychro-piezophiles) (Avagyan et al., 2019). The authors of this work advanced that protein stability ranges may be due to a non-volume-based mechanism, which could be a crucial parameter for piezophily. Other features actually impact thermodynamic stability of proteins, such as the number of hydrogen bonds, the optimization of electrostatic interactions, the changes in conformational entropies, and secondary structures and do not necessarily involved volume changes (Avagyan et al., 2019).

Differences in protein flexibilities, at a nanometer scale, of *T. barophilus* and *T. kodakarensis*, which are respectively piezophile and piezotolerant, have been evaluated by quasi-elastic neutron scattering. The authors noted that flexibility was increased in the piezophilic proteome, and proposed that it could be a mechanism for high pressure adaptation in those models, at the molecular level (Martinez et al., 2016). Similar ideas were suggested for cold-adapted piezophiles, as reviewed in (Ichiye, 2018). Low-temperature and high-pressure adaptations are also helped by the fact that salt bridge are not used for protein stability in psychrophiles (Hay et al., 2009).

Proteins of piezophiles could be as sensitive to environmental conditions as their non-piezophilic homologs, but could withstand those consequences more easily. Interestingly, crystal structures of enzymes are often similar in both types of homologs (Ohmae et al., 2013). Yet, some differences between proteins from piezophiles and from piezosensitive/piezotolerant can be noted, as for example the higher proportion of small amino acids in *P. abyssi* compared to *P. furiosus* (Di Giulio, 2005). Some quaternary structures could also be involved in high-pressure adaptations in piezophiles, as indicated by the dodecamerization (in contrast to the usual barrel-shaped proteins) of the TET3-peptidase of *P. horikoshii* (Rosenbaum et al., 2012).

Adaptations of protein against pressure could also be a matter of repair and protective mechanisms rather than of structural features. Particularly, osmolyte accumulation (so-called "piezolytes"), such as betaine and glutamate, have been reported in several cases, linked with culture pressure, and could be of importance in determining the piezophily trait of a strain (Amrani et al., 2014; Avagyan et al., 2019; Martin et al., 2002). Note that this feature has also been observed in deep-sea animals (Yancey et al., 2002). Macromolecular crowding also was shown to be likely involved in high pressure adaptation of *T. barophilus*, unexpectedly augmenting high pressure sensitivity in whole cells (Golub et al., 2018). A thermal and salinity stress-response osmolyte, mannosyl-glycerate, is accumulated in this strain when grown at sub-optimal (but not supra-optimal) pressure, and was shown to help attenuate the cellular dynamics response to pressure stress (Cario et al., 2016; Salvador-Castell et al., 2019).

Protein adaptations to high pressure thus seem to involve various mechanisms, from harboring specific structures and compositions to enhance global thermostability, to accepting changing environments thanks to wide flexibilities and external protective processes.

2.2. Effects on nucleic acids

In the range of known biotopes, DNA double-helixes are not very sensitive to pressure variations, probably as the hydrogen bonds, when disrupted, are associated to very small volume changes, positive up to 600 MPa as experimentally calculated with *Clostridium perfringens* DNA. High pressure, as encountered in known biotopes, thus stabilizes DNA

structure (Girard et al., 2007; Hawley and Macleod, 1974; Macgregor, 1998; Wilton et al., 2008). The effects induced by pressure were also shown to depend on temperature and on melting temperature of DNA. With a T_m less than 50 °C, increased pressures destabilize DNA, but hold opposite effects when T_m are above 50 °C (Dubins et al., 2001). Spatial conformation could be impacted: high pressure, as encountered by piezophiles, experimentally shown to increase supercoiling of circular DNA, and to favor B conformation over Z conformation (although higher pressures might be required) (MacGregor and Chen, 1990; Tang et al., 1998) (FIGURE 10).

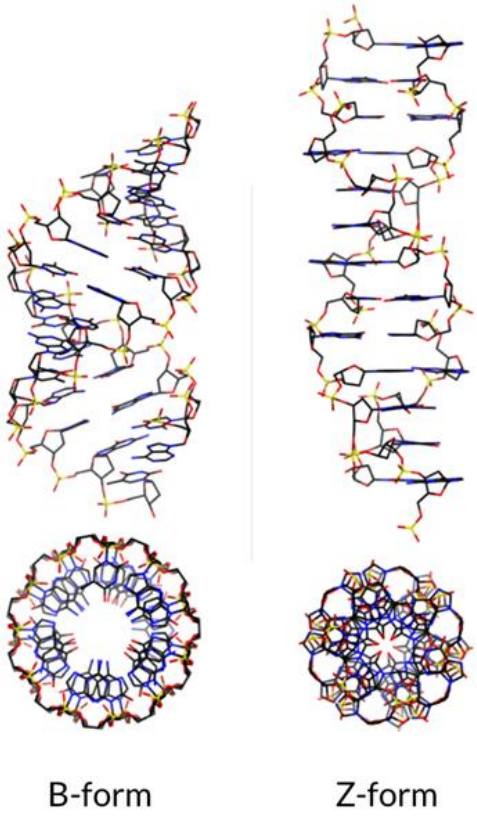

Z-form of DNA, a left-handed shape often considered non-canonical, actually plays several important physiological roles in living organisms (Lee et al., 2010). Its structure repeats every other base pair and the major and minor grooves have little width variations. B-form DNA, right-handed, can transition to this state according to environmental conditions. High pressure appear to increase supercoiling of circular DNA, as well as favoring B-form of DNA. Yet, some hyperthermophiles harbor a positive (left-handed) supercoiling (Valenti et al., 2011).

Figure 10: Structures of B-form and Z-form DNA (adapted from (Hardison, 2019))

RNA, on the other hand, also undergoes this conformational transition, but at much higher pressures (600 MPa) (Krzyżaniak et al., 1994). Simulations have shown that RNA hairpins unfold under pressure, probably because this tertiary structure is maintained by non-covalent interactions (Garcia and Paschek, 2008). Recent work on small RNA hairpins have indicated their high stability under very high pressure (400 MPa), noticing little effects on

base pairing and base stacking interactions, *i.e.* small conformational perturbations, again related to corresponding T_m (Schuabb et al., 2017).

However, protein binding to those nucleic acids, which is crucial to many important cellular processes (*e.g.* replication, transcription, recombination), can be affected, in a fashion which depends on the protein involved (Royer et al., 1990; Silva et al., 2002). 16SrRNA genes of piezophiles present more elongated helices, which could improve ribosome function at high pressure (Lauro et al., 2007). RNA-RNA interactions and the influences of co-solutes were also studied but concerned very high pressure ranges (at least 250 MPa) and were slight compared to the effects on other macromolecules (Downey et al., 2007).

Overall, few effects of high pressures have been observed on nucleic acids, in ranges concerning known biotopes, and therefore no much perspective is known on the mechanisms involved in piezophily in those specific cases. DNA repair systems have been observed to be overexpressed at low pressure in the piezophilic strain *Photobacterium profondum* SS9, an important bacterial model for piezophily, but whether this is relevant to adaptation to high pressure is still undocumented (Campanaro et al., 2005; El-Hajj et al., 2010).

2.3. Effects on lipids and membranes

Unlike nucleic acids, lipids are very sensitive to pressure, even in the living range of microorganisms. Such conditions raise the phase transition temperature (T_m) of the membrane (from liquid to gel) and encourage packing, which impairs lipid motion, and thus hinders membrane functionality. Lipids, being amphiphilic, can self-assemble; and an increased pressure leads to induced chain ordering, possibly leading to thicker membranes (FIGURE 11). This effect on membrane fluidity could be comparable to the application of low temperatures, and necessitates homeoviscous adaptation (Sinensky, 1974; Skanes et al., 2006; Winter and Jeworrek, 2009). It influences the curvature of a lipid membrane, as well as the structure of the bilayer itself, changing its micromechanic properties (Brooks, 2014; Salvador-Castell et al., 2020). Many proteins are associated to lipid membranes, and pressure can affect lipid-protein structures and interactions (Brooks, 2014; Lee, 2004).

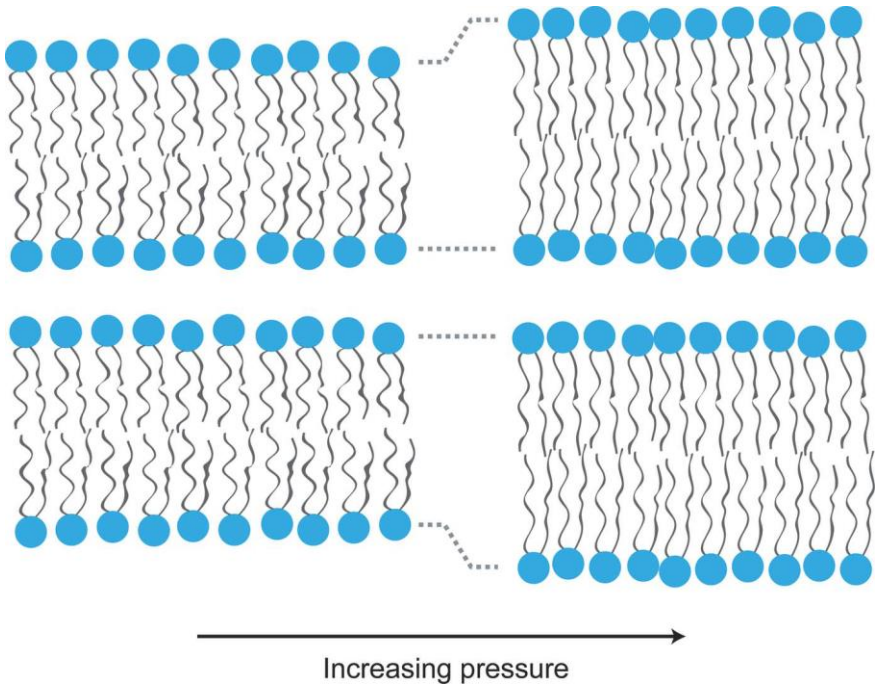

Figure 11: Pressure tends to increase chain ordering and chain extension, thereby increasing the thickness of flat bilayers (from (Brooks, 2014))

Piezophiles must adapt mechanical properties of their lipid membranes. Fluidity can be increased, lowering their T_m, due to higher unsaturated/saturated lipid *ratio*, as noted in deep-sea microorganisms (DeLong and Yayanos, 1986). Archaeal membranes, in contrast to bacteria, are composed of (bi)phytanyl hydrocarbon chains that are ether-linked to glycerol, and provide more rigidity, stability, and less permeability (Mathai et al., 2001). In *T. barophilus*, supra-optimal pressure and sub-optimal temperature for growth enhance the proportion of archaeol lipid compared to bipolar caldarchaeol, the main membrane lipid at optimal conditions. Some apolar isoprenoid lipids could also be involved in homeoviscous adaptation (Cario et al., 2015a). In *P. abyssii* however, very few or no archaeol have been detected in sub-, supra-, and optimal pressures for growth, but overall changes in phospholipid profiles were observed (Marteinsson et al., 1997). In bacteria, as shown in the piezophiles *Photobacterium profondum* SS9 and *Shewanella violacea*, increased proportions of specific mono- and poly-unsaturated lipids (*cis*-vaccenic acid and eicosapentoenoic acid (EPA), respectively) play a role in low-pressure intolerance (Allen and Bartlett, 2000; Allen et al., 1999; Usui et al., 2012).

While lipid adaptations to high pressure are well studied in different models, regulatory mechanisms of those membrane adaptations to high pressure are poorly understood, and do not seem to involve transcriptional nor translational regulation, nor *de novo* lipid synthesis. Rather, it consists in modifying existing lipids due to membrane protein activity (insaturases / conjugases) (Brooks, 2014; Oger and Cario, 2013).

2.4. Genomics and gene regulation

Some reports indicate which genetic features are associated with piezophilic life, but no single gene is responsible specifically for pressure adaptation. Rather, different gene clusters involved in various physiological functions play important roles in piezophily of specific strains, some being possibly positively selected for at high pressure (Campanaro et al., 2008). OmpH was the first protein identified as a pressure-regulated gene product, and found to be involved in periplasmic shock response, with the counterpart OmpL expressed at low pressure, in *Photobacterium profondum* SS9 (Bartlett et al., 1989; Welch and Bartlett, 1996, 1998). Since then, many other genes in different models have been revealed to be involved in high pressure adaptation, through various functions, and particularly osmoregulation (*omp*A), protein synthesis, folding and unfolding (*rpo*E, *dna*K, *gro*EL), heat or cold shock responses (*dna*K, *lon*, *gro*EL, *clp*PX, *csp*) and DNA repair machinery (*mut*T, *uvr, recN*) (Aertsen et al., 2004; Campanaro et al., 2005; Chi and Bartlett, 1995; Michoud and Jebbar, 2016; Peoples and Bartlett, 2017; Vezzi et al., 2005; Wang, 2002; Wang et al., 2008). A transcriptional study on *T. barophilus* showed that several genes of unknown function are regulated at sub- or supra-optimal pressures for growth (Vannier et al., 2015). Metagenomic studies of deep-linked microbial communities or of samples from different depths, as well as complete genome sequences of individual piezophiles, have been prone to corroborate those implications (*e.g.* (Dutta et al., 2019; Eloe et al., 2011; Liu et al., 2019)). An integrative genomic island was identified in *P. yayanosii*, holding functions of mobility, DNA repair, metabolic processes and toxin-antitoxin system, whose deletion increased biomass at high hydrostatic pressure (Li et al., 2016). Although they evolved under different environmental conditions, a genomic study on several *Pyrococcus* species hinted that *in situ* pressure is not the sole important factor driving their divergence, however (Gunbin et al., 2009). Overall, it is possible that microorganisms potentially easily evolve to endure high pressure, as shown by a directed evolution work carried out on *E. coli*, rendering the strain able to survive at more than 200

MPa, whereas it was previously not resistant to more than 70 MPa (Vanlint et al., 2011). Moreover, while still an unpublished work, upper limits for growth may have been extended by ALE experiments on *Carnobacterium* sp. AT7 over 130 generations (Tang, 2019).

Apart from genes specifically implicated in high pressure, as determined by mutational studies and ecological observations, regulations occur in order to maintain cellular activities. For several piezophilic microorganisms, atmospheric pressure induces overexpression of several genes that would be rather expressed at high pressure in piezosensitive, involved for instance in transmembrane transporters, in carbon metabolism, in signal transduction, and in DNA repair (Bartlett et al., 1995; Boonyaratanakornkit et al., 2007; Campanaro et al., 2005; Fernandes et al., 2004; Vannier et al., 2015). Such regulations seem to also occur in varied metabolic states, and thus seem to be fundamentally triggered by pressure, as for example the high pressure regulation adaptations noticed in the piezophile *Methanocaldococcus jannaschii* despite substrate-limited growth inhibition (Boonyaratanakornkit et al., 2006). Diverse mechanisms seem to be involved. Some promoters have been identified to be induced by elevated pressure, in *Thermococcales* and other models (Song et al., 2019; Tamegai et al., 2008). In *Photobacterium profondum* SS9, ToxR and ToxS protein regulate the expressions of OmpH and OmpL, and play the role of pressure sensors (Welch and Bartlett, 1998). In *T. barophilus*, the observation of the low-pressure stress protein P60 production without corresponding transcriptional adaptation indicate that regulation can occur at the post-transcriptional level. Regulation of the substrate uptake systems could also occur as high pressures downregulate the TrmB homologous expression in this model, compared to P_{atm}. In the meantime, putative ABC-transporters have been reported to be overexpressed (Marteinsson et al., 1999b; Vannier et al., 2015) (see SUBSTRATE UPTAKE, P. 71). However, contrarily to what could be observed in other strains, no notable differential stress response was observed at low pressure for the piezophile *P. abyssii* (Marteinsson et al., 1997).

Overall, such observations tend to indicate that piezophilic proteomes could be efficient at optimal pressure for growth, and differential expression patterns are placed to compensate potential stresses induced by other pressures.

2.5. Global physiological adaptations

All the local modifications described above, induced by high pressure environments, can cause global effects at the physiological level.

For example, motility seems to be affected. The stress induced by high pressure in piezosensitive microorganisms (such as *Escherichia coli* or *Photobacterium profondum* 3TCK), as well as sub- and supra-optimal pressures for growth in the piezophile *P. yayanosii*, and low pressures for *Photobacterium profundum* SS9, seem to affect the rotation of *flagella* or *archaellum*. Note that the same pressure-responsive *flagellum* systems are found in other piezotolerant bacteria, such as *Shewanella piezotolerans* WP3. The resulting cell tumbling was interpreted as a way to escape from stressful conditions and seek nutrients (Eloe et al., 2008; Michoud and Jebbar, 2016; Nishiyama et al., 2013; Wang et al., 2008). Nonetheless, in *T. barophilus*, the need for amino acid increased at optimal pressure compared to P_{atm} (Cario et al., 2015b). Cell cycles also are modulated. Filament formation has been observed in sub- or supra-optimal pressures for several piezophiles, and cell division is directly modified as some division proteins could be affected (Bartlett, 2002). Global metabolic responses to pressure were observed or hinted at in various microorganisms. Methanogenesis seem to be enhanced by pressure in *Methanocaldococcus jannaschii* (Miller et al., 1988a). Different respiratory chain proteins appear to be involved according to pressure of growth of *Shewanella violacea* (Chikuma et al., 2007). Evidences indicated that ATPase activity can be enhanced or impaired by pressure, while, *in vivo*, it is rather the state of the membrane that may be of importance in membrane ATPase activity (Kato et al., 2002; Souza et al., 2004).

Many studies have underlined the various mechanisms placed to counteract the physical effects of pressure on piezophiles, leading to lower biological activities in piezosensitive/piezotolerant strains. Rather than deep structural changes such strategies seem to mainly rely on the fine-tuning of protective systems. Probably due to the inconvenience of such experimental works, they have mainly focused on few models, and more functional data would be required to extract clear general patterns for specific groups of microorganisms.

3. Applications of high pressure in biotechnological prospects

We have established that high pressure effects on biological systems can have broad implications on various levels. Those features have been studied for biotechnological applications. High hydrostatic pressure has been applied in the food industry in order to eliminate pathogens without affecting organoleptic and nutritional properties of the products, for example (Lee et al., 2016; Mañas and Pagán, 2005; Yaldagard et al., 2008). Applying high pressure has also been investigated for other various industrial and research purposes, such as the disinfection of biomaterials, the modulation of enzymatic activities, the study of protein structures and DNA, the development of vaccine, embryo pre-conditioning, some methodological research developments (*e.g.* genetic vector preparation, and transformation, cell extraction, cryopreservation) (Demazeau and Rivalain, 2010; Jiang et al., 2016; Rivalain et al., 2010).

Piezophiles themselves have revealed interesting genetic diversity and encouraged the research community to "gamble in deep-sea" (Girguis and Holden, 2012; Ruth, 2006). Their particular features, as described in the previous paragraph (see HIGH PRESSURE EFFECTS ON PIEZOSENSITIVE AND PIEZOPHILIC ORGANISMS, P. 50), could be used in biotechnological applications, by modulating protein structure and stability, adjusting enzyme kinetics, or regulating gene expression, for example (Abe and Horikoshi, 2001). It could for example be used as substrate pre-treatment for destructuring plant biomass (Guerriero et al., 2015). Metabolic engineering could benefit from foreseeing the impacts on specific fluxes, as studied in polyketide synthesis, potentially allowing selection of metabolic route by pressure (Wright et al., 2003).

To date, no high pressure H_2 bio-production application has been reported. Yet, the energy metabolism of *Thermococcales*, a well-studied order often found around hydrothermal vents, could also be impacted by growth pressure, as hinted by -omics studies carried out in several models (Dalmasso, 2016; Le Guellec, 2019; Michoud and Jebbar, 2016; Vannier, 2012; Vannier et al., 2015). To better understand those changes and their potential implications, let us further dive into *Thermococcales* and their metabolism.

V. *Thermococcales*

Thermococcales are hyperthermophilic archaea that perform a type of dark fermentation based on sulfur and/or proton reduction, and are in part responsible for the biotic H_2 present around hydrothermal vents. They have received broad attention from the research community, as environmental works have shown that *Thermococcus* members are found ubiquitously around coastal and deep-sea hydrothermal vents (Holden et al., 2001; Orphan et al., 2000; Prieur et al., 1995). Other strains were isolated from terrestrial hot sources (thus with low salinity) (González et al., 1999; Klages and Morgan, 1994; Ronimus et al., 1997), sub-seafloor sediments (Ciobanu et al., 2014; Roussel et al., 2009), or oil reservoirs (Miroshnichenko et al., 2001; Stetter et al., 1993). They have been detected in all oceans (Rutherford, 2014), and one species may be present at several hydrothermal sites (Courtine, 2017) (FIGURE 12). Many *Thermococcales* strains are piezophiles, being isolated from deep-sea, thus living at high hydrostatic pressure (Abe and Horikoshi, 2001).

They represent an order of the *Euryarchaeota phylum*, with one class, *Thermococci*, composed of three genera: *Thermococcus* (Zillig et al., 1983), *Pyrococcus* (Fiala and Stetter, 1986), and *Palaeococcus* (Takai et al., 2000). They were discovered following a *momentum* given by the isolation of the first hyperthermophiles, and have become one of the most studied representatives of hyperthermophiles (Stetter, 2006; Zillig et al., 1983). The increasing availability of sequenced and annotated genomes (reaching 60 to date) and strain descriptions, the genetic tools developed for manipulations on well-studied representatives (see GENETIC TOOLS OF THERMOCOCCALES, P. 66), and the extensive studies on their protein structures and functions, metabolism and physiology, make *Thermococcales* a model order for the study of hyperthermophily, and piezophily, in *Archaea*. Among other laboratories, the LM2E has developed a broad expertise on culturing and characterizing those strains. Model organisms include *P. furiosus*, *T. kodakarensis*, '*T. onnurineus*', for which genetic tools are available, and on which many studies have focused (Leigh et al., 2011). At the LM2E, *T. barophilus* MP^T is a particular model to decipher piezophilic adaptations, as a genetic tool has been also set up (Birien et al., 2018; Thiel et al., 2014), and as many physiological works have been performed (see below). The LM2E also hosts the UBOCC (UBO Culture Collection), and

possesses more than 300 strains of *Thermococcales*, many of which are yet to be characterized.

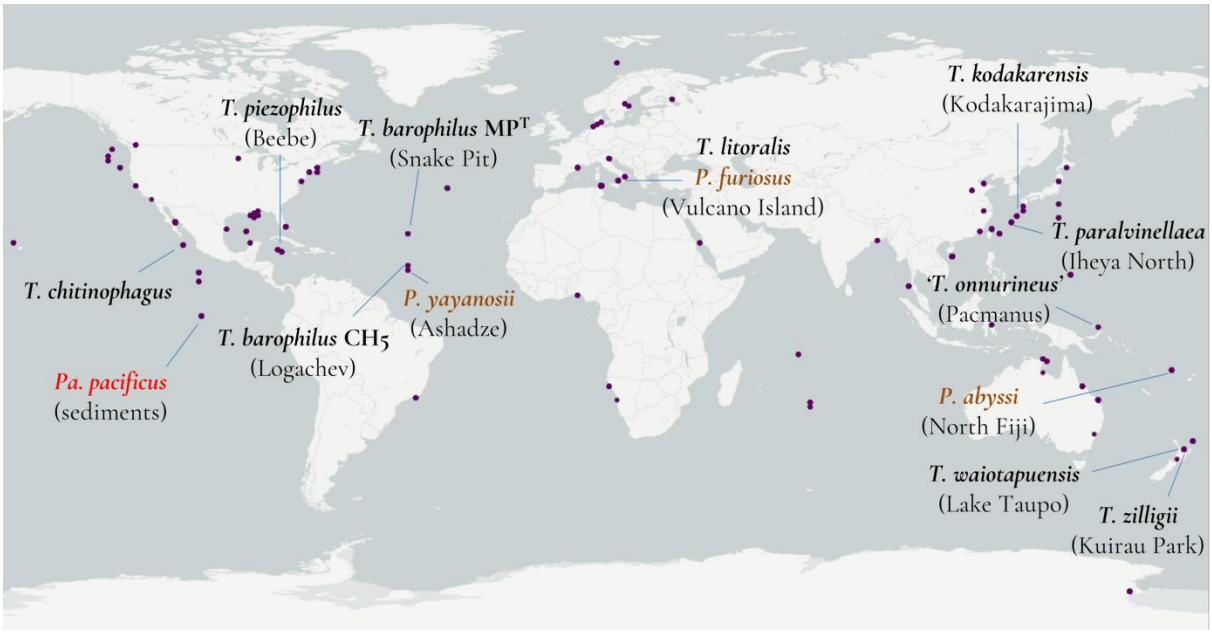

Figure 12: Origins of *Thermococcales* isolates around the world

The map of the isolation sites was generated with the Global Biodiversity Information Facility (GBIF, 2020) and names of some models mentioned in this study were added manually, along with their sampling sites (between parentheses). Colors represent genus*: **black** for* Thermococcus*, **orange** for* Pyrococcus*, and **red** for* Palaeococcus*.*

All reported *Thermococcales* strains are strictly anaerobic (with some exceptions (Amend et al., 2003; Kwan et al., 2015)) heterotrophs, with coccoid cells with or without flagella (with the morphologic exception of *T. coalescens* irregular cells (Kuwabara et al., 2005)), and neutrophilic for most. Several members have been reported to grow on a wide diversity of substrates, including simple and complex carbohydrates, simple or complex and peptides (see below) (Bertoldo and Antranikian, 2006).

1. Genetics, adaptation, and evolution in *Thermococcales* and ensuing applications

Thermococcales show wide metabolic versatilities, being able to degrade diverse substrates. They also seem to adapt quickly to survive to changing conditions encountered

around hydrothermal vents, as they harbor, particularly, a relatively short life cycle, despite having little energy available (Cossu et al., 2015). Their doubling times are comparable to *Escherichia coli* (20 – 25 min), a well-studied *bacterium* whose growth efficiency benefits from the energetic efficiency of its aerobic respiration (Gorlas et al., 2013; Sezonov et al., 2007). In addition to this low energy metabolism, apparent chromosome disorganization heightens the paradox regarding *Thermococcales*' growth efficiency. Their evolution seems to be driven by chromosome shuffling (Zivanovic et al., 2002), witnessing a wide genome plasticity, as in many other prokaryotic models (*e.g.* (López-García et al., 1995)). This shuffling has been hypothesized to allow for better adaptation in challenging environments, such as deep-sea hydrothermal vents (Cossu et al., 2015).

1.1. Genomic features and genetic evolution processes of *Thermococcales*

Genomes of *Thermococcales* are organized in one chromosome, with a mean length of about 2 Mbp. They do not have high G + C %, compared to other hyperthermophiles: *Pyrococcus* species have 42 % G + C on average, *Palaeococcus* genomes have 43 % and 53 %, and *Thermococcus* species can be divided into two groups, generally harboring around either 54 % or 42 % of G + C bases (Courtine, 2017). Several members of the order also host mobile genetic elements, in the form of plasmids (Cossu et al., 2017; Erauso et al., 1996; Krupovic et al., 2013) or viruses (Geslin et al., 2003; Gorlas et al., 2012). For example, *Thermococcus barophilus* MP^{T}, a model piezophilic strain at the LM2E, has one circular chromosome of about 2.01 Mbp and a plasmid, pTBMP1, of about 54.16 kbp (Vannier et al., 2011). Such mobile genetic elements can drive evolution by allowing horizontal gene transfer, possibly occurring intra- and inter-species, but even inter-domain, as *e.g.* between *Thermotogales* and *Thermococcales* (Le Fourn et al., 2011).

Genomic rearrangements can also happen at the strain level, along the successive generations of cells. Particularly, the pTN3 plasmid of *T. nautili* codes for a viral genome and can be transferred through membrane vesicles (Oberto et al., 2014; Soler et al., 2008, 2011). pTN3 encodes an integrase, which has been suspected to allow large-scale genomic inversions in adaptive laboratory evolution (ALE) experiments carried over less than 70 generations (see ADAPTIVE LABORATORY EVOLUTION FOR FUNDAMENTAL UNDERSTANDING AND

ENGINEERING, P. 64) (Cossu et al., 2017). Other strains, such as '*T. onnurineus*', have however shown a certain degree of genetic fidelity through generations, which was interpreted as a mechanism allowing to sustain extreme conditions (Lee et al., 2016). Nonetheless, recombination and genomic rearrangements were earlier shown to happen frequently in *Thermococcales*, and this would also mean rapid evolutions (Maeder et al., 1999; Zivanovic et al., 2002). More recent resequencing of *P. furiosus* DSM36387 have revealed improved genome stability than previously believed, so general patterns remain unclear (Grünberger et al., 2019). Yet, Cossu *et al.* (2015) have demonstrated that across *Thermococcales*, the core gene clusters are conserved in particular locations of the chromosome. Other parts of the genome are subject to abundant shuffling, which they interpreted as a possible way to adapt to changing environments for allopatric (geographical) speciation. Thus, essential, highly expressed genes (housekeeping) are located in invariant positions on the chromosome, where the position of newly acquired genes through horizontal transfer would undergo a constant adaptation and optimization (Cossu et al., 2015). *In silico* investigations, analyzing gene losses and positive Darwinian selections in three *Pyrococcus* species, led to similar conclusions, that a selection rather occurred on functional groups of genes, among others (Gunbin et al., 2009).

These rearrangements can be driven by different mechanisms. In *Thermococcales*, as well as in other archaea (*e.g.* in *Sulfolobus* (Jaubert et al., 2013)) homologous recombination can take place between numerous insertion sequence copies (*e.g.* in *P. abyssi* (Bridger et al., 2012). Such insertion sequences are however rarely found in the genus *Thermococcus* (except in, for example, *T. kodakarensis* (Sato et al., 2005)), but genome shuffling still arises. This suggests alternative recombination mechanisms, capable of producing large-scale rearrangements, which could be handled by recombinases such as the one carried by the plasmid pTN3, in *T. nautili*, mentioned earlier. It has indeed been shown to be capable of catalyzing both site-specific recombination and low sequence specificity recombination reactions, mimicking homologous recombination (Cossu et al., 2015, 2017)).

1.2. Applications: genetic tools and adaptive engineering

1.2.1. Adaptive Laboratory Evolution for fundamental understanding and engineering

Thermococcales seem to undergo rapid evolution across few generations to better adapt to changing conditions. Although the ecological interpretations are interesting by themselves, this feature has been explored for more practical applications.

Sub-culturing strains in varying conditions, in the lab, allows forcing them to grow under a controlled environment. It is, for example, one of the processes used for isolating new strains from *in situ* samples. This principle can also be applied as Adaptive Laboratory Evolution (ALE) experiments, which consist in the observation of microbial populations under particular constraints, expecting the induction of an evolution of the strains. Due to the recent technological advances in sequencing tools, which permit low-cost, high-throughput analyses, ALEs have been recognized as a way to improve fundamental knowledge on evolution processes and metabolism, but have also been applied for engineering strains to hold higher production yields of compounds of interests (Conrad et al., 2011; Sandberg et al., 2019; Shendure et al., 2017). Work in bacterial models outlined the frequent subsequent induction of single nucleotide mutations, as well as the emergence of "mutator" phenotypes in cases of general stress (such as a higher-than-optimal-for-growth temperature) in the later phases of adaptation, holding increased mutation rates (Barrick et al., 2009; Conrad et al., 2011).

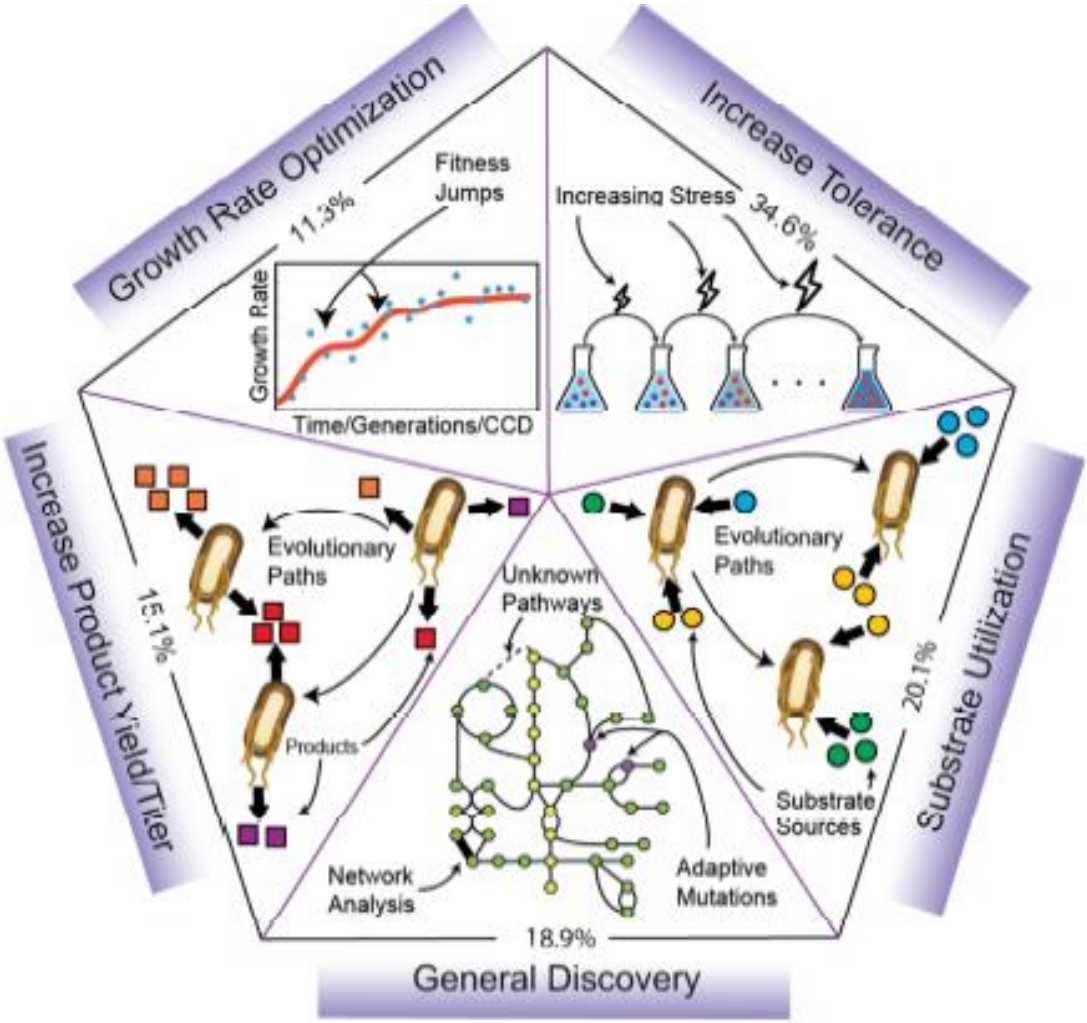

Figure 13: Categories of ALE experiments (from (Sandberg et al., 2019))

*Numbers indicate the percent makeup of the 159 studies examined. "Growth rate optimization" illustrates fitness development over the course of an ALE, with noticeable fitness jumps. "Increase tolerance" illustrates an experimental schematic of an initially mixed population acquiring beneficial mutations (cells in red) that promote cell survival in a constantly increasing external stress environment (*e.g. *pH, antibiotics, temperature, etc). "Substrate utilization" and "increase product yield/titer" illustrate evolutionary pathways enabled* via *ALE that enhance the organism's ability to make use of alternative nutrient sources (colored circles), and to increase production of metabolites of interest (colored squares), respectively. "General discovery" encompasses studies that examined ALEs at a genetic or systems level in greater detail.*

This method is powerful for constructing strains, as a complement or even a replacement of other frequently approached techniques. In rational design, for example, the resulting phenotype is generally not issued from a complete systemic context, due to the persisting lack of data, especially in archaea (Makarova et al., 2019). Indeed, inducing a

mutation while expecting a given metabolic *scenario*, often fails from incomplete foreseeing of the actual causes and effects of this change, because stressed cellular states can ensue. Some limitations can be given to directed evolution, which aims particularly at randomly mutating a gene of interest before screening for the right phenotype. For example, Xiong *et al.* (2007) used *in vitro* directed evolution to enhance the activity of β-galactosidase from *Pyrococcus woesei*, an enzyme used in a wide variety of applications, and noticeably in food industries (Panesar et al., 2006; Xiong et al., 2007). In contrast, ALE allows to randomly find at once all mutations of an evolutive *scenario*, at the genome-scale, that permit together to build up the desired phenotype (Sandberg et al., 2019; Shepelin et al., 2018). As Barrick *et al.* (2009) stated, « there may be relatively few trajectories in which fitness increases monotonically with each single mutation » (Barrick et al., 2009). This also implies that mutations can be epistatic, *i.e.* they reveal neutral or negative effects when independently considered in the ancestral genome, while being advantageous when part of the whole new cellular system (Phillips, 2008).

In *Thermococcales*, such approaches have not been widely attempted, with few exceptions, particularly on the model '*T. onnurineus*' NA1, in order to optimize growth on formate (Jung et al., 2017) or H_2 production from CO consumption (Lee et al., 2016). From the latter case, multi-omics analyses showed several levels of adaptation in addition to gene mutations, particularly at the transcriptomic and epigenetic levels.

1.2.2. Genetic tools of Thermococcales

If ALE works can be very suitable in an objective to bio-produce compounds of interest, direct mutational studies are also crucial to understand the impacts of given, targeted pieces of the cellular machinery. Several genetic tools have been developed for the modification of *Thermococcales*.

The first genetic tools available for manipulating these hyperthermophilic archaeal models were shuttle vectors (Aagaard et al., 1996; Aravalli and Garrett, 1997). The plasmid pGT5 from *P. abyssi* was used to develop a shuttle vector, transformed in *P. furiosus* to enable heterologous expression of the alcohol dehydrogenase gene from *Sulfolobus solfataricus*. The plasmid was then used as a basis for enhancement of a shuttle system between *P. furiosus*

and *E. coli* (with a patent pended), and shuttle vectors usable in *P. abyssi* (Lucas et al., 2002; Thomm et al., 2011; Waege et al., 2010). Then a markerless deletion system, based on a simvastatin positive selection and a 6-methylpurine negative selection, was used to modify the native, inactive chitinase of *P. furiosus* and to grow it on chitin (Kreuzer et al., 2013). A variant of *P. furiosus*, named COM1, was found to be naturally competent for uptake of circular and linear DNA, which, coupled to homologous recombination, allowed markerless deletions without using a shuttle vector (Lipscomb et al., 2011).

Another member of the *Thermococcales* was found among the few naturally competent *Archaea* known so far: *T. kodakarensis*. Thanks to this trait, it was one of the first hyperthermophilic *archaea* for which the chromosome was manipulated. A tool for deletion was first described and improved in *T. kodakarensis*, and based on homologous recombination and the utilization of a pop-in/pop-out system, using tryptophan and uracil for selection (Sato et al., 2003, 2005). Later, a disruption plasmid was developed, using simvastatin resistance to select for the transformants, without needing to get prior strain with a given amino acid auxotrophy or any other defect (Matsumi et al., 2007). This same system has also been applied in *'T. onnurineus'* (Kim et al., 2010). A shuttle vector system, adapted from the plasmid pTN1 from *T. nautili*, permits replication and expression of gene in both *E. coli* and *T. kodakarensis* without needing homologous recombination (Santangelo et al., 2008). Further developments have led to optimized selection protocols and more efficient deletions (Santangelo et al., 2010). Recently, a transformation tool for large-scale gene recombination was developed for *T. kodakarensis*, allowing to transfer DNA pieces of up to 75 kbp long (Sato et al., 2020).

The initial principles used in the gene disruption tools for *T. kodakarensis* have been applied to the facultative piezophile *T. barophilus* MP^T, with simvastatin for positive selection and 5-fluoroorotic acid for counter-selection (Thiel et al., 2014). It was augmented by the use of 6-methylpurine for counter-selection, granting a drop on false positives in complementation from 80 % to 15 % (Birien et al., 2018) (FIGURE 14).

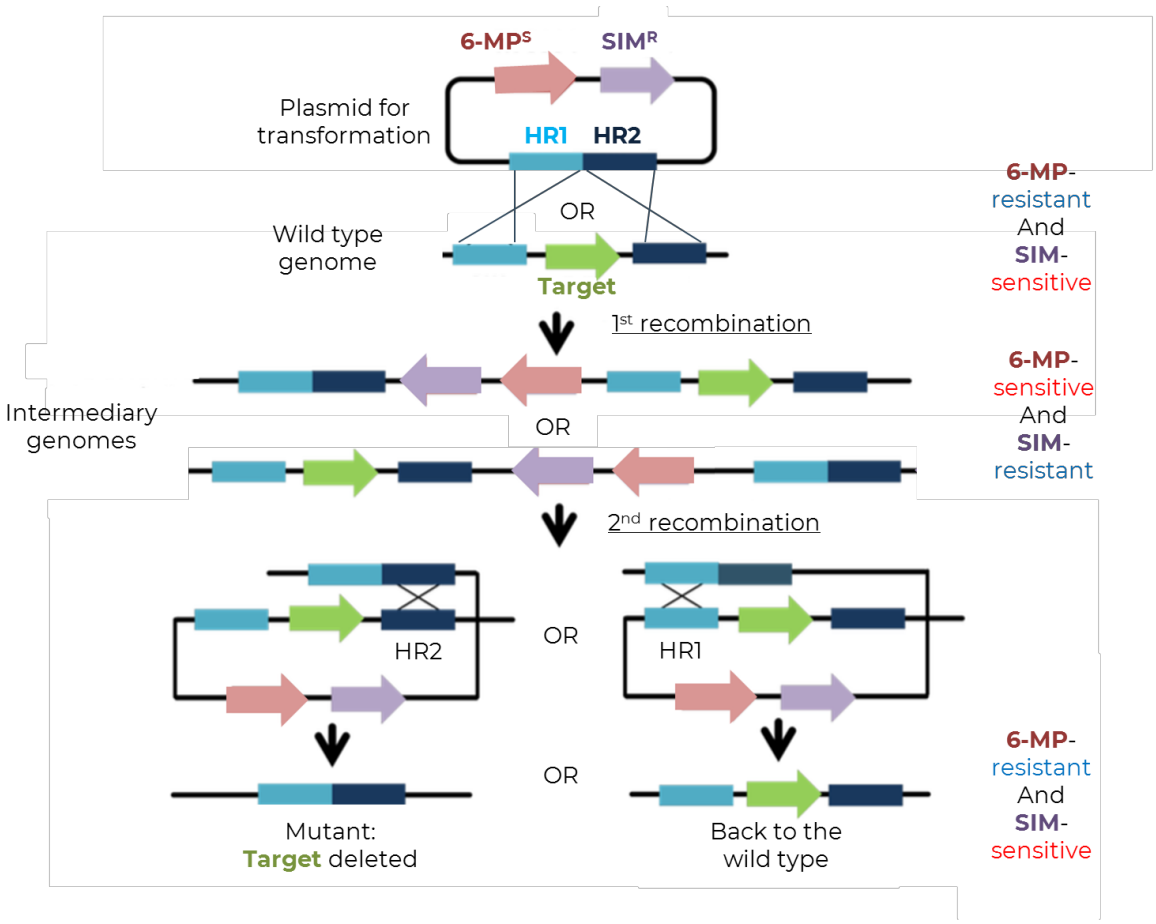

Figure 14: Schematic principle of the genetic tool for *T. barophilus*

(Birien et al., 2018; Thiel et al., 2014)

*The initial step consists in constructing a plasmid with sequences homologous to flanking regions of the **target** gene (**HR1** and **HR2**). Those are then used for transformation and a first homologous recombination with the wild type genome. This induces the acquisition of a resistance to simvastatin (**SIM**), as originally designed, and of a sensitivity to 6-methylpurine (**6-MP**), as ameliorated. A second recombination then allows to suppress the selective markers, leaving either **target**-deleted genomes or wild type genomes, which would then be verified by PCR.*

A similar system is also available for the obligate piezophile *P. yayanosii* (Li et al., 2014). The need for auxotrophic mutants and counter-selection with simvastatin was recently relieved in this latter model by the possible induction of a toxin-antitoxin system by high pressure for the pop-out recombination, permitting marker-less gene disruption (Song et al., 2019).

Those genetic tools have enabled significant advances in the comprehension of *Thermococcales* genetics, metabolism and physiology.

2. Metabolism and physiology

2.1. General concept of the fermentation in Thermococcales

Thermococcales are chemoorganotrophs, living in anaerobic conditions, and ferment peptides and/or carbohydrates, with elemental sulfur (S°) and/or protons as electron acceptors, leading to the production of H_2S and/or H_2 (Schut et al., 2014). Catabolic oxidations of a wide variety of electron donors provide energy that is not directly used by anabolic reduction reactions, but is rather transferred by electron transport chains (mainly NAD(P)H, ferredoxins). Energy can be conserved as adenosine triphosphate (ATP), thanks to a chemo-osmotic mechanism inducing the generation of an electrochemical ionic gradient (H^+, Na^+) across the cytoplasmic membrane, allowing the activity of an ATP synthase (Mayer and Müller, 2014).

Thanks to a varied set of hydrogenases, other oxidoreductases, and electron transporters, fermentation of carbohydrates and peptides allows *Thermococcales* to generate the electron fluxes that permit maintaining this ion gradient across the membrane, *i.e.* production of ATP. Energy conservation is thus linked to H_2S synthesis, and to the evolution and recycling of H_2. Though questions remain about the exact functioning of some parts of these metabolic pathways, extensive efforts have been made since the 1980's to characterize each of those parts, offering a considerable description of the systems.

2.2. A wide panel of degradation possibilities

Different substrates can be uptaken from the environment and degraded for use in metabolic pathways. Depending on their nature (carbohydrates or peptides, mainly), they will be directed towards different routes, where electron carriers are reduced. The panel of possible substrates in *Thermococcales* comprises simple and complex carbohydrates, organic acids, polyols, peptides, amino acids or other nitrogen sources, and even more complex matrices, such as milk and brewery wastes (TABLE 1). Growth on carbon monoxide as principal carbon source has also been reported in several species, such as '*T.* onnurineus' (Lee et al., 2008) and *T. barophilus* (Kozhevnikova et al., 2016). Some *Thermococcales* have also been suggested to convey exoelectrogenic abilities, *i.e.* to use extracellular electron transfer with insoluble minerals such as hydrothermal sulfides (Pillot et al., 2018).

Table 1: Examples of substrates degraded by *Thermococcales*

The information given herein does not represent an exhaustive list for the substrates nor strains concerned.

Type	Substrate	Example of species/strain	Reference
Simple and complex carbohydrates	Maltose	*T. litoralis*	(Xavier et al., 1999)
	Glucose	*T. barophilus*	(Cario et al., 2015b)
	Cellobiose	*P. furiosus*	(Oslowski et al., 2011)
	Glycogen	*P. kukulkanii*	(Callac et al., 2016)
	Starch	*P. furiosus*	(Lee et al., 2006)
	Chitin	*T. chitonophagus*	(Horiuchi et al., 2016)
	Cellulose, xylan and xyloglucan	*Thermococcus* sp. 2319x1	(Gavrilov et al., 2016)
Organic acids	Pyruvate	*T. kodakarensis*	(Kanai et al., 2005a)
	Formate	'*T. onnurineus*'	(Kim et al., 2010)
Polyol	Glycerol	*T. sibiricus*	(Mardanov et al., 2009)
Peptides, amino acids or other nitrogen sources	Casein, casamino acids and peptone	*T. barophilus* MP^T	(Marteinsson et al., 1999a)
	Tryptone	*T. peptonophilus*	(González et al., 1995)

	Urea	*P. kukulkanii*	(Callac et al., 2016)
More complex matrices	Milk and brewery waste	*T. paralvinellaea*	(Hensley et al., 2016)
	Shells and straw	*T. kodakarensis*	(Chen et al., 2019)
	Beef or yeast extracts	*T. barophilus* MP^T	(Marteinsson et al., 1999a)
	Microalgal residues	*T. eurythermalis*	(Chen et al., 2020)
Carbon monoxide		*T. barophilus* MP^T	(Kozhevnikova et al., 2016)
		'*T. onnurineus*'	(Lee et al., 2008)

All those different classes of substrates can be directed to the main metabolic pathways described below, and pass their electrons that will serve to maintain a cation gradient across the membrane, using various hydrogenases and oxidoreductases, and permit the production of ATP. Metabolism described herein has been divided into three main parts: substrate uptake, catabolism, and energy conservation.

2.3. Substrate uptake

The different substrates consumed by *Thermococcales* must enter the cell to be catabolized. To this extent, according to the nature of the concerned molecule, various mechanisms are used.

2.3.1. Carbohydrate uptake

Carbohydrates are used as carbon sources in *Thermococcales*, and may or may not allow growth without sulfur, depending on the species (see ENERGY CONSERVATION VIA HYDROGENASES IN THERMOCOCCALES, P. 86). Several members of the order have been reported to grow on monomeric sugars, but also on polymers. The latter can be degraded either intracellularly or extracellularly, before being transported inside the cell as mono- or oligomers (Verhees et al., 2003).

Transport of carbohydrates across *Thermococcales* membranes, involves ATP-binding cassette (ABC) transporters (Verhees et al., 2003). This action is specific, and not every sugar can necessarily be transported and used as a carbon source. For example, although *P. furiosus* harbors an ADP-dependent glucokinase, it is unable to uptake this monomer and grow on glucose as a carbon source and to uptake this monomer, whereas *T. barophilus* can grow on this sugar, and others (*e.g.* rhamnose) (Cario et al., 2015b; Kengen et al., 1996, 1995).

ABC transporters are widely distributed in all domains of life. They are divided into two categories, which have different substrate specificities and complex architectures: the CUT (Carbohydrate Uptake Transporter) and the Opp (di/oligopeptide transporter) (Koning et al., 2002a). Importantly however, though homologies from Opp-class ABC transporter primary sequences and domain compositions have been identified in *Thermococcales* (such as for the cellobiose/β-glucoside transport system of *P. furiosus* (Koning et al., 2001)), they rather seem to be involved, there, in carbohydrate uptake as well, and not peptides (Koning et al., 2002a). These types of transporters are, in *Bacteria*, oppositely known to be involved in the uptake of di- and oligopeptides, nickel, heme and substituted sugars (Koning et al., 2002a) (FIGURE 15).

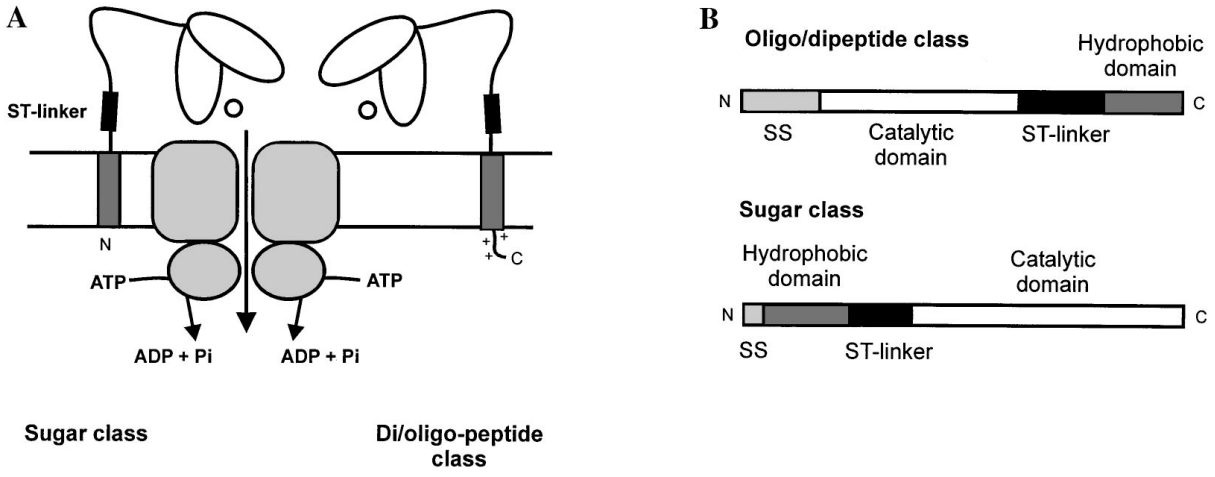

Figure 15: Domain structure of archaeal ABC transporter (from (Albers et al., 2004))

(A) Typical ABC transporter consisting of two permeases, two ATPases, and one membrane anchored substrate-binding protein. The substrate-binding proteins belong to either the sugar or the di/oligopeptide class which differ in membrane topology. (B) Representation of the domain organization of precursors of substrate-binding proteins of the sugar and di/oligopeptide class showing the signal peptide.

The function of ABC transporters involves different steps. The substrate is bound to glycosylated proteins, possibly from the S-layer, outside the cell. Those binding proteins are linked to the membrane by a hydrophobic transmembrane segment, or possibly *via* a lipid anchor, such as hypothesized in *T. litoralis* (Horlacher et al., 1998). For example, in *P. horikoshii,* some S-layer proteins bind N-acetyl glucosamine, the building block of chitin (Goda et al., 2018). After capture, the substrate is delivered to the membrane permease domains of the transporter. Then, ATP hydrolysis is thought to induce a conformational change in the ATP binding domain, thus propagating to the opening of a channel through which the substrate can pass the membrane (Diederichs et al., 2000; Koning et al., 2002a).

Unlike secondary transporters, which use electrochemical gradients of protons or sodium ions across the cytoplasmic membrane (see PEPTIDE UPTAKE, P. 74), ABC transporters can accumulate substrates inside the cell at high concentrations, and keep high affinities. They can indeed still function with substrates at sub-nanomolar concentrations, which is particularly practical in their often-changing environment, such as around hydrothermal vents (Albers et al., 2004).

In *Thermococcales* models, different sugar-specific and binding protein-dependent ABC transporters have been reported, targeting either maltose and trehalose (TM system, for which genes harbor bacterial origins, and also called Mal-I), or maltodextrin and malto-oligosaccharides (but not maltose) (MD system, for which genes arose in *Archaea*, and also called Mal-II) (Koning et al., 2002b; Noll e t al., 2008). Both the TM and MD systems have been described in *P. furiosus*, but only the TM system is found in *T. litoralis* (Horlacher et al., 1998; Xavier et al., 1996). In *P.furiosus*, a third type of ABC transporter named Cbt (cellobiose binding protein), belonging to a different class (Opp), has been shown to specifically uptake β-gluco-oligomers such as cellobiose. This function does not match with the domain homology of this Opp transporter, allowing peptide transport in some *bacteria* (Koning et al., 2001). Sugar uptake demands ATP, as ABC transporters comprise an ATPase (Albers et al., 2004; Lee et al., 2007).

Note that these transporter systems are expressed under the influence of transcriptional regulations, as explained in CARBOHYDRATE METABOLISM REGULATION, P.108.

Noticeably, a third main class of (sugar) transporters is also important in prokaryotes, namely the phosphoenolpyruvate-dependent phototransferase system (PTS). However, though it is often present in *Bacteria*, where it mediates catabolite repression, very few have been described in *Archaea* so far (and none in *Thermococcales*) (Jeckelmann and Erni, 2019; Mitchell and Moyle, 1958).

2.3.2. Peptide uptake

In addition to carbohydrates, peptide substrates can also serve as carbon source for all known *Thermococcales* (Schut et al., 2014), thanks to numerous intra- or extra-cellular proteases. Peptides additionally provide amino acids, though those constituents can directly be uptaken from the *medium* (Cario et al., 2015b). Minimal requirements in amino acids differ among *Thermococcales* members. For example, *P. abyssi* can grow on 9 amino acids (Watrin et al., 1995), whereas *T. celer* needs at least 10 (Hoaki et al., 1994), but only 4 are necessary for the growth of *T. litoralis* (Rinker and Kelly, 1996). Interestingly, in the piezophilic model *T. barophilus* MP^T, the pressure conditions change the minimal requirements for amino acids, increased at optimal pressure for growth (from 3 to 17 required) (Cario et al., 2015b).

Much less is known about the uptake of peptides and amino-acids in *Thermococcales*, compared to carbohydrates. In all domains of life, intake of small molecules, despite from harnessing ABC transporters, can be performed using ion gradients across the membrane, allowing the use of secondary active transporters, a second main type of transporters (Adelman et al., 2016). Genetic evidence suggests that in *Thermococcales*, such structures are abundant, and functional characterizations have concerned certain type of amino acid transporters and other small molecules. However, no proof of sugar transport through secondary transporters has been reported (Koning et al., 2002a).

For instance, SnatA is an alanine/glycine transporter able to hold different of L-type amino acids, driven by an electrochemical potential of H^+, and was first described in the strain *Thermococcus* sp. KS-1. It showed homologies with genes from other *Thermococcales* (such as *P. horikoshii, P. furiosus, P. abyssi*) as well as from other models (such as *Methanocaldococcus jannaschii*, *Escherichia. coli*, *Vibrio cholerae*) (Akahane et al., 2003). In *P. horikoshii*, GltPh is a homolog to a family of proteins found in mammals and called excitatory amino acid

transporters (EAATs). It is an aspartate transporter highly selective for its substrate over other amino acids, and is coupled to Na^+ (Ryan et al., 2009).

2.3.3. Other transports

Some organic acids can be used as a source of electrons in *Thermococcales*. Their import could occur through ion channels. For example, formate can pass through a transporter shown to be widespread in *Thermococcales* (Le Guellec, 2019). Two putative formate transporters have been identified in '*T. onnurineus*' NA1, but only one (encoded by TON_1573) is shown to be actually involved in growth on formate (see FORMATE HYDROGENLYASE, P. 96) (Jung et al., 2017; Kim et al., 2010). This transporter is homolog to the bacterial FocA, a formate/nitrite transporters (FNTs), holding some structural similarities with the bidirectional aquaporines (Mukherjee et al., 2017).

Other molecules that are of interest in this study follow paths of transports that are not well described in the literature, in *Thermococcales*, and would deserve further practical investigations. Indeed, few or no experimental data is available regarding, for example, how carbon monoxide is uptaken, how elemental sulfur can pass through the cellular membrane, or even how H_2 and H_2S end up in the extracellular *medium* (Gorlas et al., 2015).

2.4. Carbohydrate catabolism

2.4.1. Substrate rewiring to glycolysis

Depending on the molecule type and size, carbohydrates are degraded in different pathways, for which products are redirected towards a modified version of the Embden-Meyerhof-Parnas (EMP) pathway as a common route. Probably because monosaccharides can be quite thermolabile, growth on polymers is often preferred in *Thermococcales* (α- or β-linked glucan polysaccharides) (Driskill et al., 1999; Gao et al., 2003; Schut et al., 2014). Those polymers can be degraded extracellularly by several glycosyl hydrolases such as, for example, endoglucanases, amylases, pullulanases, chitinases, amylopullulanases (Brown and Kelly, 1993; Brown et al., 1990; Gao et al., 2003; Guo et al., 2018; Oslowski et al., 2011). For example in *P. furiosus* and *P. woeisei*, starch can lead to malto-oligosaccharides thanks to the action of α-amylases (Dong et al., 1997; Ghasemi et al., 2015).

Few strains have been reported to directly transport glucose, and it is performed by unknown mechanisms (Schut et al., 2014). Glucose, as a starting point for glycolysis (EMP pathway) can be formed from soluble polysaccharides transported into the cell, thanks to intracellular α- and β-glucosidases, as shown in *P. furiosus* and *T. litoralis* for example (Gueguen et al., 1997; Kengen et al., 1993; Xavier et al., 1999). Some *Thermococcales* use β-sugars, but the enzymes and transporters are specific and do not seem to be found in all species of the order, as for example the particular chitinolytic system of *T. kodakarensis* (Tanaka et al., 2003, 2004).

Thermococcales' metabolism of α-linked sugars is better described. Maltodextrin is a polymer of glucoses linked by α(1→4) glycosidic bonds. As a first step to its catabolism in *Thermococcales*, a 4-α-glucanotransferase induces disproportionation of maltodextrin to glucose and other shorter maltodextrins. A maltodextrin phosphorylase then forms glucose-1-P (Xavier et al., 1999). Noticeably, a specific pullulan hydrolase (TK-PUL) in *T. kodakarensis* has the ability to form maltose and glucose from maltotriose (Ahmad et al., 2014).

Maltose is a dimer of glucose with α(1→6) bonds, uptaken as such (using TM / Mal I transporter system described earlier) or resulting from polymer degradation. An α-glucosidase then splits maltose to glucose (Xavier et al., 1999). A glucanotransferase polymerizes maltoses with inorganic phosphates (rather than using ATP) to form maltooligosaccharides and glucose-1P, which would subsequently lead to glucose-6-P (then entering the glycolysis) using a phosphoglucomutase (Lee et al., 2006).

Trehalose, a dimer of glucose as well, but linked in α(1→1)α, can be uptaken from the environment thanks to the TM / Mal I transporter system, and is thought to be possibly metabolized into glucose and ADP-glucose thanks to the enzyme encoded by *treT* (in the same cluster as the transporter). The latter unit would then be re-branched to form glycogen or linear maltodextrins thanks to an uncharacterized branching enzyme (for example, TK1436 encodes putatively a branching enzyme in *T. kodakarensis* (Murakami et al., 2006)) and then glucose-1-P would form using glycogen or maltodextrin phosphorylases. This last phosphorylated sugar is taken on by glycolysis. Note that the action of the enzyme encoded by *treT* can also occur in the opposite direction, forming trehalose and ADP from ADP-glucose and glucose (Lee et al., 2008; Qu et al., 2004) (FIGURE 16).

Smaller, 5-C sugars (pentoses) are not known to be used for growth in *Thermococcales*, and the pentose phosphate pathway is absent. Instead, fructose-6-P is used as a precursor for providing pentoses to nucleic acids *via* the ribulose monophosphate pathway (Orita et al., 2006).

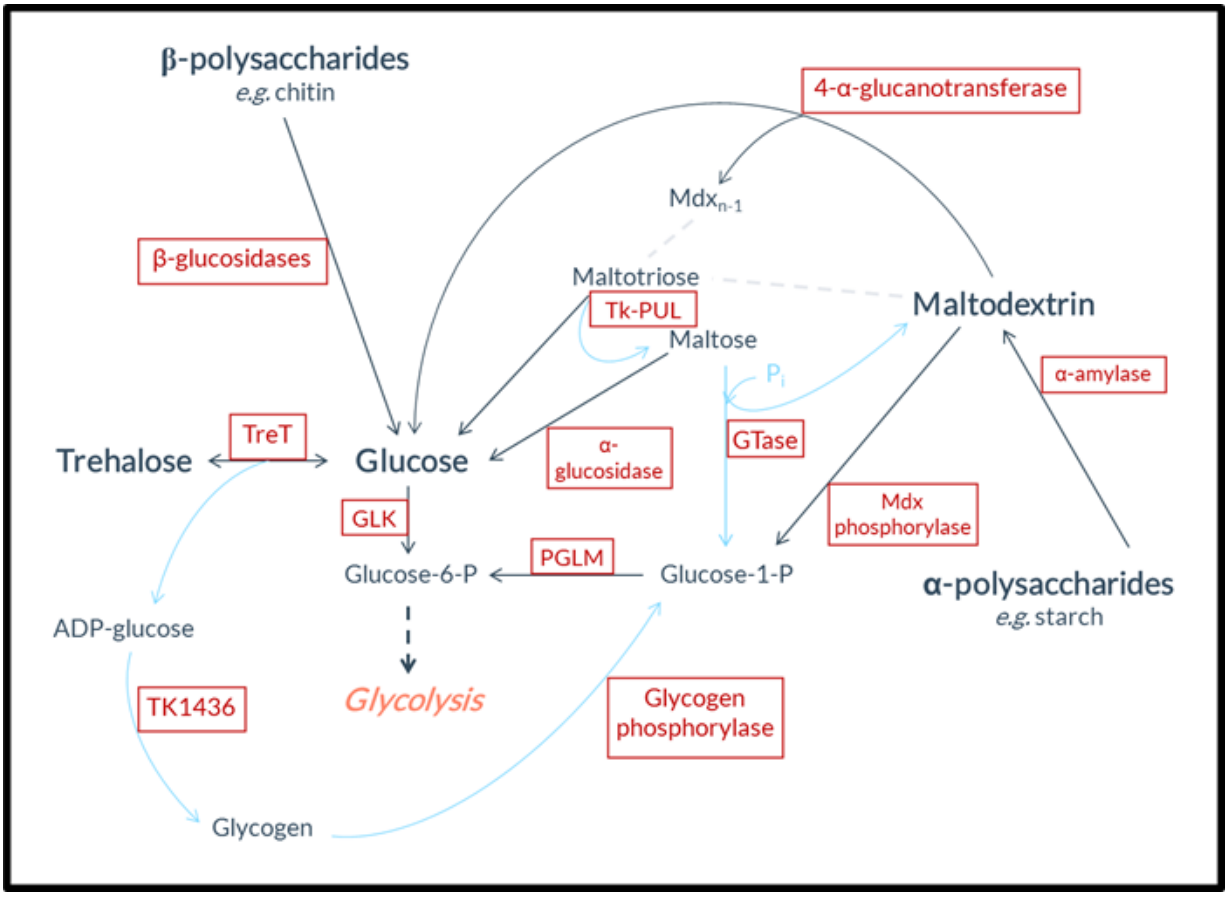

Figure 16: Carbohydrate pre-degradations for rewiring to glycolysis in *Thermococcales*

Stoichiometry was not provided. All routes are not found in all Thermococcales *models. Enzymes were represented in red squares.* ***GLK****: Glucokinase;* ***GTase****: Glucanotransferase;* ***Mdx****: Maltodextrin;* ***PGLM****: Phosphoglucomutase.*

2.4.2. Glycolysis: a modified Embden-Meyerhof-Parnas pathway

We have described how poly- and oligo-saccharides, as well as simpler monomers, enter the cell and are primarily degraded. They consequently enter the glycolytic, modified Embden-Meyerhof-Parnas pathway as 6C molecules (Sakuraba et al., 2004a; Verhees et al., 2003) (FIGURE 17).

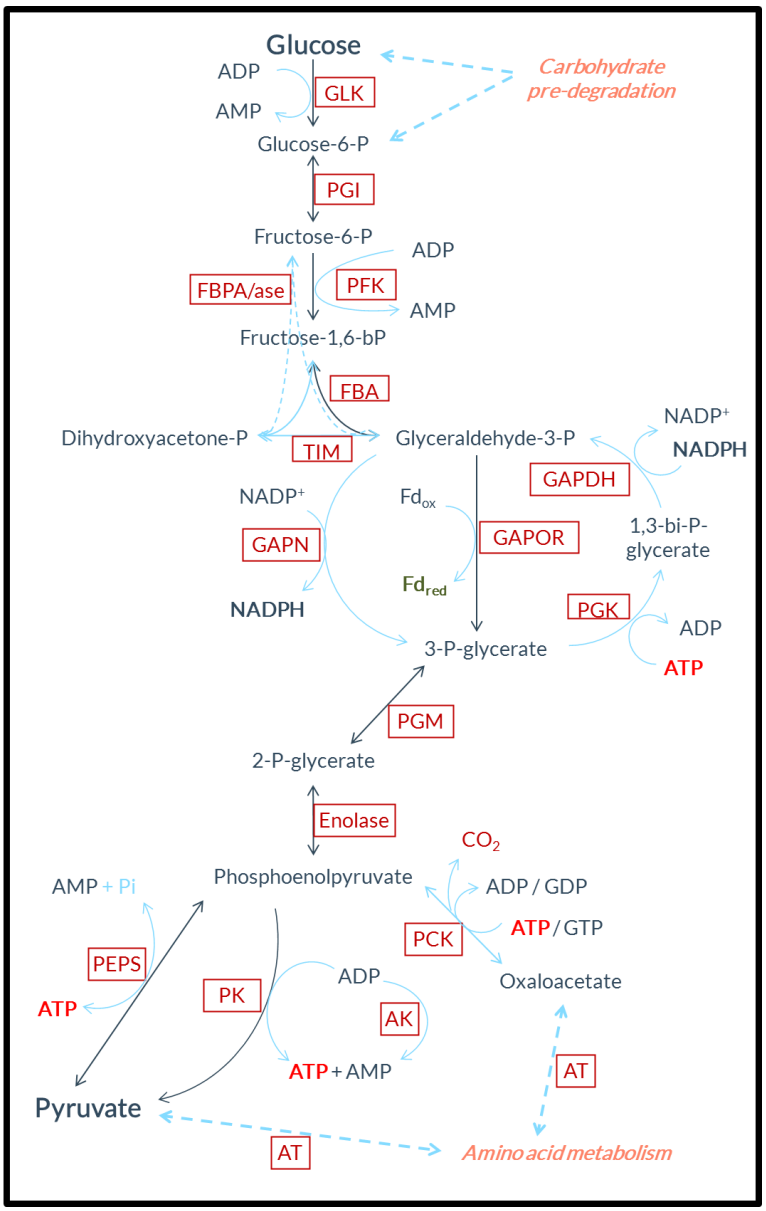

Details about gluconeogenesis are found *p. 84**. Stoichiometry was not provided. All routes are not found in all* Thermococcales *models. Enzymes were represented in red squares.*

***AK**: Adenylate kinase;*

***AT**: Aminotransferase;*

***FBA**: Fructose 1,6-biphosphate aldolase;*

***FBPA/ase**: Bifunctional fructose 1,6-biphosphatase;*

***GLK**: Glucokinase;*

***GAPDH**: Glyceraldehyde-3-phosphate dehydrogenase; **GAPN**: Non-phosphorylating GAP dehydrogenase;*

***GAPOR**: Glyceraldehyde-3-phosphate ferredoxin oxidoreductase;*

***PCK**: Phosphoenolpyruvate carboxykinase;*

***PEPS**: Phosphoenolpyruvate synthetase;*

***PFK**: Phosphofructokinase;*

***PGI**: Phosphogluco-isomerase;*

***PGK**: Phosphoglycerate kinase;*

***PGM**: Phosphoglycerate mutase;*

***PK**: Pyruvate kinase;*

***TIM**: Triose-phosphate isomerase.*

Figure 17: Glycolysis and gluconeogenesis in *Thermococcales*

The first stage of the following metabolic route is then the conversion to 3C, which is similar to what can be classically encountered in glycolysis. Glucose is first phosphorylated to glucose-6-phosphate by glucokinase (GLK), and then converted to fructose-6-phosphate by phosphogluco-isomerase (PGI). It is subsequently phosphorylated to fructose-1,6-biphosphate by phosphofructokinase (PFK) before being cleaved by a fructose-1,6-biphosphate aldolase (FBA) which allows the formation of glyceraldehyde-3-phosphate (GAP) and dihydroxyacetone-phosphate (the latter being converted again to GAP by a triose-phosphate isomerase (TIM)). For these steps, the difference with the classical route resides in the nature of the glucokinase, which is commonly found as ATP-dependent. In *Thermococcales*, several

studies have shown that the GLK is ADP-dependent (Kengen et al., 1995; Rivas-Pardo et al., 2013; Ronimus et al., 2001). Hypotheses have claimed that this could be preferred due to the better stability of ADP over ATP at high temperatures, or, more likely, that such a system would allow to quickly re-activate glycolysis after a period of starvation, which would have diminished the global ATP stocks in the cell (Guixé and Merino, 2009; Kengen et al., 1996). After this first degradation stage, the classical following conversion of GAP to 1,3-biphosphoglycerate (1,3-BPG) (by glycereraldehyde-3-phosphate dehydrogenase (GAPDH)) and to 3-phosphoglycerate (3PG) (by a phosphoglycerate kinase (PGK)) is replaced by a unique, physiologically irreversible step. It involves the specific enzyme glyceraldehyde-3-phosphate ferredoxin oxido-reductase (GAPOR), and reduces ferredoxin, an electron transporter protein (Mukund and Adams, 1995; van der Oost et al., 1998). To be more precise, GAPDH and PGK are indeed encoded in *Thermococcales'* genomes, but demonstrated very low activities in cell extracts, and are transcriptionally limited in glycolysis, rather expressed during growth on peptides, and active during gluconeogenesis (Hess et al., 1995; Jia et al., 2011; Matsubara et al., 2011; Mukund and Adams, 1995; Zwickl et al., 1990). Finally, this 3-PG formation can also occur, as shown in *T. kodakarensis, via* a third independent route (in addition to the inactive, classical GADPH/PGK route and the GAPOR route). This pathway involves a non-phosphorylating GAP dehydrogenase (GAPN)-like enzyme, for which sequence homologies (according to NCBI database) can be found in several *Thermococcales* (*e.g. P. furiosus*, *T. litoralis, T. nautili*) though that does not necessarily translate into an actual active enzyme (Matsubara et al., 2011). Importantly, GAPN is suggested to reduce $NADP^+$ during this glycolytic, irreversible step, thus compensating, in the global NADPH pool, for the lack of pentose phosphate pathway (see NO PENTOSE PHOSPHATE PATHWAY IN THERMOCOCCALES, P.86). This would contrast with the assumptions sometimes encountered in the literature that glycolysis only furnishes reduced ferredoxins for electron disposal in *Thermococcales* (*e.g.* in (Mayer and Müller, 2014; Nguyen et al., 2017; Schut et al., 2014)), although it seems, in *T. kodakarensis*, that solely using the GAPN route would not allow sustainable growth on sugars, probably due to an insufficient intrinsic NADPH generation in a glycolytic mode (Matsubara et al., 2011).

Afterwards, 3PG follows a usual conversion to 2-phosphoglycerate (2PG) by a phosphoglycerate mutase (PGM), and to phosphoenol-pyruvate using an enolase. Pyruvate is

then yielded with the generation of ATP mainly from ADP with a pyruvate kinase (PK). A subsequent acetyl-CoA formation also leads to ferredoxin reduction, and results in CO_2 and acetate end-production, concomitantly to ATP generation (see BOX 1, P. 84).

The net energy conversion of this unusual EMP pathway in *Thermococcales* varies and is tempered by the ADP-dependent sugar kinases and the possible use of PEPS and/or PK to form pyruvate (leading respectively to 2 or 0 mol ATP / glucose) (Bräsen et al., 2014). These steps does then not induce the ATP production classically found (*i.e.* 2 mol ATP / mol glucose) in EMP pathway, but the reducing equivalent have the chance to further carry on a particular oxidative phosphorylation system, thus conserving energy (Sapra et al., 2003). Ferredoxins and NADPH can be re-oxidized by hydrogenases, during which process electrons are passed to the final acceptors: either protons, thus producing H_2 (only from reduced ferredoxins), or elemental sulfur, to further produce H_2S (from reduced ferredoxins or NADPH) (see ENERGY CONSERVATION VIA HYDROGENASES IN THERMOCOCCALES, P. 86).

2.5. Peptide & amino acid catabolism

After and before their uptake in the cell (see PEPTIDE UPTAKE, P. 74), peptides are likely broken down into their constituent amino acids, thanks to the action of extracellular (Dib et al., 1998; Kannan et al., 2001; Klingeberg et al., 1995) and cytosolic (Basbous et al., 2018; Theriot et al., 2010; Ward et al., 2002a) proteases (Schut et al., 2014). Then, three main processes occur to oxidize the amino acids to their respective organic acids (FIGURE 18).

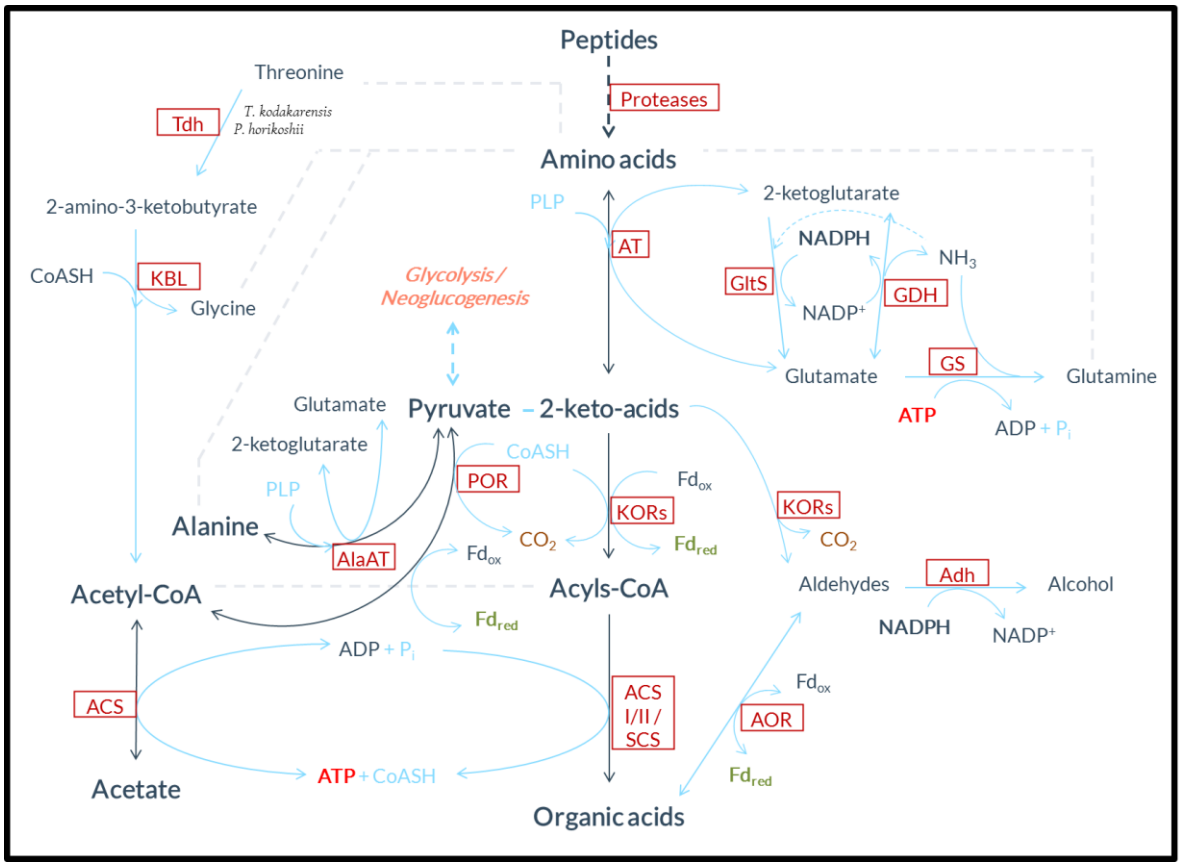

Figure 18: Peptide / amino acid metabolism in *Thermococcales*

Stoichiometry was not provided. All routes are not found in all Thermococcales *models. Enzymes were represented in red squares.* ***Adh****: Alcohol dehydrogenase;* ***ACS****: Acetyl-CoA synthetase;* ***AlaAT****: Alanine aminotransferase;* ***AOR:*** *Aldehyde ferredoxin oxidoreductase;* ***AT****: Aminotransferase;* ***GDH****: Glutamate dehydrogenase;* ***GltS****: glutamate synthase;* ***GS****: Glutamine synthetase;* ***KBL****: 2-amino-3-ketobutyrate ligase;* ***KOR****: 2-ketoacid ferredoxin oxidoreductase;* ***PLP****: Pyridoxyal 5'-phosphate;* ***SCS****: ADP-forming succinyl-CoA synthetase;* ***Tdh****: Threonine dehydrogenase.*

First, keto acids are formed through transamination/deamination. In the transamination process, amino acids are converted to the corresponding 2-keto acids by transfer of their amino group to 2-ketoglutarate, which leads to glutamate. This reaction needs an aldehyde-containing coenzyme, pyridoxal-5'-phosphate (PLP), and is catalyzed by aminotransferases, with different substrate specificities, such as alanine (AlaAT), aspartate (AspAT), aromatic amino acids (AroAT) and alanine:glyoxylate (Andreotti et al., 1994, 1995; Matsui et al., 2000; Sakuraba et al., 2004b; Ward et al., 2000, 2002b). Deamination of glutamate is then helped by a key enzyme: the glutamate dehydrogenase (GDH), highly conserved in the *Thermococcales* order. The GDH of *Thermococcales* has a central role, and estimated to constitute for more than 10 % of the total cytoplasmic protein of some strains

(Consalvi et al., 1991; Rahman et al., 1998). Note that glutamate is essential for growth in some models, as in *T. barophilus* MP^T (Cario et al., 2015b). It is oxidatively deaminated to reform 2-ketoglutarate again, allowing the processing of amino acids to continue. This recycling of glutamate by GDH forms *ammonia*, and electrons are discharged as NADPH (rather than NADH). The resulting *ammonia* can additionally be assimilated to glutamate, which permits to supply glutamine for biosynthesis, thanks to a glutamine synthetase, using ATP. A reverse synthesis of glutamate from *ammonia* can also be performed thanks to a glutamate synthase in some strains, dependent on NADPH (having very low activity with NADH) and using 2-ketoglutarate (Hudson et al., 1993; Jongsareejit et al., 1997; Robb et al., 1992; Schut et al., 2003; Yokooji et al., 2013). Other amino acid dehydrogenase activities have been observed in *T. kodakarensis* in a GDH-independent fashion, towards threonine and serine (Yokooji et al., 2013). A specific oxidoreductase, named threonine dehydrogenase (TDH), can indeed produce 2-amino-3-ketobutyrate from threonine (the third largest amino acid), and this product is further cleaved in a co-enzyme A-dependent reaction, using the catalysis performed by 2-amino-3-ketobutyrate CoA ligase (KBL). This produces glycine and acetyl-CoA (Bowyer et al., 2009). This enzyme has also been described in *P. horikoshii* (Higashi et al., 2008).

Then, 2-keto acids are decarboxylated oxidatively to the CoA derivatives. This involves, in *Thermococcales* models, at least four types of 2-keto acid oxidoreductases:ferredoxin (KORs) (Schut et al., 2001), specific to pyruvate (POR) (Blamey and Adams, 1993; Kletzin and Adams, 1996; Menon et al., 1998; Nisa et al., 2020; Nohara et al., 2014; Schut et al., 2001; Smith et al., 1994), branch chain 2-keto acids (VOR) (Heider et al., 1996; Nohara et al., 2014; Ozawa et al., 2005) , 2-ketoglutarate (KGOR, or OGOR) (Mai and Adams, 1996a), and aromatic 2-keto acids (IOR) (Mai and Adams, 1994; Ozawa et al., 2012; Siddiqui et al., 1997). Depending on the strains, this specificity to particular acids can be tempered, as the enzymes are also active towards other acids. For example, VOR from *T. litoralis* could participate, even though weakly, in pyruvate oxidation, but physiological studies in *T. kodakarensis* have not shown the occurrence of such reaction (Heider et al., 1996; Nohara et al., 2014). These 2-keto acid oxidations happen in the presence of reduced coenzyme A (CoASH), produce CO_2 and Acyl-CoA, reduce ferredoxins, and produce aldehydes, respective to each specific case.

The ensuing aldehydes are hypothesized to be potential substrates for an oxidoreductase dependent to ferredoxin (AOR), producing organic acids (Ma et al., 1997). Note that AOR contain tungsten, a metal rarely used in biological systems, but found in other enzymes in *P. furiosus*, such as formaldehyde Fd oxidoreductase and glyceraldehyde-3-phosphate Fd oxidoreductase (and transported by WtpA (Bevers et al., 2006)). AOR seems to harbor a substrate preference for acetaldehyde, phenylacetaldehyde and isovaleraldehyde, which are respectively produced by POR, IOR and VOR (Heider et al., 1996). It can function in the opposite direction, reducing organic acids, which was considered to apply to alcohol bio-production (Nissen and Basen, 2019).

Another enzyme, alcohol dehydrogenase, could indeed be involved in aldehyde consumption, but the actual activities under usual conditions are low. Maybe this could take part into limited-sulfur conditions though, as in *T. paralvinellae* ES-1. This would indeed only occur when AOR and ADH would compete for aldehydes, in the absence of electron sinking through sulfur (see ENERGY CONSERVATION VIA HYDROGENASES IN THERMOCOCCALES, P. 86). ADH reduces preferentially acetaldehyde and phenylacetaldehyde into alcohols, and uses NADPH rather than NADH as a cofactor. The ADH reaction thus oxidizes an electron carrier (produces $NADP^+$), whereas the AOR reaction reduces ferredoxin (Ma et al., 1994, 1995, 1997).

Finally, the corresponding organic acids can also be produced from the acyl-CoAs. This reaction is linked to substrate-level phosphorylation, generating ATP by the action of acetyl-CoA synthetases (ACS) I and II, hydrolyzing several acyl-CoAs (produced during the previous step) and aryl-CoAs (Yokooji et al., 2013). In the case of succinyl-CoA formation from 2-ketoglutarate by KGOR, a particular ACS-like protein, the ADP-forming succinyl-CoA synthetase (SCS), forms succinic acid, CoA and ATP, and consumes H_2O and ATP (Shikata et al., 2007).

By breaking down amino acids to their organic acid equivalents, through transamination/deamination to keto acids, oxidative decarboxylation to CoA derivatives, and substrate-level phosphorylation, *Thermococcales* thus produce reducing equivalents as both NADPH and ferredoxins. This could be in contrast with the degradation of carbohydrates, which, in some models (where GAPN is not active), seems to reduce ferredoxins only (see

GLYCOLYSIS: A MODIFIED EMBDEN-MEYERHOF-PARNAS pathway, P. 77). Note that ATP is also produced during the last step corresponding to acid synthesis (Schut et al., 2014; Yokooji et al., 2013).

Box 1: Pyruvate, an electron sink in the catabolic network

Pyruvate can thus ensue from peptide degradation, and also from glycolysis. From the peptide metabolism, alanine amino-transferase (AlaAT) reversibly transfers the amino group from glutamate to pyruvate, thus generating alanine and 2-ketoglutarate (Ward et al., 2000). In their mass balance analysis, Nohara et al., 2014, noticed that alanine formation was comparable to amino acid consumption, indicating that most amino groups in the amino acids end up transferred to pyruvate. Furthermore, GDH was suggested to form glutamate, rather than deaminating it to 2-ketoglutarate, when pyruvate is in excess (Yokooji et al., 2013). Consequently, AlaAT and GDH could importantly act coordinately to maintain the redox balance in this fermentative system, as they could modulate the relative flux of pyruvate to acetate formation towards pyruvate to alanine formation, possibly accumulated as an end-product in case of high H_2 partial pressures (Kengen and Stams, 1994a; Kobayashi et al., 1995; Mai and Adams, 1996b; Ward et al., 2000). Indeed, pyruvate oxidation to acetyl-CoA involves the reduction of ferredoxins, which can be reoxidized with hydrogenase activities (see ENERGY CONSERVATION VIA HYDROGENASES IN THERMOCOCCALES, P.86), provided that the *medium* is not H_2-saturated, hence the need for flux rather leading towards alanine. Deletion of AlaAT in *T. kodakarensis* has verily led to H_2 overproduction, forcing the acetate pathway (Kanai et al., 2015).

2.6. Other metabolic routes influencing catabolism

2.6.1. Gluconeogenesis

Producing glucose-6-phosphate from pyruvate, *via* gluconeogenesis, can also occur in archaea, however through bypassing of three irreversible EM reactions, namely the PEP-to pyruvate conversion catalyzed by PK, the GAP-to-3PG conversion catalyzed by GAPN and GAPOR and the F6P-to-F1,6bP conversion catalyzed by PFK (Bräsen et al., 2014) (FIGURE 17).

Several *Thermococcales* are capable of gluconeogenesis growth. Such a route was early demonstrated, in the order, in cell-free extracts of *P. furiosus* (Kengen et al., 1996). Conversion of pyruvate to PEP can classically be catalyzed by a phosphoenolpyruvate synthetase (PEPS). However, PEPS has shown to be essential in glycolytic conditions in *T.*

kodakarensis (Hutchins et al., 2001; Imanaka et al., 2006; Sakuraba et al., 2001). PEPS utilizes AMP produced by glycolytic ADP-dependent sugar kinases and P_i and thus permits to generate ATP. This step could be important in favoring energy yields of the overall carbohydrate catabolism, since, probably due to ATP scarcity, and as explained earlier (see

GLYCOLYSIS: A MODIFIED EMBDEN-MEYERHOF-PARNAS pathway, P. 77), sugar degradation is based on ADP-dependent kinases, and not ATP-dependent ones, encountered in classical glycolytic pathways (Bräsen et al., 2014; Imanaka et al., 2006; Kengen et al., 1994).

Alternatively, a first step to gluconeogenesis can occur through a PEP carboxykinase (PCK), which catalyzes the nucleotide-dependent, reversible decarboxylation of oxaloacetate to PEP and CO_2. It thus permits the conversion between C3 and C4 metabolites. In *T. kodakarensis*, PCK has been shown to be more transcribed in gluconeogenic conditions than in glycolytic conditions (Fukuda et al., 2004).

As shown in *T. kodakarensis*, the GAPDH/PGK couple is also essential for gluconeogenesis, where deletions of GAPOR and GAPN are not limiting to this metabolism, indicating their non-essentiality therein. Interestingly, GAPDH involves the consumption of NAD(P)H in this gluconeogenic direction (Matsubara et al., 2011). To bypass the irreversible conversion of F6P to F1,6bP, a bifunctional fructose-6-phosphate aldolase/phosphatase (FBPA/ase) is also essential in *T. kodakarensis* in the gluconeogenesis direction, directly catalyzing the formation of F6P from GAP, DHAP and FBP without any release of intermediates (Fushinobu et al., 2011; Imanaka et al., 2002; Sato et al., 2004; Say and Fuchs, 2010).

2.6.2. No Entner-Doudoroff pathway in Thermococcales

In *Bacteria* and *Eukarya*, the gluconate pathway (or Entner-Doudoroff pathway) constitutes a second major glycolytic pathway, also producing pyruvate (Flamholz et al., 2013). It is however absent in *Thermococcales* (Bräsen et al., 2014; Selig et al., 1997; Verhees et al., 2003).

2.6.3. No pentose phosphate pathway in Thermococcales

Pentoses, though abundant in nature as constituents of polymers such as nucleic acids and polysaccharides, do not seem to be catabolized by a pentose phosphate pathway in *Thermococcales*. To substitute such route, the ribulose monophosphate pathway (RuMP) has been described in *T. kodakarensis.* It involves a 3-hexulose-6-phosphate synthase and 6-phospho-hexuloisomerase fused enzyme (encoded by TK0475) able to bidirectionally fix formaldehyde and synthesize ribulose-5-phosphate from fructose 6-phosphate (Orita et al., 2006). A so-called pentose biphosphate pathway also replaces the absent pentose phosphate pathway in *T. kodakarensis* and links the pentose moieties of nucleosides or nucleotides to central carbon metabolism. Indeed, ribose-1,5-biphosphate (R-1,5-bP) issued from conversion and degradation of nucleosides and nucleosides 5'-monophosphate can be reoriented towards glycolysis *via* R-1,5-bP isomerase (in high AMP concentration) and Rubisco (ribulose-1,5-biphosphate carboxylase/oxygenase) (Aono et al., 2012, 2015). Note that those routes do not seem to involve $NADP^+$ reductions, contrarily to the classical archaeal pentose phosphate pathway (Bräsen et al., 2014).

2.7. Energy conservation *via* hydrogenases in *Thermococcales*

The two main catabolic routes described herein, *i.e.* peptide and carbohydrate fermentations, do not yield substantial net energy, but produce reducing equivalents mainly in the form of ferredoxins and NADPH. Those electron carriers are further recycled, disposing of the electrons they carry to protons or sulfur (so-called "electron sinks").This step occurs, in part, at the level of membrane-bound hydrogenases, and other membrane-bound oxidoreductases, which also translocate ions. Hydrogenases catalyze the reversible interconversion of molecular hydrogen and protons, as one of the most ancient microbial metabolic reactions (Schoelmerich and Müller, 2019; Schut et al., 2014). Such proton-translocating, proton-reducing reaction allows the maintenance of an ion gradient across the membrane, which represents, along with ATP, one of the two biological "energy currencies". Importantly, to allow converting those two "currencies", ATP synthases, also present in every living cell, catalyze the following reaction while coupling it to ion translocation across the membrane (Mayer and Müller, 2014):

$$ATP + H_2O \Leftrightarrow ADP + P_i$$

The different members of the order produce two (*e.g. P. horikoshii*) to seven (*e.g. 'T. onnurineus'* NA1) [NiFe]-hydrogenases (Lee et al., 2017). Several functions can be represented, such as: membrane-bound H_2-evolution, membrane-bound sulfane reduction, cytosolic H_2-protons electron interexchange, formate dehydrogenation, carbon monoxide dehydrogenation.

Depending on the presence or absence of elemental sulfur, which is a key player in the energy conservation system of *Thermococcales*, different set of enzymes are more involved than others in the disposal of electrons carried by the transporters mentioned before, thanks to the redox-active, master transcriptional regulator SurR. In the absence of sulfur, the regulator is reduced and can bind to specific DNA sequences in promoters and activate or repress the expression of different clusters. It has been described to be responsible for a metabolic switch in the presence of sulfur (thus in its oxidized, DNA-unbound form) from hydrogenogenic to sulfidogenic energy conservation. More details about the mechanisms involved in SurR regulation are given after the description of the individual parts of the system (SURR, A MASTER REGULATOR RESPONSIVE TO SULFUR, P.106).

Pressure can also influence this metabolic system, depending on the strain considered. Details about specific parts are given in TABLE 3, P.100.

2.7.1. H_2-evolution: Mbh

Mbh (Membrane-bound hydrogenase) is a 14-subunit hydrogenase complex, whose expression is activated by SurR (thus transcription rather occurs in lack of sulfur) (Lipscomb et al., 2017; Sapra et al., 2000; Silva et al., 2000). It is conserved within *Thermococcales*, has a tight evolutionary relationship with Complex I of the mitochondrial aerobic respiratory chain (Albracht, 1993; Sazanov, 2015; Schut et al., 2016a), and forms a membrane-bound [NiFe]-hydrogenase that is proposed to accept electrons directly from ferredoxins (although the initial published work mistakenly indicated an unknown electron carrier (Sapra et al., 2000; Silva et al., 2000)). The Mbh complex is not able to lead to H_2S synthesis and is not able to use NAD(P)H as an electron donor (Sapra et al., 2000). In the absence of elemental sulfur, it was shown in *T. kodakarensis* and in *P. furiosus* that Mbh is essential for growth (Kanai et al., 2011; Schut et al., 2012). Two functional modules can be distinguished: the hydrogenase

activity module Mbh, and the antiporter module Mrp. In *Pyrococcus furiosus*, the Mbh module is shown to have very high hydrogen evolving activity compared to other hydrogenases, and thus to produce a proton motive force (Silva et al., 2000). This exergonic reduction of protons induces a H^+ gradient across the membrane. The Mrp Na^+ / H^+ antiporter homolog subunits, encoded in the same cluster, allows the pumping of sodium cations out of the membrane, in exchange for protons, transforming the H^+ gradient in Na^+ gradient. Mrp is an important monovalent cation/proton antiporter allowing the intake of proton in exchange of a cation, and which homologs are found in most prokaryotes (Swartz et al., 2005). The antiporter function may be crucial for further energy conservation in *Thermococcales* as their ATP synthase translocates Na^+ rather than H^+, as shown from *P. furiosus* and '*T.* onnurineus' (Mayer et al., 2015; Pisa et al., 2007; Schut et al., 2012).

Box 2: ATPase or ATP synthase?

Note that in *Thermococcales* literature, ATP synthases are sometimes also termed ATPases (e.g. (Fukui et al., 2005; Santangelo et al., 2011), as archaeal ATP synthases function in both directions (synthesis and breaking of ATP), and are evolutionary closely related to eukaryal organelle ATPases (which only function towards ATP hydrolysis) (Grüber et al., 2014; Müller, 2004).

H_2 production has been shown to be linked to ATP production, with an estimated energetic yield of 0.3 mol of ATP formed per mol of H_2 in *P. furiosus* (Ma and Adams, 1994; Ma et al., 1993; Sapra et al., 2003).

2.7.2. Membrane polysulfide reduction : Mbs

In the presence of sulfur, SurR is oxidized and does not bind to DNA: Mbh expression is repressed. In that case, another important protein, whose expression is repressed by SurR, is now de-repressed and can be produced: Mbs (Membrane-Bound Sulfane reductase), previously termed Mbx (Schut et al., 2007). It is highly homologous to Mbh, with a 13-genes cluster (lacking MbhI) having conserved [FeS] binding motives and ion translocation modules, and found uniquely in *Thermococcales* (Wu et al., 2018a). However, it is believed to have issued from operon duplications of a Mbh-like respiratory system, but having switched from

proton to sulfur reduction (Sapra et al., 2003; Schut et al., 2013, 2016a). This respiration thus induces the production of H_2S rather than H_2, as measured in many studies, though the exact mechanism is unclear (Fiala and Stetter, 1986; Kozhevnikova et al., 2016; Moon et al., 2015; Schut et al., 2007).

A main structural difference, between Mbh and Mbs is that the proposed catalytic subunit of Mbs, formerly named MbxL, lacks half of the cysteine residues coordinating the active site of the enzyme in MbhL; although replacing the two missing residues in MbsL does not seem to impact growth nor H_2S production in *P. furiosus*. Mutant strains with Mbs deletion nevertheless showed growth defect in the presence of sulfur, indicating its essentiality for sulfur respiration, which was also shown in *T. kodakarensis* (Bridger et al., 2011; Kanai et al., 2011; Santangelo et al., 2011).

It was previously thought that H_2S production in *Thermococcales* was a mechanism of detoxifying H_2 (Adams, 1990; Fiala and Stetter, 1986). However, sulfur respiration, using Na^+ gradient induction, also conserves energy, and has even been calculated to be more efficient (41 kJ / mol) than generating H_2 (*i.e. via* the Mbh system) (12 kJ / mol) (Schicho et al., 1993). Physiological studies highlighted the advantage of sulfur reduction for growth, which could be linked to this efficiency (Kanai et al., 2005a; Kozhevnikova et al., 2016; Moon et al., 2015; Schut et al., 2007). It is important to precise that elemental sulfur, being quite insoluble, is not likely directly used by Mbs in *Thermococcales* as substrate for H_2S production. Rather, S°, being often octatomic, reacts with HS^- to form mainly long dianionic polysulfides (S_n^{2-}), that are soluble under hyperthermophilic conditions (Blumentals et al., 1990a; Hedderich et al., 1998; Ma et al., 1993). Organic polysulfides (with aryl or alkyl radicals) could also form from reactions of anionic polysulfides with aldehydes (Ritzau et al., 1993). Mbs is proposed to reduce the S-S bond within a trisulfide and to reduce polysulfides, producing di- and tri-sulfides, which, near neutral pH, are unstable and would spontaneously disproportionate to HS^- and S°:

$$S_n^{2-} + 2e^- \rightarrow S_{n-x}^{2-} + S_x^{2-}$$

Those reactions are thought to involve two electrons and no proton, hence the catalytic site of MbsL still functioning with only two cysteine residues and a lack of proton

path. *In vitro* experiments revealed that electrons are not ceded by NAD(P)H, but rather come from reduced ferredoxins (Wu et al., 2018a) (FIGURE 19). No Fd-dependent NADPH generation was shown *in vitro*, which partly refutes a previous hypothesis arguing that Mbs (then called Mbx) serves to reduce $NADP^+$ thanks to ferredoxin oxidation, which would then feed another NADPH-dependent sulfur reductase, Nsr (Schut et al., 2007).

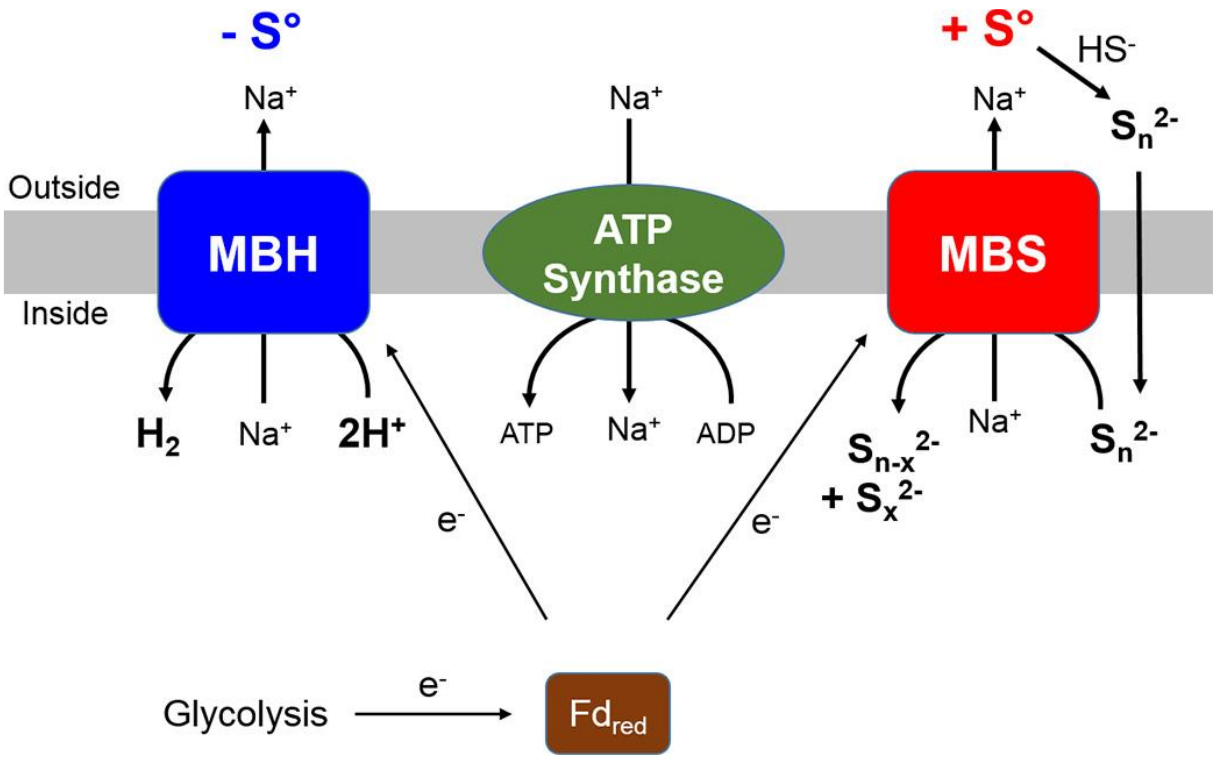

Figure 19: Proposed model for the respiration of *P. furiosus* in the presence and absence of sulfur and the role of Mbs (from (Wu et al., 2018a))

2.7.3. Cytosolic sulfidogenic system: Nsr / TK1481

Nsr is a cytosolic oxidoreductase involved in the sulfidogenic metabolism of *Thermococcales via* direct S°-reduction. It is homologous to NOX enzymes (NAD(P)H oxidase), which are involved in oxygen detoxification, suggesting similar catalytic mechanisms (Kobori et al., 2010). Its expression is negatively regulated by SurR, as for Mbs (thus upregulated in the presence of sulfur). Deletion of Nsr did not impair growths of *P. furiosus* nor *T. kodakarensis* mutants, in the presence of S°, thus confirming the position of Mbs as the major sulfidogenic enzyme in the system. However, physiological studies have shown that a *T. kodakarensis* Mbs-deleted strain still produced H_2S, though in lesser amounts, confirming the existence of another sulfidogenic route. The S°-reducing activity of Nsr, as shown *in vitro*,

produces H_2S, and uses NADPH (but not Fd_{red}) and CoA (Bridger et al., 2011; Kanai et al., 2011; Santangelo et al., 2011; Schut et al., 2007).

In *T. kodakarensis*, another cytosolic, NOX-homolog, H_2S-evolving oxidoreductase has been described, not found in *Pyrococcus spp.* nor in *T. barophilus* or '*T. onnurineus*', and encoded by **TK1481**. A SurR binding motif indicated that it may be rather expressed in the presence of sulfur (Jäger et al., 2014). *In vitro*, it oxidizes NAD(P)H and reduces polysulfides or oxygen as well, but not elemental sulfur, producing H_2S or H_2O_2. *In vivo* observations on oxygen tolerance of a TK1481-deleted strain have also shown the influence of the sulfur presence on the phenotypical outcome of the mutant. However, growth of this mutant on sulfur was not impaired, indicating that energy conservation is not a primary role of TK1481 sulfur reduction activity, or that it can be compensated by other systems (Kobori et al., 2010).

2.7.4. Cytosolic hydrogenases: SHI / SHII/ Hyh

SHI and **SHII** (SulfHydrogenase I and II) are two cytoplasmic [NiFe] hydrogenases supplying NADPH back to the metabolism as reducing equivalents by using H_2 as an electron donor. It was also shown *in vitro* that they can habor NADPH-dependent S° and polysulfide reduction activities, hence their name. Purified SHI from *P. furiosus* has shown to be stable at 100 °C and not sensitive to oxygen. It contains one large subunit, one small subunit, and two additional subunits, one with two FeS clusters and one with a FeS and a FAD clusters. Both proteins are similar in their molecular and enzymatic mechanisms, with SHI being much more active than SHII. Earlier hypotheses placed SHI and SHII (formerly simply named hydrogenases I and II) as the enzymes responsible for both H_2 and H_2S productions in *P. furiosus*. Note that these sulfhydrogenases are not to be mistaken with SuDH, the former name of NfnI, when it was first characterized as a sulfide dehydrogenase (see CYTOSOLIC REGULATION OF ELECTRON FLUXES: NFN , P. 92) (Bryant and Adams, 1989; Ma and Adams, 1994, 2001a; Ma et al., 1993).

Several arguments later tempered that belief for their *in vivo* function, however, justifying here their description in a different paragraph. Not all *Thermococcales* possess both cytoplasmic enzymes ('*T. onnurineus*' encodes both, *T. gammatolerans* encodes none). In *T. kodakarensis,* for example, an ortholog has been well studied: **Hyh** (encoded by *hyhBGSL*: TK2072-TK2069). It was shown to be involve in H_2 consumption (Kanai et al., 2003, 2017;

Moon et al., 2015). The NADP(H)-dependence of SHI/II also renders H_2 evolution thermodynamically unlikely to happen, and they do not accept ferredoxins. Note that a *mbh*-deleted strain of *P. furiosus* was shown to produce H_2 *via* SHI in low amounts, although it did not permit growth (Schut et al., 2012). They rather consume H_2, which was confirmed experimentally. *In vivo* experiments have indeed highlighted an increased H_2 production by a Hyh-deleted strain, particularly in the absence of sulfur (Haaster et al., 2008; Kanai et al., 2011; Santangelo et al., 2011). Note that without sulfur, deletion of those sulfhydrogenases did not induce growth impairment in *P. furiosus* nor in *T. kodakarensis*, though final cell densities were lower. In the presence of sulfur, however, no growth phenotype was observed due to the mutations. In addition, Hyh and SHI / SHII protein levels in *T. kodakarensis* and '*T. onnurineus*', respectively were higher in hydrogenogenic conditions than in sulfidogenic conditions. No dramatic H_2S production phenotype was observed in deletion strain, in the presence of sulfur. All this indicates that the so-called sulfhydrogenases do not seem to intervene as importantly in the sulfidogenic metabolism, or that their lack can be compensated, and that they do not actually evolve H_2 but rather catalyze the reverse reaction. Their role would consist in regulating the electron fluxes, as for example possibly reorientating electrons to biosynthesis *via* NADPH supply to alanine production, or to detoxification of free NH_3 (Kanai et al., 2011; Lipscomb et al., 2011; Ma and Adams, 2001a; Moon et al., 2015; Nohara et al., 2014; Santangelo et al., 2011; Schut et al., 2012).

2.7.5. Cytosolic regulation of electron fluxes: Nfn

NADPH can be recycled for biosynthesis thanks to other cytosolic proteins. In *P. furiosus*, another oxidoreductase, different from the sulfhydrogenases SHI and SHII (though divergently encoded from SHII), was originally described as a sulfide dehydrogenase (formerly named SuDH, and encoded by PF1327-28) and found to hold a FNOR (Ferredoxin:NADP oxidoreductase) activity (*i.e.* ferredoxin-dependent reduction of NADP). *In vitro,* this heterodimeric flavoenzyme possibly catalyzed NADPH-dependent polysulfide, elemental sulfur, or oxygen reductions, among others. However, it did not evolve nor oxidize H_2. Oxygen reduction is active at high O_2 concentrations, but it is unlikely to impact the physiology of the strain in its classical anaerobic culture conditions. It was suggested that this SuDH/FNOR is used to generate NADPH, *in vivo* (Ma and Adams, 1994, 2001b). Those potential reduction activities have not been described *in vivo*.

Rather, SuDH/FNOR then confirmed to play important roles in maintaining redox homeostasis, thanks to its NADH-dependent ferredoxin NADP+ oxidoreductase (Nfn) activity, and was renamed Nfn1, alongside with its paralog Nfn2 (later named Xfn) also found in *P. furiosus*, with which it harbors important structural and functional differences. Homologs of Nfn2/Xfn are found in all *Thermococcales*, along with either Nfn1 or a third, uncharacterized isoform, named Nfn3. Several strains encode the three isoforms, as does '*T.* onnurineus', for example (Nguyen et al., 2017).

Nfn enzymes are also encountered in numerous, mainly anaerobic, models (as for example the homolog in the bacterium *Thermotoga maritima* (Demmer et al., 2015)) and have been described as flavin-based electron-bifurcating catalysts, involved in exchanging electrons between the three main redox carriers: ferredoxins, NADH, and NADPH (Liang et al., 2019). They couple the endergonic reduction of $NADP^+$ by NADH and the exergonic reduction of $NADP^+$ by reduced ferredoxin, which allow to keep a high NADPH/$NADP^+$ ratio for biosynthesis. The mechanisms of electron-bifurcation in *P. furiosus* have been highlighted using the crystal structures of Nfn1, though this activity is less clearly defined for Nfn2 (Buckel and Thauer, 2013; Lubner et al., 2017; Wang et al., 2010). Nfn2 exhibits a good Fd-dependent $NADP^+$ reduction, without electron bifurcation. From their structures, it is likely that this FNOR activity would be catalyzed by all Nfn2 homologs in *Thermococcales*. However, the structure of Nfn2 in *P. furiosus* revealed a subunit similar to that of Nfn1. Nguyen *et al.* hypothesized that Nfn2 could hold another, unknown, bifurcating activity, using different substrates from Nfn1 (*i.e.* not harboring a NADH-dependent ferredoxin $NADP^+$ oxidoreductase activity), and that those substrates could be involved in sulfidogenic metabolism. Nfn2 would be a bifunctional enzyme with both bifurcating and non-bifurcating (FNOR) activities. Nfn2 was thus renamed Xfn, as the substrate involved in its potential bifurcating activity is unclear (Nguyen et al., 2017).

Physiological studies have allowed to better understand Nfn1 and Nfn2/Xfn functions *in vivo* in *P. furiosus*. Both enzymes were deleted (single or double deletions) and the phenotype of mutant strains revealed their importance for growth, in both hydrogenogenic and sulfidogenic conditions, consistently with both genes expression patterns in the presence or absence of sulfur. Nfn1 and Nfn2/Xfn encoding genes both possess SurR binding motives and

are both repressed by the master regulator. Interestingly, Nfn1 could likely be additionally repressed by another unknown regulator, also responsive to sulfur (Lipscomb et al., 2009, 2017) (see SurR, a master regulator responsive to sulfur, p. 106). Overall, Nfn1 seems to be rather involved in hydrogenogenic conditions, holding an important role for NADPH production, while Nfn2/Xfn would rather concern the sulfidogenic metabolic routes. Those deletions led to higher NADP(H) and NAD(H) pools, with lower NADPH/$NADP^+$ ratio (Lipscomb et al., 2017; Nguyen et al., 2017; Schut et al., 2003).

Therefore, as importantly stated by Nguyen *et al.* (2017), Nfn1 and Nfn2/Xfn hold overlapping and crucial roles in balancing the pools of three different electron carriers (ferredoxins, NADP(H) and NAD(H)); which roles are not compensated by other enzymes. In the frame of a H_2-saturated metabolism in *Thermococcales*, the excess electrons could thus be rewired to the alanine biosynthetic pathway through NADPH, thanks to glutamate dehydrogenase and alanine amino-transferase (see Peptide & amino acid catabolism, p. 80) (Kengen and Stams, 1994b; Verhaart et al., 2010).

2.7.6. A complex system with several more enzymes

Electron fluxes in the energy conservation system of *Thermococcales* can be organized thanks to the activities of many other enzymes, that are sometimes not well characterized, and add to the complexity of the general behavior described before (*e.g.* unique proteins (Tóth et al., 2008), or whole transcriptomes of unusual models (Zeng et al., 2020)). Here are brief, non-exhaustive descriptions of supplementary enzymes that can be found in some *Thermococcales* models and hold roles in the energy metabolism.

2.7.6.1. Pdo & TrxR

Pdo is a glutaredoxin-like protein disulfide oxidoreductase (an enzyme that catalyzes dithiol-disulfide exchanges) playing a role in the overall cellular redox balance. While its exact roles *in vivo* are unclear, different lines of evidence tend to indicate that it is a key factor in the hydrogen metabolism of *Thermococcales*. Its encoding gene share the same promoter region as *surR*, with SurR binding motif, and activated in the presence of sulfur (likely subject to SurR repression thus) (Pedone et al., 2004; Schut et al., 2007). Homologs of Pdo are however widespread in both *Archaea* and *Bacteria*, not uniquely in organisms reducing sulfur.

For example, in *Thermotoga maritima* (which is a member of the bacterial hyperthermophilic order *Thermotogales*), Pdo could receive electrons from NADPH thanks to a thioredoxin reductase (**TrxR**), and then serve as an electron carrier itself for ribonucleotide reductase (RNR), consequently making a link to deoxynucleotide synthesis (Yang and Ma, 2010). Homologs of such thioredoxin reductase can be found in *Thermococcales* genomes, also regulated by SurR (overexpressed in the presence of sulfur) (Schut et al., 2007, 2013). Interestingly, a *P. furiosus* ortholog of TrxR is also divergently transcribed from the Mbh operon, supporting the hypothesis of its implication in the hydrogen metabolism (Lipscomb et al., 2009). Furthermore, the disulfide oxidoreductase activity of the couple Pdo:TrxR could also serve to change the thiol/disulfide state of SurR, as shown *in vitro* from '*T. onnurineus*' NA1, and thus regulate the activity of the regulator (Lim et al., 2017). The Pdo/TrxR couple of '*T. onnurineus*' helps the reduction of cystine to cysteine, which abiotically reduces DMSO to DMS (FIGURE 20). Note that in this model, TrxR rather uses NADPH than NADH (two fold preference) (Choi et al., 2016).

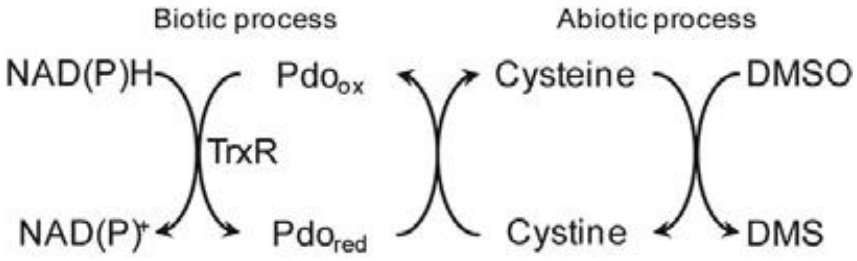

Figure 20: Principles of biotic and abiotic reactions involved in DMSO reduction in '*T. onnurineus*' NA1 (from (Choi et al., 2016))

2.7.6.2. Carbon monoxide dehydrogenase

In some *Thermococcales* species, the membrane bears a carbon monoxide dehydrogenase module (**CODH**), allowing the cell to grow on CO (TABLE 2), which is abundant near hydrothermal vents, as a carbon source (*e.g.* '*T. onnurineus*' NA1, *T. barophilus* MP^T). The CODH complex permits oxidizing CO with water to produce CO_2 and protons (Kozhevnikova et al., 2016; Lee et al., 2008, 2016a; Robb and Techtmann, 2018; Sokolova et al., 2004). In '*T. onnurineus*' NA1, this module comprises the carbon monoxide dehydrogenase, as well as a

hydrogenase and a Na^+/H^+ antiporter (Lee et al., 2008; Lim et al., 2010; Schut et al., 2016b). A putative regulator (TON_1525) could repress its transcription (Lee et al., 2016). The proteome of this well-studied strain has been characterized, in the presence of CO, revealing differentially expressed hydrogenases during carboxydotrophic growth (Moon et al., 2012).

The highest *Thermococcales* H_2 productions considered in an applied fashion, to date, are reported with this metabolic system in '*T. onnurineus*' NA1, reaching 577 mM/h in a slightly-pressurized (less than 10 bar), CO-phase gas-renewed, bioreactor (Kim et al., 2017, 2020). This strategy of using carbon monoxide has been targeted for several optimizations (*e.g.* use of a strong promoter (Kang et al., 2017; Lee et al., 2015), ALE (Lee et al., 2016)), as CO can be found as an industrial waste (e.g. from steam reforming) (Uehara, 2008).

Table 2: Growth of some *Thermococcus* strains on CO or formate in the presence of elemental sulfur (Kozhevnikova et al., 2016)

Strain	Growth and H_2 production on CO	Growth and H_2S production on CO + S^0	Growth and H_2 production on formate	Growth and H_2S production on formate + S^0
T. alcaliphilus DSM-10322^T	–	–	–	–
T. barophilus DSM-11836^T = MP^T	+	+	–	–
T. celer DSM-2476^T	–	–	–	–
T. gammatolerans DSM-15229^T	–	+	+	+
T. profundus DSM-9503^T	–	+	–	–
T. stetteri DSM 5262$_T$	–	–	–	–
T. sibiricus DSM-12597^T	–	–	–	–
Thermococcus sp. DS1	–	–	+	–
Thermococcus sp. AM4	+	+	–	–
Thermococcus sp. Ch1	+	–	–	–
T. barophilus Ch5	+	+	+	–
Thermococcus sp. DT4	–	+	+	–

2.7.6.3. Formate hydrogenlyase

Several *Thermococcales* members, such as '*T. onnurineus*' NA1, are able to grow using formate as a carbon and energy source, potentially accumulated by fermentation or entered in the cell *via* specific transporters (Kim et al., 2010; Takács et al., 2008; Topçuoğlu et al., 2018). To such extent, a formate dehydrogenase, oxidizing formate to CO_2 associated with H_2-evolution, functions in combination with a H^+/Na^+ antiporter subunit, allowing to maintain a

Na^+ gradient across the membrane for further ATP synthase activity. Together with a formate transporter, they constitute a cluster called formate hydrogenlyase (FHL). The FHL cluster of '*T. onnurineus*' (*fdh2-mfh2-mnh2*) comprises 2 dehydrogenase units, 7 [NiFe]-hydrogenase subunits, one formate transporter (TON_1573) and 7 Na^+/H^+ antiporter subunits. Its transcription has shown to be down-regulated in the presence of sulfur (Jung et al., 2017; Kim et al., 2010; Lim et al., 2010; Takács et al., 2008). As for carboxydotrophic conditions, the proteome of this model was characterized during growth on formate (Moon et al., 2012). Interestingly, as suggested in *T. paralvinellae*, FHL appears to oxidize H_2 with CO_2 reduction into formate, which could allow to relieve H_2 saturation in hydrogenogenic growth conditions, permitting a supplementary mechanism of electron disposal (Le Guellec, 2019; Topçuoğlu et al., 2018). Note that in '*T. onnurineus*' and *T. piezophilus,* SurR binding sites can be found in the promoters of the FHL encoding genes. In '*T. onnurineus*', it was found overexpressed in the absence of sulfur (Cho et al., 2017). Regarding pressure, formate measurements have also shown higher concentrations at high pressure in *T. piezophilus*, although these experiments were performed in H_2-saturated environments, likely increasing formate production (Le Guellec, 2019).

2.7.6.4. frhAGB-encoding hydrogenase

A homolog of the F_{420}-reducing hydrogenase, found in methanogenic organisms, has been reported in *Thermococcales* (*e.g. T. gammatolerans* EJ3 and '*T. onnurineus*' NA1): the cytoplasmic **frhAGB-encoding** hydrogenase. In methanogens, the F_{420}-reducing hydrogenase oxidizes H_2 to provide reduced coenzyme F_{420}, used as electron donor for CO_2 reduction in the methane metabolic pathway (Baron and Ferry, 1989; Schauer and Ferry, 1980). While its exact mechanisms remain to be demonstrated, its H_2 production during growth on CO or formate could be important for the overall redox balance. Its deletion in '*T. onnurineus*' did not drastically impair growth nor H_2 production, however its overexpression is induced by formate, and CO utilization. These expression seem to be increased by *frhA* deletion, thus leading to an increased H_2 production in those conditions (Jeon et al., 2015; Lee et al., 2017; Zivanovic et al., 2009).

2.7.7. Different types of ferredoxins

ATP production is reliant on the respiratory system set by the various oxidoreductases described in ENERGY CONSERVATION VIA HYDROGENASES IN THERMOCOCCALES. A proper supply in electron from the catabolic routes to the energy conservation pathways is thus crucial to allow the cells to thrive. Both sugar and peptide catabolism lead to reduced ferredoxins and NADPH formation (though NADPH from glycolysis would only concern strains with active GAPN, like *T. kodakarensis*) (see

GLYCOLYSIS: A MODIFIED EMBDEN-MEYERHOF-PARNAS pathway, P. 77). Particularly due to thermodynamical constraints, all types of electron carriers cannot be used indifferently in every reaction, though compensations are sometimes possible (*e.g.* the NADP(H)-dependent GDH of *T. kodakarensis* can use NAD(H), but in a less efficient fashion (Yokooji et al., 2013)) (Schut et al., 2016a). NAD(P)H are required as electron carriers for many reactions, and NAD(H) are not very stable in hot conditions (Hachisuka et al., 2017). Moreover, ferredoxins are required for some specific steps and their absence cannot be compensated sometimes, such as for the H_2-evolution catalyzed by Mbh, which, except in case of low H_2 concentration, is thermodynamically unfavorable from NAD(P)H (Verhaart et al., 2010). Ferredoxins thus need specification to maximize the electron fluxes of the metabolic system.

As shown in *T. kodakarensis*, *Thermococcales* can produce several different ferredoxins that influence the electron fluxes. Rather than representing generic shuttles, each of these small Fe-S proteins have different activities and specificities in the metabolism so critical physiological pathways can be furnished with enough energy, in particular thanks to their various mid-electric potential points (Burkhart et al., 2019; Meyer, 2008). In *Thermococcales*, ferredoxins are not only used for the supply of the respiratory system, but can also be used by cytosolic oxidoreductases for NAD(P)H generation, particularly through Nfn (Hidese et al., 2017) (see CYTOSOLIC REGULATION OF ELECTRON FLUXES: NFN, P. 92). In *T. kodakarensis*, at least three different ferredoxins are expressed differentially and have different structures.

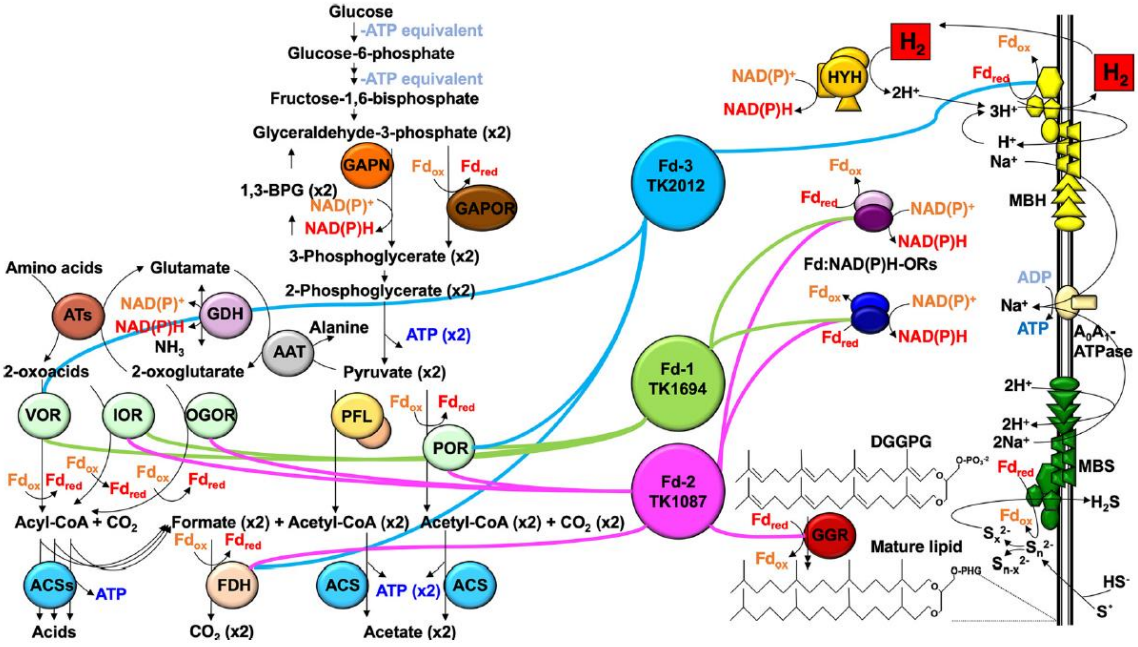

Figure 21: The distinct ferredoxin interactomes in *T. kodakarensis* (from (Burkhart et al., 2019))

*The primary electron donors that reduce oxidized Fds are shown on the left within a model glycolysis and amino acid fermentation. The primary electron acceptors that oxidize reduced Fds are shown to the right within partial representations of soluble lipid and NAD(P)H production pathways and membrane-bound respiratory and ATP-generating complexes. Each Fd is highlighted in the center of the panel, with interacting partners connected by solid, colored lines (Fd-1 in **green**; Fd-2 in **pink**; Fd-3 in **blue**).*

Interestingly, each of these proteins also has different interaction networks (FIGURE 21). From Burkhart et al., 2019, Fd-1 has been interpreted to rather be involved in NADP(H) production, particularly interacting with oxidoreductases from the amino acid catabolism routes : POR, VOR, and IOR (see PEPTIDE & AMINO ACID CATABOLISM, P. 80). It is essential and expressed independently from the presence or absence of sulfur. Fd-2 has a broader interactome, but rather concerning lipid maturation, as well as formate dehydrogenase, IOR and OGOR. It is also essential and however rather expressed when S° is available. Fd-3 is implicated in H_2-evoluting systems, particularly through Mbh subunits and possibly an ATPase, which is consistent with its expression in the absence of sulfur, and its non-essentiality (Burkhart et al., 2019). Noticeably, as explained earlier, though few data are available in the literature, coenzyme F_{420} could also serve as a low-potential electron carrier, as in methanogens, thus allowing ferredoxin-independent hydrogen-evolution (see FRHAGB-ENCODING HYDROGENASE, P. 97).

2.7.8. Summary of the principal enzymes of energy conservation metabolism

The information previously presented on the hydrogenase-linked energy conservation enzymes was summarized in TABLE 3 and FIGURE 22.

Table 3 : Summary of the main information on several enzymes involved in the principal energy conservation metabolism in *Thermococcales*

P_{opt}: optimal pressure for growth; $P_{sb\text{-}opt}$: sub-optimal pressure for growth; $P_{spr\text{-}opt}$: supra-optimal pressure for growth. +: upregulated. -: downregulated. Tb: Thermococcus barophilus*; Tk:* Thermococcus kodakarensis*; Py:* Pyrococcus yayanosii*; Tp:* Thermococcus piezophiles*. All pressure data ensued from the following references: (Dalmasso, 2016; Michoud and Jebbar, 2016; Vannier et al., 2015).*

Enzyme	Principal information at P_{atm}	Pressure influence (presence of sulfur, compared to P_{opt})	References
Mrp-Mbh	**Main functions:** H_2 evolution, Cation gradient maintenance. ***In vitro* observations:** No H_2S synthesis. **Physiological observations:** Essential for growth in the absence of sulfur. **Gene expression:** Activated by SurR. **Electron carrier or source:** Ferredoxin, No NAD(P)H.	P sb-opt spr-opt **Gene:** *Tb* + + *Tk* - *Py* - - *Tp* + + **Protein:** *Py* - -	(Kanai et al., 2011; Lipscomb et al., 2017; Sapra et al., 2000; Schut et al., 2012; Silva et al., 2000)
Mrp-Mbs (previously Mbx)	**Main functions:** H_2S synthesis, Cation gradient maintenance. ***In vitro* observations:** Polysulfide reduction. **Physiological observations:** Growth defect if deleted in the presence of sulfur. **Gene expression:** Repressed by SurR. **Electron carrier or source:** Ferredoxin, No NAD(P)H.	P sb-opt spr-opt **Gene:** *Tb* (-) (-) *Tk* + *Py* + + *Tp* + **Protein:** *Py* - -	(Schut et al., 2007; Wu et al., 2018a)

Nsr	**Main functions:** H_2S synthesis. ***In vitro* observations:** Use of CoA and elemental sulfur. **Physiological observations:** Growth defect if deleted in the presence of sulfur. **Gene expression:** Repressed by SurR. **Electron carrier or source:** NAD(P)H, No ferredoxin.	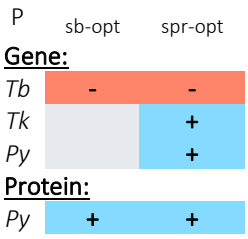	(Bridger et al., 2011; Kanai et al., 2011; Santangelo et al., 2011; Schut et al., 2007)
TK1481	**Main functions:** H2S or H2O2 synthesis. ***In vitro* observations:** Polysulfide or oxygen reduction. **Physiological observations:** No growth defect if deleted in the presence of sulfur. **Gene expression:** Potentially repressed by SurR. **Electron carrier or source:** NAD(P)H.	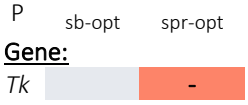	(Jäger et al., 2014; Kobori et al., 2010)
SHI / SHII / Hyh	**Main functions:** NADPH production by H_2 recycling, Potential regulation of electron fluxes. ***In vitro* observations:** NADPH-dependent S° and polysulfide reduction. **Physiological observations:** Increase in H_2 production when deleted in the absence of sulfur, No growth impairment when deleted in the presence of sulfur, No dramatic H_2S phenotype when deleted in the presence of sulfur. **Gene expression:** Activated by SurR. **Electron carrier or source:** NAD(P)H, No ferredoxin, H_2.	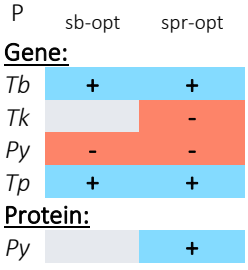	(Kanai et al., 2003, 2011; Lipscomb et al., 2011; Ma and Adams, 2001a; Moon et al., 2015; Nohara et al., 2014; Santangelo et al., 2011; Schut et al., 2012)
Nfn	**Main functions:** Redox homeostasis, Electron-bifurcating NADH- (or unknown)-dependent NADP+ reduction / ferredoxin-dependent reduction of NADP+ (FNOR). ***In vitro* observations:** Reduces (NADPH-dependent)	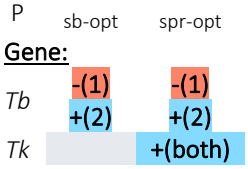	(Ma and Adams, 1994, 2001b; Nguyen et al., 2017)

	polysulfide, S°, oxygen, No H_2 reduction or oxidation. **Physiological observations:** Growth impaired when deleted in the presence and absence of sulfur with higher NADP(H) and NAD(H) pools and lower NADPH/NADP+ ratio, Nfn1 rather involved in hydrogenogenic conditions, Xfn rather involved in sulfidogenic conditions. **Gene expression:** Repressed by SurR, Nfn1 likely repressed by another unknown regulator. **Electron carrier or source:** NAD(H), NADP(H), Ferredoxin.		
Pdo	**Main functions:** Potentially implicated in H_2 metabolism. ***In vitro* observations:** Can change the redox state of SurR. **Gene expression:** Activated in the presence of sulfur. Likely repressed by SurR. **Electron carrier or source:** TrxR.	P sb-opt spr-opt **Gene:** *Tb* (-) - *Tk* + *Py* + **Protein:** *Py* +	(Choi et al., 2016; Lim et al., 2017; Pedone et al., 2004; Schut et al., 2007)
TrxR	**Main functions:** Potentially implicated in H_2 metabolism. ***In vitro* observations:** Can change the redox state of SurR. **Physiological observations:** Interacts with cysteine/cystine shuttle. **Gene expression:** Activated in the presence of sulfur. Likely repressed by SurR. **Electron carrier or source:** NADP(H) more than NAD(H).	P sb-opt spr-opt **Gene:** *Tb* - - *Tk* +	(Choi et al., 2016; Lim et al., 2017; Schut et al., 2007)
Mrp-Mbh-COdh	**Main functions:** Oxidation of CO, H2 evolution, Cation gradient maintenance. ***In vitro* observations:** No H_2S synthesis. **Physiological observations:** Essential for growth in the absence of sulfur.	P sb-opt spr-opt **Gene:** *Tb* + + *Tp* +	(Kozhevnikova et al., 2016; Lee et al., 2008, 2016b; Lim et al., 2010; Robb and Techtmann, 2018; Schut et al., 2016b;

	Gene expression: Potentially repressed by a putative regulator (TON_1525) in '*T. onnurineus*', but no SurR binding site. SurR binding site in *T. barophilus* MP^T. **Electron carrier or source:** Ferredoxin (hypothetically), CO.		Sokolova et al., 2004)
FHL	**Main functions:** Oxidation of formate and H_2 evolution, Cation gradient maintenance, H_2 oxidation to formate. **Gene expression:** Activated in the presence of sulfur, SurR binding site present. **Electron carrier or source:** Formate or H_2.		(Cho et al., 2017; Jung et al., 2017; Kim et al., 2010; Lim et al., 2010; Takács et al., 2008; Topçuoğlu et al., 2018)

Note that the proteomic characterization of *P. yayanosii* in function of pressure demonstrated that the genetic expression patterns do not necessarily translate in actual proteins, and thus in activity. It also appeared that for certain genetic expressions, the adaptation to sub- or supra-optimal pressure for growth could be different in each strain.

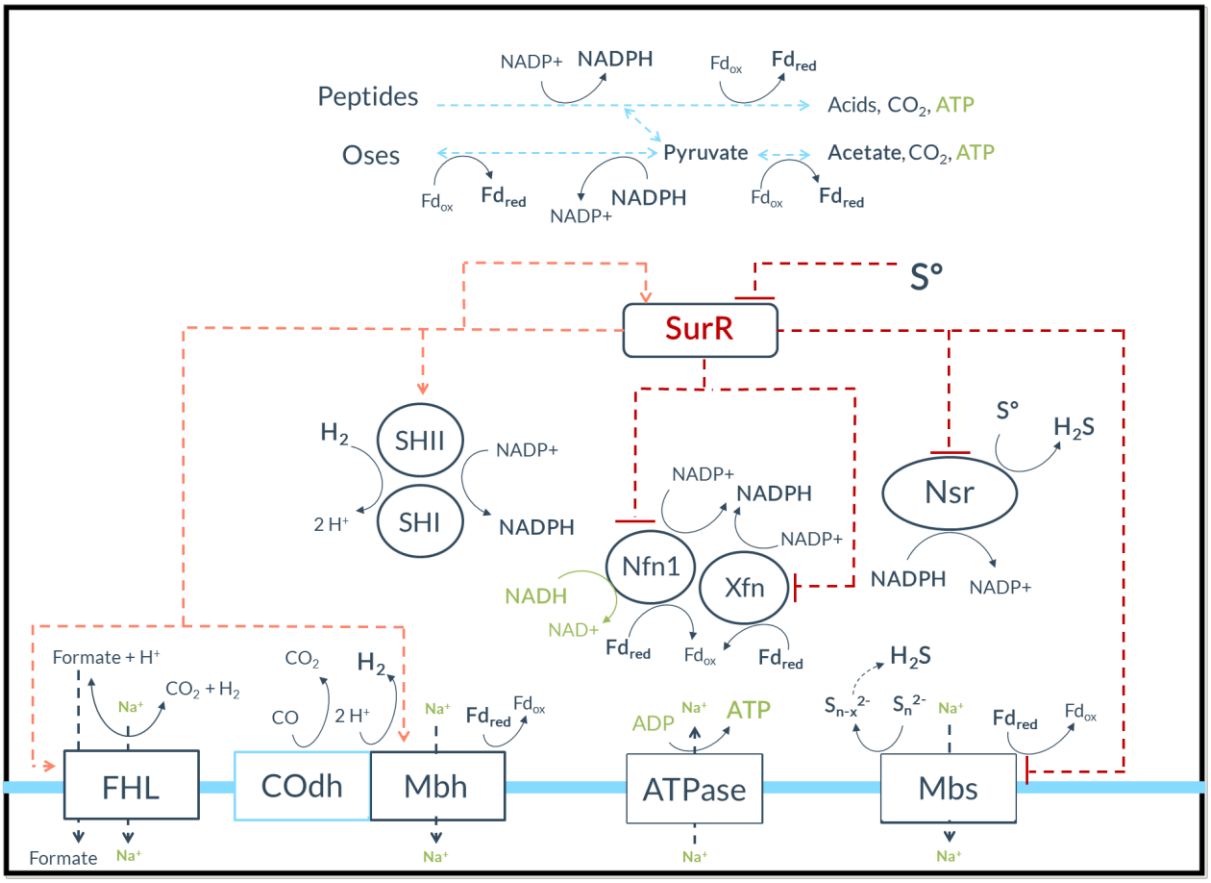

Figure 22: Simplified schematic summary of the principal energy conservation metabolism in *Thermococcales*, with the representation of SurR transcriptional regulation

Dotted lines to and from SurR represented transcriptional regulation on genetic targets: orange arrows designated expression, and red dashes showed repressions. Those were then de-regulated in the presence of sulfur, and effects on transcription were reversed. Stoichiometry was not precised. Mrp and other transporters were not displayed, but translocations were shown. H^+/Na^+ antiporters were simplified to Na^+ export. The COdh module is not present with all Mrp-Mbh clusters. All enzymes displayed herein are not present in all Thermococcales *models.*
Precisions can be found for each enzyme in the text.

2.7.9. Hydrogenase maturation

We have now clearly set that hydrogenases are key enzymes in the energy metabolism of *Thermococcales*. In order to paint this complex system as completely as possible, it is important to precise that though transcriptional regulation is indeed most involved in metabolic adaptation (see METABOLIC REGULATIONS OCCUR MAINLY AT THE TRANSCRIPTIONAL LEVEL, P. 106), hydrogenases however undergo important post-translational modifications, called

maturation, in order to reach their state of functionality. This has been of particular importance for considerations of cell-free H_2 production systems (Wu et al., 2018b).

Nickel-iron (Ni-Fe) hydrogenases, as the ones found in *Thermococcales*, usually contain two subunits, one large and one small, though this feature can vary. The large subunit hosts the catalytic center of the enzyme, where cysteine residues coordinate the Ni and the Fe atoms. The latter also harbors three unusual biological diatomic ligands (two cyanides and one carbon monoxide), allowing modulation of their electronic structure and encouraging catalysis (Pierik et al., 1999). The small subunits contain three iron-sulfur clusters to transfer electrons from outside the enzyme into the active site of the large subunit, in order to reduce protons. The catalytic center matures post-translationally, thanks to a whole set of proteins, called Hyp. This first involves the assistance of chaperones for insertion of the cations, followed by the formation and coordination of the ligands. The nickel cation acquisition cycle can be ATP-dependent, as for the activity of HypA and HypB proteins in *T. kodakarensis* (Sasaki et al., 2013; Watanabe et al., 2015). Maturation, as shown in *E. coli*, is complete only once the C-terminal region of the large subunit is degraded by specific endopeptidases, thus permitting the refolding of the hydrogenase around its active site (Kanai et al., 2017; Rossmann et al., 1995). Some C-ter-processing proteins have been described in *P. furiosus*, as for example FrxA, needed for SHI maturation, or HycI (homolog of *E. coli* HYD3), needed by its three hydrogenases (Sun et al., 2010). Note that in *T. piezophilus*, the HypE encoding gene was upregulated at optimal (50 MPa) and supra-optimal (90 MPa) pressure for growth, compared to sub-optimal pressure for growth (P_{atm}), and the HypD encoding gene was overexpressed at atmospheric pressure compared to 50 MPa and 90 MPa (Dalmasso, 2016).

At the moment of writing, few studies on hydrogenase-specific maturation endopeptidases of *Thermococcales* have been carried out, and studies on the overall maturation process and proteins concerned mostly *T. kodakarensis* (Kanai et al., 2017; Kwon et al., 2016; Sasaki et al., 2013; Tominaga et al., 2013; Watanabe et al., 2012, 2015), and *P. furiosus* (Sun et al., 2010; Wu et al., 2018b).

2.8. Metabolic regulations occur mainly at the transcriptional level

The metabolic capabilities of a cell answer to conditional needs, defined by environmental states. While these capabilities are encoded into genes, their function has to be regulated in order to be energy-efficient, by corresponding to current requirements, but also to allow rapid shifts in case of any change of settings. Whereas in other domains, enzyme activities are often under allosteric control, studies have pinpointed that in archaeal glycolytic pathways, regulation seems to happen rather at the level of gene transcription (van der Oost et al., 1998; Siebers et al., 2001; Verhees et al., 2001, 2003; van de Werken et al., 2006). For example, the three main points of allosteric controls in classical Embden-Meyerhof-Parnas pathways (towards phosphofructokinase, hexokinase and pyruvate kinase), are absent in *Archaea.* There is, however, a sole allosteric control on GAPN, which is activated by glucose-1-P in *Thermococcales* (and not by AMP nor ADP, which can control other GAPNs) (Bräsen et al., 2014; Brunner et al., 1998; Johnsen et al., 2003; Matsubara et al., 2011; Schramm et al., 2000).

2.8.1. SurR, a master regulator responsive to sulfur

The presence or absence of elemental sulfur seems to be a key factor in the metabolic "decision" towards H_2 and/or H_2S production as modes of energy conservation pathways in *Thermococcales*. For example, in *P. furiosus*, a primary response to the addition of elemental sulfur occurs within minutes, and induces a down-regulation of Mbh, SHI and SHII and a concomitant upregulation of Mbs (Schut et al., 2007). Similar differences in metabolic profiles in response to sulfur have been observed in other *Thermococcales* models (Moon et al., 2015; Santangelo et al., 2011; Zeng et al., 2020). Behind this rapid shift, in part, lies a fundamental transcriptional regulator: SurR.

This ArsR-type sulfur-response redox-active regulator, conserved and unique to *Thermococcales,* allows the hydrogenase-based respiratory system to orientate towards two types of electron disposal: H_2 or H_2S production. SurR binding motives ($GTTn_3ATC$ or $GTTn_3AACn_5GTT$) are found in many promoters of genes involved in sulfur response (Hidese et al., 2017; Lipscomb et al., 2009, 2017; Schut et al., 2013; Yang et al., 2010). Its binding activity seems to be controlled by a redox-active switch, thanks to a CxxC motif possibly affecting the conformation of the DNA-binding domain of the protein according to the

oxidation state of the cysteine residues. In its reduced free-thiol form, in the absence of S°, it has been shown to activate the expression of its own gene as well as genes involved in hydrogenogenic metabolism, as for example *mbh1* and *hydb1*, the first genes of the Mbh and SHI operons, respectively, in *P. furiosus*. SurR also represses the expression of Nsr, Mbx and other clusters involved in sulfur reduction, such as Pdo (Schut et al., 2013). However, in the presence of S°, thus in an oxidized disulfide form, the activations and repressions are limited or cancelled as SurR cannot bind to DNA targets. Indeed, as described in *T. kodakarensis*, deletion of SurR inhibits growth in the absence of sulfur but has no effect in the presence of sulfur (Lipscomb et al., 2009; Santangelo et al., 2011; Yang et al., 2010). Note as a reminder that the redox state of SurR could also be regulated by Pdo, as shown *in vitro* in '*T. onnurineus*' NA1 (Lim et al., 2017).

The activation or repression activity of SurR seems to be related to the position of its binding site in the promoter (FIGURE 23). As a general tendency, if it binds upstream of the TATA-box, it holds the role of an activator, whereas it represses transcription when bound downstream of the TATA-box. In some cases, the presence of both upstream and downstream binding sites are essential for repression, as shown for Nfn by mutational studies in *T. kodakarensis* (Hidese et al., 2017; Yang et al., 2010).

Note that in *T. kodakarensis*, *sur*R gene expression was found upregulated at supra-optimal pressure for growth (25 MPa) compared to sub-optimal pressure for growth (P_{atm}). Contrarily, it was slightly upregulated at P_{atm} (sub-optimal) in *T. barophilus* MP^T compared to 40 MPa (optimal pressure for growth) (Vannier et al., 2015).

In addition to its crucial roles in orchestrating H_2/H_2S metabolism, SurR is a global regulator of electron flow pathways, being possibly directly or indirectly linked to the regulation of other major biosynthetic pathways in the cell such as membrane lipid production, nucleotide metabolism, metal ion transfer or purine biosynthesis (Denis et al., 2018; Lipscomb et al., 2009, 2017; Yang et al., 2010; Zeng et al., 2020).

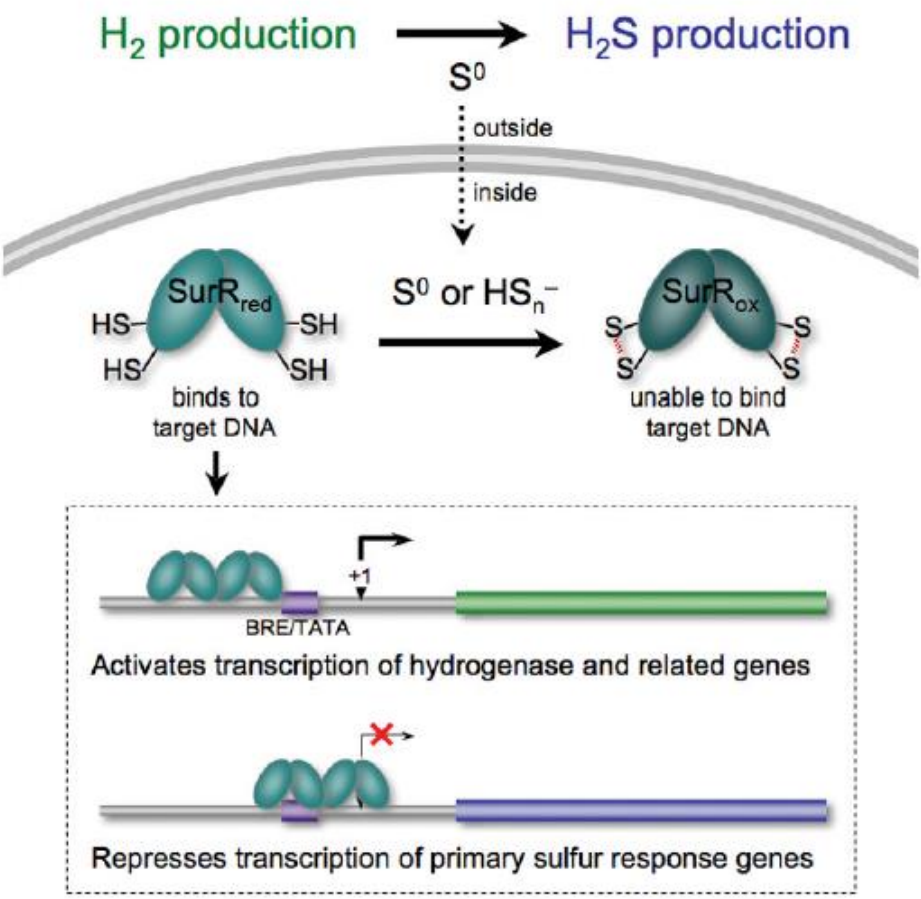

Figure 23: Representation of the physiological implications of SurR redox switch (from (Yang et al., 2010))

In the absence of sulfur, SurR remains in the reduced state ($SurR_{red}$), in which it binds DNA and elicits transcriptional control: activating hydrogenase and related genes, presumably by recruiting the basal transcription apparatus to the promoter, while repressing genes of the primary sulfur response, most likely blocking access to the promoter. Under these conditions, P. furiosus *produces H_2. However, when sulfur is available, cells shift from producing H_2 to H_2S, due at least in part to the deactivation of SurR ($SurR_{ox}$) resulting from oxidation by sulfur or polysulfide inside the cell. Once oxidizing sulfur species are depleted inside the cell, SurR is thought to be converted back to its reduced state to resume transcriptional regulation of target genes, thereby promoting the production of H_2 by the cell.*

2.8.2. Carbohydrate metabolism regulation

Other metabolic routes also undergo gene regulations in *Thermococcales*. In *T. kodakarensis*, a master regulator for glycolysis and gluconeogenesis, shown to be likely

effected by maltotriose: Tgr (*Thermococcales* glycolytic regulator), as SurR, functions both as an activator and a repressor, depending on the position of its binding motif compared to the (BRE)/TATA box (Kanai et al., 2007). While not experimentally confirmed, this could ensure the directionality of the pathway (towards glycolysis or gluconeogenesis), as observed in *P. furiosus* (van der Oost et al., 1998). Interestingly, this binding motif (TATCACN$_5$GTGATA) was already previously identified as the TGM (*Thermococcales* Glycolytic Motif) in *P. furiosus*, and found in starch-utilizing and glycolytic promoters of several *Thermococcales* (van de Werken et al., 2006). Tgr, as its homolog in *P. furiosus* (PF0124), are TrmB-like regulators. Regulation of carbohydrate metabolism can thus occur at more specific levels. TrmB (also recognizing TGMs) was first described in *T. litoralis* and *P. furiosus* as a repressor for the TM and MD transporter systems, and binding a variety of sugars, including maltose, sucrose, maltotriose and trehalose (see CARBOHYDRATE UPTAKE, P. 71) (Lee et al., 2006, 2003, 2005). Note that in *T. barophilus* MP^T, the TrmB- homolog encoding gene expression was reported to be downregulated at high pressures compared to P$_{atm}$, and two putative ABC transporters were upregulated in the same conditions (Vannier et al., 2015).

2.8.3. Several regulons in Thermococcales' metabolism

Few other transcriptional regulators have been described, among the dozens putatively identified (*e.g.* 87 in *T. kodakarensis*, according to Yamamoto et al., 2019), and concern various metabolic and cell functions. For example, Tar from *T. kodakarensis* regulates the biosynthesis of aromatic amino acids (Yamamoto et al., 2019). COrQR, in addition to another unknown factor, activates the CODH cluster in the presence of carbon monoxide in '*T. onnurineus*' (Kim et al., 2015; Lee et al., 2017). In the same model, CopR is sensitive to divalent metals such as nickel, cobalt, and mainly copper, and seems to repress the putative copper efflux system CopA (Kim et al., 2019). Responses to physical parameters are also regulated. PhR is involved in the heat-shock response in *T. kodakarensis* (Kanai et al., 2010). Though unpublished at the time of writing, a high hydrostatic pressure inducible operon seems to be controlled by the transcription factor HhpR in *P. yayanosii*, in response to HHP, as announced by the team of Jun Xu (Shangai) at the colloquium "Thermophiles 2019" (Song et al., 2019).

Important regulations - at levels different than transcription - remain seldom characterized in *Thermococcales*. In addition, epigenetic modifications could play a role in adaptation to environmental changes as suggested by an ALE experiment carried out in '*T. onnurineus*', rendering methylated sites in the SurR binding motif of a hydrogenase promoter, and thus possibly affecting the regulator's activity (Lee et al., 2016). To date, this work is however the only example of reported potential regulations at the epigenetic level in *Thermococcales*.

3. Biotechnological applications of *Thermococcales*

Thermococcales thus harbor numerous interesting features, which were noticeably studied in a biotechnological point of view, and considered early (Blumentals et al., 1990b). Just to name a few: novel metabolic pathways, involving quite thermostable proteins, were found in members of the order (*e.g.* concerning trehalose reversible synthesis, polyamine synthesis) (Sato and Atomi, 2011); alpha-amylases from *Thermococcales* were evaluated for their safety for the food industry, as heterologously expressed in a *Pseudomonas fluorescens* strain (Landry et al., 2003); several other debranching enzymes were studied, potentially useful to set up polymer degradations (Ahmad et al., 2014; Guo et al., 2018; Jung et al., 2014); and DNA polymerases of *Thermococcales* have been widely used in polymerase chain reaction (PCR) (*e.g. P. furiosus* (Lundberg et al., 1991), *T. pacificus* (Ppyun et al., 2013)).

However, as stated all along this manuscript introduction, one of the most envisioned features for biotechnological application of *Thermococcales*, as reported in the scientific literature, is their potential for hydrogen production. Studies have gathered substantial amounts of data on this topic, on various strains, from the most fundamental levels to bioreactor setup optimizations. Broad efforts were put on unravelling the metabolic capacities for degrading diverse substrates, which could be applied in a circular economy, based on extensive recycling of other industries' by-products (see A WIDE PANEL OF DEGRADATION POSSIBILITIES, P.69). Those potentials have been implemented into better described models (*e.g.* (Sun et al., 2010)). Systems were optimized to enhance their efficiencies (*e.g.* (Aslam et al., 2017; Jung et al., 2017; Lee et al., 2015, 2016a)), and even to produce other compounds of

interests along hydrogenogenic fermentation (such as thermophilic enzymes (Lee et al., 2020)).

Many *Thermococcales* originate from deep sea hydrothermal vents. Yet, among all these works on H_2 bio-production, one important aspect, which is the core of this project, prevails in the deep biosphere, and has merely been considered in such applications of *Thermococcales*: their piezophily.

VI. Studying *Thermococcales* as good chassis for high pressure H_2 bio-production

In order to contemplate a bio-production solution, one might choose the right chassis strain to constitute a sturdy base of such application (Calero and Nikel, 2018). Several advantages place *Thermococcales* as suitable candidates for a H_2 bio-production application: they grow quickly, are easy to cultivate, benefit from available genetic tools, are not pathogenic, have a metabolism already naturally optimized towards production of such compound (*e.g.* the modified EMP pathway), harbor resistances to potential toxicities of the product or co-products, have been largely described in many aspects in literature (*e.g.* physiology, genomics), are able to grow on a wide variety of (potentially low-cost) substrates, making them versatile, and are hyperthermophilic (relieving constraints of contaminations, lack of fluidity of the *medium*, and need for bioreactor cooling). In fact, as already mentioned, many academic works have prospected different *Thermococcales* strain for applied H_2 bio-production. A particular point is furthermore explored in this project: the application of high pressure to modulate H_2 bio-production.

1. Using high pressure to modulate the metabolism

In *T. barophilus* MP^T, sub- and supa-optimal pressures for growth (0.1 and 70 MPa) induced overexpression of several clusters encoding hydrogenases (Mbh, COdh), indicating a possible optimization of the hydrogenogenic metabolisms in those stressful conditions. In *T. kodakarensis*, 25 MPa (supra-optimal pressure for growth) led in contrary to a downregulation of Hyh and Mbh (Vannier et al., 2015). Overexpression of hydrogenases at

sub- and supra- optimal pressures for growth was also observed in *T. piezophilus* (Dalmasso, 2016). The obligate piezophile *P. yayanosii* seemingly globally expresses its energy conservation system more importantly than other *Pyrococcus* species, but, interestingly, while hydrogenase gene expressions seem to be downregulated at sub- and supra-optimal pressures, the corresponding proteins seem to be overexpressed at supra-optimal pressure. Nsr and Pdo have also been reported to be upregulated at supra-optimal pressures in this model (Michoud and Jebbar, 2016) (TABLE 3). It thus globally appears that in *Thermococcales*, the energy conservation metabolism is differentially regulated in function of the pressure of culture, denoting a possible interest in using high pressure as a tool for modulating H_2 production.

2. Advantages of high pressure for H_2 production

Commercial hydrogen cannot efficiently be stored at atmospheric pressure, especially for mobility usage. The most often encountered storage of gaseous hydrogen to date is in high pressure cylinders, at 20 MPa, but the most interesting energetic density is encountered at 70 MPa, where recent efforts have been concentrated. This pressurization requires important costs, hence the potential advantage of already placing the production process, which can be continuous, at high pressure, rather than compressing the product (EDF, 2017; James et al., 2016; Kelly et al., 2008; Makridis, 2016; Mayyas and Mann, 2019; Viktorsson et al., 2017; Züttel, 2003).

The project HPBioHyd was based on this assumption, together with the collaboration of the industrial partner HP Systems (La Rochelle, France). HP Systems is a company from around La Rochelle (France) specialized in mastering, design and development of diverse, state-of-the-art technology allowing to compress, store and regulate any kind of fluid (gases and liquids) under conditions of high pressure and temperature (HP/HT). The company has noticeably been working for several years with high pressure H2.

VII. Objectives

In a context of the collaboration between HP Systems, the LM2E UMR6197, and the PhD candidate, the project HPBioHyd aimed at setting up bases for optimized molecular hydrogen bio-production in *Thermococcales* at high temperature and high pressure.

This task was regarded as a way to advance knowledge about the physiological and metabolic behavior of these microorganisms under high pressure as well as to evaluate the feasibility of a solution of H_2 bio-production under high pressure in order to further envision larger-scale applications. The ensuing questions were (i) to determine what *Thermococcales* strains could be best used, on which substrates, through a screening of the UBOCC (UBO strain collection) and to broadly evaluate the behavior of the chosen fermentative system according to different culture parameters. We also (ii) explored technical solutions to produce H_2 at high pressure and to study our model. Investigating hydrogenogenic systems at high pressure indeed necessitated the adaptation of pre-existing tools and methods, for both fundamental approach and bioreactor design, concerning both continuous and discontinuous pressurization systems. In parallel, the third axis developed herein was (iii) how to biologically optimize H_2 bio-production. The related metabolism of *Thermococcus barophilus* was investigated on a more basic level, with a focus on two main branches of possible future optimizations (hence divided in two distinct chapters): adaptation to high pressure, through a mutational study, and tolerance to hydrogen, *via* an adapted laboratory evolution experiment.

This work was consequently approached both practically and fundamentally, and divided in four main topics, that will each constitute a chapter of this manuscript:

Chapter I:

Strain screening and fermentation overview

Chapter II:

Adaptation and optimization of high pressure tools and culture methods

Chapter III:

Impacts of high pressure on the hydrogeno/sulfidogenic metabolism of *Thermococcus barophilus*

Chapter IV:

Adaptive Laboratory Evolution study of hydrogen tolerance in *Thermococcus barophilus* MP^T

Dans un contexte de collaboration entre HP Systems, le LM2E UMR6197 et l'étudiant, le projet HPBioHyd visait à poser les bases d'un bio-production d'hydrogène moléculaire optimisée, chez des Thermococcales, à haute pression et haute température.

Cette tâche a été appréhendée comme une opportunité d'améliorer les connaissances fondamentales sur la physiologie et le comportement métabolique de ces microorganismes sous haute pression, ainsi que d'évaluer la faisabilité d'une solution de bio-production sous haute pression dans le but d'envisager à long terme des applications à plus haute échelle. Les questions découlant étaient (i) *de déterminer quelles souches de Thermococcales pourraient être utilisées de manière optimale, et sur quels substrats, à travers un criblage de la collection de souches de l'UBO (UBOCC) and d'évaluer plus largement le comportement du système fermentaire choisi selon différents paramètres de culture. Il s'agissait également* (ii) *de rechercher des solutions techniques pour produire de l'H_2 à haute pression et pour étudier le modèle biologique. Explorer des systèmes hydrogénogéniques à haute pression a en effet nécessité l'adaptation d'outils et de méthodes pré-existants, à la fois pour une approche fondamentale et pour la conception d'un bioréacteur, concernant une pressurisation continue et discontinue. En parallèle, le troisième axe développé ici était* (iii) *la question biologique de l'optimisation de la bio-production d'H_2. Le métabolisme associé de T. barophilus a été étudié à un niveau plus basique, s'intéressant particulièrement à deux branches principales d'optimisations potentielles (ainsi divisées en deux chapitres) : l'adaptation à la haute*

pression, à travers une étude mutationnelle, et la tolérance à l'hydrogène, via une expérience d'évolution adaptative en laboratoire.

Ce travail a donc été approché à la fois de manière pratique et fondamentale, et divisé en quatre sujets principaux, chacun constituant un chapitre de ce manuscrit :

Chapitre I:

Criblage des souches et évaluation de la fermentation

Chapitre II:

Adaptation et optimization d'outils haute pression et de methods de culture

Chapitre III:

Impacts de la haute pression sur le métabolisme hydrogéno/sulfidogénique de T. barophilus

Chapitre IV:

Etude de la tolérance à l'hydrogène chez T. barophilus *MP^T par évolution adaptative en laboratoire*

Materials & Methods - General

While the materials and methods used in this project are described for each specific case in the corresponding chapters, details on some common protocols can be found in this section.

1. Culture

Except when explicitly stated differently, all cultures were started from pre-cultures (issued from cryotubes), which were sub-cultured at the end of their exponential growth phases. Pre-cultures were started with 0.05 g/L colloidal S°, in order not to inject a significant amount of remaining sulfur when sub-culturing, which could potentially lead to false sulfur-less assays. To boost their growth, those pre-cultures could be incubated in H_2-desaturated conditions (*e.g.* with larger gas volumes, such as 20 mL of *medium* in a 1 L bottle filled with N_2).

Cultures were generally performed in anaerobic glass flasks of 50 mL filled with 20 mL *medium* and topped with 20 mm butyl stoppers (Dutscher) and sealed with 20 mm aluminum cap (VWR) to withstand overpressures. When H_2 saturation was an important parameter to consider (which was not the case, for example, for pre-cultures), flasks were incubated upside down to prevent gas leak, and stoppers were new for each experiment. Smaller or larger volumes could also be used, according to each experiment's needs. For larger volumes, Schott bottles (Duran) could be used and topped with Viton stoppers. Each piece of the system was autoclaved washed with deionized water and autoclaved 20 min at 121 °C or incubated in an Pasteur oven at 210 °C overnight before use.

When strain names were not precised, the reference strains for the considered species were used.

1.1. Anaerobic culture

In addition to liquid phase reduction with Na_2S (0.05 %), gas phases were replaced using a gas manifold allowing to direct the connection to a gas bottle (N_2 (Alphagaz 1, Airliquide) or N_2/CO_2 80/20 (Aligal 12, Airliquide)) or to a vacuum pump. Phases of pumping and injecting gases were alternated 8 times to consider the air in a butyl-stopper closed glass

flask completely removed. In addition, Gas mixes could be used to flush the flasks for 3 min as in the adapted laboratory evolution experiment (see chapter IV). Flasks were pressurized at 1.2 bar (absolute) at room temperature with their final gas phase.

1.2. *Media* and substrates

All powders for substrate tests and *media* preparations were purchased from Sigma, except Bacto Yeast Extracts (BD). For substrate tests, powders were diluted in deionized water to reach a 10 X concentration, and autoclaved individually before being added to a *medium*, concentrated at 1.1 X to compensate this dilution (typically 18 mL *medium* at 1.1 X + 2 mL substrate solution at 10 X in a 50 mL anaerobic flask). If no substrate was added more than the original composition of the *media* as described below, those ones were prepared at 1 X.

1.2.1. *Thermococcales* Rich *Medium* (TRM)

The following mix was performed in 1 L (*q.s.*) deionized water: 23 g NaCl, 5 g $MgCl_2 \cdot 6H_2O$, 1 g yeast extract, 4 g tryptone, 3.46 g PIPES disodium salt, 0.7 g KCl, 0.5 g $(NH_4)_2SO_4$, 0.05 g NaBr, 0.01 g $SrCl_2 \cdot 6H_2O$, and 1 mg resazurin. The pH was adjusted to 6.8 with HCl 3 N and the solution was autoclaved 20 min 121 °C, before the addition of the following sterile solutions: 1 mL KH_2PO_4 5 %, 1 mL K_2HPO_4 5 %, 1 mL $CaCl_2 \cdot 2H_2O$ 2 %, 1 mL Na_2WO_4 10 mM, 1 mL $FeCl_3$ 25 mM. Anaerobic conditions were then imposed following the protocol described earlier.

1.2.2. Anoxic Artificial Sea Water (ASW) *medium*

Artificial Sea Water (ASW) was used for the practical tests described in chapter I.

Prior to *medium* realization, the following solutions were prepared and autoclaved 20 min 121 °C, then stored out of light at room temperature: KBr (0.84 M), H_3BO_3 (0.4 M), $SrCl_2$ (0.15 M), NH_4Cl (0.4 M), KH_2PO_4 (0.04 M), NaF (0.07 M). A selenite-tungstate solution was made by mixing 0.4 g NaOH, 6 mg $Na_2SeO_3 \cdot 5H_2O$, and 8 mg $Na_2WO_4 \cdot 2H_2O$ in 1 L of deionized water (*q.s.*), filtrated (0.22 µm (Millex Millipore, Dutscher)) and stored at 4 °C. A trace element solution was prepared by mixing 10 mL HCl 25 %, 1500 mg $FeCl_2 \cdot 4H_2O$, 190 mg $CoCl_2 \cdot 6H_2O$, 100 mg $MnCl_2 \cdot 4H_2O$, 70 mg $ZnCl_2$, 36 mg $Na_2MoO_4 \cdot 2H_2O$, 24 mg $NiCl_2 \cdot 6H_2O$, 6 mg H_3BO_3, 2 mg

$CuCl_2 \cdot 2H_2O$, in 1 L deionized water (*q.s.*), filtrated (0.22 µm (Millex Millipore, Dutscher)) and stored at 4 °C. Balch's vitamin solution (Balch et al., 1979) was prepared by mixing 25 mg of p-aminobenzoic acid, 10 mg of folic acid, 10 mg of biotin (vit. B8), 25 mg of nicotinic acid, 25 mg of calcium pantothenate (vit. B5), 25 mg of riboflavin, 25 mg of thiamin HCl, 50 mg of pyridoxin HCl (vit. B6), 5 mg of cyanocobalamine (vit. B12), and 25 mg of lipoic acid (thioctic acid) in 1 L of deionized water (*q.s.*), filtrated (0.22 µm (Millex Millipore, Dutscher)) and stored at 4 °C. A 1M $FeCl_2$ solution was made by 19.8 g of $FeCl_2 \cdot 4H_2O$ to 100 mL (*q.s.*) of a 1 M HCl solution, prepared with deionized water sparged during 30 min with N_2. It was then autoclaved (20 min 121 °C) and stored at room temperature. A Na_2S solution was prepared with N_2-flushed deionized water, using 12 g of rinsed $Na_2S \cdot 9H_2O$ crystals per 100 mL (*q.s.* deionized water), while under a constant N_2 flux, and autoclaved at 109 °C for 30 min. A 60 mL bicarbonate solution was prepared by mixing 0.503 g $NaHCO_3$ to deionized water, in a flask flushed with N_2/CO_2 (80/20), then autoclaved 60 min at 121 °C.

The *medium* was prepared with deionized water in a 3 L flask according to a protocol modified from Widdel and Sass (Parkes et al., 2010; Widdel and Bak, 1992). The mineral base contained (in g/L): NaCl (27.2), $MgCl_2.6H_2O$ (10), $CaCl_2.H_2O$ (1.5), KCl (0.66), KBr (0.1), H_3BO_3 (0.025), $SrCl_2.6H_2O$ (0.04), NH_4Cl (0.021), KH_2PO_4 (0.0054), NaF (0,003), 0.625 mL of trace elements solution, and 0.125 mL of SeW solution. After autoclaving of the mineral base (30 min 121 °C), it was flushed for 30 min while cooling down with N_2/CO_2 (80/20) (FIGURE 24).

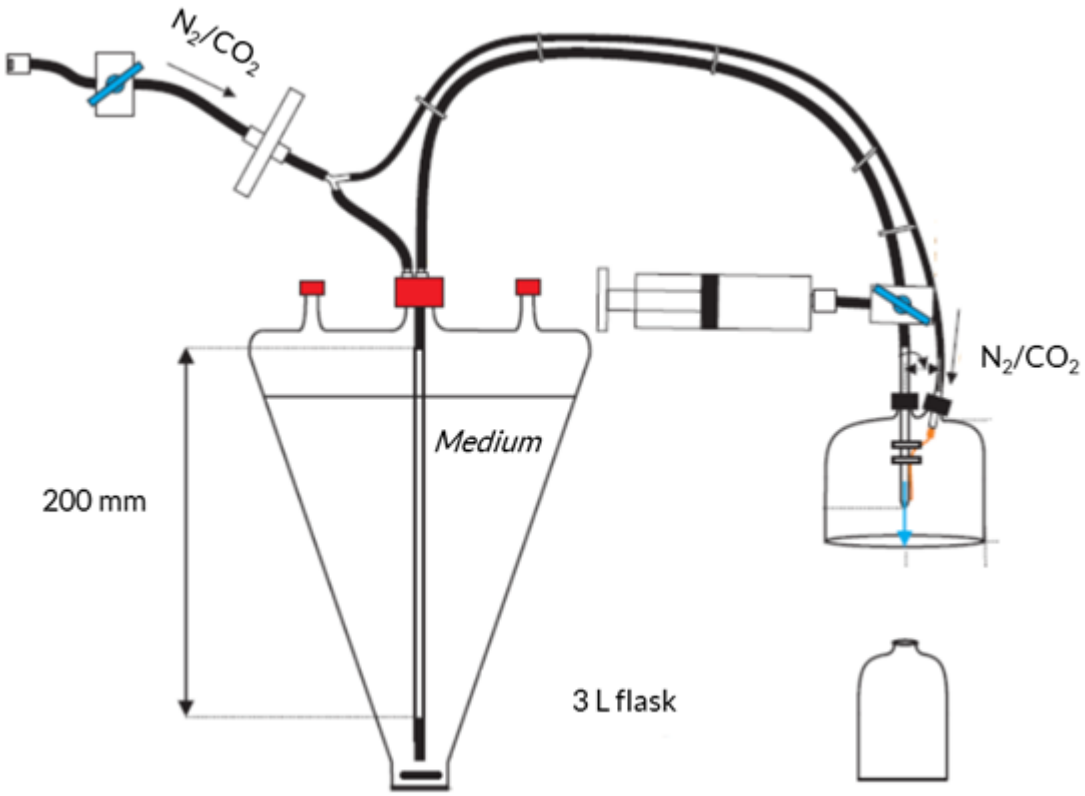

Figure 24: Schematic representation of the degassing and distribution system using Widdel flask for ASW preparation (adapted from (Le Guellec, 2019))

Then, bicarbonate solution (2 mM final) and 0.75 mL of 1 M Na_2S (1.2 mM final) were added in a sterile manner, and pH was adjusted to 6.5-6.7 with sterile 1 M HCl. It was then distributed in anaerobic glass flasks under gas flux, topped with butyl stoppers, flushed for 2 min with N_2/CO_2 (80/20), pressurized at 1.2 bar and stored at 4° C. Prior to be used, sterile yeast extracts or other substrates solutions could be added, according to the experiments.

1.2.3. Anoxic Low-Salt *medium* preparation

The *medium* used for the low salt tests described in CHAPTER I followed the same preparation method at the ASW *medium*, but using only 1.5 g/L NaCl.

1.2.4. Colloidal sulfur

Cultures in the presence of sulfur were performed with the addition of elementary sulfur in a colloidal form. To such extent, a 10 % S° solution was prepared by adding 20 g of sulfur powder, colloidal (Sigma Aldrich 13825-1KG-R) to 220 mL of ultra-pure water. It was then centrifuged for 5 min at 4 °C at 2 000 x*g*, and the supernatant was discarded. The sulfur

paste was washed as such enough times for the supernatant to be clear (about 6 times), then the last pellet was dried at room temperature (about 30 min), and the remaining powder was weighted in order to calculate the volume of water to add to reach a concentration of 10 % (w/v). Long-term storing was done at -20 °C, and each aliquot was kept at 4 °C between the experiments. Note that for lower sulfur concentrations tested (0.08 g/L and 0.16 g/L), the sulfur solution was prior diluted ten times to allow more precise volume transfers.

1.2.5. Colloidal chitin

For tests on chitin, colloidal chitin was prepared from chitin flakes (Sigma). 20 g of chitin flakes were milled, then 200 mL of 12 N HCl (*i.e.* 37 %) were slowly added, and incubated while agitating for 1 h at room temperature under a chemical hood. 4 L of deionized water was then added, and the whole volume was centrifuged at 4 °C for 15 min at 10 000 x*g*. The pellets were resuspended in deionized water, and several washes were realized until the pH reached more than 5. The mix was then neutralized with 5 N KOH, and re-centrifuged for washing and salt removal (2 L of deionized water used). The pellet was finally resuspended in 200 mL of deionized water to obtain a 10 % solution (w/v). It was then autoclaved 20 min at 121 °C and stored at 4 °C.

1.2.6. Gas mixing

Gas mixes were produced with a custom AirLiquide central with a MixLab 4 mixer, using mass flows for a 0.1 % precision on the mixes. Gas mixes could be used to flush sample flasks to replace their initial gas phases.

1.3. Cell density estimation

1.3.1. Optical counting

Cell densities of the suspensions were mainly estimated by counting on a Thoma counting chamber (0.01 mm depth, 0.0025 mm² surface) (Weber, England) at x100 magnification (Olympus BX40). If no direct counting was possible due to experimental constraints, samples were fixated by mixing 50 µL of glutaraldehyde (2.5 % final) with 450 µL of cell suspension and stored at 4 °C for an observation within one week.

Recognizing *Thermococcales* cells from *medium* artefacts can be quite tedious, particularly due to their small size. In order to get used to differentiate them, samples (5 µL) were marked with SYBR Green I (Molecular Probes Inc.) (5 µL of 10X solution) and immediately observed under UV light (Olympus BX60, WIB filter).

1.3.2. Flow cytometry

In addition to optical cell counting by Thoma cell, many samples were also checked by flow cytometry. Those experiments were realized by Erwann Vince, with the help of Stéphane L'Haridon, on a Partec FR-AIB with a blue laser.

Samples were prepared by mixing 500 µL of fresh cell suspension with glutaraldehyde (2.5 % final) and stored at -80 °C until analysis. For analysis, A SYBR Green solution was prepared by diluting 5 µL of SYBR Green 10 000 X (Invitrogen S7563) in 50 mL ultra-pure water with 9 g/L NaCl, vortexed for 30 s and kept out of light and at 4 °C if not used immediately. Cell samples were thawed on iced then serial diluted (100 µL sample in 900 µL ultra-pure water with 9 g/L NaCl) at 1/10, 1/100, and 1/1 000. The 1/100 or 1/1 000 dilutions were used to set up the photomultiplier tubes (PMT) on side scatter and forward scatter parameter. Flux speed was adjusted to discriminate cells (from 15 µL/s to 5 µL/s), in order to obtain between 500 and 3 000 event/s. Fluorescence signal was adjusted on the same principle. Ultra-pure water was used as a sheathe fluid.

2. Metabolite measurements

2.1. Following the metabolite production over time

Note that in such experiments, each flask was sacrificed for each point of measurement, in order not to change the volume of culture, which could influence the physiology regarding H_2 saturation.

2.2. H_2S assays

To measure H_2S productions, a colorimetric method (Cline assay) was adapted, based on methylene blue formation by DMPD (N,N-dimethyl-1,4-phenylenediamine) and sulfide, in

the presence of Fe(III) and acidic environment (Engel et al., 2018; Field and Oldach, 1946; Fonselius et al., 2007).

For each sample, 1.75 mL of suspension was mixed with 250 µL of 10 % (m/v) ZnAc solution and was vortexed for 5 s. 1 mL of a DMPD complex solution (20 g of DMPD and 30 g $FeCl_3$ dissolved in 1 L HCl 6 N) was then added, immediately vortexed for 5 s and precisely incubated for 50 min at room temperature. After incubation, ultra-pure water was added to reach 10 mL. It was immediately vortexed for 5 s and incubated at room temperature for precisely 5 min. 400 µL of the solution where then diluted into 10 mL of ultra-pure water, and absorbance at 670 nm was read. A 5-points calibration curve was performed using the same batches of solutions, and with Na_2S solutions, allowing a precise detection range from about 100 to 4 250 µM H_2S in the original sample (R^2 = 0.9988). Gas phases were also tested, but did not lead to detection except in highly sulfidogenic conditions (3 g/L sulfur cultures), so the gaseous part was not considered in the analyses, particularly to calculate cell-specific productions.

2.3. Gas chromatography

Gaseous H_2, N_2 and CO_2 concentrations were determined by gas chromatography using a MTI M200 micro-chromatograph (SRA Instruments, Marcy l'Etoile, France), which was equipped with two ways: a MS-5A molecular sieve and a Poraplot U column, heated at respectively 80 °C and 100 °C; and with a thermal conductivity sensor. Vector gases were helium and argon. Similar configurations were also used on a MTI R3000 machine, and on a Fusion µGC (Inficon), equipped with a Chembox (Chemlys). A pressure sensor and a thermometer allowed to determine, by application of the ideal gas law, molar concentrations of the sensed gases. Calibrations were performed using mixes of H_2, CO_2 and/or N_2. Concentrations of 0.1 %, 0.5 %, 1 %, 3 %, 5 %, 10 %, 15 %, 20 %, 30 %, 50 % and 80 % of H_2 were used, allowing to set standard curves with correlation coefficients superiors than 0.999 when considering different ranges of 4 points to treat the results. N_2 and CO_2 were each calibrated with at least 3 different points. For smaller detections, columns were flushed several times with N_2 prior to sample analysis. All sample measures were realized with a flask headspace gas pressure between the atmospheric pressure and 2 bar, at 85°C, with a 160 s

acquisition. Note that H_2S peaks could also be detected, but the correspondence to concentrations could not be calibrated. For cell-specific productions of H_2, calculations were based on the consideration that the soluble part was negligible, hence only on the gas volume.

2.4. Ionic chromatography

Soluble anion concentrations were measured thanks to a Dionex ICS-2000 Reagent-Free Ion Chromatography system (Dionex Camberley, UK) with a AS50 autosampler (Thermo Fisher Scientific, Waltham, MA, USA) as described by Roussel *et al.* (Roussel et al., 2015). Separation was performed on two AS15 columns at 30 °C and species determination was done using an Anion Self-Regenerating Suppressor (ASRS 300 4 mm) and a DS6 heated conductivity cell at 35 °C. The system was calibrated to measure fluoride, acetate, lactate, formate, 3-hydroxybutyrate, propionate, acrylate, pyruvate, chloride and nitrite, by Erwan Roussel. 1 mL of cell suspension was centrifuged for 15 min at 12 000 x*g* at room temperature, and 100 µL of the supernatant was diluted with 900 µL of ultra-pure water, then stored at -20 °C until analysis in a chromocol flask in borosilicated glass (Thermofisher). In order to prevent organic matter contamination, the flasks were heated for 6 h at 450 °C in a pyrolysis oven, and all stoppers were rinsed with ultra-pure water and autoclaved 20 min 121 °C. During sampling, nitrile gloves were worn, and filtered tips were used for transfers, which were realized under laminar flux hood. For cell-specific productions, only this soluble fraction was considered.

3. Molecular biology

3.1. Total RNA extractions

For these experiments, all surfaces were frequently cleaned with RNAseZap™ (Invitrogen), nitrile gloves were worn at all time and frequently changed, and manipulations were performed under a chemical hood, on ice and in 4 °C-cooled centrifuges (except if stated differently). Cell suspensions in mid exponential phase (or other phase if precised), with a volume sufficient to harvest 1.5 $.10^9$ cells, were placed on ice directly when taken out

from the incubator. All the necessary volume was pelleted in 50 mL RNAse free Falcon tubes (Corning), for 6 min at 7 700 x*g*. Supernatant was then discarded, and the pellet was resuspended in 1 mL TRIzol reagent (Invitrogen), then transferred in a 2 mL RNAse-free tube (Biopur Eppendorf). It could be stored at -80 °C for later extraction, or pursued directly with the "TRIzol™ reagent experimental protocol". 200 µL of chloroform (Sigma) was added, then the mix was vigorously agitated for 10 s, and let to decant for 3 min at room temperature. It was then centrifuged for 15 min at 15 000 x*g*, 4 °C. The aqueous phase was then mixed with 500 µL of isopropanol and incubated for 5 min at room temperature. It was then centrifuged for 15 min at 15 000 x*g* and the pellet was washed twice with 70 % ethanol (prepared with RNAse-free water (PCR water ultra clean, Ozyme)). The last supernatant was discarded and the pellet was dried for 5 min at room temperature, before its resuspension in 54 µL of RNAse-free water. It was then treated by DNAse, by adding 6 µL of 10X Turbo DNAse buffer (Ambion) and 1 µL of Turbo DNAse (Ambion), and incubated for 30 min at 37 °C. The reaction was then stopped by adding 5 µL of DNAse inactivation reagent (Ambion) and incubating at room temperature for 5 min. It was then centrifuged at 10 000 x*g* for 2 min, and the RNA supernatant was transferred in a new 1.5 mL RNAse-free tube (Biopur Eppendorf), and stored at -80 °C for later analysis.

3.2. Total DNA extractions

TE-Na-1X buffer (TRIS-HCl, EDTA) was prepared by mixing 50 mL of Tris-HCl 1 M, 10 mL NaCl 5 M, 50 mL EDTA 0.5 M, pH 8, with 390 mL of ultra-pure water.

Fully grown cells were pelleted for 5 min at 7 700 x*g*, 4 °C. The pellet was resuspended in 1 mL of TE-Na-1X buffer, then 100 µL of 10 % sarkosyl, 100 µL of 10 % SDS and 50 mL of 20 mg/mL (initial) K proteinase were added and gently mixed. It was incubated at 55 °C for 1 h, with slow agitation. Then 20 µL of A RNase (50 µg/mL initial) (Promega) was added, before 30 min incubation at 37 °C. The DNA extraction was performed by adding 1 mL of PCI solution (phenol/chloroform/isoamyl alcohol 25/24/1, Sigma-Aldrich). After a gentle agitation of 45 s, it was centrifuged for 15 min at 20 000 x*g*, 4 °C. The aqueous top phase was recuperated, to which 40 µL of sodium acetate 3 M, pH 5.2 was added. 0.7 volumes of -20 °C isopropanol were added, and samples were kept at -20 °C for at least 1 h. DNA was then pelleted by

centrifuging at 20 000 x*g* for 5 min at 4 °C. Pellets were dried and then resuspended in 100 to 200 µL of sterile ultra-pure water. DNA samples were stored at 4° C.

3.3. Verification of RNA and DNA quality and quantity

Qualities and concentrations of nucleic acids were checked using a Qubit fluorometer (Invitrogen). For RNA, concentrations were evaluated using the Qubit RNA HS Assay kit (Molecular Probes, Life Technology). For DNA, we used the Qubit dsDNA HS Assay Kit (Molecular Probes, Life Technology). Those parameters could also be checked using a Nanodrop spectrophotometer (Thermo Scientific).

For more complete evaluations, which were for example necessary to send samples to sequencing, RNA qualities were checked on chips using the Agilent High Sensitivity RNA 6000 Nano kit, analyzed on the Bioanalyzer Agilent system.

3.4. RT-qPCR

Reverse transcriptions of extracted RNAs were performed thanks to the qScript Flex cDNA synthesis kit (QuantaBio), in order to obtain complementary DNA (cDNA) concentrations of about 2 ng/µL. Quantitative PCR on those cDNAs were realized thanks to the PerfeCTa SYBR Green SuperMix Rox kit (QuantaBio), with 100 nM of each primer (reverse and forward) according to the gene targeted (see primer sets description in chapter III). The volumes of qPCR mixes for each samples were described in TABLE 4.

Table 4: Mixes for quantitative PCR

Component (initial concentration)	Volume (µL)
ROX mix	25
Nuclease-free water	14
Primer (reverse and forward) (10 µM)	0.5 each
cDNA (2 ng/µL)	10

Reactions were performed on a Step-One Plus instrument (Applied Biosystems), with the program described in TABLE 5.

Table 5: Time/temperature program of the quantitative PCR

Step	Temperature (°C)	Time
Holding stage	95	10 min
Cycling stage (40 cycles)	95	15 s
	60	1 min
Melt curve stage	95	15 s
	60	1 min
	95	15 s

Raw data were treated thanks to StepOne Software v2.2.2 (Life Technologies). Results with multi-peaked melt curves, or with cycle thresholds too important (typically cycle threshold (Ct) > 32) were removed. The analysis was performed thanks to the $\Delta\Delta Ct$ method, to give fold changes of expressions relatively to control targets (Livak and Schmittgen, 2001). For such calculations, variations in cycle thresholds (ΔCt) were determined as the difference between the Ct of each target gene for the mutant and for the wild type in the same conditions. As the quantitation was relative, $\Delta\Delta Ct$ were calculated as the differences between ΔCt for a target gene and ΔCt for the internal reference (30S ribosomal subunit encoding gene). Then, fold change in expression was calculated as follows:

$$Relative\ expression\ (fold\ change) = 2^{-\Delta\Delta Ct}$$

$$\Delta\Delta Ct = \Delta Ct_{target\ in\ mutant} - \Delta\, Ct_{target\ in\ wild\ type}$$

$$\Delta Ct = Ct_{target\ gene} - Ct_{30S}$$

Matériels & Méthodes – Général
French version

Les matériels et méthodes utilisés dans au cours de projet sont décrits de façon spécifique pour chacun des chapitres de ce manuscrit. Les protocoles généraux à l'étude sont détaillés dans cette section.

1. Culture

Si aucune précision n'indique de différence de traitement, les cultures sont réalisées à partir de pré-cultures (issues de cryotubes) repiquées à la fin de leur phase exponentielle de croissance. Les pré-cultures sont inoculées avec 0,05 g/L de S° colloïdal pour que la quantité maximale de soufre issue repiquage négligeable ; ainsi les potentiels biais lors des tests en conditions de culture sans soufre sont réduits. Pour stimuler leur croissance, les pré-cultures peuvent être incubées en conditions de désaturation en H_2 (*e.g.* avec de plus larges phases gazeuses : 20 mL de milieu de culture dans une bouteille d'une contenance de 1 L remplie de N_2).

Les cultures sont généralement réalisées en fioles de verre de 50 mL contenant 20 mL de milieu de culture et en conditions d'anaérobie. Les fioles sont fermées hermétiquement à l'aide bouchons butyl 20 mm (Dutscher) et scellées par des capsules d'aluminium 20 mm (VWR) pour résister aux surpressions. Lorsque la saturation en H_2 est un paramètre à prendre en considération (ce qui n'est pas le cas pour les pré-cultures par exemple), les fioles sont incubées à l'envers pour éviter les fuites de gaz et des bouchons neufs sont utilisés pour chaque expérience. Les volumes de cultures peuvent être ajustés en fonction des besoins de l'expérience. Pour de plus gros volumes, des bouteilles Schott (Duran) fermées hermétiquement à l'aide de bouchons Viton sont utilisées. Chaque élément est lavé à l'eau déionisée puis autoclavé ou placé au four Pasteur à 210 °C sur la nuit avant utilisation.

Lorsque le nom de souche n'est pas précisé, la souche de référence de l'espèce considérée est utilisée.

1.1. Culture anaérobie

La phase liquide du milieu de culture est réduite avec du Na_2S (à une concentration finale de 0,05 %). La phase gazeuse est remplacée par du N_2 (Alphagaz 1, Airliquide) ou un

mélange N_2/CO_2 80/20 (Aligal 12, Airliquide) à l'aide d'une rampe à gaz directement dirigée alternativement vers une bouteille de gaz ou une pompe à vide. Les étapes de pompage et d'injection des gaz sont réalisées 8 fois afin de complétement remplacer l'air dans les fioles surmontées d'un bouchon butyl. Des mélanges de gaz ont permis de flusher les fioles sur une période de 3 min pour les expériences d'évolution adaptatives en laboratoire (voir chapitre IV). Les fioles sont pressurisées à 1,2 bar (en absolu) à température ambiante avec leur phase gazeuse finale.

1.2. Milieux et substrats

Toutes les poudres utilisées lors des tests de substrats et dans la préparation des milieux de culture proviennent de la compagnie Sigma, à l'exception des extraits de levures Bacto (BD). Pour les tests de substrats, les poudres ont été diluées dans de l'eau déionisée pour obtenir une solution à concentration finale de 10 X, en fonction de la concentration attendue pour chaque test. Les solutions ont été autoclavées individuellement avant ajout au milieu de culture à une concentration 1,1 X pour compenser la dilution (généralement 18 mL de milieu à 1,1 X + 2 mL de la solution du substrat considéré à 10 X dans des fioles de 50 mL en conditions anaérobies). Si aucun substrat n'est ajouté à la composition classique des milieux décrits par la suite, ceux-ci sont alors préparés à une concentration 1 X.

1.2.1. TRM (*Thermococcales* Rich *Medium* – milieu riche pour *Thermococcales*)

Le mélange suivant a été réalisé pour 1 L d'eau déionisée : 23 g NaCl, 5 g $MgCl_2 \cdot 6H_2O$, 1 g d'extraits de levures, 4 g tryptone, 3.46 g PIPES sel disodium, 0.7 g KCl, 0.5 g $(NH_4)_2SO_4$, 0.05 g NaBr, 0.01 g $SrCl_2 \cdot 6H_2O$, et 1 mg de résazurine. Le pH a été ajusté à 6.8 avec du HCl 3 N puis la solution a été autoclavée 20 min à 121 °C avant ajout des solutions stériles suivantes : 1 mL KH_2PO_4 5 %, 1 mL K_2HPO_4 5 %, 1 mL $CaCl_2 \cdot 2H_2O$ 2 %, 1 mL Na_2WO_4 10 mM, 1 mL $FeCl_3$ 25 mM. L'utilisation de ce milieu de culture est réalisée en conditions anaérobies comme décrit dans plus haut.

1.2.2. ASW (Anoxic Artificial Sea Water *medium* – milieu d'eau de mer anoxique artificielle)

Le milieu d'eau de mer artificielle (ASW) a été utilisé pour les tests pratiques décrits dans le chapitre I.

En amont de la préparation du milieu, les solutions suivantes ont été préparées et autoclavées 20 min à 121 °C puis stockées à l'abri de la lumière à température ambiante : KBr (0.84 M), H_3BO_3 (0.4 M), $SrCl_2$ (0.15 M), NH_4Cl (0.4 M), KH_2PO_4 (0.04 M), NaF (0.07 M). Une solution de sélénate a été réalisée en mélangeant 0.4 g de NaOH, 6 mg de $Na_2SeO_3 \cdot 5H_2O$, et 8 mg de $Na_2WO_4 \cdot 2H_2O$ dans 1 L d'eau désionisée (Q.S.P.), puis la solution a été filtrée (0,22 µm (Millex Millipore, Dutscher)) et stockée à 4 °C. Une solution d'éléments traces a également été préparée en mélangeant 10 mL d'HCl 25 %, 1 500 mg de $FeCl_2 \cdot 4H_2O$, 190 mg de $CoCl_2 \cdot 6H_2O$, 100 mg de $MnCl_2 \cdot 4H_2O$, 70 mg de $ZnCl_2$, 36 mg de $Na_2MoO_4 \cdot 2H_2O$, 24 mg de $NiCl_2 \cdot 6H_2O$, 6 mg de H_3BO_3, 2 mg de $CuCl_2 \cdot 2H_2O$, dans 1 L d'eau déionisée (QSP), puis la solution a été filtrée (0,22 µm (Millex Millipore, Dutscher)) et stockée à 4 °C. Une solution de vitamines de Balch's (Balch et al., 1979) a été préparée en mélangeant 25 mg d'acide p-aminobenzoique, 10 mg d'acide folique, 10 mg de biotine (vit. B8), 25 mg d'acide nicotinique, 25 mg de calcium pantothénate (vit. B5), 25 mg de riboflavine, 25 mg de thiamine HCl, 50 mg de pyridoxine HCl (vit. B6), 5 mg de cyanocobalamine (vit. B12), et 25 mg d'acide lipoique (acide thioctique) dans 1 L d'eau déionisée (QSP), puis la solution a été filtrée (0,22 µm (Millex Millipore, Dutscher)) et stockée à 4 °C. Une solution à 1 M de FeCl2 a été réalisée en ajoutant 19,8 g de $FeCl_2 \cdot 4H_2O$ à 100 mL (QSP) d'une solution de HCl à 1 M préalablement préparée avec de l'eau déionisée qui a bullée pendant 30 min à l'aide de N_2. La solution a ensuite été autoclavée (20 min à 121 °C) et stockée à température ambiante. Une solution de Na_2S a été réalisée avec de l'eau déionisée bullée à l'aide de N_2 et de de cristaux de $Na_2S \cdot 9H_2O$ préalablement rincés (12 g pour 100 mL), sous un flux constant de N_2, puis la solution a été autoclavée à 109 °C pendant 30 min. Finalement, une solution de 60 mL de bicarbonate a été préparée en mélangeant 0,503 g de $NaHCO_3$ et de l'eau déionisée dans une fiole flushée avec un mélange de N_2/CO_2 (80/20), puis la solution a été autoclavée 60 min à 121 °C.

Le milieu de culture est préparé avec de l'eau déionisée dans une fiole de 3 L suivant un protocole modifié de Widdel et Sass (Parkes et al., 2010; Widdel and Bak, 1992). La base

minérale contient (en g/L) : NaCl (27,2), $MgCl_2.6H_2O$ (10), $CaCl_2.H_2O$ (1,5), KCl (0,66), KBr (0,1), H_3BO_3 (0,025), $SrCl_2.6H_2O$ (0,04), NH_4Cl (0,021), KH_2PO_4 (0,0054), NaF (0,003), 0,625 mL de solution d'éléments traces, et 0,125 mL de solution de SeW. Après autoclavage de la base minérale (30 min à 121 °C), la base est flushée pendant 30 min à l'aide de N_2/CO_2 (80/20) tout en refroidissant (FIGURE 24).

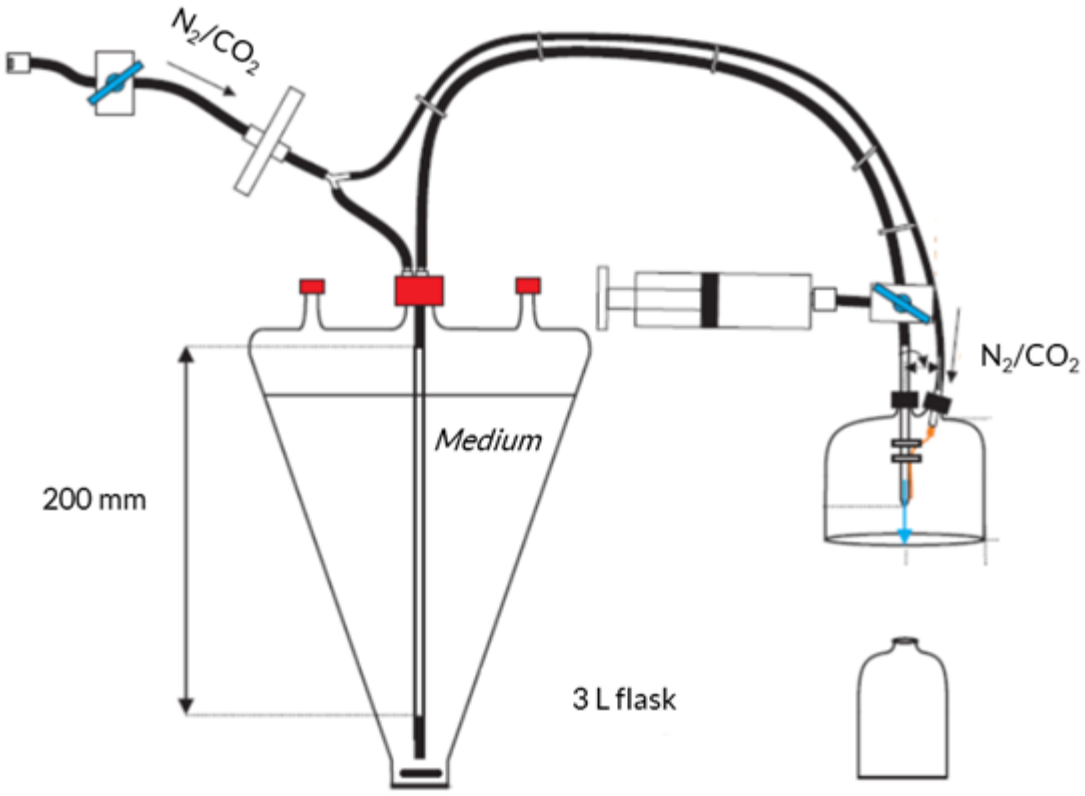

Figure 25: Représentation schématique du système de dégazage et de distribution utilisant une fiole de Widdel pour la préparation du milieu ASW (adapté de (Le Guellec, 2019))

Enfin, une solution de bicarbonate (2 mM en concentration finale) et 0.75 mL de Na_2S 1 M (1,2 mM en concentration finale) sont ajoutés stérilement. Le pH est ajusté à 6,5-6,7 avec de l'HCl 1 M stérile. Le milieu est ensuite distribué en fioles en verre anaérobies sous un flux de gaz, fermées à l'aide de bouchon butyl et flushée pendant 2 min avec du N_2/CO_2 (80/20). Les fioles sont pressurisées à 1,2 bar et stockées à 4 °C. Avant utilisation, de l'extrait de levures stérile ou d'autres substrats peuvent être ajoutés dépendamment de l'expérience.

1.2.3. Milieu anoxique à faible concentration en sels

Le milieu utilisé pour les tests de faibles concentrations en sels décrits dans le chapitre I suit la même méthode de préparation que le milieu ASW, mais ne contient qu'1,5 g/L de NaCl.

1.2.4. Soufre colloïdal

Les cultures en présence de soufre ont été réalisées avec ajout de soufre élémentaire sous forme colloïdale. Pour cela, une solution de S° à 10 % a été préparée en ajoutant 20 g de soufre en poudre, colloïdal (Sigma Aldrich 13825-1KG-R) à 220 mL d'eau ultra-pure. La solution est ensuite centrifugée pendant 5 min à 4 °C à 2 000 *xg*, et le surnageant a été vidé. La pâte de soufre a été lavée jusqu'à ce que le surnageant soit limpide (généralement 6 fois), puis le culot final a été séché à température ambiante (environ 30 min). La poudre restante a été pesée pour permettre de calculer le volume d'eau à aouter pour atteindre une concentration de 10 % (w/v). Le stockage à long terme s'est fait à -20 °C tandis que chaque aliquot est gardé à 4 °C entre chaque utilisation. Il est à noter que pour les concentrations de soufre testées les plus basses (0,08 g/L et 0,16 g/L), la solution de soufre a été préalablement diluée 10 fois pour permettre une meilleure précision pour les transferts de volume.

1.2.5. Chitine colloïdale

Pour les tests sur chitine, de la chitine colloïdale a été préparée à partir de flocons de chitine (Sigma). 20 g de flocons de chitine ont été moulus, puis 200 mL d'HCl 12 N (*i.e.* 37 %) ont été ajoutés lentement avant incubation de la solution sous agitation pendant 1 h à température ambiante sous hôte chimique. 4 L d'eau déionisée ont ensuite été ajoutés et le tout a été centrifugé à 4 °C pendant 15 min à 10 000 x*g*. Les culots ont été repris dans de l'eau déionisée et plusieurs lavages ont été réalisés jusqu'à ce que le pH soit supérieur à 5. Le mélange a ensuite été neutralisé avec du KOH 5 N et centrifugé de nouveau pour laver et se débarrasser des sels (2 L d'eau déionisé). Le culot a finalement été repris dans 200 mL d'eau déionisée pour obtenir une solution à 10 % (w/v). La solution a été autoclavée et stockée à 4 °C.

1.2.6. Les mélanges de gaz

Les mélanges de gaz ont été réalisés à l'aide d'une centrale AirLiquide à façon avec un mélangeur MixLab 4 à régulateur de débit massique pour une précision de 0,1 % sur les

mélanges. Des mélanges de gaz peuvent être utilisés pour flusher les fioles d'échantillonnage afin de remplacer leurs phases gazeuses initiales.

1.3. Estimation de la densité cellulaire

1.3.1. Comptages au microscope optique

Les densités cellulaires des suspensions ont été principalement estimées par comptage sur cellule de Thoma (0,1 mm de profondeur, 0,0025 mm² de surface) (Weber, Angleterre) à un grossissement x100 (Olympus BX40). Si le comptage n'était pas réalisable au moment de l'échantillonnage du fait de contraintes expérimentales, les échantillons ont alors été fixés en mélangeant 50 µL de glutaraldéhyde (2,5% en concentration finale) avec 450 µL de suspension cellulaire. Les échantillons ont ensuite été stockés à 4 °C pour une observation dans la semaine.

Différencier les cellules de Thermococcales des artefacts du milieu peut se révéler parfois difficile, en particulier du fait de leur petite taille. Des observations sous lampe à UV (Olympus BX60, WIB filter) à l'aide d'un marquage au SYBR Green I (Molecular Probes Inc.) (5 µL d'une solution à 10 X) ont permis d'établir une différenciation précise entre cellules et artefact.

1.3.2. Cytométrie en flux

Pour compléter les comptages en cellule de Thoma, plusieurs échantillons ont été analysés en cytométrie en flux. Ces expériences ont été réalisées par Erwann Vince, avec l'aide de Stéphane L'Haridon, sur un cytomètre Partec FR-AIB muni d'un laser bleu.

Les échantillons ont été préparés en mélangeant 500 µL d'une suspension cellulaire fraiche avec du glutaraldéhyde (à 2,5 % en concentration finale) puis ils ont été stockés à -80 °C jusqu'à analyse. Le marquage lors de l'analyse se fait à l'aide d'une solution de SYBR Green composée de 5 µL de SYBR Green 10 000 X (Invitrogen S7563) dilué dans 50 mL d'eau ultra-pure contenant 9 g/L de NaCl. Cette solution, après agitation au vortex pendant 30 s, est conservée à l'abri de la lumière et, si non utilisée immédiatement, à 4 °C. Les échantillons cellulaires, conservés à -80 °C, sont décongelés lentement sur glace, puis dilués en série (100

µL d'échantillon dans 900 µL d'eau ultra-pure contenant 9 g/L de NaCl) à 1/10, 1/100, et 1/1000. Les dilutions 1/100 et 1/1000 ont été utilisées pour configurer les tubes photomultiplicateurs (PMT) sur les paramètres de diffusion latérale et de diffusion directe. La vitesse de flux a été ajusté pour différencier les cellules (de 15 µL/s à 5 µL/s) afin d'obtenir entre 500 et 3 000 événements/s. La florescence du signal a été ajustée de la même manière. De l'eau ultra-pure a servie de liquide de gaine.

2. Mesures de métabolites

2.1. Suivi de la production de métabolites au cours du temps

Il est à noter que pour ces expériences, chaque fiole est sacrifiée pour chaque temps d'acquisition des mesures afin de ne pas modifier le volume de culture, ce qui pourrait influencer la physiologie des cellules considérant la saturation en H_2.

2.2. Tests H_2S

Afin de mesurer la production d'H_2S, une méthode colorimétrique (test de Cline) a été adaptée. Cette méthode est basée sur la formation de bleu de méthylène par le DMPD (N,N-dimethyl-1,4-phenylenediamine) et de sulfides en présence de Fe(III) dans un environnement acide (Engel et al., 2018; Field and Oldach, 1946; Fonselius et al., 2007).

Pour chaque échantillon, 1,75 mL de suspension cellulaire est mélangée à 250 µL de solution de ZnAc à 10 % puis agité au vortex pendant 5 s. 1 mL de solution de complexe DMPD (20 g de DMPD et 30 g de $FeCl_3$ dissous dans 1 L de HCl 6 N) est ensuite ajoutée à la préparation qui est immédiatement agitée au vortex pendant 5 s, puis incubée précisément pendant 50 min à température ambiante. Après incubation, de l'eau ultra-pure est ajoutée afin d'atteindre un volume de 10 mL. La préparation est immédiatement agitée au vortex pendant 5 s et incubée à température ambiante pendant exactement 5 min. 400 µL de la préparation est alors diluée dans 10 mL d'eau ultra-pure et une lecture de l'absorbance à 670 nm est effectuée. Une courbe de calibration à 5 points a été réalisée en utilisant les mêmes solutions et avec des solutions de Na_2S permettant une gamme de détection précise de 100 à 4 250 µM d'H_2S dans l'échantillon de base (R^2 = 0,9988). Les phases gazeuses ont aussi été

testées, mais n'ont pas permis de détection sauf dans des conditions hautement sulfidogéniques (3 g/L de soufre colloïdal dans les cultures). Ainsi, les phases gazeuses ne sont pas prises en considération dans les analyses, en particulier pour calculer les productions spécifiques par cellules.

2.3. Chromatographie en phase gazeuse

Les concentrations en H_2, N_2 et CO_2 gazeux ont été déterminées par chromatographie en phase gazeuse à l'aide d'un micro-chromatographe MTI 200 (SRA Instruments, Marcy l'Etoile, France) équipé de deux voies : avec un tamis moléculaire MS-5A et une colonne Poraplot U, chauffés respectivement à 80 ° C et 100 ° C ; avec un capteur de conductivité thermique. L'hélium et l'argon ont été utilisés comme gaz vecteurs. Des configurations similaires ont également été utilisées sur une machine MTI R3000 et sur un Fusion µGC (Inficon), équipé d'un Chembox (Chemlys). Un capteur de pression et un thermomètre ont permis de déterminer, par application de la loi des gaz parfaits, les concentrations molaires des gaz détectés. Les étalonnages ont été effectués en utilisant des mélanges de H_2, CO_2 et / ou N_2. Des concentrations de 0,1 %, 0,5 %, 1 %, 3 %, 5 %, 10 %, 15 %, 20 %, 30 %, 50 % et 80 % de H_2 ont été utilisées, permettant de définir des courbes standard avec des coefficients de corrélation supérieurs à 0,999 lorsque l'on considère différentes gammes de 4 points pour traiter les résultats. Le N_2 et le CO_2 ont chacun été calibrés avec au moins 3 points différents. Pour les détections plus petites, les colonnes ont été rincées plusieurs fois avec du N_2 avant l'analyse de l'échantillon. Toutes les mesures d'échantillons ont été réalisées avec une fiole dont la pression interne de la phase gazeuse est entre la pression atmosphérique et 2 bar, à 85 °C, avec une acquisition de 160 s. Il est à noter que des pics d'H_2S pouvaient également être détectés, mais la correspondance avec les concentrations n'a pas pu être calibrée. Pour les productions de H_2 spécifiques par cellules, les calculs ont été réalisés en considérant que la partie soluble était négligeable, donc uniquement sur le volume de gaz.

2.4. Chromatographie ionique

Les concentrations en anions solubles ont été mesurées grâce à un système Dionex ICS-2000 Reagent-Free Ion Chromatography (Dionex Camberley, UK) avec un échantillonneur automatique AS50 (Thermo Fisher Scientific, Waltham, MA, USA) comme décrit par Roussel et

collaborateurs (Roussel et al., 2015). La séparation a été effectuée sur deux colonnes AS15 à 30 °C et la détermination de l'espèce a été effectuée en utilisant un suppresseur d'auto-régénération anionique (ASRS 300 4 mm) et une cellule de conductivité DS6 chauffée à 35 °C. Le système a été calibré pour mesurer le fluorure, l'acétate, le lactate, le formate, le 3-hydroxybutyrate, le propionate, l'acrylate, le pyruvate, le chlorure et le nitrite, par Erwan Roussel. 1 mL de suspension cellulaire a été centrifugé pendant 15 min à 12 000 *xg* à température ambiante, et 100 µL du surnageant ont été dilués avec 900 µL d'eau ultra pure, puis la préparation a été stockée à -20 °C jusqu'à l'analyse dans une fiole chromacol en verre borosilicaté (Thermofisher). Afin d'éviter la contamination par des matières organiques, les fioles ont été chauffées pendant 6 h à 450 ° C dans un four à pyrolyse, et tous les bouchons ont été rincés à l'eau ultra pure et autoclavés 20 min à 121 °C. Pendant l'échantillonnage, des gants en nitrile ont été portés et des cônes filtrés ont été utilisés pour les transferts par pipettes, eux-mêmes été réalisés sous une hotte à flux laminaire. Pour les productions spécifiques par cellules, seule cette fraction soluble a été prise en compte.

3. Biologie moléculaire

3.1. Extractions d'ARN total

Pour ces expériences, toutes les surfaces ont été nettoyées régulièrement avec du RNAseZap™ (Invitrogen), des gants en nitrile, fréquemment changés, ont été portés à chaque étape. Les manipulations ont été effectuées sous une hotte, sur de la glace et dans des centrifugeuses refroidies à 4 °C (sauf indication contraire). Des suspensions cellulaires en en milieu de phase exponentielle (ou autre phase si précisée), avec un volume suffisant pour récolter $1{,}5.10^9$ cellules, ont été placées sur de la glace directement après avoir été retirées de l'incubateur. Le volume nécessaire a été culotté dans des tubes Falcon RNAse-free de 50 mL (Corning), pendant 6 min à 7 700 *xg*. Le surnageant a ensuite été vidé et le culot a été remis en suspension dans 1 mL de réactif TRIzol (Invitrogen), puis transféré dans un tube RNAse-free de 2 ml (Biopur Eppendorf). L'échantillon peut alors être conservé à -80 °C pour une extraction ultérieure, ou être traité directement avec le « protocole expérimental au réactif TRIzol™ ». 200 µL de chloroforme (Sigma) sont alors ajoutés à l'échantillon, puis le mélange a vigoureusement été agité pendant 10 s et laissé à décanter pendant 3 min à

température ambiante. La préparation a ensuite été centrifugée pendant 15 min à 15 000 *xg* et à 4 °C. La phase aqueuse a ensuite été mélangée avec 500 µL d'isopropanol et incubée pendant 5 min à température ambiante. Elle a ensuite été centrifugée pendant 15 min à 15 000 *xg* et le culot a été lavé deux fois avec de l'éthanol à 70 % (préparé avec de l'eau RNAse free : eau PCR ultra propre, Ozyme). Le dernier surnageant a été vidé et le culot a été séché pendant 5 min à température ambiante, avant sa remise en suspension dans 54 µL d'eau RNAase-free. La solution a ensuite été traitée par DNAse, en ajoutant 6 µL de tampon 10X Turbo DNAse (Ambion) et 1 µL de Turbo DNAse (Ambion), et incubée pendant 30 min à 37 °C. La réaction a ensuite été arrêtée en ajoutant 5 µL de réactif d'inactivation de la DNAse (Ambion) et en incubant à température ambiante pendant 5 min. Il a ensuite été centrifugé à 10 000 *xg* pendant 2 min et le surnageant d'ARN a été transféré dans un nouveau tube RNAase free de 1.5 mL (Biopur Eppendorf) et stocké à -80 ° C pour une analyse ultérieure.

3.2. Extraction d'ADN total

Le tampon TE-Na-1X (TRIS-HCl, EDTA) a été préparé en mélangeant 50 mL de Tris-HCl 1 M, 10 mL de NaCl 5 M, 50 mL d'EDTA 0,5 M à pH 8, avec 390 mL d'eau ultra-pure.

Les cellules en fin de croissance ont été culotées pendant 5 min à 7 700 *xg* à 4 ° C. Le culot a été remis en suspension dans 1 mL de tampon TE-Na-1X, puis 100 µL de sarkosyl à 10 %, 100 µL de SDS à 10 % et 50 mL de protéinase K (20 mg/mL initiale) ont été ajoutés. La préparation a été mélangée doucement. Elle a ensuite été incubée à 55 °C pendant 1 h, avec une agitation lente. Ensuite, 20 µL de RNase A (50 µg/mL initiale) (Promega) ont été ajoutés, avant 30 minutes d'incubation à 37 °C. L'extraction d'ADN a été réalisée en ajoutant premièrement 1 mL de solution PCI (phénol / chloroforme / alcool isoamylique 25/24/1, Sigma-Aldrich). Après une agitation douce de 45 s, la préparation a été centrifugée pendant 15 min à 20 000 *xg* à 4 °C. La phase supérieure aqueuse a été récupérée et 40 µL d'acétate de sodium 3 M à pH 5,2 lui ont été ajoutés. 0.7 volumes d'isopropanol préalablement refroidi à -20 °C ont été ajoutés à la préparation qui a ensuite été conservée à -20 °C pendant au moins 1 h. L'ADN a ensuite été culoté par centrifugation à 20 000 *xg* pendant 5 min à 4 °C. Les culots ont été séchés puis remis en suspension dans 100 à 200 µL d'eau ultra pure stérile. Les échantillons d'ADN ont été conservés à 4 °C.

3.3. Vérification de la quantité et de la qualité de l'ARN et de l'ADN

Les concentrations et qualités d'acides nucléiques ont été déterminées à l'aide d'un fluorimètre Qubit (Invitrogen). Pour l'ARN, les concentrations ont été évaluées à l'aide du kit Qubit RNA HS Assay (Molecular Probes, Life Technology). Pour l'ADN, c'est le kit de dosage Qubit dsDNA HS (Molecular Probes, Life Technology) qui a été utilisé. Ces paramètres pourraient également être vérifiés à l'aide d'un spectrophotomètre Nanodrop (Thermo Scientific). Pour des évaluations plus complètes qui sont notamment nécessaires, par exemple, pour l'envoi d'échantillons au séquençage, les qualités d'ARN ont été vérifiées sur puces à l'aide du kit Agilent High Sensitivity RNA 6000 Nano, analysées sur le système Bioanalyzer Agilent.

3.4. RT-qPCR

Les transcriptions inverses des ARN extraits ont été réalisées grâce au kit de synthèse d'ADNc qScript Flex (QuantaBio), afin d'obtenir des concentrations d'ADN complémentaire (ADNc) d'environ 2 ng/µL. La PCR quantitative sur ces ADNc a été réalisée grâce au kit PerfeCTa SYBR Green SuperMix Rox (QuantaBio), avec 100 nM de chaque amorce (sens et antisens) selon le gène ciblé (voir description des couples d'amorces au chapitre III). Les volumes de mélanges qPCR pour chaque échantillon ont été décrits dans la TABLE 6.

Table 6: Mélange réactionnel pour la PCR quantitative

Produits (concentration initiale)	Volume (µL)
ROX mix	25
Eau nuclease-free	14
Amorce (sens et antisens) (10 µM)	0.5 chaque
cDNA (2 ng/µL)	10

Les réactions ont été effectuées sur un instrument Step-One Plus (Applied Biosystems), avec le programme décrit dans le TABLE 7.

Table 7: Programme utilisé pour les réactions de PCR quantitative

Etapes	Température (°C)	Temps
Activation – phase native	95	10 min
Amplification (40 cycles)	95	15 s
	60	1 min
Courbe de fusion	95	15 s
	60	1 min
	95	15 s

Les données brutes ont été traitées grâce au logiciel StepOne Software v2.2.2 (Life Technologies). Les résultats avec des courbes de fusion présentant plusieurs pics ou avec des cycles seuils trop importants (généralement un cycle seuil (Ct)> 32) ont été supprimés. L'analyse a été réalisée grâce à la méthode des $\Delta\Delta Ct$, qui permet de détecter des changements d'expressions par rapport à des cibles contrôles (Livak et Schmittgen, 2001). Pour de tels calculs, les variations des cycles seuils (ΔCt) ont été déterminées comme la différence entre les Ct de chaque gène cible pour le mutant et pour le type sauvage dans les mêmes conditions. La quantification étant relative, les $\Delta\Delta Ct$ ont été calculées comme étant la différence entre un gène cible et la référence interne (gène codant pour la sous-unité ribosomale 30S). Ensuite, la différence d'expression a été calculée comme suit :

$$Expression\ relative\ (fold\ change) = 2^{-\Delta\Delta Ct}$$

$$\Delta\Delta Ct = \Delta Ct_{cible\ chez\ le\ mutant} - \Delta\, Ct_{cible\ chez\ la\ souche\ sauvage}$$

$$\Delta Ct = Ct_{gène\ cible} - Ct_{30S}$$

Chapter I: Strain screening and fermentation overview

Abstract

Thermococcales are well-studied hyperthermophilic archaea envisioned for H_2 bio-production applications. However, high pressure bio-production of H_2 has not been considered, even though it may present several possible advantages. *T. barophilus* MP^T is a good candidate for such an application, particularly due to the availability of genetic tools and previous work. The LM2E also has access to more than 300 strains of *Thermococcales via* the UBO culture collection, among which more than 110 have their genome sequenced. We organized a screening based on *in silico* predictions of metabolic pathways (MicroCyc), literature data, and previous phylogenetic analyses, in the hope of finding significantly highly H_2-producing piezophiles, with certain substrate degradation capabilities. This step confirmed the selection of *T. barophilus* MP^T as the model organism of choice; therefore, its global fermentative behavior was further investigated with an applied point of view. We varied several parameters of batch cultures (particularly sulfur, substrate, product concentrations; temperature and pressure) and measured products (H_2, H_2S, CO_2, acetate, formate and cell concentrations), from which we observed several trends. Notably, we found that CO_2 could likely be globally consumed under certain conditions, although those indications undoubtedly need confirmation. Overall, these findings would permit to propose strategies to consider for future industrial applications.

Les Thermococcales *sont des archées hyperthermophiles bien étudiées et envisagées pour des applications de bio-production d'H_2. Cependant, aucune solution à haute pression n'a été considérée, à notre connaissance, bien que ce facteur induirait plusieurs avantages.* T. barophilus *MP^T constitue un bon candidat potentiel pour de tels travaux, particulièrement grâce à la disponibilité d'un outil génétique et la profusion de données de littérature. Le LM2E a aussi accès à plus de 300 souches de* Thermococcales *via la collection de souches de l'UBO (UBOCC), parmi lesquelles 110 ont leurs génomes séquencés. Un criblage a été organisé, basé sur des prédictions in silico de voies métaboliques, sur des données de littérature, et sur résultats préalables d'analyses phylogénétiques, dans l'espoir de trouver des piézophiles montrant des productions naturelles d'H_2 significativement hautes, avec des capacités de dégradations des substrats particulièrement intéressantes. Cette étape a confirmé la sélection de* T. barophilus *MP^T comme modèle biologique de choix ; par conséquent son comportement*

fermentaire global a été étudié plus en profondeur, d'un point de vue appliqué. Plusieurs paramètres de culture en batch ont été variés (particulièrement les concentrations en soufre, substrats et produits, la température, la pression) et certains résultats de ces fermentations ont été mesurés (productions d'H_2, H_2S, CO_2, acétate, formate et densité cellulaires), à partir desquels plusieurs tendances ont été notées. De manière notable, ces résultats ont montré que du CO_2 a probablement été consommé dans certaines conditions, mais davantage de confirmations sont nécessaires. De manière générale, les conclusions de cette étude permettent de proposer des stratégies à considérer pour de futures orientations industrielles.

Introduction

The project HPBioHyd aimed to envision potential practical solutions of molecular hydrogen (H_2) bio-production in *Thermococcales* models at high pressure. Several reported works describe the use of different species, all considered near or at atmospheric pressure (P_{atm}) (*e.g. T. kodakarensis* (Aslam et al., 2017), '*T. onnurineus*' (Bae et al., 2012a; Kim et al., 2020), *T. paralvinellaea* (Hensley et al., 2016), *Pyrococcus furiosus* (Kreuzer et al., 2013)). Each species presented different advantages and drawbacks for practical application, according to various parameters, as for instance their respective metabolic pathways, regulation patterns, temperature and pressure preferences, end-product tolerances, or substrate specificities. Many works have already been reported on what could be regarded as individual optimizations on specific models (*e.g.* (Cario et al., 2015b; Choi et al., 2016; Chou et al., 2007; Santangelo et al., 2011)). In the "*Laboratoire de Microbiologie des Environnements Extrêmes*" – Laboratory of Microbiology of Extreme Environments (LM2E UMR6197), past studies have focused on the physiology of different *Thermococcales* strains, and particularly *T. barophilus* MP^T, *T. barophilus* Ch5, *P. yayanosii*, and *T. kodakarensis* (Le Guellec, 2019; Michoud, 2014; Vannier et al., 2015). Overall, *T. barophilus* MP^T is an interesting candidate for applying high pressure H_2 bio-production: in addition to the extensive knowledge about its physiology and its piezophily, a genetic tools have been developed, rendering possible the manipulation of its genome (Birien et al., 2018; Thiel et al., 2014), leading to the deletion of different clusters of the hydrogenogenic and sulfidogenic pathways. Nonetheless, before exploring the possible direct optimizations of hydrogen production with this model, verifying whether other qualities would be found in other strains could be beneficial. After several years of

oceanographic cruises, more than 300 *Thermococcales* strains were isolated at the LM2E, many of which remain uncharacterized, and are available at the UBOCC (*Université de Bretagne Occidentale* Culture Collection - https://www.univ-brest.fr/ubocc/). These isolates were obtained from different sites, and depths, hence with different physical, chemical, and biological environments, allowing us to speculate on various physiological potentials.

In order to propose one or several organisms for H_2 bio-production, a first step in this project was to determine which *Thermococcales* model organism to choose. The UBOCC was screened to predict if high H_2 productions (*i.e.* H_2 tolerances in the conditions tested), and particular substrate degradation capabilities would emerge from uncharacterized strains. If no others appealing *criteria* were revealed, such strains could still serve as bases for further investigations, envisioning to implement the particular abilities in our model of choice.

Each strain harboring its own physiological features, it was technically infeasible, in the frame of this project, to perform every necessary culture test to find the best H_2 bio-production solution (we could not have tried every strain with every possible substrate at every possible temperature and pressure, for example). Consequently, this first step was performed as a screening for the best model to focus on, based on several *criteria*, stated below. This chapter describes part of the project HPBioHyd that does not precisely explore the fundamental metabolism of *Thermococcales*, but rather strives for proposing applied solutions for the choice of model and culture conditions towards H_2 bio-production. The arrangement of our screening plan was thus based on several pre-selections.

Producing hydrogen at high pressure could present several advantages. Particularly, the need for pressurizing accounts for important costs in the process of H_2 production (Makridis, 2016; Viktorsson et al., 2017). Moreover, proteomic and transcriptomic studies have indicated that the metabolic state of the piezophiles *T. barophilus* MP^T and *T. piezophilus* could tend towards higher H_2 synthesis, due to overexpressed hydrogenases at higher pressures. Pressure of growth, according to each strain's respective piezophily, can thus modulate their metabolism (Dalmasso, 2016; Vannier et al., 2015). A first requirement for our choice of strain was its ability to grow at high pressure. Rather than directly growing every tested strain at different pressures, we screened the isolate collection based on depth of *in situ* sampling to assume this trait.

Tolerance to hydrogen, and thus potential H_2 production yields, can vary from one strain to another. Closed, batch cultures imply that H_2 becomes saturating, making hydrogenogenic metabolism inefficient. Hydrogenase activities towards hydrogen production indeed diminish with increased H_2 partial pressures (P_{H2}), which can impair, in some strains, the membrane ion gradient, and consequently hinder energy conservation *via* ATP synthases (Sapra et al., 2003). A highest H_2 overproducing strain would tend to its own saturating P_{H2}, even when working in a continuously renewed environment, hence the need for selecting a higher tolerance for our chosen solution. Since this trait could not be universally explained by a unique aspect, as it relies on each enzyme's catalytic properties, as well as a complex metabolic system with several alternative electron fluxes, we aimed to approach performances of literature-recognized good H_2 producers by targeting their phylogenetic neighbors, in the hope that the latter could also be highly H_2-tolerant. The availability of genome sequence was therefore a convenience, and it also allowed to screen for particular metabolic potentialities, where homologies for enzymes related to interesting substrate degradations could be encoded. In addition, our bio-production systems would take one of its interests in the use of low-cost substrates. As detailed in the introduction of this manuscript, many *Thermococcales* can degrade abundant biomolecules (*e.g.* chitin), or raw industrial and agricultural waste (TABLE 1, P. 70). We aimed to pre-select strains on their genome-encoded potential degradation capabilities.

This chapter thus describes the results obtained with this first screening, which led to the choice of a model strain to further investigate. Then, the fermentative system had to be characterized, to give practical answers to the question of feasibility of such a project. The corresponding experimental plan was not designed as a matter of unravelling the metabolism of our strain, but rather to give practical insights about different solutions of H_2 bio-production systems. Those insights aimed to serve a possible decision from an industrial point of view towards the orientation of further investigations. The fermentative system can be lumped into a global reaction involving several key parameters, which impact the outcomes. Such products do not only comprise H_2, but also other metabolites that can be valorized or that are, in contrary, not suitable.

The objectives of the work reported by this two-part chapter were thus to advance towards the determination of cost-effective *formulae* for applied *Thermococcales* H_2 bio-production, *via*:

- Determining which strain(s) would be most suitable as candidates for an optimized bio-H_2 production in high pressure / high temperature.
- Providing measured indications about how fermentation could be impacted by several key parameters.

Part I – Screening and choice candidate strain / substrate

Although *T. barophilus* MP^T seemed a suitable choice for pursuing applied H_2 production, we aimed to screen for significant potentialities in the UBOCC *Thermococcales* collection, for H_2 tolerances and substrate degradation capabilities. We first pre-selected which strain to focus on, among the 300 + available, and tested them for H_2 productions. Strains having shown highest H_2 productions were chosen to refine the screen followed by substrate degradation tests. Along those experiments, methodological adjustments were performed, to determine culture parameters and as limitations were faced in assessing cell densities in the presence of poorly soluble substrates. Those steps are thus also described herein, as parts of the study. The obtained data were then used to select a model of choice for further evaluation of the fermentation, which will be described hereafter.

Materials and methods

Descriptions of the general materials and methods used in this work can be read in the dedicated section of this manuscript (MATERIALS & METHODS - GENERAL). Each strain was cultivated in *Thermococcales* Rich *Medium* (TRM), at its temperature of isolation. Although this project emphasized the piezophilic aspect of *Thermococcales*, the screening was performed at atmospheric pressure, as required methods for studying H_2-production at high pressure were not yet functional and necessitated development (see chapter II). The examination of genomes for potential interesting metabolic pathway encoding genes was performed *in silico* with MicroCyc (MicroScope project, Genoscope), a pathway/genome database using the PathoLogic program to compare genome annotations to the metabolic reference database MetaCyc (MicroCyc, 2017).

To assess phylogenetic/genomic proximity, we used a tree built with the concatenation of the 16S rRNA gene and ITS sequences of 305 isolates from the UBOCC, and a phylogenomic tree based on single copies from core genomes (about 600 targets) of 113 *Thermococcales*, both from a previous work by Damien Courtine (Courtine, 2017).

A part of this work was realized with the help of Marie Naitali, a student from the *Institut Universitaire de Technologie* of Saint-Brieuc (France), during her internship at the LM2E.

Results & Discussions

A) Selection of tested strains

To organize a possible screening experiment in limited time, we needed to preselect a set of strains to test for finding substantially interesting options. To such extent, we focused on the *criteria* such as: depth of sampling, phylogenetic proximity with known good H_2 producers (literature), and interesting metabolic potential.

49 complete genome sequences were examined for potentially interesting metabolic pathways, using MicroCyc. It included the genome of *T. barophilus* MP^T and those of 48 *Thermococcales* isolates from the UBOCC obtained during a previous PhD project (Courtine, 2017) (see Appendix, TABLE 27, P. 348). 8 potentially interesting metabolic pathways were examined related to chitin, starch, lactose, melibiose, d-mannose, ethanol and glycerol degradation, and formate oxidation. 44 strains were consequently pre-selected from this analysis based on genomic predictions of metabolic features (see Appendix, TABLE 28, P. 349). From these data, a list of potentially interesting substrates was set, based on potential metabolic pathways indicated by MicroCyc results, and on reported literature degradation in other models (see TABLE 1, P. 70): maltose, cellulose, starch, pectin, keratin, glucose, glycerol, cellobiose, ramnose, chitin, ethanol, formate, and pyruvate.

Overall, in the time-frame of this project, **41 strains among the pre-selected ones were actually tested** during the first phase, emphasizing H_2 tolerances (TABLE 8). As many strains had interesting substrate degradation potentials, we chose to favor phylogenetic proximity to *T. barophilus* MP^T, which is already a model of study at the LM2E: 26 selected strains were close to *T. barophilus* MP^T and 3 strains were close to '*T. onnurineus*'. In addition to uncharacterized isolates, 5 literature-described strains were selected (*T. kodakarensis*, *T. litoralis*, '*T. onnurineus*' and *T. pacificus*, *T. barophilus* MP^T). Note that 4 strains were selected only based on their putative degradation pathways (MicroCyc), and 3 other strains were issued from the LM2E IFREMER strain collection for various interesting features (see details in TABLE 8).

Table 8: List of the 41 strains grown during the first phase of the screening

	UBOCC reference	Name	Interest	Microcyc pathways (number of missing enzymes)	Depth of origin (m)	Reference
1	**2918**	*T. barophilus* MP^T	Literature model	ethanol degradation (1), starch degradation (1 and 1)	3550	(Marteinsson et al., 1999a)
2	**2921**	*T. pacificus*	Literature model	-	Few meters	(Miroshnichenko et al., 1998)
3	**2922**	*T. litoralis*	Literature model (keratin)	-	Few meters	(Bálint et al., 2005; Neuner et al., 1990)
4	**3201**	*'T. onnurineus'*	Literature model	-	1650	(Bae et al., 2006)
5	**3203**	*T. kodakarensis*	Literature model	chitin degradation (1)	Few meters	(Atomi et al., 2004b; Morikawa et al., 1994)
6	**2236**	E2P4	16S/ITS close to *T. barophilus* MP^T	-	2301	
7	**2238**	E2P6	16S/ITS close to *T. barophilus* MP^T	-	2301	
8	**2240**	E2P8	16S/ITS close to *T. barophilus* MP^T	-	2301	
9	**2246**	E2P15	16S/ITS close to *T. barophilus* MP^T	-	2301	
10	**2248**	E4D2	16S/ITS close to *T. barophilus* MP^T	-	2273	
11	**2249**	E4D3	16S/ITS close to *T. barophilus* MP^T	-	2273	
12	**2250**	E4D5	16S/ITS close to *T. barophilus* MP^T	-	2273	
13	**2253**	E4D7	16S/ITS close to *T. barophilus* MP^T	-	2273	
14	**2254**	E4D8	16S/ITS close to *T. barophilus* MP^T	-	2273	
15	**2255**	E4D12	16S/ITS close to *T. barophilus* MP^T	-	2273	
16	**2256**	E4P13	16S/ITS close to *T. barophilus* MP^T	-	2273	
17	**2392**	CIR03a	16S/ITS close to '*T. onnurineus*'	-	-	
18	**2403**	CIR14 a	16S/ITS close to *T. barophilus* MP^T	-	-	
19	**2431**	IRI 17c	16S/ITS close to *T. barophilus* MP^T	-	2338	
20	**2432**	IRI 19c	16S/ITS close to *T. barophilus* MP^T	-	2338	
21	**2433**	IRI 21c	16S/ITS close to *T. barophilus* MP^T	-	2338	
22	**2469**	CIR 02c	16S/ITS close to *T. barophilus* MP^T	-	-	

23	**2488**	KAZA	16S/ITS close to *T. barophilus* MP^T	-	2301	
24	**2572**	GE08	16S/ITS close to *T. barophilus* MP^T	-	2000	
25	**2399**	CIR 10a	Core genome close to *T. barophilus* MP^T	-	-	
26	**2032**	IRI 33c	Core genome close to *T. barophilus* MP^T	-	2274	
27	**2049**	AMTc73	Core genome close to *T. barophilus* MP^T	-	2631	
28	**2206**	AMTc70	Core genome close to *T. barophilus* MP^T	chitin degradation (4), starch degradation (0 and 2)	2631	
29	**3178**	MC4	Core genome close to *T. barophilus* MP^T	-	Few meters	
30	**3182**	MC9	Core genome close to *T. barophilus* MP^T	-	Few meters	
31	**3182**	MC8	Core genome close to *T. barophilus* MP^T	-	Few meters	
32	**2424**	IRI 06 c	Core genome close to '*T. onnurineus*'	-	2274	
33	**IFREMER Strain collection**	MF15	Core genome close to '*T. onnurineus*'	-		(Le Guellec, 2019)
34	**2181**	AMTc 95	Potential pathways	chitin degradation (2), starch degradation (2)	2633	
35	**2211**	AMTc51	Potential pathways	glycerol degradation (1), chitin degradation (2), starch degradation (2)	-	
36	**2350**	E14P19	Potential pathways	glycerol degradation (1), chitin degradation (3), starch degradation (2)	-	
37	**2415**	EXT10 c	Potential pathways	chitin degradation (2), lactose degradation (0), starch degradation (2)	-	
38	**IFREMER Strain collection**	AT1243	Description of substrate degradations (keratin)	-	-	
39	**IFREMER Strain collection**	*T. chitonophagus*	Literature model (chitin degradation)	-	2600	(Huber et al., 1995)
40	**2421**	EXT16 c	Need for other experiment	-	2500	
41	**3296**	*T. piezophilus*	Isolated from the deepest hydrothermal vent	-	4964	(Dalmasso et al., 2016)

B) Methodological adjustments

1. Determination of screening parameters: sulfur concentration and time of incubation

Sulfur activates sulfidogenic metabolism and inhibits hydrogenogenic growth in some strains, but lack of sulfur can also lead to growth impairment. For the screening, it was necessary to determine the best sulfur conditions to obtain the highest H_2 concentrations possible, while still allowing growth. The model *T. barophilus* MP^T, as being already studied in the LM2E, was used to set up this parameter. Over 54 h, cell densities were assessed by counting on Thoma chambers, and H_2 concentrations were measured by gas chromatography, on 20 mL cultures in TRM, with 30 mL 100 % N_2 at +0.2 bar (room temperature), and at 6 different colloidal sulfur concentrations: 0; 0.025; 0.050; 0.125; 0.250 and 0.500 g/L. Results (not shown here) indicated that highest H_2 levels were observed at 48 h and 54 h, averaging around 1 mM H_2 at both times, stating a saturation. No H_2 was detected after 0; 5; 8 and 24 h of incubation, and very little H_2 (0.1 - 0.2 mM) was detected after 31 h. Growth kinetics were similar at sulfur concentrations of 0.250 g/L and 0.500 g/L but were slower at lower S° concentrations, indicating that sulfur was not sufficient anymore to ensure optimal growth of this strain.

Consequently, we chose to perform the screening at 48 h, with 0.250 g/L S°, which constituted, in *T. barophilus* MP^T, suitable conditions to obtain higher H_2 values with good growths, in minimal periods.

2. Method optimization for counting

During the screening, difficulties occurred in counting, according to the substrate used in the *medium* and to strain morphology, when using optical microscope and Thoma chambers. As cell density was an important parameter to measure during the screening, it was necessary to adjust the methodology in order to try to better count cells on those particular substrates. Some polymers, particularly, hampered the observations, as can be seen in FIGURE 26.

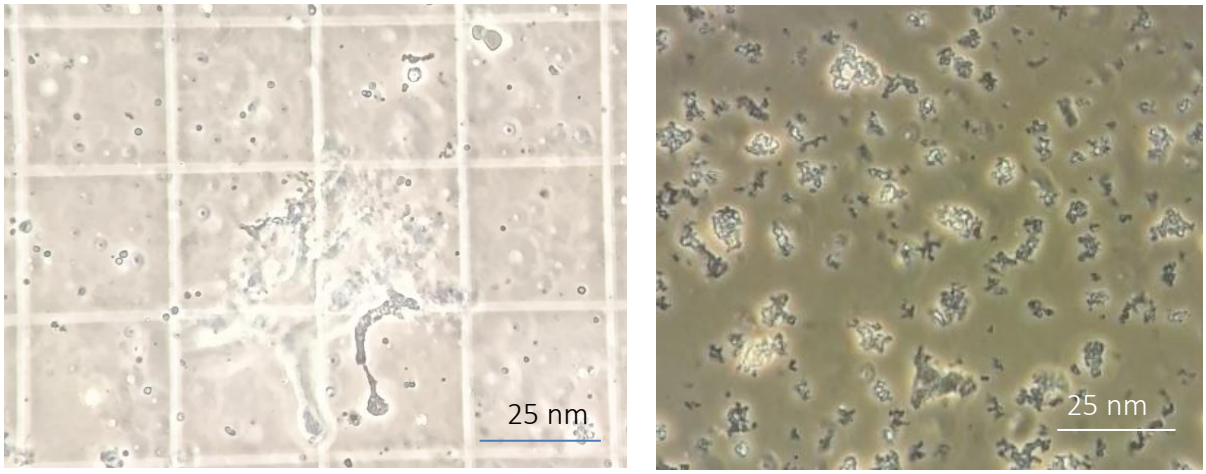

Figure 26: Examples of optical observations of *T. barophilus* MP^T cell suspensions in TRM with added substrates (left: starch 0.5 g/L; right: chitin 3 g/L)

Soluble starch forms colloidal structures of various sizes, which can be mistaken for cells (left). Colloidal chitin induces cell aggregation, and places numerous artefacts, preventing an accurate counting (right).

Numerous papers also report the use of optical density at 600 or 660 nm (OD_{600} /OD_{660}) as a way to measure growth of *Thermococcales* (*e.g.* (Kanai et al., 2011; Kengen and Stams, 1994b; Santangelo et al., 2011)). Decantation of insoluble sulfur for a pre-determined time and was sometimes reported elsewhere to be used for sampling and for measurement (personal communications from Kanai and from Lee, 2019). However, after several tests, it appeared that our use of resazurin as an oxidation indicator, of (non-decanting) colloidal sulfur, and of aggregation-inducing substrates, impaired cell density estimation by OD_{600}. Since too many methodological changes would have been necessary to shift to a working system, this idea was pushed aside.

Several tests were also performed with a flow cytometer (see MATERIALS & METHODS - GENERAL), and results were very comparable with what we could obtain by cell counting, in the absence of any particular aggregation-inducing substrate (data not shown) (samples treated by Erwann Vince, study engineer at the LM2E). We had no chance to experiment this technique with substrate-aggregated cells, but it theoretically demands separated entities to properly discriminate cells. Dilutions of cell suspensions (x 20 and x 50 tested) did not eliminate the problem of aggregation neither, from optical microscope observations. SYBR

Green staining better revealed the differences between cells and small colloids of substrates, but did not permit packs of cells around bigger substrate pieces to be counted.

As many samples were fixated with glutaraldehyde (2.5 % final) for storing several days before counting, its effect on agglomeration was tested by diminishing the final concentration of the fixator (0; 0.1; 0.25; 0.5; 1; 2.5 and 5 % final), finding no influence in our conditions (data not shown). The use of a dispersant was also tried, by adding sodium pyrophosphate at a final concentration of 5.5 mM before counting, which helped reduce the amount of cell/substrate agglomerates, but some were still remaining.

Finally, sonication was chosen as a solution (using a Vibra-cell 72408, Bioblock Scientific), allowing to reduce almost completely the aggregates, and thus to count the most accurately possible our cells. Several rhythms of sonication were tried, showing that samples were best countable when 20 µL of cell suspension were mixed with 180 µL of ultra-pure water, then sonicated on ice for a total of 30 s, each period of 5 s sonication spaced by 10 s. Cell morphologies remained similar, from microscope observations, and observations of *T. barophilus* MP^T non-aggregated cells, grown for 48 h, showed that concentrations were comparable before and after sonication. This indicates that the protocol did not induce cell lysis and could allow accurate counting (FIGURE 27).

Note that some works estimate biomass using total protein assays, but as the screening necessitated to allow quick measurements on an important number of samples, we kept the sonication solution, which was only used on aggregated suspensions.

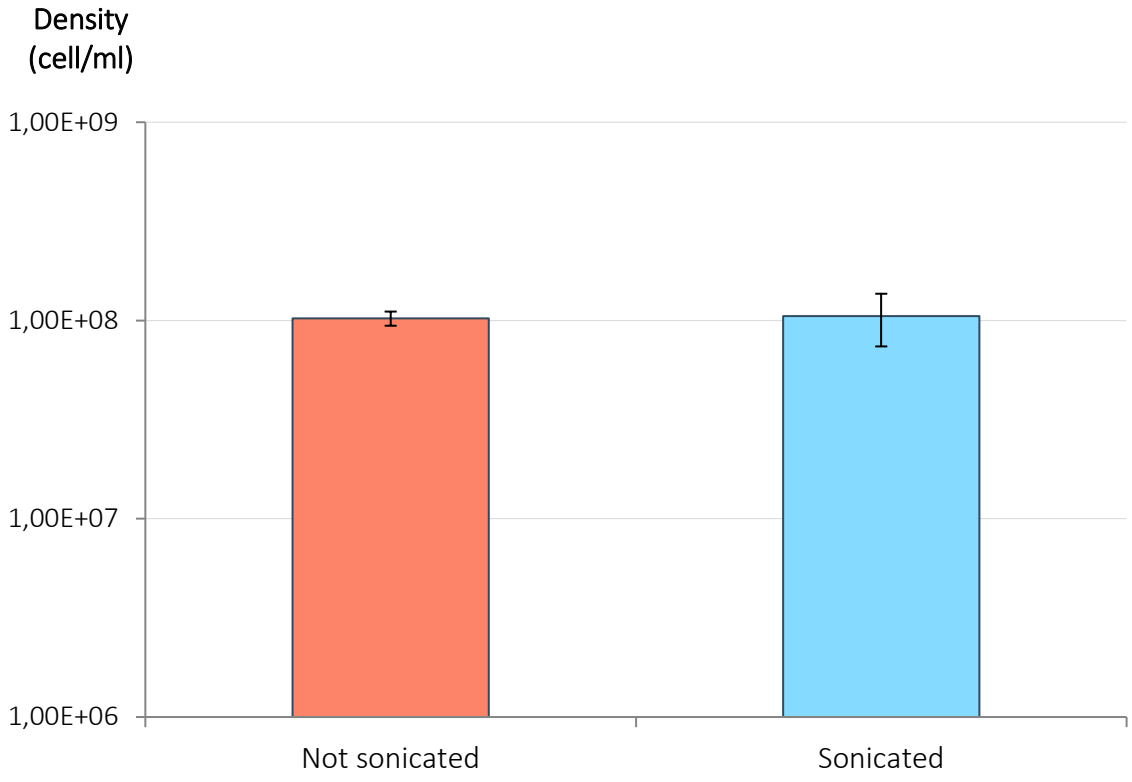

Figure 27: Effects of the described sonication protocol on cell integrity, as estimate by cell counting on Thoma chambers on sonicated and non-sonicated samples.

Samples were made in triplicates, and observed in non-aggregating conditions (TRM).

C) First phase: H_2 tolerances

The first phase of the screening consisted in looking for unusual H_2 tolerances in the 41 pre-selected strains (TABLE 8), in culture conditions determined to yield the highest H_2 concentrations while still allowing rapid growth in *T. barophilus* MP^T. To such extent, *Thermococcales* isolates, in duplicates, were incubated at their respective optimal temperatures for growth (all between 85 °C and 90 °C, see UBOCC) for 48 h in TRM at 0.25 g/L S°. H_2 productions were measured by gas chromatography and biomasses were estimated by optical microscopy (counting on Thoma chambers).

While all strains grew properly in these sulfur conditions (final densities around $1.0 .10^8$ cell/m, data not shown), no substantial H_2 production was observed, compared to the

literature models. FIGURE 28 displays the best producers obtained in these conditions: 6 UBOCC isolates compared with 4 literature models (from 0.12 mM H_2 to 2.33 mM). Despite the phylogenetic proximity of AMTc70, E4D5, E4D8, GE08 and *T. barophilus* MP^T, varied H_2 concentrations were found in those conditions, indicating that finding a dramatically more tolerant strain would not have been impossible.

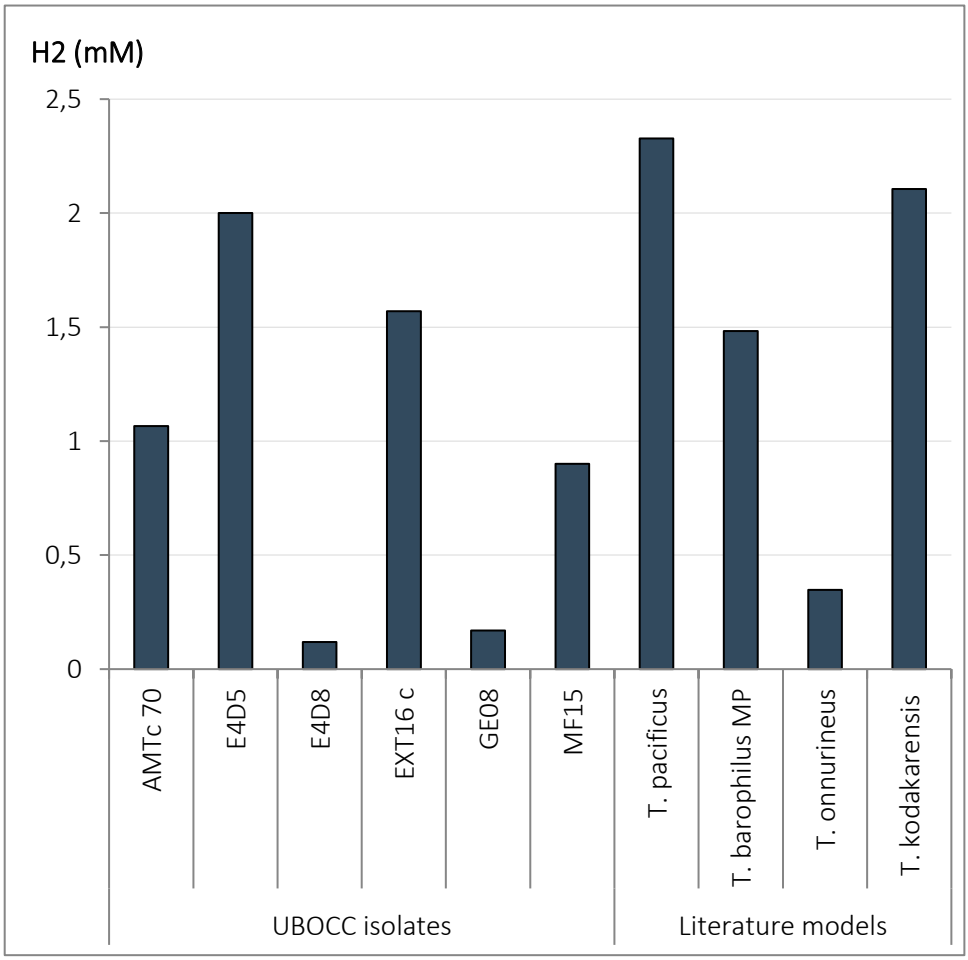

Figure 28: Highest average H_2 productions in 48 h at 0.25 g/L S° in TRM, batch cultures (duplicates) obtained from the first phase of screening

D) Second phase: substrate degradations

The second phase of the screening consisted in checking H_2 productions based on particular substrate degradations. Because time did not allow to perform all possible tests, our efforts were focused on the best H_2 producers as 4 UBOCC isolates (AMTc70, E4D5,

EXT16c, MF15) and the 4 literature models (*T. pacificus*, *T. barophilus* MP^T, '*T. onnurineus*', *T. kodakarensis*) established in the first phase, 1 strain with interesting *in silico*-predicted degradations by MicroCyc (EXT10c for chitin and starch), and 2 positive control strains, previously reported to grow on particular substrates (AT1243 for keratin and *T. chitonophagus* for chitin).

TABLE 9 reports the tests realized on those 12 strains. Samples were cultivated, in duplicate, as for the first phase, but with the addition of substrate solutions to TRM.

Table 9: Summary of the substrate/strain couples tested in the second phase of screening

Based on different reports in the literature, the following concentrations were tested: 2.5 g/L for starch, pectin, glycerol, cellulose, cellobiose, formate, and pyruvate; 1.5 g/L for keratin, 5 g/L for glucose; 3 g/L for chitin, 0.05 % and 0.5 % (v/v) for ethanol.

	Starch	Glycerol	Keratin	Cellulose	Cellobiose	Chitin	Pyruvate	Formate	Ethanol	Pectin	Glucose
AT1243	x	x	x								
E4D5	x										
EXT10c	x	x				x					
T. chitonophagus	x	x				x					
T. pacificus	x	x	x								
AMTc 70	x	x								x	
EXT16c	x	x								x	
MF15	x	x								x	
AMTc 95	x	x				x					
T. kodakarensis	x	x	x	x		x	x	x			
'*T. onnurineus*'	x	x	x	x		x	x	x			
T. barophilus MP^T	x	x	x	x	x	x	x	x	x	x	x

FIGURE 29 presents the absolute H_2 concentrations measured in gas phases after 48 h incubation in TRM with additional substrates for each of the 12 strains tested.

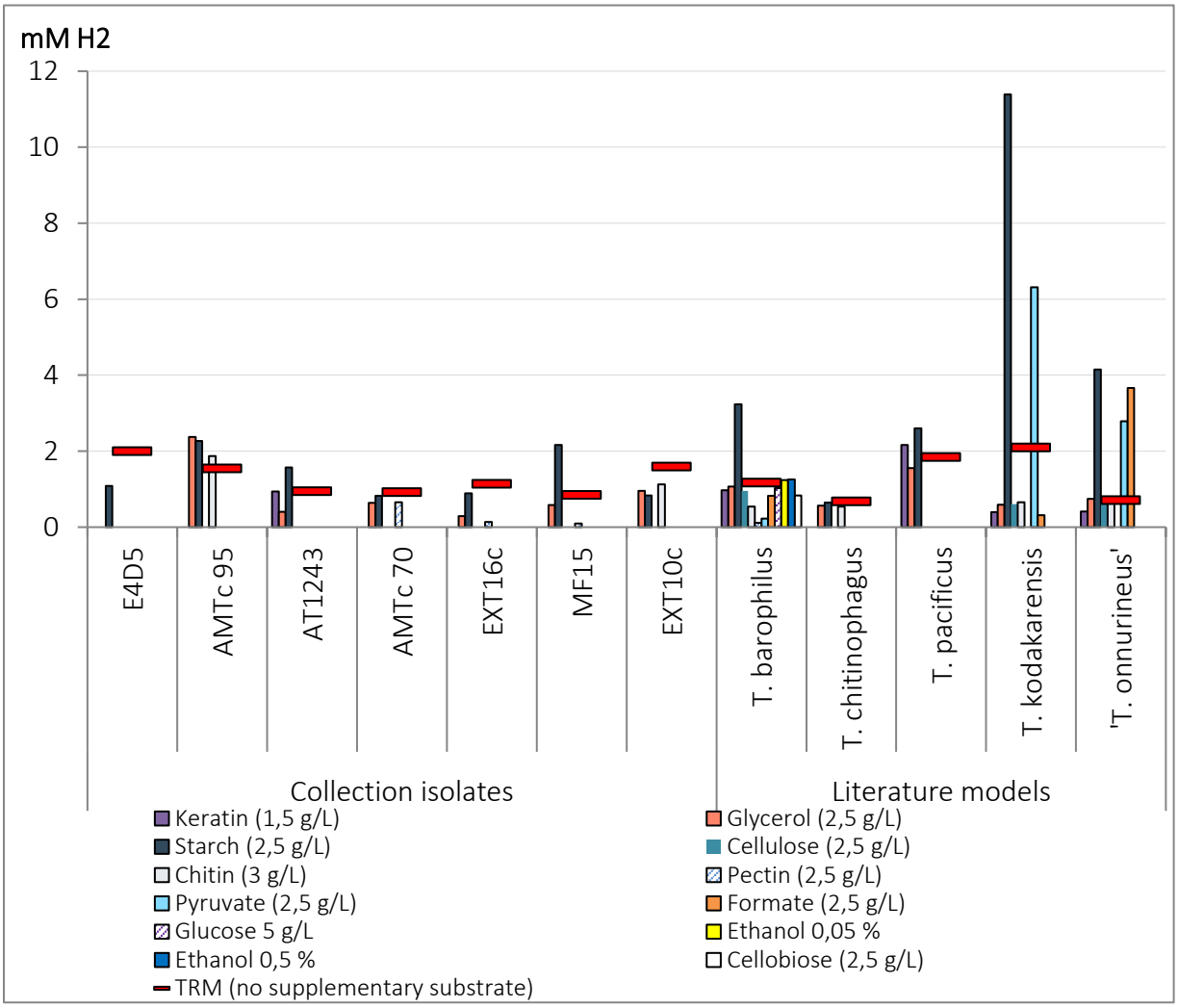

Figure 29: H_2 production for different strains in TRM (0.25 g/L S°) with added substrates after 48 h of incubation, for the second phase of screening

It hence appeared that the strains tested are not equally reacting to substrate additions. Compared to their respective behavior in classical TRM, substantial augmentations of H_2 productions occurred with starch for *T. barophilus* MP^T and MF15 (about 2.5-fold increases), *T. kodakarensis* (about 5.5-fold increase), and '*T. onnurineus*' (about 6-fold increase). Pyruvate also importantly increased H_2 production when added to cultures of *T. kodakarensis* (3-fold) or '*T. onnurineus*' (4-fold). Consistently with the literature (Bae et al., 2012a), formate can also increase H_2 production, in '*T. onnurineus*' (about 5-fold). However, other substrates did not lead to dramatic H_2 overproduction in the strains tested.

Low or TRM-equivalent H_2 productions are nonetheless inconclusive to particular abilities to degrade a specific substrate. For example, EXT10c, predicted to be able to degrade

chitin and starch, had no improvement in H_2 production compared to classical TRM conditions, when those substrates were added. Keratin did not improve AT1243 H_2 production, nor did chitin on *T. chitonophagus*. These seemingly negative results could indeed result from an equally H_2-producing compensation of a different pathway, still involving the degradation of the tested substrate. To be able to really infer on that matter (which was not the proper point of this screening) would require evaluating the amount of remaining substrate in suspension after fermentation, related to the number of cells, or a measurements of gene expression or protein levels. However, positive results can be informative. MicroCyc analyses indicated missing enzymes in the starch degradation pathways of *T. barophilus* MP^T and AMTc 95, but the addition of starch in the *medium* led to an overproduction of H_2 in both strains. It is thus possible that those strains utilize unknown enzymes or degradation pathways.

In order to verify whether those substrates could be used as principal carbon or nitrogen sources, modified *media* were also used as basis: TRM with 0.1 g/L of yeast extracts and 0.4 g/L of tryptone, or TRM with no yeast extracts nor tryptone at all. *T. barophilus* MP^T, *T. pacificus* and AMTc 95 were tested on these modified *media*. While no growth was obtained for any strain / substrate couple in the absence of tryptone and yeast extracts, diminished concentrations of the latter components led to impairments of H_2 productions (compared to a diminished medium without addition of any supplementary substrate), except for starch, which increased H_2 productions in these conditions for *T. barophilus* MP^T (7-fold) and *T. pacificus* (2.5-fold), but decreased H_2 production compared to an absence of starch, in AMTc 95 (data not shown). While those data are hardly relevant to other strains, they show that, in an applied point of view, growth of the model of choice can be envisioned on a diminished *medium*, thus optimizing the costs. The formulation of such culture conditions would require more investigations, but determining the strain model was a preliminary question to treat.

Overall, starch was an interesting substrate for H_2 overproduction in those conditions, and further experiments consequently ensued. We incubated *T. barophilus* MP^T with a double gradient of starch (0; 0.5; 1; 1.5 and 2 g/L) and colloidal sulfur (0; 0.05 and 0.25 g/L) on classical TRM, to observe the possible changes in H_2 yields (FIGURE 30).

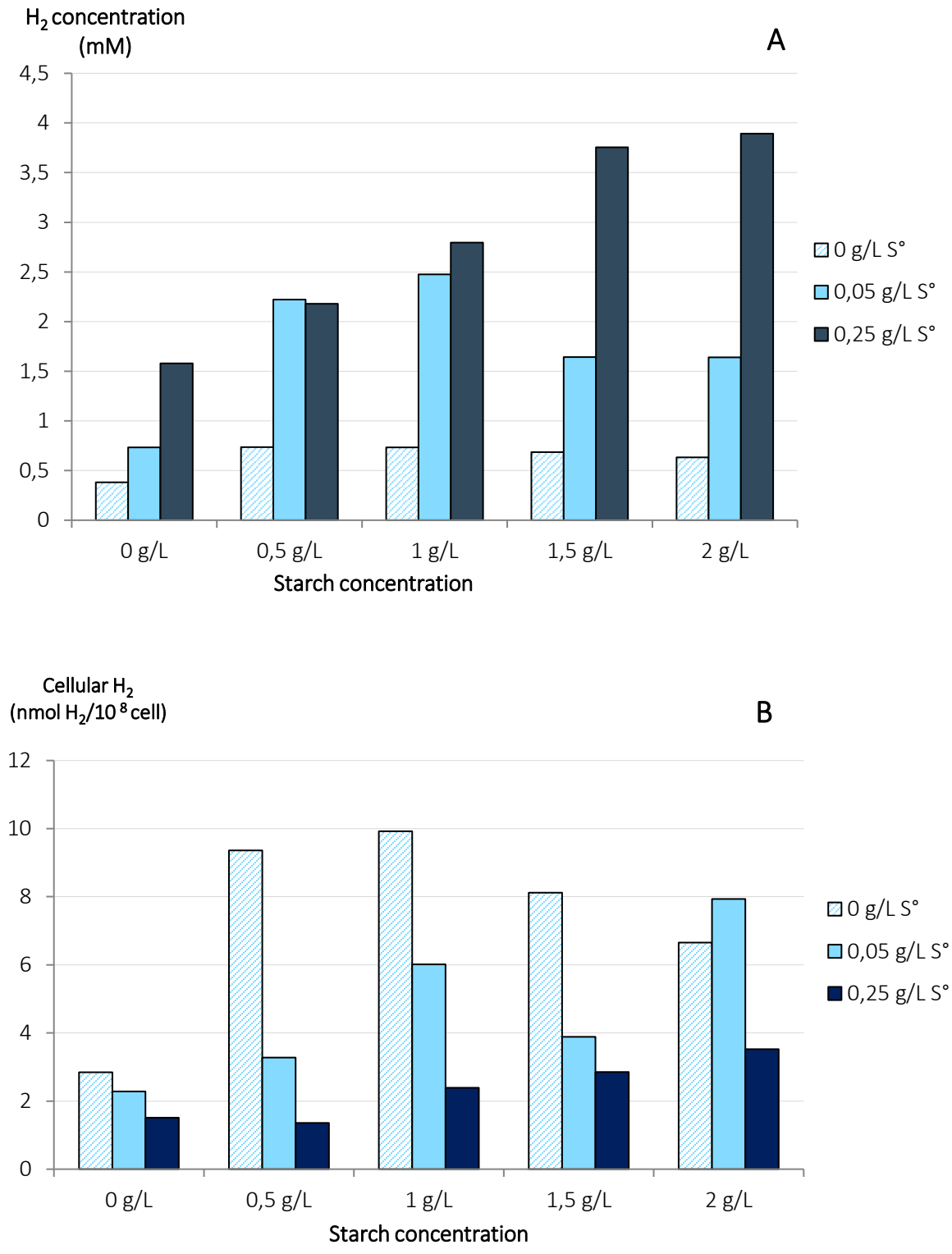

Figure 30: Absolute (A) and cellular (B) H_2 productions of *T. barophilus* MP^T at different colloidal sulfur and starch initial concentrations

Measurements of cell densities and H_2 concentrations in the gas phase performed after 48 h of incubation at 85 °C, in duplicates.

This highlighted that an optimal H_2 production requires to adjust several parameters. Much probably, sulfur and substrate concentrations are not the only aspects influencing the system. Furthermore, if cellular H_2 could be higher in sulfur-less conditions, as growth was impaired, absolute H_2 levels were substantially lower as well. The highest absolute concentrations of H_2, in this experiment, were encountered for 0.25 g/L S°, with 2 g/L starch, reaching about 3.9 mM, while only 0.6 mM H_2 were produced without sulfur in these conditions (not shown). Yet, if considering cellular productions, minimizing both sulfur and starch could be interesting, although an optimal H_2 production could be found with a small but present starch addition (between 0.5 g/L and 1 g/L). In an applied point of view, the most economically interesting solution might thus be found through a fine balance between several culture parameters. After this screening, aiming to define a candidate strain for further investigations, a more complete picture needed to be set on the chosen model, which constitutes the second part of this chapter.

E) Choice of the candidate strain

This first screening phase focused on H_2 tolerances (*via* final H_2 concentrations) and substrate degradation abilities. While it was not complete, we decided to formulate our choice for the candidate strain, in order to optimize the use of our limited time-frame.

T. kodakarensis and '*T. onnurineus*', which both gave interesting substrate-specific H_2 productions, are widely described literature models, particularly considered as applied solutions (*e.g.* (Aslam et al., 2017; Bae et al., 2012a; Kanai et al., 2015; Kim et al., 2017, 2020)). However, these strains have limited piezophily (although it was not actually tested for '*T. onnurineus*', the original isolate was sampled from a depth of 1 650 m) (Bae et al., 2006; Vannier et al., 2015). Despite those strain-associated, substrate-specific productions, the screening did not reveal outstanding features that would justify to diverge from choosing *T. barophilus* MP^T, which presents several advantages. Indeed, numerous data on the piezophilic strain's metabolism and physiology, particularly related to pressure, are available and tend to indicate a better H_2 production at high pressure (Vannier, 2012). Its genome was fully sequenced (Vannier et al., 2011), an efficient genetic tool has been developed (Birien et al., 2018; Thiel et al., 2014), and several mutants for key clusters of the energy metabolism were already created before the project HPBioHyd (Birien, 2018). The basal and substrate-specific

(especially on starch) H_2 productions are quite competitive to the other strains tested, and other interesting molecules, not tested here, have been reported to induce hydrogenogenic growth (*e.g.* carbon monoxide (Kozhevnikova et al., 2016)).

For further investigations on a potential H_2 bio-production solution (see below), as well as fundamental investigations of our model's metabolism (see chapters III and IV), we then decided to focus on *T. barophilus* MP^T.

Part II - Overview of the fermentation

Our screening tended to confirm that *T. barophilus* MP^T could be a suitable choice of strain for an applied H_2 bio-production at high pressure. Yet, its fermentative system in needed to be more thoroughly characterized, to assess whether such solutions could be energetically favorable, with a preliminary input/output assessment. This part of the project emerged from a discussion with an industrial partner, and several members of our laboratory (Raphaël Brizard, Didier Flament, Jean-Marc Daniel, Mohamed Jebbar, Erwan Roussel and myself). We aimed to propose a general evaluation of measured efficiencies for different H_2 bio-production solutions, in order for the partner to decide whether further investigations could be interesting.

Definition of the experimental plan

An experimental plan was set to rapidly gather data on various fermentative conditions, so a global behavior of the system could be approximated by extrapolating on each tendency observed. We first supposed the main parameters influencing this fermentation, as shown in FIGURE 31 then decided on which measurements to perform. It is important to highlight that this work was not focused on considering the fundamental metabolism of the model, but rather on shallowly evaluating whether further investigations would be interesting, to apply H_2 bio-production solutions. Noticeably, each measurement was realized without replicate. The interpretations given herein should be read as potential tendencies on practical systems.

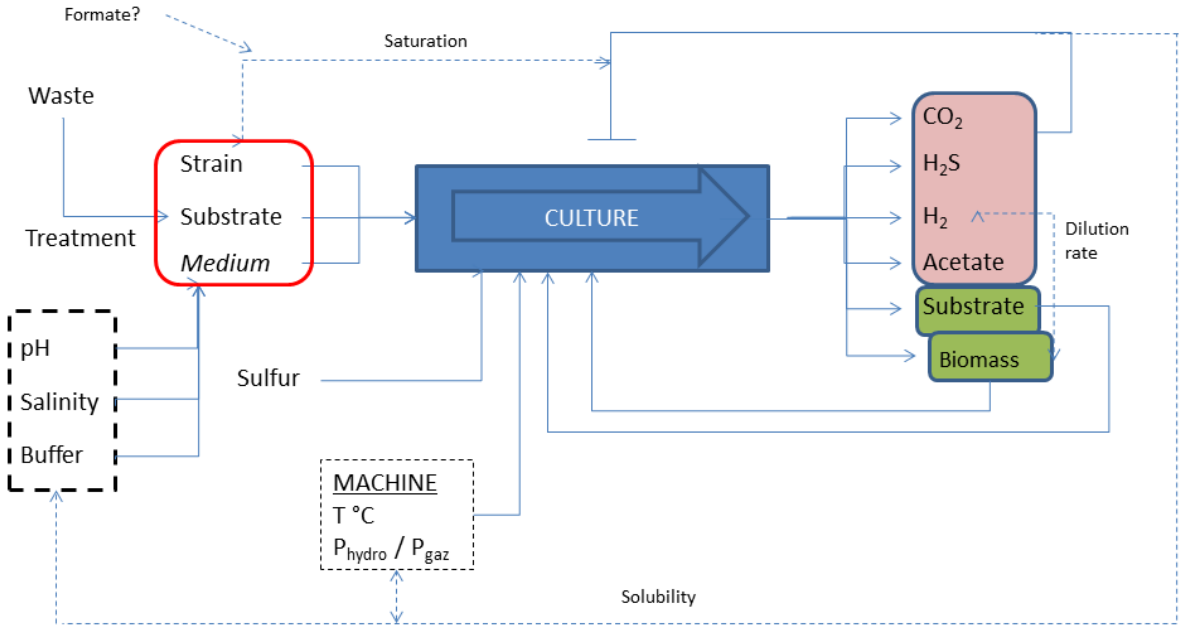

Figure 31: Schematic representation of the main parameters considered for the fermentative system

The hydrogenogenic culture could be influenced by different types of inputs (strain, substrate, medium*, temperature, pressure, product saturations, sulfur), and those variables could also be influenced themselves by other parameters (dilution rate, solubility, buffer,* etc.*). Lines with arrows indicated a positive influence, and lines with a dash indicated negative influences. Dotted lines represented indirect, inter-parameter influences.*

From the parameters considered, the experimental plan was defined. The model strain chosen from the previous phase was *T. barophilus* MP^T. Other strains were also investigated for their particular abilities: *T. barophilus* Ch5 is known to degrade formate (Oger et al., 2016), and *T. waiotapuensis* and *T. zilligii* grow on low-salt *medium* (González et al., 1999; Ronimus et al., 1997). The point here was not to reproduce a screening for strain as in the first part of this chapter, but rather to obtain tendencies with those other strains, which could serve to extrapolate to and from our main model. The use of *Thermococcales* Rich *Medium* (TRM) for the previous strain / substrate screening was mainly due to practical considerations and as a reference *medium*, but could be optimized for our actual needs. An industrial *scenario* would require cheaper and easily adjustable and accessible *medium*. We hence chose to shift towards the use of artificial sea water (ASW) (see MATERIALS & METHODS - GENERAL). This *medium* resembles the composition of sea water, which could be directly used in an applied

prototype. Low-salt water would also present the advantages to be less corrosive and sometimes more geographically accessible, so it was also tested (using the same ASW base but with a NaCl concentration of 1.5 g/L instead of 24.3 g/L NaCl). The pH of the *medium* could influence the saturation rate of some compounds in solution, which could be otherwise gaseous (*e.g.* CO_2, H_2S). The way the medium is buffered could also influence fermentation. ASW *medium* is buffered with bicarbonate (2 mM in our usual cases), which can influence CO_2 saturation in the system (initial gas-phases were composed of N_2:CO_2 80:20, if not stated differently). A weakly buffered *medium* could see pH decrease while organic acids are produced during fermentation.

The hydrogen economy paradigm finds its interest in part in the dissociation from fossil fuels, which particularly emit lots of greenhouse gases for their productions. An applied H_2 bio-production consequently has to fit this idea, but *Thermococcales* fermentative system can lead to CO_2 emissions. It was thus important to precisely assess this aspect. Other end-products (H_2S, acetate, formate) are to be considered as they can lead to metabolic saturation, constitute substrates for other metabolic routes, or could also be valorized.

The part of the initial substrate which was degraded by the fermentative system is also an interesting parameter as it could be re-used in the case of a continuous production for example. In continuous culture conditions, the biomass (cell density) parameter would also need to be precised, as well as growth dynamics, since metabolic variations could occur according to each phase, and to saturation of the *medium*. Finally, the cost of functioning of the bioreactor has to be taken into account, and would importantly depend on the needs of pressurization and heating.

Consequently, the experimental plan was set up to investigate what best substrate could be used on ASW *medium*, what effects would have substrate and sulfur concentration variations on the outcomes, what effects would ensue from product and cell density saturations, what temperature and pressure variations could change on the system, and to obtain further information on additional specific cases (utilization of formate, and low salt *medium*).

Materials and methods

Since the first screening phase was based on TRM, we needed to re-assess which best substrate to use in these new conditions to optimize H_2 production. Starch, yeast extracts, maltodextrin, maltose, and ethanol were tested, as they led to interesting yields in the previous phase. H_2 and CO_2 productions were measured by gas chromatography, H_2S concentrations were evaluated by Cline assay, cell densities were estimated by optic microscopy (Thoma counting), and acetate and formate productions were assessed by ionic chromatography.

We then varied the initial concentrations in the chosen substrate (0; 1; 2.5 g/L) and in sulfur (0; 0.25; 0.5; 3 g/L), and performed the same measurements as before. Note that H_2S variations could be estimated by both Cline assay and gas chromatography. Our µGC method was however not calibrated for H_2S, but tendencies could be observed thanks to peak areas.

The effects of potential product saturations were estimated by varying the initial concentrations of Na_2S (leading to H_2S) (1; 5; 20 mM), H_2 (1; 5; 20 %), acetate (1; 5; 20 mM), and bicarbonate (leading to CO_2) (2; 15; 30 mM), based on previous observations of the ranges of productions. The ensuing H_2, CO_2, H_2S (Cline), acetate, formate productions, and cell densities were measured. A growth curve (cell densities) was realized, with measurements of formate and acetate concentrations.

T. zilligii and *T. waiotapuensis* were grown on low-salt *medium*, and the ensuing H_2, CO_2 and H_2S (µGC) productions, and cell densities, were measured. *T. barophilus* Ch5 and *T. barophilus* MP^T were grown on formate, either in the absence or presence of the initial chosen substrate, and outcoming H_2, CO_2, H_2S (µGC), formate, acetate, and cell densities were measured.

Finally, the effects of high pressures (0.1; 20; 40; 60; 64; 71 MPa) on H_2 and CO_2 productions and cell densities were tested, thanks to the newly developed gas-phase device for discontinuous high pressure culture described in chapter II.

Note that values from uninoculated *medium* as blank controls were removed from all results displayed herein. See MATERIALS & METHODS - GENERAL for additional details.

Results

Results of the previously described experiments were summarized below. As several parameters were tested, we chose to display data into tables. For each test, absolute concentrations were given, followed by the calculated "cost" per hydrogen of each compound (in mol compound per mol H_2, or cell per mL per mol H_2 (for cell densities)). For example, in a "productions reported to H_2" table, if one line displays "2" for acetate, it means that in the concerned condition, the measured outcome of the fermentation was 2 mol acetate produced per mol H_2 produced. Note that those values can be negative, likely indicating global consumptions.

For better visual appreciation of each effect, colored bars have a length correlated to the report of each value to the maximum obtained in each series. Each column, per table, has a different maximum to which colored bars are related.

A) Choice of the substrate and H_2 tolerances

Several substrates were tested for growth of *T. barophilus* MP^T in ASW *medium,* as culture conditions were different from the first screening phase described earlier in this chapter (TABLE 10). As no growth could be obtained without, 0.2 g/L of yeast extracts were always added.

Table 10: Fermentation outcomes of *T. barophilus* MP^T grown with different substrates on ASW *medium* after 77 h of incubation, at 0.25 g/L S°

Absolute values:

Conditions	H2 (mM)	CO2 (mM)	H2S (mM)	H2S (area eq.)	Acetate (mM)	Formate (mM)	Cell density (cell/mL)
ASW	2,87	1,47	0,20		0,54	0,02	6,88E+06
Starch (2,5 g/L)	4,95	2,75	0,60		1,83	0,18	6,20E+07
YE (2,5 g/L)	6,10	2,52	0,71		1,44	0,03	6,00E+07
Maltodextrin (2,5 g/L)	5,92	2,81	0,41		2,37	0,14	5,80E+07
Ethanol (0,05 %)	3,04	1,52	0,26		0,59	0,01	4,75E+06
Maltose (2,5 g/L)	3,43	1,54	0,40		1,09	0,04	9,31E+06

Productions reported to H_2: (mol/mol H_2 or (cell/mL)/mol H_2).

Conditions	H2	CO2	H2S	H2S (area eq.)	Acetate	Formate	Cell density
ASW	1	0,511	0,069		0,188	0,007	2,39E+06
Starch (2,5 g/L)	1	0,555	0,121		0,369	0,037	1,25E+07
YE (2,5 g/L)	1	0,413	0,117		0,236	0,005	9,83E+06
Maltodextrin (2,5 g/L)	1	0,475	0,069		0,401	0,023	9,80E+06
Ethanol (0,05 %)	1	0,499	0,086		0,195	0,003	1,56E+06
Maltose (2,5 g/L)	1	0,449	0,116		0,318	0,012	2,72E+06

It appears that the addition of substrate enhances importantly all metabolite productions, together with cell densities. Dramatic absolute differences occur between several parameters, which are to be considered. For example, one could emphasize minimizing cell density in the bio-process (which probably accounts for less substrate degradation, although unfortunately this parameter could not be estimated during this work). In that case, using ethanol as a substrate may seem as an interesting option to explore, as it increased absolute H_2 production by about 6 % while decreasing final cell density by about 31 %. On the contrary, the accent could be made on H_2 production itself, considering that ensuing biomass could be valorized. To that extent, the addition of 2.5 g/L yeast extracts or maltodextrin led respectively to increases in H_2 concentration of about 112 % and 106 %, respectively. It is also essential to take into account that these experiments were performed in batch. As H_2 is itself limiting for growth (Schäfer and Schönheit, 1991), lower absolute productions and lower cell densities (as for ethanol, maltose, or without substrate) could indicate that the corresponding metabolic configurations have reached saturation. The choice of the substrate might thus depend, on one hand, on the desired type of bioreactor (continuous / batch).

While absolute productions are important to define the possible ranges to consider, one may be concerned about the respective co-productions reported to each H_2 molecule, which would define the actual "costs" in each outcome. For example, it seems that yeast extracts, which allow growth mainly based on peptide catabolism, led to less acetate (-43 %) and less formate (-78 %) but more H_2S (+70 %) and equivalent CO_2 and cell density than maltodextrin, which sensibly leads to equivalent absolute H_2 productions in our conditions.

Gas chromatography measurements (H_2, CO_2) were also performed after 24 h and 48 h of incubation. Gas reached final concentrations at 48 h (data not shown). As time, and consequently the phase of culture, is an important parameter to consider, further experiments were performed at 48 h, considering that it would display a suitable final point for batch cultures.

For further analyses, maltodextrin was chosen as a model substrate, contrarily to during the first screening phase, as it permits important absolutes productions, and thus probably more accurate measurements. In those conditions, starch and yeast extracts could also be chosen, but maltodextrin allows more accurate cell density estimations, and more precise knowledge of the substrate, respectively.

B) Influence of substrate concentration

Those experiments were performed with 0.25 g/L S°. Only two supplementary maltodextrin concentrations (0 g/L and 1 g/L) were tested, as we initially assumed that results of the first experiment (with 2.5 g/L) could be exported herein (see TABLE 11).

Table 11: Fermentation outcomes of *T. barophilus* MP^T grown on different maltodextrin concentrations after 48 h incubation on ASW 0.25 g/L S°. Results indicated in red were exported from the previous experiment.

Absolute values:

Maltodextrin (g/L)	H2 (mM)	CO2 (mM)	H2S (mM)	H2S (area eq.)	Acetate (mM)	Formate (mM)	Cell density (cell/mL)
0	0,59	-0,18	0,57	4722,57	0,72	0,02	1,27E+07
1	3,90	1,52	0,80	6133,83	2,78	0,12	8,90E+07
2,5	5,92	2,75	0,41		2,37	0,14	5,80E+07

Productions reported to H_2: (mol/mol H_2 or (cell/mL)/mol H_2):

Maltodextrin (g/L)	H2	CO2	H2S	H2S (area eq.)	Acetate	Formate	Cell density
0	1	-0,299	0,962	7946	1,203	0,027	2,14E+07
1	1	0,389	0,205	1574	0,713	0,032	2,28E+07
2,5	**1**	**0,464**	**0,069**		**0,401**	**0,023**	**9,80E+06**

Note that CO_2 resulted in negative productions in the absence of maltodextrin. This could correspond to an overall consumption of CO_2 (-0.3 mol CO_2/mol H_2), but can also likely be attributed to measurements errors, especially since differences from zero are not huge. These data are nonetheless to be taken into account, as they show a probable production quite inferior to other conditions.

The results obtained with 0 g/L maltodextrin were virtually in the same conditions as for the first experiment when testing only ASW (no substrate added). Still, important differences in absolute productions could be observed in the two experiments (*e.g.* more than 2 mM H_2, about 1.5 mM CO_2). This once again highlights the lack of statistical significance for comparing each experiment together. Consequently, the results of the first experiment in the presence of maltodextrin (2.5 g/L), written in red in TABLE 11, were to be excluded from comparison. They will not be displayed with the next results, hence reducing the number of available points for each experiment, unfortunately, as the experimental plan was designed on the surmise that data would be comparable from one experiment to the other.

Yet, from these results, it would seem that 1 g/L of maltodextrin triggers important changes in the system, overproducing absolute H_2 (+561 %). And for each mol of H_2, though equivalent biomass would be produced, less H_2S (-79 %) and less acetate (-41 %)) may be generated, and more CO_2. We can surmise that these tendencies would not be extrapolating to unlimited substrate, as each cell can only degrade maltodextrin at certain, limited maximum rate. Overall, more points should be available to reasonably conclude more about the influence of substrate concentration on fermentation outcomes.

C) Influence of sulfur concentration

Those experiments were performed with 2.5 g/L of maltodextrin, as initially planned, testing three different concentrations in sulfur (0; 0.5 and 3 g/L) (TABLE 12).

Table 12: Fermentation outcomes of *T. barophilus* MP^T grown on different sulfur concentrations on ASW at 2.5 g/L maltodextrin, after 48 h of incubation

Absolute values:

Sulfur (g/L)	H2 (mM)	CO2 (mM)	H2S (mM)	H2S (area eq.)	Acetate (mM)	Formate (mM)	Cell density (cell/mL)
0	3,00	1,13	0,02	18,59	2,65	0,12	1,43E+08
0,5	4,36	2,16	1,12	862,09	2,77	0,14	6,00E+07
3	0,67	2,00	7,54	9468,17	2,24	0,15	4,00E+07

Productions reported to H_2: (mol/mol H_2 or (cell/mL)/mol H_2):

Sulfur (g/L)	H2	CO2	H2S	H2S (area eq.)	Acetate	Formate	Cell density
0	1	0,377	0,008	6	0,884	0,041	4,76E+07
0,5	1	0,496	0,257	198	0,636	0,032	1,38E+07
3	1	2,999	11,303	14185	3,351	0,218	5,99E+07

When concerned about absolute productions, it seemed that a minimal sulfur concentration was necessary to trigger H_2 production, as H_2 values increase at low concentration from 3 mM (without sulfur) to 4.36 mM (with 0.5 g/L S°); before dropping down to 0.67 mM (at 3 g/L S°). Interestingly, a maximal growth was actually observed without any sulfur. Other products seemed not to vary much according to sulfur concentration however, except for CO_2 which seemed lower without sulfur.

In order to maximize H_2 production while minimizing H_2S production, one may thus probably use between 0 and 0.5 g/L S°, depending on the CO_2 and biomass "cost" per H_2 considered.

D) Influence of growth phase

Previous tests on different substrates (see CHOICE OF THE SUBSTRATE AND H2 TOLERANCES, P. 167) were performed at different times, and showed that this parameter could be important to consider for assessing fermentation outcomes. We aimed to evaluate the influence of growth phases, by measuring concomitant metabolite productions at different times, with 2.5 g/L maltodextrin and 0.25 g/L S°. Unfortunately, no gas chromatography or Cline assay data were available for this experiment. Acetate, formate and cell densities were measured over time. Relative productions were thus reported to cell concentrations (TABLE 13).

Table 13: Biomass, acetate and formate productions of *T. barophilus* MP^T in function of time, on ASW *medium* with 0.25 g/L S° and 2.5 g/L maltodextrin

Absolute values:

Time (h)	Acetate (mM)	Formate (mM)	Cell density (cell/mL)
0	0,055	0,001	2,19E+06
4	0,134	0,004	5,63E+06
9	0,550	0,010	4,70E+07
13	0,965	0,027	9,60E+07
48			8,90E+07

Acetate and formate productions related to cell densities (cell densities displayed in absolute values):

Time (h)	Acetate	Formate	Cell density (cell/ mL)
0	2,53E-08	6,37E-10	2,19E+06
4	2,39E-08	7,68E-10	5,63E+06
9	1,17E-08	2,18E-10	4,70E+07
13	1,01E-08	2,82E-10	9,60E+07
48			8,90E+07

Acetate and formate thus appeared to be rather produced during exponential phase of growth, since each cell produced less of these organic acids at 9 h and 13 h than earlier. Extrapolating those data to deduct patterns in H_2 productions over time by observing the acetate and formate data from other experiments would not be accurate as nothing indicates a direct correlation between acetate / formate and H_2 productions. This information is nonetheless useful to assess a link between acetate, formate, and growth phase.

E) Influence of product concentrations

Fermentations were realized with varied initial concentrations of selected known products, on 2.5 g/L maltodextrin and 0.25 g/L S°. Na_2S, in water, readily dissociates to HS^-, which equilibrates with its H_2S form, at adequate pH. Na_2S was thus used to impose initial H_2S concentrations in the assays. In the same manner, bicarbonate (which, in carbonic acid form, equilibrates with gaseous CO_2) was used to set up different initial CO_2 concentrations. Acetate and H_2 were directly injected in culture flasks.

Initially added acetate and H_2 concentrations were subtracted from final results, so the values displayed in the tables correspond to actual productions (or consumptions) (TABLE

14). It was not the case for Na_2S and bicarbonate, as the error would be greatly increased by calculating the corresponding gaseous portion, which varies with conditions of measure, and are increased by the error associated with product preparations. Tendencies could however be interpreted.

Table 14: Fermentation outcomes of *T. barophilus* MP^T grown with different product concentrations (Na_2S, H_2, acetate and bicarbonate) after 48 h of incubation in ASW with 2.5 g/L maltodextrin, and 0.25 g/ S°.

Absolute values:

Condition	Concentration	H2 (mM)	CO2 (mM)	H2S (mM)	H2S (area eq.)	Acetate (mM)	Formate (mM)	Cell density (cell/mL)
Na2S (mM)	1	3,21	1,69		4598,51	2,88	0,17	1,18E+08
	5	3,60	0,43		41116,93	2,83	0,14	1,66E+08
	20	3,67	-4,88		97819,71	2,66	0,23	1,09E+08
H2 (%)	1	1,51	1,95		6403,36	2,92	0,14	6,60E+07
	5	0,93	-2,27		2313,46	2,90	0,13	5,40E+07
	20	0,00	1,63		10818,59	2,58	0,16	3,70E+07
Acetate (mM)	1	2,86	1,35		3782,41	1,10	0,15	9,50E+07
	5	3,71	1,57		4591,59	-3,68	0,16	1,08E+08
	20	3,08	1,01		4967,01	-20,41	-	9,40E+07
Bicarbonate (mM)	2	4,10	1,96		3869,81	2,27	0,12	8,60E+07
	15	4,75	2,64		4604,89	2,47	0,16	1,07E+08
	30	3,13	2,01		2548,14	2,60	0,21	1,02E+08

Productions reported to H_2: (mol/mol H_2 or (cell/mL)/mol H_2):

Condition	Concentration	H2	CO2	H2S (mM)	H2S (area eq.)	Acetate	Formate	Cell density
Na2S (mM)	1	1	0,525		1431	0,895	0,053	3,67E+07
	5	1	0,120		11432	0,787	0,039	4,62E+07
	20	1	-1,329		26632	0,724	0,063	2,97E+07
H2 (%)	1	1	1,294		4246	1,934	0,092	4,38E+07
	5	1	-2,442		2489	3,118	0,145	5,81E+07
	20	-	-		-	-	-	-
Acetate (mM)	1	1	0,471		1321	0,385	0,051	3,32E+07
	5	1	0,424		1236	-0,990	0,043	2,91E+07
	20	1	0,328		1613	-6,627	-	3,05E+07
Bicarbonate (mM)	2	1	0,478		943	0,553	0,030	2,10E+07
	15	1	0,556		970	0,521	0,035	2,25E+07
	30	1	0,642		814	0,829	0,069	3,26E+07

When looking at absolute values, it seemed that increasing Na_2S initial concentration did not importantly impact H_2 synthesis, nor final cell densities or acetate and formate productions. However, it appeared to be negatively correlated to CO_2 production, likely leading to CO_2 consumption at high Na_2S concentrations (-4.88 mM CO_2 at 20 mM Na_2S). No conclusion could be made on H_2S production, as initial H_2S concentrations could not be removed from the measurements. Same indications are given by productions reported to H_2.

For the study of the influence of H_2, initial concentrations could be removed from the results, and H_2 results well described the saturating effect of the product: initial H_2 concentrations both diminished absolute H_2 productions and cell densities. However, while CO_2 and H_2S productions seemed decreased by initial augmentations of H_2 until 5 %, a high concentration of H_2 (20 %) seemed to lead the system back to higher CO_2 and H_2S productions. One may thus take into account that a highly saturated system possibly leads to more H_2S and CO_2 production. Oppositely, if the values presented are accurate, it appears that a lightly H_2-saturated fermentation could decrease the amount of CO_2, and to a lesser extent H_2S, synthesized for each mol of H_2 produced. Therefore, an industrial application should consider the renewing of gas phase, but its rate may be of importance for minimizing CO_2 co-production.

Interestingly, acetate and bicarbonate initial concentrations suggested the same patterns on fermentation outcomes. Absolute H_2 concentrations seemed to find an optimal with a minimal initial concentration of those products, and to decline past this threshold. High bicarbonate concentrations could induce a rise in formate production. Other parameters did not look impacted, except for acetate or bicarbonate themselves. Increased initial acetate concentrations led to increased acetate consumptions, from 0.39 mol acetate produced per mol H_2 produced at 1 mM initial acetate to 6.63 mol acetate *consumed* per mol H_2 produced at 20 mM initial acetate (initial values were removed in the tables shown). As initial CO_2 values could not be subtracted from the measurements, we can only adjudge that as the measured data did not increase substantially with higher initial bicarbonate concentrations, CO_2 might be consumed as well. If those tendencies are confirmed, the ensuing applied systems could be highly interesting as ways to fixate CO_2 and recycle other fermentation co-products.

F) Influence of temperature

Temperature is an important parameter to consider as it can constitute elevated costs for higher-scale systems, but could also provide several advantages, as for instance preventing contaminations, decreasing *medium* viscosity, ameliorating mixing, allowing otherwise thermodynamically unfavorable H_2-evolution, and cancelling the need for cooling

down a bioreactor (Pawar and Niel, 2013). Three temperatures of incubation (60, 70, and 90 °C) were tested (TABLE 15).

Table 15: Fermentation outcomes of *T. barophilus* MP^T in function of incubation temperature after 48 h in ASW with 2.5 g/L maltodextrin, 0.25 g/L S°

Absolute productions:

Temperature (°C)	H2 (mM)	CO2 (mM)	H2S (area eq.)	Acetate (mM)	Formate (mM)	Cell density (cell/mL)
60	0,52	0,77	4256,05	0,63	0,01	5,80E+07
70	1,55	1,78	2977,25	1,92	0,07	1,44E+08
90	3,57	0,20	8061,23	2,96	0,15	1,30E+08

Productions reported to H_2: (mol/mol H_2 or (cell/mL)/mol H_2):

Temperature (°C)	H2	CO2	H2S (area eq.)	Acetate	Formate	Cell density
60	1	1,482	8150	1,206	0,018	1,11E+08
70	1	1,142	1916	1,238	0,045	9,27E+07
90	1	0,055	2257	0,830	0,043	3,64E+07

Augmenting temperature thus appeared to increase absolute H_2 productions. The optimal temperature for growth of our model is 85 °C (Marteinsson et al., 1999a). Unfortunately, the experimental plan was designed in such as the 85 °C value would have been extracted from previous experiment, but we showed earlier that such comparison would not be accurate. At 60 °C, the culture yielded lower cell densities. Concentrations equivalent to what is obtained at optimal growth were reached at both 70 and 90 °C, but interestingly, more H_2 (+130 %), more H_2S, and more organic acids (+54 % acetate; +114 % formate) ensued at higher temperature, but less CO_2. Overall, it seemed that if one may choose to lower temperature in order to diminish heating costs, the CO_2, H_2S, and acetate per H_2 productions would be more important. Whether 85 °C would constitute a point where H_2 peaks would be interesting to determine. As explained earlier, in those experiments, the error is too important to be able to export data from one series to another.

G) Influence of pressure

Compression can account for 10 – 30 % of energy content for H_2 commercial storage (IEA-ETSA, 2014; Parks, 2014). The strategy developed in this project stressed a possibly interesting pressurization before culture, in order to optimize this cost, based on the assumptions that some *Thermococcales* metabolisms could yield H_2 more efficiently at high

pressure. To test this hypothesis, methods and tools were developed, as described in chapter II. Cultures were performed in our new gas-phase, leak-free high pressure devices for discontinuous culture, with 6 mL of ASW at 0.25 g/L S°, 2.5 g/L maltodextrin, and 8 mL of N_2/CO_2 (80:20), at 85 °C, for 14 h, at different hydrostatic pressures (FIGURE 32).

Absolute cell densities happen to be approximately equivalent at each pressure of culture. Optimal pressure for growth is 40 MPa, but this corresponds to the condition at which the growth rate is the highest (Marteinsson et al., 1999a; Zeng et al., 2009). Cell densities can still be similar at different pressures, and after 14 h of culture, it is not surprising that each plateau phase was attained. Yet, H_2 concentration decreased as pressure increased. In addition to hydrostatic pressure, the impact of gas pressure was also tested. As described in chapter II, we developed a high temperature / high pressure continuous bioreactor allowing gas phase, gas-pressurized incubations. Experiments were performed in the frame of the machine development, and not for this fermentation overview, so culture conditions were not comparable with the previous batches described in the second part of this chapter. A *T. barophilus* MP^T culture was incubated in classical TRM with no added substrate, and pressurized at 30 MPa with N_2 (300 mL liquid and 65 mL gas), for 48 h at 85 °C. A 570 mL suspension in 1 L anaerobic flask (Schott Duran) filled with +0.5 bar N_2 was used for atmospheric pressure control. The BHP culture was collected in a 1 L anaerobic flask (Schott Duran) previously flushed with N_2 then emptied at -0.9 bar. After collection, this flask was slightly re-pressurized with the gas remaining in the bioreactor (up to about +1.5 bar), and was let for degassing at room temperature for 24 h before µGC measurements. The obtained concentration in the flask was used to recalculate the corresponding concentration at high pressure, considering that the gas phase, being pressurized, importantly “diluted” the suspension. The equivalent volume at near atmospheric pressure would thus be virtually much more important, so the total amount of H_2, at a given concentration, is also underestimated. Atmospheric pressure H_2-production consequently was compared with a re-calculated value, mimicking the total amount of H_2 and reported in a lowed volume, according to the ideal gas law (pV=nRT). FIGURE 33 presents the obtained equivalent H_2 concentrations and shows that much higher results were obtained at high pressure.

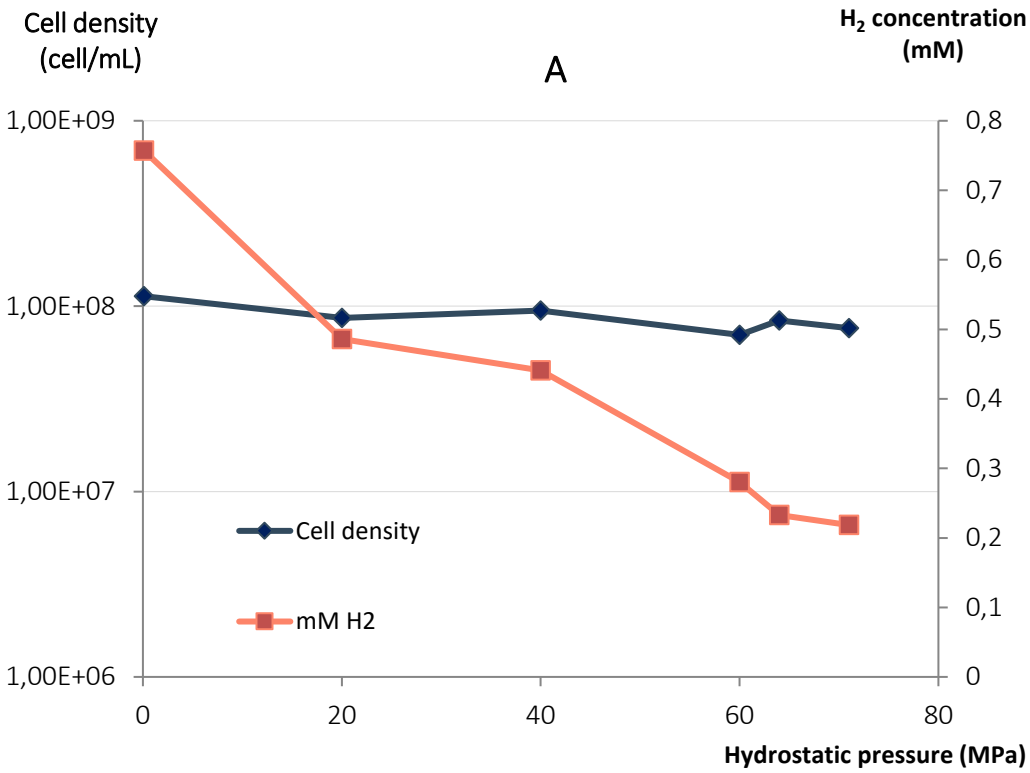

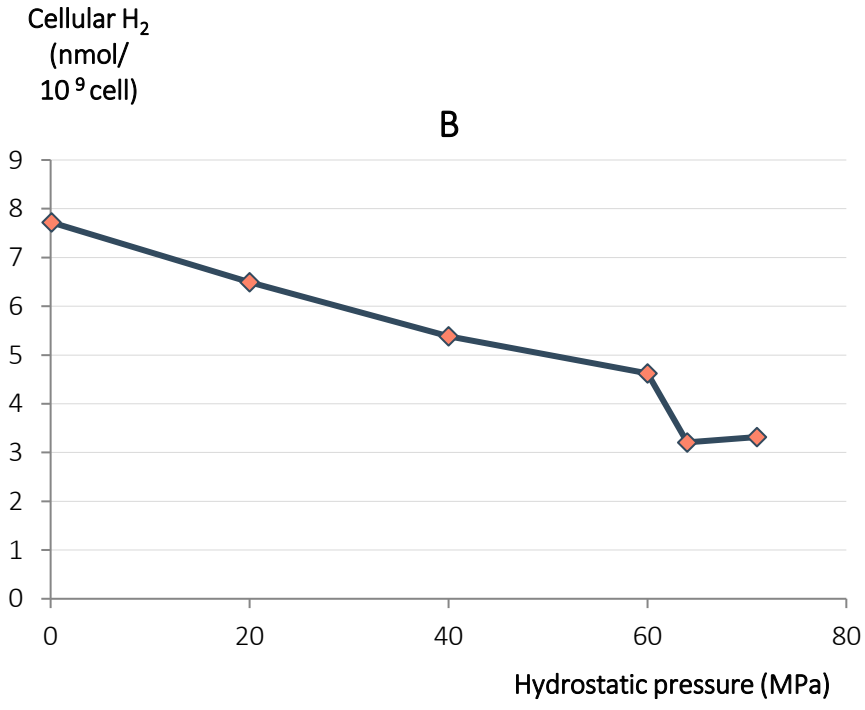

Figure 32: Absolute (A) and cellular (B) H_2 productions of *T. barophilus* MP^T in ASW with 2.5 g/L maltodextrin and 0.25 g/L S° at different pressures after 14 h of incubation

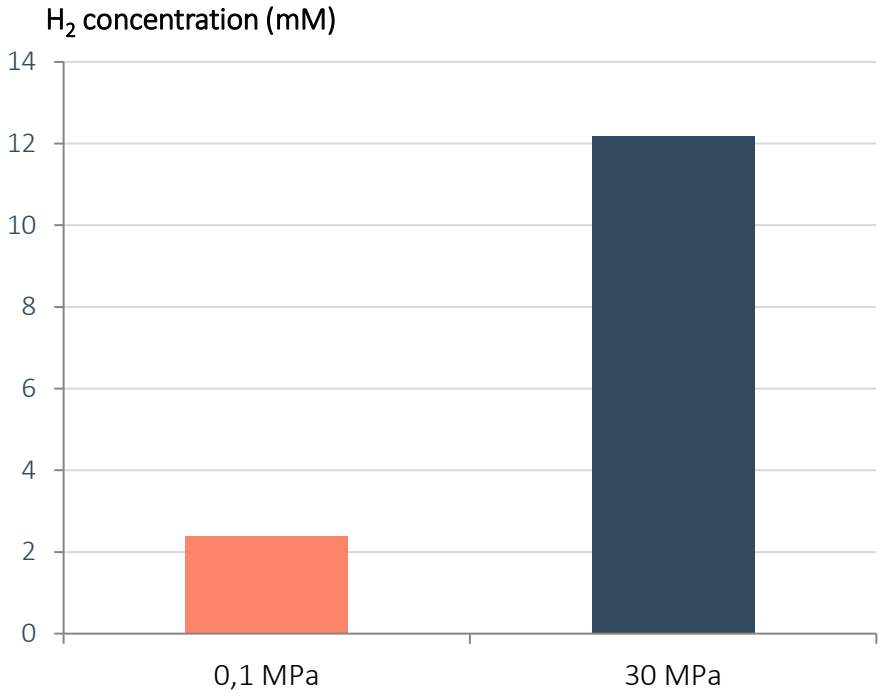

Figure 33: H_2 concentration obtained from *T. barophilus* MP^T culture in TRM at 0.25 g/L S° after 48 h of incubation at 0.1 MPa and the P_{atm}-equivalent approximated concentration of H_2 from a 30 MPa gas-pressurized culture.

Thus, contrarily to what was obtained with a compressible gas phase (*i.e.* hydrostatic pressure), this experiment indicated that high gas pressure could increase H_2 production in *T. barophilus* MP^T.

H) Other strains

T. barophilus Ch5 on formate

Formate is a product or intermediary of fermentation in many systems, and thus could be a valorized substrate to use (Crable et al., 2011). Some *Thermococcales*, such as *T. barophilus* Ch5, have been reported to grow on formate (Kim et al., 2010; Kozhevnikova et al., 2016; Oger et al., 2016; Topçuoğlu et al., 2018). Fermentation of strain Ch5 (UBOCC strain 3206) was thus compared with strain MP^T in the presence and absence of formate (30 mM) and / or maltodextrin (2.5 g/L) (FIGURE 33).

Table 16: Fermentation outcomes of *T. barophilus* MP^T and Ch5 in the presence and absence of formate (30 mM) and/or maltodextrin (2.5 g/L) after 48 h of incubation in ASW at 0.25 g/L S°

Absolute values:

Strain	Formate	Maltodextrin	H2 (mM)	CO2 (mM)	H2S (area eq.)	Acetate (mM)	Formate (mM)	Cell density (cell/mL)
MP	+	-	0,62	0,38	6352,97	0,62	-0,39	3,90E+07
Ch5	+	-	9,31	-1,97	2998,27	0,43	-3,31	3,70E+07
MP	-	-	0,69	0,36	6042,87	0,72	0,01	5,00E+07
Ch5	-	-	0,34	0,12	4193,00	0,59	0,02	5,90E+07
MP	-	+	3,80	1,35	4947,81	2,58	0,19	1,11E+08
Ch5	-	+	2,98	1,51	4230,08	2,58	0,07	1,06E+08
MP	+	+	2,86	1,93	5258,00	2,07	-0,68	5,20E+07
Ch5	+	+	13,19	1,31	3823,02	-0,01	-3,36	1,97E+08

Productions reported to H_2: (mol/mol H_2 or (cell/mL)/mol H_2):

Strain	Formate	Maltodextrin	H2	CO2	H2S (area eq.)	Acetate	Formate	Cell density
MP	+	-	1	0,618	10319	1,001	-0,628	6,33E+07
Ch5	+	-	1	-0,212	322	0,046	-0,356	3,98E+06
MP	-	-	1	0,515	8739	1,042	0,013	7,23E+07
Ch5	-	-	1	0,341	12189	1,707	0,045	1,72E+08
MP	-	+	1	0,356	1302	0,679	0,051	2,92E+07
Ch5	-	+	1	0,505	1418	0,864	0,022	3,55E+07
MP	+	+	1	0,675	1841	0,723	-0,238	1,82E+07
Ch5	+	+	1	0,099	290	-0,001	-0,254	1,49E+07

In the presence of formate, *T. barophilus* Ch5 produced considerably more H_2 than strain MP^T (+1 400 % without maltodextrin; +386 % with maltodextrin). Interestingly, in the presence of formate as principal source of carbon (without maltodextrin), Ch5 did not yield higher cell concentrations than MP^T, but substantially more H_2. Per mol of H_2, strain Ch5 produced 94 % fewer cells. This was accompanied by a slight consumption of CO_2 and, as expected, of formate, and a diminution of H_2S production. Formate seemed quite limiting for strain MP's growth, even in the presence of maltodextrin, as no high cell concentrations were reached (*maximum* of 5.2 .10^7 cell/mL). Maltodextrin seemed to rather induce acetate production, in both strains. Absolute productions tended to indicate two different metabolisms when both tested substrates were present: while *T. barophilus* MP^T seemed to tend towards acetate production with no formate degradation in order to allow hydrogenogenic growth, Ch5 rather degraded formate, but did not produce acetate, with no hampered growth. Interestingly, using maltodextrin seemed to favor CO_2 production with Ch5, although it was limited when formate was also added.

Therefore, *T. barophilus* Ch5 could be a very interesting strain to use for applied H_2 bio-production, as it seemed to allow significantly more important H_2 productions than MP^T when formate was added to the *medium*, and since it could also show negative CO_2 outcome, and limit H_2S, acetate, and biomass production.

T. waiotapuensis and T. zilligii on low-salt medium

A *medium* based on sea water (ASW), thus with high salinity, could be interesting when production units are to be located near seashores, but it still imposes important drawbacks, particularly diminishing the equipment's durability, due to corrosion (Yin et al., 2015; Zaky et al., 2018). Some *Thermococcales* can grow on low-salt *medium*, which could be interesting to save costs on equipment maintenance, and which could also permit to install production units near rivers or other fresh water reservoirs. Tests were performed on *T. zilligii* and *T. waiotapuensis* (IFREMER strain collection), using a low-salt *medium* (same as ASW but with 1.5 g/L NaCl) supplemented with either yeast extracts (2.5 g/L) or maltodextrin (2.5 g/L) (TABLE 17).

Table 17: Fermentation outcomes of *T. zilligii* and *T. waiotapuensis* in low-salt *medium* (1.5 g/L NaCl) with yeast extracts or maltodextrin (2.5 g/L) and 0.25 g/L S°, after 48 h of incubation

Absolute productions:

Substrate	Strain	H2 (mM)	CO2 (mM)	H2S (area eq.)	Cell density (cell/mL)
Maltodextrin	*T. zilligii*	0,02	0,71	15018	2,31E+06
Yeast extract	*T. zilligii*	0,06	0,75	24844	9,00E+06
Maltodextrin	*T. waiotapuensis*	0,30	1,68	32031	8,20E+07
Yeast extract	*T. waiotapuensis*	0,75	1,14	42567	8,80E+07

Productions reported to H_2: (mol/mol H_2 or (cell/mL)/mol H_2):

Substrate	Strain	H2	CO2	H2S (area eq.)	Cell density
Maltodextrin	*T. zilligii*	1	31,561	665118	102413771,2
Yeast extract	*T. zilligii*	1	12,757	422127	152920112,8
Maltodextrin	*T. waiotapuensis*	1	5,623	106914	273700126,5
Yeast extract	*T. waiotapuensis*	1	1,509	56510	116824909,3

In the conditions tested, *T. zilligii* did not yield high cell concentrations, especially on maltodextrin. Best results were obtained with *T. waiotapuensis* on yeast extracts, which maximized the amount of H_2 ensued, while limiting the associated normalized CO_2 and H_2S

co-productions. Note that *T. barophilus* MP^T did not grow in such *media* (not shown), so data cannot be compared.

Fermentation overview: discussion

The experiments described in the second part of this first chapter resulted in different data that were not statistically strong enough to allow fundamental interpretations about the involved metabolic features. Still, they permit to further project possible applied solutions in order to optimize H_2 bio-production. Optimization, in that sense, would depend on each situation, as we have shown that among the many parameters influencing fermentation, some can provide situational advantages, which translate in terms of costs. That is to say, one may not necessarily be only interested in increasing the absolute amount of H_2 concentration obtained, but rather, for example also in limiting inconvenient co-productions, or in decreasing costs associated to the conditions of culture. TABLE 18 summarizes the different tendencies observed by varying certain parameters, and TABLE 19 provides the corollaries, *i.e.* the adjustments on each individual parameter required to orientate fermentation towards four different applied questions: H_2 production optimization, and CO_2, H_2S and biomass per H_2 minimization.

Table 18: Summary of different broad tendencies observed when varying several parameters in *T. barophilus* MP^T fermentation

	Absolute	*Relative to H2*				
Increase of:	**H2**	**CO2**	**H2S**	**Acetate**	**Formate**	**Cell density**
Maltodextrin concentration	↗	↗	↘	↘	↗	↗
Sulfur concentration	↗↘	↗	↗	↗	↗	↘↗
Na2S concentration	~	↘	↗	~	~	~
H2 concentration	↘	↘	↘	↗	↗	↗
Acetate concentration	↗↘	~	~	↘	~	~
Bicarbonate concentration	↗↘	~	~	~	↗	↗
Temperature	↗	↘	↘	↘	↗	↘

Note that certain experiments were not included herein (results on different substrates, influence of pressure, tests on other strains). Tendencies are related to each parameter positive variation. Tendencies for H_2 are based on absolute values, but those for other outcomes are based on values reported to H_2.

Up arrows (↗) indicate positive variations of the measured outcome associated to increase of the concerned parameter. Down arrows (↘) indicate negative variations of the measured outcome

associated to increase of the concerned parameter. Waves (~) represent the absence of significant variations, and two arrows (↘↗ or ↗↘) represent alternatively negative and / or positive variations.

Table 19: Summary of individual parameter adjustments suggested to tend towards the different objectives, according to our results

	Objective	[Substrate]	[Sulfur]	[Na2S]	[H2]	[Acetate]	[Bicarbonate]	Temperature
Absolute	**Increase H2 production**	↗	(↘)	~	↘	(↗)	(↘)	↗
Relative to H2	**Minimize CO2 production**	↘	↘	↗	↗	~	~	↗
	Minimize H2S production	↗	↘	↘	↗	(↗)	~	↗
	Minimize biomass	~	~	~	↘	~	(↘)	↗

Note that those indications are uncomplete as there were not many different points on each gradient experiment. Furthermore, they concern T. barophilus MP^T *grown in the basic conditions described herein, on 2.5 g/L maltodextrin with 0.25 g/L sulfur, at 85 °C. Different tendencies are to be expected in different conditions, but those could still be useful indications. Absolute values were considered for the H_2 production objective, and assuming that this first had to be filled in any case, other objectives were expressed with each value reported to the corresponding H_2 concentration measured.*

Up arrows (↗) indicate that the concerned parameter has to be increased to tend towards the objective. Down arrows (↘) indicate that the concerned parameter has to be decreased to tend towards the objective. Waves (~) represent the absence of significant variations, and parentheses represent unclear patterns.

Note that we attempted to measure the amount of degraded substrate during fermentation in our experiments, by assessing the initial and final values of non-purgeable organic carbon (NPOC). These measurements were started by Jérémie Gouriou (*Laboratoire Géodynamique et enregistrement Sédimentaire*, Ifremer) on a Shimadzu TOC-L CSH. Unfortunately we could not properly calibrate the method used, at the time of writing. Therefore, these data were not considered herein. Carbon monoxide was also considered, but unfortunately, our safety conditions did not permit to obtain any data.

The reports presented herein could serve as a good basis to orientate decisions for future optimization attempts, but experiments would need to be further probed to allow accurate predictions, as errors were quite important. The addition of substrates that are not entirely soluble increases biases in volume transfers for sample preparation, as well as in microscopic counting. It also appeared that gas measurements are quite sensitive to the quality of the

individual stopper used. Overall, the lack of replicate already sets up important errors within each series of tests, which is moreover confirmed as some batches performed in similar conditions but from different series consequently gave important result differences, rendering them inaccurate to compare together.

More important uncertainties emerged from the high-pressure tests (and FIGURE 33). The fact that H2 concentration decreased as pressure increased, using our newly-developed leak-free high pressure devices for discontinuous culture (FIGURE 32) was contradictory to our expectations, especially when approaching supra-optimal pressure for growth (Vannier et al., 2015). This may be explained by the method used: although a gas phase of 8 mL was present at P_{atm}, where H_2 could desaturate, this volume was compressed as pressure increased. According to Boyle-Mariotte law, at 40 MPa, the remaining gas phase was theoretically about 20 µL. At higher pressure, H_2 saturation in the liquid phase should thus be much higher, hence the lower measured concentration when returned to P_{atm}. It is nonetheless surprising that cell densities still reached high values despite this possible H_2 saturation. Acknowledging this methodological bias, the obtained results tended to highlight, once again, that H_2 saturation would be an important parameter to consider, and that gas pressure, rather than hydrostatic pressure, should be applied in order to allow lowering of dissolved H_2.

Tests in the HP Systems continuous gas-pressurized bioreactor led to different conclusions, indicating a possible overproduction of H_2 at 30 MPa compared to at P_{atm}. While they are interesting to consider, these results also have to be tempered. They had yet to be replicated, were not performed in exact same conditions, and still included a saturation parameter for the atmospheric control. Indeed, we did not refute experimentally that a P_{atm} culture in a 300 L gas phase would lead to same H_2 absolute amounts, which would correspond to same volume-equivalent results. In that case, the overproduction would be attributed to a product-saturation relief rather than an effect of high pressure. A true evaluation of H_2 production would necessitate to perform gas-lift cultures at both high pressure and atmospheric pressure, in the same other culture conditions. Furthermore, previous studies have indicated that the hydrogenogenic metabolism of *T. barophilus* MP^T would rather be overexpressed at supra-optimal pressure for growth, and thus at 70 MPa. At 40 MPa, such system would be downregulated (Vannier et al., 2015). However, since those

works were also performed in closed, saturable environments, the associated conclusion may not apply to a gas-pressurized culture. Additionally, such mode of pressurization could also induce different physiological responses than when applying hydrostatic pressure, as reported for other models (Sturm et al., 1987; Thom and Marquis, 1984).

Yet, noticeable tendencieswere suggested. Particularly, absolute productions of H_2 seemed to depend on the substrate uptaken by the model. From our tests, it appeared that *T. barophilus* MP^T "preferred" maltodextrin over yeast extracts to that extent, but was adaptable to other types of substrates. Different strains may induce different outcomes, and could be preferably used with other substrates (*e.g.* formate with Ch5). Interestingly, we could observe, in some conditions, indications that CO_2 could be consumed, which was also suggested in the literature, but never confirmed, to my knowledge (Aono et al., 2012; Le Guellec, 2019; Moon et al., 2012). In the case of a culture of *T. barophilus* MP^T with no maltodextrin, a first experiment indicated a consumption of 0.2 mol CO_2/mol H_2 produced, whereas same conditions led to measurements of a production of 0.6 mol CO_2/mol H_2 produced (see respectively P. 169 and P. 178). But in the presence of high concentration of Na_2S (20 mM initial) and *medium* concentration of H_2 (5 % initial), more important variations were measured: respectively -1.3 mol CO_2/mol H_2 produced and -2.4 mol CO_2/mol H_2 produced (see P. 172). Determining whether those values are relevant or not would require further investigations. pH approximations were made with pH strips (Hydrion Z264784), but did not suggest any clear pattern regarding the influence of CO_2 concentrations (not shown), which could be foretold since other parameters could affect these estimations, such as, for instance, organic acid production, or unbuffered Na_2S additions.

Intriguingly, *T. barophilus* Ch5 did not yield high CO_2 concentrations when grown in the presence of formate (even seemingly negative productions, when no maltodextrin was added). This was surprising since formate oxidation leads to CO_2 and H_2 synthesis, and could exhort that issued CO_2 is re-used elsewhere in the metabolism. This strain is close to strain MP^T, so the genetic tool developed for MP^T could probably serve to modify the genome of Ch5. Furthermore, Ch5 has also been reported to grow on CO (Oger et al., 2016), and to hold a much better H_2 tolerance than strain MP^T (Le Guellec, 2019). As *T. barophilus* Ch5 is a piezophilic strain, it could also be grown at high pressure, making it a particularly appealing

model in the frame of this project. The pressure parameter could be an asset, but this fact remains to confirm. It seems that allowing a de-saturation of H_2, either thanks to a gas phase in the pressurized bioreactor or by sparging an inert gas through the incubated suspension (gas-lift) would be necessary to reach large yields.

Acetate, which can be an important end-product in certain configurations, can also be valorized. It could, for example, be re-used in the frame of a continuous culture, but might also serve to feed anaerobic cultures of methanogens, which would lead to methane, possibly further re-mixed with H_2, which could be energetically very compelling (Bergman, 2016; Jetten et al., 1992; Xue et al., 2018). Interestingly, acetate was not reported to be consumed in description of *T. barophilus* MP^T, although it was tested at lower concentrations (0.2 g/L, i.e. about 3.3 mM) (Marteinsson et al., 1999a), but other *Thermococcales* models seemed to be able to utilize it (Birrien et al., 2011; Schäfer and Schönheit, 1991; Schut et al., 2016b).

These results indicate that different states of fermentation can occur, in function of the conditions, and are promising to foresee an applied system of H_2 bio-production. There could moreover be other interesting co-products that have not been considered in this work (for example volatile fatty acids or alcohols (Schicho et al., 1993)), as well as substrates leading to better productions, or other parameters holding an influence on the system. For example, the micronutrient composition of the *medium* can effect substrate degradation, as shown with differences induced by vitamin and calcium for starch hydrolysis in *T. guaymasensis* and *T. aggregans* (Canganella et al., 2000). The actual formulation of an optimal bioprocess solution could constitute a whole new project of itself, as many parameters are to be considered. The mathematical representations of each tendencies observed could then be computed in a model describing the production of each measured compound according to given conditions, interpolating within the tested ranges of the different parameters. However, the combined effects of different parameters could be synergistic or antagonistic, and such consequences would need to be evaluated. To such extent, one would need to adopt a more fundamental point of view over the metabolism of the model.

Thermococcales, as already well emphasized in the literature, could be well-suited to apply H_2 bio-production at higher scales, as they show important versatilities in their

metabolism, allowing the manipulator to modulate the production in function of the needs, and to possibly render efficient every aspect of the process, from using waste materials as a substrate, to valorize every co-product, while fixating CO_2.

Chapter I: Screening and fermentation overview: Discussions and conclusions

The objective of the project HPBioHyd was to set bases for future optimizations of H_2 bio-production in *Thermococcales* models, particularly considering high pressure solutions. This chapter describes an applied point of view, investigating which strain and substrates could be used, and assessing a global fermentation behavior in order to orientate future decisions for further industrial solutions. While *T. barophilus* MP^T was a good *a priori* candidate for H_2 bio-production, the UBOCC screening confirmed this choice, as no apparently more interesting strain was substantially revealed by our experiments. Different outcomes of the fermentative system (H_2, H_2S, cell densities, acetate, formate and CO_2) of *T. barophilus* MP^T (as well as 3 other strains selected for their peculiar abilities) were measured in varied conditions to evaluate the global behavior of the system. These experiments, while yet to be replicated, pinpointed some strategies for optimization, according to one's interest. They indicated that outcomes result from a complex system where many parameters can hold dramatic influences. Singularly, it appeared that CO_2, a known co-product of the fermentation of *Thermococcales*, could, in certain conditions, result in negative values, indicating a possible overall consumption. This, however, needs clearer confirmation.

Several adjustments would probably have constituted benefits, in the methodology used for this work. Screening was based, on one hand, on *in silico* database analysis (MicroCyc). Such approaches often result in incomplete predictions, as based on automatic annotations, not always curated. Some pathways could be present *in vivo* whereas not predicted. For example, two starch pathways were predicted for *T. barophilus* MP^T, each missing one enzyme. Our experimental results however showed possible starch degradation by this strain. As another example, MicroCyc did not inform about an alcohol dehydrogenase described in *T. kodakarensis* (Wu et al., 2013). Nevertheless, while other examples are

probably detectable, such method remains useful to orientate a screening. In our case, however, we lacked time to test all possible inferred hypotheses (all substrates were not tested with all strains), as experimental adjustments had to be performed. Another possible critique to this screening phase would also concern the lack of applied point of view from the first steps. Indeed, assessing the practical needs of a potential industrial partner beforehand would have permitted to better orient the experiments. Particularly, the use of ASW or low-salt *media* for screening could have saved time.

The availability of adequate tools and techniques was also lacking at the beginning of this first phase, particularly for high pressure culture. As stated in the second part, our newly developed gas-phase devices for discontinuous HP incubations revealed that H_2 probably rapidly saturated when cells were grown at high pressure, due to a compressed gas volume. Nonetheless, the use of these devices could now allow to compare strains in order to reveal best H_2 producers at high pressure, as all cultures would be equally saturated. Confirmation of the observations of potential H_2 overproduction in the BHP with a gas-pressurized culture of *T. barophilus* MP^T is still awaited. If pressure eventually demonstrates not to be an asset for such bioprocess, the choice of the model strain could be re-evaluated, noticeably against the important starch-dependent H_2 overproduction of *T. kodakarensis*. Calculations should be performed to assess the costs of H_2 productions taking into account a prior-to-culture pressurization step, not necessary in the latter case.

Yet, following the first part described herein, *T. barophilus* MP^T was chosen as the model strain for this project. One could argue that Ch5, in addition to all advantages procured by strain MP^T, seemed to yield higher H_2 productions, particularly when grown on formate. Those results were however not available at the time the decision was made to emphasize MP^T for fundamental studies, described in chapter III and chapter IV. It is likely that the observations on the metabolism of MP^T could be extrapolated on strain Ch5, provided that each involved correspondence is verified to the extent possible (for example, Ch5, contrarily to MP^T, encodes a formate hydrogen lyase cluster). Therefore, a more industry-oriented application of Ch5 fermentations could benefit from all the available data on MP^T, and such a choice should not be excluded.

Results from the fermentation overview were not statistically strong, mainly due to lack of replicates. Tendencies could be true, but estimations would not permit further calculations, as for example to set up strong mathematical models. Furthermore, more practical insights would have been given if the measurements of NPOC were successful, thus allowing to estimate the part of the substrate which was consumed during each batch. Some other substrates are lacking from this analysis. Carbon monoxide, for example, has been reported to trigger high H_2 yields (Kim et al., 2017, 2020). Growing cells directly on crude waste could also have been appealing (Chen et al., 2019; Hensley et al., 2016); reaching conditions closer to what would interest an industrial partner. Other end-products were not considered, that are known to ensue from certain metabolic configurations, noticeably alanine and NH_3 (Matsubara et al., 2011). pH changes were broadly estimated here, but the actual influence of this parameter could be interesting. Other works have noted that it could indeed show changes in H_2 yields, or at more fundamental levels (*e.g.* enzymatic activities) (Bae et al., 2012a; Ma et al., 1993).

The observed tendencies (see TABLE 18), concerning our particular model, could also be compared with data from different strains reported in the literature, in order to better foresee possible extrapolations. For example, (Bae et al., 2012a) reported increased H_2 productions when increasing initial concentrations in yeast extracts, but not in starch. While our increasing concentrations in maltodextrin led to higher H_2 productions, it is likely that we would notice a similar limit if higher substrate concentrations were tried. Sulfur concentrations have been shown to influence the activity of related hydrogenases in *P. furiosus*, with an intermediate optimal concentration, which could resemble what was noted from our results (Ma et al., 1993). In batch, literature models are indicated to attain H_2 productions at the same order of magnitude, *i.e.* of several mM (*e.g.* (Bae et al., 2012a; Hensley et al., 2016; Schut et al., 2007)). But all conditions would have to be equal to accurately compare the obtained numbers. For example, (Bae et al., 2012a) reached up to almost 30 mM H_2 in 24 h with '*T. onnurineus*' on starch where we only measured about 5 mM H_2 on this substrate with *T. barophilus* MP^T, but many conditions were different (*e.g.* substrate concentration doubled and gas phase volume 5-times higher for the cited study, different *medium*). It is yet also paramount to deem that each strain can behave differently.

The fact that our data were obtained from batch reactions may be important to take into account for further application. Since some products are limiting to the different metabolic routes involved, applied solutions would probably be considered in chemostat or turbidostat, in continuous cultures. Many works on *Thermococcales* H_2 bio-productions were realized in continuous bioreactors (*e.g.* (Kim et al., 2020; Schicho et al., 1993)). As it was technically infeasible in our laboratory at the time, no data were obtained from such mode of culture, and comparisons to other literature reports would not be accurate. Considering scaling-up a H_2 bio-production solution could thus not be based precisely on the values described herein. Still, tendencies, as described in FERMENTATION OVERVIEW: DISCUSSION should be useful for setting up next experiments and orient material design choices. A first step in deciding which condition(s) to focus on would be to confirm the tendencies observed herein by reproducing the experiments described in this work in the hinted interesting *scenario*, while adding more points and replicates to be able to properly model the bioprocess.

This work consequently gave more insights into the possible applicability of *T. barophilus* cultures for applied H_2 bio-production. They did not allow to accurately estimate the costs of scaled-up productions as such, which would be better informed by a further pilot study, but gave estimations on the impact of several parameters on fermentation outcomes. They also gave considerable hope about the energetical interest of such approach, particularly if CO_2 measurements can be confirmed. Next chapters recount material and methodological adjustments made for this project (Chapter II), as well as investigations on the hydrogeno/sulfidogenic metabolism of *T. barophilus* MP^T related to high pressure (Chapter III) and to H_2 tolerance (Chapter IV), performed to be better prepared for possible fundamental optimizations of an applied culture.

Note: Part of the work presented in this chapter was valorized by a short presentation at the Gdr *Archaea* 2017 (Lyon, France).

Chapter II: Adaptation and optimization of high pressure tools and culture methods

Abstract

High pressure (HP) could be an advantageous parameter to apply for H_2 bio-production by *Thermococcales*. Several HP incubators are available at the LM2E and have allowed cultivating and studying piezophilic microorganisms. Yet, the tools and methods used for HP culture before this project, including the prototype in development of a continuous bioreactor, were not adequately applicable to envision proper study of the hydrogenogenic metabolism for practical H_2 bio-production. No *apparatus* conveniently permitted to measure gaseous outcomes of HP replicates in our discontinuous incubators, and the continuous bioreactor developed by HP Systems (La Rochelle, France) needed several optimizations. This technical chapter relates the development of glass devices for pressurized gas-phase incubations, specifically fitted to our discontinuous HP incubators, and the important modifications imposed to our continuous bioreactor in order to authorize better evaluation of the applicability of such systems in the context of H_2 bio-production. Together, those methodological progresses should allow to further appreciate the scalability of an optimized H_2 production system at high pressure by *Thermococcales*.

La haute pression (HP) pourrait être un paramètre avantageux pour la bio-production d'H_2 par les Thermococcales*. Plusieurs incubateurs HP sont disponibles au LM2E et ont permis la culture et l'étude de microorganismes piézophiles. Toutefois, les outils et méthodes utilisés pour la culture haute pression avant ce projet, comprenant le prototype en développement de bioréacteur continu, n'étaient pas utilisables de manière adéquate pour correctement étudier le métabolisme hydrogénogénique en vue d'une bio-production d'H_2 appliquée. Aucun appareil ne permettait de mesurer convenablement les produits gazeux de réplicas de haute pression dans nos incubateurs discontinus, et le bioréacteur continu développé par HP Systems (Périgny, France) nécessitait plusieurs optimisations. Ce chapitre technique décrit le développement de tubes de verre pour des incubations pressurisées à phase gazeuse, spécialement adaptées à nos incubateurs HP discontinus, ainsi que les importantes modifications imposées au bioréacteur continu, dans le but d'autoriser une meilleure évaluation de l'applicabilité de tels systèmes dans le contexte de la bio-production d'H_2. Ces progrès méthodologique devraient permettre de mieux évaluer l'adaptabilité d'une production d'H_2 à haute pression par des* Thermococcales *optimisée.*

I - Introduction

Pressure is an important parameter modulating life mechanisms. Study of the effects of pressure on biological entities, and noticeably on marine microorganisms, is a matter of interest since the end of the nineteenth century, and have been considered in both hydrostatic and gas pressures (Bert, 1878; Certes, 1884; Demazeau and Rivalain, 2010; Larson et al., 1918; Regnard, 1884). *Thermococcales* are often piezophiles, *i.e.* adapted to grow at high pressure, and have also drawn the attention of the research community as good candidates for biotechnological H_2 production (*e.g.* (Hensley et al., 2016; Kim et al., 2020; Santangelo et al., 2011; Schut et al., 2016b)). Previous studies have shown that the metabolism of some strains could be encouraged towards hydrogenogenic pathways when cultured at high pressure (Vannier et al., 2015).

Compressed gas represents one of the possible manners of storing hydrogen. Noticeably, H_2, as used in fuel cell electric vehicles, needs to hold efficient volumetric densities, in order to minimize tanks while maximizing autonomy, hence the high pressure (70 MPa often envisioned). Hydrogen production could gain efficiency if already produced at high pressure, as pressurization accounts for important costs (up to 30 %) in the processes (EDF, 2017; IEA-ETSA, 2014; Kelly et al., 2008; Makridis, 2016; Parks, 2014; Viktorsson et al., 2017).

High hydrostatic pressure *apparatus* for studying marine piezophilic microorganisms, that were described about seventy years ago by pioneers in marine piezophily studies (FIGURE 34), were quite similar to what is still currently used in specialized laboratories such as the LM2E (see PRESENTATION OF THE DISCONTINUOUS INCUBATORS AVAILABLE AT THE LM2E, P.196) (Zobell and Oppenheimer, 1950).

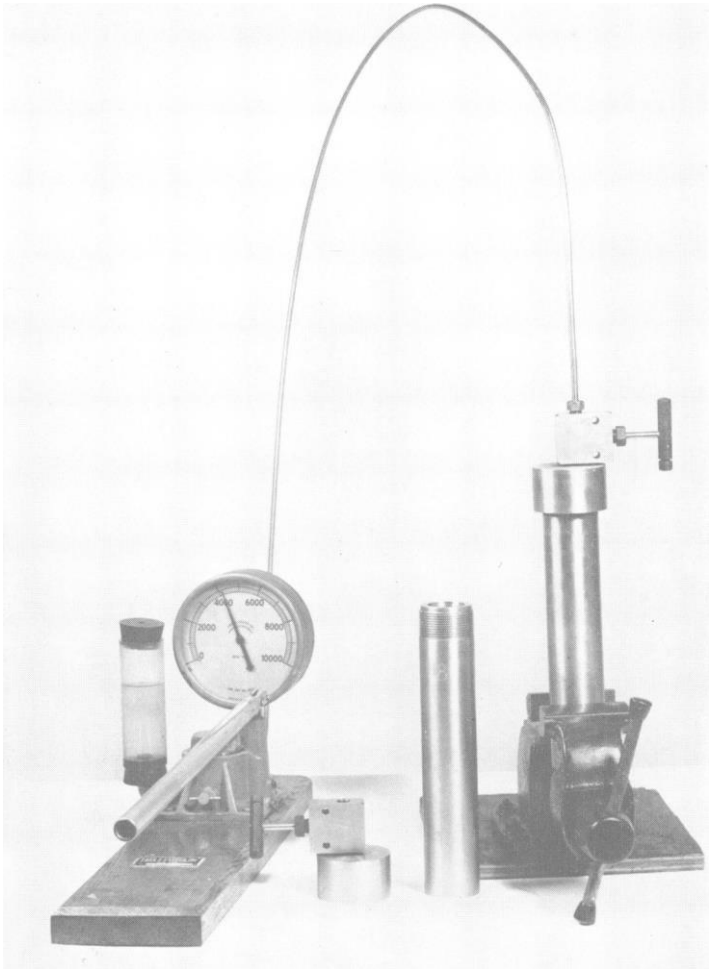

Figure 34: Assembled pressure vessel connected with hydraulic pump, used for the first studies of piezophilic microorganisms (from (Zobell and Oppenheimer, 1950))

While these systems require depressurization for sampling, other early incubators particularly focused on biochemical frames were described, which allowed to sample without depressurization, and new continuous *apparatus* were later considered for studying piezophiles (Grieger and Eckert, 1970; Parkes et al., 2009; Taylor and Jannasch, 1976; Yayanos, 1969). Systems for high gas (or barometric) pressure were described from different laboratories, some also allowing to sample without depressurization (*e.g.* (Boonyaratanakornkit et al., 2006; Miller et al., 1988b; Sauer et al., 2012; Sturm et al., 1987)). Some works have shown that the ensuing physiology from gas pressure could be differentially impacted. For example, the culture of *Sulfolobus acidocaldarius* with either hydrostatic or barometric pressures led to different temperature preferences (Sturm et al., 1987). Early observations also related potential effects with different gases on several bacterial strains (Thom and Marquis, 1984). Even at low pressures, gas solubility could be enhanced by

increased pressure, and thus gaseous substrates could become more available, which has been shown to be particularly interesting in the frame of H_2 production. In '*T. onnurineus*', slightly CO-pressurized cultures (less than 1 MPa) led to better carboxydotrophy, while an upper limit then increased CO toxicity for the cells (Jeong et al., 2016; Kim et al., 2020).

Two types of high hydrostatic culture *apparatus* were available at the LM2E: five discontinuous incubators (Top Industries, France), and one prototypical bioreactor designed to allow sampling without depressurization of the culture chamber (HP Systems, France) (see descriptions P. 196 and P. 211). However no high-pressure device was specifically intended as a H_2-producing bioreactor in our lab, nor described in literature, to our knowledge. This would require, among other features, the possibility to perform continuous culture, with a convenient regulation of various parameters, and sampling methods would need to permit to assess metabolite productions. H_2, as one of the smallest molecules, is extremely leaky as a gas, and thus materials need to be furthermore adapted. In order to allow physiological studies with many replicates, culture techniques from discontinuous reactors should be adapted for H_2 too. To the latter extent, solutions have been proposed in other laboratories, but they mainly consist in improving commercial devices for H_2-tightness, and are thus quite expensive (Takai et al., 2008).

This chapter describes the technical work achieved in parallel to what is related in the other parts of the manuscript, in order to study the effects of high pressure on our model and to foresee possible H_2 bio-production applications in such conditions. It was necessary to adapt tools and methods available at the LM2E, as specific constraints would be encountered. We aimed to advance previously employed techniques used for discontinuous high-pressure culture to study hydrogenogenic metabolism. Furthermore, based on the bioreactor manufactured by HP Systems, another objective was to further develop a new machine that would permit to evaluate the scalability of a H_2 bio-production process.

This technical chapter was thus divided into two parts describing the results of methodological optimizations:

- Adaptation and development of tools and methods for discontinuous HP culture
- Amelioration of the continuous HP bioreactor prototype

II - Discontinuous high-pressure culture

1. Presentation of the discontinuous incubators available at the LM2E

In our lab, five discontinuous incubators were available at the beginning of the HPBioHyd project. Each sampling from those devices necessitates the opening of the incubator, and thus its depressurization. Considering that frequent changes of pressure induce a stress to cell populations, following over time is not possible, and demands several different experiments. However, they allow to work with more replicates than by using the continuous bioreactor described later (see III - CONTINUOUS HP CULTURE WITH THE HIGH PRESSURE BIOREACTOR (BHP, P.211)).

Each incubator consists in one austenitic chamber of 600 mL, tightly closed with a head module comprising a manual valve, a thermocouple probe, a bursting disk and a manometer (FIGURE 35). For high temperature incubations, this system is placed in a heating slot with a three-site regulation, driven automatically by an electronic regulator and a generator. Those devices were manufactured by Top Industries (France), and can sustain up to 60 MPa of hydrostatic pressure, and be heated up to 300 °C. While pressure setting up and adjustment is manual, temperature can be set up with an accuracy of 1 °C. A manual water pump allows, connected through the manual valve on the head, to impose hydrostatic pressure inside the vessel.

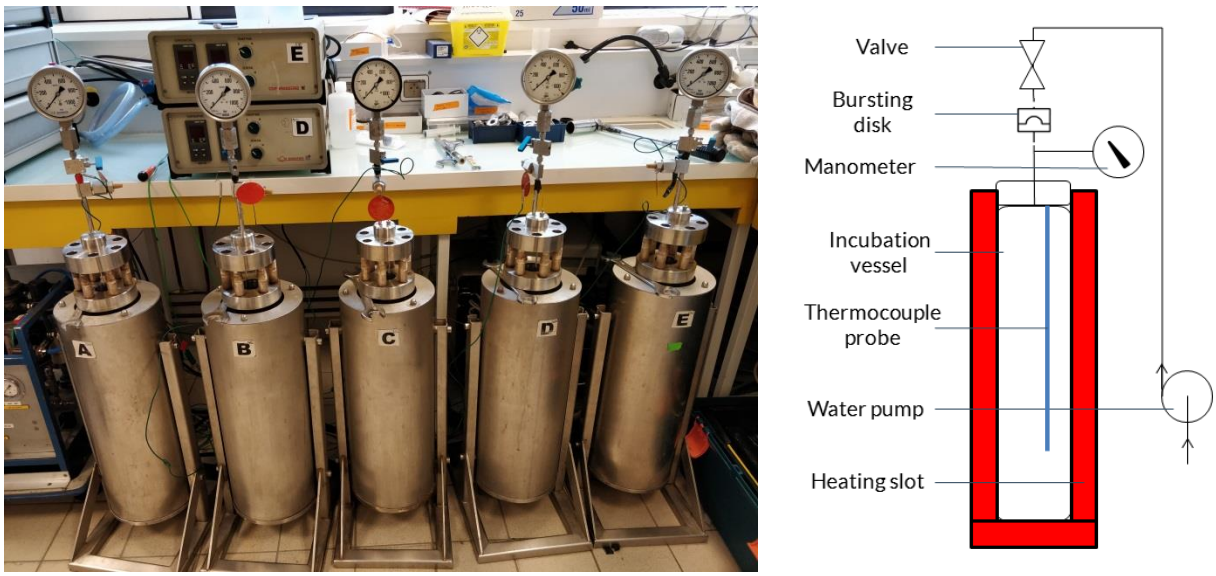

Figure 35: Photo of the five discontinuous HP/HT incubators of the LM2E and their regulators/generators at the beginning of the HPBioHyd project and schematic representation of one device

Each heating slot is about 59 cm high. A incubation vessel has a volume of about 620 cm³.

---

2. Methods for discontinuous HP culture

2.1. Initial protocols

At the beginning of this project, high pressure cultures of *Thermococcales* at the LM2E were usually realized by placing plastic Terumo syringes filled with an inoculated volume of *medium*, and closed by silicon plungers inside the HP incubators (FIGURE 37). Imposing hydrostatic pressure in the vessel *via* the manual pump, with distilled water, would then transmit to the syringe plunger, thus pressurizing the cell suspension. Each incubator can receive, for example, up to nine syringes of 2.5 mL capacity. These systems have allowed to characterize and study several piezophilic strains, in a convenient fashion (*e.g.* (Marteinsson et al., 1999a; Michoud and Jebbar, 2016)).

Nonetheless, in the context of this project, we were required to perform high pressure hydrogenogenic cultures, without sulfur, and needed to retain hydrogen. And although these usual, plastic syringes were quite practical (*e.g.* permitted a high number of replicate in each incubation), they were not gas-tight. Not even mentioning how H_2 could easily leak, a short

contact with air or oxygenated water induced oxidation of the *medium*, as indicated by the resazurin color shift.

2.2. Repeatability assessment and protocol adaptation for HP culture

Probably due to this gas permeability, many first experiments resulted in inconsistent growths, or no growth at all, in conditions previously reported as successful for growth of *T. barophilus* MP^T. To experimentally confirm that oxidation was detrimental to the physiology of our strains, growth repeatability was tested.

Cells were pre-cultured at atmospheric pressure (P_{atm}) in TRM with 0.25 g/L of colloidal sulfur (S°), for 15 h in a dry incubator at 85 °C (reaching 1.0 $.10^8$ cell/mL). Then, a volume calculated to start the experiment at 2.0 $.10^6$ cell/mL was used for inoculation in TRM with 0.25 g/L S° (see MATERIALS & METHODS - GENERAL) in an anaerobic glass flask containing enough *medium* for all samples. All syringes were vacuum emptied then refilled with 100 % N_2 eight times, and were immediately used to take up 1.5 mL of *inoculum*. 33 samples were pressurized at 40 MPa, three syringes were placed at P_{atm} in an anaerobic jar filled with N_2, and three samples were placed at P_{atm} in a dry oven (air), all for 16 h at 85 °C.

As presented in FIGURE 36, only about 57 % of pressurized samples reached expected cell concentrations, with no color shift from resazurin. About 30 % of all samples were pink from the resazurin shift (oxidation). All samples from incubator E gave poor results, though no material dysfunction was noticed. P_{atm} controls left in air did not grow, but nor did the control samples put in anaerobic jar. This could tend to indicate that time between transfer of the *inoculum* into the syringes and the placement in the jar is a key factor for further culture development.

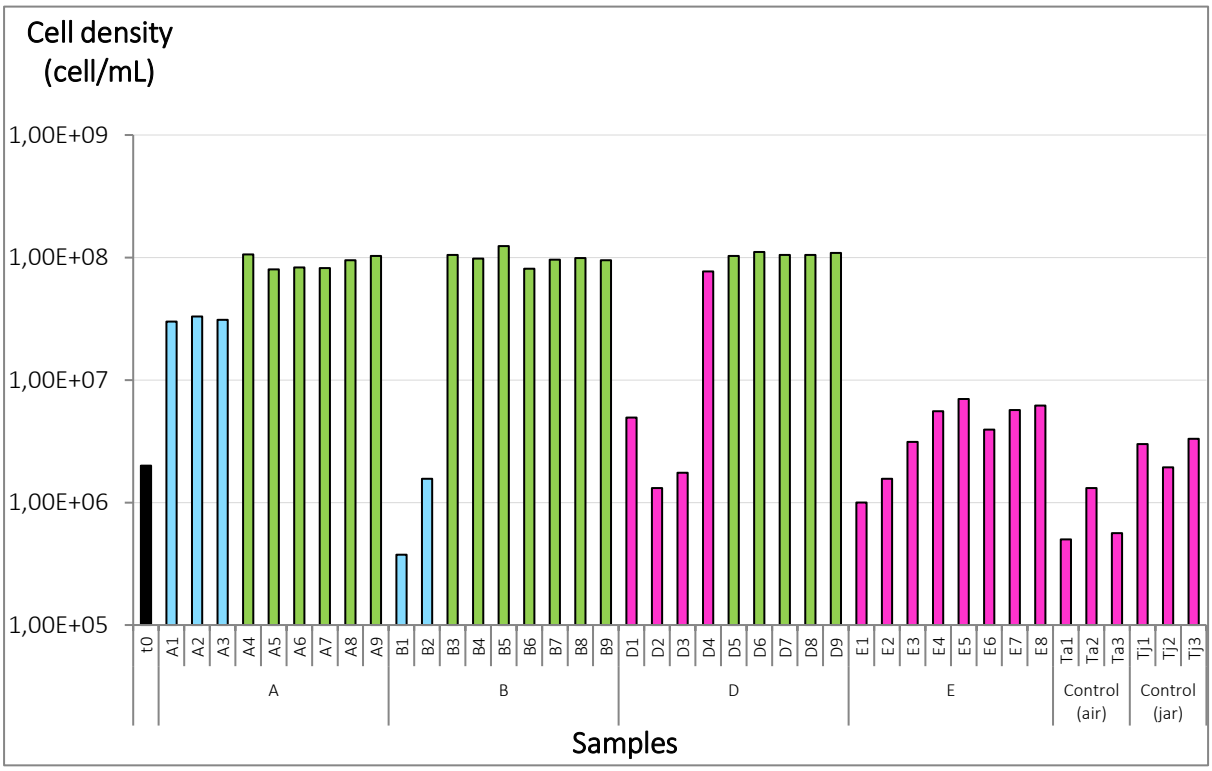

Figure 36: Cell densities of different samples of the same *inoculum* for repeatability test of the usual HP culture protocol, obtained after 16 h at 85 °C in TRM at 0.25 g/L S°, at 40 MPa (A to E) and at P_{atm} (controls)

*The **black** bar (t0) is the initial cell density of the inoculum. **Green** bars designate samples not visually oxidized (resazurin) and grown up to expected density. **Pink** bars design samples visually oxidized. **Blue** bars design samples which have not reached expected cell density but were not visually oxidized. The letter in a sample name precises the incubator used (A to E). 'Ta' samples were air P_{atm} controls, and 'Tj' samples were anaerobic jar P_{atm} controls.*

Be that as it may, this experiment showed that in those conditions, samples can be oxidized and growths cannot be considered as repeatable in triplicates, probably due to a lack of gas-tightness. And undoubtedly, if O_2 can pass through the syringe, so can H_2. The usually performed protocol for HP culture of *Thermococcales* was thus not suitable in the context of the HPBioHyd project.

In order to culture our strains in better controlled conditions, other protocols had to be adapted. Anaerobic glass flasks were consequently chosen to perform gas-tight cultures, as reported in previous works (*e.g.* (Le Guellec, 2019)). Instead of sampling the *inoculum* with plastic syringes, it was anaerobically transferred in a previously N_2-flushed, then vacuumed flask, topped with a butyl stopper (FIGURE 37).

*On the left, some syringes appeared pink after a short exposition to air (*e.g. *15 min), showing the oxidation of the* medium. *On the right, the suspensions are enclosed in fully-filled glass flasks, preventing gas exchange from the external environment.*

Figure 37 : Photos of plastic syringes (left) and fully-filled glass flasks (right)

The transfer occurred *via* two needles melted and stuck one to another, thus in an anaerobic fashion. In order to avoid glass breaking when pressurized, flasks have to be completely filled with liquid, with all the gas bubbles cautiously removed. While this method requires longer time to set up the experiment, it allows to obtain acceptable standard deviations in triplicates, and a growth rate comparable to published results (Marteinsson et al., 1999a), as shown in the growth curve of FIGURE 38.

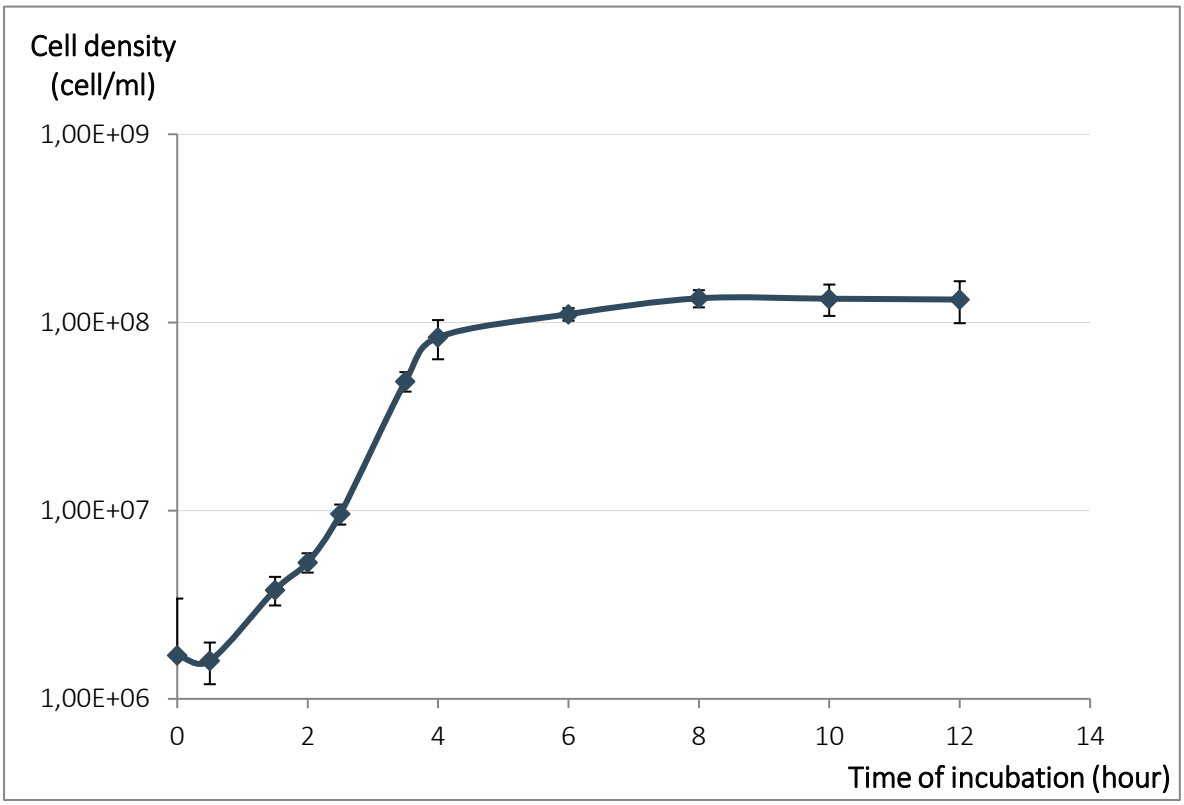

Figure 38: Growth of *T. barophilus* MP^T over time at 40 MPa, 85 °C, in TRM 0.25 g/L S°, using the fully-filled glass flask method

Error bars represent standard deviations. Samples made in triplicates. Growth rate was estimated at 1.14 h^{-1}.

While this protocol permits to study growth of our model at high pressure, and was extensively used for the work described in chapter III, measuring gas production would require a transfer in a larger volume for degassing. Several attempts of such transfer did not lead to any satisfying result. Consequently, a new tool for gas-phase, gas-tight HP incubations was developed.

3. Development of a new device for gas-phase, gas-tight HP incubations

During this project, a new, simple device for H_2-tight culture with gas phase in HP discontinuous incubators was conceived and realized. This work was done in collaboration with Raphaël Brizard (LM2E, Ifremer) and Damien Le Vourc'h (RDT, Ifremer).

In order to study the hydrogenogenic metabolism of *Thermococcales* strains using the LM2E discontinuous high-pressure incubators, several methodological needs had to be met. We developed a solution to retain properly the H_2 produced, needing limited or no gas transfer for analyses, temperature-resistant, holding a certain pressure resistance (several bar, in order to support possible variations in pressurization and depressurization phases), biologically and chemically inert, inexpensive, simple to use, simple to manufacture, and adapted to our incubators, volume-wise, to maximize the number of replicates possible while allowing sufficient volumes for our experiments. Microorganisms can sometimes be cultured in commercial gas-tight syringes (such as Hamilton™ 1000 series), but these are not perfectly adapted to our requirements. Particularly, they are quite expensive (about 120 € per 10 mL syringe and 225 € per 25 mL syringe, for Hamilton™ 1000 series at the time of writing), have a limited lifespan due to damageable plungers, are not volume-adapted to our incubators, and would require transfer for gas analysis. We thus chose to find our own solution, for which development the steps are described hereafter.

3.1. Realization: From first ideas to glass prototypes

We first drew theoretical principles for solutions. It rapidly appeared that a syringe-type system, *i.e.* a tube with a mobile plunger, would solve the need for gas-phase incubation, due to a compressible volume, preventing any breaking when pressurized (FIGURE 39). One or several joints would be mounted on the plunger to ensure gas-tightness. An initial gas volume would be set up at P_{atm}, and would then be reduced by high hydrostatic pressure, and expand again when sampling, *i.e.* returning at P_{atm}. In order to be the most comparable with our usual anaerobic culture protocols, we envisioned the top of the tube with a classical stopper for anaerobic culture. Thus, measuring gas concentrations would be possible simply by entering a needle into the tube, as typically done for anaerobic flasks (see MATERIALS & METHODS - GENERAL). Once the principle defined, glass prototypes of the tubes were manufactured by a glass-blower, Claude Calvarin (UBO) (FIGURE 39). We first attempted to fabricate our own plungers by cutting butyl stoppers and casting polytetrafluoroethylene (PTFE), without success.

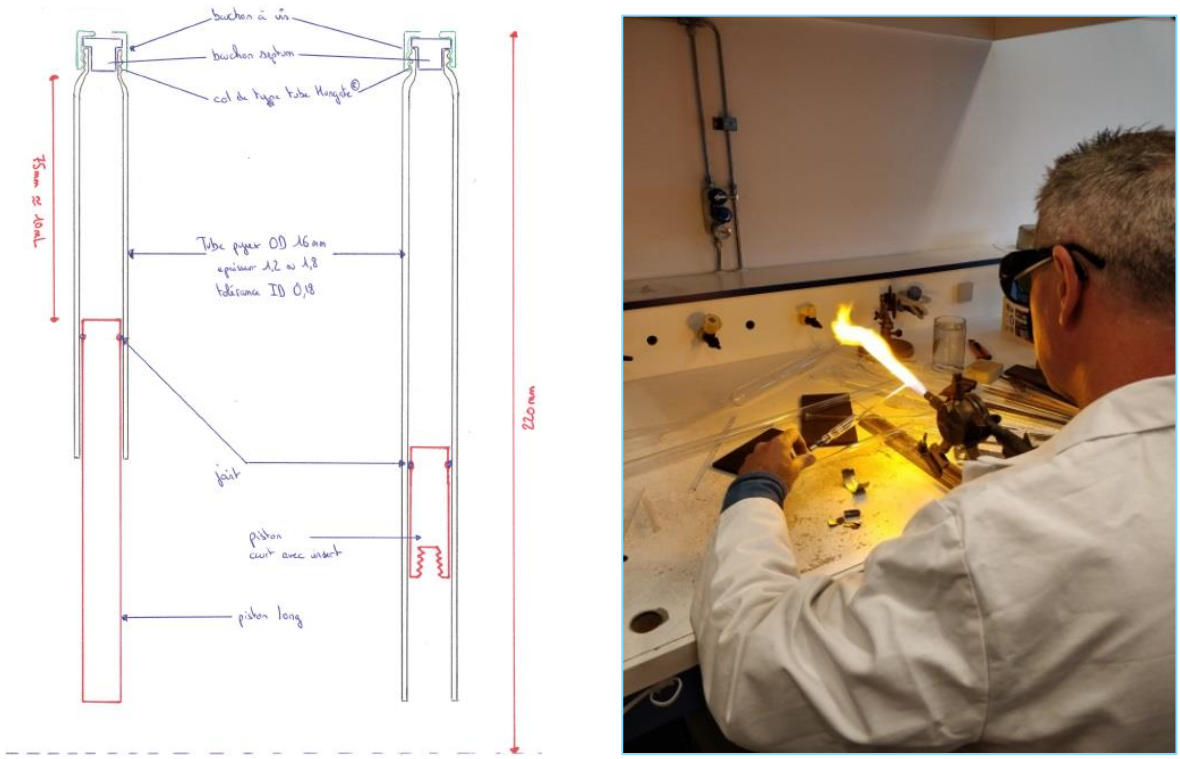

Figure 39: (Left) Example of initial hand-made drawing of the envisioned system. (Right) Claude Calvarin working on the manufacturing of the first tube prototypes.

Note that we initially thought of long plungers, then switched to more space-saving ones.

Damien Le Vourc'h (RDT, Ifremer) then calculated suitable dimensions of the tubes, tops, plungers and joints necessary, in order to be able to fit 6 such devices per HP incubator, with minimal lost volumes, and maximal gas-tightness. We used the first glass prototypes to test different joint and stopper types and materials, emphasizing noticeably how H_2 could be retained. These experiments, described below, were useful to orientate the definition of the prototypes, but due to a limited number of first tubes available, samples were not replicated. Materials were pre-selected based on their temperature resistances, and reported tightness. Four types of joints were hence considered: O-rings in nitrile rubber (acrylonitrile butadiene, NBR) or in fluoro rubber (FKM/FPM), lip seals in NBR or in polyurethane (PU). Plungers were manufactured in PEEK (polyether ether ketone), in two different versions, to handle lip seals and O-rings. Butyl stoppers are standard in anaerobic culture and have shown good H_2-tightness, provided they are new. Skirted silicon stoppers were also tried.

3.1.1. Joint friction tests

Dimensions were calculated for the joint to tightly fit the tube at all time, even when warmed up and pressurized. However, adherence to the glass tube, during plunger movement, appeared to be another critical factor for joint selection. A too adherent material could induce plunger jolts and/or delays, due to friction, during the pressurization and depressurization phases. It could thus lead to internal pressures being temporarily too different from its environment (either while increasing hydrostatic pressure or returning to P_{atm}), which could (i) cause fractures in the glass if this difference is too important, or (ii) stress the cells with too brutal pressure variations. On another hand, a joint gliding too easily would not allow any differential pressure from its environment, without plunger retention. It is however convenient, for routine microbial culture, to incubate cell suspensions with a slight overpressure (*e.g.* +0.5 bar). The adherence parameter was particularly important to consider close to P_{atm}, where the resistance induced by friction could hamper balancing of the pressure between inside and outside the tube (at higher pressures, this resistance would rapidly be overwhelmed).

To assess joint adherences, the different solutions were placed in a transparent, tightly-closed plastic bottle, submerged in water, then inflated with a manual pump up to 7 bar (FIGURE 40). Our experiments (not individually displayed herein) showed that lip seals were too adherent, inducing important jolts while pressurizing (*e.g.* quasi-instant three-fold increase of internal pressure). O-rings were tried by using one or two joints on the same plunger. The two-joint version was too adherent and induced jolts. One FPM joint still induced jolts but in a limited manner. No jolt was observed with NBR one-joint version in our experiments. Both NBR and FPM one-joint versions and retained a bit of pressure in the tube (+ 0.5 bar and +0.3 bar respectively) when returning to P_{atm}, which was interesting for gas-phase culture, even considered at P_{atm}. Note that in a dry environment, without inducing a plunger movement (for instance by depressurizing), the systems could withhold about + 1 bar of relative pressure without triggering volume adjustment.

Air could be pumped in a tightly closed bottle, where the tube with the plunger was placed. Tests were also performed with tubes pre-immerged in water.

Figure 40: Example of joint behavior observation in dry overpressure

Note that those devices were also considered as made of stainless steel, and would have been adapted by HP Systems. At the lab, we focused on a glass version, since being able to see through the tube presents several advantages for microbial cultures (*e.g.* when employing color indicators, or using the plunger position as an indicator of gas production). Stainless-steel tubes could however require other materials for joints, as adherence might be different, so further tests would have been necessary. Yet, no stainless-steel prototype was produced.

3.1.2. H_2-tightness assessments

To verify whether H_2 could be retained in the FPM or NBR O-ring systems, they were filled with 2 bar (absolute) of different gas mixes (pure H_2 or 5/95 H_2/N_2 mix). A leak detector (Restec #22655) could not be activated around the tubes, indicating that their leak rate was not important enough (< 1.0 $.10^{-5}$ mbar.L/s). Thus, the systems were incubated at room temperature and P_{atm}, overnight, and the remaining pressure inside was measured. Unfortunately, no gas chromatograph was available during that time, so gas concentrations could not be analyzed. Our experiments showed that best pressure retention was obtained with NBR joints, leading to a loss of only 50 mbar at 5 % initial H_2. FPM O-rings lost a little more (100 mbar) but were only tested with pure H_2. Lip seals were not as gas-tight (400 mbar lost with 5 % initial H_2). Interestingly, used butyl stoppers confirmed to poorly retain gas in those conditions (900 mbar lost with 5 % initial H_2), as tried on classical tube (leaks could not

be attributed to joints). Skirted silicon stoppers did not retain any pressure in those conditions, so their use was abandoned. When incubated at 40 MPa and 85 °C, with pure H_2, a slightly higher pressure lost than at P_{atm} was observed with FPM O-rings (200 mbar).

Therefore, in our conditions, a small gas leak seemed inevitable, but an adequate calibration of such pressure lost could allow to accurately assess H_2 productions in our cultures. Although FPM is supposedly a bit more resistant to autoclave than NBR, NBR O-rings were selected for further tests, as they seemed to present slightly higher pressure retention at P_{atm}, H_2-tightness, and were cheaper as consumables. Butyl stoppers seemed good solutions; however, they are to be used only once or twice, to ensure H_2-tightness.

3.1.3. Growth tests

Overnight incubations of *T. barophilus* MP^T in TRM (initial 2.0 $.10^6$ cell/ml) with 0.25 g/L S° (6 mL *medium* 8 mL N_2 at + 0.5 bar initial) at 40 MPa and 85 °C led to cell densities (concentrations around 1 $.10^8$ cell/mL), indicating that growth was possible in our system (NBR O-rings used).

3.1.4. Prototype manufacturing

Following these initial tests, and thus having formulated suitable solutions with PEEK plunger, butyl stoppers and NBR O-ring joints, more tubes were manufactured by a glass factory (Batailler, Treillers, France) allowing to perform more replicates, contrarily to the first tests. Tubes were 220 mm long, with screw top, and an external diameter of 1.3 mm (+/- 0.2 mm) and an internal diameter of 12.5 mm (+/- 0.010 mm).

In addition to a solution fitted to the volume of the incubators, the system would need to be very easily handleable, for quick and reproducible experiments. A custom mount was designed, able to hold all the devices in a safe manner as glass remains fragile, and facilitating the measurements. It had to retain the plungers in case of a too important pressure, and allow the easy re-positioning of this one, in order to match the gas chromatograph requirements for sampling. Indeed, as many instruments have a pressure limit, it is thus useful to modulate the internal pressure of our devices before performing the measure. To such extent, a threaded rod can be quickly attached to the plunger. A dynamometer could

thus be used (whereas it was not done during this project) to adjust the internal pressure in the device for sampling.

After discussing the principles with Raphaël Brizard and Damien Le Vourc'h, the latter produced technical drawing, and mounts were first printed in poly-lactic acid (PLA), a thermolabile polymer easily handled by 3D printers, at the UBO Open Factory (by Mathieu Cariou, Yves Quéré and Tomo Murovec). Once the dimensions of the prototype validated, several pieces were printed in a thermostable resin (Formlabs SLA form 2, high resistance) (FIGURE 41).

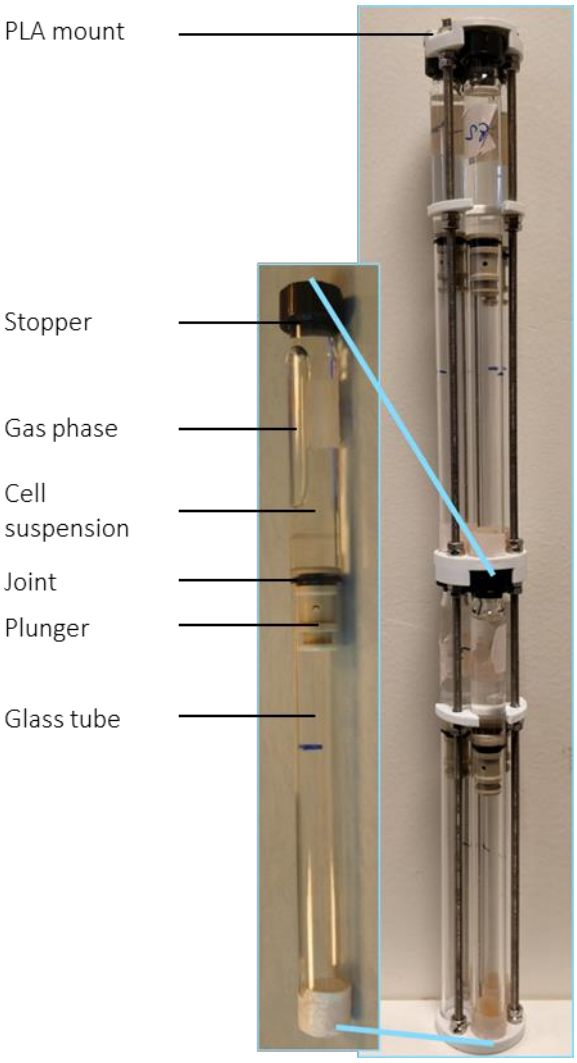

Figure 41: Prototypical system of the new device for gas-phase, gas-tight HP incubations

3.2. Tube calibration for hydrogenogenic fermentation studies

Though H_2 could be retained in the tested conditions, a small leak was inevitable, even when using materials giving our best results (NBR O-rings and butyl stoppers). However, it is possible to use the devices for accurate measurements of gas productions, as long as this leak is known and quantified. For each type of experiment, a calibration has to be performed, using known gas mixes. From previous experiments, movement of the plunger seemed to be a key factor of gas leak. As various pressures potentially impact plunger movements differently during pressurization and depressurization, calibrations have to be realized for each pressure of culture. Two important parameters are to consider: the possible loss of internal gas pressure, corresponding to global gas leaks, and the relative proportion changes for each gas, corresponding to possible more rapid leak of one molecule type over the others (for example, H_2 being smaller than N_2, it could potentially be leakier, resulting in a changing relative concentration).

A preliminary calibration experiment, in the time-frame of this PhD, consisted in incubating at high pressure typical volumes of gas in the tubes (8 mL), with different mixes (3 – 5 % and 45 – 47 % of H_2 (in N_2)) corresponding to our usual range of H_2 detection for fermentation tests. Each sample was realized in five replicates to minimize the errors. Each tube had a known initial internal pressure at a fixed volume, and gas concentrations and final internal pressure at the same initial volume were measured by gas chromatography and a pressure probe. They were incubated at 40 MPa and P_{atm}, in the discontinuous HP incubators, at 85 °C, for 16 h (FIGURE 42).

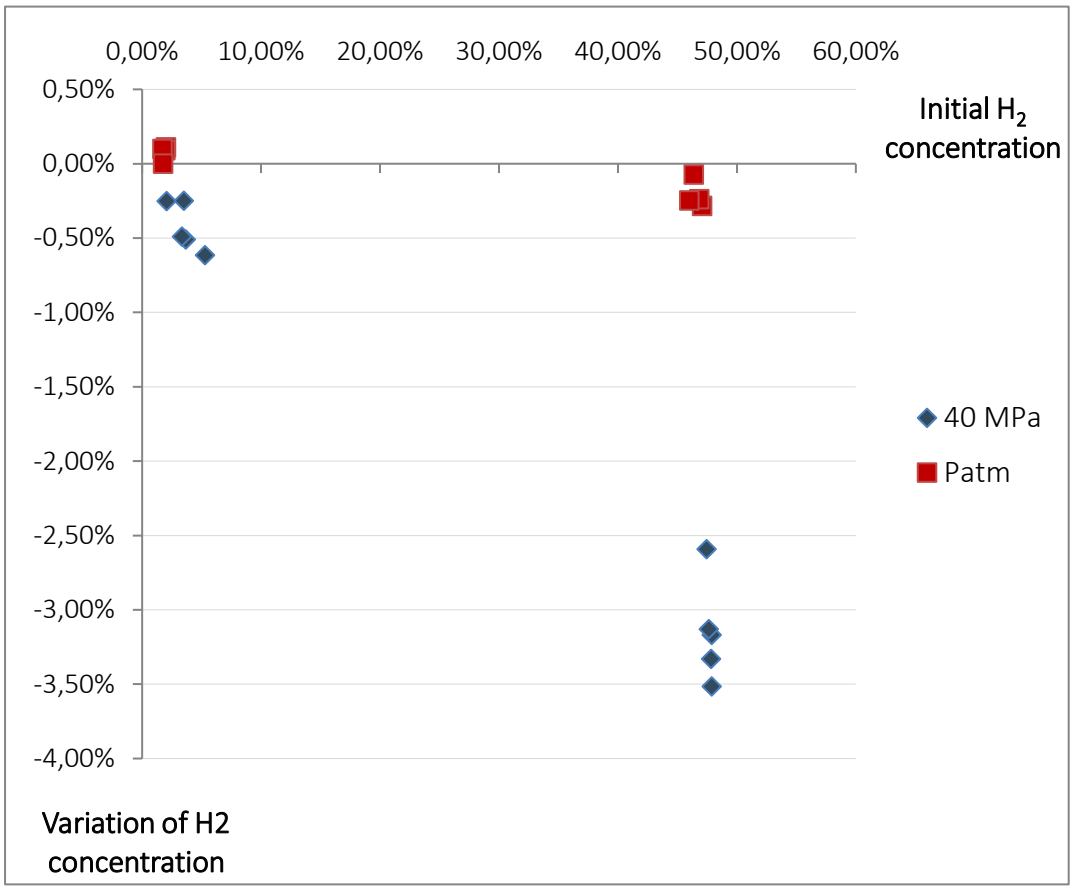

Figure 42: Representation of H2 composition variations in different H_2/N_2 mixes incubated at 40 MPa and Patm in the new device for gas-phase, gas-tight HP incubations

Each item on the graph represents a unique sample.

Note that no significant pressure loss was observed out of two series of 5 replicates incubated, at both P_{atm} and 40 MPa. This indicates that no important global gas leak occurred during incubation. Gas concentration measurements show that at P_{atm}, no significant H_2 leak occurred. At 40 MPa, thus with plunger movements, a small proportion (around 0.25 - 0.5 % H_2) of the initial H_2 was lost, which was more important at higher initial concentrations (around 2.5 – 3.5 % H_2).

Therefore, although H_2 still leaks during high pressure incubation, this loss is not important and is quantifiable, which would allow to complete an accurate calibration curve to re-calculate the actual H_2 productions in our fermentative systems. As H_2 is a saturating end-product of *Thermococcales* metabolism, a system losing hydrogen could influence the physiology of the cells, thus inducing bias in the culture observations. It is however probable

that most of the leak occurs when returning to P_{atm}, when the plunger can move with a positive pressure difference between the tube and its environment. Considering this fact, it is thus unlikely that H_2 leaks impact the cell physiology during a fermentation, as saturation would still likely occur during incubation, until depressurization.

4. Discontinuous HP culture methods and tools: Conclusions

The discontinuous high pressure incubators of the LM2E allow to perform several replicates at the same time, which can be useful for physiological studies. However, protocols used commonly in the LM2E did not allow reproducible results in the frame of this project, particularly for growth with limited sulfur and for measurements of H_2 productions. Consequently, different protocols were adapted, using fully-filled glass flasks, dramatically reducing error in replication. In order to allow gas-phase incubations, even at high pressure, new devices were developed. While commercial equivalents are available (gas-tight syringes), they present several drawbacks. The systems developed herein have been calculated to cost, at the prototype phase, around 86 € per unit, whereas equivalents are much more expensive (*e.g.* around 200 € per unit for equivalent volume). We can moreover expect the price per unit to decrease if manufactured in larger quantities. As described in this chapter and seen in chapter I, and while leak calibrations still need to be better defined, those tubes can be used to accurately measure H_2 productions at high pressure. However, since the device volume is variable, gas volume considerably diminishes when pressurized (*e.g.* around 400 times smaller at 40 MPa than at P_{atm}). As a result, gaseous end-products tend to remain more in solution, saturating the *medium*. Yet, those tubes could serve to compare piezophilic strains in similar conditions, and could also be used to quickly monitor microbial gas productions at atmospheric pressure.

III - Continuous HP culture with the high pressure bioreactor (BHP)

As described in chapter I, culture conditions influence dramatically the rate of H_2 production. Particularly, the *medium* can become saturated in products, such as H_2. In an applied point of view, H_2 bio-production would thus benefit from conditions inducing a frequent relief of such saturations. Furthermore, studying physiological dynamics under high pressure is inconvenient by using discontinuous bioreactors, as they necessitate as many incubators as sampling points. It would also benefit from the ability to maintain a given growth phase.

Consequently, a custom, prototypical high pressure/temperature (HP/HT) bioreactor was manufactured in 2014 by the company HP Systems (La Rochelle, France) for the LM2E, allowing to automatically maintain a high hydrostatic pressure, even when sampling. While originally thought as a convenient tool for studying piezophiles (*e.g.* through the possibility to enrich pressurized *in situ* samples and isolate piezophiles without decompression), this high pressure continuous bioreactor (BHP) was adapted during the project HPBioHyd in order to help considering applied H_2 bio-production at high pressure by *Thermococcales.* Much of the work described in this part was realized with the assistance of Raphaël Brizard (LM2E, Ifremer) and Erwann Vince (LM2E, CNRS). HP Systems helped in designing and realizing the modifications described, and in teaching me how to properly manipulate high pressure equipment in May 2017 at La Rochelle (particularly Hoang Nguyen Duc, Romain Avril, Romain Flamant, Serge Theodule, Jean-Mathieu Pauillacq, Gregory Caillaud, and Cedric Vadepied).

1. Presentation of the initial state of the machine and protocol for HP culture

The bioreactor (FIGURE 43) had a usable capacity of about 365 mL, a maximal operating pressure of 120 MPa and a range of operating temperatures from 10 °C to 200 °C.

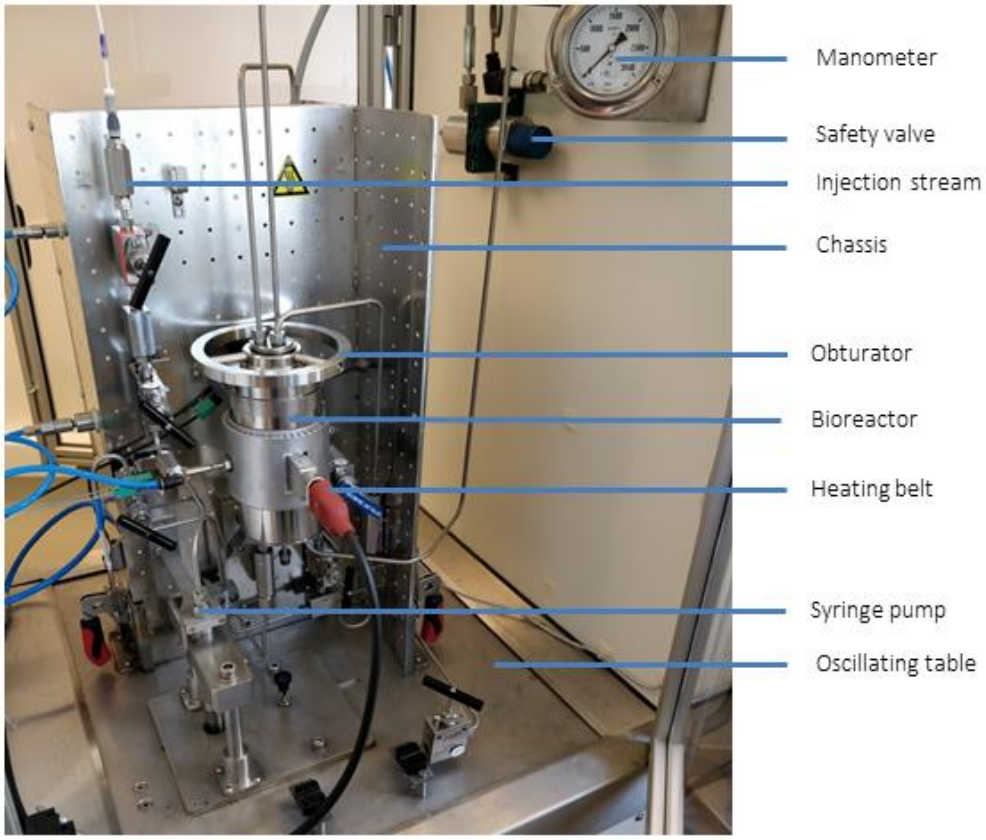

Figure 43: Initial state of the BHP with some main organs annotated

The machine is constituted of a modular aluminum/stainless steel chassis with an oscillating table and an operator desk. The bioreactor part is mounted on a detachable deck for facilitating maintenance and cleaning, which comprised a high-pressure regulatory circuit. Two electrical cabinets powered command and motorization functions, respectively. A laptop served to drive the automaton and record data, thanks to a HMI (Human-Machine Interface). The equipment was checked for safety and compliant to the European directive 97/23/CE.

The bioreactor circuits originally consisted in three main modules, as seen in FIGURE 44, functioning as described below.

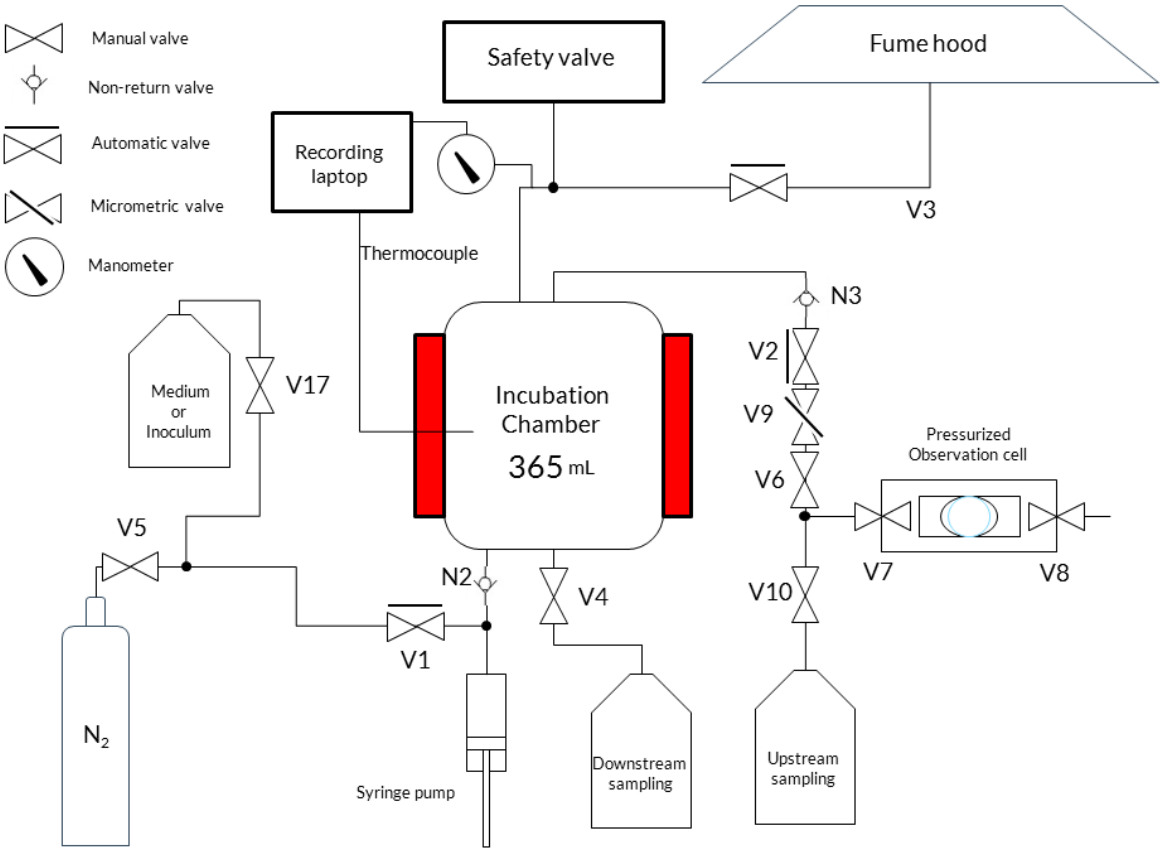

Figure 44: Schematic representation of the organization of the HP/HT continuous bioreactor manufactured by HP Systems (BHP) in its initial state

---

Box 3: Three initial functional circuits of the BHP

Injection circuit

A manual valve (V17) allowed to connect the bioreactor to a low-pressure fluid (for instance an *inoculum*, fresh *medium* or cleaning products), injected into the circuit when the automatic valve V1 was open and the syringe pump was in pulling phase. Then, V1 closed and the pump pushed the injected fluid inside the bioreactor, through the non-return valve (N2). Pumping could continue until the pressure setpoint is reached.

Downstream sampling circuit

A manual isolation valve (V4) allowed to drain the content of the bioreactor.

Upstream sampling circuit

A manual debit valve (micrometric) (V9) and a manual isolation valve (V6) allowed to sample from the top of the incubator, at a debit small enough to allow automatic pressure compensation by the syringe pump. An automatic valve (V2) and a non-return valve (N3), upstream of these organs, permitted to further set an automatic management of this sampling. It could then be taken out directly or passed in a pressurized observation cell.

During a cycle, temperature and pressure were automatically regulated thanks to the parameters set on the laptop by the user, through the HMI. *In situ* parameters were controlled thanks to a manometer and a thermocouple. Oscillations of the table could be manually set *via* a potentiometer.

Though installed three years before the project, the BHP had not really been exploited before 2017. Raphaël Brizard had managed to obtain grown cells of *T. barophilus* MP^T at 40 MPa as a proof of principle, but the bioreactor remained to be more characterized, in order to foresee a practical fermentation at high pressure. We thus aimed to evaluate the potentials and limits of this machine.

We set up a sterilization protocol, which could be performed before and after the cycle, consisting in circulating a 10 % Deconex solution (Deconex 61 DR, Borer 281238 (industrial detergent composed of gloyxal 6%, dioctyl-dimethyl ammonium chloride 2,3%, alcohol and surfactants, at neutral pH)) pre-heated at 90 °C in the circuits, for at least 2 min then rinsing three times with sterile water. Ideally, such a protocol would have to be re-confirmed by incubating sterile *medium*, to see if a microbial contaminant development would occur. However, the solution used showed no remaining observable cell on a Thoma counting chamber (*i.e.* if there were remaining cells, they were less than $1.5 .10^4$ cell/mL dense) in the rinsing water. This protocol was hence suitable for our following experiments.

1.1. Cycle for growing cells under hydrostatic pressure

We managed to reproduce cell growth, sampling on final points. For a typical *T. barophilus* MP^T culture (see FIGURE 45), after cleaning, anaerobic conditions were set up by 5 min of N_2 flushing, *via* the injection circuit (valve V5, with "sweeping" mode on the HMI). An *inoculum* was then anaerobically injected inside the bioreactor, using the HMI "filling" mode. Once the container full, the HMI was switched to "cycle" mode, where a pressure and a temperature targets were defined, and the system was automatically pressurized and heated thanks to the heating belt and by pumping more *inoculum* (or any chosen filling fluid). An automatic purge valve (V3) was triggered whenever measured pressure overcame the target, leading the pressuring fluid towards a fume hood, and the syringe pump reinjected the filling fluid whenever this measure was below the target. Thus it was possible to perform samplings (*via* upstream and downstream circuit, provided the used was careful not to open the manual valves too dramatically) while maintaining high hydrostatic pressure in the bioreactor. However, several possible or necessary optimizations were soon revealed.

1.2. Several points of optimizations

Our first experiments on the continuous HP/HT bioreactor manufactured by HP Systems outlined several points that needed to be modified and optimized in order to obtain a system better suited to our H_2 bio-production applied point of view.

1.2.1. Inhomogeneity

The oscillating table, unsurprisingly, revealed to be inefficient for mixing suspensions in the bioreactor full of liquid (FIGURE 46). Samples from upstream circuit showed significantly lower cell densities than from the downstream circuit (respectively around $5 .10^6$ and $1 .10^8$ cell/mL, for instance). Attempts were made to manufacture a floating autonomous device, which would asymmetrically move with the system oscillation, and thus induce mixing of the suspension, but we failed to obtain a functioning solution. Furthermore, though connected to fixed parts with flexible tubing, fragilities emerged after few hours of oscillation, which led to visible leaks at high pressure (from around 60 MPa).

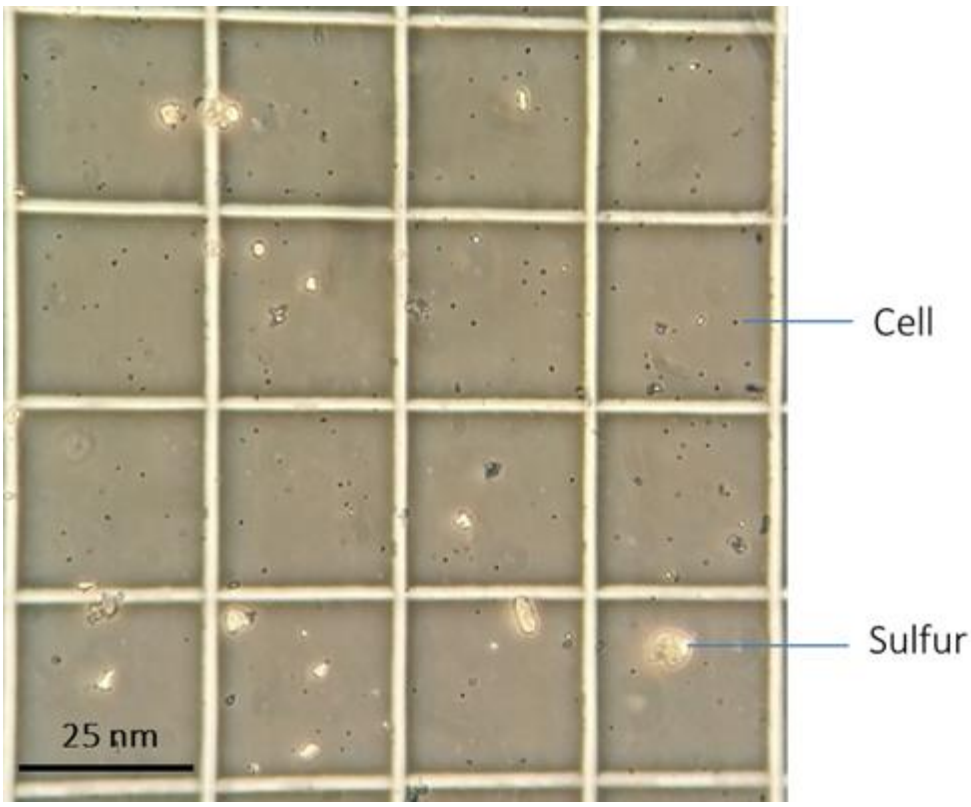

Figure 45: Microscopic observation of *T. barophilus* MP^T cells grown in the BHP at 40 MPa, 85 °C, for 6 h, in TRM 0.25 g/L S°

The photograph shows cells with normal shape, but rather small when visually compared to cells grown at Patm. The density was of about 5 – 6 .10^7 cell/mL.

Inhomogeneity in a fermenter is problematic, as it does not allow a precise measurements and control over fermentation dynamics in the whole volume of the bioreactor (Cleland and Enfors, 1987). Therefore, a functioning mixing system was necessary.

1.2.2. H_2 saturation of the medium

We attempted to measure the hydrogen produced during a high hydrostatic pressure culture (40 MPa) of *T. barophilus* MP^T in 48 h in TRM with 0.25 g/L S°. To such extent, we anaerobically sampled a known volume in usual culture flasks previously flushed with N_2, at a known initial pressure, and let the suspension degas inside the flask. On sample volumes comparable to what was usually performed at P_{atm} (20 mL of cell suspension in 50 mL flasks), we did not detect any H_2 by gas chromatography, in our first experiments.

Figure 46: Visual observation of a lack of homogeneity in the BHP

The three bottles each held approximately 50 mL of cell suspension after a downstream drain, and were successively filled from left to right. The right bottle clearly shows less opacity, and seems to show a bit of oxidation (pink color shift), indicating that colloidal sulfur probably settled down the bottom of the incubator during the culture.

We hypothesized that these failures could be attributable to the absence of gas phase, inducing a H_2 saturation of the *medium*, further enhanced by high pressure (as it was already observed in other high pressure cultures, *e.g.* (Boonyaratanakornkit et al., 2006). Interestingly, growth was still observed in these conditions (up to 10^8 cell/mL), which, at P_{atm}, would have failed, since with 0.25 g/L S°, both hydrogenogenic and sulfidogenic metabolic pathways seem to be involved in *T. barophilus* MP^T energy conservation system. It is however possible that the metabolism behaves differently at high pressure, as indicated by previous transcriptomic studies (Vannier et al., 2015). On another hand, it is possible that H_2 was indeed produced, but that the system was purged during the fermentation, thus evacuating the end-product (at the same time relieving its saturation). It is also possible, although not likely, that our gas sampling system was not adequate, involving too little amounts of H_2, thus falling beneath the limit of detection of our gas chromatography method.

In any case, these observations showed that a system for storing produced gas was necessary, and that a gas phase would also be suitable. Indeed, it would allow to relieve hydrogen saturation in the liquid phase. Sparging an inert gas, such as N_2, through the culture during a cycle would also accelerate this process and likely increase H_2 production rates. To allow such conditions, we needed to be able to prevent the system from purging when in cycle.

1.3.1. Pressure regulation precision

When sampling, even using micrometric valves, internal pressure variations could easily reach +/- 6 MPa, mainly because regulation was only triggered when a measure was 3 MPa higher or lower than the target. Depending on the volume sampled, these variations could occur several times within minutes, likely inducing a stress on cells. Growth was observed to be impaired by such manipulations, especially when performed in the first hours of incubation. Furthermore, probably due to the suspension density, the purge system (automatic action of V3, see FIGURE 44) was not adapted to all pressure ranges, as seen in FIGURE 47. While a cycle termination should have gradually purged the internal pressure, our system did not immediately succeed in returning to P_{atm} and stagnated for several minutes between 20 and 10 MPa before. Moreover, as purge could be inefficient in cycle too, pressure could easily overcome its target by up to 20 MPa, if no manual regulation was performed, when the system was pressurized before reaching its temperature target, due to heat-induced dilatation.

To correct those problems, valve opening times thus needed to be re-programmed to more accurately fit our fluids. It also needed to be adjusted for the implementation of a gas phase. The possibility to set up a consign with an accuracy of 0.1 MPa would help the system react more readily to pressure changes induced by sampling, thus limiting pressure variation. Additionally, the placement of micrometric valves at each sampling side (*i.e.* at the downstream circuit too) was necessary in order to limit sampling debit and thus permit the pump (which had a limited speed) to compensate. This was also especially necessary in the case of a gas phase.

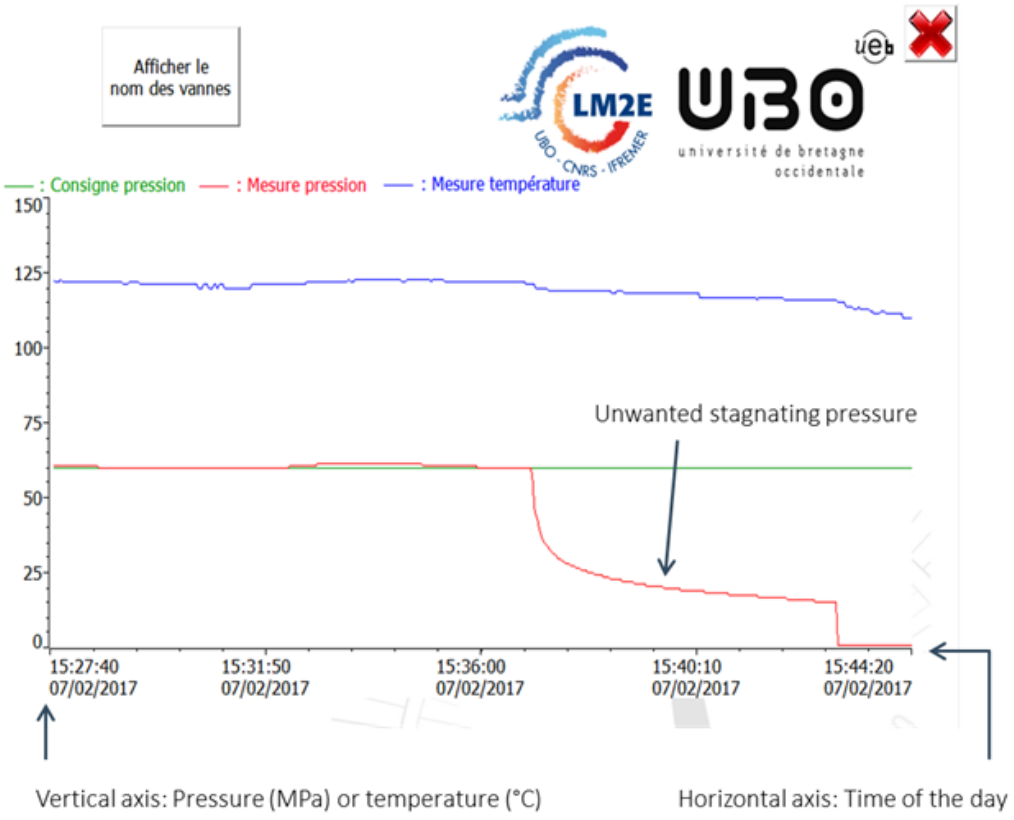

Figure 47: Screenshot of the HMI at cycle termination, showing an unwanted stagnating pressure before returning to P_{atm}

Vertical axis represents temperature (in °C) for the ***blue*** *line and pressure (in MPa) for the* ***red*** *(measured) and* ***green*** *(target) lines. Horizontal axis represents time.*

1.2.4. Non-operational observation cell

The machine developed by HP Systems was originally provided with a module intended to serve as an optical chamber for high-pressure microscopic observations. It was composed of a 590 µL container made of Inconel 718, also able to hold up to 120 MPa, and surrounded by two sapphires for optical observation. In line with two valves, it was projected to be easily disconnectable from the bioreactor, while maintaining high pressure in the chamber, in order to be carried for microscopic observation. Unfortunately, the concave conception of the bottom of the observable area rendered homogeneity in the sample, and thus accurate observations, impossible, letting the cells accumulate. A new system for high pressure observation was thus necessary.

1.3.2. Unwanted pressure accumulation

After several experiments, we observed that pressure accumulated in the low-pressure part of the injection circuit, *i.e.* the connection between the injection fluid and the V17 valve. Several bursts of the connector (HPLC valve units, WVR) occurred. This occurred during a high-pressure cycle, when the syringe pump re-filled. During this event, if the bioreactor was already pressurized, the internal pressure was also present between the pump and the non-return valve V2 (see FIGURE 44). As a re-filling of the pump implied an opening of V1 during the return to its lower position, this pressure was communicated to the whole injection circuit, consequently breaking the first weaker equipment, *i.e.* the connector. We initially tried to augment the section in this connector in order to allow a higher debit, which would have permitted to transmit the hydrostatic pressure back to the bottle, where a gas phase would absorb the surplus. However, the water hammer was too important. Therefore, a new non-return valve, upstream of V17, was necessary.

1.4. Design and realization of the BHP2

Following those experiments, we thus defined needs for changes on the continuous HP / HT bioreactor manufactured by HP Systems in order to better conform to the applied aim of H_2 bio-production by *Thermococcales*. The following points were to be optimized for better function: mixing, optic chamber, sampling, gas-shift / gas-pressure, and control of the automaton. Together with the development team of HP Systems, we designed and performed several optimizations. FIGURE 48 and FIGURE 49 represent the new version of the BHP (BHP2). For mixing, a hastelloy magnetic stirrer (model MM-20, Amar, India) with impellers at two levels, was installed, able to hold 69 MPa. Hence, a new stainless-steel (1.45.42P930) obturator was machined (SMB, France), but this piece was limited to 40 MPa. As manufacturing a new optical chamber would have been too costly, we obtained a commercial High Pressure Microscopic Cell (PMC-100-1.5-NA0.6-YAG-SUS630), from Syn-Corporation (Japan). This chamber is able to withstand 100 MPa, up to 80 °C, allowing observations through a 2 mm diameter sapphire window, with a possible temperature control system. We adapted a new system for sampling without pressure drops, as described in the previous paragraph. A gas booster (HP Biotech, France) was settled, which could impose up to 35 MPa of hydrostatic pressure, possibly augmented by heat-induced dilatation afterwards. It allows the manual injection of pressurized gas through the bottom of the incubator, consequently

creating a gas-sparging. A gas phase in our fermentative system would be rapidly purged away in case of pressure excess, thus biasing the possible subsequent measurements. In order to still be able to accurately study how imposing and renewing such a gas phase could help the fermentative system, we designed a 200 mL gas-storing chamber, supporting up to 40 MPa, for collecting purged gas and further analyzing it. Note that the gas circuit was made to prevent H_2 leaks, which were controlled by injecting pressurized helium and using a leak detector (Restec #22655). The liquid injection circuit was protected with a non-return valve. With the new gas system, better controlling pressure regulation was crucial, and the HMI was re-programmed to better fit our new setup (FIGURE 50). It was now possible to enable the purge function or not during a cycle, to choose between a gas-phase or full hydrostatic pressure (which corresponded to different times of valve opening for purge), and to modulate the pressure variation tolerance before purge was activated.

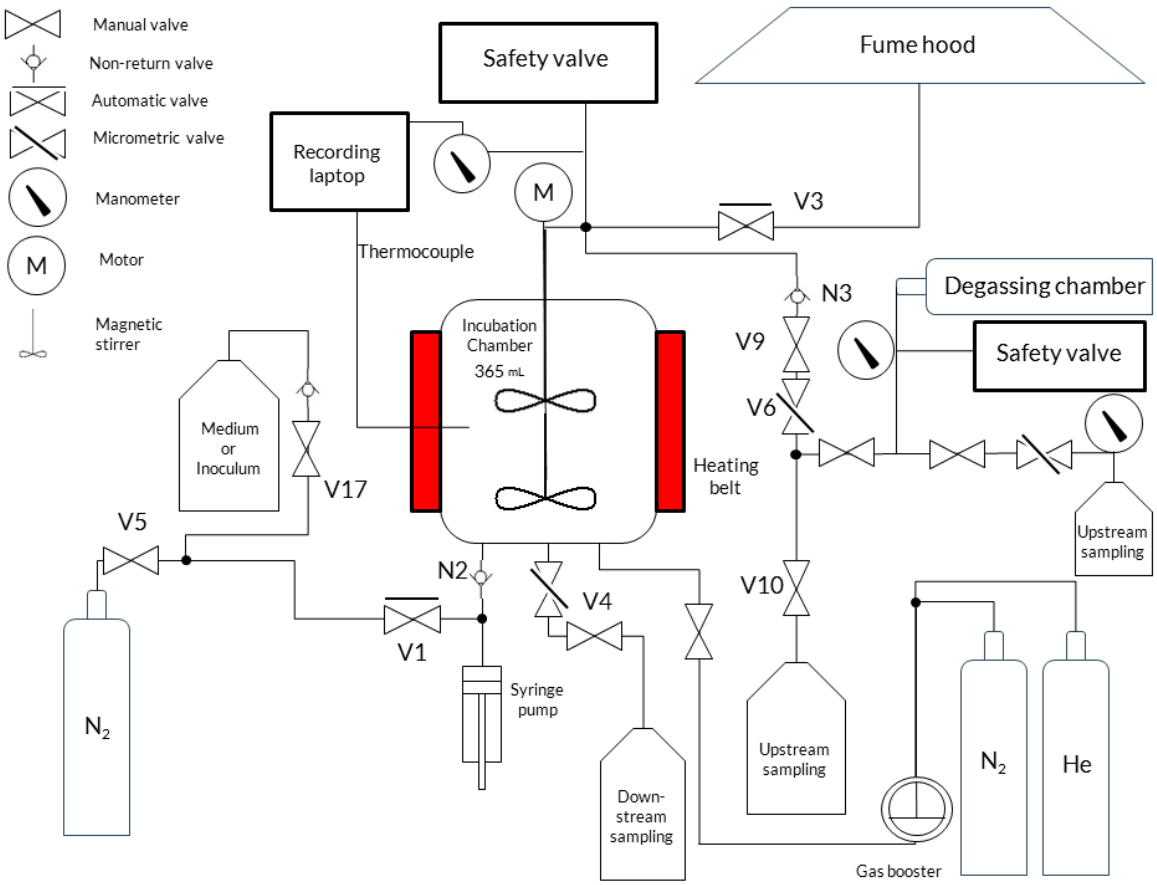

Figure 48: Schematic representation of the organization of the HP/HT continuous bioreactor manufactured by HP Systems in its modified state (BHP2)

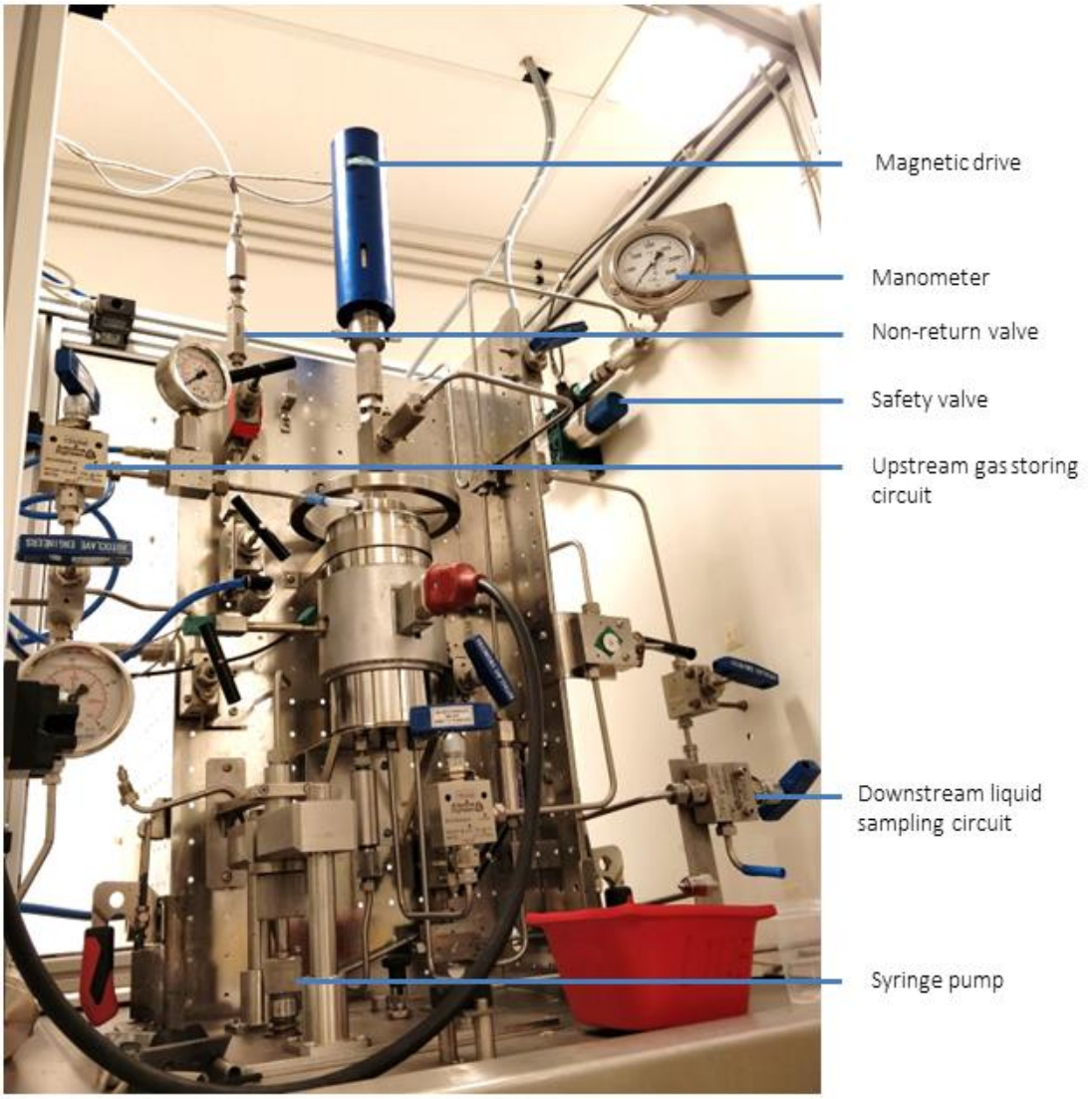

Figure 49: Modified state of the bioreactor (BHP2), with some main organs annotated

2. Results obtained on the BHP2

The modifications occurred on the BHP allowed to perform new experiments to further characterize the system.

2.1. H_2 production of *T. barophilus* MP^T at high gas pressure

H_2 production from gas-pressurized culture could be assessed and are described in chapter I. We found that such production could be more important than at P_{atm}, when reported to the equivalent unpressurized gas concentrations, but these results needed to be adequately controlled.

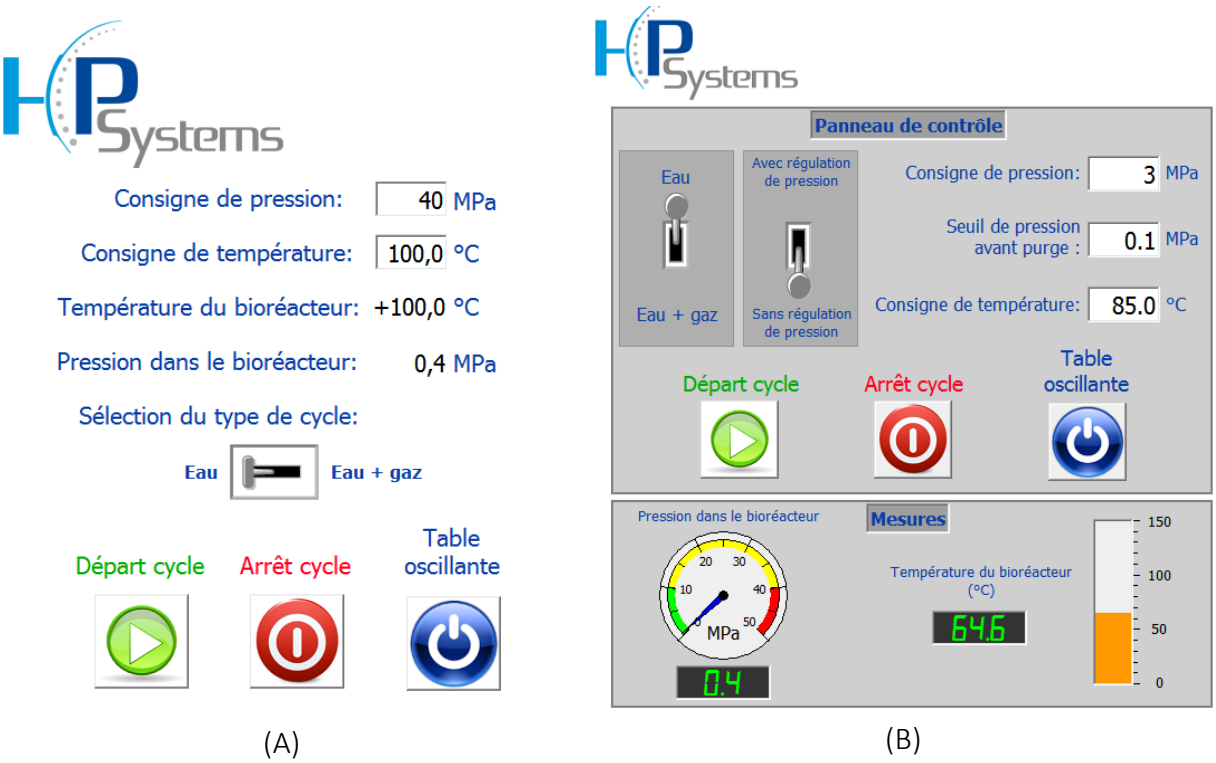

Figure 50: Screenshots of HMI of BHP1 (A) and BHP2 (B)

Left, (A): initial state (BHP1). Right, (B): modified state (BHP2). Main visible modifications were the possibility to define purge reaction treshold, and to decide whether a pressure regulation had to occur during the cycle or not.

2.2. Micrometric sampling selection of smaller cells

First attempts to set a growth curve of our model in the BHP failed. For such experiment, frequent samplings had to be performed during the culture. No growth was observed, after 8 h of culture (FIGURE 51). Note that we had determined that 30 s of mixing at minimum speed (300 rpm) was enough for reaching homogeneity from sampling (data not shown). Previous experiments had also shown that the selected mixing rhythms were not responsible for this lack of cell viability, by injecting fully grown cells into the bioreactor at high pressure (35 MPa) and $P_{atm,}$ mixing for at least 15 min, then collecting the whole content of the bioreactor: no change in morphologies or cell densities could be observed (results not shown).

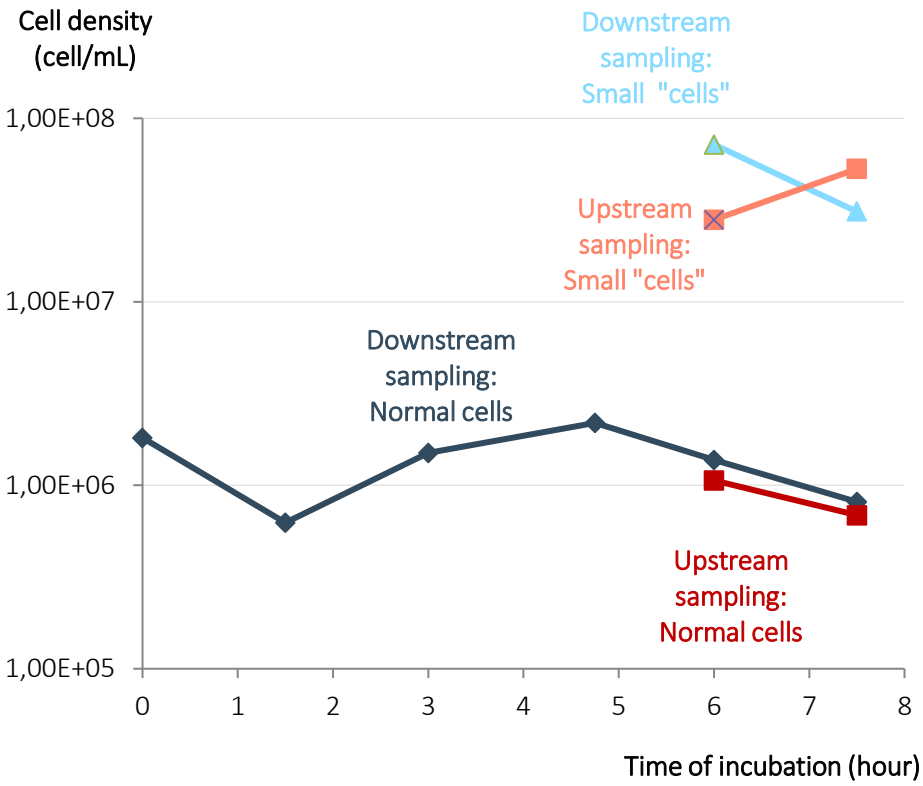

Figure 51: Example of failed growth curve obtained from the BHP culture of *T. barophilus* MP^T in TRM 0.25 g/L S°, at 40 MPa, 85 °C

The displayed failed growth curve was unexpected, compared to the HP dynamics remarked with discontinuous culture, showing that growth at 40 MPa should have reached plateau phase (see REPEATABILITY ASSESSMENT AND PROTOCOL ADAPTATION FOR HP CULTURE, P. 198). Microscopic observations of those samples revealed some particles very similar, in morphology, to *Thermococcales* cells, but approximately 5 times smaller. Those particles, hardly visible at a 400-fold magnification, could be estimated at around 3 - 7 $.10^7$ particles/mL. Even more surprisingly, the same batches showed a high cell density (equivalent to what would be expected, *i.e.* about 10^8 cell/mL) when the whole volume was retrieved, with normal cells. We tried to directly inject full-grown cells into the bioreactor, pressurized them, and also observed only smaller cells when sampling. It was thus hypothesized that micrometric sampling could induce a French press effect on cells, leading to their burst when passing from high pressure to P_{atm}, thus only allowing us to observe debris (McCarthy, 1962; Milner et al., 1950).

However, same observations were unexpectedly made when performing these experiments at P_{atm}. Rather than inducing a French press effect, we thus postulated that

micrometric valves could select for smaller particles. We assumed that those smaller particles could be present in the usual suspensions, but as they are almost invisible with our counting protocol, we never counted them.

A solution to that cell selectivity was to sample at a higher flow, *i.e.* with widely opened micrometric valves. However, that configuration led to swift drops in internal pressure, of up to 20 MPa, which could not be compensated by the pump, until finally returning to P_{atm}.

Therefore, we had to find a manner to allow sampling with larger flow without losing internal pressure. Unfortunately, adjusting the speed of pumping was not possible. We thus thought of a compensation system (FIGURE 52).

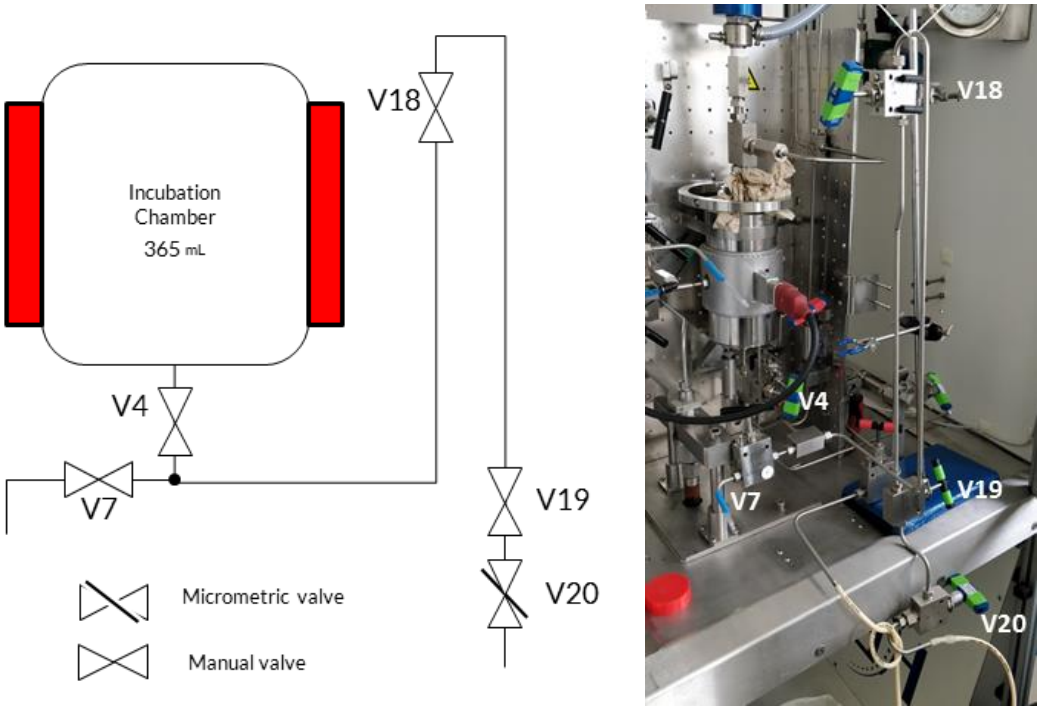

Figure 52: New sampling system for preventing pressure loss in the BHP2

Tubing volume is of about 10 mL.

This sampling system was tested during a high hydrostatic pressure experiment. For sampling, the tubing volume was filled beforehand with cold water (V4 closed, all other valves of the sampling system opened). Then, all valves were closed and V4 was opened. As the volume was already filled with liquid, the pressure lost inside the bioreactor was limited (about 0.5 MPa from 30 MPa). In order to extract the suspension, V18 and V19 (and still V4)

were fully opened and V20, a micrometric valve, was then progressively opened, in order not to let the internal pressure of the bioreactor drop. This step consisted in purging the water previously present in the tube. As the density of each liquid was different, and the tube section was small enough, mixing was limited, and a clear pycnocline could be observed after about 10 mL of liquid extraction. Once the water out, V20 and V19, then V4, could be closed, leaving the sampling volume pressurized and disconnected from the incubator. Then, V19 could be re-opened and V20 could serve to decrease pressure smoothly down to P_{atm}. That way, the sample did not undergo rapid depressurization. Once atmospheric pressure was reached, the micrometric valve V20 could be fully opened, as well as V18 and V7. The sample thus did not pass through a micrometric section. Preliminary tests showed that cell morphology was not unusual, and that cell densities were correct, with this new method of sampling. Overall, no French press effect was theoretically endured, and bioreactor pressure variation was limited. This new configuration could thus be used for performing growth curves on BHP2 cultures, although no such result was available at the time of writing. Whether it is also suited to gas-pressures still remains to be assessed, but sampling-induced pressure drops are way less likely in barometric configuration, as gas is compressible.

2.3. Safety concerns

As gas pressurization was installed, new safety concerns emerged. Hydrostatic pressure, while presenting risks of equipment bursting, will rapidly decrease in case of leak, as few milliliters lost (in our case) are enough to reach atmospheric pressure back. However, gas pressure can be more dangerous, as the energy stored is higher. If decompressed too rapidly, it can generate a blast wave, launch projectiles, and important sound (risk of ear-drum rupture for the experimenter). Furthermore, our system is mainly composed of an inert gas (N_2) which could, in case of rapid decompression, displace oxygen in the experiment room and induce risk of anoxia. Gases produced from fermentation (CO_2, H_2S, H_2), while in lower proportions, are respectively anoxic, toxic / flammable, and explosive / flammable (Paulsen, 2009).

Note that the BHP2 system can only be pressurized up to 45 MPa, as 1/16” tubing in 316L stainless-steel would probably not sustain more, in our chemical and temperature conditions (personal communication, HP Systems). The risk of vessel explosion was limited by

the safety valves installed both on the bioreactor and on the storing gas bottle, and a silencer was installed on the purge stream. In case of unexpected failure of the system (*e.g.* due to electrical or compressed air problem), the emergency stop induces a total opening of the system, *via* the purge stream, under a chemical hood. However, considering to apply this system in larger scales would require an accurate safety evaluation by accredited professionals.

3. Further experiments and optimizations envisioned: concept of a new BHP3

The development of the BHP2 was a preliminary step in to evaluate the interest of scaling up this laboratory equipment to a higher-volume solution, for assessing whether high-pressure H_2 bio-production by *Thermococcales* could be applied. Before setting up such further technology, several experiments remain to be performed on the BHP2.

The most important would be to verify whether high pressure, in our conditions would really induce H_2 overproduction. As explained in chapter I, no control could be performed on the obtained results to ensure that the effects observed were not due to desaturation of the metabolism. Moreover, those results were yet to be replicated.

Growth curves were not yet performed at the time of writing. Due to the lack of prior adequate method for accurate sampling without depressurization, no continuous culture was set up, and it would be interesting to study such dynamics at high pressure. Changes in such conditions have been reported in some others works: gas-pressurized culture of *Methanocaldococcus jannaschii*, showed a linearization of the growth curve, attributed to H_2 substrate-limitation due to its low solubility, for example (Boonyaratanakornkit et al., 2006).

At the time of writing, no test of our new, commercial, optical microscopy high pressure chamber (SynCorp, Japan), was made.

That being said, requirements for a third version of the BHP (BHP3), based on BHP2 principles, could still be imagined, in order to further test technical conditions possibly envisioned for scaling up. In biotechnological productions, scaling up often leads to

unexpected strain behavior. While it would not be economically reasonable to design a large volume bioreactor of hundreds of liter yet (which represent the biggest pressurized volumes in industrial applications (Rivalain et al., 2010)), it could still be interesting to increase the bioreactor size to start to anticipate such changes, at least by trying to reach several liters. Such system should also be adapted for higher pressures, in order to be able to explore the physiological outcomes of our biological models in wider ranges of conditions.

The solutions described in chapter I are based on the use of specific substrates that could not be entirely soluble, and thus, we would have to test if the equipment is adapted, noticeably for passage through certain smaller sections. Furthermore, CO_2 have been indicated as a possible interesting gas to use, but at high pressure, specific requirements are associated for materials, specifically joints (Paul et al., 2012). In order to prevent any pressure drop during sampling, compensation chambers with plunger systems could be manufactured, for both gas and liquid sampling. Since cultures are foreseen with gas pressure, an internal liquid level indicator could help managing a continuous culture. Automatic control of the renewal of both gas and liquid would be importantly programmed on the automaton. To facilitate measurements, in-line probes and analytical *apparatus* could be placed, on a low-pressure outstream circuit, in order to limit costs and maintenance associated. pH / redox, H_2, H_2S, CO_2, could be interesting parameters to check regularly along the fermentation. However, if the measured gas stream comes directly out of the gas phase, we could face the same dilution problem encountered herein, *i.e.* as gas is used for pressurization, the relative proportion of gaseous fermentation products would be very small. During a culture, *i.e.* not in final point, it could be so low that the analytic system could not detect it.

This problem could however be solved by another important point: the need to recycle the vector gas. Indeed, as inducing gas pressure consumes important volumes, and as most of it (except if we consider gaseous “substrates” for our fermentation systems, such as CO or CO_2) is inert to our biological reaction, it could be economically interesting to recycle the outstream gas mix. If technically feasible, it could be energy-efficient to perform a separation of the produced gases at high pressure, in order to isolate H_2 produced from the mix. Such protocol would limit the re-pressurization costs in a continuous set-up. This could occur in a separation chamber with specific membranes, but such equipment was rarely

applied at moderately high pressure, so would need technological adjustments for our needs (*e.g.* (Cholewa et al., 2018; Härtel et al., 1996)). Theoretically, condensation methods could be applicable, according to different temperature of liquefactions of the gases at given pressure. It could however be a costly process. If so, purification membranes at low pressure can separate H_2 from the rest, but induce a need for re-pressurization.

Finally, as a H_2 bio-production would conveniently be adapted to the type of substrate and *medium* (sea water or fresh water) available, designing a new BHP3 would benefit in keeping a need for adaptability, for example with portable, modular equipment.

The design of such a new device would greatly depend on calculations about the most energy-efficient processes, and would thus require deeper study.

IV – Chapter II: Conclusions and perspectives

In answer to the specific needs imposed by studying H_2 bio-production systems at high pressure, we thus developed new tubes for discontinuous culture, allowing to set gas phase to HP/HT incubations, while limiting and controlling possible H_2 leaks. Albeit similar systems may be commercially available, our solutions are much less expensive, and more adapted to our specific needs. On another hand, the initial prototypical incubator developed by HP Systems was profoundly modified to better fit requirements of a potential applied H_2-producing culture. Particularly, new mixing system was implemented, gas-pressurized incubations were made possible, and the related automaton and human-machine interface were adapted. This work represents the first description of a gas-pressurized bioreactor specifically oriented towards HP / HT H_2 bio-production, to my knowledge.

However, although our new tubes for gas-phase discontinuous HP incubation could be very practical for physiological studies of piezophiles, they still need leak calibration for each gas and pressure range considered. The BHP2 still needs several evaluations and adjustments, before being really applied in a continuous culture, H_2-producing, *scenario*. It is currently limited to the optimal pressure for growth of *T. barophilus* MP^T (about 40 MPa). Literature data indicate that H_2 overproduction could rather occur at supra-optimal pressure for growth

(70 MPa) (Vannier et al., 2015), thus our system would need material adaptation (particularly *via* the use of more resistant tubing material and magnetic drive, and a stronger gas booster) in order to verify these hypotheses. Still, even if H_2 production is less efficient than at sub- or supra-optimal pressure, we cannot exclude the possibility that working at 40 MPa could be an efficient compromise, possibly thanks to further metabolic optimizations, and since higher pressure correspond to more costs in maintenance, more energy required for pressurization, and more risks, noticeably. Projections would have to be carefully calculated, therefore.

Those technological developments could nonetheless also be considered in other applications. Diverse gas phases could be examined for both methods, allowing, for example, the culture of methanogens at high pressure, as it was described with other bioreactors (Miller et al., 1988a), or other biotechnologically interesting piezophiles. Even used at atmospheric pressure, the limited leakiness of our new tubes could allow studying any type of fermentation. They could for example be used to facilitate rapid screening of such metabolisms, by observing the position of the plunger through the glass, without any other sample. The screening described in chapter I for highly H_2-producing strains could now be performed at high pressure thanks to those devices. The BHP2 could also serve fundamental investigations by allowing transfer of *in situ* pressurized samples into the bioreactor, for isobar enrichments.

Our newly adapted bioreactor could therefore serve to develop protocols of continuous HP/HT H_2 bio-productions by *Thermococcales*, but several parameters would need to be better defined, as explained earlier, in order to permit to envision a higher bench scale bioreactor. Together with the use of our discontinuous gas-phase culture tubes, both material and biological needs for such project will be possibly assessed. The realization of a BHP3 and the application of biological optimizations rendered possible by the fundamental knowledge acquired thanks to our methods, might then permit to further evaluate the applicability of energetically efficient pilot productions.

Note: Part of the work presented in this chapter was valorized with a poster presentation at the AFEM *colloquium* 2017 (Camaret-sur-Mer, France), and with a poster presentation at the congress Thermophiles 2019 (Fukuoka, Japan).

Chapter III: Study of the hydrogeno/sulfidogenic metabolism at low and high pressure in *T. barophilus*

Abstract

Although many *Thermococcales* species are piezophiles, the impact of hydrostatic pressure on their hydrogeno/sulfidogenic energy-conserving metabolism remain elusive. This chapter describes investigations on metabolic tuning in *T. barophilus* in response to deletion of several key gene clusters involved in hydrogenogenic and sulfidogenic growth (*mbh*1, *mbh*2, *co-mbh, mbs, sh*I, *sh*II), and their relations to the sulfur absence or presence and to pressure (atmospheric and 40 MPa). Growth dynamics, end products (acetate and H_2S) and gene expressions (RT-qPCR) of main involved clusters were assessed in the wild type strain and in those mutant derivative strains, in order to analyze the role of each concerned enzyme as well as its influence regarding different metabolic configuration. We observed important differences in the metabolism of *T. barophilus*, as against other well-studied *Thermococcales*, and highlighted the strong capacity of this cellular system for reorganization to cope with missing metabolic fluxes. Although salvage patterns seemed to be highly dependent to culture condition, no clear generalization could be advanced regarding high pressure adaptation, underlining the important complexity of the system. However, those results altogether permitted to progress towards a better understanding of *Thermococcales* life at high pressure and to orientate hypotheses for future potential optimizations for high pressure H_2 bio-production.

Bien que de nombreuses espèces de Thermococcales soient piézophiles, les impacts de la pression hydrostatique sur leur métabolisme hydrogéno/sulfidogénique de conservation de l'énergie restent imprécis. Ce chapitre décrit l'étude de compensations métaboliques chez T. barophilus *en réponse à la délétion de plusieurs clusters de gènes clés impliqués dans la croissance hydrogénogénique et sulfidogénique (mbh1, mbh2, co-mbh, mbs, shI, shII), et leurs relations à la présence ou absence de soufre et à la pression (atmosphérique et 40 MPa). La dynamique de croissance, les produits (acétate et H_2S) et l'expression génétique (RT-qPCR) de groupes principalement impliqués ont été mesurés dans la souche sauvage et dans ces mutants, dans le but d'analyser le rôle de chaque enzyme concernée ainsi que son influence au sein des différentes configurations métaboliques. D'importantes différences dans le métabolisme de* T. barophilus *ont été observées, par rapport à d'autres* Thermococcales *modèles, et l'importante capacité de ce système cellulaire à se réorganiser pour s'adapter à*

des flux métaboliques manquants a été mise en lumière. Si les patterns de compensation ont semblé être très dépendants des conditions de culture, une généralisation au regard de l'adaptation à la haute pression n'a toutefois pas pu en être proposée, soulignant l'importante complexité du système. Cependant, ces résultats ont permis de progresser vers une meilleure compréhension de la vie à haute pression des Thermococcales et d'orienter des hypothèses pour des possibles futures optimisations de la bio-production d'H_2 à haute pression.

Introduction

Thermococcales have been studied for H_2 bio-production applications for many years, as they harbor a hydrogenogenic metabolism based on various, possibly interesting substrate degradations (Schut et al., 2014). Many reports have described investigations and optimizations of the concerned metabolic systems in diverse species, and particularly, at the fundamental level, in '*T. onnurineus*', *T. kodakarensis*, and *P. furiosus* (*e.g.* (Kanai et al., 2011; Moon et al., 2015; Santangelo et al., 2011; Schut et al., 2012)). Most of the *Thermococcales* known to date have been isolated from the vicinity of deep-sea hydrothermal vents, and may be piezophilic (although this strait has only been characterized in a few strains) (NCBI, 2020; Schut et al., 2014). As the post-production pressurization of hydrogen represents important costs, it could be economically beneficial to design high pressure (HP) hydrogenogenic fermentors, taking advantage of the *Thermococcales*' piezophily (EDF, 2017; James et al., 2016; Kelly et al., 2008; Makridis, 2016; Mayyas and Mann, 2019; Viktorsson et al., 2017; Züttel, 2003). For this project, we chose to advance such investigations on *T.barophilus* MP^T as determined during the first phase of this project. This facultative piezophile grows optimally at 40 MPa, an can also grow atmospheric pressure and 70 MPa (Marteinsson et al., 1999a; Zeng et al., 2009). It reached interesting H_2 yields (see chapter I) and benefits from many other advantages, such as the availability of its genome sequence (Vannier et al., 2011), of a functional genetic tool (Birien et al., 2018; Thiel et al., 2014), and of several past studies on its adaptation to high pressure (Cario et al., 2015b, 2015d, 2016; Marteinsson et al., 1997; Vannier et al., 2015). H_2 production in *Thermococcales* is linked to energy conservation, using routes that concomitantly allow to dispose of electrons, carried from substrate degradation by different transporters. Those transporters can thus be reoxidized by membrane-bound and cytosolic hydrogenases and oxidoreductases, leading to H_2 or H_2S production, which feed a

Na^+ gradient across the membrane, allowing to further activate ATP synthases (Sapra et al., 2003).

Although more thoroughly detailed in the introduction of this manuscript, main principles of the system are described in FIGURE 53.

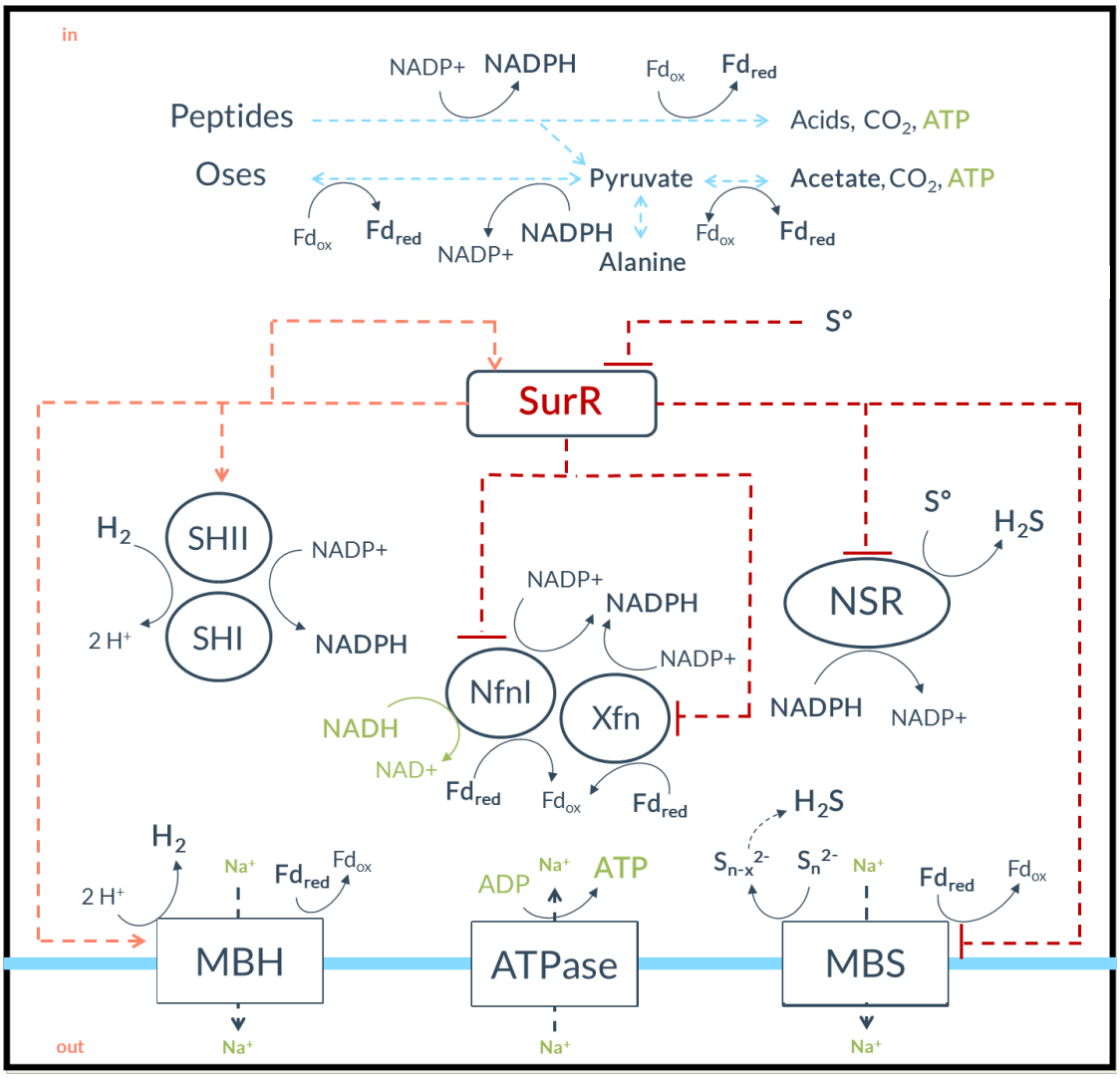

Figure 53: Simplified representation of the energy conservation metabolism of *T. barophilus* MP^T

Attention, the influences of the transcriptional regulator SurR, represented by orange dotted lines and arrows for activation or red dotted lines and dashes for repression, are on gene expressions and not on protein directly. Stoichiometry was not displayed here. The blue line represented cellular membrane, with the extracellular compartment in the lower part of the figure. Note that Xfn was also designated as Nfn2, in this chapter.

Depending on the nature of the degraded substrate, the involved catabolic pathway can lead, in *T. barophilus* MP^T, to reduction of both $NADP^+$ and ferredoxins (Fd) (in the case of peptide degradation), or to reduction of only Fd (in the case of sugar degradation) (Bräsen et al., 2014; Schut et al., 2014).

The membrane-bound hydrogenase (Mbh) uses reduced Fd (and not NADPH) and produces H_2. An associated antiporter, Mrp, couples this reaction with the translocation of a sodium ion across the membrane (Sapra et al., 2000; Silva et al., 2000). In the genome of *T. barophilus* MP^T, two Mrp-Mbh complexes are encoded, namely *mrp-mbh*1 (TERMP_1485-98) and *mrp-mbh*2 (TERMP_1471-84). Note that only one Mrp-Mbh complex is encoded in *P. furiosus*, *T. kodakarensis* and '*T. onnurineus*' (Fukui et al., 2005; Lee et al., 2008; Robb et al., 2001). In our model, an additional enzyme is associated with a carbon monoxide dehydrogenase (COdh) module, constituting the *mrp-mbh-codh* cluster (TERMP_1139-54), whose homolog cannot be found in *P. furiosus* or *T. kodakarensis*, but is present in '*T. onnurineus*', among others (Kozhevnikova et al., 2016; Lee et al., 2008; Oger et al., 2016). In the presence of elemental sulfur, a membrane-bound sulfane reductase (Mbs, previously known as Mbx), conserved in our considered models, indirectly produces H_2S from polysulfides, also using Fd_{red} as electron donor. A translocation module also maintains an ion gradient, in association to the activity of the sulfane reductase (Wu et al., 2018a). Sodium can then re-enter the cell through an ATP synthase, allowing energy conservation (Mayer et al., 2015; Pisa et al., 2007; Schut et al., 2012).

Cytosolic enzymes are also involved in the system. SHI and SHII have been shown to consume H_2 to produce NADPH, which can be used by Nsr (NADPH-dependent sulfur reductase) to reduce elemental sulfur, leading to H_2S production (Haaster et al., 2008; Kanai et al., 2011; Santangelo et al., 2011; Schut et al., 2007). Note that the SHI (TERMP_00536-39) and SHII (TERMP_0067-70) of *T. barophilus* MP^T are the homologs of respectively SHII (PF1329-32; TON_0052-55) and SHI (PF0891-94; TON_0534-37) as designated in *P. furiosus* or '*T. onnurineus*', respectively (Birien, 2018). NADH-dependent ferredoxin:$NADP^+$ oxidoreductase (Nfn) proteins are also found in all *Thermococcales*, and have been described in *P. furiosus* to produce NADPH from Fd_{red} and NADH or another substrate thanks to electron

bifurcation. They consequently allow to transfer electrons between both important types of carriers in this system (Nguyen et al., 2017).

Sulfur has been demonstrated to play an important role in this metabolism. Growth in the absence of sulfur is diminished in several strains, and the sulfidogenic energy conservation system has been calculated to be more efficient than the hydrogenogenic conservation system (Sapra et al., 2003; Schicho et al., 1993; Schut et al., 2016b). Sulfur also importantly changes the metabolic flux organizations, thanks to the master regulator SurR. This transcriptional factor can activate or repress several genes in the absence of sulfur, but is oxidized in the presence of sulfur, which induces a de-regulation. Particularly, in the metabolism presented here, SurR has been shown to activate Mbh, SHI and SHII expression as well as its own, and to repress Nfn, Nsr and Mbs (Lipscomb et al., 2009, 2017; Yang et al., 2010).

Mutational studies in *P. furiosus* and *T. kodakarensis* have determined the importance of several enzymes for growth in function of sulfur (Kanai et al., 2011; Santangelo et al., 2011; Schut et al., 2012). In the absence of sulfur, it has been shown that Mbh is essential for growth, while SHI or SHII deletions did not induce phenotype change. In the presence of sulfur, Mbs deletion impairs growth, while the Nsr absence could be compensated. Deletions of Nfn1 and Nfn2 in *P. furiosus* impact growth and NAD(P)H concentrations in both the presence and absence of sulfur (Nguyen et al., 2017). In *T. kodakarensis*, deletion of the gene encoding the master regulator SurR impairs growth, but only in the absence of sulfur (Santangelo et al., 2011). In *P. furiosus*, a *sur*R-deletion induced growth impairment in the absence of sulfur, but less dramatically, and did not affect the growth phenotype in the presence of sulfur (Lipscomb et al., 2017).

Although the question of the pressure-induced modifications of the metabolism has been raised long ago (Zobell, 1952), how this parameter precisely affects the hydrogenogenic metabolism of piezophilic *Thermococcales* is still unclear. Previous works have shown certain influences in *T. barophilus* MP^{T}. In our model, *mrp-mbh*1, *mrp-mbh*2, *mrp-mbh-codh*, *sh*I, and *sh*II expressions (as well as *sur*R to a minor extent) were upregulated at atmospheric pressure (sub-optimal pressure for growth) compared to 40 MPa. *mbs* was slightly overexpressed at this optimal pressure for growth, as was *nsr*. It is yet important to precise that those

transcriptomic analyses were performed in excess of sulfur (5 – 10 g/L). Different expression variations were observed in the piezotolerant *T. kodakarensis,* where *mbh* and *hyh* (homolog of SHII in *T. barophilus*) were upregulated at optimal pressure for growth (P_{atm}) (Vannier et al., 2015). Importantly, pressure-induced variations in gene expression patterns are not necessarily correlated to actual proteomic profiles, as shown in *P. yayanosii* (Michoud and Jebbar, 2016). In those studies, no metabolite productions were obtained, allowing no indication of actual ensuing metabolic activities.

Past projects at the LM2E have led to production of several strains of *T. barophilus* MP^T deleted of key energy conservation metabolism genes, namely *mrp-mbh*1/*mrp-mbh*2, *sh*I, *sh*II, *mbs*, and the *mbh* coding sequence of *mrp-mbh-codh* (Birien, 2018). In the perspective of an applied H_2 bio-production, we aimed to gain insight in the hydrogenogenic metabolism of *T. barophilus* strain at high pressure. Since the sulfur presence or absence seems to be of paramount importance in the orientation of the electron fluxes in *Thermococcales*, it was interesting to study its concomitant influence with HP. The objectives of this work were to further our comprehension of the respective roles of each enzyme of the system in the metabolism, to observe in which ways the strain could compensate their absence, and to better appreciate how the presence/absence of sulfur as well as low or high pressure could influence these compensation patterns. To such extent, physiological changes induced by the available deletions were studied on the aforementioned mutant strains, *via* growth dynamics, H_2S and acetate concentrations measurements, and gene expression of several related genes. We thus provided analyses that completed previous assumptions based on HP gene expressions, but also showed likely important differences in the functioning of *T. barophilus* metabolism compared to other *Thermococcales* models.

Materials and methods

More detailed description of the materials and methods used in this work can be found in the MATERIALS & METHODS - GENERAL section of this manuscript.

Thermococcus barophilus strains

The mutant strains used herein, which were constructed prior to this project and are available at the UBO Culture Collection (https://www.univ-brest.fr/ubocc), are presented in TABLE 20. The strain Δ517 corresponded to the necessary removal of 6-methylpurine sensitivity for an effective application of the genetic tool and was considered as a wild type phenotype in this study (Birien et al., 2018). To avoid any confusion, the Mbh subunit encoding gene of the Mrp-Mbh-COdh complex will be designated herein as "*co-mbh*". Note again that in our model, *sh*I and *sh*II are respectively homologous to *sh*II and *sh*I of *P. furiosus*.

Table 20: List of the mutant strains used in this study

Name	*Loci* mutated	UBOCC ID	Reference
Δ517(WT)	Deletion of: TERMP_00517	UBOCC-M-3300	(Birien et al., 2018)
Δ*mbh*	Deletions of: TERMP_01471 to TERMP_01498 (both *mbh2* and *mbh*1 complexes)	UBOCC-M-3311	(Birien, 2018)
Δ*co-mbh*	Deletions of: TERMP_01146 to TERMP_01150 (hydrogenase unit of the Mrp-Mbh-COdh complex (*co-mbh*)).	UBOCC-M-3312	
Δ*mbs* (previously called Δmbx)	Deletions of: TERMP_00853 to TERMP_00865 (whole complex)	UBOCC-M-3315	
Δ*shI*	Deletions of: TERMP_00067 to TERMP_00070 (whole complex)	UBOCC-M-3313	
Δ*shII*	Deletions of: TERMP_00536 to TERMP_00539 (whole complex)	UBOCC-M-3314	

Culture conditions and physiological measurements

All tests were realized in *Thermococcales* Rich *Medium* (TRM), in fully-filled anaerobic glass flasks of 14 mL topped with new butyl stoppers, as described in chapter II, both at atmospheric pressure and at 40 MPa. Cultures were performed in Top Industrie discontinuous incubators, pressurized or not, and cell densities were evaluated by optical counting (Thoma cell). As this methodology imposed discontinuous cultures with a maximum of 5 time points per series, several experiment results (between 1 and 4 series per mutant, each point being realized in triplicate) were gathered into unique growth curves. Note that in the curves, final cell densities always designated verified plateau phases. Growth rates were calculated on the merged curves (hence no error was calculated) but were to be considered only indicatively in some cases, where the number of points to delimit the exponential phase was not sufficient. In order to ensure the absence of elemental sulfur in the *medium*, pre-cultures were performed in 0.05 g/L S°, and ensuing cell inoculations in assay cultures did not exceed 5 % (vol./vol.). For the condition "presence of sulfur", a final concentration of 0.25 g/L of added colloidal sulfur was used, as determined optimal in our model for normal growth with an active hydrogenogenic metabolism (see chapter I). Na_2S was added for *medium* reduction at a final concentration of 0.05 % (wt./vol.).

Acetate and H_2S concentrations were measured in culture triplicates at the beginning of the plateau phase of growth in each case, using respectively ionic chromatography and Cline assay, and were reported to cell numbers of the corresponding samples, after removal of non-inoculated *medium* values. Note that in the absence of sulfur, H_2S productions could still be measured, but the corresponding absolute amounts were low and close to our detection limit, which was attributed to the presence of Na_2S in the *medium*, which leads to sulfide, allowing biological reduction to H_2S.

Gene expressions were assessed by RT-qPCR, using relative comparison ($\Delta\Delta$Ct method (Livak and Schmittgen, 2001)) of each mutant's expressions to the levels of the wild type strain (Δ517(WT)) in given conditions. As no inter-plate calibrator was applied to such extent, comparisons of each mutant's expression data in different culture conditions were impossible; they were always reported to the wild type strain. RNA samples were extracted at

the middle-end of the exponential phases for each mutant, when possible, according to the pre-established growth curves in each condition (data not shown). RNA qualities and concentrations were checked by Nanodrop and/or Bioanalyzer (Agilent), then cDNAs were produced by reverse transcription, thanks to a qScript Flex cDNA synthesis kit (Quantabio). Quantitative PCR reactions were performed thanks to a PerfeCTa SYBR Green Supermix ROX kit (Quantabio), and analyzed on a StepOne Real-Time PCR system (Thermo-Fisher).

A list of the primers used and the targeted regions is displayed in TABLE 21. The 30S ribosomal subunit was used as an internal reference for normalization. Each value was obtained in biological triplicate, however, due to a lack of technical replicate and the inherent variability of RT-qPCR protocols, some data remained unavailable and need to be confirmed.

Note that the work presented herein would have taken a much longer time without the help on many levels from several colleagues and collaborators: Yann Moalic (assistant professor / researcher), Erwan Roussel (researcher), Madina Ahmed (master student), Guillaume Lannuzel (technician), Pauline Grippon (undergraduate student), Anaïs Sire de Vilar (master student) and Kateline Letoquart (master student), and Mohamed Jebbar (professor). Unfortunately, at the time of writing, measurements could not be yet obtained for all conditions in some mutants.

Results

T. barophilus strain Δ517 (wild type)

Δ517 was the strain equivalent to the wild type *T. barophilus* MP^T as adapted for the use of the genetic tool (Birien et al., 2018). Both growth phenotypes in the presence and absence of sulfur of *T. barophilus* MP^T and strain Δ517 were tested at atmospheric pressure and 40 MPa and were found to be equivalent (not shown). The latter was used for comparison with mutant derivative strains, and was designated herein as Δ517(WT).

Table 21: List of the primers used for RT-qPCR and the corresponding region targeted in this study

Target name	*Locus* targeted	Forward primer sequence (5'to 3')	Reverse primer sequence (5'to 3')	Amplicon size (bp)
*sh*I	TERMP_00068	TACCTACCGGCCAGGTCAGT	GGTCCCCGAATGCCCACA	180
*sh*II	TERMP_00536	GCATAGCTGACCC TTCCATTCTT	AACAACGCTGATCTGCTCTATGG	284
*mbh*2	TERMP_01480	GTTCACGCTCTTCCTCCTTG	GTCGCTTCGCCAAGAGTATC	174
*mbh*1	TERMP_01494	AGTGGCTTCTCCAAGGG TATCATAAC	ATCCTTGGTGTGCTCTTAATA GTAGCTAACC	195
mbs	TERMP_00865	GCAGCACTCTGTAG GCAACATC	TTCCTGACGAGCAGCCTTGATC	205
*sur*R	TERMP_00656	CGTCCAGCTTTATGCCCCTGT	CCTCAACGGCAGTCTCAAAACA	180
co-mbh	TERMP_01140	TGGTGTTGGCTTGCTTGTAG	ATAGCTGCCCGTGATTGTTC	163
nsr	TERMP_02185	CTGATGCACTATCCCCC AGAATTCTTC	CTCCCTTATCGCAACTGCATCG	246
*nfn*1	TERMP_00066	GTGCATGAGTTGTGAATC CTTTCATTCC	GCCAAGCCACATAGACAGGTTTG	239
*nfn*2	TERMP_01522	TTCCGCTTAATCCAG AGAAGAGCT	TTGATCTGTCCTCCA ACAGTAACCCT	256
30S	TERMP_00095 (ribosomal subunit for internal standard)	AGTGGTGGCCGCTATTATTG	TAGGATTTCACCCCTACCCC	156

We first observed some phenotypical differences of this wild type strain according to culture conditions: in the presence (0.25 g/L) or absence of colloidal sulfur, and at atmospheric pressure and 40 MPa (optimal pressure for growth at 85 °C) (FIGURE 54). Results for metabolite productions were always displayed as reported to the corresponding cell number, as more significant to the metabolic behavior of a cell. No gene expression could be displayed for comparing the effects of each condition on this wild type strain, which served as a reference for other mutants' gene expressions.

The absence of sulfur, in our culture conditions, limited both growth rates and *maximum* cell densities of Δ517(WT). In both the presence or absence of sulfur, growth was also affected by pressure. Growth rates seemed enhanced both in the presence and absence of sulfur at 40 MPa compared to P_{atm}. The rates in the presence of sulfur were slightly inferior herein (1.11 h^{-1} at 40 MPa and 0.53 h^{-1} at P_{atm}) compared to the literature description of *T. barophilus* MP^T (about 1.55 h^{-1} at 40 MPa and 0.6 h^{-1} at P_{atm}), but culture conditions (*e.g.* different *medium*) were not strictly similar, and our results did not allow precise calculations due to insufficient samples number in exponential phase (Marteinsson et al., 1999a). In our results, *maximum* cell densities were however not significantly different at low and high pressures, for each respective sulfur condition.

It appeared that in the presence of sulfur at P_{atm}, cellular productions of acetate and H_2S were almost equivalent (9 – 11 µmol/10^9cell), but different in the absence of sulfur, where no H_2S could be detected and acetate was over-produced. At high pressure, each cellular H_2S production was more important than at P_{atm}, in the presence of sulfur, but was not detected without sulfur.

As expected, pressure shifted the phenotype of the wild type strain. Consequently all mutants were then compared to this wild type strain, as the outcomes of low and high pressure conditions of culture could not be solely attributable to the effect of the mutation, but also of sulfur and pressure.

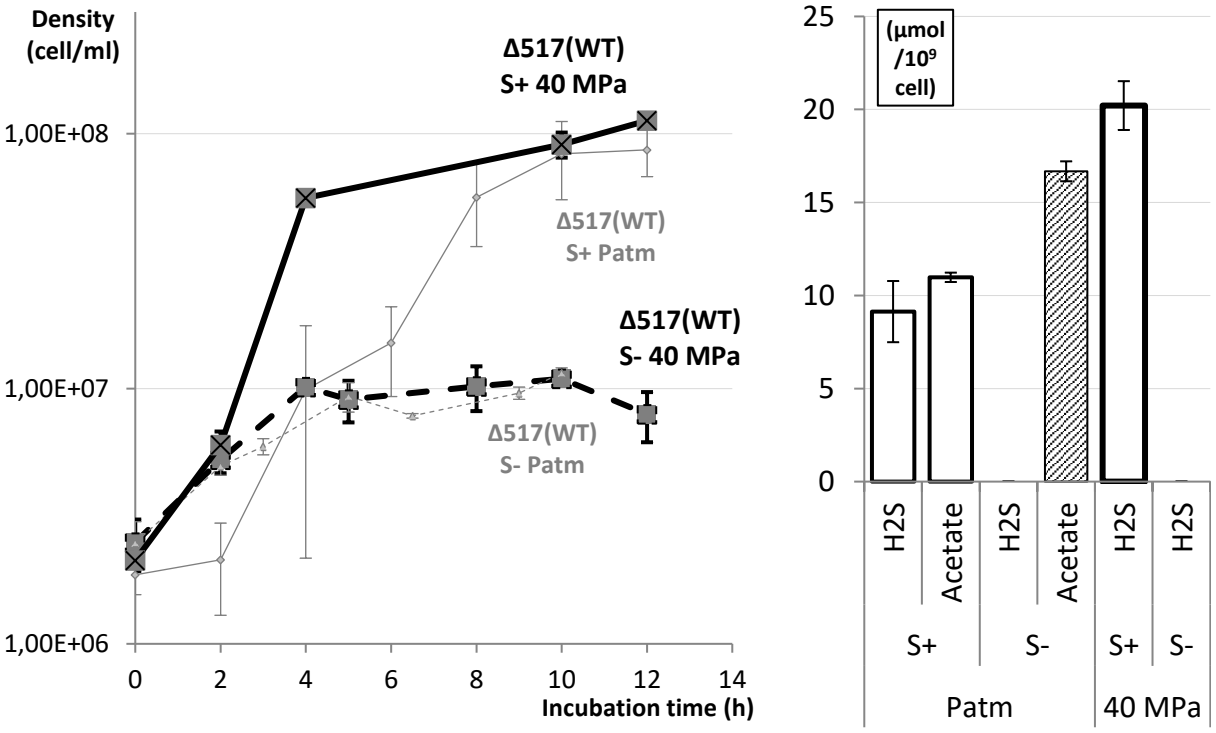

	P_{atm}		40 MPa	
Max. density .10^6 cell/mL (rate h^{-1})	**S+**	**S-**	**S+**	**S-**
Δ517(WT)	86 (0.53)	10 (0.26)	113 (1.11)	12 (0.37)

Figure 54: Growth curves and characteristics, cellular acetate and cellular H_2S productions of *T. barophilus* Δ517(WT) in the presence (0.25 g/L) or absence of sulfur, at atmospheric pressure and 40 MPa

Acetate productions could not be assayed at 40 MPa at the time of writing. Error bar represent standard deviations. Note that the important error bar in the growth curve at 4 h is for P_{atm} Δ 517(WT) with sulfur, and not the confounded point of 40 MPa Δ517(WT) without sulfur, for which the error is small enough not to be seen on this graph.

When absolute metabolite concentrations were below our detection method thresholds, corresponding reported concentrations were consequently indicated as null.

In the table, maximum *densities were expressed in .10^6 cell/mL, and the corresponding growth rates in exponential phase were displayed in parentheses (in h^{-1}).*

Δ*mbh*

A previously constructed Δ*mbh* mutant strain, with both *mbh*1 and *mbh*2 deleted, was examined in this study. Mbh has been reported to be important for H_2 evolution, using reduced ferredoxin. Growth, H_2S cellular productions were assessed in the presence (0.25 g/L) and absence of sulfur, at atmospheric pressure and 40 MPa, and acetate productions were measured at atmospheric pressure (FIGURE 55). Gene expressions of different key clusters of the energy conservation metabolism of Δ*mbh* compared to Δ517(WT) were assessed by RT-qPCR, in the presence and absence of sulfur at atmospheric pressure, and in the presence of sulfur at high pressure (FIGURE 56).

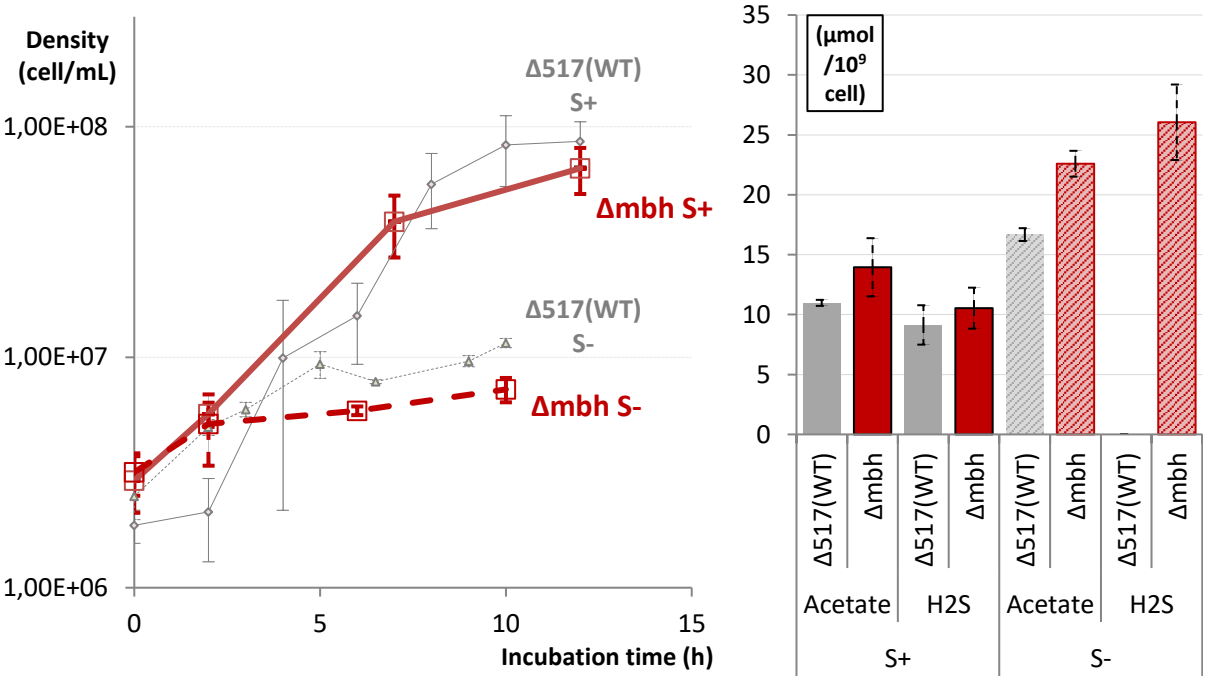

Atmospheric pressure

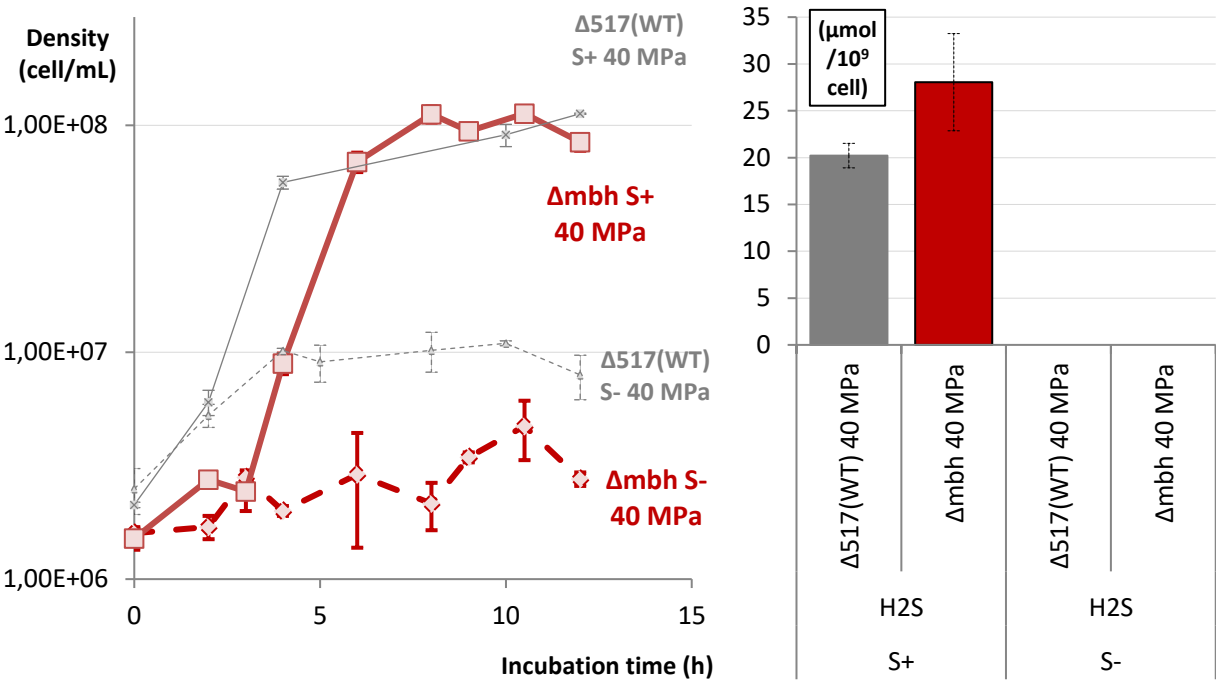

40 MPa

	P_{atm}		40 MPa	
Max. density .10^6 cell/mL (rate h^{-1})	**S+**	**S-**	**S+**	**S-**
Δ517(WT)	86 (0.53)	10 (0.26)	113 (1.11)	12 (0.37)
Δmbh	66 (0.37)	7 (0.24)	113 (1.11)	5 (0.10)

Figure 55: Growth curves and characteristics, cellular acetate and cellular H_2S productions of *T. barophilus* Δ517(WT) and *Δmbh* in the presence (0.25 g/L) or absence of sulfur, at atmospheric pressure and 40 MPa

Error bars represent standard deviations.

In the table, maximum *densities were expressed in .10^6 cell/mL, and the corresponding growth rates in exponential phase were displayed in parentheses (in h^{-1}). When absolute metabolite concentrations were below our detection method thresholds, corresponding reported concentrations were consequently indicated as null.*

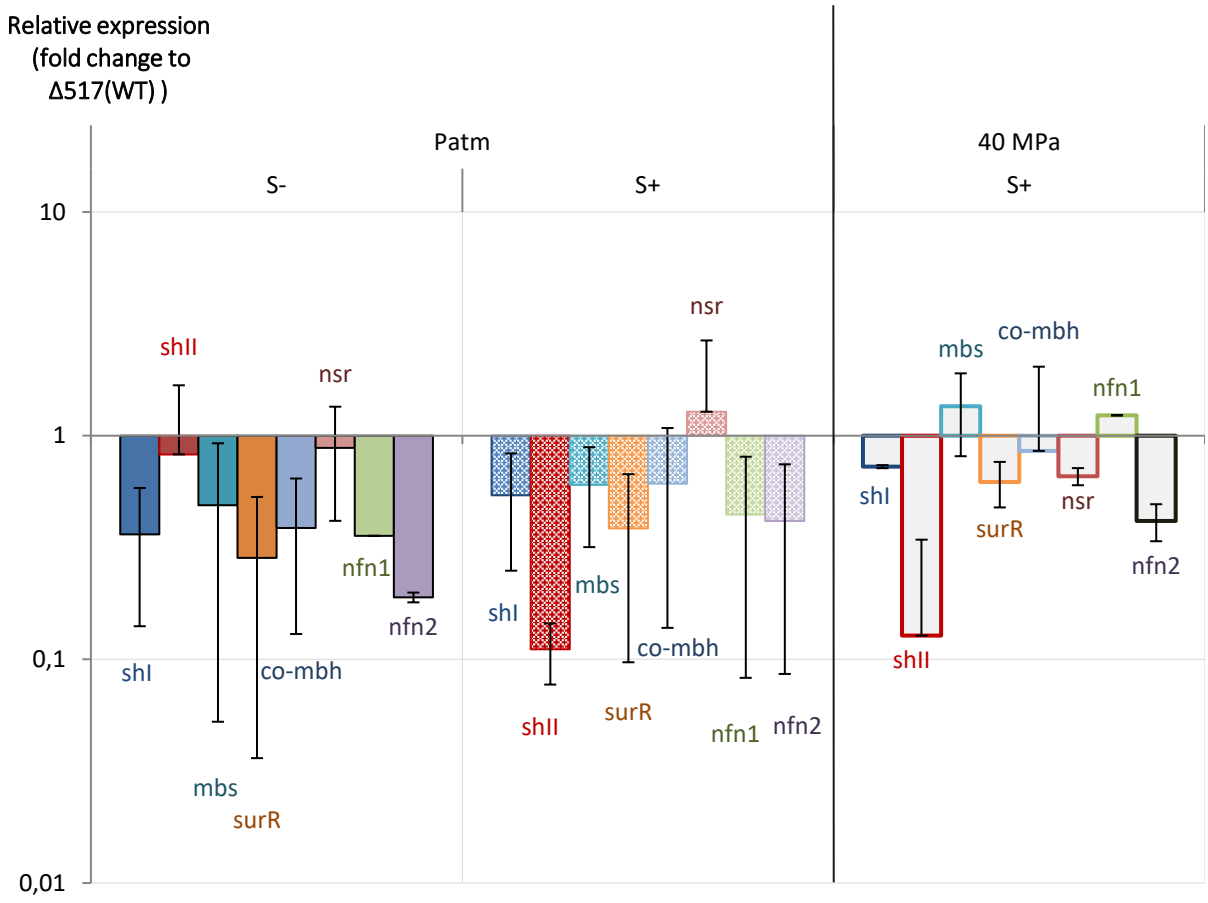

Figure 56: Expression of different genes in Δ*mbh*, relative to Δ517(WT) in the presence (0.25 g/L) or absence of sulfur, at atmospheric pressure and 40 MPa

Vertical axis is in logarithmic scale and represents fold changes between expression values for given targets of Δmbh compared to Δ517(WT) (level 1 of expression). Error bars represent standard deviations.

At atmospheric pressure, in the presence of sulfur, growth of Δ*mbh* strain seemed to reach almost equivalent rate (0.37 h^{-1}) to Δ517(WT) (0.53 h^{-1}), yet imprecisely calculated. The observable higher cell density after 2 h of incubation could be interpretable as a result of a slightly higher starting cell density, although more points should be obtained to better conclude on this small shift. *Maximum* cell concentrations seemed almost equivalent (6.6 $.10^7$ cell/mL for the mutant and 8.6 $.10^7$ cell/mL for the wild type strain). This was in contrast to the absence of sulfur, where practically no growth was observed in the mutant strain, with a final biomass even more limited than for the wild type (respectively 7.25 $.10^6$ cell/mL and 1.15

.10^7 cell/mL). Levels of H_2S produced per cell were equivalent in the mutant in the presence of sulfur (around 10.5 µmol/10^9cell) but higher for the mutant strain in the absence of sulfur (26.0 µmol/10^9cell for Δ*mbh*, not detected for Δ517(WT)). Acetate was also overproduced by the mutant strain in both the presence (14.0 *vs.*11.0 µmol/10^9cell) and absence (22.6 *vs*. 16.7 µmol/10^9cell) of sulfur. Expression patterns of many targeted genes were affected, showing a global metabolic adaptation induced by the mutation, regardless whether strain growth was impaired or not. The presence of sulfur seemed to induce two important differences compared to the absence of sulfur. Compared to the wild type strain, Δ*mbh* underexpressed *sh*II (9-fold) and slightly overexpressed *nsr* (1.3-fold) in the presence of sulfur, while those transcriptions seemed equivalent to the wild type in the absence of sulfur.

At 40 MPa, Δ*mbh* mutant strain showed a similar growth to the wild type strain (*i.e.* same growth rate (1.11 h^{-1}) and *maximum* densities (1.13 .10^8 cell/mL)), but with a 2 h shift, and thus a more important lag phase (FIGURE 55). In the absence of sulfur however, very little growth was observed, compared to the wild type, hardly exceeding the initial cell concentration. The corresponding acetate levels could unfortunately not be measured, but H_2S cellular production was higher in Δ*mbh* (28.1 µmol/10^9cell) than in the wild type strain (20.2 µmol/10^9cell) in the presence of sulfur, but was not detected in the absence of sulfur, probably due to the very low cell density associated. Interestingly, in the presence of sulfur, high pressure did not lead to the same expression patterns in all the tested *loci*. *mbs*, *nsr* and *nfn*1 expression patterns in the Δ*mbh* strain were reversed at high pressure *versus* atmospheric pressure in the presence of sulfur, compared to the wild type strain.

In *T. barophilus*, *mbh* thus seems to be non-essential for growth in the presence of sulfur, where acetate is rather used for compensatory electron sink (at P_{atm} at least), through a genetic circuit involving expressions of more *nsr* and less *sh*II than in the absence of sulfur. But *mbh* deletion significantly impairs growth in the absence of sulfur, where both H_2S and acetate are used for compensation. At high pressure, the effects of Mbh seem more dramatic: while growth is not prevented in the presence of sulfur, an extra time is necessary, probably to acclimatize and compensate (with H_2S overproduction, probably *via mbs*

overexpression and *nsr* underexpression, compared to atmospheric pressure), and the membrane hydrogenase gene seems essential for growth without sulfur.

Δ*co-mbh*

The Δ*co-mbh* strain lacks the hydrogenase encoding gene of the Mrp-Mbh-COdh cluster. Same measurements as for Δ*mbh* were realized (FIGURE 57 and FIGURE 58). Note that for gene expressions, the targeted gene (*mrp*) was not deleted in the Δ*co-mbh* mutant.

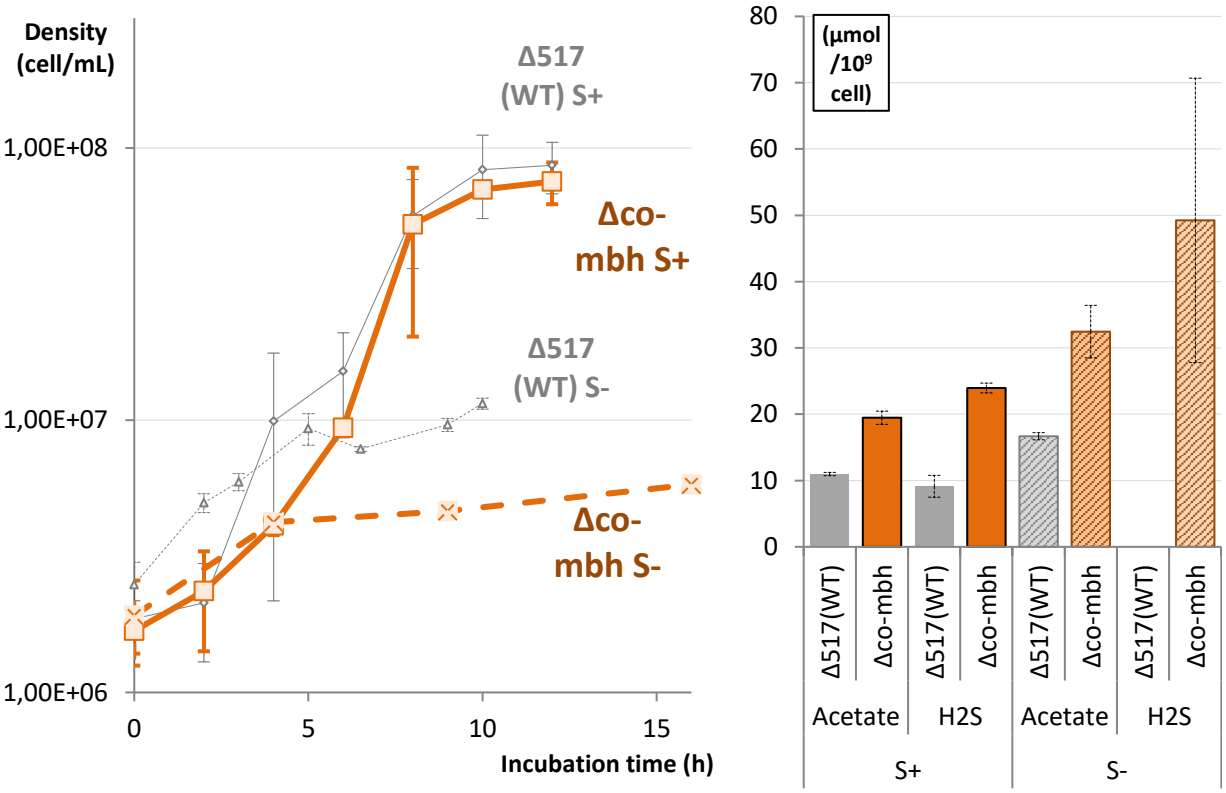

Atmospheric pressure

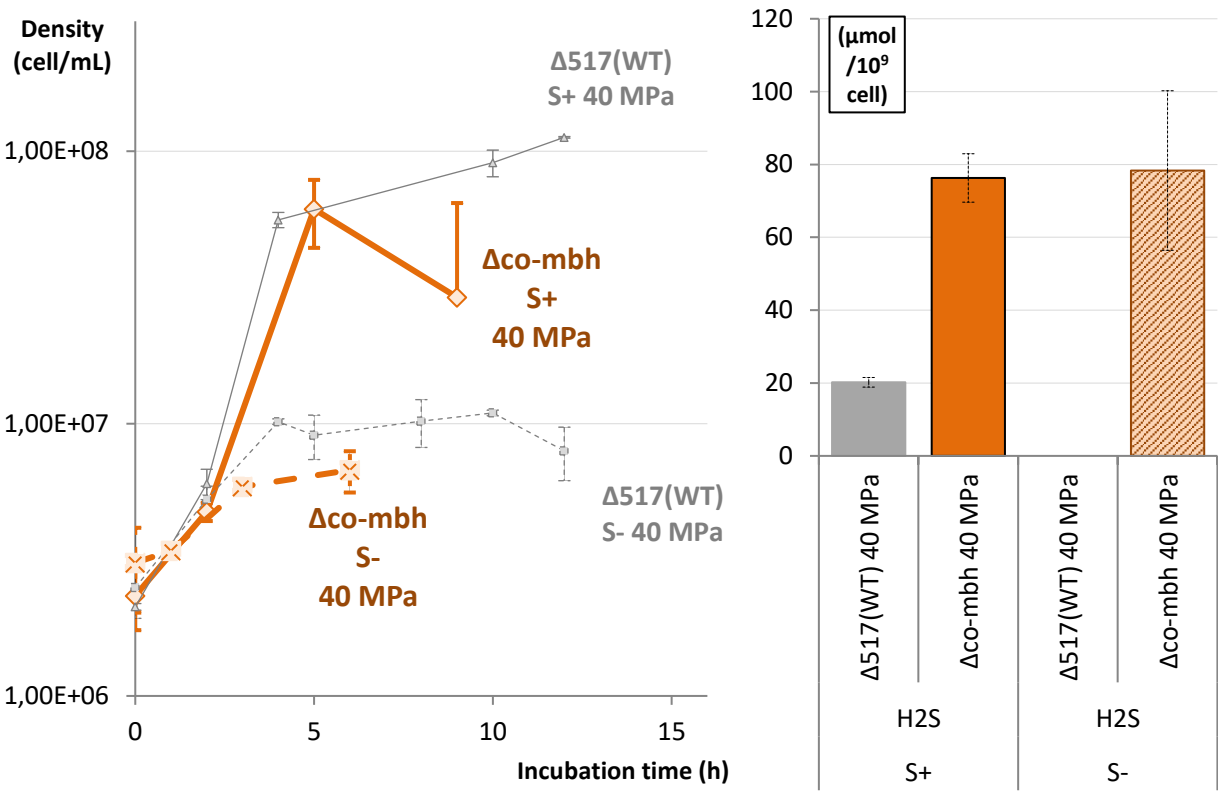

40 MPa

	P_{atm}		40 MPa	
Max. density .10^6 cell/mL (rate h^{-1})	**S+**	**S-**	**S+**	**S-**
Δ517(WT)	86 (0.53)	10 (0.26)	113 (1.11)	12 (0.37)
Δco-mbh	75 (0.52)	6 (0.20)	91 (0.67)	7 (0.21)

Figure 57: Growth curves and characteristics, cellular acetate and cellular H_2S productions of *T. barophilus* Δ517(WT) and *Δmo-mbh* in the presence (0.25 g/L) or absence of sulfur, at atmospheric pressure and 40 MPa

Error bars represent standard deviations. In the table, maximum *densities were expressed in .10^6 cell/mL, and the corresponding growth rates in exponential phase were displayed in parentheses (in h^{-1}). When absolute metabolite concentrations were below our detection method thresholds, corresponding reported concentrations were consequently indicated as null.*

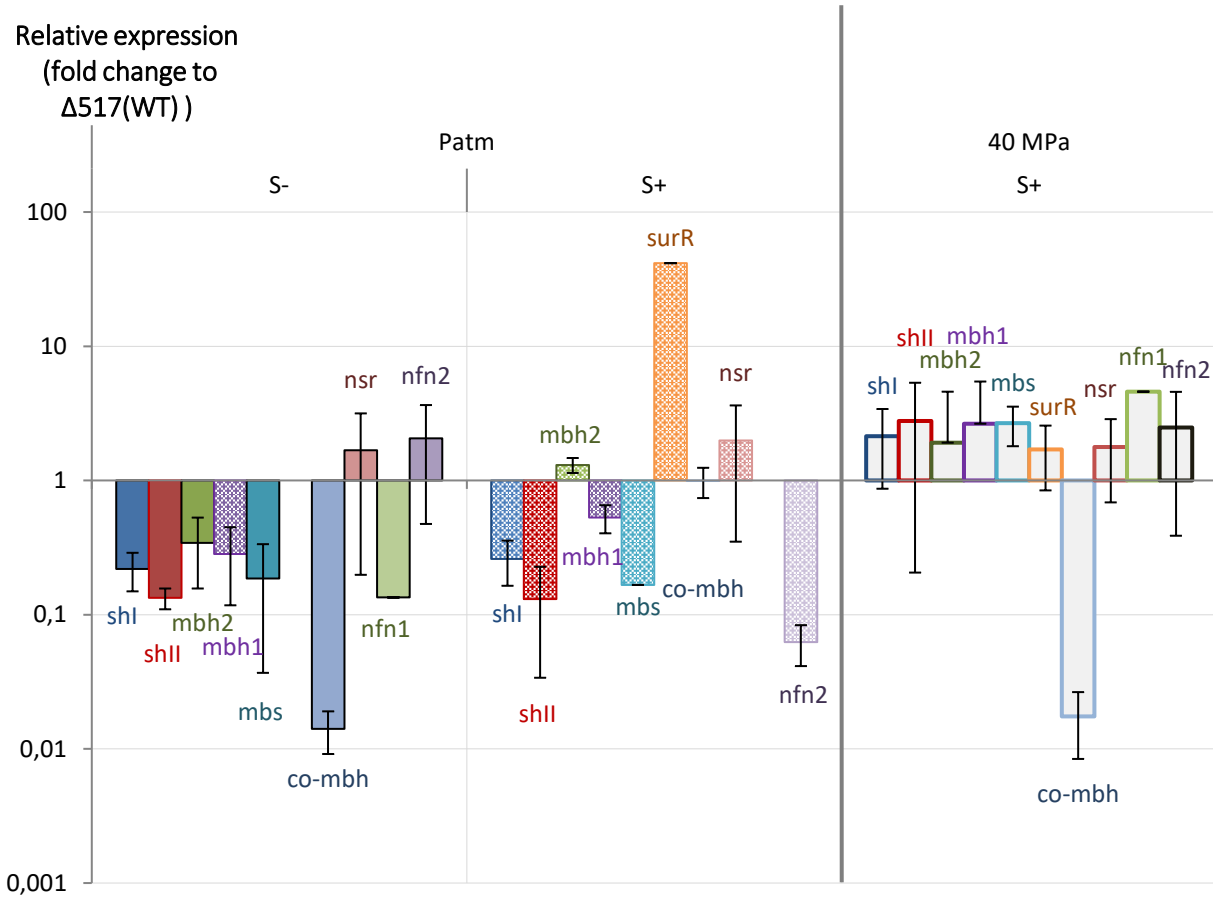

Figure 58: Expression of different genes in Δ*co-mbh*, relative to Δ517(WT) in the presence (0.25 g/L) or absence of sulfur, at atmospheric pressure and 40 MPa

*Vertical axis is in logarithmic scale and represents fold changes between expression values for given targets of Δ*co-mbh *compared to Δ517(WT) (level 1 of expression). Error bars represent standard deviations.*

No sur*R and no* nfn*1 expression data could be obtained at atmospheric pressure, respectively in the absence and presence of sulfur.*

Note that co-mbh *expression was displayed here, since the RT-qPCR-targeted part of the cluster was not deleted (primers targeted* mrp *while only* mbh *was deleted).*

At atmospheric pressure, deletion of *co-mbh* did not dramatically impact growth in the presence of sulfur, although significantly higher cellular levels of acetate (19.5 µmol/10^9cell) and H_2S (24.0 µmol/10^9cell) were observed, compared to the wild type strain (11.0 µmol/10^9cell acetate and 9.1 µmol/10^9cell H_2S). In the absence of sulfur, growth of the Δ*co-*

mbh strain was impaired (rate of 0.20 h^{-1}) compared to the wild type, in a similar fashion to Δ*mbh*. In the latter conditions, Δ*co-mbh* cells also significantly overproduced acetate (32.5 µmol/10^9cell) and H_2S (49.2 µmol/10^9cell). Main differences in gene expressions between the presence and absence of sulfur at P_{atm} could be noted for *mbh*2, which was underexpressed (3.6-fold) in Δ*co-mbh* compared to Δ517(WT) in the absence of sulfur, but overexpressed (1.3-fold) in the presence of sulfur. Inversely, *nfn*2 was not significantly differentially expressed compared to Δ517(WT) in the absence of sulfur, but underexpressed (16.5-fold) in the presence of sulfur. Additionally, the *mrp* coding sequence of *co-mbh* was underexpressed (71-fold) in the absence of sulfur in the mutant compared to the wild type strain, contrarily to in the presence of sulfur where it was not regulated. Note that no *sur*R expression data could be obtained in the absence of sulfur, but that in the presence of sulfur, it was overexpressed (41-fold) in the mutant compared to the wild type.

At 40 MPa, growth rates of Δ*co-mbh* were slightly inferior to Δ517(WT), and Δ*co-mbh* likely led to lower *maximum* cell densities. Those conclusions could however benefit from more points to add precision to the curves. This growth pattern was associated to an important H_2S cellular overproduction (almost 4-fold) compared to the wild type strain. Unfortunately, acetate concentrations could not be measured here. In the absence of sulfur, growth was even more limited in the Δ*co-mbh* mutant compared to the wild type, as low final cell densities were reached (6.75 $.10^6$ cell/mL), and cellular H_2S was overproduced. Unfortunately, no acetate data were available for these experiments. Gene expressions, compared to the wild type strain, seemed differently affected at high pressure than at atmospheric pressure, in the presence of sulfur. *sh*I, *sh*II, and *nfn*2 were no more underexpressed. *mbh1* and *mbs*, while underexpressed (respectively 1.9-fold and 6-fold) at atmospheric pressure in the presence of sulfur in Δ*co-mbh* compared to Δ517(WT), were now overexpressed (2.6-fold and 2.7-fold). The gene encoding the master regulator SurR was no more overexpressed in the mutant compared to the wild type strain, at high pressure. The *mrp* coding sequence of *co-mbh* was also much underexpressed at high pressure (57.5-fold)

but not differentially regulated at atmospheric pressure in the mutant strain compared to the wild type, in the presence of sulfur.

Overall, *co-mbh* seemed to be non-essential for growth of *T. barophilus* in the presence of sulfur, although high pressure appeared to mitigate this tendency, which could be the result of different gene expression patterns. In the absence of sulfur, *co-mbh* was not essential but its deletion greatly impaired growth. In all cases, H_2S (and maybe acetate) productions were probably used to compensate the enzyme's absence.

Δ*mbs*

Mbs is known to be involved in indirect H_2S synthesis in *Thermococcales*. The whole *mbs* complex gene was previously deleted, and same measurements on Δ*mbs* mutant strain than for Δ*mbh* and Δ*co-mbh* mutants were performed (FIGURE 59 and FIGURE 60).

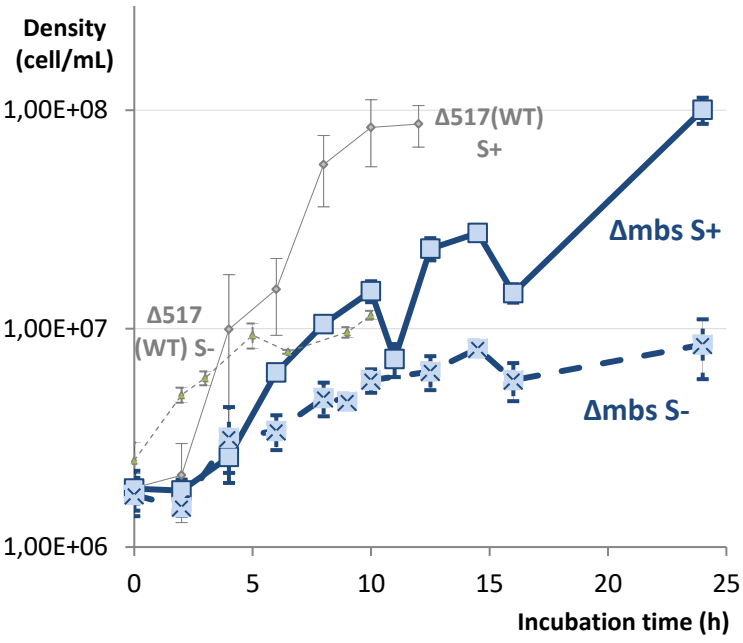

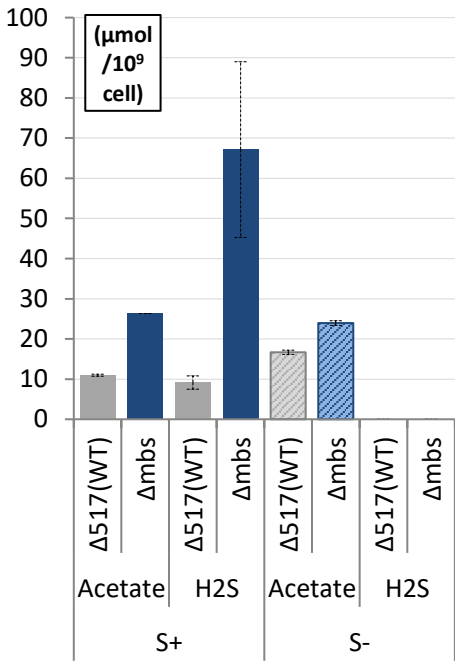

Atmospheric pressure

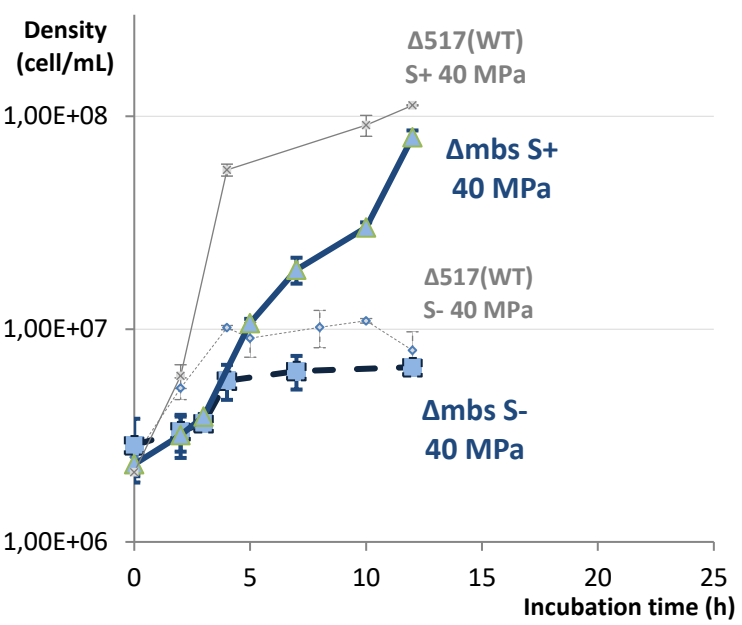

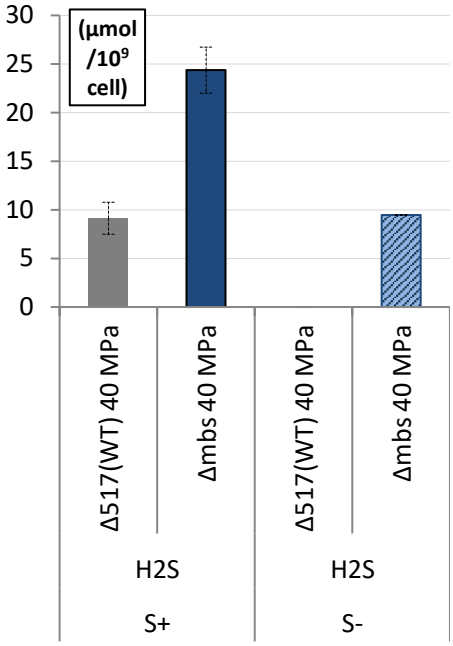

40 MPa

	P_{atm}		40 MPa	
Max. density .10^6 cell/mL (rate h^{-1})	**S+**	**S-**	**S+**	**S-**
Δ517(WT)	86 (0.53)	10 (0.26)	113 (1.11)	12 (0.37)
Δmbs	100 (0.18)	8 (0.13)	80 (0.30)	7 (0.29)

Figure 59: Growth curves and characteristics, cellular acetate and cellular H_2S productions of *T. barophilus* Δ517(WT) and *Δmbs* in the presence (0.25 g/L) or absence of sulfur, at atmospheric pressure and 40 MPa

Error bars represent standard deviations. In the table, maximum *densities were expressed in .10^6 cell/mL, and the corresponding growth rates in exponential phase were displayed in parentheses (in h^{-1}). When absolute metabolite concentrations were below our detection method thresholds, corresponding reported concentrations were consequently indicated as null.*

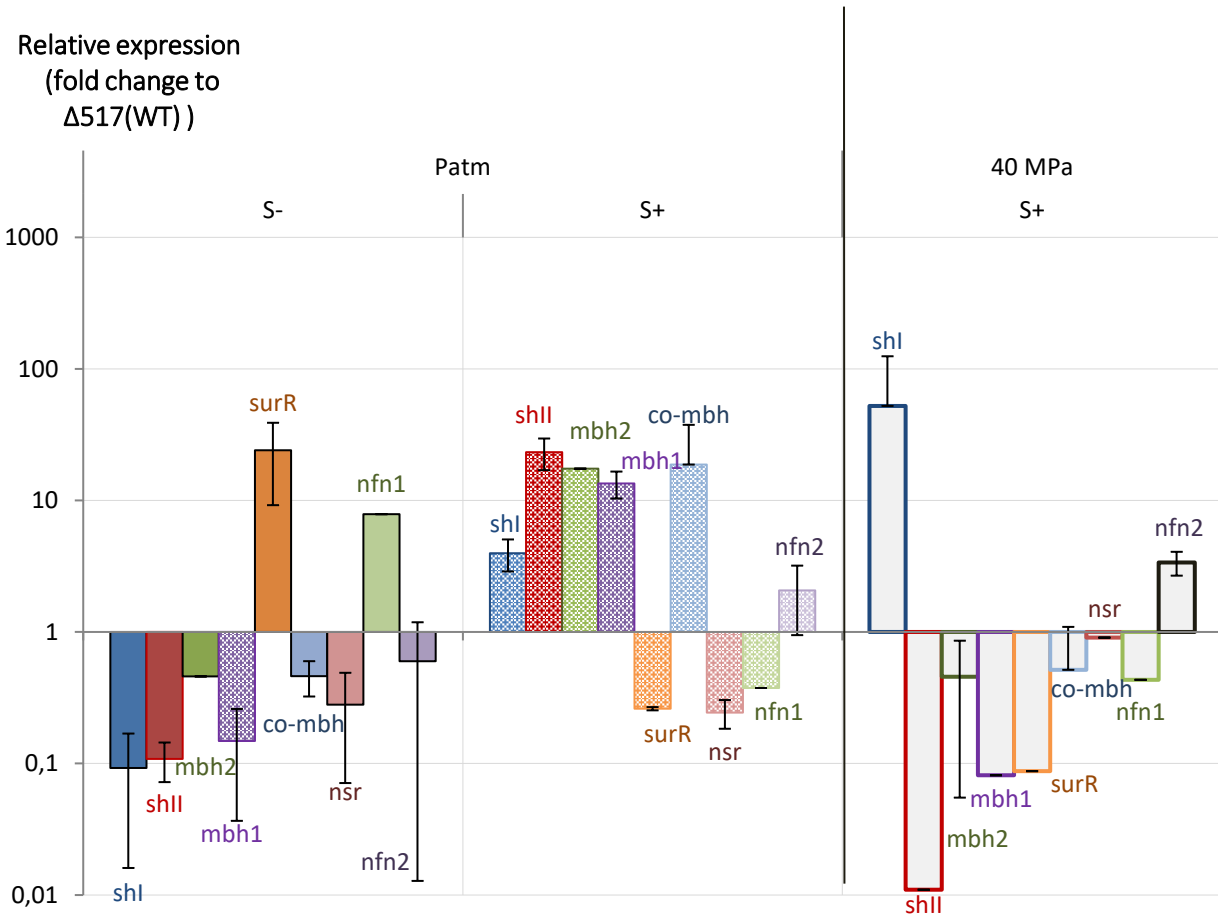

Figure 60: Gene expression of different genes in Δ*mbs*, relative to Δ517(WT) in the presence (0.25 g/L) or absence of sulfur, at atmospheric pressure and 40 MPa

Vertical axis is in logarithmic scale and represents fold changes between expression values for given targets of Δmbs compared to Δ517(WT) (level 1 of expression). Error bars represent standard deviations.

At atmospheric pressure, growths of Δ*mbs* were significantly impaired as against the wild type strain both in the presence and absence of sulfur. *Maximum* cell densities were equivalent in both cases, but growth rates seemed dramatically lower in the mutant strain (3-fold and 2-fold in the presence and absence of sulfur). Those phenotypes were accompanied by higher cellular productions of acetate and H_2S (more than 7-fold H_2S overproduction in the presence of sulfur). Interestingly, all tested target expression patterns (except *nsr*), compared to the wild type, were reversed between the presence and absence of sulfur at atmospheric pressure. While *sh*I, *sh*II, *mbh*1, *mbh*2, *co-mbh* and *nfn*2 expressions were downregulated, *sur*R and *nfn*1 expressions were upregulated compared to Δ517(WT) in the absence of sulfur.

nsr was underexpressed in the mutant strain compared to the wild type at atmospheric pressure both in the absence and presence of sulfur. Note that these results do not indicate that *nsr* expression was inhibited in the mutant strain, but only that its expression was less important than in the wild type strain.

Same observations could be made at high pressure, comparing Δ*mbs* and Δ517(WT) in the presence of sulfur for growth and cellular H_2S productions (unfortunately, acetate productions could not be measured at high pressure). In the absence of sulfur, the Δ*mbs* strain produced more H_2S per cell that at atmospheric pressure (as no levels could be detected with our method in the latter condition). High pressure induced changes in expressions patterns of several genes, related to their expression levels in the wild type strain in same conditions (presence of sulfur) and compared to the relations observed at atmospheric pressure between both strains. Noticeably, *sh*II, *mbh*1, *mbh*2, and *co-mbh* were underexpressed (while overexpressed at P_{atm}) compared to Δ517(WT) , and *sh*I and *nsr* were significantly more expressed compared to the wild type strain, at high pressure. *nfn*1 and *nfn2* relative expressions did not vary much at high pressure compared to their relative expressions at atmospheric pressure.

Consequently, it seemed that, regardless of the pressure, Mbs is not essential in *T. barophilus* in both the presence and absence of sulfur, but that its deletion can be compensated at the price of a slower growth and higher acetate and H_2S cellular productions, which does not ensue from same gene expression compensation patterns at sub-optimal and optimal pressure for growth (in the presence of sulfur, sulfidogenic system rather overexpressed at high pressure, while hydrogenogenic system overexpressed at atmospheric pressure).

Δ*sh*I

SHI (similarly to SHII) has been described in other models as a cytoplasmic enzyme consuming H_2 and supplying NADPH back to the metabolic system. A previously constructed Δ*sh*I mutant strain was examined in this study. Growth, acetate and H_2S cellular productions

were assessed in the presence (0.25 g/L) and absence of sulfur, at atmospheric pressure and 40 MPa (FIGURE 61). Gene expressions of different key clusters of the energy conservation metabolism of Δ*sh*I compared to Δ517(WT) were assessed by RT-qPCR, in the presence and absence of sulfur at atmospheric pressure, and in the presence of sulfur at high pressure (FIGURE 62).

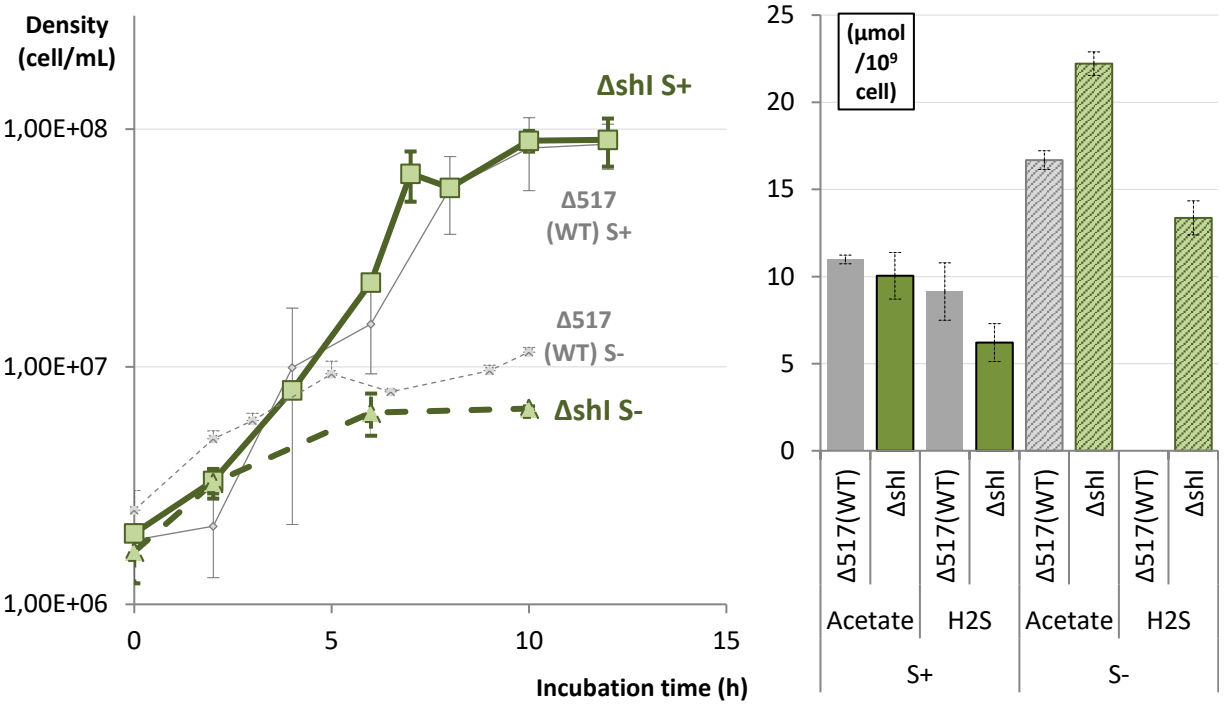

Atmospheric pressure

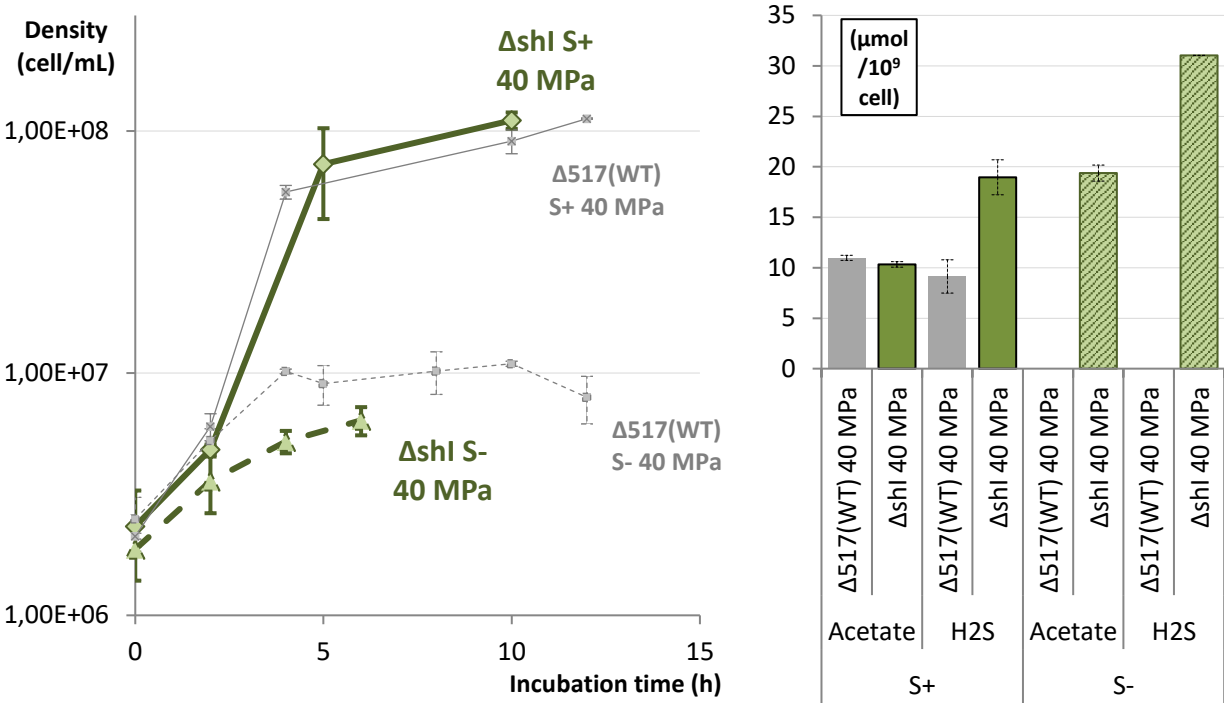

40 MPa

	P_{atm}		40 MPa	
Max. density .10^6 cell/mL (rate h^{-1})	**S+**	**S-**	**S+**	**S-**
Δ517(WT)	86 (0.53)	10 (0.26)	113 (1.11)	12 (0.37)
Δ*sh*I	90 (0.60)	7 (0.22)	111 (0.91)	6 (0.20)

Figure 61: Growth curves and characteristics, cellular acetate and cellular H_2S productions of *T. barophilus* Δ517(WT) and Δ*sh*I in the presence (0.25 g/L) or absence of sulfur, at atmospheric pressure and 40 MPa

No acetate value was available for Δ517(WT) at high pressure. Error bars represent standard deviations. In the table, maximum *densities were expressed in .10⁶ cell/mL, and the corresponding growth rates in exponential phase were displayed in parentheses (in h^{-1}). When absolute metabolite concentrations were below our detection method thresholds, corresponding reported concentrations were consequently indicated as null.*

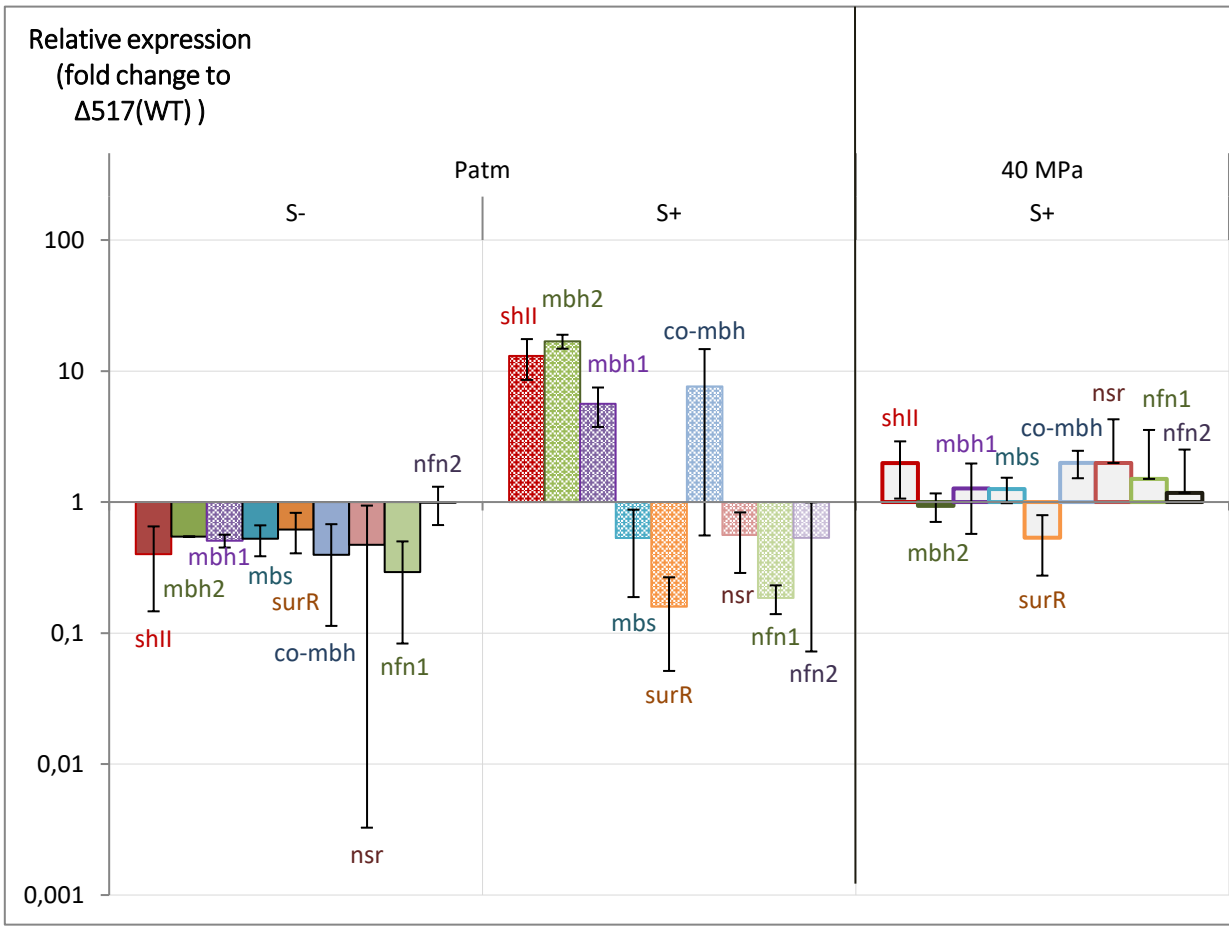

Figure 62: Expression of different genes in Δ*sh*I, relative to Δ517(WT) in the presence (0.25 g/L) or absence of sulfur, at atmospheric pressure and 40 MPa

Vertical axis is in logarithmic scale and represents fold changes between expression values for given targets of ΔshI compared to Δ517(WT) (level 1 of expression). Error bars represent standard deviations.

At atmospheric pressure, deletion of *sh*I seemed to lead to similar growth dynamics as for the wild type strain in the presence of sulfur, although a slight higher growth rate (0.60 h^{-1}) could be possible for the mutant. In those conditions, cellular acetate levels were equivalent for both strains (around 10 – 11 µmol/10^9cell), but Δ*sh*I tended to produce slightly less H_2S (6.2 µmol/10^9cell). In the absence of sulfur, growth of the mutant was less rapid than the wild type strain, and final cell densities were reduced (6.67 .10^6 cell/mL for Δ*shI versus* 1.15 .10^7 cell/mL for Δ517(WT)). In addition, both cellular acetate and H_2S were overproduced in that case in the mutant strain. The associated differences in gene

expressions in these two culture conditions were noticeably that all tested genes were underexpressed compared to the wild type in the absence of sulfur (except for *nfn*2 which showed roughly the same levels of expression), but in the presence of sulfur, *sh*II, *mbh*1, *mbh*2, and probably *co-mbh*, were overexpressed compared to in Δ517(WT)).

At 40 MPa, growth rates of the mutant were slightly lower than the wild type strain, both in the presence and absence of sulfur. However, different levels of metabolites were measured: while in the presence of sulfur, cellular acetate concentrations were still equivalent in both strains (10 – 11 µmol/10^9cell), H_2S was overproduced at 40 MPa (19.0 µmol/10^9cell), contrarily to at P_{atm}. Indeed, in the latter condition, *mbs* was no more underexpressed, and *nsr* was overexpressed (around 2-fold), compared to the wild type. Concomitantly, *mbh*1 and *mbh*2 expressions were equivalent to those of Δ517(WT)), and *sh*II and *co-mbh* were less overexpressed compared to the wild type than at atmospheric pressure. Interestingly, *nfn*1 and *nfn*2 showed also reversed patterns of expression relative to the wild type strain, being slightly upregulated at high pressure (respectively 1.5-fold and 1.2-fold).

In the absence of sulfur, at 40 MPa, we noted same tendencies as at P_{atm} for cellular H_2S and acetate productions when compared to the wild type, but noticeably, the relative proportion of acetate and H_2S levels in Δ*sh*I were reversed at both pressures.

Thus, at both tested pressures, SHI seemed non-essential in the presence of sulfur, but slightly hampered growth in the absence of sulfur. Pressure of growth seemed to influence the compensation routes employed, leading to more cellular H_2S at 40 MPa, and differences in other targeted gene expressions appeared to be more dramatic for the P_{atm} Δ*sh*I compensation.

Δ*sh*II

SHII (similarly to SHI) has been described in other models as a cytoplasmic enzyme consuming H_2 and supplying NADPH back to the metabolic system. A previously constructed Δ*sh*II mutant strain was examined in this study, with same measurements as for the Δ*sh*I mutant (FIGURE 63 and FIGURE 64).

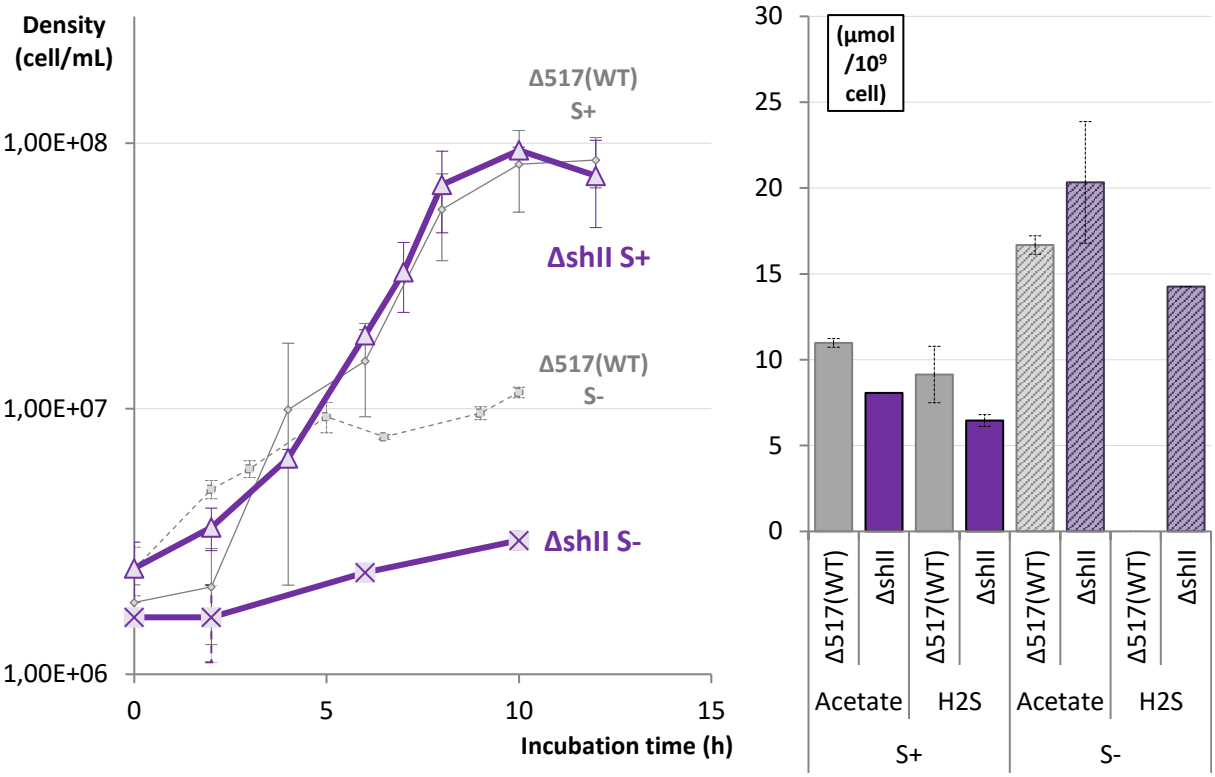

Atmospheric pressure

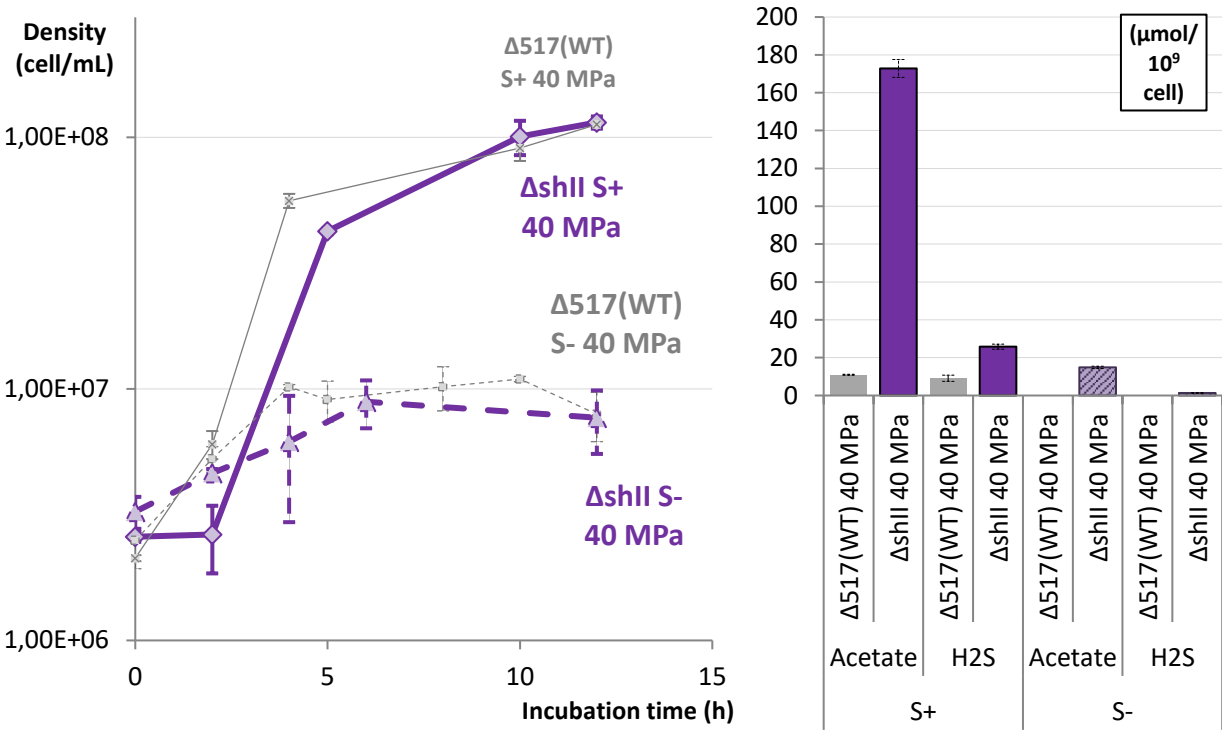

40 MPa

	P_{atm}		40 MPa	
Max. density .10^6 cell/mL (rate h^{-1})	**S+**	**S-**	**S+**	**S-**
Δ517(WT)	86 (0.53)	10 (0.26)	113 (1.11)	12 (0.37)
Δ*sh*I	94 (0.50)	3 (0.07)	115 (0.92)	9 (0.17)

Figure 63: Growth curves and characteristics, cellular acetate and cellular H_2S productions of *T. barophilus* Δ517(WT) and Δ*sh*II in the presence (0.25 g/L) or absence of sulfur, at atmospheric pressure and 40 MPa

No acetate value was available for Δ517(WT) at high pressure. Error bars represent standard deviations. In the table, maximum *densities were expressed in .10^6 cell/mL, and the corresponding growth rates in exponential phase were displayed in parentheses (in h^{-1}). When absolute metabolite concentrations were below our detection method thresholds, corresponding reported concentrations were consequently indicated as null.*

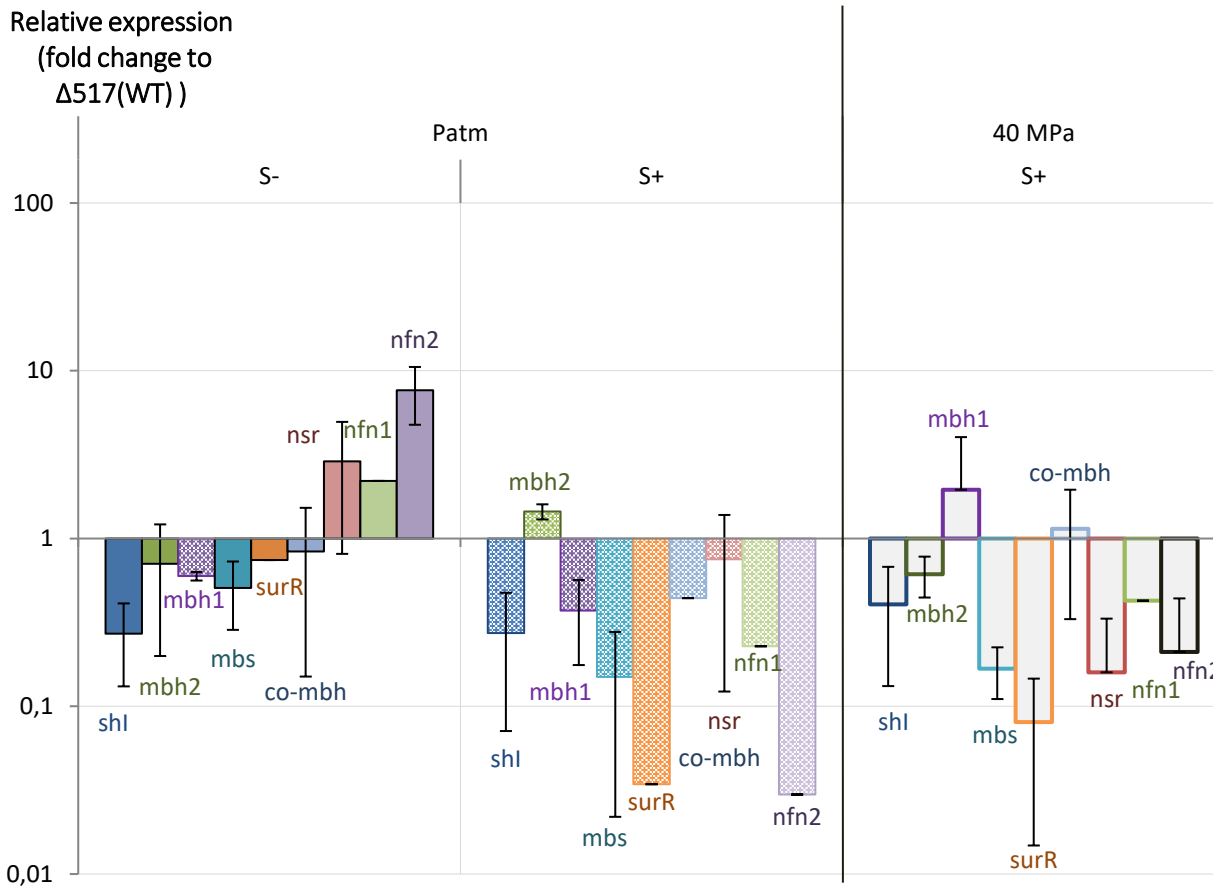

Figure 64: Expression of different genes in Δ*sh*II, relative to Δ517(WT) in the presence (0.25 g/L) or absence of sulfur, at atmospheric pressure and 40 MPa

Vertical axis is in logarithmic scale and represents fold changes between expression values for given targets of ΔshII compared to Δ517(WT) (level 1 of expression). Error bars represent standard deviations.

At atmospheric pressure, in the presence of sulfur, deletion of *shII* did not change significantly the growth phenotype, although cellular levels of acetate (8.1 µmol/10^9cell) and H_2S (6.5 µmol/10^9cell) were lowered compared to the wild type strain. However, in the absence of sulfur, growth of the mutant was completely impaired. The associated cellular levels of acetate and H_2S were not informative, consequently, and ensuing gene expression profiles were also to be confirmed. Main differences in the compensation to *sh*II deletion in gene expression compared to the wild type strain, in the absence and presence of sulfur, seemed to appear in the lower expression of all tested target in the functional phenotype (presence of sulfur), except *mbh*2, which was rather slightly upregulated (1.5-fold) compared

to Δ517(WT) in the presence of sulfur, contrarily to in the absence of sulfur (1.7-fold downregulation).

At high pressure, the growth defect observed in the absence of sulfur at P_{atm} was corrected, and was just slightly slower in the mutant (0.17 h^{-1}) than in the wild type strain (0.37 h^{-1}), but reached almost equivalent final cell densities. The measured metabolites reported to cell concentrations did not vary in those conditions in both strains. In the presence of sulfur, Δ*shI* seemed to show similar growth features than Δ517(WT), but with a supplementary lag phase of about 1 h. Importantly, the associated cellular acetate production was strikingly higher in the mutant strain (about 16-fold augmentation). High pressure seemed surprisingly to induce similar relative expression patterns in the tested target genes in the presence of sulfur, compared to the respective expression profiles of Δ517(WT). However, *mbh*1 and *mbh*2 relative expression patterns were reversed compared to at P_{atm}, and *co-mbh* was equivalently expressed at high pressure in the mutant than in the wild type strain.

Therefore, SHI seemed to be essential in the absence of sulfur, only at atmospheric pressure. At high pressure, the restored growth was associated to a very important acetate overproduction, which seemed to compensate for a lack of *sh*I, and which was also associated with the changes in membrane-bound hydrogenase expressions.

Discussions

This work reports various phenotypical observations made on strains harboring several deletions of key genes of the energy conservation metabolism of *T. barophilus*. We aimed to gather information on the respective roles of each of the deleted enzymes, as well as to investigate what adaptations could occur to compensate those absences. Additionally, we cared to evaluate the possible impacts of the presence or absence of sulfur and of high pressure.

The functions of the different parts of the metabolic system, their interactions, and the associated effects of sulfur and pressure, were discussed hereafter. Note that growths of those mutants were described in previous works in our laboratory, but were not performed in similar conditions as in this project (*e.g.* plastic syringes, uncontrolled sulfur excess for "sulfur presence" condition), and were thus not entirely comparable. For these reasons, the associated H_2 measurements could not be applied in this discussion neither (Birien, 2018). In the following interpretations, growth dynamics were considered as a proxy for ATP production.

In this work, the RT-qPCR experiment design was set up to allow observations of the expression compensations in place in each condition, compared to the wild type strain. We were however not able to formulate the expressions of each tested gene compared to itself at different conditions. Thereupon, no correlation with previous works on *T. barophilus* MP^T or other models expressions at different pressure could be accurately assessed, and the impact of pressure or sulfur were rather deducted from the whole set of data. The following hypotheses could ensue from the analysis of the results presented in this chapter. The interpretations discussed herein remain to some extent quite speculative and need to be next experimentally evidenced.

Hydrogenogenic system

. Both *mbh* and *co-mbh* could be required in the absence of sulfur

Two main systems, present in *T. barophilus* MP^T, have been described as directly responsible for hydrogenogenic growth: Mrp-Mbh (being duplicated) and Mrp-Mbh-COdh (Sapra et al., 2000; Schut et al., 2016b; Silva et al., 2000). In this work, deletion of genes encoding one or the other seemed to impact growth in the absence of sulfur (FIGURE 55), indicating that **both were necessary for the metabolism to be efficient, and that their role completed each other in these conditions.** Expression patterns tended to confirm this assumption, as compensations in gene expressions were different in relation to each condition for both enzymes (FIGURE 56), showing that they were not interchangeable in the

system, as they held different influences. In the presence of sulfur at atmospheric pressure, while the growth phenotype of both Δ*mbh* and Δ*co-mbh* (FIGURE 57) mutants were unaffected compared to the wild type strain, *mbh* deletion was compensated through a slight increase of acetate production, but none of H_2S production. On the other hand, the absence of *co-mbh* led, in those conditions, to more important productions of both metabolites. Those compensations could be regarded as different routes for ATP productions. Thus, in the absence of *co-mbh*, it could mean that a more important lack of ATP needed to be compensated. While no data was actually available to verify this assumption, **this could indicate that in the presence of sulfur at atmospheric pressure, *co-mbh* was associated to a more important H_2 production than *mbh*1 and *mbh*2**. As observed elsewhere (Kengen and Stams, 1994a; Kobayashi et al., 1995; Mai and Adams, 1996b; Ward et al., 2000), electrons could also be sunk into other routes, leading to alanine accumulation instead of H_2 however, or another unknown end-product, which would need to be verified by more exhaustive metabolomics assessment.

. The hydrogenogenic system could be more influent at optimal pressure for growth

At high pressure, both *mbh*1 and *mbh*2 clusters seemed to hold important roles in the energy metabolism of *T. barophilus*, as their deletions induced differential growth phenotype both in the presence and absence of sulfur. *mbh* was actually essential for growth in the absence of sulfur at high pressure. The fact that the effects were mitigated at atmospheric pressure (particularly in the presence of sulfur) compared to high pressure, along with the more notable difference in H_2S production at high pressure, **could indicate that sub-optimal pressure for growth diminishes the importance of Mbh in energy production.** Note that in the piezotolerant *T. kodakarensis*, deletion of *mbh* at atmospheric pressure induced total growth impairment in the absence of sulfur, as described in previous works, contrarily to what was obtained here (Kanai et al., 2011; Santangelo et al., 2011). This ensuing phenotypical difference could hypothetically be explained as the genome of *T. kodakarensis* encodes only one Mrp-Mbh complex (TK2080-93) and no Mrp-Mbh-COdh, so no hydrogenogenic system could compensate such a deletion.

Moreover in the absence of *co-mbh*, the other gene of the system known to encode H_2-evolving enzyme, H_2S productions were herein more increased (compared to the wild type strain) at high pressure than at P_{atm}. In the Δ*mbh* mutant, compensation through *co-mbh* occurred *via* its overexpression at high pressure, but not at atmospheric pressure. Additionally, Δ*co-mbh* growth was limited at high pressure in the presence of sulfur, but not at atmospheric pressure. One could thus further hypothesize that **the overall hydrogenogenic system could be more important at high pressure**. Such surmises would necessitate actual H_2 measurements. A direct comparison of *mbh* expressions in different cases could also add up to this argument. It did not however lead to a global pattern herein, but the sulfur presence may have also intervened.

This comes in complement to previous observations indicating that *mbh* and *co-mbh* were overexpressed at atmospheric pressure compared to 40 MPa and were thus probably more important in these conditions (Vannier et al., 2015): as stated earlier, these results were obtained in different culture conditions (excess of sulfur and use of plastic syringe, and growth), allowing to presuppose divergent results. Moreover, transcriptional levels do not necessarily mean that actual productions will be similarly affected, especially since the activity of the proteome may be higher at optimal pressure for growth (40 MPa). Therefore, the "importance" of those clusters in the system has to be confirmed experimentally by metabolomics measurements.

. *mbh*1 and *mbh*2 could be involved in different sulfur conditions

While they constituted a duplication of the *mrp-mbh* cluster, **the respective roles of *mbh*1 and *mbh*2 could be related to different sulfur conditions at atmospheric pressure**, as their expression patterns varied in compensation to deletions of *sh*II (FIGURE 63) or *co-mbh* (FIGURE 57) in the presence of sulfur (both leading to unaffected growth phenotype), but were similar in the absence of sulfur in all mutants.

However, high pressure reversed the respective levels of expressions in the compensation scheme of *mbh*1 and *mbh*2 in response to the absence of *sh*II (FIGURE 64). This showed that **high pressure changes the metabolic configuration** of the system. It also

suggested **that both genes were differentially regulated**, which could have been expected, as although two SurR binding sites were identified around the *mbh*2 promoter (positions 1286949 and 1287033), none was found at the vicinity of the *mbh*1 promoter. SurR could thus be involved in the regulation of *mbh*2 expression, but less likely of *mbh*1. We could also hypothesize that **another transcription factor** could intervene in both gene expressions, as no clear pattern would be identified regarding the influence of the tested conditions on the respective relations between *mbh*1 and *mbh*2. Moreover, in the Δ*mbs* mutant at atmospheric pressure, when sulfur was present and should have impaired *mbh*2 expression *via* SurR de-activation, it was upregulated compared to the wild type (FIGURE 60). This does not mean that it was overall not downregulated compared to the absence of sulfur (the results are displayed as relative to wild type expressions), but there was still a factor counteracting any SurR-induced downregulation. Physiological comparisons of this double mutant with two simple mutants (Δ*mbh*1 and Δ*mbh*2) would further allow better understanding of their possible respective roles.

. co-mbh could function without COdh activity

Growth phenotype at atmospheric pressure in the presence of sulfur was not impaired by *co-mbh* deletion, while it was accompanied by increases of H_2S and acetate productions. This compensation could indicate that H_2 was probably less produced in the mutant, if we considered an unchanged global electron pool to dispose of, and hence that the wild type strain possibly produced H_2 *via* the Mrp-Mbh-COdh cluster. Since no carbon monoxide was added to the *medium*, this would suggest that **the COdh activity would not be required for H_2 production by this enzyme**. This was surprising, since in a *P. furiosus* strain heterologously producing the Mrp-Mbh-COdh complex from *'T. onnurineus'*, the absence of carbon monoxide (*i.e.* of COdh activity) considerably limited H_2 production, however. Yet, as the CO oxidation activity was shown to be mainly located in the cytoplasm, it is possible that the coupling to Mrp-Mbh modules requires the intervention of ferredoxins for electron transfer, as proposed by Schut *et al.*, 2016. In that sense, in is not unreasonable to advance that COdh activity could be facultative in our system thanks to the electron supply *via* ferredoxins, and to explain the difference of phenotype in *P. furiosus* by a possible substrate limitation, since CO was not provided in our experiments (Schut et al., 2016b). Our results thus tended to

corroborate the possibility of use of ferredoxin as electron transporter for the activity of the Mrp-Mbh-COdh complex, independently from CO oxidation. However, although not characterized, another putative carbon monoxide dehydrogenase can be found encoded in *T. barophilus* MP^{T}'s genome, by TERMP_02146. We could consequently also imagine that CO_2 would be reduced to CO by the ensuing enzyme, and that this CO would be reused by the Mrp-Mbh-COdh cluster concerned by this study. A double mutant of both TERMP_02146 and TERMP_1146-50 (*co-mbh* herein) would help precise this question.

The *mrp* coding sequence of *co-mbh* was also much less expressed at high pressure than at atmospheric pressure in the mutant strain compared to the wild type in the presence of sulfur. There seemed to be a reaction of downregulation in correlation with the absence of hydrogenase activity, which could not be explained here. We could surmise for example that as Mrp influences exchange of sodium ion and proton exchanges with the extracellular environment, it could change the pH of the cell, and we could thus hypothesize that it would necessitate an adequate regulation even in the absence of activity of the associated hydrogenase function. No evidence from our data allowed any confirmation of such interpretation, nonetheless, and it is possible that transcription of the whole cluster was affected by the deletion, in an undetermined fashion. Physiological tests of mutant strains deleted of the whole Mrp-Mbh-COdh cluster, as well as enzymatic assessments of the possible use of ferredoxin by the Mbh cluster, without the involvement of CODH, may permit to further explore those hypotheses.

Sulfidogenic system

. *mbs* could be more important at atmospheric pressure

As described in other models and observed earlier in this project (see chapter I), the presence of sulfur benefitted for the growth of *T. barophilus* MP^{T} at both high pressure and P_{atm}. At atmospheric pressure, compensation of all deletions except *mbs* could completely occur in the presence of sulfur while they were not entirely functional in the absence of sulfur. This indicated that *mbs* might be the most important gene for sulfidogenic growth, at atmospheric pressure, conformingly to its description from *P. furiosus* and *T. kodakarensis* (Bridger et al., 2011; Kanai et al., 2011; Santangelo et al., 2011). At high pressure, other genes

were concerned by an impairment of potential for compensation to deletion, in the presence of sulfur, indicating that in those conditions, *mbs* was no more the only important feature among those tested. Consequently, those data suggested that **Mbs could be more important in the sulfidogenic energy conservation system at atmospheric pressure than at 40 MPa.** In *P. yayanosii*, sub- and supra-optimal pressures for growth seemed to induce *mbs* overexpression, in the presence of sulfur (Michoud and Jebbar, 2016). However, in *T. barophilus*, expression profiles of *mbs* in the presence of sulfur seemed almost equivalent at 40 MPa and P_{atm}, with a slight overexpression at high pressure. Once again, these results are hard to put in relation to the present work, as the experimental conditions differed greatly, noticeably because of the excess sulfur and lack of H_2-tightness (Vannier et al., 2015).

. *mbs* might be important regardless of the sulfur presence

Unexpectedly, *mbs* deletion was also impacting in the absence of sulfur, at both pressures (FIGURE 59), meaning that **Mbs may play an important role in the absence of sulfur, contrarily to what was observed in other models** (*e.g.* in *T. kodakarensis* and *P. furiosus* (Bridger et al., 2011; Kanai et al., 2011; Santangelo et al., 2011)). In these conditions, SurR should have repressed *mbs* expression, and thus we would have expected the absence of the gene to be silent on the ensuing phenotype. Since Mbh and Mbs have similar structures (Wu et al., 2018a), one could surmise that in our system, in contrast to other *Thermococcales*, **Mbs could be involved in both H_2S synthesis and H_2 evolution**. However, more experimental evidences, *e.g.* from enzymatic tests, would be necessary to conclude on that assumption. This phenotype could also be explained by a possible cooperation, in our conditions, of both hydrogenogenic and sulfidogenic routes in the energy conservation of the cells. Measurements of H_2 could better inform on such ideas.

. sulfidogenic energy conservation could only function with *mbs*

Production of H_2S as described in other *Thermococcales* models is the direct result of the action of Mbs or Nsr, using reduced ferredoxin and NADPH as electron carriers, respectively. It is linked, in the case of Mbs, to ATP production (Wu et al., 2018a). Surprisingly though, *mbs* deletion was associated with an increase in cellular productions of H_2S in all

conditions, compared to the wild type strain, opposite to what was observed in other models ((*e.g.* in *T. kodakarensis* (Kanai et al., 2011)). We could attempt to explain this fact by arguing that **the production of H_2S *via* Mbs could possibly be the only efficient sulfidogenic energy conservation**. It would not be surprising since Nsr does not directly support the cation gradient across the membrane, linked with ATP synthesis, while Mbs is associated with an ion translocation module (Wu et al., 2018a). In the case of Δ*mbs*, energy conservation would necessitate a more indirect route, hence the observed slower growth rate. The role of Nsr could be limited to NADPH regeneration, balancing electron fluxes between electron carriers and thus allowing a better functioning of the catabolic routes, also producing ATP by substrate-level phosphorylation, but not to directly lead to ATP production itself through a cation gradient across the membrane. Note that normal or reduced rates were elsewhere noticed in *T. kodakarensis* or *P. furiosus* deleted of *mbs* in the presence of sulfur, while final biomasses were lower (Bridger et al., 2011; Santangelo et al., 2011) or equivalent (Kanai et al., 2011), depending on culture conditions. Expression patterns in compensation to *mbs* deletion were not exactly similar in *P. furiosus*, with noticeably an unaffected expression of *mbh* in the latter model (Bridger et al., 2011), while it was found overexpressed in our work (FIGURE 60). This highlights the possibility of different metabolic organizations, also indicating that conclusions on the roles of the enzymes must be considered carefully with respect to culture conditions.

In the absence of *mbs*, at atmospheric pressure, *nsr* expression was downregulated in compensation, which was inconsistent with the increased H_2S production, but consistent with what was observed in *P. furiosus* (Bridger et al., 2011). Note that in our case, this did not necessarily mean that no Nsr was produced, as the levels of expression in the wild type could have been high (which was the case in other species). We could speculate several explanations, which would however need experimental evidences: **another enzyme could be involved in H_2S biosynthesis**, and/or maybe low levels of *nsr* expressions were actually sufficient to hold an important activity, provided that enough electrons were carried towards the enzyme. In that case, it would imply that the system was not easily saturated, as even low amounts of enzymes could perform larger amounts of sulfur reduction. That **H_2S production would still be a way to refurnish $NADP^+$ to other parts of the metabolism**, which would need it for ATP productions. Acetate production was also enhanced in the mutant strain showing a

reorganization of the electron fluxes in the metabolic system. *mbs* deletion was associated with *nfn*1 and *nfn*2 expression compensations, as well as *sh*I overexpression at high pressure, which could support the theory of a need for H_2S overproduction, in the absence of *mbs*, only to supply back electron carriers. Those assumptions are highly speculative, and would need further confirmation, for example through the measurements of NADP(H) and ferredoxin pools.

Maintenance of the redox balance

. The different influences of SHI and SHII depend on culture condition

The differences in the roles of SHI and SHII are unclear as described in the literature, except that the SHI homolog seems more active than the SHII homolog (Schut et al., 2012). As a reminder, the *sh*I homolog in *T. barophilus* MP^T corresponds to *sh*II in *P. furiosus*, and conversely (Birien, 2018).

In the presence of sulfur at atmospheric pressure, both Δ*sh*I and Δ*sh*II growth phenotypes were similar to the wild type (FIGURE 61 and FIGURE 63), indicating **SHII and SHI non-essentialities in these conditions**. Yet, they did not lead to the same amount of end-products. While deletion of *sh*I did not affect H_2S and acetate productions, deletion of *sh*II led to diminished cellular levels in those conditions.

The ensuing expression patterns were also different (FIGURE 62 and FIGURE 64). While *sh*II was overexpressed in the Δ*sh*I mutant, the opposite was not true: *sh*I was underexpressed in the Δ*sh*II mutant, **indicating that the two enzyme functions do not completely overlap**. In the case of the *sh*I deletion, both *mbh1* and *mbh2* were overexpressed, as well *co-mbh*. In the case of *sh*II deletion, all other targets were underexpressed compared to the WT, except for *mbh*2, which levels were slightly enhanced. These different compensation strategies highlighted that **SHI and SHII, although each not essential at atmospheric pressure in the presence of sulfur, may hold different roles in the energy metabolism of *T. barophilus*.**

*sh*II overexpression was used to compensate the *sh*I absence in the presence of sulfur at atmospheric pressure, but *sh*I was downregulated in the *sh*II absence. SHII thus seemed to be able to lead to a functional phenotype without SHI, but in the absence of SHII, *sh*I also needed to be downregulated. **This could indicate that SHI and SHII hold antagonist influences in the metabolism of our model at atmospheric pressure, in the presence of sulfur**. Since the absence of *sh*I was associated to *sh*II overexpression and led to higher cellular H_2S concentrations, while conversely, the absence of *sh*II seemed to be associated with lower H_2S production (with *sh*I underexpression), **SHII could be linked to H_2S production**. *In vitro* experiments previously showed possible actual H_2S production (Bryant and Adams, 1989; Ma and Adams, 2001a; Ma et al., 1993). In our model, Δ*sh*II, in contrast to other mutants, at P_{atm} and in the presence of sulfur, led to compensation with lower H_2S and acetate.

The impact of *sh*II on *T. barophilus* sulfidogenic metabolism could also be indirect, by helping supplying NADPH to Nsr. As growth was not affected, it is possible that more H_2 or alanine was produced in the mutant strain. To extrapolate further, we could argue that SHII could also be implicated in H_2 consumption in these conditions, which would be consistent with literature reports on other species (Haaster et al., 2008; Kanai et al., 2003, 2011, 2017; Moon et al., 2015; Santangelo et al., 2011). However, in the absence of *mbs*, *nsr*, the other H_2S-producing enzyme in the system, was measured as underexpressed in the presence of sulfur at atmospheric pressure, but H_2S cellular productions were increased in the Δ*mbs* mutant compared to Δ517(WT), along with overexpressions of *sh*I and *sh*II (FIGURE 59 and FIGURE 60). This would be congruous with the hypothesis of a direct H_2S production by SHII, but the rationale for energy conservation is unclear. Since producing H_2S would consume NADPH, we could further advance that it would serve to regenerate electron carriers to allow a better turnover in other ATP-synthesizing parts of the metabolism, such substrate catabolism, favoring them over the activity of membrane ATP synthases, to still lead to a functional phenotype. More data would be required to examine this *scenario*, possibly *via* the measurements of changes in NADPH pools.

Note that conversely, Δ*sh*I overproduced acetate and H_2S in these conditions, which does not conflict with the possibility of two distinct roles of SHI and SHII in the metabolism.

At atmospheric pressure in the absence of sulfur, SHII was essential, as *sh*II deletion completely prevented growth. This result contrasted with deletion studies in *P. furiosus* showing no different phenotype in the absence of sulfur in a *sh*II-deleted strain (nor in the absence of both *sh*I and *sh*II), but the described tests were realized in the presence of sugar (maltose), which thus corresponded to a different, incomparable metabolic configuration (Lipscomb et al., 2011; Schut et al., 2012). *shII* was, in our work, the only mutated enzyme tested here to show essentiality in those conditions. *sh*I deletion led to lower biomass, but the phenotype was not as dramatic as for *sh*II deletion. This tended to confirm **the paramount importance of SHII at atmospheric pressure**, compared to SHI. Interestingly, SHII homologs have been shown as more active than SHI in other models as well (SHII in *T. barophilus* MP^T corresponds to SHI in *P. furiosus*) (Schut et al., 2012). Moreoever, contrarily to *sh*I, *sh*II did not seem to be linked to Mbh function at atmospheric pressure in the absence of sulfur, as the deletion of the membrane-bound hydrogenase led to no change in *sh*II expression.

At high pressure, SHII was not essential, either in the absence or presence of sulfur, as its deletion could be compensated completely, although a small lag phase seemed to occur before the exponential growth of the Δ*sh*II mutant. In the presence of sulfur, the *sh*II deletion seemed **correlated with very high acetate overproduction**, accompanied by a slight H_2S overproduction. Electrons should thus have been disposed elsewhere in the wild type, through H_2 or alanine. It is consequently not impossible that **at high pressure and in the presence of sulfur, the metabolic configuration occurring in the presence of SHII could increase H_2 tolerance, and thus H_2 production** (contrarily to at P_{atm} in the presence of sulfur). However, such hypothesis would need experimental confirmation (H_2 measurements). In the presence of sulfur at high pressure, a lag phase was added to the growth dynamics of the Δ *sh*II mutant but not in the absence of *sh*I. This change in phenotype also indicated that **SHII could be important for the overall energy metabolism of *T. barophilus*, but, at high pressure, even more in the presence of sulfur.** High pressure tended to change the parameter influencing *sh*II essentiality, while the *sh*I absence could be compensated in all situations. As for other culture conditions, high pressure expressions of *sh*I and *sh*II in compensation of the *mbs* absence were different, *sh*I being upregulated and *sh*II being downregulated. As deletion of *sh*II, in these conditions, led to an increase in H_2S production, it is also possible that SHII

impairs sulfidogenic metabolism at high pressure in the presence of sulfur, contrarily to *sh*I. This further evidenced for the fact that the two oxidoreductases might have different places in the metabolic scheme of *T. barophilus*.

Hence, our results thus indicated that SHII and SHI probably exert different functions in *T. barophilus* energy metabolism, which vary according to culture conditions. SHII seemed more influent than SHI both at high and low pressure, and even essential at P_{atm} in the absence of sulfur, but the impact of sulfur on *sh*II essentiality was inverted at 40 MPa. *sh*II seemed important for high pressure adaptation in the presence of sulfur. We hypothesized that the respective effects of each enzyme on the metabolic fluxes could be antagonistic, that *sh*II could rather favor sulfidogenic metabolism at atmospheric pressure but could hinder it at high pressure, and that its overproduction could be a lead for H_2 production optimization studies through its possible involvement in H_2 tolerance. The possibility that *sh*II could hamper sulfidogenic metabolism in the presence of sulfur would also be interesting for H_2 high pressure production, as we could further foresee the deletion of a possible alternative electron sink pathway (towards alanine production for example) to force H_2 production. Evidently, those assumptions would require additional experimental investigations, as other compensations could occur in unexpected manners, if the system is additionally modified by another deletion.

. Nfn1 and Nfn2 could have different specificities

Nfn proteins in *Thermococcales* have been described to play important roles in maintaining redox homeostasis. They are particularly interesting in our system as they can transfer electrons from reduced ferredoxins to $NADP^+$.

In our results, *nfn*1 and *nfn*2 expression patterns were different in many compensation cases, including those which were functional (presence of sulfur), showing that they could have different roles in the metabolism, as their regulation was different. Same conclusions were inferred in *P. furiosus* (Nguyen et al., 2017). From our data, it seemed that *nfn*1 expression was only downregulated in all mutant strains, compared to the wild type strain, at atmospheric pressure in the presence of sulfur. *nfn*1 expression seemed to be involved in the compensation of every deletion concerned, while *nfn*2 was not differentially

regulated compared to the wild type strain at atmospheric pressure in the absence of *co-mbh*, *mbs*, and *sh*I without sulfur, and *mbs* and *sh*I in the presence of sulfur. **We could suppose that Nfn2 does not intervene in Mbs and SHI functions at atmospheric pressure**, but a Δ*nfn*2 mutant would be necessary to explore this possibility. Although this is completely hypothetical, it could occur through different electron carrier specificities, as it was shown for the ferredoxins of *T. kodakarensis* (Burkhart et al., 2019). In *P. furiosus*, Nfn1 uses NADH for its bifurcating activity, while another substrate for Nfn2 has not yet been clearly identified (Buckel and Thauer, 2013; Lubner et al., 2017; Wang et al., 2010). If those features are similar in *T. barophilus*, the respective implications of the two enzymes in the metabolic system could logically be expected to be indeed different.

High pressure tended to change the compensation patterns on *nfn*1 and *nfn*2 expressions, as for all other genes targeted in this study. For example, *nfn*2 expression seemed to compensate the *mbs* absence at high pressure, whereas it was involved in the *co-mbh* absence compensation only at P_{atm} (in the presence of sulfur). Other works in the piezotolerant *P. furiosus* have tended to indicate that Nfn2 would actually be related to the sulfidogenic system at P_{atm} (Nguyen et al., 2017). We could imagine a generalization where Nfn2 would intervene in sulfidogenic growth in optimal growth conditions, but that sub-optimal pressure would have modified this metabolic organization in our model. Yet, *nfn*1 expression seemed to play a role in the *mbh* absence compensation only at atmospheric pressure, *i.e.* at sub-optimal pressure for growth, whereas it was shown to be rather linked to the hydrogenogenic system of *P. furiosus* at P_{atm}, *i.e.* at optimal pressure for growth (Nguyen et al., 2017). The relations between Nfn1 or Nfn2 involvements in metabolism and culture conditions thus seem to be more complex and remain unclear, and deletions of those genes could help understanding their respective roles.

SurR regulation

SurR is described as a master regulator of the electron flow in *Thermococcales* metabolism, globally affecting the transcription of the energy conservation pathway genes, by activating the expression of its own gene as well as hydrogenogenic clusters and repressing the expression of sulfidogenic clusters (Lipscomb et al., 2017). Expressions of *sh*I and *sh*II are

supposed to be activated by SurR, but in *T. barophilus* MP^T, the *sh*I promoter shows an absence of binding site for the regulator (unpublished work, Y. Moalic, 2018). SurR represses *nfn*1 and *nfn*2 expressions. The presence of sulfur is known to induce deregulation of SurR (Lipscomb et al., 2009, 2017; Yang et al., 2010).

. SurR seems important for the energy conservation system

From our data, it appeared that in the absence of sulfur (at atmospheric pressure), expressions of *sur*R in compensation to absences of all genes tested except *co-mbh* and *mbs* were downregulated. This could indicate a **global diminution of regulation by SurR in those conditions**. All growth phenotypes were affected in the absence of sulfur, and the less impacted was obtained in the absence of *mbs*, for which *sur*R expression was actually upregulated. This tended to indirectly confirm the **importance of the master regulator for the energy conservation system**.

. SurR regulation may be different from other models and/or it may not be the only important transcription factor for the energy conservation system

In the absence of sulfur, SurR has been described to activate transcription of numerous hydrogenogenic genes and to repress clusters associated with sulfidogenic metabolism. However, our results showed that in the absence of sulfur (at atmospheric pressure), in the Δ*mbs* mutant, compensation occurred through the overexpression of *sur*R compared to the wild type strain, accompanied by a downregulation of *mbh*, *sh*I, *sh*II, and *co-mbh*. Only *nfn*2 and *nsr* expression compensations were as expected *via* SurR effect in this case. Note that although described as both repressed by SurR, the compensation patterns of expressions of *nfn*1 and *nfn2* were opposed in these conditions (Nguyen et al., 2017). Moreover, our results showed that the absence of *mbh* or *co-mbh* impacted growth even in the presence of sulfur, at high pressure, meaning that those enzymes may be active in the wild type in those conditions. This was in contradiction to the expected SurR regulation outcomes, in respect to other models.

Admitting that a *sur*R expression would in fact lead to more translation of active SurR (which was not verified), **we could surmise that** those expression patterns showed that **the regulatory effect of SurR of each concerned gene would be different from what was**

described in other models, or else that another transcription regulation system, *e.g.* another transcription factor, may importantly intervene in those conditions.

The first assumption could be justified as different motives of SurR binding sites have been identified for several gene homologs in various *Thermococcales* strains, in addition to promoters showing binding sites in some strains while not in others (unpublished work from Yann Moalic, 2018). These mutated binding sites could maybe explain other features, as for example the differences in importance of *mbh* and *co-mbh* in the presence of sulfur: if acknowledged that they function similarly (which has not been shown), they then appeared more or less sensitive to the sulfur presence, and consequently possibly to SurR regulation. Concomitantly, *mbh* promoter was associated to a long SurR binding motif ($GTTn_3AACn_5GTT$), whereas *co-mbh* promoter showed a short SurR binding motif ($GTTn_3AAC$). Nonetheless, it is also likely that this observation was anecdotal; more data from other genes with different SurR binding motives would be required to argue on this potential correlation.

The second hypothesis of other transcription systems involved, incidentally not incompatible with the first one, would not be surprising neither, as many transcription factors seem to orchestrate *Thermococcales* metabolism, some being also responsive to sulfur or to high pressure (Clarkson et al., 2010; Denis et al., 2018; Song et al., 2019). Furthermore, different sub-complexes of the concerned enzymes could be under the influence of different promoters, not necessarily SurR-dependent, and similar unexpected reactions to the sulfur presence were observed, as for Mbs in *P. furiosus* (Wu et al., 2018a).

. SurR may not be important for pressure adaptation

Expression patterns of *sur*R at 40 MPa and atmospheric pressure in compensation to all tested gene deletions followed similar tendencies compared to the wild type. The ensuing growth phenotypes were however different in many cases at both pressures, indicating that SurR may not be of crucial importance in adaptation to high pressure.

Those results thus indicated that the importance of SurR could be mitigated and would be integrated in a much more complex regulatory system. SurR itself could be regulated by other parts; for example, the couple TrxR/Pdo has been shown to possibly impact its redox

state (and thus its regulatory activity) (Lim et al., 2017). A deleted *sur*R strain could help better link expression data to actual activities and thus confirm or infirm these hypotheses.

Intermediate sulfur conditions may have induced uncomplete metabolic switch

Some of those unexpected results regarding usual SurR regulation could also be explained by an additional idea. Since it was determined as an optimal concentration for maximizing both growth and H_2 production, the "presence of sulfur" condition was based on 0.25 g/L sulfur (see chapter I), which is much less than the excess used in most studies (generally using more than 2 g/L S°). The experiments described herein may thus have occurred in an intermediate sulfur condition allowing both hydrogenogenic and sulfidogenic growth. **Such layout would mean that the sulfur-induced, SurR-orchestrated metabolic switch was not responding in an "all-or-nothing" configuration**, and could allow gradient response, more adapted to an often-fluctuating natural environment, where energy conservation would ensue from a hybrid metabolism involving both H_2S and H_2 productions. That could possibly explain how *mbh* and *co-mbh* were important even in the presence of sulfur, at high pressure. Yet, it would not permit to justify the significance of *mbs* in the absence of sulfur, for example, and might not be the only reason for all of the aforementioned unanticipated phenotypes. In order to better compare *T. barophilus* with other strains, obtaining similar data in sulfur excess should be informative. As a control where sulfur would less impact the metabolism, producing similar data in conditions allowing a proper growth without sulfur (with sugar) could also be interesting to better understand the system.

Conclusions

Several hypotheses were formulated herein regarding the metabolic behavior of *T. barophilus*. Doubtlessly, many other hints on possible correlations were missed in this analysis. However, a definitive overall conclusion to this work would argue that compensations occur in complex manners, and may involve many yet to be characterized regulation systems, which could directly affect certain pathway; or indirectly influence other outcomes. While some patterns could be extracted from our data on the potential roles and

interactions of certain distinct parts, as well as on the possible effects of changing environmental conditions on the whole cellular organization, no precise global description of pressure-induced variations could be surmised here. Although previous reports (*e.g.* (Cario et al., 2015b; Michoud and Jebbar, 2016; Vannier et al., 2015)) have indicated punctual physiological outcomes depending on pressure, a generalization cannot yet be reasonably advanced, as acclimatization patterns appeared diverse and dependent to many factors. Particularly, our results indicated that the hydrogenogenic system may be important at optimal pressure for growth, and that the sulfidogenic system would rather be influent at atmospheric pressure, which came in contradiction to transcriptional observations made in excess of sulfur (Vannier et al., 2015). Our data also confirmed that high pressure adaptations are a question of global reorganizations, for which no single gene influence has been identified yet, to my knowledge.

In our model *T. barophilus*, physiological behaviors regarding different enzymes studied herein have shown that some parts may function differently to what was observed in other models (*e.g.* the essentiality of *sh*II in the absence of sulfur at atmospheric pressure). We also advanced in the identification of respective functions and interactions of the studied modules. The fact that there were gene expression acclimations in each case showed that regulation of the metabolism of *T. barophilus* is highly dynamic, likely occurring largely at the transcriptomic levels.

Several confirmations would be necessary beforehand however. It is important to remind that most assumptions extracted from our work were based on gene expression data, which do not necessarily correspond to actual translated proteins. Regulatory systems could still impact the system post-transcriptionally/translationally. For example, *T. barophilus* MP^T was shown to produce the stress protein P60 at low pressure, while no corresponding genetic regulation was observed (Marteinsson et al., 1999a; Vannier et al., 2015). In the frame of our project, measurements of some additional possible end-products (alanine and H_2) would help giving more indications about actual activities. Acetate has been demonstrated to be possibly consumed in various strains, although the mechanisms involved are unclear (*e.g.* (Birrien et al., 2011; Schut et al., 2016b)). If such route is present in *T. barophilus* MP^T, as tended to indicate the results in chapter I, it would have to be taken into account when interpreting

electron disposals. Note that H_2 measurements at high pressure would now be possible thanks to the new device developed during this project, as described in chapter II. We could also benefit from other mutants. Particularly, a deletion of *sur*R would permit to unravel whether other potential transcription factors could be at play. Multiple deletions in same strains could also inform on the interactions between each system. Some other works have evaluated the impacts of various deletions on different *medium*, based on sugar degradation rather than peptides (*e.g.* (Lipscomb et al., 2011)). In several strains, those conditions would allow growth in the absence of sulfur, as for our model on artificial sea water with maltodextrin (see chapter I). Phenotypical comparisons in such metabolic state could allow different perspectives on the roles of the considered proteins. Moreover, it would permit to better appreciate actual contrasts with the wild type strain, since our reference growth was already impaired on TRM without sulfur here.

This work opened many other fundamental interrogations. We focused here on specific parts of the energy conservation metabolism, but it is also likely that the whole upstream pathways could be involved in adaptation. We often hypothesized further on our results by considering end-products as electron sinks, admitting that for similar growth phenotypes, equivalent levels of electrons were to be disposed of. However, there remained missing information on the possible compensations made by other metabolic keystones of the energy conservation system, such as ATPases, substrate transport or degradation. For example, it was previously shown that several amino acid transporters, uptaking the substrates which constitute the sources of electrons, could be overexpressed at atmospheric pressure (Vannier et al., 2015). Full understanding of high pressure adaptation would require a systemic consideration. Additionally, although it appeared that the absence of sulfur was detrimental in all cases, the reasons why compensation of a deletion was sometimes possible and sometimes not remain unconfirmed. From these inefficient but actually regulated pathways, we could presuppose thermodynamical incompatibilities, accumulation of toxic metabolites, or for example substrate specificities to be actual blocking points in some metabolic nodes, but the precise identification of those keystones have yet to be unraveled.

Such evaluation would however be important in the prevision of applied high pressure H_2 bio-production systems. Indeed, a good knowledge of the metabolic pathways (which

could even be questioned in *Thermococcales* models) would enable mathematical prediction of fluxes changes and orientate future genetic modifications, but as shown in this chapter, some compensation would not be adequately foreseen without a better understanding of the regulations and interactions at stake.

Nonetheless, with this work, we advanced towards a more precise comprehension of our model in relation to high pressure, and could highlight some ideas of strategies potentially allowing H_2 overproduction, as for example the overexpression of *sh*II to increase H_2 tolerance at high pressure. Indeed, unravelling the metabolic pathways involved and their regulation to force the system towards H_2 production would be necessary, but understanding how to increase tolerance to this potentially saturating end-product would also be necessary. The next chapter hence describes an adaptive laboratory evolution experiment that has focused on that matter.

Note: Part of the work presented in this chapter was valorized with an oral presentation at the congress Thermophiles 2019 (Fukuoka, Japan), by Mohamed Jebbar. Complementary data are expected to allow the writing of a scientific paper in a near future.

Chapter IV: Adaptive laboratory evolution study of hydrogen tolerance in *T. barophilus* MP^{T}

Abstract

High hydrogen concentrations have been reported to inhibit hydrogenogenic energy conservation in *Thermococcales*, limiting growth. Different species can harbor various tolerance to H_2, but the exact mechanisms at stake remain unclear. Because H_2 inhibition would inhibit the optimization of applied H_2 bio-production application, we aimed to investigate the systemic features of H_2 tolerance in *T. barophilus* MP^T. Through adaptive laboratory evolution (ALE), we produced a super-tolerant strain, named "Evol", by gradually habituating our cell population to sulfur-depleted conditions, then to increased initial H_2 concentrations (up to 10 % in gas phase), in closed conditions, through 22 successive sub-cultures (about 76 generations).

The resulting adapted strain showed dramatically better growth in the absence of sulfur than the *T. barophilus* MP^T reference strain, reaching about the same biomass as in the presence of sulfur, and leading to higher absolute H_2 concentrations in its absence. We investigated metabolite productions and found only slight differences in acetate accumulation, but lower H_2 and H_2S yields in "Evol". The whole genome of the evolved strain was sequenced and showed 119 point mutations, which were predicted to affect various physiological processes. Additionally, transcriptomic profiles under different H_2 saturation conditions were produced, although not yet sequenced at the time of writing.

Based on the discussion of available results, we hypothesized that the "Evol" strategy to tolerate high H_2 concentrations could reside in a more rapid division rate based on an energy metabolism less sensitive to sulfur and less hydrogenogenic overall, due to more optimal electron fluxes, resulting in a rebalanced redox potential. Further investigations on "Evol" should allow to better grasp H_2 tolerance, to predict strategies for applied H_2 bio-production.

La conservation de l'énergie chez les Thermococcales *peut être inhibée par de fortes concentrations en hydrogène, limitant leur croissance. Des tolérances à l'H_2 variées ont été*

observées chez différentes espèces, mais les mécanismes engagés demeurent incomplètement définis. Un tel paramètre interviendrait probablement de manière importante dans l'optimisation d'une application de bio-production d'H_2. Par conséquent, les caractéristiques systémiques de la tolérance à l'H_2 chez T. barophilus *MP^T ont été étudiées, à travers une expérience d'évolution adaptative en laboratoire. La souche a été graduellement habituée à une absence de soufre, puis à des concentrations d'H_2 croissantes (jusqu'à 10 % en phase gaz), en conditions fermées à travers 22 repiquages successifs (environ 76 générations) produisant ainsi un variant super-tolérant, nommé « Evol ».*

Ce dernier a montré une croissance en absence de soufre nettement supérieure à la souche de référence T. barophilus *MP^T, atteignant une biomasse équivalente à des conditions de présence de soufre, et menant à des concentrations d'H_2 absolues plus importantes en absence de soufre. Les productions spécifiques cellulaires de métabolites ont été évaluées, montrant de faibles différences dans l'accumulation d'acétate, mais des productions d'H_2 et d'H_2S plus basses chez « Evol ». Le génome complet de la souche évoluée a été séquencé, révélant 119 mutations ponctuelles, estimées comme affectant différents processus physiologiques. Afin de mieux appréhender ces données au regard des observations phénotypiques, des profils transcriptomiques dans différentes conditions de saturation d'H_2 ont été obtenus, quoique non séquencés à ce jour.*

Les résultats disponibles ont découlé sur l'hypothèse que la stratégie d'« Evol » pour mieux tolérer de hautes concentrations d'H_2 s'expliquerait par un taux de division cellulaire plus rapide, basée sur un métabolisme énergétique moins sensible au soufre et moins hydrogénogénique globalement, grâce à une optimisation des flux d'électrons, résultant sur un potentiel redox rééquilibré. « Evol » constitue une base intéressante pour de futurs travaux visant à mieux comprendre la tolérance à l'hydrogène, dans le but de prévoir des stratégies de bio-production d'H_2 appliquée.

Introduction

The project HPBioHyd explored possible ways of optimizing H_2 bio-production by *Thermococcales*. Those hyperthermophilic *Archaea* have been demonstrated to produce H_2 to dispose of electrons while maintaining a cation gradient across their cell membrane, allowing energy conservation *via* the activity of membrane ATPases. However, high H_2 concentrations inactivate hydrogenases (Fourmond et al., 2013). Consequently, high H_2 levels can lead to cell toxicity by inhibiting this energy conservation metabolism. As a result, growth of *Thermococcales* can be impaired, lowering molecular hydrogen production, which can be problematic in certain configurations in the frame of our applied objective (Blumentals et al., 1990b; Bonch-Osmolovskaya and Stetter, 1991; Fiala and Stetter, 1986).

Different strains harbor varied tolerances to H_2, as shown in chapter I and in several literature descriptions. These H_2 saturations have been shown to be related to closed culture conditions, and can be relieved by interspecies transfer or gas-phase renewal (Bonch-Osmolovskaya and Miroshnichenko, 1994; Bonch-Osmolovskaya and Stetter, 1991; Canganella and Jones, 1994; Fiala and Stetter, 1986; Topçuoğlu et al., 2019). Specific metabolic features can also help tolerating high H_2 productions. Formate synthesis from H_2, as performed by a membrane-bound formate hydrogen lyase complex in *T. paralvinellae*, among others, was proposed as a mechanism of H_2-detoxification. Yet, growth on formate as an energy source could also constitute a strategy allowing to improve H_2 production, since it also generates a sodium-motive force, able to further activate membrane ATPases, and has proven to induce higher H_2 yields (Le Guellec, 2019; Topçuoğlu et al., 2018). All species are not able to use or produce formate, and we observed that no such mechanisms seemed to be present in our model *T. barophilus* strain MP^T, unlike strain *T. barophilus* Ch5 (see chapter I). Soluble hydrogenases are also involved in H_2 consumption, which could help hydrogenogenic energy conservation while limiting H_2 saturation (Haaster et al., 2008).

The H_2-based system is not the only one involved in energy conservation of *Thermococcales*. In the presence of sulfur, following de-regulation of the master transcriptional regulator SurR, a metabolic shift has been observed in several models towards H_2S production, as a mean for disposing of electrons, while efficiently conserving energy. In

the presence of sulfur, *Thermococcales* generally harbor better growth since H_2, replaced by H_2S, is no longer inhibitory (Lipscomb et al., 2017; Sapra et al., 2003; Schicho et al., 1993; Schut et al., 2013, 2016a). Other metabolic pathways can lead to ATP generation, and their use can allow to compensate for inhibitory H_2 conditions. When degrading carbohydrates, degradation of phosphoenolpyruvate to pyruvate produces ATP, as does the formation of organic acids from 2-keto acids, issued from amino acid transamination (Schut et al., 2014). It has been observed in several models that growth could occur properly in the absence of sulfur if sugars or pyruvate were added, although corresponding H_2 level differences were unclear, as for example in *P. furiosus* (Schut et al., 2012), *T. kodakarensis* (Kanai et al., 2011; Santangelo et al., 2011; Yokooji et al., 2013), or '*T.* onnurineus' (Bae et al., 2012b).

Peptide catabolism leads to both NADPH and reduced ferredoxin formation, while glycolysis induces reduction of ferredoxin, but not of $NADP^+$ (except if a non-phosphorylating glyceraldehyde-3-phosphate dehydrogenase is produced, which has been shown in *T. kodakarensis* but is seemingly lacking in *T. barophilus* MP^T (Matsubara et al., 2011; Vannier et al., 2011)). Although H_2 evolution by membrane-bound hydrogenases is thermodynamically less favorable with electrons carried by NADPH than with electrons carried by ferredoxins (Verhaart et al., 2010), the implication of those specific electron transporters in H_2 tolerance has not been investigated, to my knowledge. Such an interpretation would be particularly tedious as they are part of a complex system of many pathways, involving different regulations and specificities, still not completely characterized (Burkhart et al., 2019; Hidese et al., 2017; Nohara et al., 2014). For example, at high H_2 levels, alanine accumulation has also been observed, synthesized from pyruvate by the activities of an alanine aminotransferase and a glutamate dehydrogenase (Nohara et al., 2014; Ward et al., 2000). Gluconeogenesis could also occur, which would then lead to NADPH formation by the synthesis of glyceraldehyde-3-phosphate from 1,3-biphosphoglycerate by GADPH (Bräsen et al., 2014).

Hence, in the aim for future H_2 bio-production optimization, a more systemic approach was necessary to better understand which particular metabolic configurations could intervene in hydrogen tolerance in *Thermococcales*, in addition to the few identified specific reactions, as aforementioned (*e.g.* formate consumption).

Adaptive laboratory evolution (ALE), consisting in prolonged culturing or sub-culturing of a given strain in selective conditions, has revealed to be an efficient tool for inducing a beneficial phenotype and studying the changes associated (Sandberg et al., 2019). Ensuing genomic modifications are frequently single nucleotide mutations, leading to physiological adaptations on different levels (Conrad et al., 2011). ALE experiments were performed on '*T. onnurineus*' to force the evolution of the strain towards higher formate and carbon monoxide uses, accompanied with higher H_2 yields. In the first case, 11 mutations were found on the genome, and a specific mutation highlighted the crucial importance of the formate transporter (Jung et al., 2017). In the second case, 10 mutations were found, but a more complex adaptation was at stake, involving important and regulated genomic, epigenetic and transcriptomic changes, with about 500 differentially expressed genes, concerning various functions, including in the membrane hydrogenase energy conservation system (Lee et al., 2016).

In the frame of H_2 bio-production optimization, H_2 tolerance is an important parameter to understand, to be able to maximally favor hydrogenogenic growth and increase H_2 yields. In order to investigate possible ways of modulating H_2 tolerance, other than the few previously mentioned, we aimed to perform an adaptive laboratory evolution experiment to produce a *T. barophilus* strain super-tolerant to H_2, and to study the involved changes that occurred. We gradually acclimatized *T. barophilus* MP^T to sulfur-less culture, then to increasing initial H_2 concentrations, and characterized the ensuing strain, "Evol". Growth phenotypes, H_2, H_2S, and acetate productions were compared to the parent strain in various conditions. Whole-genome sequence of the new strain was analyzed, and transcriptome profiles were established to compare saturating or non-saturating conditions in both strains.

Materials and methods

More details on materials and methods used in this chapter can be found in MATERIALS & METHODS - GENERAL.

Culture

All cultures described in this chapter were grown in *Thermococcales* Rich *Medium* (TRM). Unless otherwise stated, each culture was started from a pre-culture (issued from a cryo-conserved strain) with 0.05 g/L colloidal sulfur. Cultures were started at about 2 $.10^6$ cell/mL. The presence of sulfur corresponded to 0.25 g/L colloidal sulfur. All incubations occured in dry ovens at 85 °C, with flasks upside-down in order to maximize H_2 retention. Except for the ALE experiment, all gas phases were initially at 100 % N_2 (+0.2 bar at room temperature). Cell concentrations were estimated by Thoma counting on optical microscopy. High pressure cultures were performed in fully-filled anaerobic glass flasks in Top Industrie discontinuous bioreactors, as described in chapter II.

Adaptive laboratory evolution experiment

The initial strain used in this study was *T. barophilus* MP^T from UBO Culture Collection (UBOCC-M-3107). Its genome was constituted of a circular chromosome of 2 010 078 bp encoding 2212 genes and a circular plasmid, pTBMP1, of 54 159 bp encoding 57 genes (Vannier et al., 2011).

For adapting the strain "Evol", sub-cultures were performed to reach stationary phase each 24, 48 or 72 h, and were stopped depending on the evolution of the measured cell density. They were re-inoculated at about 2 $.10^6$ cell/mL. Increasingly H_2-concentrated gas mixes were produced by a custom AirLiquide mass flow mixer, at a 0.1 % precision, and were used to flush gas phases for at least 5 min to ensure proper replacement.

For testing potential adaptation loss, "Evol" was sub-cultured up to stationary phase 6 or 9 times with 1 g/L sulfur, then re-cultured twice without sulfur before assessing the growth phenotype, in order to ensure that no colloidal sulfur was remaining in the final culture.

Metabolite concentrations

H_2 concentrations in the headspaces were measured using gas chromatography, H_2S concentrations were measured using the Cline assay, and organic acid concentrations

(glycolate, acetate, formate, propionate, chloride, sulphate, thiosulphate, bromide) were estimated using ionic chromatography. All samples were performed in triplicate.

DNA extraction, sequencing and analysis

Total DNA was extracted from a 24 h culture of "Evol" without sulfur, and its concentration was checked by Nanodrop spectrophotometer (Thermo Scientific) and Qubit fluorometer (Invitrogen). It was then sequenced by Fasteris (Plan-les-Ouates, Switzerland) on an Illumina MiSeq for identification of the single nucleotide variants. The company provided reads trimmed of their 3' adapters, which were aligned and mapped against the original strain sequence (Genbank accession number CP002372 (chromosome) and CP002373 (plasmid)), using Burrows-Wheeler Aligner (Li and Durbin, 2010). Variant calling was then performed with LoFreq (Wilm et al., 2012), and putative effects of the mutations were annotated thanks to snpEff (Cingolani et al., 2012). Protein homologies with other models were calculated with blastp (NCBI).

RNA extraction, sequencing and RT-qPCR

For RNA extractions, volumes of cell suspensions were pooled together in order to obtain 1.5 $.10^9$ cells in total. For example, if the cell density at a given point of interest was 4.5 10^6 cell/mL, approximately 320 mL were necessary to reach the objective cell number, so the extractions were based on 2x 200 mL cultures in 500 mL Schott bottles (in order to keep comparable liquid/gas *ratio* than in the usual culture flasks), from which 320 mL were pelleted.

RNA qualities and quantities were controlled on BioAnalyzer chip (Agilent) and Qubit fluorometer (Invitrogen) before being shipped to Fasteris for sequencing (Fasteris, Switzerland). Unfortunately, at the time of writing, transcriptomic profiles were sent but data were not received yet.

Gene expression was also assessed by RT-qPCR, using relative comparison ($\Delta\Delta$Ct method (Livak and Schmittgen, 2001)) of "Evol"'s expressions to the levels of the wild type strain (*T. barophilus* MP^T) in given conditions (absence or presence (0.25 g/L) of colloidal

sulfur). RNA samples were extracted at the end of the exponential phases for each strain, according to the pre-established growth curves in each condition. RNA qualities and concentrations were checked by Nanodrop fluorometer (Thermo Scientific), then cDNAs were produced by reverse transcription, using a qScript Flex cDNA synthesis kit (Quantabio). qPCR reactions were performed using a PerfeCTa SYBR Green Supermix ROX kit (Quantabio), and analyzed on a StepOne Real-Time PCR system (Thermo-Fisher).

Primers used were same as for chapter III. The 30S ribosomal RNA subunit was used as an internal reference for normalization. Each value was obtained in biological triplicate, however, due to a lack of technical replicate and the inherent variability of RT-qPCR protocols, some data remained unavailable and need to be confirmed.

Note that the work presented herein would have taken a much longer time without the help on many levels from several colleagues and collaborators: Yann Moalic (assistant professor / researcher), Erwan Roussel (researcher), Madina Ahmed (master student), Guillaume Lannuzel (technician), Emeline Vidal (master student), Pauline Grippon (undergraduate student), Hamza El Khati (master student) and Mohamed Jebbar (professor).

Results

Adaptive laboratory evolution of *T. barophilus* towards higher H_2 tolerance

In order to gradually increase *T. barophilus* MP^T's tolerance to hydrogen, the strain was first adapted to the absence of sulfur, a culture condition which should stimulate hydrogenogenic metabolism (FIGURE 65). Initially, a culture inoculated with 2 $.10^6$ cell/mL only reached 1 $.10^7$ cell/mL of cell yield. After about 27 generations (8 sub-cultures, 316 h of incubation in total) growing without sulfur, final cell concentrations reached about 4.2 $.10^7$ cell/mL (4.2-fold increase of growth yield). Then, sub-culturing was continued with gradually increasing initial H_2 concentrations (from 0 to 10 %), in the absence of sulfur. After about 49

more generations, *i.e.* 14 more sub-cultures (total of about 76 generations, *i.e.* 22 sub-cultures, 1049 h of incubation in total), the resulting strain, named "Evol", reached about 1 $.10^8$ cell/mL with 10 % initial H_2 (*i.e.* about 6.05 mM in gas). The initial *T. barophilus* MP^T would not grow in such conditions, demonstrating that "Evol" underwent adaptive evolution towards H_2 tolerance.

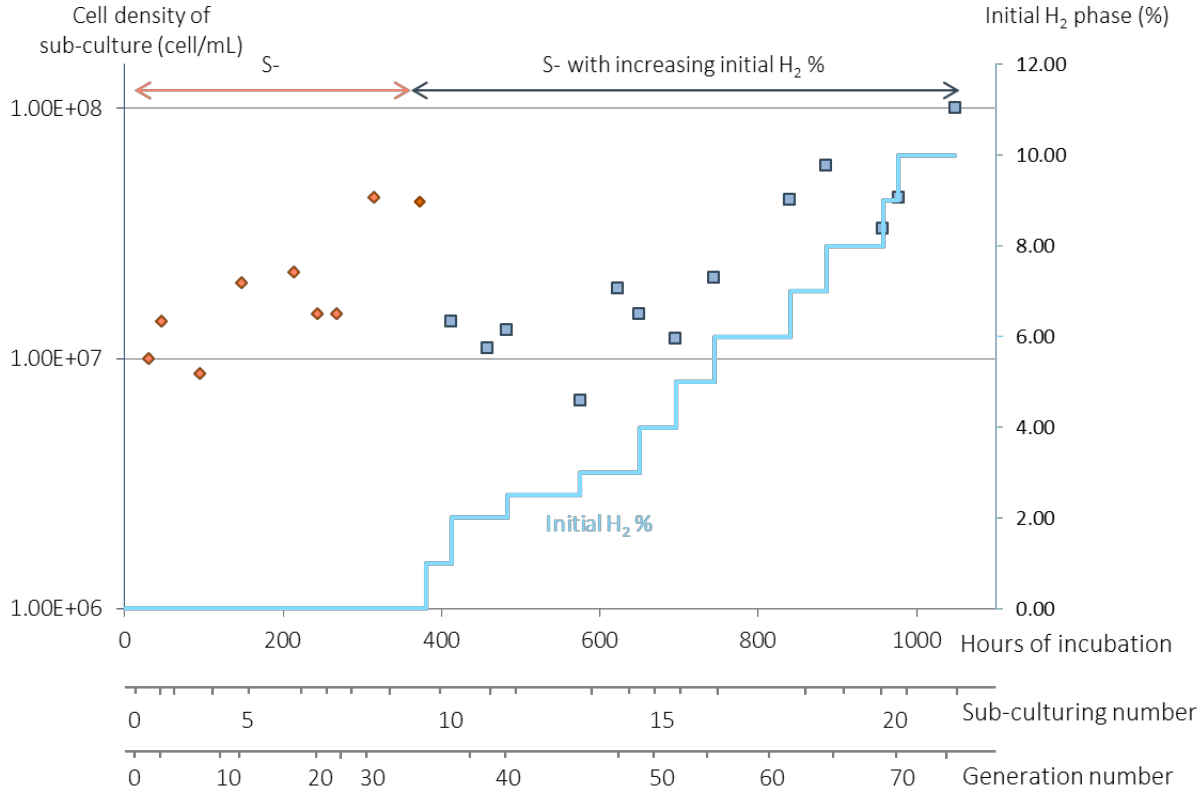

Figure 65: History of the adapted laboratory evolution of the strain "Evol"

Each point represents a final cell density after a sub-culture from the precedent, started at around 2 $.10^6$ cell/mL. Orange diamonds constitute a first adaptation phase without sulfur and without initial hydrogen. Blue squares represent the second phase, where initial H_2 concentration was gradually increased (light blue line) at each sub-culture.

Further investigations on "Evol" were then conducted to better understand this H_2 tolerance.

Growth phenotype and adaptation

Phenotypical observations further indicated differences between "Evol" and the initial *T. barophilus* MP^T (hereafter designated as wild type (WT)). Growths were assessed both in the absence and presence (0.25 g/L) of colloidal sulfur, with no initial H_2 added (FIGURE 66).

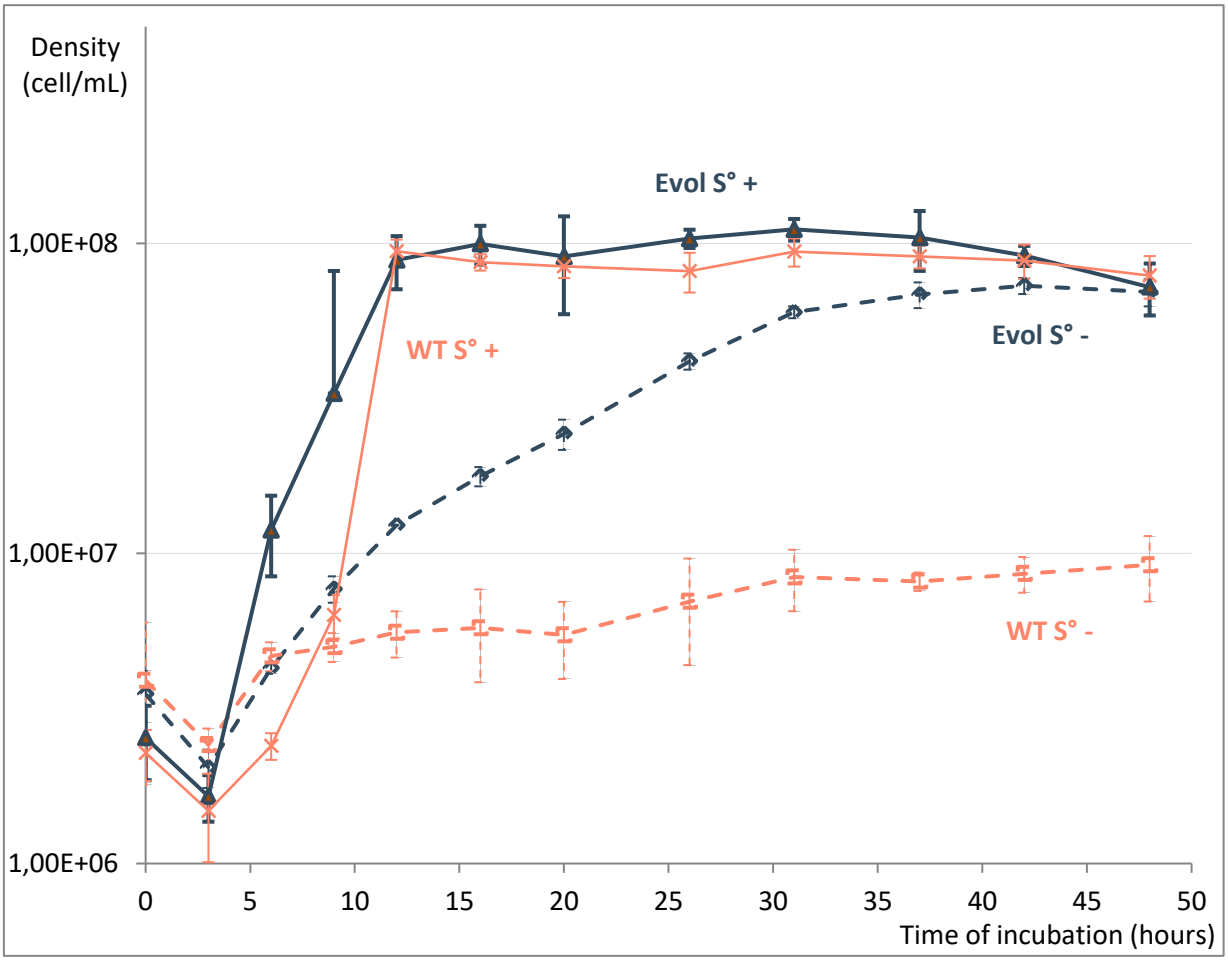

Figure 66: Growth curves of "Evol" and the wild type strain *T. barophilus* MP^T in the absence or presence (0.25 g/L) of colloidal sulfur

Samples were realized in triplicate. These graphs represent on series, but tendencies were confirmed in four different series.

Orange curves represent growths of the wild type strain. Blue curves represent growths of "Evol". Plain lines designate the presence of colloidal sulfur (0.25 g/L) while dotted lines designate the absence of colloidal sulfur. Error bars represent standard deviations (n=3).

It appeared that in the presence of 0.25 g/L sulfur, growth of "Evol" was equivalent in final cell density to the wild type (around 10^8 cell/mL), but showed a slightly earlier-occurring

exponential phase. Both grow rates were approximately 0.45 h^{-1}. Phenotypic differences were observed in the absence of sulfur, where biomass was rapidly limited in the wild type (with a maximum at about 10^7 cell/mL), but reached almost the same levels as in the presence of sulfur in "Evol" (*i.e.* almost 10^8 cell/mL), although with a much slower growth rate (about three-fold slower in "Evol"). Note that in the absence of sulfur, both strains showed two steps in their exponential growth phase, with distinct rates. For the wild type, the first phase was barely remarkable between 3 h and 6 h of incubation, but it continued until about 10 h of incubation for "Evol", both at a rate of about 0.22 h^{-1}. The second phase seemed to stop when plateau was reached, at around 32 h for both strains, although it was almost inexistent for the WT (rates of 0.08 h^{-1} for "Evol" and 0.02 h^{-1} for *T. barophilus* MP^T).

Interestingly, visual differences in cell morphology could be observed with optical microscopy between both strains (FIGURE 67). In the absence of sulfur, cells often appeared swollen all along growth for the wild type, whereas such morphologies could only be observed until 6 h of incubation in "Evol", which corresponds to the point where both curves dissociated. After 6 h, cells appeared in a "normal" shape, comparable to what was observed in the presence of sulfur in both strains.

In order to test if these phenotypical changes could be reversed, both strains were sub-cultured up to 9 times with sulfur excess (1 g/L), before being tested again in 2 sub-cultures in the absence of sulfur to ensure that no colloidal sulfur was remaining from dilutions (FIGURE 68). No differences were found in final cell densities in the absence of sulfur between "Evol" before and after those sub-cultures (around $7 – 8 .10^7$ cell/mL). The wild type strain also led to lower biomass than "Evol" (around 10^7 cell/mL). This indicated that the adaptation of "Evol" was not easily reversible in our test conditions.

A

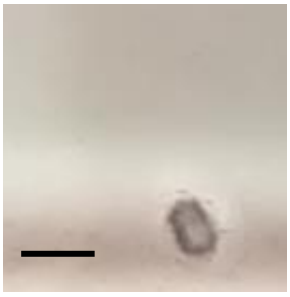

B

Figure 67: Photo of microscopic observations of "normal" and swollen *Thermococccales* cells

Cells A, appearing smaller and denser, were typically observed during growth in the presence of sulfur in both “Evol” and the WT, and during growth in the absence of sulfur after at least 6 h of incubation in “Evol”.

Cells B, appearing bigger and emptier, were typically observed during growth in the absence of sulfur in “Evol” (prior to 6 h of incubation) and in the WT (all along incubation).

Scale bars represent 3 µm.

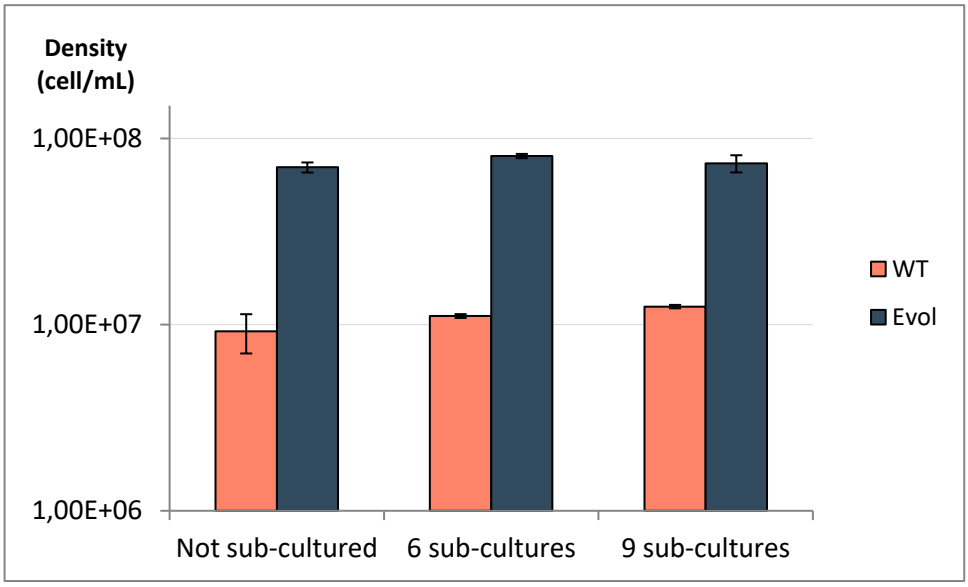

Figure 68: Final cell densities of "Evol" and the wild type strain in the absence of sulfur after 6 and 9 sub-cultures in sulfur excess (1 g/L), compared to the initial "Evol" phenotype

“Not sub-cultured” designated the initial strains, without any excess sulfur sub-culturing. Error bars represent standard deviations (n=3).

As preference for growth at high pressure was an important aspect in this project, "Evol" growth dynamics were tested in the presence of sulfur at 40 MPa. It showed that the piezophilic trait was not lost during the ALE experiment, as growth curves were almost identical between "Evol" and the wild type strain, in those conditions (data not shown).

H_2 tolerance

The adaptive laboratory evolution experiment performed enabled "Evol" to sustain high H_2 concentrations, compared to the initial strain *T. barophilus* MP^T, based on the hypothesis that H_2 tolerance was a key parameter for H_2 production.

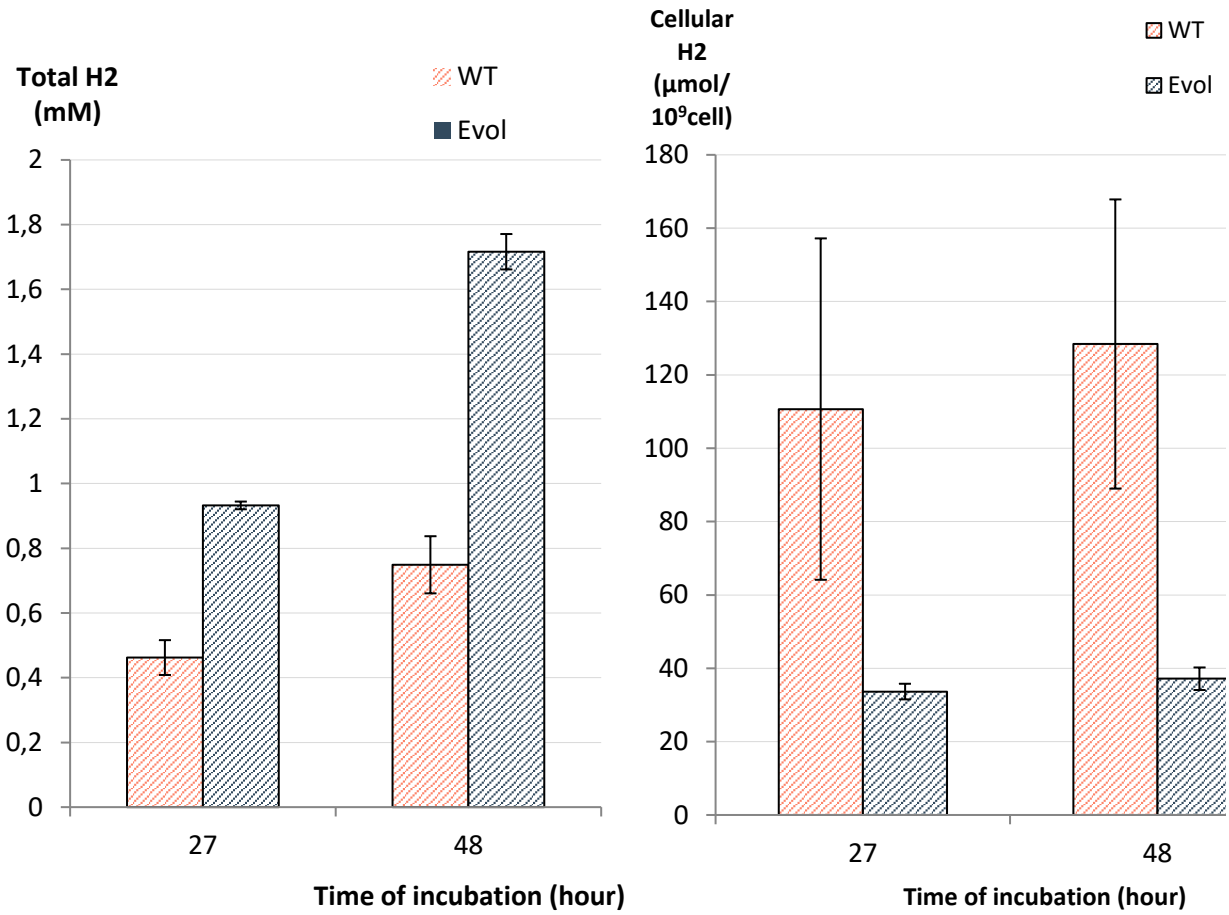

Figure 69: Absolute (left) and cellular (right) H_2 concentrations in gas phase from cultures of WT and "Evol" after 27 or 48 h of incubation at 85 °C, in the absence of sulfur

Samples were realized in triplicates. Error bars represent standard deviations (n=3).

FIGURE 69 presents absolute and cellular H_2 productions in the wild type strain and in "Evol", in 50 mL, N_2-filled anaerobic flasks with 20 mL TRM. It appeared that "Evol" cultures produced more than twice as much absolute H_2 as the WT (respectively 1.72 mM and 0.75 mM after 48 h). Envisioning an optimized H_2 bio-production application would however require the fundamental understanding of metabolic implications concerned by this seemingly over-producing configuration. It was thus necessary to consider cellular productions. Those were however significantly more important in the wild type, showing that cells led to higher H_2 concentrations thanks to their higher number, but that each cell produced less H_2, statistically (128 µmol/10^9cell for WT and 37 µmol/10^9cell for "Evol" after 48 h). The high H_2-tolerance of "Evol" thus seemed to concern the whole culture, for which each cell did not need to be more tolerant, as it produced less H_2, or recycled it better.

To better understand how H_2 saturation could influence growth dynamics of our strains, they were cultured with different gas phase volumes, allowing different levels of H_2 saturation, in the absence of sulfur (FIGURE 70). Higher gas phase volumes corresponded to less H_2-saturated cultures.

These graphs showed that the volume of gas phase, directly linked to H_2-desaturation potential of the culture, induced changes in growth dynamics of WT, while "Evol"'s phenotype was similar in all cases. In each condition, both strains' growths were similar in the first phase of culture, until they reached a dissociation point from where "Evol" continued to grow, though at a slower rate (generally in plateau phase at 30 h), and the wild type reached a plateau phase (generally in the first 15 h). This dissociation point corresponded to higher cell densities, with bigger gas phases (about 8 .10^6 cell/mL in 50 mL flasks; 1.3 .10^7 cell/mL in 120 mL; 1.7 .10^7 cell/mL in 160 mL; 2.9 .10^7 cell/mL at 250 mL), until "Evol" and WT phenotypes were quite similar (from 500 mL flasks).

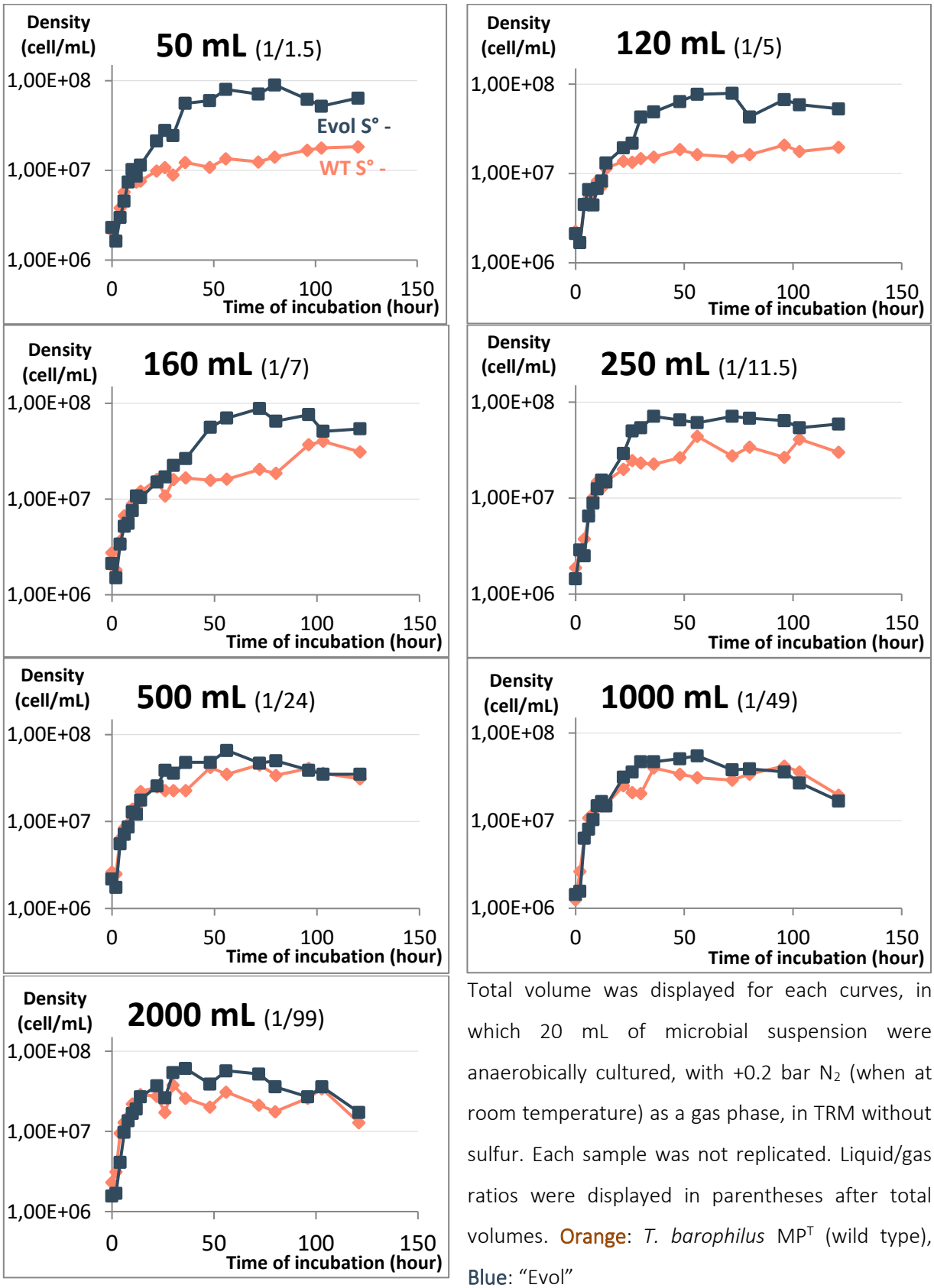

Total volume was displayed for each curves, in which 20 mL of microbial suspension were anaerobically cultured, with +0.2 bar N_2 (when at room temperature) as a gas phase, in TRM without sulfur. Each sample was not replicated. Liquid/gas ratios were displayed in parentheses after total volumes. Orange: *T. barophilus* MP^T (wild type), Blue: "Evol"

Figure 70: Growth over time of "Evol" and the wild type strain with different volumes of gas phase, in the absence of sulfur

Sulfidogenic system

Sulfur is known in *Thermococcales* to trigger a metabolic switch in the energy conservation system, leading to H_2S synthesis rather than H_2 evolution (Lipscomb et al., 2017). While less H_2 was produced in "Evol" cells in the absence of sulfur, compared to the WT strain, we aimed to explore the outcomes of the adapted strain when sulfur was added to the *medium*.

Cellular H_2 and H_2S productions were measured after 20 h of incubation with a gradient of initial colloidal sulfur concentration (from 0 to 3 g/L), in usual culture conditions (50 mL flasks) (FIGURE 71).

In the lower sulfur concentrations, *i.e.* between 0 g/L and 0.5 – 1 g/L, each "Evol" cell produced less H_2 and H_2S than for the WT strain. While the wild type *T. barophilus* MP^T rapidly reacted towards more H_2S and less H_2 with increased sulfur concentrations, "Evol" cells seemed to be fixed in similar metabolite productions at lower sulfur concentrations, before reaching a shifted switching point. Their H_2 productions declined from 0.5 g/L sulfur, while H_2S production began to increase. In contrast, the wild type strain seemed more sensitive to colloidal sulfur regarding its metabolite productions.

In order to better understand the relations between phase of culture and metabolic configurations, H_2S productions were also observed over time, in the absence and presence (0.25 g/L) of initial colloidal sulfur (FIGURE 72).

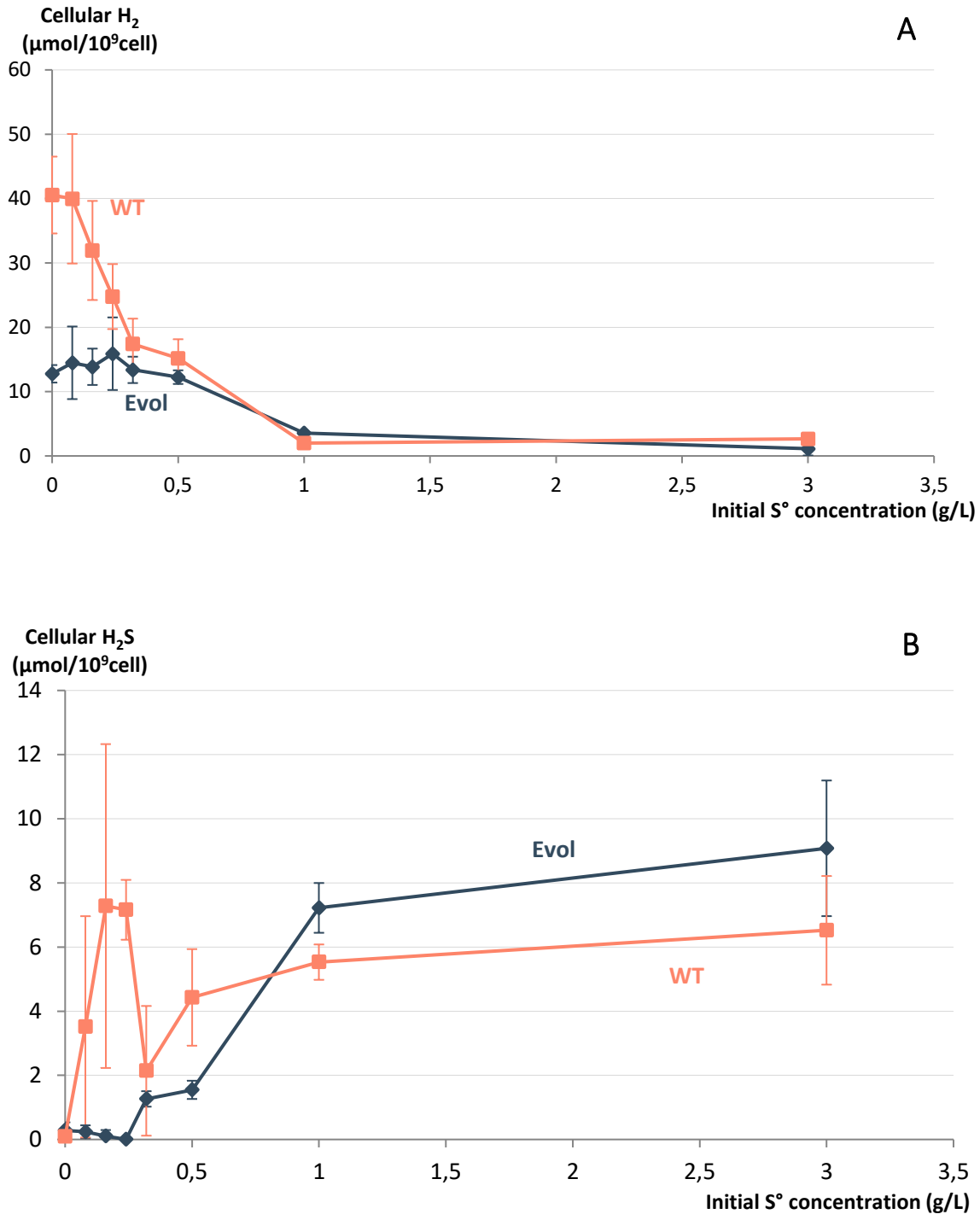

Figure 71: Cellular H_2 (A) and H_2S (B) concentrations obtained after 20 h of incubation, for different sulfur concentrations

Error bars represent standard deviations (n=3).

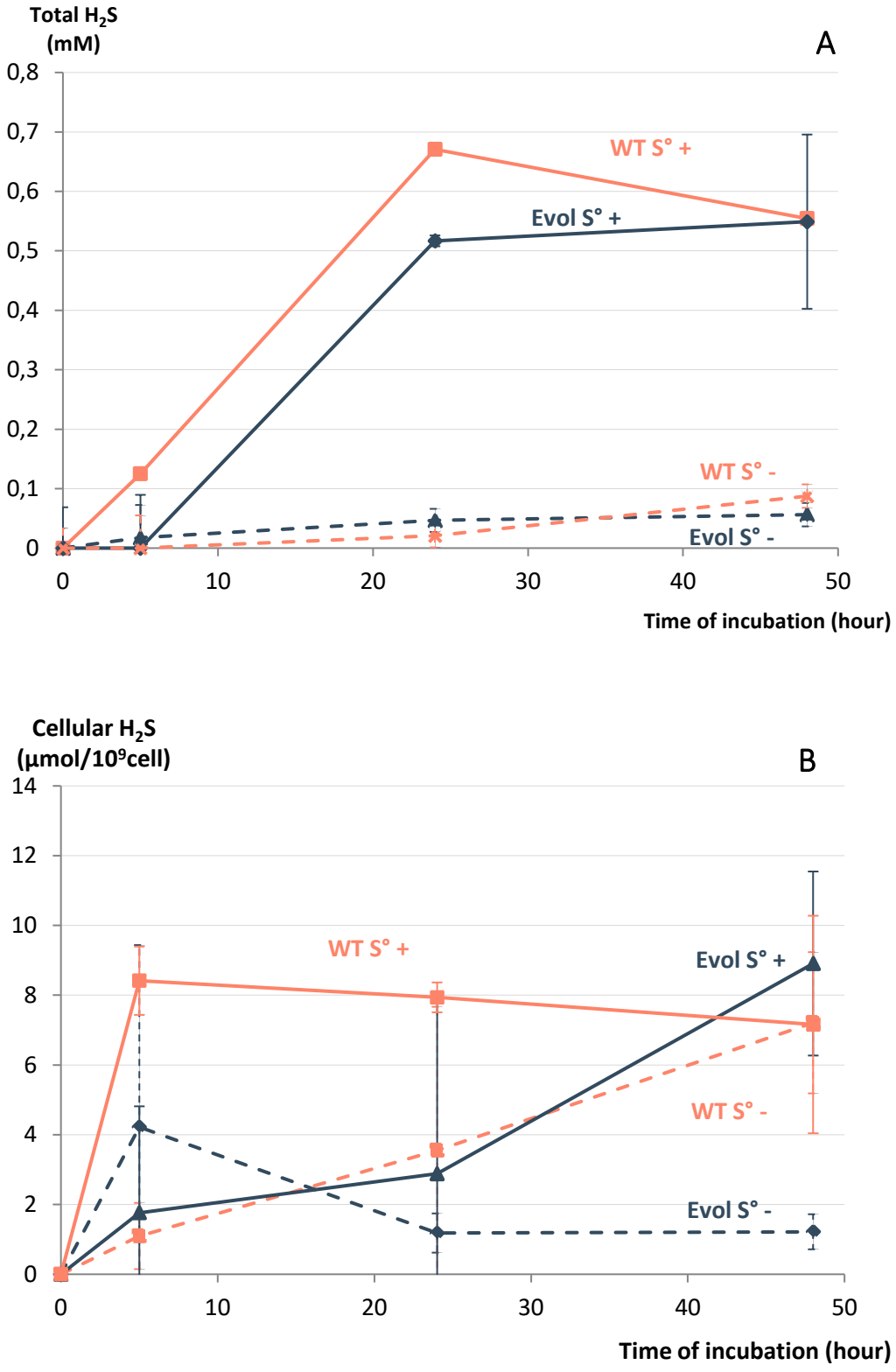

Figure 72: Absolute (A) and cellular (B) H_2S concentrations of "Evol" and *T. barophilus* MP^T cultures over time, in the absence and presence (0.25 g/L) of initial colloidal sulfur

Error bars represent standard deviation (n=3).

It appeared that absolute H_2S productions did not follow growth phenotypes. In the presence of sulfur, the wild type strain seemed to produce H_2S slightly more rapidly than "Evol", but final concentrations were equivalent in both strains (about 0.55 mM). In the absence of sulfur, no difference of absolute production could be observed between both strains (about 0.07 mM final). Yet, when reported to cell concentrations, several phases over time could be distinguished, although errors were quite important, indicating a need to confirm the results. During the first 24 h, "Evol" cells did not produce more H_2S in the presence than in the absence of sulfur (around 2 – 4 µmol/10^9cell), while cellular production had already peaked at 5 h for the WT strain in the presence of sulfur (8.4 µmol/10^9cell). Then, between 24 h and 30 h of incubation, cellular production increased importantly for "Evol" in presence of sulfur, to reach the levels of the WT strain. Interestingly, in the absence of sulfur, the phenotypes of "Evol" and the WT strain were also different: H_2S production of the ALE-issued strain remained at lower levels, while the WT followed the same trends as "Evol" in the presence of sulfur.

Accumulation of organic acids

As cultures were grown on TRM, peptides represented the main energy sources (although carbohydrates were also present in the yeast extracts used herein at about 14 %, according to the manufacturer (Bacto Yeast Extracts, BD), and organic acids would ensue from their degradations. Among the acids detected by our ionic chromatography method (glycolate, acetate, formate, propionate, sulphate, thiosulphate,), only acetate was found accumulated in "Evol" and the WT strain, in the absence and presence (0.25 g/L) of colloidal sulfur (FIGURE 69).

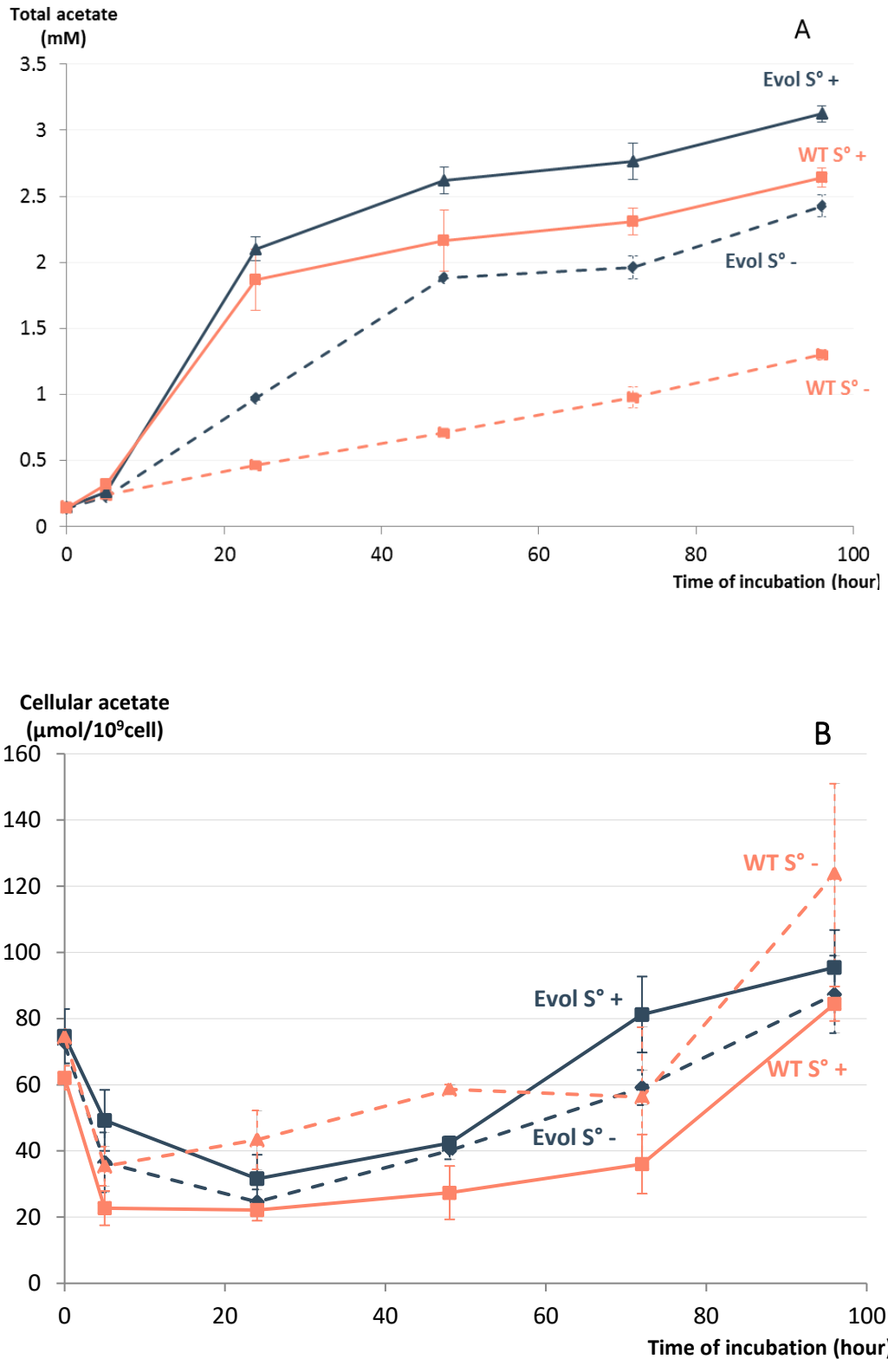

Figure 73: Absolute (A) and cellular (B) acetate concentrations of "Evol" and *T. barophilus* MP^T cultures over time, in the absence and presence (0.25 g/L) of initial colloidal sulfur

Error bars represent standard deviations (n=3).

Total acetate values continued to increase during the 96 h of incubation in all cases. Absolute tendencies seemed to be similar to that of growth dynamics, except that accumulation was still observed once stationary growth phase was reached. However, when looking at cellular concentrations, slight differences appeared between "Evol" and the wild type strain. In the presence of sulfur, "Evol" seemed to produce a little more acetate per cell (*e.g.* about 2.25 times more at 72 h), except at the last point (96 h), which could be attributed to the decline of cell density. In the absence of sulfur, the WT strain produced more acetate per cell than "Evol", but only at 24 h and 48 h, which could thus be the result of the fact that the WT strain had already attained its plateau phase of growth, while the ALE-issued strain was still actively dividing (see FIGURE 66).

Genomic modifications

Since the adaptations could be observed thanks to marked phenotypes, and did not seem to be easily reversed, possible modifications at the genomic level were verified. Total DNA of "Evol" was extracted from a 48 h culture on TRM without S°, then sequenced by Fasteris (Switzerland) on Illumina MiSeq, and single mutations and their effects on the complete genome of "Evol" were analyzed.

Compared to the wild-type genome, 119 mutations (insertions, deletions and substitutions) were found in "Evol" chromosome, located in 43 genes (out of 2212) and 8 non-coding sequences. On the pTBMP1 plasmid, 9 sites were mutated, concerning one coding sequence (out of 57) and 8 non-coding sequences (TABLE 22). Note that quality scores, in these tables, are inversely correlated to the probability that a variant call in Evol is wrong (*i.e.* the higher the quality score, the higher the confidence that a given site holds a variation). The function column was filled with NCBI annotations.

A snpEff analysis showed the potential impacts of each mutation on several genes, estimating that a total of 1394 effects could hit 511 other genes on the chromosome and

found effects on 27 other genes on the plasmid. snpEff estimates the effects of the mutations and quantify them as different types of impacts: LOW, MODERATE, HIGH, and MODIFIER (Cingolani et al., 2012). A list of the possible biological meaning of each quantifier can be found in the snpEff documentation (Sourceforge, 2020). For example in our case, a LOW impact could designate synonymous variants, or codon change without further effect identification; MODERATE could concern codon insertion or deletion, or unspecified non-synonymous variant; HIGH could correspond to mutations of codons important for protein structure or protein-protein interactions, or leading to rare amino acid (likely impairing protein function), or a loss or gain of stop codon or a loss of start codon; and MODIFIER broadly designated less precise impacts on coding or non-coding sequences which can also be downstream or upstream the mutated site. While those estimations remain putative, they could still be helpful for formulating hypotheses on possible genomic outcomes in our adapted strain. While most genes were only concerned by a limited number of predicted effects, snpEff estimations calculated up to 35 effects on a single gene. The most putatively impacted genes are presented in TABLE 23.

Furthermore, although mutations were not directly positioned in their reading frame, some genes, which were predicted by snpEff to be affected, could also find interesting literature-described homologs, as displayed in TABLE 24.

Table 22: Description of the 128 mutations found in "Evol" genome compared to the WT strain

Note that for mutations in non-coding sequences, only genes with predicted effects different than "MODIFIER" were presented in these tables, as each were predicted to impact several upstream and downstream genes. "HIGH" impacts were displayed in red (25 in the chromosome and 1 in the plasmid). 25 "HIGH", 23 "MODERATE", 63 "LOW", and 8 "MODIFIER" impacts for the chromosome, and 1 "HIGH" and 8 "MODIFIER" impacts for the plasmid were shown herein. 63 mutations led to a synonymous variant, 23 to a reading frame shift (1 in the plasmid), 23 to a missense variant, and 3 induced a gain of a stop codon.

A) Chromosome:

Position	WT	Evol	Region mutated	Locus concerned	Function	QUALITY	EFFECT	IMPACT
4377	T	C	Coding	TERMP_00006	Oligopeptide transporter ATP-binding protein Oppf	81	upstream_gene_variant	MODIFIER
50244	TG	T	Non-coding	TERMP_00058	hypothetical protein	62	frameshift_variant	HIGH
52630	A	AT	Coding	TERMP_00059	PQQ-binding-like beta-propeller repeat protein	8452	frameshift_variant	HIGH
139312	G	T	Coding	TERMP_00178	RNA ligase	136	missense_variant	MODERATE
139316	G	T	Coding			102	missense_variant	MODERATE
139395	T	G	Coding			133	synonymous_variant	LOW
150887	C	A	Non-coding	TERMP_00190	cell division protein FtsZ	81	missense_variant	MODERATE
189891	T	C	Coding	TERMP_00234	PrsW family intramembrane metalloprotease	84	missense_variant	MODERATE
217884	AT	A	Non-coding	-	-	5128	-	MODIFIERs
246233	G	T	Coding	TERMP_00291	dicarboxylate/amino acid:cation symporter	88	stop_gained	HIGH
304957	GA	G	Coding	TERMP_00366	hypothetical protein	64	frameshift_variant	HIGH
323309	T	TA	Coding	TERMP_00393	DNA-directed RNA polymerase subunit F	2300	frameshift_variant	HIGH
327435	G	A	Coding	TERMP_00398	Glu-tRNA(Gln) amidotransferase subunit GatE	549	missense_variant	MODERATE

345822	AT	A	Coding	TERMP_00416	aspartate kinase	2750	frameshift_variant	HIGH
349448	T	G	Coding	TERMP_00420	3-deoxy-7-phosphoheptulonate synthase	88	missense_variant	MODERATE
349460	G	A	Non-coding	TERMP_00420	3-deoxy-7-phosphoheptulonate synthase	90	missense_variant	MODERATE
349481	G	A	Coding	TERMP_00421	3-dehydroquinate synthase	81	synonymous_variant	LOW
413779	A	C	Coding	TERMP_00499 (top6B)	DNA topoisomerase VI subunit B	81	missense_variant	MODERATE
504184	G	GT	Non-coding	-	-	89	-	MODIFIERs
545147	TA	T	Coding	TERMP_00634	ATPase	66	frameshift_variant	HIGH
602406	TA	T	Coding	TERMP_00697	CBS domain-containing protein	61	frameshift_variant	HIGH
636592	C	T	Coding	TERMP_00730	sulfite exporter TauE/SafE family protein	81	missense_variant	MODERATE
683744	C	A	Coding	TERMP_00782	DUF2202 domain-containing protein	95	stop_gained	HIGH
685747	AT	A	Coding	TERMP_00783	hypothetical protein	64	upstream_gene_variant	MODIFIER
813063	A	G	Coding	TERMP_022095	16S ribosomal RNA	170	upstream_gene_variant	MODIFIER
832307	TA	T	Non-coding	-	-	72	-	MODIFIERs
862195	AAC	A	Coding	TERMP_00983	Lrp/AsnC family transcriptional regulator	131	frameshift_variant	HIGH
911882	A	C	Coding	TERMP_01044	NAD(P)-dependent glycerol-1-phosphate dehydrogenase	88	missense_variant	MODERATE
956935	T	C	Coding	TERMP_01099	transcription initiation factor 2B	5517	synonymous_variant	LOW
956938	T	C	Coding			5739	synonymous_variant	LOW
956959	C	T	Coding			6763	synonymous_variant	LOW
956962	C	T	Coding			6889	synonymous_variant	LOW
957001	C	T	Coding			7162	synonymous_variant	LOW
957019	T	C	Coding			5519	synonymous_variant	LOW
957022	A	G	Coding			5343	synonymous_variant	LOW
957025	G	A	Coding			5372	synonymous_variant	LOW
957033	G	C	Coding			5490	missense_variant	MODERATE
957034	A	G	Coding			5345	synonymous_variant	LOW

957040	C	T	Coding			5703	synonymous_variant	LOW
957043	C	T	Coding			5949	synonymous_variant	LOW
957055	A	C	Coding			5174	synonymous_variant	LOW
957058	G	A	Coding			4817	synonymous_variant	LOW
957061	T	C	Coding			4876	synonymous_variant	LOW
957064	T	C	Coding			5037	synonymous_variant	LOW
957068	T	C	Coding			5269	synonymous_variant	LOW
957085	C	T	Coding			7156	synonymous_variant	LOW
957106	C	T	Coding			7352	synonymous_variant	LOW
957112	C	T	Coding			7378	synonymous_variant	LOW
957115	G	A	Coding			7451	synonymous_variant	LOW
957194	C	T	Coding			6702	synonymous_variant	LOW
1048426	G	T	Coding	TERMP_01192	CGP-CTERM sorting domain-containing protein	82	missense_variant	MODERATE
1159505	TC	T	Coding	TERMP_01333	metal-sulfur cluster assembly factor	71	frameshift_variant	HIGH
1173050	A	C	Coding	TERMP_01353	cation:proton antiporter	80	missense_variant	MODERATE
1301219	A	T	Non-coding	TERMP_01508	hypothetical protein	87	upstream_gene_variant	MODIFIER
1378632	T	C	Coding			5531	synonymous_variant	LOW
1378634	A	G	Coding			5562	synonymous_variant	LOW
1378646	G	A	Coding			5052	synonymous_variant	LOW
1378647	T	G	Coding			4986	synonymous_variant	LOW
1378650	T	C	Coding			5114	synonymous_variant	LOW
1378662	T	C	Coding			5667	synonymous_variant	LOW
1378665	A	T	Coding	TERMP_01587	EVE-domain containing protein	5551	synonymous_variant	LOW
1378697	A	G	Coding			5628	synonymous_variant	LOW
1378698	T	A	Coding			5580	synonymous_variant	LOW
1378707	T	C	Coding			5539	synonymous_variant	LOW
1378710	A	G	Coding			5437	synonymous_variant	LOW
1378713	T	G	Coding			5570	synonymous_variant	LOW
1378719	T	C	Coding			5522	synonymous_variant	LOW

1378722	T	C	Coding			5542	synonymous_variant	LOW
1378740	A	T	Coding			6892	synonymous_variant	LOW
1378755	A	G	Coding			6421	synonymous_variant	LOW
1378761	A	G	Coding			6021	synonymous_variant	LOW
1378764	C	T	Coding			6212	synonymous_variant	LOW
1378776	G	A	Coding			5319	synonymous_variant	LOW
1378779	T	G	Coding			5309	synonymous_variant	LOW
1378782	T	A	Coding			5189	synonymous_variant	LOW
1378785	G	A	Coding			5252	synonymous_variant	LOW
1378788	T	C	Coding			5409	synonymous_variant	LOW
1378812	C	T	Coding			5421	synonymous_variant	LOW
1378830	A	G	Coding			4416	synonymous_variant	LOW
1378836	A	T	Coding			4291	synonymous_variant	LOW
1378848	G	A	Coding			3776	synonymous_variant	LOW
1378852	G	A	Coding			3799	missense_variant	MODERATE
1378876	T	C	Coding			3665	missense_variant	MODERATE
1378887	T	C	Coding			2945	synonymous_variant	LOW
1378890	A	C	Coding			2691	synonymous_variant	LOW
1378893	G	A	Coding			2458	synonymous_variant	LOW
1378899	A	G	Coding			2769	synonymous_variant	LOW
1378907	T	C	Coding			2613	missense_variant	MODERATE
1378911	C	T	Coding			2367	synonymous_variant	LOW
1438439	C	CT	Coding	TERMP_01652	TrmB family transcriptional regulator	287	frameshift_variant	HIGH
1454558	AT	A	Coding	TERMP_01664	DUF890 domain-containing protein	64	frameshift_variant	HIGH
1520235	CT	C	Coding	TERMP_01729	diphthamide biosynthesis enzyme Dph2	59	frameshift_variant	HIGH
1567906	C	T	Coding	TERMP_01776	Lrp/AsnC family transcriptional regulator	387	missense_variant	MODERATE
1568162	GA	G	Coding	TERMP_01777	serine/threonine protein kinase	60	frameshift_variant	HIGH
1646423	A	G	Coding	TERMP_01859	EVE domain-containing protein	891	synonymous_variant	LOW
1646432	C	T	Coding			897	synonymous_variant	LOW

1646454	A	G	Coding			874	missense_variant	MODERATE
1646460	A	G	Coding			886	missense_variant	MODERATE
1646468	A	T	Coding			853	synonymous_variant	LOW
1646474	A	G	Coding			882	synonymous_variant	LOW
1646483	C	T	Coding			784	synonymous_variant	LOW
1646485	A	G	Coding			737	missense_variant	MODERATE
1646498	A	C	Coding			594	synonymous_variant	LOW
1646504	C	A	Coding			633	synonymous_variant	LOW
1646509	C	T	Coding			530	missense_variant	MODERATE
1646525	C	A	Coding			611	synonymous_variant	LOW
1662344	TG	T	Non-coding	-	-	64	-	MODIFIERs
1667513	CT	C	Coding	TERMP_01872	DNA-directed DNA polymerase II large subunit	60	frameshift_variant	HIGH
1692537	TG	T	Coding	TERMP_01897	DUF515 domain-containing protein	61	frameshift_variant	HIGH
1745134	GA	G	Coding	TERMP_01949	cation:proton antiporter	58	frameshift_variant	HIGH
1758349	A	AT	Coding	TERMP_01964	radical SAM protein	4263	frameshift_variant&stop_gained	HIGH
1764407	C	T	Coding	TERMP_01969	sugar ABC transporter permease	1422	missense_variant	MODERATE
1791606	GC	G	Coding	TERMP_02001	polyhydroxyalkanoate depolymerase	64	frameshift_variant	HIGH
1819165	TA	T	Coding	TERMP_02034	phosphoribosylaminoimidazolesuccinocarboxamide synthase	61	frameshift_variant	HIGH
1891337	CT	C	Coding	TERMP_02119	flippase	83	frameshift_variant	HIGH
1930243	AT	A	Coding	TERMP_02146	4Fe-4S dicluster domain-containing protein	63	frameshift_variant	HIGH
1941872	CT	C	Coding	TERMP_02156	radical SAM protein	62	frameshift_variant	HIGH
1956257	G	A	Coding	TERMP_02169	beta-CASP ribonuclease aCPSF1	3257	missense_variant	MODERATE
1982105	AT	A	Coding	TERMP_02187	MFS transporter	65	frameshift_variant	HIGH

B) Plasmid :

Position	WT	Evol	Region mutated	Locus concerned	Function	QUALITY	EFFECT	IMPACT
8102	GA	G	Non-coding	-	-	7117	-	MODIFIER
8385	A	C	Non-coding	-	-	10683	-	MODIFIER
47760	T	TA	Coding	TERMP_02259	hypothetical protein	8639	frameshift_variant	**HIGH**
47825	A	AT	Non-coding	-	-	10685	-	MODIFIER
47846	AC	A	Non-coding	-	-	1100	-	MODIFIER
47850	C	CA	Non-coding	-	-	1074	-	MODIFIER
47893	G	GT	Non-coding	-	-	9391	-	MODIFIER
47901	C	CT	Non-coding	-	-	10059	-	MODIFIER
50671	CT	C	Non-coding	-	-	62	-	MODIFIER

Table 23: Other most impacted genes by mutation effects in « Evol » but not directly mutated

Impacted gene	Number of effects	Function
TERMP_01091	13	50S ribosomal protein L31e
TERMP_01092	22	50S ribosomal protein L39e
TERMP_01093	22	hypothetical protein
TERMP_01094	22	YhbY family RNA-binding protein
TERMP_01095	22	30S ribosomal protein S19e
TERMP_01096	22	hypothetical protein
TERMP_01097	22	DNA-binding protein
TERMP_01098	22	hypothetical protein
TERMP_01100	22	flap endonuclease-1
TERMP_01101	22	hypothetical protein
TERMP_01102	22	Acetyl-coA synthetase
TERMP_01103	22	hypothetical protein
TERMP_01104	22	hypothetical protein
TERMP_01583	35	ABC transporter permease
TERMP_01584	35	ATP-binding protein
TERMP_01585	35	glycine cleavage system aminomethyltransferase GcvT
TERMP_01586	35	hypothetical protein
TERMP_01588	35	M48 family metallopeptidase
TERMP_01589	35	HsdR family type I site-specific deoxyribonuclease
TERMP_01590	35	PIN domain-containing protein
TERMP_01591	35	DUF104 domain-containing protein
TERMP_01592	35	hypothetical protein
TERMP_01854	8	hypothetical protein
TERMP_01855	12	DUF1156 domain-containing protein
TERMP_01856	12	hypothetical protein
TERMP_01857	12	hypothetical protein
TERMP_01858	12	hypothetical protein
TERMP_01860	12	DNA double-strand break repair nuclease NurA
TERMP_01861	12	ATP-binding protein
TERMP_01862	12	hypothetical protein
TERMP_01863	12	DNA repair exonuclease

Table 24: Examples of notable genes less impacted, but with interesting literature-described homologs manually compared

Impacted gene	NCBI annotation	Protein homolog as described in literature	Gene in other model	Reference
TERMP_00417	hypothetical protein	Tar (*Thermococcales* aromatic amino acid regulator)	TK0271	(Yamamoto et al., 2019)
TERMP_00960	FAD-dependent oxidoreductase	Cytosolic NADPH polysulfide oxydoreductase	TK1481	(Kobori et al., 2010)
TERMP_01652	TrmB family transcriptional regulator	TrmB	PF1743	(Lee et al., 2005)
TERMP_01653	neopullulanase	Tgr	TK1769	(Kanai et al., 2007)
TERMP_01654	extracellular solute-binding protein	Mal-II	PF1938	(Lee et al., 2006)
TERMP_01655	sugar ABC transporter permease	Mal-II	PF1937	
TERMP_01658	ABC transporter ATP-binding protein	Mal-II	PF1933	
TERMP_01944	DUF1926 domain-containing protein	4-alpha glucanotransferase	PF0272	
TERMP_01966	carbohydrate kinase	fructokinase	PF1738	(Bräsen et al., 2014)
TERMP_01967	DUF2139 domain-containing protein	alpha-glucosidase	PF0132	(Lee et al., 2008)
TERMP_01971	glycosyltransferase	TreT, trehalose synthase	PF1742	(Qu et al., 2004)
TERMP_01972	TrmB family transcriptional regulator	TrmB	PF1743	(Lee et al., 2008)
TERMP_02160	DUF1957 domain-containing protein	Branching enzyme of the GH-57 family	TK1436	(Murakami et al., 2006)
TERMP_02166	Glu/Leu/Phe/Val dehydrogenase	Glutamate dehydrogenase	TK1431	(Nohara et al., 2014)
TERMP_02174	phosphoenolpyruvate synthase	Phosphoenolpyruvate synthase	TON_0311	(Moon et al., 2015)
TERMP_02185	CoA-disulfide reductase	NADPH-dependent sulfur reductase (Nsr)	TK1299	(Santangelo et al., 2011)

Note that those comparisons were only based on homologies on protein sequences, but would require functional confirmation. For instance, two genes, TERMP_01972 and TERMP_01652, resembled TrmB in *P. furiosus*, but only shared 32.45 % of protein sequence homologies between themselves, and possibly represented functional paralogs of TrmB-like proteins. Yet, looking for homologs described in the literature could help assuming new metabolic configurations.

On the chromosome, most of the variations occurred in coding sequence, and this analysis was thus mainly based on their direct effects on the mutated genes.

Unfortunately, many concerned proteins remained predicted as putative, although some were estimated to be highly impacted (as for example the ones encoded by TERMP_00058, TERMP_00366, or TERMP_02259). This underlines the need for a better knowledge of the global metabolism, but also a better curation of annotation databases, since some estimation can be given by analyzing literature (*e.g.* TERMP_01652, annotated as a hypothetical protein but homologous to the regulator Tar of *T. kodakarensis* (Yamamoto et al., 2019)).

Importantly, LOW impacts have to be taken into account, as they can simply correspond to a lack of information. Some regions were particularly affected by several LOW impact mutations, with synonymous variants, for example. It was the case, for instance, for TERMP_01099 (annotated as transcription initiation factor 2B) and the two putative EVE-domain proteins encoded by TERMP_01587 and TERMP_01859. While synonymous variants might not change the resulting protein sequence, they can still have important roles in the normal processing of transcription, and translation, among others (Zeng and Bromberg, 2019; Zhang et al., 2013). In our examples, the mutations were more likely to be biologically relevant as they presented high quality scores.

Genes associated to several different functions seemed to be affected by those mutations, with various levels of confidence, such as substrate uptake (*e.g.* TERMP_00006 (ABC transporter ATP binding protein), TERMP_00291 (dicarboxylate amino acid:cation transporter)), cell division (*e.g.* TERMP_00190 (FtsZ)), amino acid catabolism (*e.g.* TERMP_02166 (glutamate dehydrogenase)), replication (*e.g.* TERMP_01872 (DNA-directed DNA polymerase II large subunit)), glycolysis (*e.g.* TERMP_02174 (PEP synthase)), transcriptional regulation (*e.g.* TERMP_01652 (TrmB family regulator)), cation translocation (*e.g.* TERMP_01949 (cation:proton antiporter)), lipid transport (*e.g.* TERMP_02119 (flippase)), and polymer degradation (*e.g.* TERMP_02001 (polyhydroxyalkanoate depolymerase)).

Noticeably, no mutations or their effects were found on the best characterized modules of the energy conservation system, as described in chapter III. For example, genes

encoding SurR (TERMP_00656), Mrp-Mbh1 and 2 (TERMP_01471-98), Mrp-Mbh-COdh (TERMP_001139-54), Mbs (TERMP_00853-65), SHI (TERMP_00067-70), or SHII (TERMP_00536-9), were not mutated or predicted as affected. The exception was for the gene encoding the Nsr homolog (TERMP_02185), which was predicted to receive a MODIFIER impact by a T deletion at position 1982105, in the TERMP_02187 gene. Yet, since this mutation showed a low quality score, this prediction has to be interpreted as very hypothetical.

Transcriptomic adaptation

As genomic modifications only represent a first level of adaptation, we aimed to better characterize the changes justifying the new phenotype in "Evol" by also looking at transcriptional differences, in the hope to correlate them with gene mutations.

In order to characterize the differences in transcriptomes in the original and adapted strains, total RNA were extracted in five different conditions for each strain, in triplicate. Based on the growth curves presented earlier (FIGURE 66 and FIGURE 70), the objectives were to compare cells in different states of H_2-saturation stress, and at different growth phases, as described in TABLE 25. We aimed to compare the transcriptomic configurations of both strains in different situations: (A) when growth dynamics were different in the absence of sulfur (when H_2 was saturating but "Evol" still grew), (B) using the references of a "both not stressed" (before H_2 saturation, in the first phase of exponential growth), as well as (C) "both stationary" conditions. In the presence of sulfur, both (D) exponential and (E) stationary phase references were also assessed.

At the time of writing, total RNA samples are being sequenced by Fasteris (Switzerland) on Illumina MiSeq, and will thus not be displayed in this report.

Table 25: Description of the conditions tested for transcriptomic comparisons of "Evol" and the wild type strain, with usual 1/1.5 (liquid/gas) volume ratio

Condition		State / Phase	Strain	Time of incubation
Without suflur	A	Stressed	Evol	20 h
		Not stressed	WT	20 h
	B	Not stressed	Evol	6 h
		Not stressed	WT	6 h
	C	Stationary	Evol	50 h
		Stationary	WT	50 h
With sulfur (0.25 g/L)	D	Exponential	Evol	8 h
		Exponential	WT	8 h
	E	Stationary	Evol	16 h
		Stationary	WT	16 h

Prior to begin the assessment of these configurations, in order to verify that changes in transcription could occur, relative gene expression of few clusters of the energy conservation metabolism of *T. barophilus* MP^T were evaluated by RT-qPCR in both strains, in the presence (0.25 g/L) and absence of colloidal sulfur (FIGURE 74). For these experiments, triplicates of RNA samples of both strains were extracted after 8 h of incubation in the presence of sulfur (end of exponential growth phase), and 24 h of incubation in the absence of sulfur (later H_2-saturated exponential growth for "Evol", and H_2-saturated stationary phase for the WT strain).

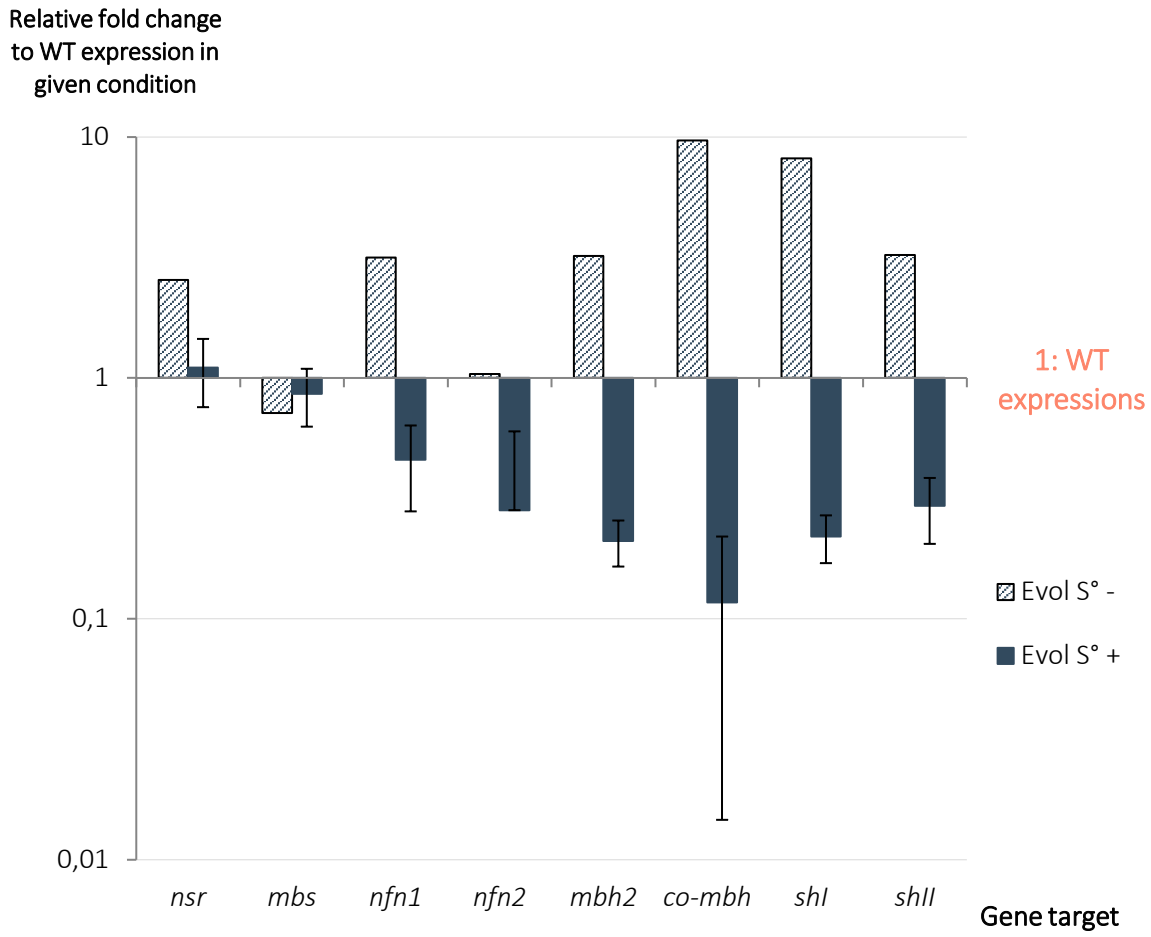

Figure 74: Relative gene expressions of several gene targets in "Evol" compared to the wild type strain, in the presence (0.25 g/L) or absence of colloidal sulfur

RT-qPCR data were analyzed with the 2-ΔΔCT method (Livak and Schmittgen, 2001). Error bar represent standard deviations (n=3). Vertical axis is displayed in logarithmic scale.

Changes in gene expression between both strains were observed in almost all cases, reaching maximally 10-fold in over- or under-expression. As a general tendency, it appeared that targeted genes were overexpressed in "Evol" in the absence of sulfur, and underexpressed in the presence of sulfur, compared to the wild type strain (except for *nsr* and *mbs*, which were not differentially expressed in the presence of sulfur, and for *nfn*2, which was not differentially expressed in the absence of sulfur).

Discussions & conclusions

In this study, the mechanisms of H_2 tolerance were considered using adaptive laboratory evolution of *T. barophilus* MP^T, leading to the production of the strain "Evol". Such variant was able to grow significantly more than the wild-type train in the absence of sulfur. It was found to induce higher total H_2 levels in these conditions, while less cell-specific H_2 was produced. We examined how sulfur concentration influenced H_2 and H_2S productions, and compared to organic acid productions, genomic modifications and some gene expressions of the new strain with the wild type. While transcriptomic profiles were still expected at the time of writing, the results of the investigations were discussed herein, proposing various hypothetical lines of thoughts to characterize the process associated to this new physiology.

An energy conservation less based on hydrogenases and less sensitive to sulfur

The adapted strain, « Evol », clearly showed differences in growth dynamics in the absence of sulfur, compared to the wild type strain (FIGURE 66). Those differences were observable only after a certain time of incubation, before which growth rates were similar in both strains. Although actual H_2 measurements were missing for these precise times, we could suppose that the observed changes in growth rate were due to H_2 saturation in the *medium*. It was also indirectly confirmed by the correction of these defects in the wild type strain when gas phase volume was increased (*i.e.* H_2 product partial pressure decreased) (FIGURE 70), and as it was observed for example in early works on other strains (*T. celer*, *T. litoralis*, *T. stetteri*) (Bonch-Osmolovskaya and Miroshnichenko, 1994). Cells in saturating conditions seemed to show swollen morphologies (FIGURE 67), which were also interestingly observed in other strains during the screening phase of this project (chapter I) when cultures led to high H_2 concentrations (data not shown). However, "Evol" cells, while dividing, remained in a "normal" morphological state (as observed in the presence of sulfur) all along growth in the absence of sulfur. Moreover, H_2 productions have revealed to be less important for each "Evol" cell in these conditions, compared to WT (FIGURE 69). Note that some *Thermococcales* are able to produce formate from H_2 oxidation as a proposed supplementary mechanism of reductant disposal (Le Guellec, 2019; Topçuoğlu et al., 2018), but no such

observation was made herein, which is not surprising as *T. barophilus* MP^T genome does not encode the specific formate hydrogen lyase cluster (Vannier et al., 2011).

Consequently, it appeared that "Evol" cultures led to high total H_2 concentrations thanks to lower cell-specific H_2 productions, yet accompanied by a more important cell division. Assuming that energy conservation is important in order to result in cell division, it would imply that **ATP could be produced from other metabolic routes than the well-described cytosolic and membrane-bound hydrogenase system, involving the maintenance of a sodium gradient across the membrane**. Most of the energy produced could come from other pathways.

To investigate this option, measuring other possible catabolic end-products could be informative. We first verified whether this impairment of hydrogenogenic energy conservation could be compensated by the sulfidogenic system. Elemental sulfur is known to induce a metabolic switch in *Thermococcales*, thanks to the action of the master regulator SurR, as mentioned previously. Note that, as in chapter III, a small H_2S production could be observed even in the absence of colloidal sulfur, which was attributed to the presence of Na_2S. Globally, cellular H_2S levels were yet also lower over time in "Evol" than in the wild type, both in the presence and absence of sulfur, showing that **H_2 underproduction was not compensated by H_2S overproduction**. Noticeably, these conclusions only concerned intermediate sulfur concentrations (tested at 0.25 g/L). With more sulfur, "Evol" reached the cellular H_2S production levels of the WT strain, which also corresponded to an entirely sulfidogenic configuration in both strains (no more H_2 production). The sulfidogenic system seemed to be triggered from higher minimum sulfur concentrations (between 0.5 and 1 g/L) than for the WT strain (from 0.08 g/L). These measurements in different concentrations of sulfur, along with the lower H_2S cellular production in the presence of sulfur over time, **tended to indicate that "Evol" is less sensitive to the sulfur presence**. Whether the effect of mutations predicted on TERMP_02185 had significance in such phenotype would be interesting to verify. This gene encodes the Nsr homolog in *T. barophilus*, described to be involved in cytosolic H_2S production while reoxidizing NADPH (Kanai et al., 2011; Schut et al., 2007).

Nonetheless, H_2 production was also less important in "Evol" than in WT in low sulfur concentrations (up to 0.32 g/L), where the hydrogenogenic system was predominant in WT. Another preliminary experiment (data not shown) indicated that cellular H_2 rates in "Evol" did not increase when N_2 volume (*i.e.* H_2 desaturation potential) increased, contrarily to the wild type strain. We could hence advance that in "Evol", not only the **hydrogenase-dependent energy conservation mechanisms** were less sensitive to sulfur, but **they also might have been less generally active, independently of the sulfur presence or saturation conditions.** Many mutations concerned putative cation-proton antiporters (*e.g.* TERMP_01949). While none of them were reported to possibly affect known Mrp subunits of the hydrogenase system, they could still influence the maintenance of an ion gradient across the membrane, and further, ATP production by membrane ATPases. Interestingly, TERMP_00634, encoding a putative ATPase, was mutated in its coding sequence, which was estimated to render a high impact. However, TMHMM (http://www.cbs.dtu.dk/services/TMHMM/) predictions indicated that the corresponding protein do not harbor any transmembrane helix and is thus unlikely a membrane ATPase. No hint on the possible functional outcomes of these mutations could yet be advanced here, and would require further investigations, such as physiological observations of "Evol" after modification of this gene back to the WT genotype, along with a comparison of ATP/ADP/AMP pools.

One could also advance a possibly complementary assumption that the hydrogenogenic energy conservation metabolism would still be active, thanks to a more important recycling of the ensuing H_2 by SHI/II activity, relieving cellular H_2 saturation. However, while gene expression has shown an increase in "Evol" in *sh*I expression of 8.1-fold and in *sh*II expression of 3.2-fold in the absence of sulfur compared to the WT, tending to add credit to this surmise, we also noted that imposing a 20 % H_2 gas-phase to *T. barophilus* MP^T did not lead to any measurable H_2 consumption (see chapter I). Deleting membrane ATPase encoding genes (TERMP_01694-1702) or diminishing their expression in both "Evol" and WT, then comparing the ensuing effects on growth phenotype would allow to verify whether energy conservation still occurs importantly *via* membrane ATPase in "Evol". Nonetheless, the many mutations in "Evol"'s genome also encouraged to explore other hypotheses.

A possible implication of acetate metabolism in the presence of sulfur

If not involving membrane ATPases, synthesis of ATP could also occur *via* substrate catabolism. In that case, many studies on other *Thermococcales* models have underlined an accumulation of acetate, ensuing from pyruvate, regardless of its origin (mainly from amino acid or carbohydrate catabolism) (*e.g.* (Nohara et al., 2014; Schicho et al., 1993)). Yet, if cellular acetate seemed slightly more important in "Evol" in the presence of sulfur compared to the wild type strain, the opposite tendency was remarked in the absence of sulfur. It thus appeared that if ATP was rather produced towards other metabolic routes for electron disposal than H_2 or H_2S production in "Evol", **compensation through a disposal of electron leading to acetate accumulation could only occur in the sulfur presence**. **In the absence of sulfur, the lack of hydrogeno- and sulfidogenic energy conservation did not seem to be corrected by higher acetate accumulation.** Still, contrarily to H_2S, acetate absolute and cellular productions increased all along the 96 h of stationary phase, in both strains, in the presence and absence of sulfur. This showed that catabolic routes and their likely associated ATP productions were still employed, in both strains.

A possible line of thought to explain slight differences in acetate production could come from the observation that TERMP_00417 was predicted as affected by the mutations in "Evol", and the encoded protein showed homologies with the amino acid regulator Tar in *T. kodakarensis* (Yamamoto et al., 2019). Thus, a modification of the amino acid pools in "Evol" due to these putative effects could be imagined, possibly ensuing on different acetate levels.

Nevertheless, another end-product was measured in certain literature reports, ensuing from pyruvate: alanine (Kengen and Stams, 1994a; Kobayashi et al., 1995; Mai and Adams, 1996b; Ward et al., 2000). It was shown that an alanine amino-transferase and a glutamate dehydrogenase allowed this turnover (Yokooji et al., 2013). Note that in our results TERMP_02166, encoding a glutamate dehydrogenase, was predicted to be affected by genomic variants of "Evol". Nonetheless, this pathway would compete with another pyruvate-involved pathway, leading to ATP formation: synthesis of acetate from acetyl-CoA (with acetyl-coA synthetase, ACS), itself issued from pyruvate. It would thus render an apparently

energetically disadvantageous metabolic strategy. Actual flux calculations at the whole-metabolism scale would be necessary to better apprehend this assumption. Those observations as reported in literature were realized in high H_2 concentrations. Herein, we were unable to provide any alanine concentration measurements at the time of writing.

We also showed in chapter I that acetate could likely be consumed by *T. barophilus* MP^T, similarly to in other strains, even though the exact mechanisms implied are unclear (Birrien et al., 2011; Slobodkin et al., 2001). Early works in *P. furiosus* have demonstrated that ACS activity could occur in both directions, *i.e.* possibly an ATP-dependent formation of acetyl-CoA, but mass balance analyses in *T. kodakarensis* have also advanced that other unknown routes might additionally be involved in acetate synthesis (Nohara et al., 2014; Schäfer and Schönheit, 1991). In our results, an ACS homolog encoding gene (TERMP_01102) was interestingly found to be impacted by 22 mutations, which could allow to hypothesize its implication in the phenotype of "Evol". Upcoming transcriptomic data should allow better hints on that matter.

Divide more to saturate less?

A complementary hypothesis to explain "Evol"'s tolerance to sulfur-less conditions could be that **cells would shift in a physiological mode encouraging rapid cell division over cell mass production**, as hinted by the observed morphological differences between both strains in usually H_2-saturating conditions. Such *scenario* may require different amounts of ATP per cell, hence the variations in metabolite productions. A missense mutation at position 150887 (non-coding sequence) was estimated to moderately impact TERMP_00190, annotated as encoding a FtsZ homolog. This protein has been described to play important roles in bacterial cell division machinery, and was also likely involved in cytokinesis of *Euryarchaeota* (Caspi and Dekker, 2018; Makarova et al., 2010). Speculatively, one could imagine that this mutation would impact the rate of cell division of "Evol", but more experimental evidence, *e.g.* from mutational studies in WT, would be necessary.

A fine-tuning of a complex system based on electron flux balance?

The numerous mutations on the genome of "Evol" and their expected effects could lead to many different interpretations, which would each be highly hypothetical and would require more experimental confirmation. Note that no large-scale genomic rearrangement was observed, but the number of punctual mutations in "Evol" (119) was much more important than the 10 and 11 mutations found in an ALE works performed on '*T. onnurineus*', which were based on the enhancement of unique, precise reactions of CO or formate consumptions (Jung et al., 2017; Lee et al., 2016). The fact that re-culturing "Evol" several times in excess of sulfur did not induce a loss of sulfur-less adaptation indicated that the modifications were likely anchored in the genome. Yet, since high pressure growth phenotype, *i.e.* another likely systemic function, did not seem changed, **it appeared that those modifications could rather be targeted at the concerned function in the absence of sulfur, and not be randomly present**. It is thus possible that many different functional parts of the systems were modified, in addition to the ones previously mentioned in this discussion, which all compiled into a global physiological adaptation.

As possible examples of implications, we noticed several mutations or effects on glycolysis-related genes. A study on bacterial model *Corynebacterium glutamicum* has demonstrated that a single point mutation could change the net ATP gain of the EMP pathway by modifying the electron carrier preference of an oxidoreductase (NDH-II), allowing it to oxidize NADPH and thus to re-balance its pools (Komati Reddy et al., 2015). We could imagine similar effects on the glycolytic metabolism of "Evol". Moreover, several genes encoding potential transporters for carbohydrates and amino-acids (*e.g.* TERMP_01654,55,58, encoding a Mal-II homolog), as well as related transcriptional regulators (e.g. TERMP_01652, encoding a TrmB-like regulator) appeared indirectly affected by numerous mutations.

In the adapted strain, a gain of stop codon possibly highly impacted the function encoded by TERMP_00291. The ensuing protein has a homolog encoded by TON_0901, which was advanced in '*T. onnurineus*' to be involved in cystine uptake. In this model, a thioredoxin

reductase (TrxR), able to oxidize NAD(P)H, was demonstrated to be likely linked to cysteine/cysteine redox shuttle *via* a glutaredoxin-like protein disulfide oxidoreductase (Pdo) (Choi et al., 2016). We could thus extrapolate that the mutation of TERMP_00291 may be indirectly influent in redox carrier pools, although experimental measurements of those pools would be needed for confirmation. Additionally, Nsr has been described to oxidize NADPH while producing H_2S, and its encoding gene (TERMP_02185) was predicted to be affected by mutations in "Evol". If this predicted effect ensues on a different Nsr activity, NADPH pools would thus be likely affected. As the cell has to maintain its redox balance to continue functioning, and if acknowledged that the usual electron sinks (noticeably H_2 and H_2S) were not similarly used in "Evol", **we could surmise that the metabolic system was reorganized to allow proper electron shuttling to maintain viable metabolic fluxes.** This hypothesis of re-balanced electron flows could also be supported by the fact that almost all our RT-qPCR-tested gene targets were expressed differently in the adapted strain, each of them being implicated electron carrier redox transfers.

ADP and AMP pools could also be involved in differential ATP productions. TERMP_02174 was found potentially affected by mutations, and the encoded protein is homolog to the phosphoenolpyruvate synthetase of '*T. onnurineus*' (encoded by TON_0311) (Moon et al., 2015). In *Thermococcales* glycolysis, degradation of PEP to pyruvate can either occur through PEP synthetase, producing ATP from AMP, or through pyruvate kinase, producing ATP from ADP (Bräsen et al., 2014; Hutchins et al., 2001). As the upstream glucokinase would rather be ADP-dependent than ATP-dependent, modulating ADP pools could be important for the functioning of the EMP pathway (Kengen et al., 1995; Rivas-Pardo et al., 2013; Ronimus et al., 2001).

However, those assumptions remain theoretical, and would need to be verified in order to separate random variations from the ones actually responsible for high H_2-concentration tolerance. Interpretations are all the more tedious, since other potentially involved pathways were not considered, such as for instance gluconeogenesis, which is able to regenerate NADPH through GAPDH activity (Bräsen et al., 2014). Transcriptome profiles should allow better apprehension on that matter, to orientate future potential mutational verifications.

More hints on *T. barophilus* SurR

The the absence of mutation in the many genes implicated in the membrane-bound energy conservation system, and particularly in SurR, was surprising, since H_2 and H_2S productions were dissimilar and differential expressions were observed from the wild type strain, both in the absence and presence of sulfur. Tendencies in expression patterns in the absence of sulfur could not be correlated by an increase or decrease of SurR activity, as not all consistent or inconsistent with the expected outcomes as described in FIGURE 53, P. 234, in chapter III. These observations would once again tend to mitigate the influence of the master regulator in our model compared to literature reports on other strains (Lipscomb et al., 2017). This could possibly be justified by the competitive effects of other hypothetical transcriptional regulators, or different, unknown regulatory effects of SurR on the concerned genes. The latter explanation would be less likely verified, since we found no mutation or effect of another mutation in TERMP_00656, encoding SurR.

Conclusive remarks

The results presented herein consequently allowed to formulate several hypotheses on the mechanisms involved in H_2 tolerance in "Evol". Its metabolism seemed less sensitive to sulfur, and overall less relying on the hydrogenase-associated energy conservation system. We advanced that these features could be accompanied by a cell cycle strategy to divide quicker, as allowed by an energy metabolism possibly more efficient thanks to many points of electron fluxes re-balancing. Several arguments would however necessitate clarification or confirmation.

The impacts of genomic modifications would benefit from deeper analyses and more information. Several automatically predicted proteins remained inaccurately annotated, and a literature analysis has shown that some homologs were identified in other *Thermococcales* models. A more complete comparison of the 538 putatively affected genes with other literature references could help grasp a complete picture of the system. Quality scores of each mutation could also be interesting to take into account, keeping in mind that clonal interference, *i.e.* statistically discarding of beneficial mutations at the profit of the highest number of mutants in the population during a sub-culture, was likely high in our experiment,

and therefore that less represented mutations could still be important (Barrick et al., 2009). Non-coding sequences were also poorly characterized in our model, and although they did not represent the majority of mutation sites, they could impact genet expression, for example.

A more complete story would be helped by alanine measurements, in order to better assume electrons fate. Substrate consumption assessment would permit to normalize those data. ATP, ADP and AMP would also be interesting to quantify, in order to verify a possible relation with cell morphology. Overall, more complete metabolomic profiles in different conditions would allow better precision in formulating possible explanations for the "Evol" adaptation, as many other factors could still be unknown or incompletely characterized herein. For example, a triose-phosphate isomerase from *P. furiosus* has been shown to likely harbor a promiscuous cellulase/endoglucanase activity (Sharma and Guptasarma, 2017). Epigenetic modifications could also be at stake, as observed in an ALE work on '*T. onnurineus*' (Lee et al., 2016). Actual measurements of cell sizes in different conditions could more precisely assess morphological differences between both strain cells.

We only tested herein metabolic organizations when cultured in TRM, a *medium* based on yeast extracts and tryptones. It would be interesting to assess similar changes, but in a *medium* based on carbohydrates as a principal source of electrons, which has been shown in *T. barophilus* MP^T to allow growth in the absence of sulfur (see chapter II).

At the time of writing, transcriptomic data were still expected, and should give better comprehension of the system. Particularly, many transcriptional regulators were estimated to be involved in *Thermococcales* gene expressions (Denis et al., 2018). Ensuing hypotheses on the respective implications of given enzymes or regulators should then be confirmed by mutational studies. Yet, despite those efforts, "Evol", rather than *T. barophilus* MP^T, should serve as a basis for future metabolic engineering works, in short-terms interests. Even if keystone nodes in H_2-tolerance are identified in a near future, many epistatic mutations could probably remain hidden (Barrick et al., 2009). As a consequence, simply implementing obvious modifications could potentially result in an incompletely optimized system.

Overall, “Evol”, the strain issued from this adaptive laboratory evolution experiment to grow at high concentrations of H_2, represents an interesting subject to deconstruct and further understand how *Thermococcales* could cope with these usually hampering conditions. By doing so, we could better design strategies for optimized applied H_2 production, considering that even in a renewed (thus de-saturated) environment, each cell would locally potentially face H_2 saturation on a certain level. Unravelling how “Evol” cells managed to control their H_2 yields to finally reach more important concentrations at the level of the cell population should allow us to extrapolate on optimal physiological states in diverse metabolic configurations, and to thus propose adaptable solutions for various bio-production needs.

Note: Part of the work presented in this chapter was valorized with a poster at the congress Thermophiles 2019 (Fukuoka, Japan). Complementary data are expected to allow the writing of a scientific paper in a near future.

General discussion – conclusion

Molecular hydrogen, a promising energy carrier envisioned by many as a key for future developments, remains nowadays mainly produced from fossil fuel sources, but can also be naturally synthesized by diverse groups of microorganisms. *Thermococcales* are one of them, and their hydrogenogenic energy conservation metabolism has been quite well-studied in different strains. Their use for such an application would benefit from several advantages, as for example the possibility to degrade various substrates, and their hyperthermophily. Many members of this anaerobic group of *Euryarchaeota* have been isolated from deep-sea hydrothermal vents and are thus recognized or potential piezophiles. Nonetheless, their metabolic adaptation to pressure, if witnessed in several studies, remains incompletely explained, particularly regarding routes leading to H_2 production. Yet, pressurization is often a necessary but costly part of the process in commercial H_2 storage, hence the hypothesis that a biological production after pressurization could be economically beneficial, if such protocols require less energy.

In this context, we wanted to advance towards possible bases for optimization of high pressure H_2 bio-production in *Thermococcales*. Three different directions were explored. Firstly, we produced basic data to allow further estimation of the feasibility of applied solutions on our chosen model, *T. barophilus* MP^T, in order for an industrial partner to evaluate the interest of continuing with such a project. Such assumptions could not be completed without the additional development of new methodologies and tools for high pressure culture. The third part of this project resided in the actual emphasizing of biological optimization, through better comprehension of the metabolism of our model, *T. barophilus* MP^T, focusing on high pressure adaptation and tolerance to hydrogen. This last manuscript part aims at refining our discussion in perspective of our initial objectives.

I - Would our bioreactor solutions be used for applied H_2 bio-production?

1. The costs of bio-hydrogen production

At the time of writing, the cost of commercial hydrogen for larger scale production varied between 0.91 and 6.19 €/kg, according to the method involved (Collins, 2020). Thanks to the re-use of organic waste, dark fermentation processes at larger scale, present quite competitive cost-effectiveness (around 2.25 €/kg), showing that biological H_2 bio-production is feasible (Han et al., 2016; Nikolaidis and Poullikkas, 2017).

The results presented herein did not allow estimating commensurate costs, since much information would be lacking. For example, we would not be able to foresee the costs of utilization of the bioreactor, since an actual H_2 production application would be based on the exploitation of a different machine, which would take more into account actual needs for future industrialization evaluation (*e.g.* bigger volumes, high pressure gas recycling and separation, with adapter materials) (BHP3, see P. 227). Moreover, calculating costs of production would need to take into account infrastructure and energy demands, human resources, substrate pre-treatment in some cases, product separation, hydrogen storage, and more, which all depend on the strategy chosen for pilot scale (Bergman, 2016). As highlighted in chapter I, many culture conditions would induce variations in H_2 productivities, and metabolic optimization could be envisioned thanks to the data described in chapter III and chapter IV. The application of continuous culture could also be considered, which was not technically validated at high pressure herein but proved to possibly increase yields (Kanai et al., 2005b). A precise estimation of the cost of hydrogen production by *Thermococcales* would thus require further data and constitute another study of itself, beyond the frame of the project HPBioHyd.

Considering our laboratory-scale experiments, we could roughly evaluate the price of *medium* preparation according to commercial chemical suppliers (not ordered in bulk), and then report the absolute H_2 concentrations obtained to estimate normalized costs of a kg of H_2 produced in our flasks, as displayed in TABLE 26.

Table 26: Examples of costs of H_2 productions from this project, considering *medium* price

	Medium		Pressure (MPa)	Substrate			Sulfur	mM H_2 in sample	cost of H_2 production (€/kg)
Strain	**ASW**	**TRM**		**Yeast extracts**	**Maltodextrin**	**Formate**			
MP	.		0.1	2.5 g/L			0.25 g/L	6.1	242.43
MP	.		0.1	0.2 g/L	2.5 g/L		0.25 g/L	5.9	288.03
CH5	.		0.1	0.2 g/L	2.5 g/L	30 mM	0.25 g/L	13.19	141.52
MP		.	0.1	*(in TRM)*				0.75	5835.77
"Evol"		.	0.1	*(in TRM)*				1.72	2544.67
MP		.	0.1	*(in TRM)*			0.25 g/L	2.39	1891.19
MP		.	30	*(in TRM)*			0.25 g/L	12.18	371.10

ASW: Artificial Sea Water. TRM: Thermococcales *Rich* Medium.

Again, such assumptions were highly approximate, and would be far from representing actual production costs at higher scales. They concerned final concentrations, without taking into account the price of gas (which could be important in the frame of a gas-pressurized culture, but would also be diminished in the case of re-utilization of product-separated N_2), nor heating or pressurizing, but just the *media* price with their respective substrates. This table highlights the dramatic differences in costs according to the chosen culture solution. We obtained the "cheapest" production using *T. barophilus* strain Ch5 in the presence of formate and maltodextrin on ASW *medium* with 0.25 g/L S°, and the "most expensive" one by using *T. barophilus* MP^T in TRM in the absence of sulfur. Noticeably, if high pressure results were confirmed, they would indicate an important lowering of H_2 cost relative to *medium* price (here from 1891.19 to 371.10 €/kg), but the pressurization cost would need to be taken into account too.

Overall, those differences principally mean that there is room for optimization. Similarly, Lee *et. al* recently demonstrated that a reformulation of the *medium*, suppressing reagent-grade salts and high quality nitrogen sources by sea salts and fish meal in '*T. onnurineus*' cultures could reduce normalized hydrogen cost by more than 90 % (Lee et al., 2019). Direct use of sea water as a *medium* formulation simplification has also proved efficient for bio-H_2 production by the bacterial model *Thermotoga maritima* (Saidi et al., 2017). Herein, the production of TRM was estimated to cost 6.51 €/L, whereas ASW cost about 1.45 €/L.

Considering a case where the mineral base for ASW would be taken directly from the sea, its price would be diminished down to about 0.51 €/L (though not considering the associated cost of sea water sampling and pre-treatment).

Applied studies on *T. onnurineus* are among the most advanced towards the application of H_2 bio-production by *Thermococcales* models to date (Kim et al., 2013, 2015; Lee et al., 2015, 2016a, 2019). Although they were mainly performed in bioreactors and reached high H_2 concentrations, *medium*-normalized hydrogen production costs of these bioreactor cultures would be comparable to our results (between about 1500 and 2500 €/kg, except for the use of cost-optimized *medium*, which lowered their normalized H_2 costs under 150 €/kg). Such comparisons are fostering for the application of *T. barophilus* for H_2 bio-production, since our optimization is not yet as pushed on as for '*T. onnurineus*'. We furthermore observed that our model would tend to be more productive than '*T. onnurineus*' in basic TRM conditions, as hinted by the results displayed in chapter I. It is thus not impossible that *T. barophilus* could lead to competitive yields if properly cultured, which would deserve further investigations.

Yet, relatively to the hydrogen prices mentioned earlier, and although they are not properly comparable to pilot-scale or larger scales of production, laboratory-scale costs of production in *Thermococcales* are very high. Considerable efforts for lowering them would be necessary to ever envision actual practical applications. Fortunately, many strategies could be explored to that extent, as hinted in chapter I, and in chapters III and IV at a more fundamental level.

2. Many other possibilities for improvements

Other important factors have been highlighted during this project, which could improve the cost-efficiency of a future process. A noticeable argument would be the yet-to-be-confirmed possibility of CO_2 fixation in certain configurations. Our results with *T. barophilus* Ch5 in the presence of formate, or *T. barophilus* MP^T in the presence of high initial Na_2S concentrations, tended to indicate that each mol of H_2 produced was accompanied by a consumption of CO_2 (see chapter I). Such feature could be very interesting, noticeably if we imagine coupling our future bioreactor solutions to other processes which produce undesirable CO_2. For example, a plant could associate the streams of different *Thermococcales* bioreactors, some producing H_2 and CO_2, the others re-consuming the

produced CO_2 to also synthesize more H_2. Furthermore, those strategies would be fitted with the current political efforts to reduce global CO_2 emissions, which could constitute further funding opportunities, besides the obvious global service that they would represent (H2020, 2019; SNBC, 2019). Note that steam methane reforming, the current predominant method of H_2 production, emits more than 7 kg CO_2 per kg H_2 produced (Soltani et al., 2014; Transitions Energies, 2020).

Moreover, to render cost-effective solutions, it would be worth assessing any possible material way to optimize input costs (*e.g. medium* or gas-stream re-circulation) as well as to treat co-products. For example, as explained earlier, ensuing organic acids could serve for methanogenic systems. Spent biomass could also be envisioned as fertilizer (Andersen et al., 2001; Sullivan et al., 2017).

The metabolic configuration will also necessarily be associated to different costs. Although carbon monoxide has proven to be effective for H_2 production in other strains (noticeably '*T. onnurineus*'), its use would be accompanied by risks for the worker's safety. Handling those risks would induce additional practical costs, for example *via* the installation of hoods and detection systems. Same observations could be made for highly sulfidogenic configurations. H_2S, despite from being importantly toxic, is also corrosive, and would increase material or maintenance costs. To that extent, the strain "Evol" could be interesting to emphasize, since it was shown to rather orientate metabolic routes towards non-sulfidogenic energy conservation. Similarly, the use of fresh water instead of sea water (and the corresponding strains) could be advantageous for material life expectancy regarding corrosion, but also for geographical implantation of our practical solutions. The pressure chosen for fermentation would also greatly influence material costs, not only H_2 yields (which could be *e.g.* 5-fold higher at 30 MPa, if our results are confirmed). It is also important to keep in mind that a pressurization step, upstream or downstream hydrogen production, is necessary for commercial use anyways.

Consequently, many *criteria* will have to be taken into account in a further work for evaluating larger-scale application feasibility.

II - How to approach the fundamental comprehension of *T. barophilus* metabolism?

1. A highly dynamic metabolic organization

1.1. A better understanding of our model strain

Apart from more practical assessments realized in chapter I, indirect investigations on possible optimizations of H_2 bio-production were also described in chapter III and chapter IV, towards a better knowledge of our model regarding its physiological relations to high pressure and to H_2 saturation. *T. barophilus* metabolic features seemed different in many ways to other models, as reflected by physiological outcomes. For example, in *T. kodakarensis*, among others, using pyruvate as a substrate leads to increased H_2 production, contrarily to what we observed in *T. barophilus* MP^T (Kanai et al., 2005b). Our results have thus allowed formulating several hypotheses on the functioning of the concerned parts of the metabolism, ensuing on various assumed strategies for H_2 production optimization.

Yet, some observations made on deletion strains still need confirmations or complementary explanations. For example, SHII (TERMP_0036-39) was hypothesized in chapter III to be possibly involved in H_2 tolerance, but no mutation or putative effect was noticed on the corresponding gene in "Evol". Expression of *sh*II as evaluated by RT-qPCR seemed slightly more important in "Evol" in the absence of sulfur (about 3-fold), but as it was the case for most targeted genes, RNA-Seq data are still awaited for better distinguishing patterns. Additionally, considering the sulfidogenic system, the gene encoding Nsr (TERMP_02185) was found affected by genomic mutations in "Evol", but no difference was found regarding TERMP_00853-65, encoding Mbs. This would be consistent with a surmise ensued from the study of our mutant strains, placing Mbs as the most important player in this system, if we extrapolate that a variation of Nsr would be more easily tolerated. This would not be surprising since Nsr is not directly linked to ATP production, while Mbs activity maintains a Na^+ gradient allowing to trigger ATPase ATP production. Additionally, both *mbs* and *nsr* expressions seemed to be slightly affected in "Evol" compared to the wild type in the absence but not in the presence of sulfur. In "Evol", the sulfidogenic system seemed

impacted, even in the presence of sulfur, as shown in chapter IV, FIGURE 71, P. 300. While those assumptions still wait for full transcriptomic confirmations, it would appear that the differences in "Evol" sulfidogenic energy conservation may not occur at the level of gene expression, and also only meagerly from genomic modifications. Since activities seemed different, it is possible that post-transcriptional/-translational modifications are at stake, even though these assumptions would need more experimental evidence. Similarly, the hydrogenogenic metabolism was clearly impacted in "Evol", but no mutation or putative effect was found at the genomic level on any *mbh* module. Their implication in the system, as hinted in chapter III, could be confirmed from more complete transcriptomic profiles.

The regulatory impact of SurR over the system is particularly interesting, since this transcriptional activator or repressor was described as the master regulator for the electron flow in energy conservation metabolism of *Thermococcales* (Lipscomb et al., 2017). From the results presented in chapter III and chapter IV, it appeared that the metabolism of *T. barophilus* could be differently regulated by SurR than in other models. This would not be surprising since the concerned gene homologs harbor various types of SurR binding sites (long or short) in different strains (Yang et al., 2010). For example, the SHI-encoding homolog in *P. furiosus* has a long SurR binding motif ($GTTn_3AACn_5GT$) in its promoter, whereas no such sites could be found in *T. barophilus* MP^T or '*T. onnurineus*'. The gene encoding Mbs also presents a short binding motif ($GTTn_3AAC$) whereas *T. barophilus* MP^T and '*T. onnurineus*' have long ones (Moalic, 2018, unpublished).

1.2. The importance of elemental sulfur

Another reason could also explain some differences observed in our results. It is probable that the low sulfur concentration for the "sulfur presence" condition (0.25 g/L), compared to the excess used in other studies (often at least 2 g/L, *e.g.* (Kanai et al., 2011; Santangelo et al., 2011)), placed our model in a poorly studied intermediary physiological state where both hydrogenogenic and sulfidogenic systems are at stake. Phenotypical differences between 0.5 g/L and 2 g/L S° were also observed in mutational studies of *P. furiosus* (Schut et al., 2012). This hypothesis could also be supported by the sulfur gradient experiments described in chapter IV, showing that the sulfidogenic system fully replaced the hydrogenogenic system only between 0.5 and 1 g/L of initial colloidal sulfur. Our work likely involved situations where

both hydrogeno- and sulfidogenic energy conservation mechanisms are at stake, which is not the case in sulfur excess, and in most literature descriptions. This however showed that the sulfur-induced, SurR-orchestrated metabolism switch is not "all-or-nothing" at the population level, but supports an important range of sulfur concentrations (from no sulfur to 0.5 - 1 g/L in our case) for which an intermediary state is engaged. It would be interesting to reproduce our results in excess of sulfur. Additionally, many works reported in the literature did not accurately describe what precautions were taken regarding sulfur concentration in *medium* preparation, but also through inoculation in sub-cultures (*e.g.* (Burkhart et al., 2019; Michoud and Jebbar, 2016; Vannier et al., 2015)). We observed that in excess of tyndallized sulfur powder in a pre-culture, a sub-culture inoculated at 2 % of its volume could grow up to a biomass equivalent to in the presence of sulfur, even though no initial sulfur was added in the sub-culture flask (results not shown). In this study, we ensured that no remaining sulfur significantly impacted our samples by using pre-cultures with only 0.05 g/L S°. Consequently, differences in this work and in literature descriptions regarding the amounts of sulfur used clearly hamper physiological comparisons between the different models and cases described. It could be possible that a part of our divergent conclusions would ensue from those potential methodological differences.

1.3. High pressure adaptations

More insights into the adaptation to high pressure were obtained from the results described in chapter III. It appeared that this new parameter added a level of complexity to the regulation of the metabolic network. It was clearly stated that pressure variation has an influence over the metabolism of *Thermococcales*, as remarked in several works (*e.g.* (Cario et al., 2015b; Michoud and Jebbar, 2016; Vannier et al., 2015)). Herein, many compensation patterns in response to various deletions were affected by those changes, although data at supra-optimal pressure for growth (70 MPa) would have been interesting to gather in order to better assess general patterns observed regarding to pressure stress. Encouraging results for H_2 production at optimal pressure for growth were reported: mutational studies allowed to infer that the hydrogenogenic system may be enhanced at 40 MPa, and preliminary tests in the continuous HP bioreactor (BHP) in gas pressure (30 MPa) tended to show higher H_2 yields. Yet, the actual influence of pressure (as opposed to gas-phase-induced H_2-desaturation) remained to confirm in the BHP. Furthermore, thanks to the study of our mutants at high

pressure, we were only able to infer indirectly what would occur to the hydrogenogenic system, not through actual measurements of H_2-evolving activities. With the new device for discontinuous gas-phase high pressure described in chapter II, we are now materially able to pursue this study and verify our results. Relations of the metabolism to gas-pressure could also be studied at a more fundamental level in the BHP3 as conceptualized earlier.

In addition to a possible natural propensity to overproduce H_2 at high pressure, the comprehension of the adaptations of given parts of the system could allow to further set up optimization *scenarii*. For example, we hypothesized that SHII could hinder H_2S production at high pressure in the presence of sulfur. Such observation is a first step to propose other possible knock-outs of alternative electron sinks, in order to orientate fluxes towards H_2 overproduction, and dissociate from a maximum of other ways of producing ATP. Of course, since any reorientation could be incompatible with a functional phenotype, due to inefficient energy conservation, such predictions would not be practical without a proper evaluation of H_2 tolerance. H_2-tolerant configurations could be delimited thanks to the future studies of "Evol", for example through metabolomics measurements coupled to the expected transcriptomics, or mutational work, and applied in those pressurized systems.

1.4. A dynamic energy conservation system

As a main conclusion to the fundamental studies presented in this manuscript, we could state that the variety of compensatory organizations observed in our mutant strains as well as in "Evol" clearly showed that the energy conservation metabolism of *T. barophilus* is a highly dynamic system, with many differently involved parts. Each one would probably preferentially be implicated in a specific role, but adaptable to various situations. In the wild, *Thermococcales* are quite ubiquitously found around hydrothermal vents (Holden et al., 2001; Orphan et al., 2000; Prieur et al., 1995). Those environments impose rapidly varying physical and chemical conditions, and each vent harbors its own characteristics (Charlou et al., 2002; Deborah S. Kelley et al., 2002; Dick et al., 2013; Fouquet et al., 1988; Gartman et al., 2011; Haymon, 1983). Their populations can thus be subjected to dramatic environmental fluctuations, at the scale of one or few generations. It is hence not surprising that they are capable of rapid effectual adaptations to face new physiological configurations, not answering to "all-or-nothing" switches. Yet, while this important potential for dynamic acclimation is

probably crucial for *Thermococcales* evolutionary success in nature, it magnifies the complexity of an artificial application of bio-production. Unraveling the roles and interactions of specific parts of the metabolism (*e.g.* reactions, regulations) at different levels (*e.g.* genomic, transcriptomic) is a necessary step to define *T. barophilus* as a model for applied H_2 bio-production at high pressure, especially since those features can differ from other literature models.

2. An unequivocal need for systemic consideration

Indeed, many possible strategies for increasing H_2 production could be deduced from our work and from the abundant literature on *Thermococcales* metabolism. For instance, we could try to increase the expression of specific parts of the genome with strong promoters, such as ones encoding hydrogenogenic modules, as it was performed in '*T. onnurineus*' for Mrp-Mbh-COdh, or as substrate degradation systems as in *T. kodakarensis* (Aslam et al., 2017; Lee et al., 2015). We could hypothesize that *mbs* deletion would be compensated by the hydrogenogenic electron route, as was observed in *T. kodakarensis* (Kanai et al., 2013). But although apparently logical, these outcomes could vary if different metabolic fluxes are at stake. Indeed, in *T. barophilus*, *mbs* deletion induced surprising sulfidogenic compensation, producing even more H_2S per cell. As another example of unexpected results, we deducted from our mutational study that SHII could be important to increase H_2 production at high pressure in the absence of sulfur. However, in *T. kodakarensis*, deletion of its homolog encoding gene (*hyh*) led to H_2 overproduction (Nohara et al., 2014).

Consequently, to foresee a possible application in shorter terms, one has to take into account that mutational studies, especially at high pressure, are very time-consuming, from the production of the deleted strain to its physiological characterization. It is thus important to orientate the choice of the strategy adopted, and not only to practice the most easily deduced or most accessible solution. As we have seen in this work, H_2 production is the result of a complex system: metabolic compensations could hinder the realization of our initial objectives, and unexpected outcomes could ensue from some mutations. Observations from both chapter III and chapter IV tended to indicate that a fine-tuning of the redox balance would be at stake for regulating hydrogenogenic energy conservation. Consequently, without

actual calculations, such metabolic fluxes, connected to the whole-cell metabolism through the use of various electron carriers, would be impossible to accurately predict. To that extent, *in silico* estimations would constitute an important tool for orientating wet-lab efforts. To my opinion, one should minimally rely only on human-mind-directed assumptions to try to build H_2-overproducing strains based. The most efficient way to conduct strain engineering to find the best compromises according to each conditions would be through an actual design-build-test-learn cycle, which would emphasize designing and learning, and not only building and testing.

Such an approach would require to consider the whole metabolic system. Thanks to the exploitation of the –omics data obtained from this work, among possible future others (*e.g.* metabolomic and proteomic profiles) and comparisons from the literature and databases, we should be able to infer actual key metabolic nodes, while controlling the global constraints imposed by a hydrogenogenic energy conservation. A metabolic model could be calibrated thanks to the observation of the compensation patterns in our mutants and in "Evol". Moreover, pressure adaptation seems to ensue more from an entanglement of effects at many levels rather than from the influence of a single or a handful of genes. Understanding such adaptation with an aim of favoring H_2 production would thus also require systemic modelling, especially since high pressure wet-lab experiments are particularly materially tedious.

Genome-scale metabolic models (GEMs) have been used for varying purpose such as studying and developing chemicals and materials productions, targeting drugs in pathogens, predicting enzyme functions and interactions (Gu et al., 2019). They express stoichiometry-based, mass-balanced metabolic reactions in a given system by associating reactions to proteins and genes. As a most widely-used mathematical tool for analyzing GEMs, Flux Balance Analysis (FBA) allows to optimize metabolic fluxes towards an objective function (for example ATP or H_2 production) using linear programming (Orth et al., 2010). Such method could allow to evaluate possible ways of answering practical questions of minimizing or maximizing co-products of a fermentation as formulated in chapter I, for example. It could help to predict global behaviors in function of culture conditions, and if particular genomic modifications. While archaeal metabolic models represent merely more than 2 % of the

available GEMs, and although many genes remain unknown, the analysis of multi-omics data such as the ones produced in the project HPBioHyd should help render such representations useful (Gu et al., 2019). *Thermococcales* are furthermore a well-studied order, and FBA have been applied to a GEM of *T. paralvinellae* to analyze the electron route during H_2 inhibition (in relation formate production), showing the possibility of using them in our context (Topçuoğlu et al., 2018). Some methods also enable the integration of regulatory activities in GEMs, which could be fed by transcriptomic profiles such as the ones obtained studying "Evol" (Banos et al., 2017). We could imagine to further integrate relations to growth phases, as we started to study the associated phenotypical variations in our super-tolerant ALE-produced strain. Such modelling approaches would thus be a suitable initial way to accentuate both "learn" and "design" steps of the process, while enforcing the position of *T. barophilus* as a model for high pressure H_2 production application thanks to the integration of already-acquired knowledge.

III - Final conclusion

The goal of the project HPBioHyd was to set up bases to optimize H_2 bio-production in *Thermococcales* at high pressure. The subject was approached in different manners: a material and methodological points of view, described in chapter II, and a biological point of view, described in an applied fashion in chapter I and in a more fundamental way in chapter III and chapter IV. We successfully advanced towards the global objective, which will permit in the near future to design experiments allowing to evaluate the feasibility of pilot-scale applications, encouraged by our results, as well as to set up knowledge foundations that will permit efficient metabolic engineering of *T. barophilus* towards H_2 overproduction at high pressure. Overall, a better understanding of our model should authorize to more accurately estimate changes in yields induced by future scaled-up studies. While such works have been realized for other bio-producers (*e.g.* (Balachandar et al., 2020; Bergman, 2016; Lu et al., 2020)), none have been reported for *Thermococcales* to date.

H_2 is envisioned as a potential « swiss army knife » vector for storing, transforming, and transporting energy, but remains almost exclusively produced from fossil fuels. Unfortunately, the "hydrogen economy" still rarely relies on biological production in the

public opinion, preferring other “green” methods, such as wind or solar electrolyzers. Yet, such a paradigm shift will demand enormous amounts of hydrogen in order to fulfill the goals of the Paris Agreement on Climate Change (Collins, 2020). It is now ours to provide the necessary effort to entrench our models over the industrial scene. At the time of writing, biological H_2 productions technologies are at their infancy, but it is my hope that we marked here a supplementary step towards a new global system where *Thermococcales* could be part of the mix for a sustainable energy transition.

Valorization

While no teaching mission was realized, this work involved the training and management of a team of interns and technicians during certain phases. At the time of writing, the results presented herein were not yet valorized as original articles, for which complementary data on chapter III and on chapter IV were awaited. Other types of valorizations ensued, described hereafter.

Oral presentations

-*Thermophiles 2019 (Fukuoka, Japan)*: "**The Influence of hydrogenases and the SurR regulator on the adaptation to high hydrostatic pressures in *Thermococcus barophilus* MP**". Yann Moalic, Jordan Hartunians, Madina Ahmed, Anaïs Sire de Vilar, Kateline Letoquart, Guillaume Lannuzel, Mohamed Jebbar.

-*GdR* Archaea *2018 (Brest, France)*: "**Exploration of the potential physiological functions of the master regulator SurR at high pressure in *Thermococcales***". Jordan Hartunians, Yann Moalic, Mohamed Jebbar.

-*GdR* Archaea *2017 (Lyon, France)*: "**Looking for organic substrate degradation pathways in *Thermococcales***". (Short presentation). Jordan Hartunians, Raphaël Brizard, Frédéric Fragne, Mohamed Jebbar.

-*Thematic School: "Cellule Energies et Recherches CNRS 2018" (Roscoff, France)* : "**Producing hydrogen thanks to microorganisms from the bottom of the sea**". (Short presentation). Jordan Hartunians, Frédéric Fragne & Mohamed Jebbar.

Posters

-*Thermophiles 2019 (Fukuoka, Japan)*: "**How to Grow Without Sulfur - Investigations on a Sulfur-Less, H2-Saturated, Adapted Metabolism of *Thermococcus barophilus***". Jordan Hartunians, Yann Moalic, Madina Ahmed, Pauline Grippon, Guillaume Lannuzel, Mohamed Jebbar. (Awarded for Best Poster).

-*Thermophiles 2019 (Fukuoka, Japan)*: "How to keep the pressure on? Continuous anaerobic culture of *Thermococcales* using a unique high pressure / high temperature bioreactor". Jordan Hartunians, Raphaël Brizard, Frédéric Fragne et coll. & Mohamed Jebbar.

-*AFEM 2017 (Camaret-sur-Mer, France)*: "How to stay under pressure? Precising high hydrostatic pressure metabolic adaptations in *Thermococcales* using a unique high pressure / high temperature anaerobic bioreactor". Jordan Hartunians, Raphaël Brizard, Frédéric Fragne et coll. & Mohamed Jebbar.

Articles as secondary author in preparation

-"Transcriptomics reveals a fine-tuning adaptation to pressure of hydrogen metabolism in the pizeophile *Thermococcus piezophilus*". Yann Moalic, Cécile Dalmasso, Damien Courtine, Jordan Hartunians, Myriam Georges, Philippe Oger, Zongze Shao, Mohamed Jebbar & Karine Alain.

-Characterization of strain *Pyrococcus* EXT16: HP culture for Gaël Erauso (Mediterranean Institute of Oceanography, Marseille, France).

Book chapters in preparation

-Karine Alain, Marc Cozannet, Maxime Allioux, Sarah Thiroux, Jordan Hartunians. "Archées: habitats et physiologies associées". In Clouet d'Orval, B., Franzetti, B., Oger, P. (eds), Biologie des archées, Volume 3: Les archées dans leur environnement. Editions ISTE. (submitted)

-Anne Godfroy, David François, Jordan Hartunians, Yann Moalic and Karine Alain. "Physiology, metabolism, and ecology of thermophiles from deep-sea vents". In Vetriani, C., Giovannelli, D. (eds.), The Microbiology of Deep-Sea. Editions Springer International. (in press)

-Jordan Hartunians, Mohamed Jebbar. "Microbiology of piezophiles". In Vetriani, C., Giovannelli, D. (eds.), The Microbiology of Deep-Sea. Editions Springer International. (in press)

Other types of scientific involvements during this project

- Implication in iGEM competition (international genetically engineered machine): Advices in scientific communication for iGEM Evry 2017 and iGEM Nantes 2019. Attendance to the European iGEM Meetup 2017 (Delft).
- Organization of Pint of Science Brest (2017 & 2018) & various pub quizzes.
- Special event animations for the AFEM colloquium 2017 (Camaret-sur-Mer) and GdR *Archaea* 2018 (Brest)
- Organization of animations for the European Researchers Night (*Nuit Européenne des Chercheurs*) in 2017 and 2018 with the LM2E and with Oceanopolis.

Notable courses followed during this project

- qPCR: theory & practice (2 days) (by Valérie Cueff-Gauchard, LM2E)
- Valorization of public research, intellectual property and collaborative project management (3 days) (by SATT)
- Autoclave operator (1 day) (by APAVE)
- Flux cytometry: theory (2.5 h) (by Christophe Lambert, LEMAR)
- Inov'days, Entrepreneurship (8 days) (by IFREMER, ENSTA)
- Career development (1 day) (Euraxess)

Appendix

Table 27: List of the isolates of the UBOCC for which complete genomes were analyzed with MicroCyc

Those genomes were sequenced during the project of Damien Courtine (2017). T. barophilus MP^T genome was omitted herein.

AMTc09	AMTc79	E15P25	EXT12c	IRI09c	IRI29c
AMTc102	AMTc85	E15P29	EXT13c	IRI10c	IRI35c
AMTc19	AMTc94	E15P30	IRI06c	IRI14c	IRI35c2
AMTc29	AMTc95	E15P35	AMTc70	IRI15c	IRI36c
AMTc30	E10P11	E15P6	AMTc71	IRI24c	MC4 55
AMTc51	E10P7	EXT08c	AMTc72	IRI25c	MC5
AMTc52	E10P8	EXT10c	AMTc73	IRI26c	MC8 57 I
AMTc67	E14P19	EXT11c	IRI07c	IRI27c2	MC9

Table 28: List of the strains preselected according to their potentially interesting metabolic pathways

Reference UBOCC	Name	Depth(m)	Pathways							
			1	2		2	4	5	6	7	8
2179	AMTc09	2597	3	2							
2048	AMTc102	/	2	2							
3107(piezo)/	*T. barophilus* MP			1	1				1		
3208	*T. kodakarensis* KOD1	/	1								
-	*T. sibiricus* MM 739	/									
2213	AMTc19	2633	3	2							
2196	AMTc30	2626	3	2							
2211	AMTc51	/	3	2						1	
2204	AMTc52	/		2						1	
2209	AMTc67	/	3	2							
2219	AMTc79	2634	3	2						1	
2210	AMTc85	/	3	2							
2220	AMTc94	2633	3	2						1	
2181	AMTc95	2633	2	2							
2297	E10P11	2628	2	2						1	
2293	E10P7	806	2	2						1	
2294	E10P8	806	3	2						1	
2350	E14P19	/	3	2						1	
2383	E15P29	/	2	2						1	
2384	E15P30	/	2	2						1	
2389	E15P35	/	3	2						1	
2360	E15P6	/	3	2						1	
2443	IRI35c2	806	4		1						
2444	IRI36c	806	4		1						
2171	AMTc29	2628	2	2							
2206	AMTc70	2631	4		2						
2205	AMTc71	2631	4		2						
2172	AMTc72	2631	4		2						
2049	AMTc73	2631	4		2						
2413	EXT08c	/	3	2							
2415	EXT10c	/	2	2							
2416	EXT11c	/	2	2							
2417	EXT12c	/	2	2							
2418	EXT13c	/	2	2							
2425	IRI07c	2274	3		1						
2427	IRI09c	2274	3		1						
2021	IRI14c	2274	3		1						
2022	IRI15c	2274	3		1						
2028	IRI24c	2274	3		1						
2029	IRI25c	2274	3		1						
2436	IRI26c	2274			1						
2030	IRI27c2	2274	3		1						
2439	IRI29c	2274	3		1						
2026	IRI35c	806	3		1						

Full pathway
Partial pathway (number of missing enzymes)
Not detected

(1) Chitin degradation, (2) Starch -2 pathways possible, (3) Lactose, (4) Melibiose, (5) d-mannose, (6) ethanol, (7), glycerol, (8) formate oxidation

Bibliography

Aagaard, C., Leviev, I., Aravalli, R.N., Forterre, P., Prieur, D., and Garrett, R.A. (1996). General vectors for archaeal hyperthermophiles: strategies based on a mobile intron and a plasmid. FEMS Microbiol. Rev. *18*, 93–104.

Abe, F., and Horikoshi, K. (2001). The biotechnological potential of piezophiles. Trends Biotechnol. *19*, 102–108.

Adam, N., and Perner, M. (2018a). Novel hydrogenases from deep-sea hydrothermal vent metagenomes identified by a recently developed activity-based screen. ISME J. *12*, 1225-1236.

Adam, N., and Perner, M. (2018b). Microbially mediated hydrogen cycling in deep-sea hydrothermal vents. Front. Microbiol. *9*:2873.

Adams, M.W.W. (1990). The metabolism of hydrogen by extremely thermophilic, sulfur-dependent bacteria. FEMS Microbiol. Lett. *75*, 219–237.

Adelman, J.L., Ghezzi, C., Bisignano, P., Loo, D.D.F., Choe, S., Abramson, J., Rosenberg, J.M., Wright, E.M., and Grabe, M. (2016). Stochastic steps in secondary active sugar transport. Proc. Natl. Acad. Sci. *113*, E3960–E3966.

Aertsen, A., Vanoirbeek, K., Spiegeleer, P.D., Sermon, J., Hauben, K., Farewell, A., Nyström, T., and Michiels, C.W. (2004). Heat shock protein-mediated resistance to high hydrostatic pressure in *Escherichia coli*. Appl. Environ. Microbiol. *70*, 2660–2666.

AFP (2018). Plan hydrogène : Les industriels satisfaits d'une "première étape." Imaz Press La Réun.

Ahmad, N., Rashid, N., Haider, M.S., Akram, M., and Akhtar, M. (2014). Novel maltotriose-hydrolyzing thermoacidophilic type III pullulan hydrolase from *Thermococcus kodakarensis*. Appl. Environ. Microbiol. *80*, 1108–1115.

Ahmadi, P. (2019). Environmental impacts and behavioral drivers of deep decarbonization for transportation through electric vehicles. J. Clean. Prod. *225*, 1209–1219.

Akahane, S., Kamata, H., Yagisawa, H., and Hirata, H. (2003). A novel neutral amino acid transporter from the hyperthermophilic archaeon *Thermococcus* sp. KS-1. J. Biochem. *133*, 173–180.

Albers, S.-V., Koning, S.M., Konings, W.N., and Driessen, A.J. (2004). Insights into ABC transport in *archaea*. J. Bioenerg. Biomembr. *36*, 5–15.

Albracht, S.P. (1993). Intimate relationships of the large and the small subunits of all nickel hydrogenases with two nuclear-encoded subunits of mitochondrial NADH: ubiquinone oxidoreductase. Biochim. Biophys. Acta *1144*, 221–224.

Allen, E.E., and Bartlett, D.H. (2000). FabF is required for piezoregulation of *cis*-vaccenic acid levels and piezophilic growth of the deep-sea bacterium *Photobacterium profundum* strain SS9. J. Bacteriol. *182*, 1264–1271.

Allen, E.E., Facciotti, D., and Bartlett, D.H. (1999). Monounsaturated but not polyunsaturated fatty acids are required for growth of the deep-sea bacterium *Photobacterium profundum* SS9 at high pressure and low temperature. Appl. Environ. Microbiol. *65*, 1710–1720.

Amend, J.P., and LaRowe, D.E. (2019). Mini-Review: Demystifying Microbial Reaction Energetics. Environ. Microbiol. *21*:10, 3539-3547.

Amend, J.P., and Plyasunov, A.V. (2001). Carbohydrates in thermophile metabolism: calculation of the standard molal thermodynamic properties of aqueous pentoses and hexoses at elevated temperatures and pressures. Geochim. Cosmochim. Acta *65*, 3901–3917.

Amend, J.P., and Shock, E.L. (2001). Energetics of overall metabolic reactions of thermophilic and hyperthermophilic *Archaea* and *Bacteria*. FEMS Microbiol. Rev. *25*, 175–243.

Amend, J.P., Meyer-Dombard, D.R., Sheth, S.N., Zolotova, N., and Amend, A.C. (2003). *Palaeococcus helgesonii* sp. nov., a facultatively anaerobic, hyperthermophilic archaeon from a geothermal well on Vulcano Island, Italy. Arch. Microbiol. *179*, 394–401.

Amrani, A., Bergon, A., Holota, H., Tamburini, C., Garel, M., Ollivier, B., Imbert, J., Dolla, A., and Pradel, N. (2014). Transcriptomics reveal several gene expression patterns in the piezophile *Desulfovibrio hydrothermalis* in response to hydrostatic pressure. PloS One *9*:9, e106831.

Andersen, J.T., Schäfer, T., Jørgensen, P.L., and Møller, S. (2001). Using inactivated microbial biomass as fertilizer: the fate of antibiotic resistance genes in the environment. Res. Microbiol. *152*, 823–833.

Andreotti, G., Cubellis, M.V., Nitti, G., Sannia, G., Mai, X., Marino, G., and Adams, M.W. (1994). Characterization of aromatic aminotransferases from the hyperthermophilic archaeon *Thermococcus litoralis*. Eur. J. Biochem. *220*, 543–549.

Andreotti, G., Cubellis, M.V., Nitti, G., Sannia, G., Mai, X., Adams, M.W., and Marino, G. (1995). An extremely thermostable aromatic aminotransferase from the hyperthermophilic archaeon *Pyrococcus furiosus*. Biochim. Biophys. Acta *1247*, 90–96.

Aono, R., Sato, T., Yano, A., Yoshida, S., Nishitani, Y., Miki, K., Imanaka, T., and Atomi, H. (2012). Enzymatic characterization of AMP phosphorylase and ribose-1,5-bisphosphate isomerase functioning in an archaeal AMP metabolic pathway. J. Bacteriol. *194*, 6847–6855.

Aono, R., Sato, T., Imanaka, T., and Atomi, H. (2015). A pentose bisphosphate pathway for nucleoside degradation in Archaea. Nat. Chem. Biol. *11*, 355–360.

Aravalli, R.N., and Garrett, R.A. (1997). Shuttle vectors for hyperthermophilic archaea. Extrem. Life Extreme Cond. *1*, 183–191.

Arrhenius, S. (1889). Über die dissociationswärme und den einfluss der temperatur auf den dissociationsgrad der elektrolyte. Z. Für Phys. Chem. *4U*, 96–116.

Aslam, M., Horiuchi, A., Simons, J.-R., Jha, S., Yamada, M., Odani, T., Fujimoto, R., Yamamoto, Y., Gunji, R., Imanaka, T., et al. (2017a). Engineering of a hyperthermophilic archaeon, *Thermococcus kodakarensis*, that displays chitin-dependent hydrogen production. Appl. Environ. Microbiol.

Atomi, H., Matsumi, R., and Imanaka, T. (2004a). Reverse gyrase is not a prerequisite for hyperthermophilic life. J. Bacteriol. *186*, 4829–4833.

Atomi, H., Fukui, T., Kanai, T., Morikawa, M., and Imanaka, T. (2004b). Description of *Thermococcus kodakaraensis* sp. nov., a well studied hyperthermophilic archaeon previously reported as *Pyrococcus* sp. KOD1. Archaea Vanc. BC *1*, 263–267.

Auzanneau, M. (2015). Or noir. La grande histoire du pétrole. La Découverte.

Avagyan, S., Vasilchuk, D., and Makhatadze, G.I. (2019). Protein adaptation to high hydrostatic pressure: computational analysis of the structural proteome. Proteins Struct. Funct. Bioinforma. *88*:4, 584-592.

Bae, S.S., Kim, Y.J., Yang, S.H., Lim, J.K., Jeon, J.H., Lee, H.S., Kang, S.G., Kim, S.-J., and Lee, J.-H. (2006). *Thermococcus onnurineus* sp. nov., a hyperthermophilic archaeon isolated from a deep-sea hydrothermal vent area at the pacmanus field. J. Microbiol. Biotechnol., *16*:11, 1826-1831.

Bae, S.S., Kim, T.W., Lee, H.S., Kwon, K.K., Kim, Y.J., Kim, M.-S., Lee, J.-H., and Kang, S.G. (2012). H_2 production from CO, formate or starch using the hyperthermophilic archaeon, *Thermococcus onnurineus*. Biotechnol. Lett. *34*, 75–79.

Balachandar, G., Varanasi, J.L., Singh, V., Singh, H., and Das, D. (2020). Biological hydrogen production *via* dark fermentation: A holistic approach from lab-scale to pilot-scale. Int. J. Hydrog. Energy *45*, 5202–5215.

Balch, W.E., Fox, G.E., Magrum, L.J., Woese, C.R., and Wolfe, R.S. (1979). Methanogens: reevaluation of a unique biological group. Microbiol. Rev. *43*, 260–296.

Bálint, B., Bagi, Z., Tóth, A., Rákhely, G., Perei, K., and Kovács, K.L. (2005). Utilization of keratin-containing biowaste to produce biohydrogen. Appl. Microbiol. Biotechnol. *69*, 404–410.

Ballard, R.D., Bryan, W.B., Heirtzler, J.R., Keller, G., Moore, J.G., and van Andel, Tj. (1975). Manned submersible observations in the FAMOUS area: Mid-Atlantic Ridge. Science *190*, 103–108.

Banos, D.T., Trébulle, P., and Elati, M. (2017). Integrating transcriptional activity in genome-scale models of metabolism. BMC Syst. Biol. *11*, 134.

Baron, S.F., and Ferry, J.G. (1989). Purification and properties of the membrane-associated coenzyme F420-reducing hydrogenase from *Methanobacterium formicicum*. J. Bacteriol. *171*, 3846–3853.

Barrick, J.E., Yu, D.S., Yoon, S.H., Jeong, H., Oh, T.K., Schneider, D., Lenski, R.E., and Kim, J.F. (2009). Genome evolution and adaptation in a long-term experiment with *Escherichia coli*. Nature *461*, 1243–1247.

Bartlett, D.H. (2002). Pressure effects on in vivo microbial processes. Biochim. Biophys. Acta BBA - Protein Struct. Mol. Enzymol. *1595*, 367–381.

Bartlett, D., Wright, M., Yayanos, A.A., and Silverman, M. (1989). Isolation of a gene regulated by hydrostatic pressure in a deep-sea bacterium. Nature *342*, 572–574.

Bartlett, D.H., Kato, C., and Horikoshi, K. (1995). High pressure influences on gene and protein expression. Res. Microbiol. *146*, 697–706.

Basbous, H., Appolaire, A., Girard, E., and Franzetti, B. (2018). Characterization of a glycyl-specific tet aminopeptidase complex from *pyrococcus horikoshii*. J. Bacteriol. *200*:17, e00059-18.

Bergman, E. (2016). Evaluation of the software SuperPro Designer through simulation of a biohydrogen production process. Master thesis, Lund University.

Bernander, R. (2000). Chromosome replication, nucleoid segregation and cell division in *Archaea*. Trends Microbiol. *8*, 278–283.

Bert, P. (1878). La pression barométrique: recherches de physiologie expérimentale (G. Masson).

Bertoldo, C., and Antranikian, G. (2006). The order *Thermococcales*. In The Prokaryotes, (Springer, New York, NY), pp. 69–81.

Bevers, L.E., Hagedoorn, P.-L., Krijger, G.C., and Hagen, W.R. (2006). Tungsten transport protein a (WtpA) in *Pyrococcus furiosus*: the first member of a new class of tungstate and molybdate transporters. J. Bacteriol. *188*, 6498–6505.

Birien, T. (2018). Génétique et génomique des microorganismes piézophiles des sources hydrothermales océaniques profondes (Adaptation aux hautes pressions hydrostatiques chez l'archée piézo-hyperthermophile : *Thermococcus barophilus*, apport de la génétique et impact des hydrogénases).

Birien, T., Thiel, A., Henneke, G., Flament, D., Moalic, Y., and Jebbar, M. (2018). Development of an effective 6-methylpurine counterselection marker for genetic manipulation in *Thermococcus barophilus*. Genes *9*:2, 77-90.

Birrien, J.-L., Zeng, X., Jebbar, M., Cambon-Bonavita, M.-A., Quérellou, J., Oger, P., Bienvenu, N., Xiao, X., and Prieur, D. (2011). *Pyrococcus yayanosii* sp. nov., an obligate piezophilic hyperthermophilic archaeon isolated from a deep-sea hydrothermal vent. Int. J. Syst. Evol. Microbiol. *61*, 2827–2881.

Blamey, J.M., and Adams, M.W.W. (1993). Purification and characterization of pyruvate ferredoxin oxidoreductase from the hyperthermophilic archaeon *Pyrococcus furiosus*. Biochim. Biophys. Acta *1161*, 19–27.

Blöchl, E., Rachel, R., Burggraf, S., Hafenbradl, D., Jannasch, H.W., and Stetter, K.O. (1997). *Pyrolobus fumarii*, gen. and sp. nov., represents a novel group of archaea, extending the upper temperature limit for life to 113 degrees C. Extrem. Life Extreme Cond. *1*, 14–21.

Blumentals, I.I., Itoh, M., Olson, G.J., and Kelly, R.M. (1990a). Role of polysulfides in reduction of elemental sulfur by the hyperthermophilic archaebacterium *Pyrococcus furiosus*. Appl. Environ. Microbiol. *56*, 1255–1262.

Blumentals, I.I., Brown, S.H., Schicho, R.N., Skaja, A.K., Costantino, H.R., and Kelly, R.M. (1990b). The hyperthermophilic archaebacterium, *Pyrococcus furiosus*. Ann. N. Y. Acad. Sci. *589*, 301–314.

Bolatkhan, K., Kossalbayev, B.D., Zayadan, B.K., Tomo, T., Veziroglu, T.N., and Allakhverdiev, S.I. (2019). Hydrogen production from phototrophic microorganisms: Reality and perspectives. Int. J. Hydrog. Energy *44*, 5799–5811.

Bonch-Osmolovskaya, E.A., and Miroshnichenko, M.L. (1994). Effect of molecular hydrogen and elemental sulfur on metabolism of extremely thermophilic archaebacteria of the genus *Thermococcus*. Mikrobiologiya *63*, 777–782.

Bonch-Osmolovskaya, E.A., and Stetter, K.O. (1991). Interspecies hydrogen transfer in cocultures of thermophilic *Archaea*. Syst. Appl. Microbiol. *14*, 205–208.

Boonyaratanakornkit, B., Córdova, J., Park, C.B., and Clark, D.S. (2006). Pressure affects transcription profiles of *Methanocaldococcus jannaschii* despite the absence of barophilic growth under gas-transfer limitation. Environ. Microbiol. *8*, 2031–2035.

Boonyaratanakornkit, B.B., Park, C.B., and Clark, D.S. (2002). Pressure effects on intra- and intermolecular interactions within proteins. Biochim. Biophys. Acta BBA - Protein Struct. Mol. Enzymol. *1595*, 235–249.

Boonyaratanakornkit, B.B., Miao, L.Y., and Clark, D.S. (2007). Transcriptional responses of the deep-sea hyperthermophile *Methanocaldococcus jannaschii* under shifting extremes of temperature and pressure. Extremophiles *11*, 495–503.

Bothe, H., Schmitz, O., Yates, M.G., and Newton, W.E. (2010). Nitrogen fixation and hydrogen metabolism in *cyanobacteria*. Microbiol. Mol. Biol. Rev. *74*, 529–551.

Bowyer, A., Mikolajek, H., Stuart, J.W., Wood, S.P., Jamil, F., Rashid, N., Akhtar, M., and Cooper, J.B. (2009). Structure and function of the l-threonine dehydrogenase (TkTDH) from the hyperthermophilic archaeon *Thermococcus kodakaraensis*. J. Struct. Biol. *168*, 294–304.

Bräsen, C., Esser, D., Rauch, B., and Siebers, B. (2014). Carbohydrate metabolism in *Archaea*: current insights into unusual enzymes and pathways and their regulation. Microbiol. Mol. Biol. Rev. *78*, 89–175.

Bridger, S.L., Clarkson, S.M., Stirrett, K., DeBarry, M.B., Lipscomb, G.L., Schut, G.J., Westpheling, J., Scott, R.A., and Adams, M.W.W. (2011). Deletion strains reveal metabolic roles for key elemental sulfur-responsive proteins in *Pyrococcus furiosus*. J. Bacteriol. *193*, 6498–6504.

Bridger, S.L., Lancaster, W.A., Poole, F.L., Schut, G.J., and Adams, M.W.W. (2012). Genome sequencing of a genetically tractable *Pyrococcus furiosus* strain reveals a highly dynamic genome. J. Bacteriol. *194*, 4097–4106.

Bridgman, P.W. (1914). The coagulation of albumen by pressure. J. Biol. Chem. 511–512.

Brock, T.D., and Freeze, H. (1969). *Thermus aquaticus* gen. n. and sp. n., a nonsporulating extreme thermophile. J. Bacteriol. *98*, 289–297.

Brooks, N.J. (2014). Pressure effects on lipids and bio-membrane assemblies. IUCrJ *1*, 470–477.

Brown, S.H., and Kelly, R.M. (1993). Characterization of amylolytic enzymes, having both alpha-1,4 and alpha-1,6 hydrolytic activity, from the thermophilic archaea *Pyrococcus furiosus* and *Thermococcus litoralis*. Appl. Environ. Microbiol. *59*, 2614–2621.

Brown, S.H., Costantino, H.R., and Kelly, R.M. (1990). Characterization of amylolytic enzyme activities associated with the hyperthermophilic archaebacterium *Pyrococcus furiosus*. Appl. Environ. Microbiol. *56*, 1985–1991.

Brunner, N.A., Brinkmann, H., Siebers, B., and Hensel, R. (1998). NAD^+-dependent glyceraldehyde-3-phosphate dehydrogenase from *Thermoproteus tenax*. The first identified archaeal member of the aldehyde dehydrogenase superfamily is a glycolytic enzyme with unusual regulatory properties. J. Biol. Chem. *273*, 6149–6156.

Bryant, F.O., and Adams, M.W.W. (1989). Characterization of hydrogenase from the hyperthermophilic archaebacterium, *Pyrococcus furiosus*. J. Biol. Chem. *264*, 5070–5079.

Buckel, W., and Thauer, R.K. (2013). Energy conservation via electron bifurcating ferredoxin reduction and proton/Na(+) translocating ferredoxin oxidation. Biochim. Biophys. Acta *1827*, 94–113.

Burke, J. (2018). Are we really on the cusp of a “hydrogen economy”? Infrastruct. - BusinessGreen.

Burkhart, B.W., Febvre, H.P., and Santangelo, T.J. (2019). Distinct physiological roles of the three ferredoxins encoded in the hyperthermophilic archaeon *Thermococcus kodakarensis*. MBio *10*, e02807-18.

Calero, P., and Nikel, P.I. (2018). Chasing bacterial chassis for metabolic engineering: a perspective review from classical to non-traditional microorganisms. Microb. Biotechnol. *12*, 98–124.

Callac, N., Oger, P., Lesongeur, F., Rattray, J.E., Vannier, P., Michoud, G., Beauverger, M., Gayet, N., Rouxel, O., Jebbar, M., and Anne Godfroy (2016). *Pyrococcus kukulkanii* sp. nov., a hyperthermophilic, piezophilic archaeon isolated from a deep-sea hydrothermal vent. Int. J. Syst. Evol. Microbiol. *66*, 3142–3149.

Campanaro, S., Vezzi, A., Vitulo, N., Lauro, F.M., D’Angelo, M., Simonato, F., Cestaro, A., Malacrida, G., Bertoloni, G., Valle, G., et al. (2005). Laterally transferred elements and high pressure adaptation in Photobacterium profundum strains. BMC Genomics *6*, 122.

Campanaro, S., Treu, L., and Valle, G. (2008). Protein evolution in deep sea bacteria: an analysis of amino acids substitution rates. BMC Evol. Biol. *8*, 313.

Canganella, F., and Jones, W.J. (1994). Fermentation studies with thermophilic *Archaea* in pure culture and in syntrophy with a thermophilic methanogen. Curr. Microbiol. *28*, 293–298.

Canganella, F., Kato, C., and Horikoshi, K. (2000). Effects of micronutrients on growth and starch hydrolysis of *Thermococcus guaymasensis* and *Thermococcus aggregans*. Microbiol. Res. *154*, 307–312.

Cario, A., Grossi, V., Schaeffer, P., and Oger, P.M. (2015a). Membrane homeoviscous adaptation in the piezo-hyperthermophilic archaeon *Thermococcus barophilus*. Front. Microbiol. *6*.

Cario, A., Lormières, F., Xiang, X., and Oger, P. (2015b). High hydrostatic pressure increases amino acid requirements in the piezo-hyperthermophilic archaeon *Thermococcus barophilus*. Res. Microbiol. *166*, 710–716.

Cario, A., Jebbar, M., Thiel, A., Kervarec, N., and Oger, P.M. (2016). Molecular chaperone accumulation as a function of stress evidences adaptation to high hydrostatic pressure in the piezophilic archaeon *Thermococcus barophilus*. Sci. Rep. *6*, 29483.

Caspi, Y., and Dekker, C. (2018). Dividing the archaeal way: the ancient Cdv cell-division machinery. Front. Microbiol. *9*:174.

Catchpole, R.J., and Forterre, P. (2019). The evolution of reverse gyrase suggests a nonhyperthermophilic last universal common ancestor. Mol. Biol. Evol. *36*:12, 2737-2747.

Certes, A. (1884). Note relative à l’action des hautes pessions sur la vitalité des microorganismes d’eau douce et d’eau de mer. Comptes Rendus Soc. Biol. *36*, 220–222.

Charlou, J.L., Donval, J.P., Fouquet, Y., Jean-Baptiste, P., and Holm, N. (2002). Geochemistry of high H_2 and CH_4 vent fluids issuing from ultramafic rocks at the Rainbow hydrothermal field (36°14′N, MAR). Chem. Geol. *191*, 345–359.

Chen, C.R., and Makhatadze, G.I. (2017). Molecular determinant of the effects of hydrostatic pressure on protein folding stability. Nat. Commun. *8*, 1–9.

Chen, L., Wei, Y., Shi, M., Li, Z., and Zhang, S.-H. (2019). An archaeal chitinase with a secondary capacity for catalyzing cellulose and its biotechnological applications in shell and straw degradation. Front. Microbiol. *10*:1253.

Chen, S., Qu, D., Xiao, X., and Xiaoling, M. (2020). Biohydrogen production with lipid-extracted Dunaliella biomass and a new strain of hyper-thermophilic archaeon *Thermococcus eurythermalis* A501. Int. J. Hydrog. Energy *45*, 12721–12730.

Chi, E., and Bartlett, D.H. (1995). An rpoE-like locus controls outer membrane protein synthesis and growth at cold temperatures and high pressures in the deep-sea bacterium *Photobacterium* sp. strain SS9. Mol. Microbiol. *17*, 713–726.

Chikuma, S., Kasahara, R., Kato, C., and Tamegai, H. (2007). Bacterial adaptation to high pressure: a respiratory system in the deep-sea bacterium *Shewanella violacea* DSS12. FEMS Microbiol. Lett. *267*, 108–112.

Cho, S., Kim, M.-S., Jeong, Y., Lee, B.-R., Lee, J.-H., Kang, S.G., and Cho, B.-K. (2017). Genome-wide primary transcriptome analysis of H2-producing archaeon *Thermococcus onnurineus* NA1. Sci. Rep. *7*.

Choi, A.R., Kim, M.-S., Kang, S.G., and Lee, H.S. (2016). Dimethyl sulfoxide reduction by a hyperhermophilic archaeon *Thermococcus onnurineus* NA1 via a cysteine-cystine redox shuttle. J. Microbiol. *54*, 31–38.

Cholewa, M., Dürrschnabel, R., Boukis, N., and Pfeifer, P. (2018). High pressure membrane separator for hydrogen purification of gas from hydrothermal treatment of biomass. Int. J. Hydrog. Energy *43*, 13294–13304.

Chou, C.-J., Shockley, K.R., Conners, S.B., Lewis, D.L., Comfort, D.A., Adams, M.W.W., and Kelly, R.M. (2007). Impact of substrate glycoside linkage and elemental sulfur on bioenergetics of and hydrogen production by the hyperthermophilic archaeon *Pyrococcus furiosus*. Appl. Environ. Microbiol. *73*, 6842–6853.

Cingolani, P., Platts, A., Wang, L.L., Coon, M., Nguyen, T., Wang, L., Land, S.J., Lu, X., and Ruden, D.M. (2012). A program for annotating and predicting the effects of single nucleotide polymorphisms, SnpEff. Fly (Austin) *6*, 80–92.

Ciobanu, M.-C., Burgaud, G., Dufresne, A., Breuker, A., Rédou, V., Maamar, S.B., Gaboyer, F., Vandenabeele-Trambouze, O., Lipp, J.S., Schippers, A., et al. (2014). Microorganisms persist at record depths in the subseafloor of the Canterbury Basin. ISME J. *8*, 1370–1380.

Clarkson, S.M., Newcomer, E.C., Young, E.G., and Adams, M.W.W. (2010). The elemental sulfur-responsive protein (SipA) from the hyperthermophilic archaeon *Pyrococcus furiosus* is regulated by sulfide in an iron-dependent manner. J. Bacteriol. *192*, 5841–5843.

Cleland, N., and Enfors, S.-O. (1987). A biological system for studies on mixing in bioreactors. Bioprocess Eng. *2*, 115–120.

Collins, L. (2020). A wake-up call on green hydrogen: the amount of wind and solar needed is immense. Recharge.

Colman, D.R., Poudel, S., Stamps, B.W., Boyd, E.S., and Spear, J.R. (2017). The deep, hot biosphere: Twenty-five years of retrospection. Proc. Natl. Acad. Sci. *114*, 6895–6903.

Conrad, T.M., Lewis, N.E., and Palsson, B.Ø. (2011). Microbial laboratory evolution in the era of genome-scale science. Mol. Syst. Biol. *7*, 509.

Consalvi, V., Chiaraluce, R., Politi, L., Vaccaro, R., De Rosa, M., and Scandurra, R. (1991). Extremely thermostable glutamate dehydrogenase from the hyperthermophilic archaebacterium *Pyrococcus furiosus*. Eur. J. Biochem. *202*, 1189–1196.

Corliss, J.B., Dymond, J., Gordon, L.I., Edmond, J.M., von Herzen, R.P., Ballard, R.D., Green, K., Willilams, D., Bainbridge, A., Crane, K., et al. (1979). Submarine thermal sprirngs on the galapagos rift. Science *203*, 1073–1083.

Cossu, M., Da Cunha, V., Toffano-Nioche, C., Forterre, P., and Oberto, J. (2015). Comparative genomics reveals conserved positioning of essential genomic clusters in highly rearranged *Thermococcales* chromosomes. Biochimie *118*, 313–321.

Cossu, M., Badel, C., Catchpole, R., Gadelle, D., Marguet, E., Barbe, V., Forterre, P., and Oberto, J. (2017). Flipping chromosomes in deep-sea archaea. PLOS Genet. *13*, e1006847.

Courtine, D. (2017). Génomique comparative d'isolats phylogénétiquement proches appartenant au genre *Thermococcus*, une archée hyperthermophile. PhD thesis. Université Bretagne Loire.

Crable, B.R., Plugge, C.M., McInerney, M.J., and Stams, A.J.M. (2011). Formate formation and formate conversion in biological fuels production. Enzyme Res. 2011:532536.

Dalmasso, C. (2016). Approches physiologiques et génomiques d'une archée thermo-piézophile *Thermococcus piezophilus*. PhD thesis. Université de Bretagne Loire.

Dalmasso, C., Oger, P., Selva, G., Courtine, D., L'Haridon, S., Garlaschelli, A., Roussel, E., Miyazaki, J., Reveillaud, J., Jebbar, M., et al. (2016). *Thermococcus piezophilus* sp. nov., a novel hyperthermophilic and piezophilic archaeon with a broad pressure range for growth, isolated from a deepest hydrothermal vent at the Mid-Cayman Rise. Syst. Appl. Microbiol. *39*, 440–444.

De Maio, A., Santoro, M.G., Tanguay, R.M., and Hightower, L.E. (2012). Ferruccio Ritossa's scientific legacy 50 years after his discovery of the heat shock response: a new view of biology, a new society, and a new journal. Cell Stress Chaperones *17*, 139–143.

Kelley D.S., Baross J.A., and Delaney, J.R. (2002). Volcanoes, fluids, and life at mid-ocean ridge spreading centers. Annu. Rev. Earth Planet. Sci. *30*, 385–491.

Dębowski, M., Korzeniewska, E., Filipkowska, Z., Zieliński, M., and Kwiatkowski, R. (2014). Possibility of hydrogen production during cheese whey fermentation process by different strains of psychrophilic bacteria. Int. J. Hydrog. Energy *39*, 1972–1978.

DeLong, E.F., and Yayanos, A.A. (1986). Biochemical function and ecological significance of novel bacterial lipids in deep-sea procaryotes. Appl. Environ. Microbiol. *51*, 730–737.

Demazeau, G., and Rivalain, N. (2010). High hydrostatic pressure and biology: a brief history. Appl. Microbiol. Biotechnol. *89*, 1305–1314.

Deming, J.W., and Baross, J.A. (1993). Deep-sea smokers: Windows to a subsurface biosphere? Geochim. Cosmochim. Acta *57*, 3219–3230.

Demmer, J.K., Huang, H., Wang, S., Demmer, U., Thauer, R.K., and Ermler, U. (2015). Insights into flavin-based electron bifurcation via the nadh-dependent reduced ferredoxin:nadp oxidoreductase structure. J. Biol. Chem. *290*, 21985–21995.

Denis, A., Martínez-Núñez, M.A., Tenorio-Salgado, S., and Perez-Rueda, E. (2018). Dissecting the repertoire of dna-binding transcription factors of the archaeon *Pyrococcus furiosus* DSM 3638. Life Basel Switz. *8*:4, 40.

Desbruyéres, D., Almeida, A., Biscoito, M., Comtet, T., Khripounoff, A., Bris, N.L., Sarradin, P.M., and Segonzac, M. (2000). A review of the distribution of hydrothermal vent communities along the northern Mid-Atlantic Ridge: dispersal vs. environmental controls. Hydrobiologia *440*, 201–216.

Di Giulio, M. (2005). A comparison of proteins from *Pyrococcus furiosus* and *Pyrococcus abyssi*: barophily in the physicochemical properties of amino acids and in the genetic code. Gene *346*, 1–6.

Dib, R., Chobert, J.-M., Dalgalarrondo, M., Barbier, G., and Haertlé, T. (1998). Purification, molecular properties and specificity of a thermoactive and thermostable proteinase from *Pyrococcus abyssi*, strain st 549, hyperthermophilic archaea from deep-sea hydrothermal ecosystem. FEBS Lett. *431*, 279–284.

Dick, G.J. (2019a). The microbiomes of deep-sea hydrothermal vents: distributed globally, shaped locally. Nat. Rev. Microbiol. *17*, 271.

Dick, J.M. (2019b). CHNOSZ: Thermodynamic calculations and diagrams for geochemistry. front. Earth Sci. *7*:180.

Dick, G.J., Anantharaman, K., Baker, B.J., Li, M., Reed, D.C., and Sheik, C.S. (2013). The microbiology of deep-sea hydrothermal vent plumes: ecological and biogeographic linkages to seafloor and water column habitats. Front. Microbiol. *4*, 124.

Diederichs, K., Diez, J., Greller, G., Müller, C., Breed, J., Schnell, C., Vonrhein, C., Boos, W., and Welte, W. (2000). Crystal structure of MalK, the ATPase subunit of the trehalose/maltose ABC transporter of the archaeon *Thermococcus litoralis*. EMBO J. *19*, 5951–5961.

Diender, M., Stams, A.J.M., and Sousa, D.Z. (2015). Pathways and bioenergetics of anaerobic carbon monoxide fermentation. Front. Microbiol. *6* :1275.

Dong, G., Vieille, C., Savchenko, A., and Zeikus, J.G. (1997). Cloning, sequencing, and expression of the gene encoding extracellular alpha-amylase from *Pyrococcus furiosus* and biochemical characterization of the recombinant enzyme. Appl. Environ. Microbiol. *63*, 3569–3576.

Downey, C.D., Crisman, R.L., Randolph, T.W., and Pardi, A. (2007). Influence of hydrostatic pressure and cosolutes on RNA tertiary structure. J. Am. Chem. Soc. *129*, 9290–9291.

Driessen, R.P.C., Sitters, G., Laurens, N., Moolenaar, G.F., Wuite, G.J.L., Goosen, N., and Dame, R.Th. (2014). Effect of temperature on the intrinsic flexibility of dna and its interaction with architectural proteins. Biochemistry *53*, 6430–6438.

Driskill, L.E., Kusy, K., Bauer, M.W., and Kelly, R.M. (1999). Relationship between glycosyl hydrolase inventory and growth physiology of the hyperthermophile *Pyrococcus furiosus* on carbohydrate-based media. Appl. Environ. Microbiol. *65*, 893–897.

Dubins, D.N., Lee, A., Macgregor, R.B., and Chalikian, T.V. (2001). On the stability of double stranded nucleic acids. J. Am. Chem. Soc. *123*, 9254–9259.

Dutta, A., Peoples, L.M., Gupta, A., Bartlett, D.H., and Sar, P. (2019). Exploring the piezotolerant/piezophilic microbial community and genomic basis of piezotolerance within the deep subsurface Deccan traps. Extrem. Life Extreme Cond. *23*, 421–433.

Eckermann, E. (2001). World History of the Automobile (Society of Automotive Engineers).

EDF (2017). Le stockage de l'électricité, un défi pour la transition énergétique (Lavoisier).

El-Emam, R.S., and Özcan, H. (2019). Comprehensive review on the techno-economics of sustainable large-scale clean hydrogen production. J. Clean. Prod. *220*, 593–609.

El-Hajj, Z.W., Allcock, D., Tryfona, T., Lauro, F.M., Sawyer, L., Bartlett, D.H., and Ferguson, G.P. (2010). Insights into piezophily from genetic studies on the deep-sea bacterium, Photobacterium profundum SS9. Ann. N. Y. Acad. Sci. *1189*, 143–148.

Eloe, E.A., Lauro, F.M., Vogel, R.F., and Bartlett, D.H. (2008). The deep-sea bacterium *Photobacterium profundum* SS9 utilizes separate flagellar systems for swimming and swarming under high-pressure conditions. Appl. Environ. Microbiol. *74*, 6298–6305.

Eloe, E.A., Shulse, C.N., Fadrosh, D.W., Williamson, S.J., Allen, E.E., and Bartlett, D.H. (2011). Compositional differences in particle-associated and free-living microbial assemblages from an extreme deep-ocean environment. Environ. Microbiol. Rep. *3*, 449–458.

Engel, L., Tarantik, K.R., Pannek, C., and Wöllenstein, J. (2018). Colorimetric detection of hydrogen sulfide in ambient air. Proceedings *2*:13, 804.

Erauso, G., Marsin, S., Benbouzid-Rollet, N., Baucher, M.F., Barbeyron, T., Zivanovic, Y., Prieur, D., and Forterre, P. (1996). Sequence of plasmid pGT5 from the archaeon *Pyrococcus abyssi*: evidence for rolling-circle replication in a hyperthermophile. J. Bacteriol. *178*, 3232–3237.

Fang, J., Zhang, L., and Bazylinski, D.A. (2010). Deep-sea piezosphere and piezophiles: geomicrobiology and biogeochemistry. Trends Microbiol. *18*, 413–422.

FAO (2020). Definitions | Vulnerable Marine Ecosystems | Food and Agriculture Organization of the United Nations. http://www.fao.org/in-action/vulnerable-marine-ecosystems/definitions/en/

FCHEA (2020). Fuel Cell Basics. http://www.fchea.org/fuelcells

Fernandes, P.M.B., Domitrovic, T., Kao, C.M., and Kurtenbach, E. (2004). Genomic expression pattern in *Saccharomyces cerevisiae* cells in response to high hydrostatic pressure. FEBS Lett. *556*, 153–160.

Fiala, G., and Stetter, K.O. (1986). *Pyrococcus furiosus* sp. nov. represents a novel genus of marine heterotrophic archaebacteria growing optimally at 100°C. Arch. Microbiol. *145*, 56–61.

Field, E., and Oldach, C.S. (1946). Determination of hydrogen sulfide in gases. Ind. Eng. Chem. Anal. Ed. *18*, 665–667.

Fiore, M. (2019). The origin and early evolution of life: prebiotic chemistry. Life *9*, 73.

Flamholz, A., Noor, E., Bar-Even, A., Liebermeister, W., and Milo, R. (2013). Glycolytic strategy as a tradeoff between energy yield and protein cost. Proc. Natl. Acad. Sci. *110*, 10039–10044.

Fonselius, S., Dyrssen, D., and Yhlen, B. (2007). Determination of hydrogen sulphide. In Methods of Seawater Analysis, (John Wiley & Sons, Ltd), pp. 91–100.

Forterre, P. (2002). A hot story from comparative genomics: reverse gyrase is the only hyperthermophile-specific protein. Trends Genet. TIG *18*, 236–237.

Fortunato, C.S., Larson, B., Butterfield, D.A., and Huber, J.A. (2018). Spatially distinct, temporally stable microbial populations mediate biogeochemical cycling at and below the seafloor in hydrothermal vent fluids. Environ. Microbiol. *20*, 769–784.

Fouquet, Y., Auclair, G., Cambon, P., and Etoubleau, J. (1988). Geological setting and mineralogical and geochemical investigations on sulfide deposits near 13°N on the East Pacific Rise. Mar. Geol. *84*, 145–178.

Fourmond, V., Baffert, C., Sybirna, K., Dementin, S., Abou-Hamdan, A., Meynial-Salles, I., Soucaille, P., Bottin, H., and Léger, C. (2013). The mechanism of inhibition by H_2 of H_2-evolution by hydrogenases. Chem. Commun. *49*, 6840–6842.

Franc, P.-E., and Mateo, P. (2015). Hydrogène : la transition énergétique en marche!. Manifestô.

Lesongeur, F., Briand, P., Godfroy, A., Crassous, P., Byrne, N., and Khripounoff, A. (2014). Export of deep-sea hydrothermal particles, indigenous thermophilic microorganisms and larvae to the surrounding Ocean. Cahiers de Biologie Marine (0007-9723), *5*:4, 109-420.

Frankfurt School-UNEP Collaborating Centre (2018). Global trends in renewable energy investment report 2018.

Fukuda, W., Fukui, T., Atomi, H., and Imanaka, T. (2004). First characterization of an archaeal gtp-dependent phosphoenolpyruvate carboxykinase from the hyperthermophilic archaeon *Thermococcus kodakaraensis* KOD1. J. Bacteriol. *186*, 4620–4627.

Fukui, T., Atomi, H., Kanai, T., Matsumi, R., Fujiwara, S., and Imanaka, T. (2005). Complete genome sequence of the hyperthermophilic archaeon Thermococcus kodakaraensis KOD1 and comparison with Pyrococcus genomes. Genome Res. *15*, 352–363.

Fung, M. (2005). Energy Density of Hydrogen. The Physics Factbook. https://hypertextbook.com/facts/2005/MichelleFung.shtml

Fushinobu, S., Nishimasu, H., Hattori, D., Song, H.-J., and Wakagi, T. (2011). Structural basis for the bifunctionality of fructose-1,6-bisphosphate aldolase/phosphatase. Nature *478*, 538–541.

Gao, J., Bauer, M.W., Shockley, K.R., Pysz, M.A., and Kelly, R.M. (2003). Growth of hyperthermophilic archaeon *Pyrococcus furiosus* on chitin involves two family 18 chitinases. Appl. Environ. Microbiol. *69*, 3119–3128.

Garcia, A.E., and Paschek, D. (2008). Simulation of the pressure and temperature folding/unfolding equilibrium of a small RNA hairpin. J. Am. Chem. Soc. *130*, 815–817.

Gartman, A., Yücel, M., Madison, A.S., Chu, D.W., Ma, S., Janzen, C.P., Becker, E.L., Beinart, R.A., Girguis, P.R., and Luther, G.W. (2011). Sulfide oxidation across diffuse flow zones of hydrothermal vents. Aquat. Geochem. *17*, 583–601.

Gavrilov, S.N., Stracke, C., Jensen, K., Menzel, P., Kallnik, V., Slesarev, A., Sokolova, T., Zayulina, K., Bräsen, C., Bonch-Osmolovskaya, E.A., et al. (2016). Isolation and characterization of the first xylanolytic hyperthermophilic euryarchaeon *Thermococcus* sp. strain 2319x1 and its unusual multidomain glycosidase. Front. Microbiol. *7*.

GBIF (2020). *Thermococcales* in GBIF Secretariat. GBIF Backbone Taxon.

Geslin, C., Le Romancer, M., Erauso, G., Gaillard, M., Perrot, G., and Prieur, D. (2003). PAV1, the first virus-like particle isolated from a hyperthermophilic euryarchaeote, "*Pyrococcus abyssi*." J. Bacteriol. *185*, 3888–3894.

Ghasemi, A., Ghafourian, S., Vafaei, S., Mohebi, R., Farzi, M., Taherikalani, M., and Sadeghifard, N. (2015). cloning, expression, and purification of hyperthermophile α-amylase from *Pyrococcus woesei*. Osong Public Health Res. Perspect. *6*, 336–340.

Ghiasian, M. (2019). Biophotolysis-based hydrogen production by cyanobacteria. In Prospects of Renewable Bioprocessing in Future Energy Systems, A.A. Rastegari, A.N. Yadav, and A. Gupta, eds. (Cham: Springer International Publishing), pp. 161–184.

Ghimire, A., Frunzo, L., Pirozzi, F., Trably, E., Escudie, R., Lens, P.N.L., and Esposito, G. (2015). A review on dark fermentative biohydrogen production from organic biomass: Process parameters and use of by-products. Appl. Energy *144*, 73–95.

Gibbs, J.W., Josiah W., Tyndall, J (1874). On the equilibrium of heterogeneous substances. Connecticut Academy of Arts and Sciences and Burndy Library.

Girard, E., Prangé, T., Dhaussy, A.-C., Migianu-Griffoni, E., Lecouvey, M., Chervin, J.-C., Mezouar, M., Kahn, R., and Fourme, R. (2007). Adaptation of the base-paired double-helix molecular architecture to extreme pressure. Nucleic Acids Res. *35*, 4800–4808.

Girguis, P.R.., and Holden, J.F. (2012). On the potential for bioenergy and biofuels from hydrothermal vent microbes. Oceanography *25*, 213–217.

Glenk, G., and Reichelstein, S. (2019). Economics of converting renewable power to hydrogen. Nat. Energy *4*, 216–222.

Goda, S., Koga, T., Yamashita, K., Kuriura, R., and Ueda, T. (2018). A novel carbohydrate-binding surface layer protein from the hyperthermophilic archaeon *Pyrococcus horikoshii*. Biosci. Biotechnol. Biochem. *82*:8, 1327-1334.

Golub, M., Martinez, N., Michoud, G., Ollivier, J., Jebbar, M., Oger, P., and Peters, J. (2018). The effect of crowding on protein stability, rigidity, and high pressure sensitivity in whole cells. Langmuir ACS J. Surf. Colloids *34*, 10419–10425.

González, J.M., Sheckells, D., Viebahn, M., Krupatkina, D., Borges, K.M., and Robb, F.T. (1999). *Thermococcus waiotapuensis* sp. nov., an extremely thermophilic archaeon isolated from a freshwater hot spring. Arch. Microbiol. *172*, 95–101.

Gorlas, A., Koonin, E.V., Bienvenu, N., Prieur, D., and Geslin, C. (2012). TPV1, the first virus isolated from the hyperthermophilic genus *Thermococcus*. Environ. Microbiol. *14*, 503–516.

Gorlas, A., Alain, K., Bienvenu, N., and Geslin, C. (2013). *Thermococcus prieurii* sp. nov., a hyperthermophilic archaeon isolated from a deep-sea hydrothermal vent. Int. J. Syst. Evol. Microbiol. *63*, 2920–2926.

Gorlas, A., Marguet, E., Gill, S., Geslin, C., Guigner, J.-M., Guyot, F., and Forterre, P. (2015). Sulfur vesicles from *Thermococcales*: A possible role in sulfur detoxifying mechanisms. Biochimie *118*, 356–364.

Green, L. (1982). An ammonia energy vector for the hydrogen economy. Int. J. Hydrog. Energy *7*, 355–359.

Gregory, S.P., Barnett, M.J., Field, L.P., and Milodowski, A.E. (2019). Subsurface microbial hydrogen cycling: natural occurrence and implications for industry. Microorganisms *7*:2, 53.

Grieger, R.A., and Eckert, C.A. (1970). A new technique for chemical kinetics at high pressures. AIChE J. *16*, 766–770.

Grogan, D.W. (1998). Hyperthermophiles and the problem of DNA instability. Mol. Microbiol. *28*, 1043–1049.

Grosjean, H., and Oshima, T. (2007). How nucleic acids cope with high temperature. 39–56. *In* Gerday C, Glansdorff N (ed), *Physiology and Biochemistry of Extremophiles*. ASM Press, Washington, DC.

Gross, M., and Jaenicke, R. (1994). Proteins under pressure. The influence of high hydrostatic pressure on structure, function and assembly of proteins and protein complexes. Eur. J. Biochem. *221*, 617–630.

Gross, M., Lehle, K., Jaenicke, R., and Nierhaus, K.H. (1993). Pressure-induced dissociation of ribosomes and elongation cycle intermediates. Stabilizing conditions and identification of the most sensitive functional state. Eur. J. Biochem. *218*, 463–468.

Grüber, G., Manimekalai, M.S.S., Mayer, F., and Müller, V. (2014). ATP synthases from archaea: The beauty of a molecular motor. Biochim. Biophys. Acta BBA - Bioenerg. *1837*, 940–952.

Grünberger, F., Reichelt, R., Bunk, B., Spröer, C., Overmann, J., Rachel, R., Grohmann, D., and Hausner, W. (2019). Next generation DNA-seq and differential RNA-seq allow re-annotation of the *Pyrococcus furiosus* DSM 3638 genome and provide insights into archaeal antisense transcription. Front. Microbiol. *10*:1603.

Gu, C., Kim, G.B., Kim, W.J., Kim, H.U., and Lee, S.Y. (2019). Current status and applications of genome-scale metabolic models. Genome Biol. *20*, 121.

Gueguen, Y., Voorhorst, W.G., van der Oost, J., and de Vos, W.M. (1997). Molecular and biochemical characterization of an endo-beta-1,3- glucanase of the hyperthermophilic archaeon *Pyrococcus furiosus*. J. Biol. Chem. *272*, 31258–31264.

Guerriero, G., Hausman, J.F., Strauss, J., Ertan, H., and Siddiqui, K.S. (2015). Destructuring plant biomass: focus on fungal and extremophilic cell wall hydrolases. Plant Sci. *234*, 180–193.

Guixé, V., and Merino, F. (2009). The ADP-dependent sugar kinase family: kinetic and evolutionary aspects. IUBMB Life *61*, 753–761.

Gunbin, K.V., Afonnikov, D.A., and Kolchanov, N.A. (2009). Molecular evolution of the hyperthermophilic archaea of the *Pyrococcus* genus: analysis of adaptation to different environmental conditions. BMC Genomics *10*, 639.

Guo, J., Coker, A.R., Wood, S.P., Cooper, J.B., Keegan, R.M., Ahmad, N., Muhammad, M.A., Rashid, N., and Akhtar, M. (2018). Structure and function of the type III pullulan hydrolase from *Thermococcus kodakarensis*. Acta Crystallogr. Sect. Struct. Biol. *74*, 305–314.

H2020 (2019). Appels 2019 Réduction des émissions de CO2. Horizon 2020 Appel H2020-LC-SC3-NZE-2019.

Haaster, D.J. van, Silva, P.J., Hagedoorn, P.-L., Jongejan, J.A., and Hagen, W.R. (2008). Reinvestigation of the steady-state kinetics and physiological function of the soluble nife-hydrogenase I of *Pyrococcus furiosus*. J. Bacteriol. *190*, 1584–1587.

Hachisuka, S., Sato, T., and Atomi, H. (2017). Metabolism dealing with thermal degradation of NAD+ in the hyperthermophilic archaeon *Thermococcus kodakarensis*. J. Bacteriol. JB.00162-17.

Hallenbeck, P.C., and Ghosh, D. (2009). Advances in fermentative biohydrogen production: the way forward? Trends Biotechnol. *27*, 287–297.

Han, W., Yan, Y., Gu, J., Shi, Y., Tang, J., and Li, Y. (2016). Techno-economic analysis of a novel bioprocess combining solid state fermentation and dark fermentation for H_2 production from food waste. Int. J. Hydrog. Energy *41*, 22619–22625.

Hardison, R. (2019). 2.5: B-Form, A-Form, and Z-Form of DNA. In Biology, LibreTexts.

Härtel, G., Rompf, F., and Püschel, T. (1996). Separation of a CO_2/H_2 gas mixture under high pressure with polyethylene terephthalate membranes. J. Membr. Sci. *113*, 115–120.

Hawley, S.A., and Macleod, R.M. (1974). Pressure–temperature stability of DNA in neutral salt solutions. Biopolymers *13*, 1417–1426.

Hay, S., Evans, R.M., Levy, C., Loveridge, E.J., Wang, X., Leys, D., Allemann, R.K., and Scrutton, N.S. (2009). Are the catalytic properties of enzymes from piezophilic organisms pressure adapted? Chembiochem Eur. J. Chem. Biol. *10*, 2348–2353.

Haymon, R.M. (1983). Growth history of hydrothermal black smoker chimneys. Nature *301*, 695–698.

Hedderich, R., Klimmek, O., Kröger, A., Dirmeier, R., Keller, M., and Stetter, K.O. (1998). Anaerobic respiration with elemental sulfur and with disulfides. FEMS Microbiol. Rev. *22*, 353–381.

Hei, D.J., and Clark, D.S. (1994). Pressure stabilization of proteins from extreme thermophiles. Appl. Environ. Microbiol. *60*, 932–939.

Heider, J., Mai, X., and Adams, M.W.W. (1996). Characterization of 2-ketoisovalerate ferredoxin oxidoreductase, a new and reversible coenzyme A-dependent enzyme involved in peptide fermentation by hyperthermophilic archaea. J. Bacteriol. *178*, 780–787.

Hensley, S.A., Moreira, E., and Holden, J.F. (2016). Hydrogen production and enzyme activities in the hyperthermophile *Thermococcus paralvinellae* grown on maltose, tryptone, and agricultural waste. Front. Microbiol. *7*, 167.

Hess, D., Krüger, K., Knappik, A., Palm, P., and Hensel, R. (1995). Dimeric 3-phosphoglycerate kinases from hyperthermophilic *Archaea*. Cloning, sequencing and expression of the 3-phosphoglycerate kinase gene of *Pyrococcus woesei* in *Escherichia coli* and characterization of the protein. Structural and functional comparison with the 3-phosphoglycerate kinase of *Methanothermus fervidus*. Eur. J. Biochem. *233*, 227–237.

Hidese, R., Yamashita, K., Kawazuma, K., Kanai, T., Atomi, H., Imanaka, T., and Fujiwara, S. (2017). Gene regulation of two ferredoxin:NADP+ oxidoreductases by the redox-responsive regulator SurR in *Thermococcus kodakarensis*. Extrem. Life Extreme Cond. *21*, 903–917.

Higashi, N., Tanimoto, K., Nishioka, M., Ishikawa, K., and Taya, M. (2008). Investigating a catalytic mechanism of hyperthermophilic L-threonine dehydrogenase from *Pyrococcus horikoshii*. J. Biochem. *144*, 77–85.

Higashibata, H., Fujiwara, S., Takagi, M., and Imanaka, T. (1999). Analysis of DNA compaction profile and intracellular contents of archaeal histones from *Pyrococcus kodakaraensis* KOD1. Biochem. Biophys. Res. Commun. *258*, 416–424.

Hoaki, T., Nishijima, M., Kato, M., Adachi, K., Mizobuchi, S., Hanzawa, N., and Maruyama, T. (1994). Growth requirements of hyperthermophilic sulfur-dependent heterotrophic archaea isolated from a shallow submarine geothermal system with reference to their essential amino acids. Appl. Environ. Microbiol. *60*, 2898–2904.

Holden, J.F., and Baross, J.A. (1995). Enhanced thermotolerance by hydrostatic pressure in the deep-sea hyperthermophile Pyrococcus strain ES4. FEMS Microbiol. Ecol. *18*, 27–33.

Holden, J.F., Breier, J., Rogers, K., Schulte, M., and Toner, B. (2012). Biogeochemical processes at hydrothermal vents: microbes and minerals, bioenergetics, and carbon fluxes. Oceanography *25*, 196–208.

Holden, J.F., Summit, M., and Baross, J.A. (1998). Thermophilic and hyperthermophilic microorganisms in 3–30°C hydrothermal fluids following a deep-sea volcanic eruption. FEMS Microbiol. Ecol. *25*, 33–41.

Holden, J.F., Takai, K., Summit, M., Bolton, S., Zyskowski, J., and Baross, J.A. (2001). Diversity among three novel groups of hyperthermophilic deep-sea *Thermococcus* species from three sites in the northeastern Pacific Ocean. FEMS Microbiol. Ecol. *36*, 51–60.

Horiuchi, A., Aslam, M., Kanai, T., and Atomi, H. (2016). A structurally novel chitinase from the chitin-degrading hyperthermophilic archaeon *Thermococcus chitonophagus*. Enzymol. Protein Eng. *82*, 3554–3562.

Horlacher, R., Xavier, K.B., Santos, H., DiRuggiero, J., Kossmann, M., and Boos, W. (1998). Archaeal binding protein-dependent ABC transporter: molecular and biochemical analysis of the trehalose/maltose transport system of the hyperthermophilic archaeon *Thermococcus litoralis*. J. Bacteriol. *180*, 680–689.

Houghton, J.L., Gilhooly, W.P., Kafantaris, F.-C.A., Druschel, G.K., Lu, G.-S., Amend, J.P., Godelitsas, A., and Fike, D.A. (2019). Spatially and temporally variable sulfur cycling in shallow-sea hydrothermal vents, Milos, Greece. Mar. Chem. *208*, 83–94.

Huber, R., Stöhr, J., Hohenhaus, S., Rachel, R., Burggraf, S., Jannasch, H.W., and Stetter, K.O. (1995). *Thermococcus chitonophagus* sp. nov., a novel, chitin-degrading, hyperthermophilic archaeum from a deep-sea hydrothermal vent environment. Arch. Microbiol. *164*, 255–264.

Hudson, R.C., Ruttersmith, L.D., and Danie, R.M. (1993). Glutamate dehydrogenase from the extremely thermophilic archaebacterial isolate AN1. Biochim. Biophys. Acta BBA - Protein Struct. Mol. Enzymol. *1202*, 244–250.

Hutchins, A.M., Holden, J.F., and Adams, M.W.W. (2001).Phosphoenolpyruvate synthetase from the hyperthermophilic archaeon *Pyrococcus furiosus*. J. Bacteriol. *183*, 709–715.

Ichiye, T. (2018). Enzymes from piezophiles. Semin. Cell Dev. Biol. *84*, 138–146.

IEA (2018). Scenarios. https://www.iea.org/weo2018/scenarios/

IEA (2019a). CETP. https://www.iea.org/cetp/

IEA (2019b). Hydrogen – Tracking Energy Integration – Analysis. https://www.iea.org/reports/tracking-energy-integration/hydrogen

IEA-ETSA (2014). Hydrogen Production & Distribution. https://iea-etsap.org/index.php/energy-technology-data/energy-supply-technologies-data

Imanaka, T. (2011). Molecular bases of thermophily in hyperthermophiles. Proc. Jpn. Acad. Ser. B Phys. Biol. Sci. *87*, 587–602.

Imanaka, H., Fukui, T., Atomi, H., and Imanaka, T. (2002). Gene cloning and characterization of fructose-1,6-bisphosphate aldolase from the hyperthermophilic archaeon *Thermococcus kodakaraensis* KOD1. J. Biosci. Bioeng. *94*, 237–243.

Imanaka, H., Yamatsu, A., Fukui, T., Atomi, H., and Imanaka, T. (2006). Phosphoenolpyruvate synthase plays an essential role for glycolysis in the modified Embden-Meyerhof pathway in *Thermococcus kodakarensis*. Mol. Microbiol. *61*, 898–909.

Imanaka, T., Shibazaki, M., and Takagi, M. (1986). A new way of enhancing the thermostability of proteases. Nature *324*, 695–697.

l'MTech (2017). Energy transitions: The challenge is a global one, the solutions are local. https://blogrecherche.wp.imt.fr/en/2017/07/07/energy-transitions-challenge-global/

International Seabed Authority (2020). https://www.isa.org.jm/fr

IPCC (2018). Global Warming of 1.5 °C - Special report. https://www.ipcc.ch/sr15/

Jäger, D., Förstner, K.U., Sharma, C.M., Santangelo, T.J., and Reeve, J.N. (2014). Primary transcriptome map of the hyperthermophilic archaeon *Thermococcus kodakarensis*. BMC Genomics *15*, 684.

James, B.D., Houchins, C., Huya-Kouadio, J.M., and DeSantis, D.A. (2016). Final Report: Hydrogen Storage System Cost Analysis.

Jan, C., Petersen, J.M., Werner, J., Teeling, H., Huang, S., Glöckner, F.O., Golyshina, O.V., Dubilier, N., Golyshin, P.N., Jebbar, M., et al. (2014). The gill chamber epibiosis of deep-sea shrimp *Rimicaris exoculata*: an in-depth metagenomic investigation and discovery of *Zetaproteobacteria*. Environ. Microbiol. *16*, 2723–2738.

Jannasch, H.W., and Taylor, C.D. (1984). Deep-Sea microbiology. Annu. Rev. Microbiol. *38*, 487–487.

Jaubert, C., Danioux, C., Oberto, J., Cortez, D., Bize, A., Krupovic, M., She, Q., Forterre, P., Prangishvili, D., and Sezonov, G. (2013) Genomics and genetics of *Sulfolobus islandicus* LAL14/1, a model hyperthermophilic archaeon. Open Biol. *3*, 130010.

Jeckelmann, J.-M., and Erni, B. (2019). Carbohydrate transport by group translocation: the bacterial phosphoenolpyruvate: sugar phosphotransferase system. In Bacterial Cell Walls and Membranes, A. Kuhn, ed. (Cham: Springer International Publishing), pp. 223–274.

Jeon, J.H., Lim, J.K., Kim, M.-S., Yang, T.-J., Lee, S.-H., Bae, S.S., Kim, Y.J., Lee, S.H., Lee, J.-H., Kang, S.G., et al. (2015). Characterization of the frhAGB-encoding hydrogenase from a non-methanogenic hyperthermophilic archaeon. Extrem. Life Extreme Cond. *19*, 109–118.

Jeong, Y., Jang, N., Yasin, M., Park, S., and Chang, I.S. (2016). Intrinsic kinetic parameters of *Thermococcus onnurineus* NA1 strains and prediction of optimum carbon monoxide level for ideal bioreactor operation. Bioresour. Technol. *201*, 74–79.

Jetten, M.S.M., Stams, A.J.M., and Zehnder, A.J.B. (1992). Methanogenesis from acetate: a comparison of the acetate metabolism in *Methanothrix soehngenii* and *Methanosarcina* spp. FEMS Microbiol. Rev. *8*, 181–197.

Jia, B., Linh, L.T., Lee, S., Pham, B.P., Liu, J., Pan, H., Zhang, S., and Cheong, G.-W. (2011). Biochemical characterization of glyceraldehyde-3-phosphate dehydrogenase from *Thermococcus kodakarensis* KOD1. Extrem. Life Extreme Cond. *15*, 337–346.

Jiang, Z., Harrington, P., Zhang, M., Marjani, S.L., Park, J., Kuo, L., Pribenszky, C., and Tian, X. (Cindy) (2016). Effects of high hydrostatic pressure on expression profiles of *in vitro* produced vitrified bovine blastocysts. Sci. Rep. *6*:21215.

Johnsen, U., Hansen, T., and Schonheit, P. (2003). Comparative analysis of pyruvate kinases from the hyperthermophilic archaea *Archaeoglobus fulgidus*, *Aeropyrum pernix*, and *Pyrobaculum aerophilum* and the hyperthermophilic bacterium *Thermotoga maritima*: unusual regulatory properties in hyperthermophilic archaea. J. Biol. Chem. *278*, 25417–25427.

Jongsareejit, B., Rahman, R.N., Fujiwara, S., and Imanaka, T. (1997). Gene cloning, sequencing and enzymatic properties of glutamate synthase from the hyperthermophilic archaeon *Pyrococcus* sp. KOD1. Mol. Gen. Genet. MGG *254*, 635–642.

Jung, H.-C., Lee, S.H., Lee, S.-M., An, Y.J., Lee, J.-H., Lee, H.S., and Kang, S.G. (2017). Adaptive evolution of a hyperthermophilic archaeon pinpoints a formate transporter as a critical factor for the growth enhancement on formate. Sci. Rep. *7*, 6124.

Jung, J.-H., Seo, D.-H., Holden, J.F., and Park, C.-S. (2014). Maltose-forming α-amylase from the hyperthermophilic archaeon *Pyrococcus* sp. ST04. Appl. Microbiol. Biotechnol. *98*, 2121–2131.

Kanai, T., Ito, S., and Imanaka, T. (2003). Characterization of a Cytosolic NiFe-Hydrogenase from the Hyperthermophilic Archaeon *Thermococcus kodakaraensis* KOD1. J. Bacteriol. *185*, 1705–1711.

Kanai, T., Imanaka, H., Nakajima, A., Uwamori, K., Omori, Y., Fukui, T., Atomi, H., and Imanaka, T. (2005a). Continuous hydrogen production by the hyperthermophilic archaeon, *Thermococcus kodakaraensis* KOD1. J. Biotechnol. *116*, 271–282.

Kanai, T., Imanaka, H., Nakajima, A., Uwamori, K., Omori, Y., Fukui, T., Atomi, H., and Imanaka, T. (2005b). Continuous hydrogen production by the hyperthermophilic archaeon, *Thermococcus kodakaraensis* KOD1. J. Biotechnol. *116*, 271–282.

Kanai, T., Akerboom, J., Takedomi, S., Werken, H.J.G. van de, Blombach, F., Oost, J. van der, Murakami, T., Atomi, H., and Imanaka, T. (2007). A global transcriptional regulator in *Thermococcus kodakaraensis* controls the expression levels of both glycolytic and gluconeogenic enzyme-encoding genes. J. Biol. Chem. *282*, 33659–33670.

Kanai, T., Takedomi, S., Fujiwara, S., Atomi, H., and Imanaka, T. (2010). Identification of the Phr-dependent heat shock regulon in the hyperthermophilic archaeon, *Thermococcus kodakaraensis*. J. Biochem. (Tokyo) *147*, 361–370.

Kanai, T., Matsuoka, R., Beppu, H., Nakajima, A., Okada, Y., Atomi, H., and Imanaka, T. (2011). Distinct physiological roles of the three [NiFe]-hydrogenase orthologs in the hyperthermophilic archaeon *Thermococcus kodakarensis*. J. Bacteriol. *193*, 3109–3116.

Kanai, T., Imanaka, T., and Atomi, H. (2013). Hydrogen production by the hyperthermophilic archaeon *Thermococcus kodakarensis*. J. Jpn. Pet. Inst. *56*, 267–279.

Kanai, T., Simons, J.-R., Tsukamoto, R., Nakajima, A., Omori, Y., Matsuoka, R., Beppu, H., Imanaka, T., and Atomi, H. (2015). Overproduction of the membrane-bound [NiFe]-hydrogenase in *Thermococcus kodakarensis* and its effect on hydrogen production. Front. Microbiol. *6*:847.

Kanai, T., Yasukochi, A., Simons, J.-R., Scott, J.W., Fukuda, W., Imanaka, T., and Atomi, H. (2017). Genetic analyses of the functions of [NiFe]-hydrogenase maturation endopeptidases in the hyperthermophilic archaeon *Thermococcus kodakarensis*. Extrem. Life Extreme Cond. *21*, 27–39.

Kaneko, H., Takami, H., Inoue, A., and Horikoshi, K. (2000). Effects of hydrostatic pressure and temperature on growth and lipid composition of the inner membrane of barotolerant *Pseudomonas* sp. BT1 isolated from the deep-sea. Biosci. Biotechnol. Biochem. *64*, 72–79.

Kang, S.G., Lee, J.H., Lee, H.S., Kwon, K.K., Kim, T.W., Kim, Y.J., Kim, M.S., LEE, S.H., Bae, S.S., and CHOI, A.R. (2017). *Thermococcus onnurineus* MC02 and method of hydrogen production using thereof. Patentt 10-2012-0103238.

Kannan, Y., Koga, Y., Inoue, Y., Haruki, M., Takagi, M., Imanaka, T., Morikawa, M., and Kanaya, S. (2001). Active subtilisin-like protease from a hyperthermophilic archaeon in a form with a putative prosequence. Appl. Environ. Microbiol. *67*, 2445–2452.

Kato, M., Hayashi, R., Tsuda, T., and Taniguchi, K. (2002). High pressure-induced changes of biological membrane. Study on the membrane-bound Na(+)/K(+)-ATPase as a model system. Eur. J. Biochem. *269*, 110–118.

Keese, A.M., Schut, G.J., Ouhammouch, M., Adams, M.W.W., and Thomm, M. (2010). Genome-wide identification of targets for the archaeal heat shock regulator phr by cell-free transcription of genomic DNA. J. Bacteriol. *192*, 1292–1298.

Kelly, N.A., Gibson, T.L., and Ouwerkerk, D.B. (2008). A solar-powered, high-efficiency hydrogen fueling system using high-pressure electrolysis of water: Design and initial results. Int. J. Hydrog. Energy *33*, 2747–2764.

Kengen, S.W.M., and Stams, A.J.M. (1994a). Formation of l-alanine as a reduced end product in carbohydrate fermentation by the hyperthermophilic archaeon *Pyrococcus furiosus*. Arch. Microbiol. *161*, 168–175.

Kengen, S.W.M., and Stams, A.J.M. (1994b). Growth and energy conservation in batch cultures of *Pyrococcus furiosus*. FEMS Microbiol. Lett. *117*, 305–310.

Kengen, S.W.M., Stams, A.J.M., and de Vos, W.M. (1996). Sugar metabolism of hyperthermophiles. FEMS Microbiol. Rev. *18*, 119–137.

Kengen, S.W., Luesink, E.J., Stams, A.J., and Zehnder, A.J. (1993). Purification and characterization of an extremely thermostable beta-glucosidase from the hyperthermophilic archaeon *Pyrococcus furiosus*. Eur. J. Biochem. *213*, 305–312.

Kengen, S.W., de Bok, F.A., van Loo, N.D., Dijkema, C., Stams, A.J., and de Vos, W.M. (1994). Evidence for the operation of a novel Embden-Meyerhof pathway that involves ADP-dependent kinases during sugar fermentation by *Pyrococcus furiosus*. J. Biol. Chem. *269*, 17537–17541.

Kengen, S.W., Tuininga, J.E., de Bok, F.A., Stams, A.J., and de Vos, W.M. (1995). Purification and characterization of a novel ADP-dependent glucokinase from the hyperthermophilic archaeon *Pyrococcus furiosus*. J. Biol. Chem. *270*, 30453–30457.

Kim, M.-S., Bae, S.S., Kim, Y.J., Kim, T.W., Lim, J.K., Lee, S.H., Choi, A.R., Jeon, J.H., Lee, J.-H., Lee, H.S., et al. (2013). CO-dependent H_2 production by genetically engineered *Thermococcus onnurineus* NA1. Appl. Environ. Microbiol. *79*, 2048–2053.

Kim, M.-S., Choi, A.R., Lee, S.H., Jung, H.-C., Bae, S.S., Yang, T.-J., Jeon, J.H., Lim, J.K., Youn, H., Kim, T.W., et al. (2015). A Novel CO-Responsive Transcriptional Regulator and Enhanced H2 Production by an Engineered *Thermococcus onnurineus* NA1 Strain. Appl. Environ. Microbiol. *81*, 1708–1714.

Kim, M.-S., Fitriana, H.N., Kim, T.W., Kang, S.G., Jeon, S.G., Chung, S.H., Park, G.W., and Na, J.-G. (2017). Enhancement of the hydrogen productivity in microbial water gas shift reaction by *Thermococcus onnurineus* NA1 using a pressurized bioreactor. Int. J. Hydrog. Energy *42*, 27593–27599.

Kim, M.-S., Moon, M., Fitriana, H.N., Lee, J.-S., Na, J.-G., and Park, G.W. (2020). Pressurized cultivation strategies for improved microbial hydrogen production by *Thermococcus onnurineus* NA1. Bioprocess Biosyst. Eng. *43*:6, 1119-1122.

Kim, S.-Y., Jeong, H.J., Kim, M., Choi, A.R., Kim, M.-S., Kang, S.G., and Lee, S.-J. (2019). Characterization of the copper-sensing transcriptional regulator CopR from the hyperthermophilic archeaon *Thermococcus onnurineus* NA1. BioMetals. *32*:6, 923-937.

Kim, Y.J., Lee, H.S., Kim, E.S., Bae, S.S., Lim, J.K., Matsumi, R., Lebedinsky, A.V., Sokolova, T.G., Kozhevnikova, D.A., Cha, S.-S., et al. (2010). Formate-driven growth coupled with H_2 production. Nature *467*, 352–355.

Klages, K.U., and Morgan, H.W. (1994). Characterization of an extremely thermophilic sulphur-metabolizing archaebacterium belonging to the *Thermococcales*. Arch. Microbiol. *162*, 261–266.

Kletzin, A., and Adams, M.W. (1996). Molecular and phylogenetic characterization of pyruvate and 2-ketoisovalerate ferredoxin oxidoreductases from *Pyrococcus furiosus* and pyruvate ferredoxin oxidoreductase from *Thermotoga maritima*. J. Bacteriol. *178*, 248–257.

Klingeberg, M., Galunsky, B., Sjoholm, C., Kasche, V., and Antranikian, G. (1995). Purification and properties of a highly thermostable, sodium dodecyl sulfate-resistant and stereospecific proteinase from the extremely thermophilic archaeon *Thermococcus stetteri*. Appl. Environ. Microbiol. *61*, 3098–3104.

Kobayashi, H., Takaki, Y., Kobata, K., Takami, H., and Inoue, A. (1998). Characterization of α-maltotetraohydrolase produced by *Pseudomonas* sp. MS300 isolated from the deepest site of the Mariana Trench. Extremophiles *2*, 401–407.

Kobayashi, T., Higuchi, S., Kimura, K., Kudo, T., and Horikoshi, K. (1995). Properties of glutamate dehydrogenase and its involvement in alanine production in a hyperthermophilic archaeon, *Thermococcus profundus*. J. Biochem. *118*, 587–592.

Kobori, H., Ogino, M., Orita, I., Nakamura, S., Imanaka, T., and Fukui, T. (2010). Characterization of NADH oxidase/NADPH polysulfide oxidoreductase and its unexpected participation in oxygen sensitivity in an anaerobic hyperthermophilic archaeon. J. Bacteriol. *192*, 5192–5202.

Koga, Y. (2012). Thermal Adaptation of the Archaeal and Bacterial Lipid Membranes. Archaea *2012*:789652.

Komati Reddy, G., Lindner, S.N., and Wendisch, V.F. (2015). Metabolic engineering of an ATP-neutral Embden-Meyerhof-Parnas pathway in *Corynebacterium glutamicum*: growth restoration by an adaptive point mutation in NADH dehydrogenase. Appl. Environ. Microbiol. *81*, 1996–2005.

Koning, S.M., Elferink, M.G.L., Konings, W.N., and Driessen, A.J.M. (2001). Cellobiose uptake in the hyperthermophilic archaeon *Pyrococcus furiosus* is mediated by an inducible, high-affinity ABC transporter. J. Bacteriol. *183*, 4979–4984.

Koning, S.M., Albers, S.-V., Konings, W.N., and Driessen, A.J.M. (2002a). Sugar transport in (hyper)thermophilic archaea. Res. Microbiol. *153*, 61–67.

Koning, S.M., Konings, W.N., and Driessen, A.J.M. (2002b). Biochemical evidence for the presence of two α-glucoside ABC-transport systems in the hyperthermophilic archaeon *Pyrococcus furiosus*.

Kowalak, J.A., Dalluge, J.J., McCloskey, J.A., and Stetter, K.O. (1994). The role of posttranscriptional modification in stabilization of transfer RNA from hyperthermophiles. Biochemistry *33*, 7869–7876.

Kozhevnikova, D.A., Taranov, E.A., Lebedinsky, A.V., Bonch-Osmolovskaya, E.A., and Sokolova, T.G. (2016). Hydrogenogenic and sulfidogenic growth of *Thermococcus* archaea on carbon monoxide and formate. Mikrobiologiia *85*, 381–392.

Krajačić, G., Martins, R., Busuttil, A., Duić, N., and da Graça Carvalho, M. (2008). Hydrogen as an energy vector in the islands' energy supply. Int. J. Hydrog. Energy *33*, 1091–1103.

Kreuzer, M., Schmutzler, K., Waege, I., Thomm, M., and Hausner, W. (2013). Genetic engineering of *Pyrococcus furiosus* to use chitin as a carbon source. BMC Biotechnol. *13*, 9.

Krupovic, M., Gonnet, M., Hania, W.B., Forterre, P., and Erauso, G. (2013). Insights into dynamics of mobile genetic elements in hyperthermophilic environments from five new *Thermococcus* plasmids. PLOS ONE *8*, e49044.

Krzyżaniak, A., Barciszewski, J., Fürste, J.P., Bald, R., Erdmann, V.A., Salański, P., and Jurczak, J. (1994). A-Z-RNA conformational changes effected by high pressure. Int. J. Biol. Macromol. *16*, 159–162.

Kumar, S., and Nussinov, R. (2001). How do thermophilic proteins deal with heat? Cell. Mol. Life Sci. CMLS *58*, 1216–1233.

Kuwabara, T., Minaba, M., Iwayama, Y., Inouye, I., Nakashima, M., Marumo, K., Maruyama, A., Sugai, A., Itoh, T., Ishibashi, J., et al. (2005). *Thermococcus coalescens* sp. nov., a cell-fusing hyperthermophilic archaeon from Suiyo Seamount. Int. J. Syst. Evol. Microbiol. *55*, 2507–2514.

Kwan, P., McIntosh, C.L., Jennings, D.P., Hopkins, R.C., Chandrayan, S.K., Wu, C.-H., Adams, M.W.W., and Jones, A.K. (2015). The [NiFe]-hydrogenase of *Pyrococcus furiosus* exhibits a new type of oxygen tolerance. J. Am. Chem. Soc. *137*, 13556–13565.

Kwon, S., Nishitani, Y., Watanabe, S., Hirao, Y., Imanaka, T., Kanai, T., Atomi, H., and Miki, K. (2016). Crystal structure of a [NiFe] hydrogenase maturation protease HybD from *Thermococcus kodakarensis* KOD1. Proteins *84*, 1321–1327.

Lambros, R.J., Mortimer, J.R., and Forsdyke, D.R. (2003). Optimum growth temperature and the base composition of open reading frames in prokaryotes. Extrem. Life Extreme Cond. *7*, 443–450.

Landry, T.D., Chew, L., Davis, J.W., Frawyley, N., Foley, H.H., Stelman, S.J., Thomas, J., Wolt, J., and Hanselman, D.S. (2003). Safety evaluation of an alpha-amylase enzyme preparation derived from the archaeal order *Thermococcales* as expressed in *Pseudomonas fluorescens* biovar I. Regul. Toxicol. Pharmacol. *37*, 149–168.

Larson, W.P., Hartzell, T.B., and Diehl, H.S. (1918). The effect of high pressures on *Bacteria*. J. Infect. Dis. *22*, 271–279.

Lauro, F.M., Chastain, R.A., Blankenship, L.E., Yayanos, A.A., and Bartlett, D.H. (2007). The unique 16S rRNA genes of piezophiles reflect both phylogeny and adaptation. Appl. Environ. Microbiol. *73*, 838–845.

Le Fourn, C., Brasseur, G., Brochier-Armanet, C., Pieulle, L., Brioukhanov, A., Ollivier, B., and Dolla, A. (2011). An oxygen reduction chain in the hyperthermophilic anaerobe *Thermotoga maritima* highlights horizontal gene transfer between *Thermococcales* and *Thermotogales*. Environ. Microbiol. *13*, 2132–2145.

Le Guellec, S. (2019). Identification et caractérisation fonctionnelle des communautés microbiennes en interaction avec les minéralisations hydrothermales. PhD thesis. Université Bretagne Loire.

Lee, A.G. (2004). How lipids affect the activities of integral membrane proteins. Biochim. Biophys. Acta *1666*, 62–87.

Lee, H.-S., Shockley, K.R., Schut, G.J., Conners, S.B., Montero, C.I., Johnson, M.R., Chou, C.-J., Bridger, S.L., Wigner, N., Brehm, S.D., et al. (2006). Transcriptional and biochemical analysis of starch metabolism in the hyperthermophilic archaeon *Pyrococcus furiosus*. J. Bacteriol. *188*, 2115–2125.

Lee, H.S., Kang, S.G., Bae, S.S., Lim, J.K., Cho, Y., Kim, Y.J., Jeon, J.H., Cha, S.-S., Kwon, K.K., Kim, H.-T., et al. (2008). The complete genome sequence of *Thermococcus onnurineus* NA1 reveals a mixed heterotrophic and carboxydotrophic metabolism. J. Bacteriol. *190*, 7491–7499.

Lee, J., Kim, Y.-G., Kim, K.K., and Seok, C. (2010). Transition between b-dna and z-dna: free energy landscape for the B-Z junction propagation - PubMed. J. Phys. Chem. B *114*, 9872–9881.

Lee, S.H., Kim, M.-S., Jung, H.C., Lee, J., Lee, J.-H., Lee, H.S., and Kang, S.G. (2015). Screening of a novel strong promoter by RNA sequencing and its application to H_2 production in a hyperthermophilic archaeon. Appl. Microbiol. Biotechnol. *99*, 4085–4092.

Lee, S.H., Kim, M.-S., Lee, J.H., Kim, T.W., Bae, S.S., Lee, S.-M., Jung, H.C., Yang, T.-J., Choi, A.R., Cho, Y.-J., et al. (2016). Adaptive engineering of a hyperthermophilic archaeon on CO and discovering the underlying mechanism by multi-omics analysis. Sci. Rep. *6*.

Lee, S.H., Kim, M.-S., Kim, Y.J., Kim, T.W., Kang, S.G., and Lee, H.S. (2017). Transcriptomic profiling and its implications for the H2 production of a non-methanogen deficient in the frhAGB-encoding hydrogenase. Appl. Microbiol. Biotechnol. *101*, 5081–5088.

Lee, S.H., Lee, S.-M., Lee, J.-H., Lee, H.S., and Kang, S.G. (2020). Biological process for coproduction of hydrogen and thermophilic enzymes during CO fermentation. Bioresour. Technol. *305*, 123067.

Lee, S.-J., Engelmann, A., Horlacher, R., Qu, Q., Vierke, G., Hebbeln, C., Thomm, M., and Boos, W. (2003). TrmB, a sugar-specific transcriptional regulator of the trehalose/maltose ABC transporter from the hyperthermophilic archaeon *Thermococcus litoralis*. J. Biol. Chem. *278*, 983–990.

Lee, S.-J., Moulakakis, C., Koning, S.M., Hausner, W., Thomm, M., and Boos, W. (2005). TrmB, a sugar sensing regulator of ABC transporter genes in *Pyrococcus furiosus* exhibits dual promoter specificity and is controlled by different inducers. Mol. Microbiol. *57*, 1797–1807.

Lee, S.J., Böhm, A., Krug, M., and Boos, W. (2007). The ABC of binding-protein-dependent transport in *Archaea*. Trends Microbiol. *15*, 389–397.

Lee, S.-J., Surma, M., Hausner, W., Thomm, M., and Boos, W. (2008c). The role of TrmB and TrmB-like transcriptional regulators for sugar transport and metabolism in the hyperthermophilic archaeon *Pyrococcus furiosus*. Arch. Microbiol. *190*, 247.

Lee, S.-M., Lee, J., Lee, S.H., Kim, J.Y., Lee, H.S., and Kang, S.G. (2019). Formulation of a low-cost medium for improved cost-effectiveness of hydrogen production by *Thermococcus onnurineus* NA1. Biotechnol. Bioprocess Eng. *24*, 833–838.

Lee, S.Y., Choi, M.-J., Cho, H.-Y., and Davaatseren, M. (2016c). Effects of high-pressure, microbial transglutaminase and glucono-δ-lactone on the aggregation properties of skim milk. Korean J. Food Sci. Anim. Resour. *36*, 335–342.

Leigh, J.A., Albers, S.-V., Atomi, H., and Allers, T. (2011). Model organisms for genetics in the domain Archaea: methanogens, halophiles, *Thermococcales* and *Sulfolobales*. FEMS Microbiol. Rev. *35*, 577–608.

Li, H., and Durbin, R. (2010). Fast and accurate long-read alignment with Burrows-Wheeler transform. Bioinforma. Oxf. Engl. *26*, 589–595.

Li, X., Fu, L., Li, Z., Ma, X., Xiao, X., and Xu, J. (2014). Genetic tools for the piezophilic hyperthermophilic archaeon *Pyrococcus yayanosii*. Extrem. Life Extreme Cond. *19*.

Li, Z., Li, X., Xiao, X., and Xu, J. (2016). An integrative genomic island affects the adaptations of the piezophilic hyperthermophilic archaeon *Pyrococcus yayanosii* to high temperature and high hydrostatic pressure. Front. Microbiol. *7*:1927.

Liang, J., Huang, H., and Wang, S. (2019). Distribution, evolution, catalytic mechanism, and physiological functions of the flavin-based electron-bifurcating NADH-dependent reduced ferredoxin: $NADP^+$ oxidoreductase. Front. Microbiol. *10*:373.

Lim, J.K., Kang, S.G., Lebedinsky, A.V., Lee, J.-H., and Lee, H.S. (2010). Identification of a novel class of membrane-bound [NiFe]-hydrogenases in *Thermococcus onnurineus* NA1 by *in silico* analysis. Appl. Environ. Microbiol. *76*, 6286–6289.

Lim, J.K., Bae, S.S., Kim, T.W., Lee, J.-H., Lee, H.S., and Kang, S.G. (2012). thermodynamics of formate-oxidizing metabolism and implications for H_2 production. Appl. Environ. Microbiol. *78*, 7393–7397.

Lim, J.K., Jung, H.-C., Kang, S.G., and Lee, H.S. (2017). Redox regulation of SurR by protein disulfide oxidoreductase in *Thermococcus onnurineus* NA1. Extremophiles *21*, 491–498.

Lindahl, T., and Andersson, A. (1972). Rate of chain breakage at apurinic sites in double-stranded deoxyribonucleic acid. Biochemistry *11*, 3618–3623.

Lindahl, T., and Karlstrom, O. (1973). Heat-induced depyrimidination of deoxyribonucleic acid in neutral solution. Biochemistry *12*, 5151–5154.

Linde Stories (2019). Hydrogen-powered drone lasts three times longer.

Lipscomb, G.L., Keese, A.M., Cowart, D.M., Schut, G.J., Thomm, M., Adams, M.W.W., and Scott, R.A. (2009). SurR: a transcriptional activator and repressor controlling hydrogen and elemental sulphur metabolism in *Pyrococcus furiosus*. Mol. Microbiol. *71*, 332–349.

Lipscomb, G.L., Stirrett, K., Schut, G.J., Yang, F., Jenney, F.E., Scott, R.A., Adams, M.W.W., and Westpheling, J. (2011). Natural competence in the hyperthermophilic archaeon *Pyrococcus* furiosus facilitates genetic manipulation: construction of markerless deletions of genes encoding the two cytoplasmic hydrogenases. Appl. Environ. Microbiol. *77*, 2232–2238.

Lipscomb, G.L., Schut, G.J., Scott, R.A., and Adams, M.W.W. (2017). SurR is a master regulator of the primary electron flow pathways in the order *Thermococcales*. Mol. Microbiol. *104*, 869–881.

Liu, P., Ding, W., Lai, Q., Liu, R., Wei, Y., Wang, L., Xie, Z., Cao, J., and Fang, J. (2019). Physiological and genomic features of *Paraoceanicella profunda* gen. nov., sp. nov., a novel piezophile isolated from deep seawater of the Mariana Trench. Microbiology Open *9*:2, e966.

Livak, K.J., and Schmittgen, T.D. (2001). Analysis of relative gene expression data using real-time quantitative PCR and the $2^{-\Delta\Delta CT}$ method. Methods *25*, 402–408.

López-García, P., St Jean, A., Amils, R., and Charlebois, R.L. (1995). Genomic stability in the archaeae *Haloferax volcanii* and *Haloferax mediterranei*. J. Bacteriol. *177*, 1405–1408.

Lu, C., Zhang, H., Zhang, Q., Chu, C., Tahir, N., Ge, X., Jing, Y., Hu, J., Li, Y., Zhang, Y., et al. (2020). An automated control system for pilot-scale biohydrogen production: Design, operation and validation. Int. J. Hydrog. Energy *45*, 3795–3806.

Lubner, C.E., Jennings, D.P., Mulder, D.W., Schut, G.J., Zadvornyy, O.A., Hoben, J.P., Tokmina-Lukaszewska, M., Berry, L., Nguyen, D.M., Lipscomb, G.L., et al. (2017). Mechanistic insights into energy conservation by flavin-based electron bifurcation. Nat. Chem. Biol. *13*, 655–659.

Lucas, S., Toffin, L., Zivanovic, Y., Charlier, D., Moussard, H., Forterre, P., Prieur, D., and Erauso, G. (2002). Construction of a shuttle vector for, and spheroplast transformation of, the hyperthermophilic archaeon *Pyrococcus abyssi*. Appl. Environ. Microbiol. *68*, 5528–5536.

Lundberg, K.S., Shoemaker, D.D., Adams, M.W.W., Short, J.M., Sorge, J.A., and Mathur, E.J. (1991). High-fidelity amplification using a thermostable DNA polymerase isolated from *Pyrococcus furiosus*. Gene *108*, 1–6.

Ma, K., and Adams, M.W.W. (1994). Sulfide dehydrogenase from the hyperthermophilic archaeon *Pyrococcus furiosus*: a new multifunctional enzyme involved in the reduction of elemental sulfur. J. Bacteriol. *176*, 6509–6517.

Ma, K., and Adams, M.W. (2001a). Hydrogenases I and II from *Pyrococcus furiosus*. Methods Enzymol. *331*, 208–216.

Ma, K., and Adams, M.W.W. (2001b). Ferredoxin:NADP oxidoreductase from *Pyrococcus furiosus*. Methods Enzymol. *334*, 40–45.

Ma, K., Schicho, R.N., Kelly, R.M., and Adams, M.W.W. (1993). Hydrogenase of the hyperthermophile *Pyrococcus furiosus* is an elemental sulfur reductase or sulfhydrogenase: evidence for a sulfur-reducing hydrogenase ancestor. Proc. Natl. Acad. Sci. U. S. A. *90*, 5341–5344.

Ma, K., Robb, F.T., and Adams, M.W.W. (1994). Purification and characterization of NADP-specific alcohol dehydrogenase and glutamate dehydrogenase from the hyperthermophilic archaeon *Thermococcus litoralis*. Appl. Environ. Microbiol. *60*, 562–568.

Ma, K., Loessner, H., Heider, J., Johnson, M.K., and Adams, M.W. (1995). Effects of elemental sulfur on the metabolism of the deep-sea hyperthermophilic archaeon *Thermococcus* strain ES-1: characterization of a sulfur-regulated, non-heme iron alcohol dehydrogenase. J. Bacteriol. *177*, 4748–4756.

Ma, K., Hutchins, A., Sung, S.J., and Adams, M.W. (1997). Pyruvate ferredoxin oxidoreductase from the hyperthermophilic archaeon, *Pyrococcus furiosus*, functions as a CoA-dependent pyruvate decarboxylase. Proc. Natl. Acad. Sci. U. S. A. *94*, 9608–9613.

Macedo-Ribeiro, S., Darimont, B., Sterner, R., and Huber, R. (1996). Small structural changes account for the high thermostability of 1[4Fe-4S] ferredoxin from the hyperthermophilic bacterium *Thermotoga maritima*. Struct. Lond. Engl. 1993 *4*, 1291–1301.

Macgregor, R.B. (1998). Effect of hydrostatic pressure on nucleic acids. Biopolymers *48*, 253–263.

MacGregor, R.B., and Chen, M.Y. (1990). Delta V0 of the Na(+)-induced B-Z transition of poly[d(G-C)] is positive. Biopolymers *29*, 1069–1076.

Madigan, M.T., Bender, K.S., Buckley, D.H., Sattley, W.M., and Stahl, D.A. (2017). Brock Biology of Microorganisms (NY, NY: Pearson).

Maeder, D.L., Weiss, R.B., Dunn, D.M., Cherry, J.L., González, J.M., DiRuggiero, J., and Robb, F.T. (1999). Divergence of the hyperthermophilic archaea *Pyrococcus furiosus* and *P. horikoshii* inferred from complete genomic sequences. Genetics *152*, 1299–1305.

Magnabosco, C., Lin, L.-H., Dong, H., Bomberg, M., Ghiorse, W., Stan-Lotter, H., Pedersen, K., Kieft, T.L., van Heerden, E., and Onstott, T.C. (2018). The biomass and biodiversity of the continental subsurface. Nat. Geosci. *11*, 707–717.

Mai, X., and Adams, M.W.W. (1994). Indolepyruvate ferredoxin oxidoreductase from the hyperthermophilic archaeon *Pyrococcus furiosus*. A new enzyme involved in peptide fermentation. J. Biol. Chem. *269*, 16726–16732.

Mai, X., and Adams, M.W.W. (1996a). Characterization of a fourth type of 2-keto acid-oxidizing enzyme from a hyperthermophilic archaeon: 2-ketoglutarate ferredoxin oxidoreductase from *Thermococcus litoralis*. J. Bacteriol. *178*, 5890–5896.

Mai, X., and Adams, M.W.W. (1996b). Purification and characterization of two reversible and ADP-dependent acetyl coenzyme A synthetases from the hyperthermophilic archaeon *Pyrococcus furiosus*. J. Bacteriol. *178*, 5897–5903.

Makarova, K.S., Yutin, N., Bell, S.D., and Koonin, E.V. (2010). Evolution of diverse cell division and vesicle formation systems in *Archaea*. Nat. Rev. Microbiol. *8*, 731–741.

Makarova, K.S., Wolf, Y.I., and Koonin, E.V. (2019). Towards functional characterization of archaeal genomic dark matter. Biochem. Soc. Trans. *47*, 389–398.

Makridis, S.S. (2016). Hydrogen storage and compression. Methane Hydrog. Energy Storage 1–28.

Mañas, P., and Pagán, R. (2005). Microbial inactivation by new technologies of food preservation. J. Appl. Microbiol. *98*, 1387–1399.

Mandal, T.K., and Gregory, D.H. (2010). Hydrogen: A future energy vector for sustainable development. Proc. Inst. Mech. Eng. Part C J. Mech. Eng. Sci. *224*, 539–558.

Mardanov, A.V., Ravin, N.V., Svetlitchnyi, V.A., Beletsky, A.V., Miroshnichenko, M.L., Bonch-Osmolovskaya, E.A., and Skryabin, K.G. (2009). Metabolic Versatility and Indigenous Origin of the Archaeon *Thermococcus sibiricus*, Isolated from a Siberian Oil Reservoir, as Revealed by Genome Analysis. Appl. Environ. Microbiol. *75*, 4580–4588.

Marteinsson, V.T., Moulin, P., Birrien, J., Gambacorta, A., Vernet, M., and Prieur, D. (1997). Physiological responses to stress conditions and barophilic behavior of the hyperthermophilic vent archaeon *Pyrococcus abyssi*. Appl. Environ. Microbiol. *63*, 1230–1236.

Marteinsson, V.T., Birrien, J.-L., Reysenbach, A.-L., Vernet, M., Marie, D., Gambacorta, A., Messner, P., Sleytr, U.B., and Prieur, D. (1999a). *Thermococcus barophilus* sp. nov., a new barophilic and hyperthermophilic archaeon isolated under high hydrostatic pressure from a deep-sea hydrothermal vent. Int. J. Syst. Evol. Microbiol. *49*, 351–359.

Marteinsson, V.T., Reysenbach, A.L., Birrien, J.L., and Prieur, D. (1999b). A stress protein is induced in the deep-sea barophilic hyperthermophile *Thermococcus barophilus* when grown under atmospheric pressure. Extremophiles *3*, 277–282.

Martin, D., Bartlett, D.H., and Roberts, M.F. (2002). Solute accumulation in the deep-sea bacterium *Photobacterium profundum*. Extremophiles *6*, 507–514.

Martin, W., Baross, J., Kelley, D., and Russell, M.J. (2008). Hydrothermal vents and the origin of life. Nat. Rev. Microbiol. *6*, 805–814.

Martinez, N., Michoud, G., Cario, A., Ollivier, J., Franzetti, B., Jebbar, M., Oger, P., and Peters, J. (2016). High protein flexibility and reduced hydration water dynamics are key pressure adaptive strategies in prokaryotes. Sci. Rep. *6*, 32816.

Mathai, J.C., Sprott, G.D., and Zeidel, M.L. (2001). Molecular mechanisms of water and solute transport across archaebacterial lipid membranes. J. Biol. Chem. *276*, 27266–27271.

Matsubara, K., Yokooji, Y., Atomi, H., and Imanaka, T. (2011). Biochemical and genetic characterization of the three metabolic routes in *Thermococcus kodakarensis* linking glyceraldehyde 3-phosphate and 3-phosphoglycerate. Mol. Microbiol. *81*, 1300–1312.

Matsui, I., Matsui, E., Sakai, Y., Kikuchi, H., Kawarabayasi, Y., Ura, H., Kawaguchi, S., Kuramitsu, S., and Harata, K. (2000). The molecular structure of hyperthermostable aromatic aminotransferase with novel substrate specificity from *Pyrococcus horikoshii*. J. Biol. Chem. *275*, 4871–4879.

Matsumi, R., Manabe, K., Fukui, T., Atomi, H., and Imanaka, T. (2007). Disruption of a sugar transporter gene cluster in a hyperthermophilic archaeon using a host-marker system based on antibiotic resistance. J. Bacteriol. *189*, 2683–2691.

Mayer, F., and Müller, V. (2014). Adaptations of anaerobic archaea to life under extreme energy limitation. FEMS Microbiol. Rev. *38*, 449–472.

Mayer, F., Lim, J.K., Langer, J.D., Kang, S.G., and Müller, V. (2015). Na+ transport by the a1ao-atp synthase purified from *Thermococcus onnurineus* and reconstituted into liposomes. J. Biol. Chem. *290*, 6994–7002.

Mayyas, A., and Mann, M. (2019). Manufacturing competitiveness analysis for hydrogen refueling stations. Int. J. Hydrog. Energy *44*, 9121–9142.

McCarthy, B.J. (1962). The effects of magnesium starvation on the ribosome content of *Escherichia coli.* Biochim. Biophys. Acta *55*, 880–889.

McCollom, T.M. (2007). Geochemical constraints on sources of metabolic energy for chemolithoautotrophy in ultramafic-hosted deep-sea hydrothermal systems. Astrobiology *7*, 933–950.

McMahon, S., Parnell, J., and Blamey, N.J.F. (2016). Evidence for Seismogenic Hydrogen Gas, a Potential Microbial Energy Source on Earth and Mars. Astrobiology *16*, 690–702.

Mehta, R., Singhal, P., Singh, H., Damle, D., and Sharma, A.K. (2016). Insight into thermophiles and their wide-spectrum applications. 3 Biotech *6*.

Meillaud, L. (2020). Dijon lance une station de production d'hydrogène en circuit court.

Menini, E., and Van Dover, C.L. (2019). An atlas of protected hydrothermal vents. Mar. Policy *108*, 103654.

Menon, A.L., Hendrix, H., Hutchins, A., Verhagen, M.F., and Adams, M.W.W. (1998). The delta-subunit of pyruvate ferredoxin oxidoreductase from *Pyrococcus furiosus* is a redox-active, iron-sulfur protein: evidence for an ancestral relationship with 8Fe-type ferredoxins. Biochemistry *37*, 12838–12846.

Meyer, J. (2008). Iron-sulfur protein folds, iron-sulfur chemistry, and evolution. J. Biol. Inorg. Chem. JBIC Publ. Soc. Biol. Inorg. Chem. *13*, 157–170.

Michoud, G. (2014). Etude des effets des hautes pressions hydrostatiques sur *Pyrococcus yayanosii* un piézophile extrême par une approche multi "omics.". PhD thesis. Université de Bretagne Occidentale.

Michoud, G., and Jebbar, M. (2016). High hydrostatic pressure adaptive strategies in an obligate piezophile *Pyrococcus yayanosii*. Sci. Rep. *6*.

MicroCyc (2017). Metabolism - MicroScope - Web interface system & specialized databases for (re)annotation and analysis of microbial genomes.

Miller, J.F., Shah, N.N., Nelson, C.M., Ludlow, J.M., and Clark, D.S. (1988a). Pressure and temperature effects on growth and methane production of the extreme thermophile *Methanococcus jannaschii*. Appl. Environ. Microbiol. *54*, 3039–3042.

Miller, J.F., Almond, E.L., Shah, N.N., Ludlow, J.M., Zollweg, J.A., Streett, W.B., Zinder, S.H., and Clark, D.S. (1988b). High-pressure-temperature bioreactor for studying pressure-temperature relationships in bacterial growth and productivity. Biotechnol. Bioeng. *31*, 407–413.

Milner, H.W., Lawrence, N.S., and French, C.S. (1950). Colloidal dispersion of chloroplast material. Science *111*, 633–634.

Miroshnichenko, M.L., Gongadze, G.M., Rainey, F.A., Kostyukova, A.S., Lysenko, A.M., Chernyh, N.A., and Bonch-Osmolovskaya, E.A. (1998). *Thermococcus gorgonarius* sp. nov. and Thermococcus pacificus sp. nov.: heterotrophic extremely thermophilic archaea from New Zealand submarine hot vents. Int. J. Syst. Bacteriol. *48*, 23–29.

Miroshnichenko, M.L., Hippe, H., Stackebrandt, E., Kostrikina, N.A., Chernyh, N.A., Jeanthon, C., Nazina, T.N., Belyaev, S.S., and Bonch-Osmolovskaya, E.A. (2001). Isolation and characterization of *Thermococcus sibiricus* sp. nov. from a Western Siberia high-temperature oil reservoir. Extrem. Life Extreme Cond. *5*, 85–91.

Mitchell, P., and Moyle, J. (1958). Group-translocation: a consequence of enzyme-catalysed group-transfer. Nature *182*, 372–373.

Moon, Y.-J., Kwon, J., Yun, S.-H., Lim, H.L., Kim, M.-S., Kang, S.G., Lee, J.-H., Choi, J.-S., Kim, S.I., and Chung, Y.-H. (2012). Proteome analyses of hydrogen-producing hyperthermophilic archaeon *Thermococcus onnurineus* NA1 in different one-carbon substrate culture conditions. Mol. Cell. Proteomics *11*.

Moon, Y.-J., Kwon, J., Yun, S.-H., Lim, H.L., Kim, J., Kim, S.J., Kang, S.G., Lee, J.-H., Kim, S.I., and Chung, Y.-H. (2015). Proteomic insights into sulfur metabolism in the hydrogen-producing hyperthermophilic archaeon *Thermococcus onnurineus* NA1. Int. J. Mol. Sci. *16*, 9167–9195.

Morikawa, M., Izawa, Y., Rashid, N., Hoaki, T., and Imanaka, T. (1994). Purification and characterization of a thermostable thiol protease from a newly isolated hyperthermophilic *Pyrococcus* sp. Appl. Environ. Microbiol. *60*, 4559–4566.

Morris, B.E.L., Henneberger, R., Huber, H., and Moissl-Eichinger, C. (2013). Microbial syntrophy: interaction for the common good. FEMS Microbiol. Rev. *37*, 384–406.

Mozhaev, V.V., Heremans, K., Frank, J., Masson, P., and Balny, C. (1996). High pressure effects on protein structure and function. Proteins *24*, 81–91.

Mukherjee, M., Vajpai, M., and Sankararamakrishnan, R. (2017). Anion-selective Formate/nitrite transporters: taxonomic distribution, phylogenetic analysis and subfamily-specific conservation pattern in prokaryotes. BMC Genomics *18*, 560.

Mukund, S., and Adams, M.W.W. (1995). Glyceraldehyde-3-phosphate ferredoxin oxidoreductase, a novel tungsten-containing enzyme with a potential glycolytic role in the hyperthermophilic archaeon *Pyrococcus furiosus*. J. Biol. Chem. *270*, 8389–8392.

Müller, V. (2004). An exceptional variability in the motor of archael A1A0 ATPases: from multimeric to monomeric rotors comprising 6-13 ion binding sites. J. Bioenerg. Biomembr. *36*, 115–125.

Murakami, T., Kanai, T., Takata, H., Kuriki, T., and Imanaka, T. (2006). A novel branching enzyme of the gh-57 family in the hyperthermophilic archaeon *Thermococcus kodakaraensis* KOD1. J. Bacteriol. *188*, 5915–5924.

NCBI (2020). Taxonomy browser (Thermococcales).

Neal, C., and Stanger, G. (1983). Hydrogen generation from mantle source rocks in Oman. Earth Planet. Sci. Lett. *66*, 315–320.

Neuner, A., Jannasch, H.W., Belkin, S., and Stetter, K.O. (1990). *Thermococcus litoralis* sp. nov.: A new species of extremely thermophilic marine archaebacteria. Arch. Microbiol. *153*, 205–207.

Neves, C., da Costa, M.S., and Santos, H. (2005). Compatible solutes of the hyperthermophile *Palaeococcus ferrophilus*: osmoadaptation and *Thermoadaptation* in the order *Thermococcales*. Appl. Environ. Microbiol. *71*, 8091–8098.

Nguyen, D.M.N., Schut, G.J., Zadvornyy, O.A., Tokmina-Lukaszewska, M., Poudel, S., Lipscomb, G.L., Adams, L.A., Dinsmore, J.T., Nixon, W.J., Boyd, E.S., et al. (2017). Two functionally distinct NADP+-dependent ferredoxin oxidoreductases maintain the primary redox balance of *Pyrococcus furiosus*. J. Biol. Chem. *292*, 14603–14616.

Nikolaidis, P., and Poullikkas, A. (2017). A comparative overview of hydrogen production processes. Renew. Sustain. Energy Rev. *67*, 597–611.

Nisa, K., Ashraf, S., Siddiqui, M.A., Taj, N., Habib-ur-Rehman, Bano, A., and Rashid, N. (2020). Purification and characterization of a thermostable pyruvate ferredoxin oxidoreductase/pyruvate decarboxylase from *Thermococcus kodakaraensis*. Pak. J. Zool. *52*, 1149–1156.

Nishiyama, M., Sowa, Y., Kimura, Y., Homma, M., Ishijima, A., and Terazima, M. (2013). High hydrostatic pressure induces counterclockwise to clockwise reversals of the *Escherichia coli* flagellar motor. J. Bacteriol. *195*, 1809–1814.

Nissen, L.S., and Basen, M. (2019). The emerging role of aldehyde:ferredoxin oxidoreductases in microbially-catalyzed alcohol production. J. Biotechnol. *306*, 105–117.

Nivin, V.A. (2019). Occurrence forms, composition, distribution, origin and potential hazard of natural hydrogen–hydrocarbon gases in ore deposits of the Khibiny and Lovozero massifs: a review. Minerals *9*, 535.

Nohara, K., Orita, I., Nakamura, S., Imanaka, T., and Fukui, T. (2014). Genetic examination and mass balance analysis of pyruvate/amino acid oxidation pathways in the hyperthermophilic archaeon *Thermococcus kodakarensis*. J. Bacteriol. *196*, 3831–3839.

Noll, K.M., Lapierre, P., Gogarten, J.P., and Nanavati, D.M. (2008). Evolution of mal ABC transporter operons in the *Thermococcales* and *Thermotogales*. BMC Evol. Biol. *8*, 7.

Nuttall, W.J., and Bakenne, A.T. (2020). Small-scale local hydrogen production. In Fossil Fuel Hydrogen: Technical, Economic and Environmental Potential, W.J. Nuttall, and A.T. Bakenne, eds. (Cham: Springer International Publishing), pp. 95–100.

Oberto, J., Gaudin, M., Cossu, M., Gorlas, A., Slesarev, A., Marguet, E., and Forterre, P. (2014). Genome sequence of a hyperthermophilic archaeon, *Thermococcus nautili* 30-1, that produces viral vesicles. Genome Announc. *2*:2, e00243-14.

Oger, P.M., and Cario, A. (2013). Adaptation of the membrane in *Archaea*. Biophys. Chem. *183*, 42–56.

Oger, P.M., and Jebbar, M. (2010). The many ways of coping with pressure. Res. Microbiol. *161*, 799–809.

Oger, P., Sokolova, T.G., Kozhevnikova, D.A., Taranov, E.A., Vannier, P., Lee, H.S., Kwon, K.K., Kang, S.G., Lee, J.-H., Bonch-Osmolovskaya, E.A., et al. (2016). complete genome sequence of the hyperthermophilic and piezophilic archaeon *Thermococcus barophilus* Ch5, capable of growth at the expense of hydrogenogenesis from carbon monoxide and formate. Genome Announc. *4*:1, e01534-15.

Ohmae, E., Miyashita, Y., and Kato, C. (2013). Thermodynamic and functional characteristics of deep-sea enzymes revealed by pressure effects. Extrem. Life Extreme Cond. *17*, 701–709.

Ohnsman, A. (2020). Hydrogen on the rise at CES, from drones and daimler trucks to Toyota's city of the future. Forbes.

van der Oost, J., Schut, G., Kengen, S.W., Hagen, W.R., Thomm, M., and de Vos, W.M. (1998). The ferredoxin-dependent conversion of glyceraldehyde-3-phosphate in the hyperthermophilic archaeon *Pyrococcus furiosus* represents a novel site of glycolytic regulation. J. Biol. Chem. *273*, 28149–28154.

Orita, I., Sato, T., Yurimoto, H., Kato, N., Atomi, H., Imanaka, T., and Sakai, Y. (2006). The ribulose monophosphate pathway substitutes for the missing pentose phosphate pathway in the archaeon *Thermococcus kodakaraensis*. J. Bacteriol. *188*, 4698–4704.

Orphan, V.J., Taylor, L.T., Hafenbradl, D., and Delong, E.F. (2000). Culture-dependent and culture-independent characterization of microbial assemblages associated with high-temperature petroleum reservoirs. Appl. Environ. Microbiol. *66*, 700–711.

Orth, J.D., Thiele, I., and Palsson, B.Ø. (2010). What is flux balance analysis? Nat. Biotechnol. *28*, 245–248.

Ortiz Cebolla, R., and Navas, C. (2019). Supporting hydrogen technologies deployment in EU regions and Member States: The Smart Specialisation Platform on Energy (S3PEnergy). Int. J. Hydrog. Energy *44*, 19067–19079.

Oslowski, D.M., Jung, J.-H., Seo, D.-H., Park, C.-S., and Holden, J.F. (2011). production of hydrogen from α-1,4- and β-1,4-linked saccharides by marine hyperthermophilic archaea. Appl. Environ. Microbiol. *77*, 3169–3173.

Ozawa, Y., Nakamura, T., Kamata, N., Yasujima, D., Urushiyama, A., Yamakura, F., Ohmori, D., and Imai, T. (2005). *Thermococcus profundus* 2-ketoisovalerate ferredoxin oxidoreductase, a key enzyme in the archaeal energy-producing amino acid metabolic pathway. J. Biochem. (Tokyo) *137*, 101–107.

Ozawa, Y., Siddiqui, M.A., Takahashi, Y., Urushiyama, A., Ohmori, D., Yamakura, F., Arisaka, F., and Imai, T. (2012). Indolepyruvate ferredoxin oxidoreductase: An oxygen-sensitive iron-sulfur enzyme from the hyperthermophilic archaeon *Thermococcus profundus*. J. Biosci. Bioeng. *114*, 23–27.

Panesar, P.S., Panesar, R., Singh, R.S., Kennedy, J.F., and Kumar, H. (2006). Microbial production, immobilization and applications of β-D-galactosidase. J. Chem. Technol. Biotechnol. *81*, 530–543.

Parkes, R.J., Sellek, G., Webster, G., Martin, D., Anders, E., Weightman, A.J., and Sass, H. (2009). Culturable prokaryotic diversity of deep, gas hydrate sediments: first use of a continuous high-pressure, anaerobic, enrichment and isolation system for subseafloor sediments (DeepIsoBUG). Environ. Microbiol. *11*, 3140–3153.

Parkes, R.J., Sass, H., Webster, G., Watkins, A.J., Weightman, A.J., O'Sullivan, L.A., and Cragg, B.A. (2010). Methods for studying methanogens and methanogenesis in marine sediments. In Handbook of Hydrocarbon and Lipid Microbiology, K.H. Timmis, ed. (Springer), pp. 3799–3827.

Parks, G. (2014). Hydrogen Station Compression, Storage, and Dispensing Technical Status and Costs Independent Review (National Renewable Energy Laboratory).

Parnell, J., and Blamey, N. (2017a). Global hydrogen reservoirs in basement and basins. Geochem. Trans. *18*.

Parnell, J., and Blamey, N. (2017b). hydrogen from radiolysis of aqueous fluid inclusions during diagenesis. Minerals *7*, 130.

Paul, S., Sheperd, R., and Woollin, P. (2012). Selection of materials for high pressure CO_2 transport.

Paulsen, S. (2009). Pressure systems stored-energy threshold risk analysis (Richland, WA: Pacific Northwest National Laboratory).

Pawar, S.S., and Niel, E.W.J. van (2013). Thermophilic biohydrogen production: how far are we? Appl. Microbiol. Biotechnol. *97*, 7999–8009.

Pedone, E., Ren, B., Ladenstein, R., Rossi, M., and Bartolucci, S. (2004). Functional properties of the protein disulfide oxidoreductase from the archaeon *Pyrococcus furiosus*: a member of a novel protein family related to protein disulfide-isomerase. Eur. J. Biochem. *271*, 3437–3448.

Peoples, L.M., and Bartlett, D.H. (2017). Chapter 2 Ecogenomics of Deep-Ocean Microbial Bathytypes.

Peters, J.W., Miller, A.-F., Jones, A.K., King, P.W., and Adams, M.W.W. (2016). Electron bifurcation. Curr. Opin. Chem. Biol. *31*, 146–152.

Petersen, S., Krätschell, A., Augustin, N., Jamieson, J., Hein, J.R., and Hannington, M.D. (2016). News from the seabed – Geological characteristics and resource potential of deep-sea mineral resources. Mar. Policy *70*, 175–187.

Phillips, P.C. (2008). Epistasis--the essential role of gene interactions in the structure and evolution of genetic systems. Nat. Rev. Genet. *9*, 855–867.

Pierik, A.J., Roseboom, W., Happe, R.P., Bagley, K.A., and Albracht, S.P. (1999). Carbon monoxide and cyanide as intrinsic ligands to iron in the active site of [NiFe]-hydrogenases. NiFe(CN)2CO, Biology's way to activate H2. J. Biol. Chem. *274*, 3331–3337.

Pillot, G., Frouin, E., Pasero, E., Godfroy, A., Combet-Blanc, Y., Davidson, S., and Liebgott, P.-P. (2018). Specific enrichment of hyperthermophilic electroactive *Archaea* from deep-sea hydrothermal vent on electrically conductive support. Bioresour. Technol. *259*, 304–311.

Pisa, K.Y., Huber, H., Thomm, M., and Müller, V. (2007). A sodium ion-dependent A1AO ATP synthase from the hyperthermophilic archaeon *Pyrococcus furiosus*. FEBS J. *274*, 3928–3938.

Popov, S., and Baldynov, O. (2018). The hydrogen energy infrastructure development in japan. E3S Web Conf. *69*, 02001.

Ppyun, H., Kim, I., Cho, S.S., Seo, K.J., Yoon, K., and Kwon, S.-T. (2013). Improved PCR performance using mutant Tpa-S DNA polymerases from the hyperthermophilic archaeon *Thermococcus pacificus*. J. Biotechnol. *164*, 363–370.

Prieur, D., Erauso, G., and Jeanthon, C. (1995). Hyperthermophilic life at deep-sea hydrothermal vents. Planet. Space Sci. *43*, 115–122.

Prinzhofer, A., Tahara Cissé, C.S., and Diallo, A.B. (2018). Discovery of a large accumulation of natural hydrogen in Bourakebougou (Mali). Int. J. Hydrog. Energy *43*, 19315–19326.

Qu, Q., Lee, S.-J., and Boos, W. (2004). TreT, a novel trehalose glycosyltransferring synthase of the hyperthermophilic archaeon *Thermococcus litoralis*. J. Biol. Chem. *279*, 47890–47897.

Rahman, R.N., Fujiwara, S., Takagi, M., and Imanaka, T. (1998). Sequence analysis of glutamate dehydrogenase (GDH) from the hyperthermophilic archaeon *Pyrococcus* sp. KOD1 and comparison of the enzymatic characteristics of native and recombinant GDHs. Mol. Gen. Genet. MGG *257*, 338–347.

Ramachandran, R., and Menon, R.K. (1998). An overview of industrial uses of hydrogen. Int. J. Hydrog. Energy *23*, 593–598.

Regnard, P. (1884). Recherches expérimentales sur l'influence des très hautes pressions sur les organismes vivants. Comptes Rendus Hebd. Académie Sci. *98*, 754–747.

Rekadwad, B., and Khobragade, C. (2017). Marine polyextremophiles and their biotechnological applications. In Microbial Applications, (Springer, Cham), pp. 319–331.

Reungsang, A., Zhong, N., Yang, Y., Sittijunda, S., Xia, A., and Liao, Q. (2018). Hydrogen from photo fermentation. In Bioreactors for Microbial Biomass and Energy Conversion, Q. Liao, J. Chang, C. Herrmann, and A. Xia, eds. (Singapore: Springer), pp. 221–317.

Rinker, K.D., and Kelly, R.M. (1996). Growth physiology of the hyperthermophilic archaeon *Thermococcus litoralis*: development of a sulfur-free defined medium, characterization of an exopolysaccharide, and evidence of biofilm formation. Appl. Environ. Microbiol. *62*, 4478–4485.

Ritchie, H., and Roser, M. (2018). Energy production & changing energy sources. Our World Data.

Ritossa, F. (1962). A new puffing pattern induced by temperature shock and DNP in drosophila. Experientia *18*, 571–573.

Ritzau, M., Keller, M., Wessels, P., Stetter, K.O., and Zeeck, A. (1993). Secondary metabolites by chemical screening, 25. new cyclic polysulfides from hyperthermophilic archaea of the genus *Thermococcus*. Liebigs Ann. Chem. *1993*, 871–876.

Rivalain, N., Roquain, J., and Demazeau, G. (2010). Development of high hydrostatic pressure in biosciences: pressure effect on biological structures and potential applications in biotechnologies. Biotechnol. Adv. *28*, 659–672.

Rivas-Pardo, J.A., Herrera-Morande, A., Castro-Fernandez, V., Fernandez, F.J., Vega, M.C., and Guixé, V. (2013). Crystal structure, saxs and kinetic mechanism of hyperthermophilic adp-dependent glucokinase from *Thermococcus litoralis* reveal a conserved mechanism for catalysis. PLOS ONE *8*, e66687.

Robb, F.T., and Techtmann, S.M. (2018). Life on the fringe: microbial adaptation to growth on carbon monoxide. F1000Research *7*, 1981.

Robb, F.T., Park, J.B., and Adams, M.W. (1992). Characterization of an extremely thermostable glutamate dehydrogenase: a key enzyme in the primary metabolism of the hyperthermophilic archaebacterium, *Pyrococcus furiosus*. Biochim. Biophys. Acta *1120*, 267–272.

Robb, F.T., Maeder, D.L., Brown, J.R., DiRuggiero, J., Stump, M.D., Yeh, R.K., Weiss, R.B., and Dunn, D.M. (2001). Genomic sequence of hyperthermophile, *Pyrococcus furiosus*: implications for physiology and enzymology. Methods Enzymol. *330*, 134–157.

Ronimus, R.S., Reysenbach, A., Musgrave, D.R., and Morgan, H.W. (1997). The phylogenetic position of the *Thermococcus* isolate AN1 based on 16S rRNA gene sequence analysis: a proposal that AN1 represents a new species, *Thermococcus zilligii* sp. nov. Arch. Microbiol. *168*, 245–248.

Ronimus, R.S., de Heus, E., and Morgan, H.W. (2001). Sequencing, expression, characterisation and phylogeny of the ADP-dependent phosphofructokinase from the hyperthermophilic, euryarchaeal *Thermococcus*. Biochim. Biophys. Acta BBA - Gene Struct. Expr. *1517*, 384–391.

Rosenbaum, E., Gabel, F., Durá, M.A., Finet, S., Cléry-Barraud, C., Masson, P., and Franzetti, B. (2012). Effects of hydrostatic pressure on the quaternary structure and enzymatic activity of a large peptidase complex from *Pyrococcus horikoshii*. Arch. Biochem. Biophys. *517*, 104–110.

Rossmann, R., Maier, T., Lottspeich, F., and Böck, A. (1995). Characterisation of a Protease from *Escherichia coli* Involved in Hydrogenase Maturation. Eur. J. Biochem. *227*, 545–550.

Roussel, E.G., Sauvadet, A.-L., Chaduteau, C., Fouquet, Y., Charlou, J.-L., Prieur, D., and Cambon Bonavita, M.-A. (2009). Archaeal communities associated with shallow to deep subseafloor sediments of the New Caledonia Basin. Environ. Microbiol. *11*, 2446–2462.

Roussel, E.G., Cragg, B.A., Webster, G., Sass, H., Tang, X., Williams, A.S., Gorra, R., Weightman, A.J., and Parkes, R.J. (2015). Complex coupled metabolic and prokaryotic community responses to increasing temperatures in anaerobic marine sediments: critical temperatures and substrate changes. FEMS Microbiol. Ecol. *91*.

Royer, C.A., Chakerian, A.E., and Matthews, K.S. (1990). Macromolecular binding equilibria in the lac repressor system: studies using high-pressure fluorescence spectroscopy. Biochemistry *29*, 4959–4966.

Ruth, L. (2006). Gambling in the deep sea. EMBO Rep. *7*, 17–21.

Rutherford, A. (2014). abundance and distribution of major and understudied archaeal lineages at globally distributed deep-sea hydrothermal vents. Diss. Theses.

Ryan, R.M., Compton, E.L.R., and Mindell, J.A. (2009). Functional characterization of a Na+-dependent aspartate transporter from *Pyrococcus horikoshii*. J. Biol. Chem. *284*, 17540–17548.

Sağır, E., and Hallenbeck, P.C. (2019). Chapter 6 - Photofermentative hydrogen production. in biohydrogen (Second Edition), A. Pandey, S.V. Mohan, J.-S. Chang, P.C. Hallenbeck, and C. Larroche, eds. (Elsevier), pp. 141–157.

Saidi, R., Liebgott, P.P., Gannoun, H., Ben Gaida, L., Miladi, B., Hamdi, M., Bouallagui, H., and Auria, R. (2017). Biohydrogen production from hyperthermophilic anaerobic digestion of fruit and vegetable wastes in seawater: Simplification of the culture medium of *Thermotoga maritima*. Waste Manag.

Saiki, R.K., Gelfand, D.H., Stoffel, S., Scharf, S.J., Higuchi, R., Horn, G.T., Mullis, K.B., and Erlich, H.A. (1988). Primer-directed enzymatic amplification of DNA with a thermostable DNA polymerase. Science *239*, 487–491.

Sakuraba, H., Utsumi, E., Schreier, H.J., and Ohshima, T. (2001). Transcriptional regulation of phosphoenolpyruvate synthase by maltose in the hyperthermophilic archaeon, *Pyrococcus furiosus*. J. Biosci. Bioeng. *92*, 108–113.

Sakuraba, H., Goda, S., and Ohshima, T. (2004a). Unique sugar metabolism and novel enzymes of hyperthermophilic archaea. Chem. Rec. *3*, 281–287.

Sakuraba, H., Kawakami, R., Takahashi, H., and Ohshima, T. (2004b). Novel Archaeal Alanine:Glyoxylate Aminotransferase from *Thermococcus litoralis*. J. Bacteriol. *186*, 5513–5518.

Salvador-Castell, M., Golub, M., Martinez, N., Ollivier, J., Peters, J., and Oger, P. (2019). The first study on the impact of osmolytes in whole cells of high temperature-adapted microorganisms. Soft Matter *15*, 8381–8391.

Salvador-Castell, M., Brooks, N.J., Peters, J., and Oger, P. (2020). Induction of non-lamellar phases in archaeal lipids at high temperature and high hydrostatic pressure by apolar polyisoprenoids. Biochim. Biophys. Acta BBA - Biomembr. *1862*, 183130.

Sandberg, T.E., Salazar, M.J., Weng, L.L., Palsson, B.O., and Feist, A.M. (2019). The emergence of adaptive laboratory evolution as an efficient tool for biological discovery and industrial biotechnology. Metab. Eng. *56*, 1–16.

Santangelo, T.J., Čuboňová, L., and Reeve, J.N. (2008). Shuttle Vector Expression in *Thermococcus kodakaraensis*: contributions of cis elements to protein synthesis in a hyperthermophilic archaeon. Appl. Environ. Microbiol. *74*, 3099–3104.

Santangelo, T.J., Čuboňová, L., and Reeve, J.N. (2010). *Thermococcus kodakarensis* genetics: TK1827-encoded β-glycosidase, new positive-selection protocol, and targeted and repetitive deletion technology. Appl. Environ. Microbiol. *76*, 1044–1052.

Santangelo, T.J., Cuboňová, L., and Reeve, J.N. (2011). Deletion of alternative pathways for reductant recycling in *Thermococcus increases* hydrogen production. Mol. Microbiol. *81*, 897–911.

Santos, H., Lamosa, P., Borges, N., Gonçalves, L.G., Pais, T., and Rodrigues, M.V. (2011). Organic compatible solutes of prokaryotes that thrive in hot environments: the importance of ionic compounds for thermostabilization. In Extremophiles Handbook, (Springer, Tokyo), pp. 497–520.

Sapra, R., Verhagen, M.F.J.M., and Adams, M.W.W. (2000). Purification and characterization of a membrane-bound hydrogenase from the hyperthermophilic archaeon *Pyrococcus furiosus*. J. Bacteriol. *182*, 3423–3428.

Sapra, R., Bagramyan, K., and Adams, M.W.W. (2003). A simple energy-conserving system: Proton reduction coupled to proton translocation. Proc. Natl. Acad. Sci. *100*, 7545–7550.

Sarrazin, J., and Juniper, S. (1999). Biological characteristics of a hydrothermal edifice mosaic community. Mar. Ecol. Prog. Ser. *185*, 1–19.

Sasaki, D., Watanabe, S., Matsumi, R., Shoji, T., Yasukochi, A., Tagashira, K., Fukuda, W., Kanai, T., Atomi, H., Imanaka, T., et al. (2013). Identification and structure of a novel archaeal HypB for [NiFe] hydrogenase maturation. J. Mol. Biol. *425*, 1627–1640.

Sato, T., and Atomi, H. (2011). Novel metabolic pathways in *Archaea*. Curr. Opin. Microbiol. *14*, 307–314.

Sato, T., Fukui, T., Atomi, H., and Imanaka, T. (2003). Targeted gene disruption by homologous recombination in the hyperthermophilic archaeon *Thermococcus kodakaraensis* KOD1. J. Bacteriol. *185*, 210–220.

Sato, T., Imanaka, H., Rashid, N., Fukui, T., Atomi, H., and Imanaka, T. (2004). Genetic evidence identifying the true gluconeogenic fructose-1,6-bisphosphatase in *Thermococcus kodakaraensis* and other hyperthermophiles. J. Bacteriol. *186*, 5799–5807.

Sato, T., Fukui, T., Atomi, H., and Imanaka, T. (2005). Improved and versatile transformation system allowing multiple genetic manipulations of the hyperthermophilic archaeon *Thermococcus kodakaraensis*. Appl. Environ. Microbiol. *71*, 3889–3899.

Sato, T., Takada, D., Itoh, T., Ohkuma, M., and Atomi, H. (2020). Integration of large heterologous DNA fragments into the genome of *Thermococcus kodakarensis*. Extremophiles. *24*:3, 339-353.

Sauer, P., Glombitza, C., and Kallmeyer, J. (2012). A System for incubations at high gas partial pressure. Front. Microbiol. *3*:25.

Say, R.F., and Fuchs, G. (2010). Fructose 1,6-bisphosphate aldolase/phosphatase may be an ancestral gluconeogenic enzyme. Nature *464*, 1077–1081.

Sazanov, L.A. (2015). A giant molecular proton pump: structure and mechanism of respiratory complex I. Nat. Rev. Mol. Cell Biol. *16*, 375–388.

Schäfer, T.M., and Schönheit, P. (1991). Pyruvate metabolism of the hyperthermophilic archaebacterium *Pyrococcus furiosus*. Arch. Microbiol. *155*, 366–377.

Schauer, N.L., and Ferry, J.G. (1980). Metabolism of formate in *Methanobacterium formicicum*. J. Bacteriol. *142*, 800–807.

Schicho, R.N., Ma, K., Adams, M.W.W., and Kelly, R.M. (1993). Bioenergetics of sulfur reduction in the hyperthermophilic archaeon *Pyrococcus furiosus*. J. Bacteriol. *175*, 1823–1830.

Schoelmerich, M.C., and Müller, V. (2019). Energy-converting hydrogenases: the link between H_2 metabolism and energy conservation. Cell. Mol. Life Sci. *77*:8, 1461-1481.

Schramm, A., Siebers, B., Tjaden, B., Brinkmann, H., and Hensel, R. (2000). Pyruvate kinase of the hyperthermophilic crenarchaeote *Thermoproteus tenax*: physiological role and phylogenetic aspects. J. Bacteriol. *182*, 2001–2009.

Schuabb, C., Pataraia, S., Berghaus, M., and Winter, R. (2017). Exploring the effects of temperature and pressure on the structure and stability of a small RNA hairpin. Biophys. Chem. *231*, 161–166.

Schut, G.J., Menon, A.L., and Adams, M.W.W. (2001). 2-keto acid oxidoreductases from *Pyrococcus furiosus* and *Thermococcus litoralis*. Methods Enzymol. *331*, 144–158.

Schut, G.J., Brehm, S.D., Datta, S., and Adams, M.W.W. (2003). Whole-genome dna microarray analysis of a hyperthermophile and an archaeon: *Pyrococcus furiosus* grown on carbohydrates or peptides. J. Bacteriol. *185*, 3935–3947.

Schut, G.J., Bridger, S.L., and Adams, M.W.W. (2007). Insights into the metabolism of elemental sulfur by the hyperthermophilic archaeon *Pyrococcus furiosus*: characterization of a coenzyme a- dependent nad(p)h sulfur oxidoreductase. J. Bacteriol. *189*, 4431–4441.

Schut, G.J., Nixon, W.J., Lipscomb, G.L., Scott, R.A., and Adams, M.W.W. (2012). Mutational analyses of the enzymes involved in the metabolism of hydrogen by the hyperthermophilic archaeon *Pyrococcus furiosus*. Front. Microbiol. *3*.

Schut, G.J., Boyd, E.S., Peters, J.W., and Adams, M.W.W. (2013). The modular respiratory complexes involved in hydrogen and sulfur metabolism by heterotrophic hyperthermophilic archaea and their evolutionary implications. FEMS Microbiol. Rev. *37*, 182–203.

Schut, G.J., Lipscomb, G.L., Han, Y., Notey, J.S., Kelly, R.M., and Adams, M.M.W. (2014). The order *Thermococcales* and the family *Thermococcaceae*. In The Prokaryotes: Other Major Lineages of Bacteria and The Archaea, E. Rosenberg, E.F. DeLong, S. Lory, E. Stackebrandt, and F. Thompson, eds. (Berlin, Heidelberg: Springer Berlin Heidelberg), pp. 363–383.

Schut, G.J., Zadvornyy, O., Wu, C.-H., Peters, J.W., Boyd, E.S., and Adams, M.W.W. (2016a). The role of geochemistry and energetics in the evolution of modern respiratory complexes from a proton-reducing ancestor. Biochim. Biophys. Acta BBA - Bioenerg. *1857*, 958–970.

Schut, G.J., Lipscomb, G.L., Nguyen, D.M.N., Kelly, R.M., and Adams, M.W.W. (2016b). Heterologous production of an energy-conserving carbon monoxide dehydrogenase complex in the hyperthermophile *Pyrococcus furiosus*. Front. Microbiol. *7*.

Scott, M.R., Scott, R.B., Rona, P.A., Butler, L.W., and Nalwalk, A.J. (1974). Rapidly accumulating manganese deposit from the Median Valley of the Mid-Atlantic Ridge. Geophys. Res. Lett. *1*, 355–358.

Sekar, N. (ORCID:0000000166006032), Wu, C.-H., Adams, M.W.W., and Ramasamy, R.P. (2017). Electricity generation by *Pyrococcus furiosus* in microbial fuel cells operated at 90°C: Electricity generation by *Pyrococcus furiosus*. Biotechnol. Bioeng. *114*:7, 1419-1427.

Selig, M., Xavier, K.B., Santos, H., and Schönheit, P. (1997). Comparative analysis of Embden-Meyerhof and Entner-Doudoroff glycolytic pathways in hyperthermophilic archaea and the bacterium *Thermotoga*. Arch. Microbiol. *167*, 217–232.

Sezonov, G., Joseleau-Petit, D., and D'Ari, R. (2007). *Escherichia coli* physiology in luria-bertani broth. J. Bacteriol. *189*, 8746–8749.

Sharma, P., and Guptasarma, P. (2017). Endoglucanase activity at a second site in *Pyrococcus* furiosus triosephosphate isomerase-Promiscuity or compensation for a metabolic handicap? FEBS Open Bio *7*, 1126–1143.

Shendure, J., Balasubramanian, S., Church, G.M., Gilbert, W., Rogers, J., Schloss, J.A., and Waterston, R.H. (2017). DNA sequencing at 40: past, present and future. Nature *550*, 345–353.

Shepelin, D., Hansen, A.S.L., Lennen, R., Luo, H., and Herrgård, M.J. (2018). Selecting the best: evolutionary engineering of chemical production in microbes. Genes *9*.

Shikata, K., Fukui, T., Atomi, H., and Imanaka, T. (2007). A novel ADP-forming succinyl-CoA synthetase in *Thermococcus kodakaraensis* structurally related to the archaeal nucleoside diphosphate-forming acetyl-CoA synthetases. J. Biol. Chem. *282*, 26963–26970.

Siddiqui, M.A., Fujiwara, S., and Imanaka, T. (1997). Indolepyruvate ferredoxin oxidoreductase from *Pyrococcus* sp. KOD1 possesses a mosaic structure showing features of various oxidoreductases. Mol. Gen. Genet. MGG *254*, 433–439.

Siebers, B., Brinkmann, H., Dörr, C., Tjaden, B., Lilie, H., van der Oost, J., and Verhees, C.H. (2001). Archaeal fructose-1,6-bisphosphate aldolases constitute a new family of archaeal type class I aldolase. J. Biol. Chem. *276*, 28710–28718.

Silva, J.L., Oliveira, A.C., Gomes, A.M.O., Lima, L.M.T.R., Mohana-Borges, R., Pacheco, A.B.F., and Foguel, D. (2002). Pressure induces folding intermediates that are crucial for protein–DNA recognition and virus assembly. Biochim. Biophys. Acta BBA - Protein Struct. Mol. Enzymol. *1595*, 250–265.

Silva, P.J., van den Ban, E.C., Wassink, H., Haaker, H., de Castro, B., Robb, F.T., and Hagen, W.R. (2000). Enzymes of hydrogen metabolism in *Pyrococcus furiosus*. Eur. J. Biochem. *267*, 6541–6551.

Sinensky, M. (1974). Homeoviscous adaptation—a homeostatic process that regulates the viscosity of membrane lipids in *Escherichia coli*. Proc. Natl. Acad. Sci. *71*, 522–525.

Skanes, I.D., Stewart, J., Keough, K.M.W., and Morrow, M.R. (2006). Effect of chain unsaturation on bilayer response to pressure. Phys. Rev. E *74*, 051913.

Slobodkin, A., Campbell, B., Cary, S.C., Bonch-Osmolovskaya, E., and Jeanthon, C. (2001). Evidence for the presence of thermophilic Fe(III)-reducing microorganisms in deep-sea hydrothermal vents at 13 degrees N (East Pacific Rise). FEMS Microbiol. Ecol. *36*, 235–243.

Smil, V. (2019). Energy In World History (Routledge).

Smith, E.T., Blamey, J.M., and Adams, M.W. (1994). Pyruvate ferredoxin oxidoreductases of the hyperthermophilic archaeon, *Pyrococcus furiosus*, and the hyperthermophilic bacterium, *Thermotoga maritima*, have different catalytic mechanisms. Biochemistry *33*, 1008–1016.

SNBC (2019). Stratégie Nationale Bas-Carbone (SNBC).

Sokolova, T.G., Jeanthon, C., Kostrikina, N.A., Chernyh, N.A., Lebedinsky, A.V., Stackebrandt, E., and Bonch-Osmolovskaya, E.A. (2004). The first evidence of anaerobic CO oxidation coupled with H2 production by a hyperthermophilic archaeon isolated from a deep-sea hydrothermal vent. Extrem. Life Extreme Cond. *8*, 317–323.

Soler, N., Marguet, E., Verbavatz, J.-M., and Forterre, P. (2008). Virus-like vesicles and extracellular DNA produced by hyperthermophilic archaea of the order *Thermococcales*. Res. Microbiol. *159*, 390–399.

Soler, N., Gaudin, M., Marguet, E., and Forterre, P. (2011). Plasmids, viruses and virus-like membrane vesicles from *Thermococcales*. Biochem. Soc. Trans. *39*, 36–44.

Soltani, R., Rosen, M.A., and Dincer, I. (2014). Assessment of CO2 capture options from various points in steam methane reforming for hydrogen production. Int. J. Hydrog. Energy *39*, 20266–20275.

Song, Q., Li, Z., Chen, R., Ma, X., Xiao, X., and Xu, J. (2019). Induction of a toxin-antitoxin gene cassette under high hydrostatic pressure enables markerless gene disruption in the hyperthermophilic archaeon *Pyrococcus yayanosii*. Appl. Environ. Microbiol. *85*.

Sourceforge (2020). SnpEff Manual.

Souza, M.O., Creczynski-Pasa, T.B., Scofano, H.M., Gräber, P., and Mignaco, J.A. (2004). High hydrostatic pressure perturbs the interactions between CF0F1 subunits and induces a dual effect on activity. Int. J. Biochem. Cell Biol. *36*, 920–930.

Stetter, K.O. (2006). History of discovery of the first hyperthermophiles. Extrem. Life Extreme Cond. *10*, 357–362.

Stetter, K.O., Huber, R., Blöchl, E., Kurr, M., Eden, R.D., Fielder, M., Cash, H., and Vance, I. (1993). Hyperthermophilic archaea are thriving in deep North Sea and Alaskan oil reservoirs. Nature *365*, 743–745.

Sturm, F.J., Hurwitz, S.A., Deming, J.W., and Kelly, R.M. (1987). Growth of the extreme thermophile Sulfolobus acidocaldarius in a hyperbaric helium bioreactor. Biotechnol. Bioeng. *29*, 1066–1074.

Sullivan, C.T., Harman, R.M., Eash, N.S., Zahn, J.A., Goddard, J.J., Walker, F.R., Saxton, A.M., Lambert, D.M., McIntosh, D.W., Hart, W.E., et al. (2017). Utilization of spent microbial biomass as an alternative crop nitrogen source. Agron. J. *109*, 1870–1879.

Summit, M., and Baross, J.A. (1998). Thermophilic subseafloor microorganisms from the 1996 North Gorda Ridge eruption. Deep Sea Res. Part II Top. Stud. Oceanogr. *45*, 2751–2766.

Summit, M., Scott, B., Nielson, K., Mathur, E., and Baross, J. (1998). Pressure enhances thermal stability of DNA polymerase from three thermophilic organisms. Extrem. Life Extreme Cond. *2*, 339–345.

Sun, Y., and Shirouzu, N. (2019). China's "father of EV" urges more hydrogen infrastructure to develop fuel cell vehicles. Reuters.

Sun, J., Hopkins, R.C., Jr, F.E.J., McTernan, P.M., and Adams, M.W.W. (2010). Heterologous expression and maturation of an NADP-Dependent [NiFe]-hydrogenase: a key enzyme in biofuel production. PLOS ONE *5*, e10526.

Sun, M.M., Tolliday, N., Vetriani, C., Robb, F.T., and Clark, D.S. (1999). Pressure-induced thermostabilization of glutamate dehydrogenase from the hyperthermophile *Pyrococcus furiosus*. Protein Sci. Publ. Protein Soc. *8*, 1056–1063.

Sun, M.M.C., Caillot, R., Mak, G., Robb, F.T., and Clark, D.S. (2001). Mechanism of pressure-induced thermostabilization of proteins: Studies of glutamate dehydrogenases from the hyperthermophile *Thermococcus litoralis*. Protein Sci. Publ. Protein Soc. *10*, 1750–1757.

Sun, P., Young, B., Elgowainy, A., Lu, Z., Wang, M., Morelli, B., and Hawkins, T. (2019). criteria air pollutants and greenhouse gas emissions from hydrogen production in u.s. steam methane reforming facilities. Environ. Sci. Technol. *53*, 7103–7113.

Swartz, T.H., Ikewada, S., Ishikawa, O., Ito, M., and Krulwich, T.A. (2005). The Mrp system: a giant among monovalent cation/proton antiporters? Extremophiles *9*, 345–354.

Taebi, B., and Roeser, S. (2019). The Ethics of Nuclear Energy: Its Past, Present and Future. In In Search of Good Energy Policy, (Cambridge University Press), pp. 101–119.

Takács, M., Tóth, A., Bogos, B., Varga, A., Rákhely, G., and Kovács, K.L. (2008). Formate hydrogenlyase in the hyperthermophilic archaeon, *Thermococcus litoralis*. BMC Microbiol. *8*, 88.

Takai, K., Sugai, A., Itoh, T., and Horikoshi, K. (2000). *Palaeococcus ferrophilus* gen. nov., sp. nov., a barophilic, hyperthermophilic archaeon from a deep-sea hydrothermal vent chimney. Int. J. Syst. Evol. Microbiol. *50 Pt 2*, 489–500.

Takai, K., Nakamura, K., Toki, T., Tsunogai, U., Miyazaki, M., Miyazaki, J., Hirayama, H., Nakagawa, S., Nunoura, T., and Horikoshi, K. (2008). Cell proliferation at 122 degrees C and isotopically heavy CH_4 production by a hyperthermophilic methanogen under high-pressure cultivation. Proc. Natl. Acad. Sci. U. S. A. *105*, 10949–10954.

Takami, H., Takaki, Y., Chee, G.-J., Nishi, S., Shimamura, S., Suzuki, H., Matsui, S., and Uchiyama, I. (2004). Thermoadaptation trait revealed by the genome sequence of thermophilic *Geobacillus kaustophilus*. Nucleic Acids Res. *32*, 6292–6303.

Tamegai, H., Chikuma, S., Ishii, M., Nakasone, K., and Kato, C. (2008). The narQP genes for a two-component regulatory system from the deep-sea bacterium *Shewanella violacea* DSS12. DNA Seq. *19*, 308–312.

Tanaka, T., Fukui, T., Atomi, H., and Imanaka, T. (2003). Characterization of an exo-β-d-glucosaminidase involved in a novel chitinolytic pathway from the hyperthermophilic archaeon *Thermococcus kodakaraensis* KOD1. J. Bacteriol. *185*, 5175–5181.

Tanaka, T., Fukui, T., Fujiwara, S., Atomi, H., and Imanaka, T. (2004). concerted action of diacetylchitobiose deacetylase and exo-β-d-glucosaminidase in a novel chitinolytic pathway in the hyperthermophilic archaeon *Thermococcus kodakaraensis* KOD1. J. Biol. Chem. *279*, 30021–30027.

Tang, F. (2019). Adaptive laboratory evolution of Gram-positive *Carnobacterium* sp. AT7 under high hydrostatic pressure. PhD thesis. UC San Diego.

Tang, G.-L., Huang, J., Sun, Z.-J., Tang, Q.-Q., Yan, C.-H., and Liu, G.-Q. (2008). Biohydrogen production from cattle wastewater by enriched anaerobic mixed consortia: influence of fermentation temperature and pH. J. Biosci. Bioeng. *106*, 80–87.

Tang, G.Q., Tanaka, N., and Kunugi, S. (1998). In vitro increases in plasmid DNA supercoiling by hydrostatic pressure. Biochim. Biophys. Acta *1443*, 364–368.

Taylor, C.D., and Jannasch, H.W. (1976). Subsampling technique for measuring growth of bacterial cultures under high hydrostatic pressure. Appl. Environ. Microbiol. *32*, 355–359.

Thangakani, A.M., Kumar, S., Velmurugan, D., and Gromiha, M.S.M. (2012). How do thermophilic proteins resist aggregation? Proteins *80*, 1003–1015.

Thauer, R.K., Jungermann, K., and Decker, K. (1977). Energy conservation in chemotrophic anaerobic bacteria. Bacteriol. Rev. *41*, 100–180.

Theriot, C.M., Tove, S.R., and Grunden, A.M. (2010). Characterization of two proline dipeptidases (prolidases) from the hyperthermophilic archaeon *Pyrococcus horikoshii*. Appl. Microbiol. Biotechnol. *86*, 177–188.

Thiel, A., Michoud, G., Moalic, Y., Flament, D., and Jebbar, M. (2014). Genetic manipulations of the hyperthermophilic piezophilic archaeon *Thermococcus barophilus*. Appl. Environ. Microbiol. *80*, 2299–2306.

Thom, S.R., and Marquis, R.E. (1984). Microbial growth modification by compressed gases and hydrostatic pressure. Appl. Environ. Microbiol. *47*, 780–787.

Thomm, M., Hausner, W., and Waege, I. (2011). Shuttle vector based transformation system for *Pyrococcus furiosus*. Appl. Environ. Microbiol. *76*:10, 3308-13.

Tominaga, T., Watanabe, S., Matsumi, R., Atomi, H., Imanaka, T., and Miki, K. (2013). Crystal structures of the carbamoylated and cyanated forms of HypE for [NiFe] hydrogenase maturation. Proc. Natl. Acad. Sci. U. S. A. *110*, 20485–20490.

Topçuoğlu, B.D., Meydan, C., Orellana, R., and Holden, J.F. (2018). Formate hydrogenlyase and formate secretion ameliorate H_2 inhibition in the hyperthermophilic archaeon *Thermococcus paralvinellae*. Environ. Microbiol. *20*, 949–957.

Topçuoğlu, B.D., Meydan, C., Nguyen, T.B., Lang, S.Q., and Holden, J.F. (2019). Growth kinetics, carbon isotope fractionation, and gene expression in the hyperthermophile *Methanocaldococcus jannaschii* during hydrogen-limited growth and interspecies hydrogen transfer. Appl. Environ. Microbiol. *85*.

Tóth, A., Takács, M., Groma, G., Rákhely, G., and Kovács, K.L. (2008). A novel NADPH-dependent oxidoreductase with a unique domain structure in the hyperthermophilic Archaeon, *Thermococcus litoralis*. FEMS Microbiol. Lett. *282*, 8–14.

Touran, N. (2020). Computing the energy density of nuclear fuel. https://whatisnuclear.com/energy-density.html

Toxvaerd, S. (2019). A Prerequisite for Life. J. Theor. Biol. *474*, 48–51.

Transitions Energies, L. (2020). L'hydrogène peut-il remplacer le pétrole? https://www.transitionsenergies.com/hydrogene-remplacer-petrole/

Tunnicliffe, V.J. (1991). The biology of hydrothermal vents : Ecology and evolution. Oceanogr. Mar. Biol. *29*, 319–407.

Uehara, I. (2008). Separation and Purification of Hydrogen. In Energy Carriers and Conversion System. Vol. 1.

U.S. DOE Hydrogen and Fuel Cells Program (2020). DOE Hydrogen and Fuel Cells Program: About the Hydrogen and Fuel Cells Program.

Usui, K., Hiraki, T., Kawamoto, J., Kurihara, T., Nogi, Y., Kato, C., and Abe, F. (2012). Eicosapentaenoic acid plays a role in stabilizing dynamic membrane structure in the deep-sea piezophile *Shewanella violacea*: A study employing high-pressure time-resolved fluorescence anisotropy measurement. Biochim. Biophys. Acta BBA - Biomembr. *1818*, 574–583.

Valenti, A., Perugino, G., Rossi, M., and Ciaramella, M. (2011). Positive supercoiling in thermophiles and mesophiles: of the good and evil. Biochem. Soc. Trans. *39*, 58–63.

Van Dover, C.L., Arnaud-Haond, S., Gianni, M., Helmreich, S., Huber, J.A., Jaeckel, A.L., Metaxas, A., Pendleton, L.H., Petersen, S., Ramirez-Llodra, E., et al. (2018). Scientific rationale and international obligations for protection of active hydrothermal vent ecosystems from deep-sea mining. Mar. Policy *90*, 20–28.

Vanlint, D., Mitchell, R., Bailey, E., Meersman, F., McMillan, P.F., Michiels, C.W., and Aertsen, A. (2011). Rapid acquisition of gigapascal-high-pressure resistance by *Escherichia coli*. MBio *2*, e00130-10.

Vannier, P. (2012). Bases génomiques, protéomiques et transcriptomiques de l'adaptation aux hautes pressions hydrostatiques d'une archée hyperthermophile : *Thermococcus barophilus*. PhD thesis. Université de Bretagne Occidentale.

Vannier, P., Marteinsson, V.T., Fridjonsson, O.H., Oger, P., and Jebbar, M. (2011). Complete genome sequence of the hyperthermophilic, piezophilic, heterotrophic, and carboxydotrophic archaeon *Thermococcus barophilus* MP. J. Bacteriol. *193*, 1481–1482.

Vannier, P., Michoud, G., Oger, P., Marteinsson, V.Þ., and Jebbar, M. (2015). Genome expression of *Thermococcus barophilus* and *Thermococcus kodakarensis* in response to different hydrostatic pressure conditions. Res. Microbiol. *166*, 717–725.

Verhaart, M.R.A., Bielen, A.A.M., van der Oost, J., Stams, A.J.M., and Kengen, S.W.M. (2010). Hydrogen production by hyperthermophilic and extremely thermophilic bacteria and archaea: mechanisms for reductant disposal. Environ. Technol. *31*, 993–1003.

Verhees, C.H., Huynen, M.A., Ward, D.E., Schiltz, E., Vos, W.M. de, and Oost, J. van der (2001). The phosphoglucose isomerase from the hyperthermophilic archaeon *Pyrococcus furiosus* is a unique glycolytic enzyme that belongs to the cupin superfamily. J. Biol. Chem. *276*, 40926–40932.

Verhees, C.H., Kengen, S.W.M., Tuininga, J.E., Schut, G.J., Adams, M.W.W., De Vos, W.M., and Van Der Oost, J. (2003). The unique features of glycolytic pathways in *Archaea*. Biochem. J. *375*, 231–246.

Verne, J. (1875). L'Ile mystérieuse. Magasin d'éducation et de recreation.

Vetriani, C., Maeder, D.L., Tolliday, N., Yip, K.S.-P., Stillman, T.J., Britton, K.L., Rice, D.W., Klump, H.H., and Robb, F.T. (1998). Protein thermostability above 100°C: A key role for ionic interactions. Proc. Natl. Acad. Sci. U. S. A. *95*, 12300–12305.

Vezzi, A., Campanaro, S., D'Angelo, M., Simonato, F., Vitulo, N., Lauro, F.M., Cestaro, A., Malacrida, G., Simionati, B., Cannata, N., et al. (2005). Life at depth: *Photobacterium profundum* genome sequence and expression analysis. Science *307*, 1459–1461.

Vieille, C., and Zeikus, J.G. (1996). Thermozymes: Identifying molecular determinants of protein structural and functional stability. Trends Biotechnol. *14*, 183–190.

Vierke, G., Engelmann, A., Hebbeln, C., and Thomm, M. (2003). A novel archaeal transcriptional regulator of heat shock response. J. Biol. Chem. *278*, 18–26.

Viktorsson, L., Heinonen, J.T., Skulason, J.B., and Unnthorsson, R. (2017). A step towards the hydrogen economy—a life cycle cost analysis of a hydrogen refueling station. Energies *10*, 763.

Waege, I., Schmid, G., Thumann, S., Thomm, M., and Hausner, W. (2010). Shuttle vector-based transformation system for *Pyrococcus furiosus*. Appl. Environ. Microbiol. *76*, 3308–3313.

Wang, H. (2012). Hydrogen Evolution Reaction. Stanford University.

Wang, Y. (2002). The function of OmpA in *Escherichia coli*. Biochem. Biophys. Res. Commun. *292*, 396–401.

Wang, F., Wang, J., Jian, H., Zhang, B., Li, S., Wang, F., Zeng, X., Gao, L., Bartlett, D.H., Yu, J., et al. (2008). Environmental adaptation: genomic analysis of the piezotolerant and psychrotolerant deep-sea iron reducing bacterium *Shewanella piezotolerans* WP3. PloS One *3*, e1937.

Wang, S., Huang, H., Moll, J., and Thauer, R.K. (2010). NADP+ reduction with reduced ferredoxin and $NADP^+$ reduction with NADH are coupled via an electron-bifurcating enzyme complex in *Clostridium kluyveri*. J. Bacteriol. *192*, 2115–2123.

Ward, D.E., Kengen, S.W., van Der Oost, J., and de Vos, W.M. (2000). Purification and characterization of the alanine aminotransferase from the hyperthermophilic Archaeon *Pyrococcus furiosus* and its role in alanine production. J. Bacteriol. *182*, 2559–2566.

Ward, D.E., Shockley, K.R., Chang, L.S., Levy, R.D., Michel, J.K., Conners, S.B., and Kelly, R.M. (2002a). Proteolysis in hyperthermophilic microorganisms. Archaea *1*:1, 63-74.

Ward, D.E., de Vos, W.M., and van der Oost, J. (2002b). Molecular analysis of the role of two aromatic aminotransferases and a broad-specificity aspartate aminotransferase in the aromatic amino acid metabolism of *Pyrococcus furiosus*. Archaea Vanc. BC *1*, 133–141.

Watanabe, S., Matsumi, R., Atomi, H., Imanaka, T., and Miki, K. (2012). Crystal structures of the HypCD complex and the HypCDE ternary complex: transient intermediate complexes during [NiFe] hydrogenase maturation. Struct. Lond. Engl. 1993 *20*, 2124–2137.

Watanabe, S., Kawashima, T., Nishitani, Y., Kanai, T., Wada, T., Inaba, K., Atomi, H., Imanaka, T., and Miki, K. (2015). Structural basis of a Ni acquisition cycle for [NiFe] hydrogenase by Ni-metallochaperone HypA and its enhancer. Proc. Natl. Acad. Sci. U. S. A. *112*, 7701–7706.

Watrin, L., Martin-Jezequel, V., and Prieur, D. (1995). Minimal amino acid requirements of the hyperthermophilic archaeon *Pyrococcus abyssi*, isolated from deep-sea hydrothermal vents. Appl. Environ. Microbiol. *61*, 1138–1140.

Weatherall, P., Marks, K.M., Jakobsson, M., Schmitt, T., Tani, S., Arndt, J.E., Rovere, M., Chayes, D., Ferrini, V., and Wigley, R. (2015). A new digital bathymetric model of the world's oceans. Earth Space Sci. *2*, 331–345.

Welch, T.J., and Bartlett, D.H. (1996). Isolation and characterization of the structural gene for OmpL, a pressure-regulated porin-like protein from the deep-sea bacterium *Photobacterium* species strain SS9. J. Bacteriol. *178*, 5027–5031.

Welch, T.J., and Bartlett, D.H. (1998). Identification of a regulatory protein required for pressure-responsive gene expression in the deep-sea bacterium *Photobacterium* species strain SS9. Mol. Microbiol. *27*, 977–985.

van de Werken, H.J.G., Verhees, C.H., Akerboom, J., de Vos, W.M., and van der Oost, J. (2006). Identification of a glycolytic regulon in the archaea *Pyrococcus* and *Thermococcus*. FEMS Microbiol. Lett. *260*, 69–76.

Whitman, W.B., Coleman, D.C., and Wiebe, W.J. (1998). Prokaryotes: the unseen majority. Proc. Natl. Acad. Sci. U. S. A. *95*, 6578–6583.

Widdel, F., and Bak, F. (1992). Gram-negative mesophilic sulfate-reducing bacteria. In The Prokaryotes. A Handbook on the Biology of Bacteria: Ecophysiology, Isolation, Identification, Applications. Balows, (Springer Verlag, New York), pp. 3352–3378.

Wilm, A., Aw, P.P.K., Bertrand, D., Yeo, G.H.T., Ong, S.H., Wong, C.H., Khor, C.C., Petric, R., Hibberd, M.L., and Nagarajan, N. (2012). LoFreq: a sequence-quality aware, ultra-sensitive variant caller for uncovering cell-population heterogeneity from high-throughput sequencing datasets. Nucleic Acids Res. *40*, 11189–11201.

Wilton, D.J., Ghosh, M., Chary, K.V.A., Akasaka, K., and Williamson, M.P. (2008). Structural change in a B-DNA helix with hydrostatic pressure. Nucleic Acids Res. *36*, 4032–4037.

Winter, R., and Jeworrek, C. (2009). Effect of pressure on membranes. Soft Matter *17*, 3157–3173.

Wirth, R., Luckner, M., and Wanner, G. (2018). Validation of a hypothesis: colonization of black smokers by hyperthermophilic microorganisms. Front. Microbiol. *9*, 524.

Wright, P.C., Westacott, R.E., and Burja, A.M. (2003). Piezotolerance as a metabolic engineering tool for the biosynthesis of natural products. Biomol. Eng. *20*, 325–331.

Wu, C.-H., Schut, G.J., Poole II, F.L., Haja, D.K., and Adams, M.W.W. (2018a). Characterization of membrane-bound sulfane reductase: A missing link in the evolution of modern day respiratory complexes. J. Biol. Chem. *293*, 16687–16696.

Wu, C.-H., Ponir, C.A., Haja, D.K., and Adams, M.W.W. (2018b). Improved production of the NiFe-hydrogenase from *Pyrococcus furiosus* by increased expression of maturation genes. Protein Eng. Des. Sel. PEDS *31*, 337–344.

Wu, X., Zhang, C., Orita, I., Imanaka, T., Fukui, T., and Xing, X.-H. (2013). thermostable alcohol dehydrogenase from *Thermococcus kodakarensis* KOD1 for enantioselective bioconversion of aromatic secondary alcohols. Appl. Environ. Microbiol. *79*, 2209–2217.

Xavier, K.B., Martins, L.O., Peist, R., Kossmann, M., Boos, W., and Santos, H. (1996). High-affinity maltose/trehalose transport system in the hyperthermophilic archaeon *Thermococcus* litoralis. J. Bacteriol. *178*, 4773–4777.

Xavier, K.B., Peist, R., Kossmann, M., Boos, W., and Santos, H. (1999). Maltose metabolism in the hyperthermophilic archaeon *Thermococcus litoralis*: purification and characterization of key enzymes. J. Bacteriol. *181*, 3358–3367.

Xiong, A.-S., Peng, R.-H., Zhuang, J., Li, X., Xue, Y., Liu, J.-G., Gao, F., Cai, B., Chen, J.-M., and Yao, Q.-H. (2007). Directed evolution of a beta-galactosidase from *Pyrococcus woesei* resulting in increased thermostable beta-glucuronidase activity. Appl. Microbiol. Biotechnol. *77*, 569–578.

Xu, L., Wu, Y.-H., Zhou, P., Cheng, H., Liu, Q., and Xu, X.-W. (2018). Investigation of the thermophilic mechanism in the genus *Porphyrobacter* by comparative genomic analysis. BMC Genomics *19*, 385.

Xue, Q., Wu, M., Zeng, X.C., and Jena, P. (2018). Co-mixing hydrogen and methane may double the energy storage capacity. J. Mater. Chem. A *6*, 8916–8922.

Yaldagard, M., Mortazavi, S.A., and Tabatabaie, F. (2008). The principles of ultra high pressure technology and its application in food processing/preservation: A review of microbiological and quality aspects. Afr. J. Biotechnol. *7*.

Yamamoto, Y., Kanai, T., Kaneseki, T., and Atomi, H. (2019). The TK0271 protein activates transcription of aromatic amino acid biosynthesis genes in the hyperthermophilic archaeon *Thermococcus kodakarensis*. MBio *10*.

Yancey, P.H., Blake, W.R., and Conley, J. (2002). Unusual organic osmolytes in deep-sea animals: adaptations to hydrostatic pressure and other perturbants. Comp. Biochem. Physiol. A. Mol. Integr. Physiol. *133*, 667–676.

Yang, X., and Ma, K. (2010). Characterization of a thioredoxin-thioredoxin reductase system from the hyperthermophilic bacterium *Thermotoga maritima*. J. Bacteriol. *192*, 1370–1376.

Yang, H., Lipscomb, G.L., Keese, A.M., Schut, G.J., Thomm, M., Adams, M.W.W., Wang, B.C., and Scott, R.A. (2010). SurR regulates hydrogen production in *Pyrococcus furiosus* by a sulfur-dependent redox switch. Mol. Microbiol. *77*, 1111–1122.

Yayanos, A.A. (1969). A technique for studying biological reaction rates at high pressure. Rev. Sci. Instrum. *40*, 961–963.

Yayanos, A.A., Dietz, A.S., and VAN Boxtel, R. (1981). Obligately barophilic bacterium from the Mariana trench. PNAS *78*, 5212–5215.

Yin, Y., Ding, Y., Feng, G., Li, J., Xiao, L., Karuppiah, V., Sun, W., Zhang, F., and Li, Z. (2015). Modification of artificial sea water for the mass production of (+)-terrein by *Aspergillus terreus* strain PF26 derived from marine sponge *Phakellia fusca*. Lett. Appl. Microbiol. *61*, 580–587.

Yokooji, Y., Sato, T., Fujiwara, S., Imanaka, T., and Atomi, H. (2013). Genetic examination of initial amino acid oxidation and glutamate catabolism in the hyperthermophilic archaeon *Thermococcus kodakarensis*. J. Bacteriol. *195*, 1940–1948.

Zaky, A.S., Greetham, D., Tucker, G.A., and Du, C. (2018). The establishment of a marine focused biorefinery for bioethanol production using seawater and a novel marine yeast strain. Sci. Rep. *8*, 1–14.

Zeng, Z., and Bromberg, Y. (2019). Predicting functional effects of synonymous variants: a systematic review and perspectives. Front. Genet. *10*.

Zeng, X., Birrien, J.-L., Fouquet, Y., Cherkashov, G., Jebbar, M., Querellou, J., Oger, P., Cambon-Bonavita, M.-A., Xiao, X., and Prieur, D. (2009). *Pyrococcus* CH1, an obligate piezophilic hyperthermophile: extending the upper pressure-temperature limits for life. ISME J. *3*, 873–876.

Zeng, X., Zhang, X., Jiang, L., Alain, K., Jebbar, M., and Shao, Z. (2013). *Palaeococcus pacificus* sp. nov., an archaeon from deep-sea hydrothermal sediment. Int. J. Syst. Evol. Microbiol. *63*, 2155–2159.

Zeng, X., Zhang, X., and Shao, Z. (2020). Metabolic adaptation to sulfur of hyperthermophilic *Palaeococcus pacificus* DY20341T from deep-sea hydrothermal sediments. Int. J. Mol. Sci. *21*, 368.

Zeng, Y., Luo, M., and Liu, Y. (2018). Future energy consumption prediction based on grey forecast model. ArXiv151005248 Stat.

Zeppilli, D., Leduc, D., Fontanier, C., Fontaneto, D., Fuchs, S., Gooday, A.J., Goineau, A., Ingels, J., Ivanenko, V.N., Kristensen, R.M., et al. (2018). Characteristics of meiofauna in extreme marine ecosystems: a review. Mar. Biodivers. *48*, 35–71.

Zhang, Y.-M., Shao, Z.-Q., Yang, L.-T., Sun, X.-Q., Mao, Y.-F., Chen, J.-Q., and Wang, B. (2013). Non-random arrangement of synonymous codons in archaea coding sequences. Genomics *101*, 362–367.

Zillig, W., Holz, I., Janekovic, D., Schäfer, W., and Reiter, W.D. (1983). The archaebacterium *Thermococcus celer* represents, a novel genus within the thermophilic branch of the archaebacteria. Syst. Appl. Microbiol. *4*, 88–94.

Zillig, W., Holz, I., Klenk, H.-P., Trent, J., Wunderl, S., Janekovic, D., Imsel, E., and Haas, B. (1987). *Pyrococcus woesei*, sp. nov., an ultra-thermophilic marine archaebacterium, representing a novel order, *Thermococcales*. Syst. Appl. Microbiol. *9*, 62–70.

Zinder, S., and Koch, M. (1984). Non-aceticlastic methanogenesis from acetate: acetate oxidation by a thermophilic syntrophic coculture. Arch. Microbiol. *138*, 263–272.

Zivanovic, Y., Lopez, P., Philippe, H., and Forterre, P. (2002). *Pyrococcus* genome comparison evidences chromosome shuffling-driven evolution. Nucleic Acids Res. *30*, 1902–1910.

Zivanovic, Y., Armengaud, J., Lagorce, A., Leplat, C., Guérin, P., Dutertre, M., Anthouard, V., Forterre, P., Wincker, P., and Confalonieri, F. (2009). Genome analysis and genome-wide proteomics of *Thermococcus gammatolerans*, the most radioresistant organism known amongst the *Archaea*. Genome Biol. *10*, R70.

Zobell, C.E. (1952). Bacterial life at the bottom of the Philippine Trench. Science *115*, 507–508.

Zobell, C.E., and Oppenheimer, C.H. (1950). Some effects of hydrostatic pressure on the multiplication and morphology of marine bacteria. J. Bacteriol. *60*, 771–781.

Züttel, A. (2003). Materials for hydrogen storage. Mater. Today *6*, 24–33.

Zwickl, P., Fabry, S., Bogedain, C., Haas, A., and Hensel, R. (1990). Glyceraldehyde-3-phosphate dehydrogenase from the hyperthermophilic archaebacterium *Pyrococcus woesei*: characterization of the enzyme, cloning and sequencing of the gene, and expression in *Escherichia coli*. J. Bacteriol. *172*, 4329–4338.

(2017). Extremely thermophilic energy metabolisms: biotechnological prospects. Curr. Opin. Biotechnol. *45*, 104–112.

DOCTORAT SCIENCES BRETAGNE DE LA MER LOIRE ET DU LITTORAL

UBO Université de Bretagne Occidentale

Titre : Bio-production d'H_2 à haute température chez des modèles de *Thermococcales* : bases pour des solutions de haute pression optimisées (HPBioHyd)

Mots clés : Hydrogène, *Thermococcales*, haute pression, bioréacteur, métabolisme, évolution adaptative en laboratoire.

Résumé : L'H_2, vecteur d'énergie prometteur, peut être synthétisé par les *Thermococcales*. La haute pression (HP) influencerait le métabolisme associé, mais n'a pas été envisagée en pratique. Après criblage d'isolats pour dégradations de substrats et productions d'H_2, *T. barophilus* MP^T, croissant préférentiellement à 40 MPa, a été choisi comme modèle, et sa fermentation a été décrite dans un contexte appliqué. Des méthodes HP ont été optimisées pour étudier l'H_2. Un bioréacteur de 400 mL de culture continue a été amélioré, maintenant des fluides corrosifs à HP hydrostatique (jusqu'à 120 MPa) et gazeuse (jusqu'à 40 MPa) jusqu'à 150 °C. Il a permis de mesurer la production d'H_2 de notre souche à HP gazeuse. Un tube compressible pour culture discontinue à phase gaz étanche a été inventé, et a servi à mesurer la production d'H_2 de *T. barophilus* en HP hydrostatique. Le métabolisme HP de la souche a été étudié grâce à des délétions préalables de gènes clés (*mbh*, *mbs*, *co-mbh*, *sh*I, *sh*II). Les rôles des enzymes liées ont été précisés via des mesures de croissances, produits (H_2, H_2S, acétate) et expressions génétiques des mutants, à 0,1 et 40 MPa. La tolérance à l'H_2 de *T. barophilus* a été augmentée par évolution adaptative en laboratoire. « Evol », la souche fille acclimatée durant 76 générations à une saturation d'H_2, a crû dans 10% d'H_2, contrairement à la souche mère. Pour comprendre ces adaptations, les produits (H_2, H_2S, acétate), transcriptomes et génomes des deux souches ont été comparés. Avec 119 mutations génomiques, le métabolisme de l'H_2 a été modifié dans le variant. Ce projet souligne l'intérêt du caractère piézophile des *Thermococcales* dans la bio-production d'H_2 et permet de proposer des stratégies d'H_2 et permet de proposer des stratégies d'optimisation.

Title: High temperature H2 bio-production in *Thermococcales* models: setting up bases for optimized high pressure solutions

Keywords: Hydrogen *Thermococcales*, high pressure, bioreactor, metabolism, adaptive laboratory evolution.

Abstract: H_2, a promising energetic vector, can be synthesized by *Thermococcales*. High pressure (HP) could influence the associated metabolism, but was not practically considered. After having screened isolates for assets in substrate degradation and H_2 yields, *T. barophilus* MP^T, growing optimally at 40 MPa, was chosen as a model and its metabolism was characterized in an applied context. Methods for HP culture were optimized for H_2 studies. Our HP bioreactor for continuous culture underwent major improvements. This 400 mL container, able to maintain corrosive fluids at hydrostatic (up to 120 MPa) and gas (up to 40 MPa) pressures, at up to 150 °C, served to assess H_2 production of our strain at high gas pressure. We also created a compressible device for discontinuous leak-free gas-phase incubations, allowing to measure *T. barophilus* HP H_2 production (hydrostatic). HP adaptations of *T. barophilus* were observed thanks to previous deletions of key genes (*mbh*, *mbs*, *co-mbh*, *sh*I, *sh*II). We refined the roles of each concerned enzyme by assessing growths, end-products (H_2, H_2S, acetate), and gene expressions of the mutants, at 0.1 and 40 MPa. Additionally, we enhanced H_2 tolerance in our model by adaptive laboratory evolution. "Evol", the ensuing strain acclimatized to H_2-saturating conditions for 76 generations, grew in 10% H_2, contrarily to the parent strain. To understand such adaptation, we compared both strains' end-products (H_2, H_2S, acetate), transcriptomes, and genomes. 119 mutations were detected and the H_2 metabolism was changed in the new variant. This work underlines the interest of *Thermococcales*' piezophily for H_2 bio-production and permits to propose optimization strategies.